

Open Research Online

The Open University's repository of research publications and other research outputs

Nutrient availability modulating physiology and pathogenicity of *Legionella pneumophila*

Thesis

How to cite:

James, Brian William (1997). Nutrient availability modulating physiology and pathogenicity of *Legionella pneumophila*. PhD thesis The Open University.

For guidance on citations see [FAQs](#).

© 1997 The Author



<https://creativecommons.org/licenses/by-nc-nd/4.0/>

Version: Version of Record

Link(s) to article on publisher's website:

<http://dx.doi.org/doi:10.21954/ou.ro.0000e15d>

Copyright and Moral Rights for the articles on this site are retained by the individual authors and/or other copyright owners. For more information on Open Research Online's data [policy](#) on reuse of materials please consult the policies page.

oro.open.ac.uk

UNRESTRICTED

**NUTRIENT AVAILABILITY MODULATING PHYSIOLOGY AND
PATHOGENICITY OF *LEGIONELLA PNEUMOPHILA***

BRIAN WILLIAM JAMES

**A thesis submitted in partial fulfilment of the requirements
of the Open University for the degree of**

Doctor of Philosophy

February 1997

Authors no. P9272116
Date of award: 3rd September 1997

**Centre for Applied Microbiology and Research,
Porton Down, Salisbury, Wiltshire SP4 0JG.**

**Collaborating Establishment:
Thames Water Utilities plc**

ABSTRACT

A virulent strain of *Legionella pneumophila* serogroup 1 was established in continuous culture under defined iron-replete conditions at pH 6.9. Iron-limitation and extremes of pH (6.0 and 7.8) influenced the growth and metabolism of *L. pneumophila*, as manifested by increased metabolic activity, impaired energy coupling, and altered metabolic fluxes. In particular, the physiological versatility of *L. pneumophila* was demonstrated by a significant decrease in the iron content of biomass (6-fold increase in Y_{iron}), coupled with reduced metabolic efficiency (Y_{carbon}), in response to iron-limited growth. Iron limitation promoted the accumulation of significant intracellular reserves of poly- β -hydroxybutyrate (16 % cell dry wt.), which supported long-term survival of *L. pneumophila* under starvation conditions.

Expression of the important pathogenicity factor, the zinc metalloprotease, was regulated by iron availability. Common iron acquisition mechanisms, such as siderophores and transferrin receptors, were not elaborated by iron-limited cells. However, human transferrin was identified as a potential iron source for *L. pneumophila*, with the zinc metalloprotease mediating transferrin digestion and possibly iron acquisition. Iron-limitation and extremes of pH also influenced cellular morphology and the surface properties of *L. pneumophila*, promoting the formation of uniform cultures of short rod-shaped bacteria, with altered fatty acid, phospholipid and protein composition.

In addition to morphological and physiological adaptation, iron limitation had a significant effect on the virulence of *L. pneumophila*. Iron-replete cells grown at pH 6.9 and 6.0 were highly virulent in a guinea pig model. However, the virulence of *L. pneumophila* was significantly attenuated ($P < 0.05$) in response to iron-limited growth. This phenomenon was reversible, and correlated with reduced phagocytosis and / or reduced intracellular survival following infection. Decreasing the pH of iron-limited cultures to 6.0 did not stimulate recovery of culture virulence. Therefore, this study clearly demonstrates that environmental stresses, including iron limitation and extremes of pH, play an important role in modulating the physiology and virulence of *L. pneumophila*, inducing the expression of distinct phenotypes differing in their ability to persist in nature and cause infection.

DECLARATION

No portion of the work referred to in this thesis has been submitted in support of an application for another degree or qualification of this university, or any other institute of learning.

ACKNOWLEDGEMENTS

I wish to express my sincere gratitude to Dr. C. W. Keevil, Dr. S. A. Leach and Dr. P. J. Dennis for their constant support and encouragement. I would also like to thank Dr. R. B. Fitzgeorge for his guidance and enthusiasm until his retirement, and Professor P. D. Marsh for his encouragement and understanding. Special thanks are owed to Mr. R. Wait for assistance with fatty acid and phospholipid analysis, and helpful discussion; Dr. A. Williams for the provision of antibodies, expert tuition with the macrophage assay, and critical appraisal of the introduction; Mr M. S. Lever and Dr. R. B. Fitzgeorge for performing aerosol challenge experiments; Mr. A. Hiscott for assistance with flow cytometry, and Dr. B. Mulloy, NIBSC, for providing NMR analysis. I also gratefully acknowledge Mr. M. Riches and his staff for medium preparation; Mr. M. Randles and Ms. M. Welsh for providing analytical support; Mr. A. B. Dowsett for performing electron microscopy, and the CAMR Library staff for their assistance. Finally, thanks to Lorna who cooked, cleaned, ironed, did the shopping and made my lunch, under extreme duress.

DEDICATION

TO LORNA

PUBLICATIONS

James, B. W., W. S. Mauchline, R. B. Fitzgeorge, P. J. Dennis, and C. W. Keevil. 1995. Influence of iron-limited continuous culture on physiology and virulence of *Legionella pneumophila*. Infect. Immun. 63:4224-4230.

James, B. W., W. S. Mauchline, P. J. Dennis, and C. W. Keevil. 1997. A study of iron acquisition mechanisms of *Legionella pneumophila* grown in chemostat culture. Curr. Microbiol. In press.

CONTENTS

Abstract	II
Declaration	III
Acknowledgements	IV
Dedication	V
Publications	VI
Contents	VII
Table of Contents	VIII
List of Figures	XVII
List of Tables	XXIII
Glossary of Abbreviations	XXV
Introduction	1
Materials and Methods	27
Results	69
Discussion	215
References	262

TABLE of CONTENTS

INTRODUCTION	1
1.1 Legionnaires' Disease.	1
1.1.1 Historical background.	1
1.1.2 Clinical features and diagnosis.	1
1.1.3 Epidemiology.	2
1.1.4 Source and mode of transmission.	3
1.1.5 <i>Legionella</i> identification and classification.	4
1.2 <i>Legionella</i> Physiology.	5
1.2.1 Morphology.	5
1.2.2 Biochemical activity.	6
1.2.3 Nutrition.	6
1.2.4 Culture media and growth conditions.	7
1.3 <i>Legionella</i> Ecology.	8
1.3.1 Interactions with other micro-organisms.	8
1.3.2 Physico-chemical properties of the source environment.	9
1.4 Cell Biology of <i>Legionella</i> Pathogenesis.	10
1.4.1 Attachment and phagocytosis.	11
1.4.2 Intracellular Response.	12
1.4.3 Immunity.	12
1.5 Virulence Determinants.	13
1.5.1 Virulence loci and cell associated factors.	13
1.5.2 Extracellular enzymes.	15
1.5.3 Toxins.	16

1.6 Environmental Regulation of <i>Legionella</i> Virulence.	16
1.6.1 Intra-amoebic growth.	17
1.6.2 Environmental temperature and pH.	18
1.6.3 Nutrient limitation.	18
1.6.4 Iron limitation.	19
1.6.5 Control of gene expression.	21
1.7 Studying Environmental Regulation of Microbial Physiology and Virulence.	22
1.7.1 Continuous culture	23
1.7.2 Virulence models.	24
1.8 Aims of this Study.	25
 MATERIALS and METHODS	 27
 2.1 Organism.	 27
2.2 Culture Media.	27
2.3 Continuous Culture.	31
2.3.1 Culture apparatus.	31
2.3.2 Chemostat inoculation and culture.	34
2.4 Culture Analyses.	34
2.4.1 Culture purity.	34
2.4.2 Optical density determination.	34
2.4.3 Dry weight determination.	35
2.4.4 Enumeration of colony forming units.	35
2.4.5 Total Cell Count.	35
2.4.6 Sample collection and storage.	35

	X
2.5 Chemical Analysis of Culture Supernatant and Medium Samples.	36
2.5.1 Amino acid analysis.	36
2.5.2 Ammonium and phosphate determination.	37
2.5.3 Iron and zinc determination.	37
2.5.4 Organic carbon analysis.	38
2.6 Monitoring Cellular and Colony Morphology.	38
2.6.1 Light microscopy.	38
2.6.2 Electron microscopy.	38
2.6.3 Indirect fluorescent antibody staining.	39
2.6.4 Nile red staining.	39
2.7 Protein Determination.	40
2.8 Preparation of Concentrated Culture Supernatants.	41
2.9 Fast Pressure Liquid Chromatography (FPLC) of Extracellular Proteins.	41
2.10 Azocasein Hydrolytic Activity of Culture Supernatants.	41
2.10.1 Determination of azocasein hydrolytic activity.	41
2.10.2 Inhibition of azocasein hydrolysis with EDTA.	42
2.10.3 Recovery of hydrolytic activity.	43
2.10.4 Inhibition of azocasein hydrolysis by anti-zinc-metalloprotease IgG.	43
2.10.5 Caseinase assay.	44
2.11 Phospholipase C Activity.	45
2.12 Human Transferrin Utilisation as a Source of Iron.	46
2.12.1 Preparation of diferric human transferrin.	46
2.12.2 Growth response of iron-limited cultures to diferric transferrin.	46
2.12.3 Transferrin receptor assay.	47
2.12.4 Digestion of human transferrin by <i>L. pneumophila</i> culture supernatants.	47

2.13 Siderophore Assays.	48
2.13.1 Universal siderophore assay.	48
2.13.2 Ferric chloride binding assay.	49
2.13.3 Emery and Neilands assay.	49
2.13.4 Csaky assay.	49
2.13.5 Arnow assay.	50
2.14 Determination of Ferric Citrate Reductase Activity.	50
2.15 Analysis of Serogroup Antigen.	50
2.15.1 Extraction of serogroup antigen.	50
2.15.2 Keto-2-3-deoxyoctonate determination.	51
2.15.3 Carbohydrate determination.	52
2.15.4 Protein determination.	52
2.15.5 SDS-PAGE of serogroup antigen.	52
2.16 Analysis of Cellular Protein Expression.	53
2.16.1 Preparation of cell proteins.	53
2.16.2 SDS-PAGE of protein preparations.	54
2.17 Analysis of Membrane Lipid Composition.	54
2.17.1 Extraction of fatty acids.	54
2.17.2 Polar lipid extraction.	55
2.17.3 Gas chromatography and mass spectrometry of fatty acid methyl esters.	55
2.17.4 Fast atom bombardment (FAB) mass spectrometry of polar lipids.	56
2.18 Virulence and Intracellular Growth.	57
2.18.1 Virulence testing.	57
2.18.2 <i>In vitro</i> macrophage assay.	58
2.18.3 <i>In vivo</i> infection and multiplication assay.	59

2.19 Poly- β -hydroxybutyrate Formation.	60
2.19.1 Poly- β -hydroxybutyrate extraction.	60
2.19.2 PHB determination.	60
2.19.3 NMR spectroscopy.	61
2.20 PHB Determination by Nile Red Spectrofluorimetry.	61
2.20.1 Determination of excitation and emission maxima.	62
2.20.2 Optimum incubation time.	63
2.20.3 Relationship between cell density and fluorescence.	64
2.20.4 Influence of Nile red concentration on fluorescence.	64
2.20.5 Spectrofluorometric determination of the PHB content of samples.	65
2.20.6 Relationship between PHB yield and Nile red fluorescence.	65
2.21 Survival of <i>L. pneumophila</i> in a Low-Nutrient Aquatic Environment.	66
2.21.1 Analysis of starved cells.	66
2.21.2 Nile red spectrofluorometric analysis of starved cells.	66
2.21.3 Flow cytometry analysis of starved cells stained with Nile red.	67
2.21.4 Heat shock treatment of starved cells.	67

RESULTS 69

3.1 Influence of Iron Limitation on the Physiology of <i>L. pneumophila</i> .	69
3.1.1 Growth of <i>L. pneumophila</i> in iron-replete continuous culture.	69
3.1.2 Influence of iron limitation on the growth of <i>L. pneumophila</i> .	69
3.1.3 Nutrient utilisation by iron-limited and -replete cultures.	71
3.1.4 Growth characteristics of iron-limited and -replete cultures.	72
3.1.5 Influence of iron concentration on the growth of iron-limited cultures.	75
3.2 Influence of Iron Limitation on the Morphology of <i>L. pneumophila</i> .	77

3.3 Extracellular Protein Production.	77
3.3.1 Influence of iron limitation on extracellular protein production.	77
3.3.2 Separation of extracellular proteins by anion-exchange FPLC.	82
3.3.3 SDS-PAGE of FPLC fractions.	84
3.3.4 Zinc metalloprotease activity of iron-limited and -replete supernatants.	85
3.3.5 Phospholipase C activity of iron-limited and -replete cultures.	88
3.4 Iron Acquisition by <i>L. pneumophila</i> .	88
3.4.1 Ferric citrate reductase activity of iron-replete and -limited cultures.	88
3.4.2 Growth response of iron-limited cultures to human transferrin.	91
3.4.3 Surface associated transferrin receptors.	92
3.4.4 Transferrin digestion by <i>L. pneumophila</i> culture supernatants.	93
3.4.5 Zinc metalloprotease and transferrin digestion.	98
3.4.6 Universal siderophore assay.	101
3.4.7 Csaky assay for hydroxymates.	101
3.4.8 Emery and Neilands assay for hydroxymates.	102
3.4.9 Arnow assay for phenolate type siderophores.	104
3.4.10 Ferric chloride assay for iron-binding activity.	104
3.5 Influence of Iron Limitation on Membrane Lipid Composition.	107
3.5.1 Membrane fatty acid composition of iron-limited and -replete cells.	107
3.5.2 Membrane phospholipid composition of iron-limited and -replete cells.	108
3.5.3 Analysis of individual phospholipid species.	113
3.6 Analysis of Cellular Protein Expression.	118
3.6.1 Whole cell protein profiles of iron-limited and -replete cells.	118
3.6.2 Cytoplasmic membrane proteins.	118
3.6.3 Outer membrane proteins.	119
3.7 Influence of Iron Limitation on Serogroup Antigen Expression.	124
3.7.1 Analysis of serogroup antigen by SDS-PAGE.	124
3.7.2 Chemical analyses of serogroup antigen.	125

3.8 Virulence and Intracellular Growth of <i>L. pneumophila</i> .	126
3.8.1 Influence of iron limitation on the virulence of <i>L. pneumophila</i>	126
3.8.2 Intracellular growth of iron-limited and -replete cells.	127
3.8.3 Growth of iron-limited and -replete cultures <i>in vivo</i> .	129
3.9 Influence of Culture pH on Physiology of Iron-Replete Cultures of <i>L. pneumophila</i> .	132
3.9.1 Influence of pH on the growth of iron-replete cultures.	132
3.9.2 Nutrient utilization by iron-replete cultures grown at extremes of pH.	135
3.9.3 Growth characteristics of iron-replete cultures at extremes of pH.	135
3.10 Influence of pH on the Morphology of Iron-Replete cultures.	138
3.10.1 Cellular morphology.	138
3.10.2 Colony morphology.	141
3.11 Influence of Culture pH on the Physiology of Iron-limited <i>L. pneumophila</i> .	143
3.11.1 Growth response of iron-limited cultures to low and high pH.	143
3.11.2 Nutrient utilization by iron-limited cultures at different pH values.	146
3.11.3 Growth characteristics of iron-limited cultures at extremes of pH.	149
3.12 Influence of pH on the Morphology of Iron-Limited <i>L. pneumophila</i> .	151
3.12.1 Cellular morphology.	151
3.12.2 Colony morphology.	153
3.13 Influence of pH on Extracellular Protein Production by Iron-Limited and -Replete Cultures.	156
3.14 Influence of pH on Expression of Azocasein Hydrolytic Activity.	156
3.15 Influence of Growth at pH 6.0 on the Virulence of <i>L. pneumophila</i> .	158

3.16 Influence of pH on Membrane Lipid Composition of Iron-Replete Cells.	160
3.16.1 Lipid composition of replete pH 6.0 cultures with different colony phenotypes.	160
3.16.2 Influence of culture pH on the membrane fatty acid composition of iron-replete cells.	162
3.16.3 Effect of culture pH on the phospholipid composition of iron-replete cells.	164
3.16.4 Analysis of individual phospholipid species.	166
3.17 Influence of pH on Cellular Protein Expression by Iron-Replete Cells.	170
3.18 Serogroup Antigen Expression by Iron-Replete Cultures at Extremes of pH.	173
3. 19 Physiology of Poly- β -hydroxybutyrate Formation by <i>L. pneumophila</i> .	176
3. 19.1 Intracellular granule formation by iron-limited and -replete cells.	176
3.19.2 Nile red staining of intracellular inclusions.	177
3.19.3 Analysis of PHB by ^1H NMR spectroscopy.	179
3.19.4 Comparison of the PHB content of iron-limited and -replete cells.	181
3.19.5 Relationship between Nile red fluorescence and PHB content.	182
3.19.6 Spectrofluorometric analysis of iron-limited and -replete samples.	185
3.19.7 Relationship between PHB content and culture biomass yield.	187
3.19.8 Influence of culture pH on PHB accumulation by <i>L. pneumophila</i> .	188
3.20 Survival of <i>L. pneumophila</i> in a Low Nutrient Environment.	192
3.20.1 PHB content and the survival of <i>L. pneumophila</i> in a low nutrient environment.	192
3.20.2 Flow Cytometry analysis of starved cells.	200
3.20.3 Morphological examination of starved cells.	209
3.20.4 Heat shock treatment of nutrient stressed <i>L. pneumophila</i> .	214

DISCUSSION	215
4.1 Physiology of <i>L. pneumophila</i> Grown in Chemostat Culture.	215
4.1.1 Influence of iron limitation on growth and metabolism of <i>L. pneumophila</i> .	215
4.1.2 Influence of pH on growth and metabolism of iron-replete <i>L. pneumophila</i> .	220
4.1.3 Growth response of iron-limited cultures to changes in culture pH.	224
4.2 Influence of Growth Environment on Cellular and Colony Morphology.	225
4.3 Influence of Iron Limitation and pH on the Virulence of <i>L. pneumophila</i> .	228
4.4 Extracellular Protein Production and Iron Acquisition Mechanisms.	232
4.4.1 Pigment formation.	232
4.4.2 Extracellular protein production.	233
4.4.3 Zinc metalloprotease.	233
4.4.4 Phospholipase C activity.	235
4.4.5 Ferric citrate reductase.	236
4.4.6 Human transferrin as a potential iron-source.	238
4.4.6 Siderophore activity.	240
4.5 Influence of Growth Environment on Membrane Composition.	242
4.5.1 Membrane lipid composition.	242
4.5.2 Membrane protein expression.	245
4.5.3 Serogroup antigen expression.	250
4.6 The Physiology of Poly- β -hydroxybutyrate Accumulation.	251
4.7 Relationship between PHB Reserves and Survival of <i>L. pneumophila</i> in a Low-Nutrient Environment.	255
4.8 Conclusion.	259
4.9 Future work.	260
REFERENCES	262

LIST of FIGURES

Figure 1. Schematic of the continuous culture apparatus.	32
Figure 2. Continuous culture apparatus housed within a class III cabinet.	33
Figure 3. Caseinase assay.	44
Figure 4. Excitation and emission fluorescence spectra of <i>L. pneumophila</i> stained with Nile red.	62
Figure 5. Relationship between Nile red fluorescence and incubation time.	63
Figure 6. Relationship between sample optical density and Nile red fluorescence.	64
Figure 7. Influence of Nile red concentration on fluorescence.	65
Figure 8. Batch growth of <i>L. pneumophila</i> , strain Corby, in ABCD medium.	70
Figure 9. Growth response of a steady state iron-replete culture to iron limitation.	70
Figure 10. Growth response of an iron-limited chemostat culture to ferrous sulphate.	71
Figure 11. Relationship between the molar growth yield for iron (Y_{iron}) and the concentration of iron metabolised by iron-limited cultures.	75
Figure 12. Cultures of <i>L. pneumophila</i> as viewed by DIC microscopy.	78
Figure 13. Transmission electron micrographs of <i>L. pneumophila</i> .	79
Figure 14. Indirect fluorescent antibody staining of <i>L. pneumophila</i> cultures with serogroup 1 specific polyclonal antiserum.	80
Figure 15. Colony morphology of <i>L. pneumophila</i> chemostat cultures.	81
Figure 16. FPLC anion exchange elution profiles of culture supernatants.	83
Figure 17. Silver stained SDS-PAGE of FPLC fractions	84
Figure 18. Relationship between the azocasein hydrolytic activity of iron-limited cultures and the concentration of iron metabolised.	87
Figure 19. Increase in the azocasein hydrolytic activity and the optical density of an iron-limited chemostat culture, in response to iron addition.	87
Figure 20. Growth response of a steady state iron-limited chemostat culture to 2.5 μM iron, supplied as human diferric-transferrin or ferrous sulphate.	91
Figure 21. Analysis of <i>L. pneumophila</i> for the expression of human transferrin receptors.	92

Figure 22. SDS-PAGE of iron-saturated human transferrin incubated in iron-replete culture supernatant.	94
Figure 23. SDS-PAGE of iron-saturated human transferrin incubated in iron-limited culture supernatant.	95
Figure 24. SDS-PAGE of iron-free human transferrin incubated in iron-replete culture supernatant.	96
Figure 25. SDS-PAGE of human lactoferrin incubated in iron-replete culture supernatant.	97
Figure 26. SDS-PAGE of human transferrin incubated in iron-replete supernatant, demonstrating inhibition of Hu-Tf digestion by anti-zinc metalloprotease antiserum.	99
Figure 27. SDS-PAGE of human transferrin incubated in iron-replete supernatant, demonstrating inhibition of Hu-Tf digestion by anti-zinc metalloprotease IgG.	100
Figure 28. Comparison of desferroxamine standard calibration curves for the Universal siderophore assay.	102
Figure 29. Differential absorption spectra of culture supernatant and standard samples following periodate oxidation.	103
Figure 30. Differential absorption spectra of culture supernatant and standard samples reacted with acidified ferric chloride.	105
Figure 31. Relationship between sample volume and absorbance at 470 nm, following reaction with acidified ferric chloride.	106
Figure 32. Positive ion FAB mass spectra of <i>L. pneumophila</i> .	109
Figure 33. The structure of phospholipids most commonly found in legionellae.	110
Figure 34. Comparison of the relative intensities of the protonated molecules of phosphatidylethanolamines and phosphatidylcholines from iron-limited and -replete samples.	111
Figure 35. Negative ion FAB mass spectra of <i>L. pneumophila</i> .	112
Figure 36. Comparison of the relative intensities of the deprotonated molecules of phosphatidylethanolamines and phosphatidylglycerols, from the negative ion spectra of iron-replete and -limited cultures.	113
Figure 37. Constant neutral loss spectra recorded for individual phospholipid species extracted from iron-replete samples of <i>L. pneumophila</i> .	115

Figure 38. Phosphatidylethanolamine and <i>N</i> -methylphosphatidylethanolamine profiles of iron-replete and-limited <i>L. pneumophila</i> .	116
Figure 39. Di- <i>N</i> -methylphosphatidylethanolamine and phosphatidylglycerol profiles of iron-replete and -limited <i>L. pneumophila</i> .	117
Figure 40. Silver stained SDS-PAGE total cell protein profiles.	120
Figure 41. Silver stained SDS-PAGE cytoplasmic membrane protein profiles.	121
Figure 42. Silver stained SDS-PAGE outer membrane protein profiles.	122
Figure 43. SDS-PAGE separation of <i>L. pneumophila</i> serogroup antigen.	124
Figure 44. Uptake and intracellular growth of iron-limited and -replete cultures in guinea pig alveolar macrophages cultured <i>in vitro</i> .	130
Figure 45. Comparison of the growth of iron-limited and -replete <i>L. pneumophila</i> in guinea-pig lungs.	131
Figure 46. Growth response of a steady state iron-replete culture to an incremental decrease in culture pH from 6.9 to 6.0.	133
Figure 47. Growth response of a steady state pH 6.0 iron-replete culture to the addition of 10 mM serine into the culture.	133
Figure 48. Growth response of a steady state iron-replete culture to an incremental increase in culture pH from 6.9 to 7.8.	134
Figure 49. Growth response of a steady state pH 7.8 iron-replete culture to the addition of 10 mM serine into the culture.	134
Figure 50. Residual amino acid concentrations in samples of clarified supernatant, from iron-replete cultures grown at different pH values.	137
Figure 51. Cellular morphology of iron-replete cultures of <i>L. pneumophila</i> grown at (a) pH 6.0, and (b) pH 7.8, as viewed by DIC microscopy.	140
Figure 52. (a) Normal and variant colony morphologies of iron-replete pH 6.0 cells; (b) indirect fluorescent antibody staining of the pH 6.0 culture.	142
Figure 53. Normal and variant colony morphologies of iron-replete pH 7.4 cells, when grown on BCYE agar.	143
Figure 54. Growth response of a steady state iron-limited chemostat culture to an incremental decrease in culture pH from 6.9 to 6.0.	144
Figure 55. Growth response of a steady state iron-limited (pH 6.0) culture to the addition of 2.5 μ M ferrous sulphate.	144

- Figure 56. Growth response of a steady state iron-limited chemostat culture to an incremental increase in culture pH from 6.9 to 7.8. 145
- Figure 57. Growth response of a steady state iron-limited (pH 7.8) chemostat culture to the addition of 2.5 μ M ferrous sulphate. 146
- Figure 58. Comparison of residual amino acid concentrations in samples of supernatant collected from iron-limited cultures grown at different pH values. 148
- Figure 59. Cellular morphology of *L. pneumophila* cultured under iron-limited conditions at pH 6.0, as viewed by DIC microscopy. 151
- Figure 60. Indirect fluorescent antibody labelling of iron-limited pH 6.0 cultures of *L. pneumophila* with serogroup 1 specific polyclonal antiserum. 152
- Figure 61. Cellular morphology of *L. pneumophila* cultured under iron-limited conditions at pH 7.8, as viewed by DIC microscopy. 152
- Figure 62. Normal and variant colony morphologies observed in iron-limited pH 6.0 cultures, when grown on BCYE agar. 154
- Figure 63. Indirect fluorescent antibody staining of cells from normal and variant colonies. 155
- Figure 64. Fatty acid profiles of iron-replete (pH 6.0) cultures which exhibited different colony morphologies on BCYE agar. 161
- Figure 65. Comparison of the relative intensities of the protonated molecules of phosphatidylethanolamines and phosphatidylcholines, for two iron-replete pH 6.0 cultures which displayed different colony morphologies. 161
- Figure 66. Influence of culture pH on the membrane fatty acid composition of iron-replete cultures of *L. pneumophila*. 163
- Figure 67. Influence of culture pH on the relative intensities of the protonated molecules of phosphatidylethanolamines and phosphatidylcholines of iron-replete cultures. 165
- Figure 68. Influence of culture pH on the relative intensities of deprotonated phosphatidylglycerols, from the negative ion spectra of iron-replete cultures. 166
- Figure 69. Influence of culture pH on the phosphatidylethanolamine and *N*-methylphosphatidylethanolamine profiles of iron-replete cultures. 168

Figure 70. Influence of pH on the di- <i>N</i> -methylphosphatidylethanolamine and phosphatidylglycerol profiles of iron-replete cultures of <i>L. pneumophila</i> .	169
Figure 71. Comparison of silver stained SDS-PAGE whole cell protein profiles of <i>L. pneumophila</i> , grown in iron-replete culture at different pH values.	171
Figure 72. SDS-PAGE profiles of <i>L. pneumophila</i> serogroup antigen.	174
Figure 73. Electron micrograph of chemostat grown cells revealing the presence of intracellular granule-like inclusions.	176
Figure 74. Laser confocal microscopic examination of <i>L. pneumophila</i> stained with the fluorescent lipophilic dye, Nile red, and counter stained with FITC.	177
Figure 75. Laser confocal microscopic examination of <i>L. pneumophila</i> stained with the fluorescent lipophilic dye, Nile red.	178
Figure 76. ¹ H NMR spectrum at 500 MHz of PHB.	180
Figure 77. Relationship between Nile red spectrofluorescence and PHB yield.	183
Figure 78. Relationship between Nile red spectrofluorescence and PHB yield.	184
Figure 79. Relationship between PHB content of <i>L. pneumophila</i> samples and Nile red fluorescence.	184
Figure 80. Comparison of NR spectrofluorescence values for iron-limited and -replete samples of <i>L. pneumophila</i> .	186
Figure 81. Relationship between PHB content and the biomass yield of iron-limited cultures of <i>L. pneumophila</i> .	187
Figure 82. Relationship between calculated PHB content and the concentration of iron metabolised, by iron-limited cultures of <i>L. pneumophila</i> .	188
Figure 83. Fluorescent microscopic examination of culture samples grown at pH 6.0 and stained with NR.	189
Figure 84. Fluorescent microscopic examination of culture samples grown at pH 7.8 and stained with NR.	190
Figure 85. Influence of starvation on the culturability, total cell count, and NR spectrofluorescence, of a suspension of <i>L. pneumophila</i> incubated in filter sterilized tap water.	193
Figure 86. The relationship between the decline in culturability and NR spectrofluorescence.	194

Figure 87. Influence of starvation on the optical density (540 nm), and NR spectrofluorescence of a suspension of <i>L. pneumophila</i> .	195
Figure 88. Relationship between the decrease in NR spectrofluorescence and optical density.	195
Figure 89. Influence of nutrient starvation on the culturability and NR spectrofluorescence of a suspension of <i>L. pneumophila</i> .	197
Figure 90. The relationship between the decline in culturability and NR spectrofluorescence.	198
Figure 91. Comparison of the relationship between culturability and NR spectrofluorescence, for two cultures of <i>L. pneumophila</i> incubated under starvation conditions.	199
Figure 92. Flow cytometry analysis of the changes in cellular NR fluorescence in response to nutrient starvation.	201
Figure 93. Influence of nutrient starvation on the NR fluorescence of <i>L. pneumophila</i> , as determined by flow cytometry.	203
Figure 94. Relationship between the decline in culturability, and mean cellular fluorescence.	204
Figure 95. Comparison of dot plots representing the relative cell complexity and size distribution for <i>L. pneumophila</i> .	206
Figure 96. Influence of starvation on mean cell length and mean cell complexity.	207
Figure 97. Relationship between the percentage decrease in mean cellular fluorescence and mean cell complexity, in response to starvation.	208
Figure 98. Relationship between the decrease in culturability and mean cell complexity.	208
Figure 99. Fluorescent microscopic examination of NR stained samples of starved.	210
Figure 100. Fluorescent microscopic examination of starved cells stained with serogroup 1 specific polyclonal antiserum.	211
Figure 101. Influence of starvation on the cellular morphology of <i>L. pneumophila</i> , as viewed by DIC microscopy.	212
Figure 102. Colony morphology of starved cells after growth on BCYE agar.	213
Figure 103. Recovery of <i>L. pneumophila</i> on BCYE agar after heat shock treatment at 45°C for up to 60 minutes.	214

LIST of TABLES

Table I. Formulation of buffered charcoal yeast extract (BCYE) agar.	28
Table II. Stock solution formulations for ACES-Buffered Chemically Defined (ABCD) medium.	29
Table III. Preparation of ABCD medium.	30
Table IV. Concentration of nutrients (mM) in unused ABCD medium and in iron-limited and -replete culture supernatants.	73
Table V. Comparison of the growth characteristics of iron-replete and -limited cultures of <i>L. pneumophila</i> .	74
Table VI. Influence of iron concentration on the growth characteristics of iron-limited cultures.	76
Table VII. Comparison of the extracellular protein content of iron-limited and -replete cultures.	82
Table VIII. Comparison of the azocasein hydrolytic activity of iron-limited and -replete culture supernatants.	86
Table IX. Hydrolysis of <i>p</i> -nitrophenylphosphorylcholine by iron-limited and -replete culture supernatant and cell samples.	89
Table X. Comparison of the specific ferric citrate reductase activity of cell fractions from iron-limited and -replete <i>L. pneumophila</i> .	90
Table XI. Influence of iron limitation on the membrane fatty acid composition of <i>L. pneumophila</i> grown in chemostat culture.	107
Table XII. Comparison of iron-regulated proteins in the whole cell, inner and outer membrane fractions of iron-replete and -limited <i>L. pneumophila</i> .	123
Table XIII. Chemical composition of saline extracts of serogroup antigen from iron-limited and -replete cultures.	125
Table XIV. Comparison of the LD ₅₀ values for <i>L. pneumophila</i> grown in iron-limited and -replete continuous culture.	126
Table XV. LD ₅₀ values and their 95% confidence intervals for <i>L. pneumophila</i> grown in chemostat culture, under iron-limited and -replete conditions.	128

Table XVI. Association of iron-limited and -replete cells with host phagocytic cells <i>in vivo</i> .	131
Table XVII. Concentration of nutrients in unused medium and samples from iron-replete cultures grown at different pH values.	136
Table XVIII. Comparison of the growth properties of iron-replete chemostat cultures grown at pH 6.9, 6.0 and 7.8.	139
Table XIX. Comparison of the concentration of nutrients in unused culture medium and iron-limited cultures grown at different pH values.	147
Table XX. Comparison of the growth properties of iron-limited cultures grown at pH 6.9, 6.0, and 7.8.	150
Table XXI. Influence of culture pH on extracellular protein production by iron-limited and -replete cultures of <i>L. pneumophila</i> .	157
Table XXII. Influence of culture pH on the azocasein hydrolytic activity of iron-limited and -replete cultures.	157
Table XXIII. Comparison of LD ₅₀ values for <i>L. pneumophila</i> cultured under iron-replete conditions at pH 6.9 and 6.0.	159
Table XXIV. Comparison of LD ₅₀ values for <i>L. pneumophila</i> cultured under iron-limited conditions at pH 6.9 and 6.0.	159
Table XXV. Summary of alterations in whole cell protein expression by iron-replete cultures of <i>L. pneumophila</i> in response to pH.	172
Table XXVI. Influence of culture pH on the chemical composition of saline extracts of serogroup antigen from iron-replete cultures.	175
Table XXVII. Comparison of the chemical shifts and coupling constants from ¹ H NMR spectra of purified hot chloroform extracts.	181
Table XXVIII. Comparison of the PHB content of iron-replete and -limited samples of <i>L. pneumophila</i> .	182
Table XXIX. Comparison of the mean NR spectrofluorescence and calculated PHB content for iron-replete and -limited samples of <i>L. pneumophila</i> .	185
Table XXX. Influence of culture pH on the mean NR spectrofluorescence and calculated PHB content of iron-replete and -limited cultures.	191
Table XXXI. Influence of starvation on NR fluorescence, intracellular complexity and cell length of <i>L. pneumophila</i> , as determined by flow cytometry.	207

GLOSSARY of ABBREVIATIONS

ABCD	ACES-buffered chemically defined
BCYE	Buffered charcoal yeast extract
BSA	Bovine serum albumin
CAS	Chrome azurol S
CFU	Colony forming units
4CN	4-Chloro-1-naphthol
CNL	Constant neutral loss
DIC	Differential interference contrast
DMSO	Dimethyl sulphoxide
EDDA	Ethylenediamine-N,N-diacetic acid
EDTA	Ethylenediaminetetraacetic acid
FAB-MS	Fast atom bombardment mass spectrometry
FITC	Fluorescein isothiocyanate
FPLC	Fast pressure liquid chromatography
FSC	Forward scatter
HEPES	N-2-Hydroxyethylpiperazine-N-2-ethanesulphonic acid
HPLC	High pressure liquid chromatography
Hu-Tf	Human transferrin
IgG	Immunoglobulin G
KDO	Keto-2-3-deoxyoctonate
LPS	Lipopolysaccharide
MGT	Mean generation time
MIP	Macrophage infectivity potentiator
NMR	Nuclear magnetic resonance
NR	Nile red (9-diethylamino-5H-benzo[α]phenoxazine-5-one)

PAGE	Polyacrylamide gel electrophoresis
PBS	Phosphate buffered saline
PHB	Poly- β -hydroxybutyrate
PITC	Phenyl isothiocyanate
SCV	Small colony variant
SDS	Sodium dodecyl sulphate
SSC	Side scatter
TCA	Trichloroacetic acid
TOC	Total organic carbon
UHQ	Ultra high quality

INTRODUCTION

1.1 Legionnaires' Disease.

1.1.1 Historical background.

The Legionnaires' disease bacterium was first identified following an epidemic of severe respiratory illness which occurred during the 1976 Legionnaires' convention in Philadelphia. Of 4500 delegates attending the convention, 182 developed illness, with a fatality rate of 16% (Fraser *et al.*, 1977). Isolation and identification of the causative agent was hampered by an inability to culture the organism from infected lungs onto agar. After months of intensive epidemiological and microbiological investigations, a Gram-negative-negative bacillus, subsequently named *Legionella pneumophila*, species nova, was isolated in guinea pigs and embryonated chicken eggs. Immunochemical studies with patient sera confirmed the aetiological role of the Legionnaires' disease bacterium (McDade *et al.*, 1977; Brenner *et al.*, 1979).

With the development of immunological reagents, previously unsolved cases of legionellosis were identified (Thacker *et al.*, 1978; McDade *et al.*, 1979; Winn & Myerowitz, 1981). Additional members of the genera such as the "Pittsburgh Pneumonia agent" subsequently named *L. micdadei*, were also identified as agents of respiratory disease (Myerowitz *et al.*, 1979; Pasculle *et al.*, 1980).

1.1.2 Clinical features and diagnosis.

Legionnaires' disease is an acute pneumonia with multisystemic manifestations, which develops within 2 to 10 days after infection. The disease develops slowly with non-specific symptoms of headaches, weakness and malaise. High fever (39.5 to 40.5°C), recurrent chills and a dry cough normally develop within the first couple of days. Gastrointestinal abnormalities occur in approximately 50% of

cases, while approximately 25% of cases experience central nervous system manifestations including disorientation, confusion and delirium (Fraser *et al.*, 1977; Thacker *et al.*, 1978; Meyer, 1983; Winn, 1988).

Pathological characteristics of infected lung tissue include inflammation of alveoli, respiratory bronchioles and interstitial regions, with infiltration of neutrophils, macrophages, fibrin and red blood cells. Lysis of inflammatory cells and necrosis of alveolar epithelium are a common feature. Large numbers of bacilli can be visualized intracellularly in alveolar macrophages within the inflamed alveoli (Carrington, 1979; Blackmon *et al.*, 1979; Winn & Myerowitz, 1981).

Diagnosis of *Legionella* infections is performed in many laboratories by demonstrating a four-fold rise in patient antibody titre, usually by indirect immunofluorescent antibody testing. Detection of *Legionella* antigen in urine either by enzyme immunoassay or latex agglutination is also becoming a common diagnostic tool (Leland & Kohler, 1991). Although less commonly used, diagnosis can also be achieved by using culture methods and / or direct immunofluorescent staining with polyvalent antisera to demonstrate the organism in specimen samples (Bartlett *et al.*, 1986).

1.1.3 Epidemiology.

Legionella is an important cause of both community-acquired and nosocomial pneumonia infections. In addition to the many well publicised epidemics, such as the Stafford District General Hospital outbreak, *Legionella* is also a common cause of sporadic pneumonia infections (Bartlett *et al.*, 1986). While the attack rate for Legionnaires' disease is low, normally less than 5 % in epidemics, *Legionella* species are responsible for 1 to 5% of community acquired pneumonia infections, with a fatality rate approaching 20%. Increased prevalence and mortality rates have been reported for nosocomial infections of immunocompromised individuals (Davis *et al.*, 81; Bartlett *et al.*, 1986; Marston *et al.*, 1993).

As well as being the most prevalent species in nature, *L. pneumophila*, in particular serogroup 1, is responsible for approximately 85% of community acquired *Legionella* infections. *L. micdadei* is the second most common *Legionella* species to cause pneumonia, with an increased prevalence among nosocomial infections (Fliermans *et al.*, 1981; Reingold *et al.*, 1984; Watkins *et al.*, 1985; Bartlett *et al.*, 1986). Predisposing factors for the development of Legionnaires' disease include smoking, alcohol abuse, underlying chronic disease and immunosuppression, with males and the elderly more susceptible.

L. pneumophila serogroups 1 and 6, and *L. feeleyi* have also been linked to a clinically and epidemiologically distinct non-pneumonic form of respiratory illness, termed Pontiac fever. In comparison to Legionnaires' disease, the attack rate for Pontiac fever is significantly higher, approaching 100%, and usually affects previously healthy individuals (Glick *et al.*, 1978; Herwaldt *et al.*, 1984; Friedman *et al.*, 1987; Mayaud & Dournon, 1988).

1.1.4 Source and mode of transmission.

Legionellae are ubiquitous in natural fresh water environments and readily colonize modern man-made installations such as cooling towers, hot water systems and whirlpools. These installations provide a favorable environment for the amplification of legionellae, and readily disseminate aerosolized legionellae to susceptible hosts (Dondero *et al.*, 1980; Fliermans *et al.*, 1981; Kaufmann *et al.*, 1981; Bartlett *et al.*, 1983; Friedman *et al.*, 1987; Collville *et al.*, 1993; Miller & Kenep, 1993). Evidence supporting the aerosol route of infection has been provided by animal experiments. Administration of *L. pneumophila* in fine particle aerosols of 5 µm or less to guinea pigs produced fatal bronchopneumonia (Fitzgeorge *et al.*, 1983). Within plumbing systems, fixtures such as aerators, faucet spouts, shower heads and hot water tanks maintained below 54°C are common sources of *Legionella*, and have been linked to nosocomial infections (Tobin *et al.*, 1980; Arnow *et al.*, 1982; Wadowsky *et al.*, 1982; Ciesielski *et al.*, 1984; Muder *et al.*, 1986; Woo *et al.*,

1992). Both water faucets and shower heads have been demonstrated to generate aerosols containing *Legionella* spp. (Dennis *et al.*, 1984; Bollin *et al.*, 1985a). Moist soil and compost samples have also been identified as a source of legionellae (Steele, 1993; Hughes & Steele, 1994).

1.1.5 *Legionella* identification and classification.

Identification and classification of legionellae is complicated by their limited biochemical reactivity and serological diversity. Phenotypic characteristics, namely requirement for L-cysteine and ferric iron, colony morphology and catalase activity, provide a preliminary indication that an organism is a member of the genus *Legionella*. Although cellular fatty acid analysis, isoprenoid quinone determination and serological reactions are useful classification tools, they do not accurately differentiate all species. Furthermore, panels of monoclonal antibodies capable of differentiating the majority of *Legionella* species and serogroups are not commercially available for routine use (Thacker *et al.*, 1985; Watkins *et al.*, 1985; Wait, 1988; Harrison & Saunders, 1994). Analysis of DNA relatedness remains the most satisfactory and accepted method of *Legionella* identification and classification (Brenner, 1986).

Analysis of DNA homology and phenotypic traits supported the original classification of the Legionnaires' disease bacterium as a new species, *Legionella pneumophila* in the family *Legionellaceae* (Brenner *et al.*, 1979). Since the genus *Legionella* was proposed, a total of 39 *Legionella* species with 61 individual serogroups have been isolated from clinical and environmental samples (Brenner *et al.*, 1979; Brenner, 1986; Dennis *et al.*, 1993). Currently, 14 serogroups of *L. pneumophila* have been identified, and *L. pneumophila* serogroup 1 can be further subtyped by monoclonal antibody panels (Watkins *et al.*, 1985; Joly *et al.*, 1986; Harrison & Saunders, 1994). Although the formation of two additional genera was proposed, *Tatlockia* for *L. micdadei* and *Fluoribacter* for the blue-white autofluorescent species (*L. dumoffii*, *L. gormanii* and *L. bozemanii*), analysis of 16S

rRNA gene sequences supported the formation of a monophyletic group of species (Garritty *et al.*, 1980; Brenner, 1986; Harrison & Saunders, 1994).

1.2 *Legionella* Physiology.

1.2.1 Morphology.

Legionella are Gram-negative non-sporeforming bacteria which vary morphologically depending on the source environment. Clinical isolates are typically short coccobacilli 0.5 μM in width by 1 - 2 μM long, while cells grown on culture media vary from short coccobacilli to long filamentous cells at least 20 μM in length (Chandler *et al.*, 1979; Pine *et al.*, 1979). Most *Legionella* species are motile by means of one or two polar flagella and division proceeds by a process of non-septate pinching (Chandler *et al.*, 1979; Brenner, 1986). On charcoal yeast extract based agar, *Legionella* produce round glistening colonies with a distinctive ground glass texture and a blue-white to pinkish colour after 3 days growth (Feeley *et al.*, 1979; Dournon, 1988).

The cell envelope of *L. pneumophila* is characteristic of Gram-negative bacteria, with outer and cytoplasmic membranes separated by a thin highly cross-linked peptidoglycan layer (Chandler *et al.*, 1979; Amano & Williams, 1983). *L. pneumophila* possesses a unique smooth-type lipopolysaccharide, with an O-polysaccharide side chain composed of nonulosonic acid residues (Nolte *et al.*, 1986; Otten *et al.*, 1986; Knirel *et al.*, 1994). The membrane lipid composition of legionellae is unusual among Gram-negative bacteria, with a high proportion of phosphatidylethanolamines and phosphatidylcholines, along with a predominance of branched chain fatty acids and a complex pattern of hydroxylated fatty acids (Moss & Dees, 1979; Hindahl & Iglewski, 1984; Wait, 1988; Moll *et al.*, 1992; Jantzen *et al.*, 1993). Legionellae also possess an unusual pattern of respiratory quinones, with ubiquinones containing between 10 to 15 isoprene units (Wait, 1988; Lambert & Moss, 1989).

1.2.2 Biochemical activity.

Biochemically, legionellae are oxidase variable, catalase positive, nitrate and urease negative, and positive for β -lactamase and gelatinase production. Hippurate hydrolysis is a distinguishing characteristic of *L. pneumophila*. Many species produce a brown diffusible melanin-like pigment on media supplemented with tyrosine, the formation of which is encoded by the *lly* (legiolysin) locus (Baine *et al.*, 1978; Feeley & Gorman, 1980; Wintermeyer *et al.*, 1994). A range of extracellular enzymes including esterases, phosphatases, DNase, proteases and aminopeptidases are elaborated (Müller, 1981; Conlan *et al.*, 1986). Amino acid metabolism proceeds by the Krebs' cycle with a functional Embden-Meyerhof-Parnas pathway fulfilling the role of gluconeogenesis. Respiration is achieved by a branched respiratory chain composed of cytochromes of c, b, a, and d types, and ubiquinones possessing isoprene units of 10 to 15 carbon atoms (Hoffman & Pine, 1982; Hoffman, 1984).

1.2.3 Nutrition.

Legionellae were originally considered to be nutritionally fastidious due to an inability to grow on common laboratory media. Cysteine and iron were identified as essential nutrients in early complex media formulations (Feeley *et al.*, 1978 & 1979). Amino acids in particular arginine, cysteine, isoleucine, leucine, methionine, serine, threonine and valine are essential for the growth of *L. pneumophila*. Proline, glutamate, phenylalanine and tyrosine also help promote growth. Of these, serine, glutamate, threonine and glutamine are the principal sources of carbon and energy (Pine *et al.*, 1979; George *et al.*, 1980; Ristroph *et al.*, 1980; Tesh & Miller, 1981; Tesh *et al.*, 1983). Carbohydrates are not actively metabolised as a source of carbon or energy. Purines and pyrimidines, especially guanine stimulate the growth of legionellae in chemically defined media (Pine *et al.*, 1986a). Pyruvate and α -ketoglutarate also promote growth in some media formulations by reducing the rate of cysteine oxidation, and inhibiting superoxide formation by photochemical oxidation (Pine *et al.*, 1986b). *Legionella* have a high requirement for trace elements in

particular iron, zinc, magnesium and potassium. Other stimulatory elements include calcium, cobalt, copper, manganese, molybdenum, nickel and vanadium (Reeves *et al.*, 1981; Tesh & Miller, 1982).

1.2.4 Culture media and growth conditions.

Muller-Hinton agar supplemented with haemoglobin and isovitalex was the first bacteriological culture medium which supported the growth of *L. pneumophila* (Feeley *et al.*, 1978). Identification of L-cysteine and iron as essential nutrients led to the development of a modified Feeley-Gorman agar, which produced visible colonies of *L. pneumophila* after 4 days growth in an atmosphere of 2.5 % CO₂ in air at 37°C and pH 6.9 (Feeley *et al.*, 1978). Improved growth and recovery was achieved with the development of charcoal yeast extract agar which was further enhanced by the addition of ACES buffer and α -ketoglutarate (Feeley *et al.*, 1979; Pasculle *et al.*, 1980; Edelstein, 1981). Buffered charcoal yeast extract (BCYE) agar remains the most routinely used bacteriological medium for the growth of legionellae.

Early formulations of chemically defined liquid media, containing mainly amino acids, vitamins and trace metals, failed to support satisfactory growth of many strains and species (Pine *et al.*, 1979; Warren & Miller, 1979; George *et al.*, 1980). Subsequently, Pine and colleagues (1986a & b) demonstrated that the growth of legionellae in synthetic medium could be enhanced by incorporating pyruvate and alpha-ketoglutarate, which inhibited cysteine oxidation and photochemically promoted superoxide formation. Guanine was also identified as essential for the growth of several *Legionella* species. These studies resulted in the development of an ACES buffered chemically defined (ABCD) medium which supported satisfactory growth of a range of *Legionella* species and strains (Pine *et al.*, 1986a & b).

Although *in vitro* growth of *L. pneumophila* has been demonstrated between 24 and 42°C, optimum growth is normally achieved between 35 and 37°C, within a pH range of 6.5 to 6.9, and at a dissolved oxygen tension of 4.5% (v/v) air saturation at 37°C (Feeley *et al.*, 1978; Warren & Miller, 1979; Mauchline *et al.*, 1992).

1.3 *Legionella* Ecology.

Legionellae are specialized aquatic microorganisms. Their ability to adapt to different ecological niches as intracellular parasites of protozoa, free-living members of biofilm communities and as freely suspended planktonic cells, is believed to be central to their persistence in aquatic environments under stressful physico-chemical conditions.

1.3.1 Interactions with other micro-organisms.

Early *in vitro* experiments demonstrated that legionellae and associated non-*Legionellaceae* survive and multiply in potable water (Yee & Wadowsky, 1982; Wadowsky & Yee, 1985; Wadowsky *et al.*, 1985; Stout *et al.*, 1985). Subsequently, aquatic amoebae were identified as ecologically important hosts supporting the growth of *L. pneumophila* in these environments. Thirteen species of amoebae and two species of ciliated protozoa have been demonstrated to support the intracellular multiplication of legionellae *in vitro* (Rowbotham, 1980; Tyndall & Domingue, 1982; Anand *et al.*, 1983; Barbaree *et al.*, 1986; Rowbotham, 1986; Wadowsky *et al.*, 1988; Fields, 1993). In addition to providing a suitable intracellular growth environment, protozoa may aid persistence under suboptimal growth conditions, and provide protection against biocide treatment processes (Kuchta *et al.*, 1983; Barbaree *et al.*, 1986; Barker *et al.*, 1992). Legionellae trapped within encysted *Acanthamoeba polyphaga*, survived exposure to 50 mg l⁻¹ free chlorine (Kilvington & Price, 1990). Furthermore, the increased protection afforded to legionellae in amoebal cysts may aid dissemination in aerosols and transfer from raw water into potable water supplies.

Amoebae may also contribute to the persistence of legionellae by promoting the formation of intracellular reserves of poly- β -hydroxybutyrate, thereby inducing a phenotype more physiologically prepared for extracellular survival. A number of studies have noted the formation of intracellular inclusions resembling PHB granules during intracellular growth in amoebae (Anand *et al.*, 1983; Rowbotham, 1986;

Vandenesch *et al.*, 1990). PHB is a homopolymer of β -hydroxybutyric acid, which is accumulated during unbalanced growth, and is recognized as an important endogenous carbon and energy source capable of supporting microbial survival during starvation (Dawes, 1986b; Steinbüchel & Schlegel, 1991). Indeed, *in vitro* experiments have demonstrated the ability of *L. pneumophila* to adapt to starvation conditions, and survive for prolonged periods in tap water without growth (Skaliy & McEachern, 1979; Hussong *et al.*, 1987; West *et al.*, 1993).

Outside the amoebal host, legionellae interact with other bacterial species within complex biofilm communities, and can be found in relatively high numbers on the internal surfaces of fixtures such as faucet spouts and pipes (Wadowsky *et al.*, 1982). Rogers and Keevil (1992) demonstrated the presence of microcolonies of *L. pneumophila* within biofilms in the absence of amoebae, suggesting extracellular multiplication in this ecosystem. Biofilms formation may lead to the induction of stress resistant phenotypes, as well as providing protection against adverse environmental conditions and disinfectants (Rogers & Keevil, 1992, Costerton *et al.*, 1995). Furthermore, other bacterial species present in these communities may provide essential nutrients, helping to support the growth of legionellae. Interaction with other bacterial genera has also been confirmed *in vitro*. Strains of *Flavobacterium*, *Pseudomonas*, *Alcaligenes* and *Acinetobacter* supported satellite growth of *L. pneumophila* colonies on culture media deficient in L-cysteine (Wadowsky & Yee, 1983; Stout *et al.*, 1985).

1.3.2 Physico-chemical properties of the source environment.

Another important feature of legionellae is their ability to survive stressful environmental conditions outside the amoebal host. *L. pneumophila* is a thermotolerant organism that inhabits fresh waters with temperatures ranging from 5.7 to 63°C, hydrothermal waters and hot water distribution systems (Fliermans *et al.*, 1981; Wadowsky *et al.*, 1982; Plouffe *et al.*, 1983; Tison & Seidler, 1983; Veríssimo *et al.*, 1991). Fliermans *et al.* (1981) noted increased prevalence of *L. pneumophila* at

temperatures between 40 and 60°C. The ability of *Legionella* to survive at elevated temperature has been confirmed *in vitro*, with little loss of viability at 50°C (Dennis *et al.*, 1984). Legionellae also encounter a wide range of environmental pH values (5.5 to 8.1), and can multiply between pH 5.5 to 9.2, as part of a naturally occurring water culture (Fliermans *et al.*, 1981; Wadowsky *et al.*, 1985).

The chemical composition of water is likely to contribute to the growth and survival of *L. pneumophila* in nature (States *et al.*, 1985). States *et al.* (1987) demonstrated a positive correlation between the total organic carbon content and turbidity of municipal water samples, and their ability to support the growth of *Legionella*. Furthermore, stagnant waters such as those from the corners of water reservoirs, plumbing dead ends and in the sediment of hot water tanks are believed to provide favorable niches for *Legionella* growth (Stout *et al.*, 1985; States *et al.*, 1987 & 1994). These physico-chemical properties of the source environment, together with intracellular reserves of poly- β -hydroxybutyrate which are accumulated during intra-amoebic growth, are likely to make an important contribution to the long-term persistence of legionellae in aquatic habitats. Reports have also suggested that *L. pneumophila* may survive starvation conditions by entering a dormant state of low endogenous metabolic activity (Hussong *et al.*, 1987). Colbourne and Dennis (1989) demonstrated that heat shock treatment rendered IFA positive, culture negative water distribution samples, positive for low numbers of *L. pneumophila*. However, West *et al.* (1993) failed to revive non-culturable *L. pneumophila* by heat shock treatments.

1.4 Cell Biology of *Legionella* Pathogenesis.

L. pneumophila is a facultative intracellular pathogen, dependent on the intracellular environment of non-activated mononuclear phagocytes for multiplication *in vivo* (Horwitz and Silverstein, 1980; Nash *et al.*, 1984; Elliott & Winn, 1986; Winn, 1988). Intracellular multiplication has also been demonstrated *in vitro* in a range of mammalian macrophage cultures and eukaryotic cell lines (Oldham &

Rodgers, 1985; Elliott & Winn, 1986; Cianciotto *et al.*, 1989; Marra *et al.*, 1990; McCusker *et al.*, 1991). The recognition that an important component of the human defence system preferentially supports the growth of virulent legionellae *in vivo*, prompted investigations to elucidate the molecular basis of infection and intracellular multiplication.

1.4.1 Attachment and phagocytosis.

Opsonisation of *L. pneumophila* by human monocytes is mediated by both the alternative and classical complement pathways. Activation of the alternative pathway is promoted by the major outer membrane protein (MOMP) which fixes complement components C3b and C3bi (Bellinger-Kawahara & Horwitz, 1990; Payne & Horwitz, 1987; Summersgill *et al.*, 1990). Improved opsonisation occurs in the presence of both complement and antibody through activation of the classical pathway by lipopolysaccharide (Horwitz & Silverstein, 1981b; Verbrugh *et al.*, 1985; Mintz *et al.*, 1992). Both specific antibody and complement are required for ingestion by neutrophils (Horwitz & Silverstein, 1981a). Opsonin independent uptake by mononuclear phagocytes has also been reported and may be important during the early stages of infection (Elliott & Winn, 1986; Rechnitzer & Blom, 1989; King *et al.*, 1991; Gibson *et al.*, 1994).

The uptake of *L. pneumophila*, Philadelphia 1, by human phagocytic cells occurs by an unusual coiling mechanism which is independent of cell viability, and may be inhibited by anti-*Legionella* antibodies, suggesting a receptor mediated process (Horwitz, 1984). However, other strains of *L. pneumophila* and species such as *L. micdadei* are phagocytosed by the classical microfilament-dependent process (Oldham & Rodgers, 1985; Elliott & Winn, 1986; Rechnitzer & Blom, 1989). The significance of these differences in mode of entry remains unclear and appears to be independent of the virulence of the ingested organism.

1.4.2 Intracellular Response.

Following phagocytosis *L. pneumophila* enters a membrane bound phagosome which interacts sequentially with host cell smooth-vesicles, mitochondria and ribosomes, producing a unique ribosome-lined replicative vacuole (Horwitz, 1983a & b; Oldham & Rodgers, 1985). This replicative vacuole is associated with membranes derived from the host endoplasmic reticulum, producing a structure resembling a nascent autophagosome (Swanson & Isberg, 1995). Normal phagocytic events, i.e., phagosome acidification and fusion with host cell lysosomes, do not occur (Horwitz & Maxfield, 1984). Virulent legionellae multiply in this intracellular environment with a doubling time of approximately 2 h, until the cell ruptures releasing the bacteria (Horwitz & Silverstein, 1980). However, inhibition of phagosome-lysosome fusion is not universal among *L. pneumophila* strains. Fusion was reported following ingestion of the Knoxville 1 strain, and *L. micdadei*, although neutrophil and monocyte activation was significantly impaired (Rechnitzer & Blom, 1989).

1.4.3 Immunity.

Humoral immunity does not play a prominent role in host protection against *L. pneumophila*. Although antibody and complement promote *L. pneumophila* phagocytosis by human mononuclear phagocytic cells, they do not induce killing nor inhibit intracellular multiplication (Horwitz & Silverstein, 1981a - c; Nash *et al.*, 1984). By contrast, development of Th1 cell mediated immunity following exposure to *Legionella* antigens, plays a critical function in the control of *Legionella* infections (Horwitz & Silverstein, 1981c; Horwitz, 1992). Both gamma-interferon (IFN- γ) and tumour necrosis factor alpha (TNF α) appear to mediate host resistance by promoting the anti-bacterial activity of neutrophils, as well as inhibiting the intracellular growth of *L. pneumophila* in mononuclear phagocytic cells (Nash *et al.*, 1988; Klein *et al.*, 1991; Skerrett & Martin, 1992; Matsiota-Bernard *et al.*, 1993). In addition, cytokines such as IL2, enhance the ability of natural killer cells to kill infected macrophages,

thereby controlling *L. pneumophila* infections (Blanchard *et al.*, 1988; Yamamoto *et al.*, 1994).

The mechanism employed by macrophages to inhibit intracellular multiplication of *L. pneumophila* is not fully understood. Reactive oxygen metabolites do not appear to be of significance (Friedman *et al.*, 1982; Rechnitzer, 1994). Two modes of lymphokine-activated inhibition of *Legionella* in human monocytes have been proposed. These are, reduced phagocytosis thereby restricting access to the intracellular environment, and inhibition of intracellular multiplication by limiting the availability of intracellular iron (Byrd & Horwitz, 1989; Skerrett & Martin, 1991). However, Gebran *et al.* (1994b) demonstrated that ferric iron did not completely relieve inhibition of *L. pneumophila* growth, and proposed that inhibition was only partially nutritionally dependent. It is likely that additional mechanisms contribute to the inhibitory activity of activated macrophages.

1.5 Virulence Determinants.

1.5.1 Virulence loci and cell associated factors.

Recent emphasis on the use of molecular genetics has identified a number of loci which play an essential role in the pathogenesis of *L. pneumophila*. These include the *dotA* (defect in organelle trafficking) and *icm* (intracellular multiplication) loci, which encode determinants essential for establishment of the replicative phagosome and intracellular multiplication (Marra *et al.*, 1992; Berger & Isberg, 1993; Berger *et al.*, 1994; Brand *et al.*, 1994). The *eml* (early-stage macrophage induced) locus is also essential for survival of *L. pneumophila* within macrophages and amoebae, and appears to be induced intracellularly during the early stages of infection (Abu Kwaik & Pederson, 1996). The *mip* gene (macrophage infectivity potentiator) encodes a 24 kDa surface antigen which promotes optimum infection of human alveolar macrophages and differentiated U937 cells, and is required for full virulence in the guinea pig model. Studies suggest that Mip contributes to intracellular survival rather

than uptake or growth (Cianciotto *et al.*, 1989; Cianciotto *et al.*, 1990; Wintermeyer *et al.*, 1995).

Additional proteins induced during infection have been identified, and possibly facilitate adaptation to the intracellular environment. These include a 19 kDa global stress protein (GspA) induced during intracellular infection and upon exposure to several stress stimuli *in vitro*, and a 44 kDa *Legionella* intracellular growth antigen (LIGA), which is expressed exclusively during intracellular growth (Abu Kwaik & Engleberg, 1994; Susa *et al.*, 1996). The major cytoplasmic membrane protein is a 60 kDa member of the Hsp60 family of heat shock proteins, which exhibits homology with the *Escherichia coli* GroEL heat shock protein. Expression of this protein is triggered during intracellular growth in macrophages and may play an important role in stress response (Hoffman *et al.*, 1989 & 1990). The major outer membrane protein has a molecular mass of 28 kDa and forms a cation-selective porin composed of 4 monomers stabilized by disulphide linkages (Gabay *et al.*, 1985; Gabay & Horwitz, 1985; Hindahl & Iglewski, 1986). Although this protein promotes complement fixation and phagocytosis, expression occurs independent of virulence (Butler *et al.*, 1985).

Flagella expression has been linked to *L. pneumophila* pathogenicity. Mutants deficient in the 47 kDa flagellum subunit failed to multiply in human monocyte-like U937 cells, and were attenuated for intracellular multiplication in amoebae. However, flagella expression is not required for virulence in the guinea pig model, leading researchers to postulate an indirect link between the expression of flagella and other virulence determinants, possibly through coordinated regulation with a virulence determinant (Pruckler *et al.*, 1995).

Lipopolysaccharide (LPS) is the major carbohydrate component of Gram-negative bacteria, and is an integral component of the outer membrane. As with other bacterial species, *L. pneumophila* LPS is highly antigenic and represents the principal serogroup antigen (Gabay & Horwitz, 1985; Ciesielski *et al.*, 1986). However, *L. pneumophila* LPS possesses low endotoxic activity and induces a weak pyrogenic

response in rabbits (Wong *et al.*, 1979; Otten *et al.*, 1986). Conlan and Ashworth (1986) observed that the SDS-PAGE profile of LPS from four *L. pneumophila* strains of difference virulence was similar, and concluded that *Legionella* LPS was unlikely to be a virulence factor.

1.5.2 Extracellular enzymes

Legionella species elaborate a number of extracellular enzymes including proteases, aminopeptidase, phospholipase, phosphatase, catalase and superoxide dismutase. However, none of these factors have been confirmed as essential pathogenicity factors. The major extracellular enzyme produced by *L. pneumophila* is a 38 kDa zinc metalloprotease, sharing considerable structural and functional homology with *Pseudomonas aeruginosa* elastase (Dreyfus & Iglewski, 1986; Black *et al.*, 1990). This enzyme was first identified as a possible virulence determinant due to its haemolytic activity and cytotoxicity for tissue culture cells (Rosenfeld, *et al.*, 1986; Keen & Hoffman, 1989; Quinn & Tompkins, 1989), ability to induce protective immunity in guinea pigs (Blander & Horwitz, 1989a, 1989b), *in vivo* production during experimental legionellosis, and its ability to elicit pulmonary necrosis in guinea pigs (Baskerville *et al.*, 1986; Williams *et al.*, 1987; Conlan *et al.*, 1988). Many also believe that this enzyme aids pathogenesis by disrupting the host immune response, through digestion of important immunoregulatory molecules, such as tumor necrosis factor- α (TNF- α), interleukin-2 (IL-2) and CD4 on human T cells, as well as inhibiting natural killer cell activity by blocking attachment to target cells (Hell *et al.*, 1993; Mintz *et al.*, 1993; Rechnitzer & Kharazmi, 1992; Rechnitzer, 1994). However, protease deficient mutants were found to be competent for tissue destruction and killing of guinea-pigs (Szeto & Shuman, 1990; Blander *et al.*, 1990). By contrast, Moffat *et al.* (1994) demonstrated that the virulence of a protease deficient isogenic mutant was attenuated for the guinea pig model, although it was not defective for intracellular multiplication.

Phospholipase C and phosphatase activities are recognized as potential virulence determinants due to their ability to impair respiratory activity and mammalian cell signal transduction (Müller, 1981; Thorpe & Miller, 1981; Nolte *et al.*, 1982; Baine, 1985; Baine, 1988). *L. micdadei* acid phosphatase has been demonstrated to block super anion production by neutrophils *in vitro* (Saha *et al.*, 1985). However, these enzymes do not appear to make a significant contribution to *L. pneumophila* pathogenesis. Purified Phospholipase C failed to produce haemolysis, and phosphate- (Pho-) mutants were not attenuated for infection and intracellular growth in U937 cells (Baine, 1985; Kim *et al.*, 1994).

1.5.3 Toxins.

Several *L. pneumophila* toxins have been proposed as potential virulence factors. Friedman *et al.* (1980) identified a methanol soluble heat-labile peptide toxin of 1.3 kDa that was cytotoxic for CHO cells, and impaired neutrophil bactericidal activity by disrupting the oxygen-dependent response of the cell (Friedman *et al.*, 1982). Hedlund (1981) isolated a 3.4 kDa acid-soluble toxin which was active against mouse macrophages, while McCusker *et al.* (1991) demonstrated inhibition of protein synthesis in CHO cells by a heat labile cell associated factor. However, none of these potential toxins have been purified to homogeneity, preventing studies on their mode of action and pathophysiological significance.

1.6 Environmental Regulation of *Legionella* Virulence.

Although legionellae are ubiquitous in nature, the incidence rate of Legionnaires' disease is low, with a spectrum of illness observed during outbreaks. Researchers have postulated that in addition to extrinsic factors such as dose, host health status, and transmission, this may reflect the presence of environmental legionellae which manifest differences in their ability to cause disease (Barker & Brown, 1995). Differences in the virulence of environmental isolates of *L.*

pneumophila has been confirmed (Plouffe *et al.*, 1983; Bollin *et al.*, 1985b). As previously discussed, legionellae reside in a number of distinct ecological niches with potential exposure to a wide range of environmental conditions. Such conditions have a significant impact on microbial physiology and biochemistry, and may induce a range of *Legionella* phenotypes differing in their ability to survive and cause infection (Brown & Williams, 1985; Barker & Brown, 1994 & 1995; Costerton *et al.*, 1995; Fields, 1996).

1.6.1 Intra-amoebic growth.

Intra-amoebic growth influences the physiology of *L. pneumophila*, producing alterations in cellular morphology and envelope composition, as well as promoting polymer formation and increased resistance to antimicrobial agents (Rowbotham, 1986; Barker *et al.*, 1992 & 1993; Barker & Brown, 1995; Barker *et al.*, 1995). Growth in amoebae also promotes enhanced invasion of macrophages and epithelial cells, while *L. pneumophila* retains its virulent phenotype when grown in co-culture with *Acanthamoeba* sp. (Vandenesch *et al.*, 1990; Cirillo *et al.*, 1994).

Although the uptake of *L. pneumophila* by mammalian cells and protozoa occurs by different mechanisms, a number of similarities have been identified in the intracellular pathway of *L. pneumophila* in both host cells. The ability of *L. pneumophila* to parasitize amoebae is dependent on the formation of a specialized replicative phagosome, by a process analogous to that observed in alveolar macrophages (King *et al.*, 1991; Abu Kwaik *et al.*, 1994; Abu Kwaik, 1996; Bozue & Johnson, 1996). The *mip*, *dotA* and *eml* loci which are essential for infection of mammalian cells, are also required for amoebal infection (Cianciotto & Fields, 1992; Abu Kwaik & Pederson, 1996). These observations have prompted many to propose that the ability of *Legionella* to infect mammalian cells and cause human disease, arises as a direct result of its ability to parasitize protozoa (Barker & Brown, 1994; Abu Kwaik, 1996; Fields, 1996).

1.6.2 Environmental temperature and pH.

As previously stated, legionellae inhabit aquatic environments with a wide range of temperature and pH values (Fliermans *et al.*, 1981). Temperature has been demonstrated to influence the physiology and virulence of *L. pneumophila* grown *in vitro* under defined culture conditions. The virulence of chemostat cells was significantly attenuated when the growth temperature was reduced from 37 to 24°C (Mauchline *et al.*, 1992; Mauchline *et al.*, 1994). The ability of *L. pneumophila* to infect free-living amoebae also appears to be influenced by temperature. Intra-amoebal growth was observed at 37°C, whereas internalized legionellae were digested at 20°C (Rowbotham, 1980; Anand *et al.*, 1983). In agreement with these reports, multiplication of legionellae in hot water systems was found to correlate with temperatures between 30 and 54°C, and free-living amoebal isolates supported axenic growth of legionellae at temperatures $\leq 42^\circ\text{C}$ (Wadowsky *et al.*, 1982; Plouffe *et al.*, 1983; Stout *et al.*, 1985; Fields *et al.*, 1989). Therefore, environmental temperature is likely to influence both the persistence of *Legionella* as well as its ability to cause human disease.

Although of potential importance, the influence of pH stress on the physiology of *L. pneumophila* has received little attention. Studies with other bacteria have demonstrated that maintenance of a constant intracellular pH, by the action of primary proton pumps as well as Na^+/H^+ and K^+/H^+ antiporters, is an essential feature of microbial adaptation to environmental pH changes. Adaptation to pH stress influences microbial physiology and virulence, by modulating essential cellular processes such as ATP formation, solute transport and motility, and the expression of virulence systems such as the *phoP/phoQ* regulon of *S. typhimurium* (Zilberstein *et al.*, 1984; Booth, 1985; Gross, 1993; Olson, 1993).

1.6.3 Nutrient limitation.

Nutrient limitation is another common environmental stress which microbes are likely to encounter both in their natural reservoir as well as during infection, and

is recognized as an important regulator of microbial physiology and virulence (Tempest & Neijssel, 1976; Harder & Dijkhuizen, 1983; Brown *et al.*, 1984; Brown & Williams, 1985). *Legionella* are frequently isolated from low nutrient environments (Fliermans *et al.*, 1981). Furthermore, *L. pneumophila* survives starvation conditions for long periods *in vitro*, possibly reflecting its ability to enter a dormant hypometabolic state (Skaliy & McEachern, 1979; Hussong *et al.*, 1987; Colbourne & Dennis, 1989; West *et al.*, 1993). Therefore, these conditions are likely to have a significant impact on the physiology of environmental *L. pneumophila*, producing stress resistant phenotypes as well as modulating their pathogenicity (Barker & Brown, 1995).

1.6.4 Iron limitation.

Iron is an essential nutrient for microbial growth, participating in a wide range of biochemical reactions including cellular respiration and DNA replication. The importance of iron arises from its versatile catalytic properties generated by the wide redox potential connecting its two stable valencies (Neilands, 1974; Griffiths, 1987a). However, the concentration of soluble ferric iron is restricted in nature, due to spontaneous formation of insoluble ferric hydroxides and oxy-hydroxides at neutral pH. In humans most iron is located intracellularly as ferritin or haem-containing compounds, while extracellular iron is tightly bound to the iron binding and transport glycoproteins, transferrin and lactoferrin. This restricts iron availability to concentrations usually below 10^{-18}M , which is too low to satisfy normal bacterial requirements; for example, Gram-negative bacteria usually need 0.3 to 1.8 μM iron for growth (Weinberg, 1974; Griffiths, 1987b). The human host also responds to infection by reducing the amount of available iron, through increased synthesis and release of lactoferrin by neutrophils, and ferritin in the liver (Otto *et al.*, 1992). Furthermore, the concentration of available iron is likely to be restricted in the intra-amoebal environment.

Therefore, legionellae may constantly encounter severe iron-limited conditions both in nature as well as *in vivo* during infection. In order to survive and compete in these iron-restricted environments, micro-organisms elaborate specific mechanisms for solubilizing and transporting extracellular iron to the cell. These include low molecular weight, high affinity iron chelators called siderophores, and specific cell surface receptors which extract iron directly from host iron-loaded glycoproteins (Simonson *et al.*, 1982; Griffiths, 1987b; Otto *et al.*, 1992).

However, little is known about the iron acquisition and transport mechanisms elaborated by *L. pneumophila*. Numerous studies have confirmed the importance of iron for the intracellular and extracellular growth of *Legionella pneumophila*, with iron chelators and serum iron-binding proteins growth inhibitory (Feeley *et al.*, 1978; Reeves *et al.*, 1983; Bortner *et al.*, 1986; Quinn & Weinberg, 1988; Byrd & Horwitz, 1989 & 1991; Gebran *et al.*, 1994a). Furthermore, mutants defective for iron acquisition and assimilation are also impaired for intracellular infection in both mammalian cells and protozoa (Pope *et al.*, 1996), confirming that iron is essential for intracellular growth of *L. pneumophila*.

Byrd and Horwitz (1989) proposed that the intracellular labile pool is the primary source of iron within alveolar macrophages. Periplasmic and cytoplasmic ferric reductases have been identified as important components of the iron transport machinery elaborated by *L. pneumophila* (Johnson *et al.*, 1991; Poch & Johnson, 1993). Haemin binding, promoted by the locus *hbp* stimulates the growth of *L. pneumophila* in iron-deficient media, although it is not required for intracellular infection. Other common bacterial iron-acquisition mechanisms, namely, siderophores and transferrin receptors are not elaborated by *L. pneumophila* (Reeves *et al.*, 1983, Quinn & Weinberg, 1988; Liles & Cianciotto, 1996). Furthermore, investigations by Barker *et al.* (1993) using cells grown within amoebae and in iron-deficient batch culture failed to detect the induction of specific membrane associated iron-uptake systems.

1.6.5 Control of gene expression.

Micro-organisms have limited control over their environment and therefore, have developed specialized mechanisms to sense and respond to changing conditions. This adaptation is partly achieved by regulating gene expression at the level of transcription in response to specific stimuli such as, temperature, pH, osmolarity and iron availability (Mekalanos, 1992). Genes required to respond to a particular stimulus are normally grouped into specialized regulatory units termed regulons, which facilitates coordinated expression. Many bacteria employ two component signal transduction systems to regulate gene expression in response to specific stimuli. These systems are typically composed of a transmembrane sensor/transmitter protein and a cytoplasmic regulator protein. The extracytoplasmic sensor domain transfers the signal to the cytoplasmic transmitter domain, which upon activation phosphorylates the amino terminus of the regulatory protein. Once phosphorylated the regulator binds to DNA through its carboxyl-terminal region and regulates gene expression (Miller *et al.*, 1989; Gross, 1993; Dorman, 1994). In complex environments, multiple stimuli may induce the expression of multiple regulons, producing a global stress response, as has been observed during the intracellular growth of *Salmonella typhimurium* and *L. pneumophila* (Buchmeire & Heffron, 1990; Abshire & Neidhardt, 1993; Abu Kwaik *et al.*, 1993). Sigma factors and DNA supercoiling are also recognized as important global regulators of large subsets of genes required to respond to environmental stimuli, such as starvation and pH shock (Drlica, 1992; Loewen & Hengge-Aronis, 1994).

The concentration of free iron in the environment regulates the expression of iron transport systems, and other virulence determinants such as toxins and haemolysins in many pathogens (Neilands, 1982; Bagg & Neilands, 1987; Gross, 1993). In Gram-negative bacteria such as *Escherichia coli*, *Yersinia pestis*, *Neisseria meningitidis*, *Vibrio cholerae* and *P. aeruginosa*, the regulatory action of iron is mediated by the iron responsive regulatory locus *fur*, for ferric uptake regulator (Hantke, 1984; Staggs & Perry, 1991; Thomas & Sparling, 1994; Litwin *et al.*, 1992;

Prince *et al.*, 1993). In *E. coli*, Fur is a 17 kDa iron-responsive cytoplasmic regulatory protein, which in the presence of ferrous iron represses transcription of several loci by interacting with the promoter region, the "iron-box" (Dorman, 1994). The Fur protein performs both sensory and regulatory roles, with the iron being transported into the cytoplasm before the sensing event occurs (Gross, 1993). A *L. pneumophila fur* gene has been cloned and sequenced, and encodes a protein which is structurally similar to *E. coli* Fur. Further studies are necessary to determine its significance for *Legionella* physiology and virulence (Hickey & Cianciotto, 1994 & 1997).

1.7 Studying Environmental Regulation of Microbial Physiology and Virulence.

It is widely acknowledged that environmental conditions have a significant impact on microbial physiology and virulence. The host-microbe interaction which occurs during infection is a dynamic process which induces the expression of a unique virulent phenotype. Recent genetic approaches have advanced our understanding of the molecular basis of pathogenesis, however, the physiological state and response of bacteria *in vivo* remains poorly characterized. This is partly due to the inherent complexity of the host-microbe interaction which is difficult to reproduce during *in vitro* experiments. Hence, much of our understanding of the *in vivo* behaviour of bacteria is based on *in vitro* studies of organisms which may not completely express the virulent phenotype (Brown & Williams, 1985; Williams, 1988)

Traditionally, studies of microbial physiology and virulence have used bacteria grown in batch cultures. Although batch cultivation is an effective means of producing biomass and studying microbial nutritional requirements, this method has major disadvantages for physiology studies. Firstly, cultures pass through a number of phases in which the growth environment and the physiological and biochemical composition of the cells are constantly changing. Consequently, the effect of individual growth parameters including growth rate, cannot be determined. Secondly,

this method is particularly unsuitable for nutrient limitation studies as the culture is exposed to nutritional extremes, that is, growth with excess nutrient followed by sudden starvation. Therefore, the culture does not become physiologically adapted to nutrient-limited growth. Hence, the significance of parameters such as slow growth rates and iron deprivation which are important *in vivo*, is poorly understood (Pirt, 1972 & 1975; Brown & Williams, 1985; Brown *et al.*, 1990). These inherent problems of batch cultivation can be overcome by the application of continuous culture techniques.

1.7.1 Continuous culture

The concept of continuous culture was first introduced by Monod (1950) and Novick and Szilard (1950). They described a single stage culture system into which sterile culture medium was fed at a constant flow rate (f), and from which culture was dispelled at the same rate, producing a constant culture volume. This system where, the specific growth rate (μ) is controlled by the rate of addition of the growth-limiting nutrient (D), is termed a chemostat. Under steady state conditions $\mu = D$ (Herbert *et al.*, 1956; Pirt, 1975). The important feature of this culture system is that microbial growth occurs at a constant rate in a controlled and defined environment. This facilitates studies of the effect of different growth rates on microbial physiology, independently of changes in other environmental conditions. Alternatively, other growth parameters such as pH or temperature can be varied separately, while a constant growth rate is maintained. Therefore, chemostat culture allows the effects of growth rate and individual environmental parameters to be studied separately. This system is particularly useful for studying the influence of nutrient limitation at constant growth rate (Pirt, 1975).

1.7.2 Virulence models.

Elucidation of the molecular basis of microbial pathogenicity depend on suitable models to assess virulence, and complement culture and molecular genetic studies. In view of the apparent significance of airborne transmission of the pathogen in aerosols, Baskerville *et al.* (1981) successfully developed an experimental Legionnaires' disease model in guinea pigs, based on aerosol infection. This system produces a pneumonic illness that mimics Legionnaires' disease in humans, both clinically and pathologically. This model has been widely used and has proved successful in differentiating between virulent and avirulent strains of *L. pneumophila* (Fitzgeorge *et al.*, 1983; Mauchline *et al.*, 1994).

Many groups have sought easier and less expensive assays for routine assessment of the infectivity and intracellular growth of *Legionella* isolates. This has resulted in the development of a number of assays based on mammalian and protozoan cell culture, such as human monocytes, guinea pig alveolar macrophages, *Tetrahymena pyriformis*, *A. castellanii* and eukaryotic cell lines, including MRC-5, Hep-2, Vero, and differentiated U937 and HL-60 cells (Oldham & Rodgers, 1985; Fields *et al.*, 1986; Horwitz, 1987; Pearlman *et al.*, 1988; Marra *et al.*, 1990; Moffat & Tompkins, 1992). These cultures have proved suitable hosts for the intracellular growth of *L. pneumophila*, capable of distinguishing between virulent and avirulent cultures, and are widely used in studies to elucidate the molecular basis of interactions with mammalian cells and protozoa (Fields *et al.*, 1986).

1.8 Aims of this Study.

L. pneumophila manifests a highly complex ecology which is believed to contribute to its ability to cause human disease. However, the effects of important environmental stresses, such as nutrient deprivation and extremes of pH, on the physiology and pathogenicity of this organism are poorly understood. With this in mind, a continuous culture system of non-ferrous design will be used to grow a virulent strain of *L. pneumophila* serogroup 1 in a controlled iron-limited environment. The physiological effects of iron limitation on the growth and metabolism of *L. pneumophila* will be investigated by performing chemical analyses on culture supernatant and cell samples. Changes in cellular morphology will be monitored by electron and differential interference contrast microscopy. Biochemical assays will be employed to evaluate the expression of potential virulence determinants, including extracellular zinc metalloprotease and phospholipase C activities and iron acquisition mechanisms, which may be induced in response to iron limitation. Phenotypic changes in the composition of the cell envelope will be evaluated by analysing protein, lipopolysaccharide, fatty acid, and polar lipid expression. These physiology studies will be complemented by using the guinea-pig aerosol model and an *in vitro* macrophage assay to assess the influence of iron limitation on the virulence of *L. pneumophila*.

The study will be extended to assess the role of environmental pH in phenotypic modulation of *L. pneumophila*. The physiological impact of pH will be assessed by investigating the response of steady-state iron-replete cultures growing at pH 6.9, to a change in pH to 6.0 and 7.8. In addition, the influence of growth at sub-optimal pH in combination with iron limitation on physiology and virulence will be studied, as this is a combination of environmental stresses that may be encountered in the intracellular environment of the host cell.

Many groups have postulated that the formation of intracellular energy reserves, and entry into a state of low endogenous metabolic activity, contributes to

the long-term persistence of *L. pneumophila* in low-nutrient environments. However, apart from reports of enhanced granule formation during intracellular growth, the physiology of poly- β -hydroxybutyrate (PHB) accumulation by *L. pneumophila* and its contribution to survival, has not been addressed. Therefore, both chemical and physical analyses will be performed to investigate PHB formation by chemostat cultures. A spectrofluorometric assay employing the fluorescent lipophilic probe, Nile red, will be evaluated for PHB determination, and will be used to investigate the influence of growth environment on PHB formation. This assay will also be used to investigate the relationship between PHB utilization and the survival of *L. pneumophila* in a low-nutrient tap water environment. Spectrofluorometric analyses of the starved population will be complemented by the use of flow cytometry to determine changes in granularity, size and Nile red fluorescence at the cellular level in response to starvation.

It is hoped these studies will improve our understanding of the effects of two important environmental parameters, iron availability and pH, on the physiology, and virulence of *L. pneumophila*, and clarify the role of storage polymers in long-term environmental persistence.

MATERIALS and METHODS

2.1 Organism.

Physiology studies were conducted with a *Legionella pneumophila* serogroup 1, monoclonal subgroup Pontiac strain, Corby. This clinical isolate was originally supplied by Dr R. A. Swann, John Radcliffe Hospital, Oxford, (Fitzgeorge, 1985). The isolate was sub-cultured three times on buffered charcoal yeast extract agar (BCYE, Edelstein, 1981) before storage as frozen pellets at -70°C.

2.2 Culture Media.

BCYE agar was used to prepare inoculum cultures from frozen stocks, enumerate the number of culturable bacteria in chemostat samples, and to assess culture purity. Table I outlines the formulation of BCYE agar. A modified version of this medium deficient in cysteine, NCM, was used as a negative control for culture purity, due to its inability to support the growth of *L. pneumophila*.

The ACES-buffered chemically defined (ABCD) medium of Pine *et al.* (1986a) was used for chemostat culture. Stock solution formulae and preparation of this medium are outlined in Tables II and III. Serine was present at a concentration at least 15-fold higher than any of the other amino acids, while iron was provided in the form of ferrous sulphate and haemin. The final pH of the medium was adjusted to 6.75, and the medium was filter sterilized by passage through a 0.2 µm pore size, cellulose acetate membrane filter capsule (Sartorius, Ltd). For iron-limited growth this formulation was modified by the removal of the iron sources, ferrous sulphate and haemin. All amino acids used for medium preparation were of ultrapure quality

(Sigma Chem. Co.). High quality deionised water prepared by a Millipore water purification system, was used for media preparation.

Table I. Formulation of buffered charcoal yeast extract (BCYE) agar (Edelstein, 1981).

Chemical	Quantity
ACES Buffer (Sigma)	10.0 g dissolved in 500 ml water
Potassium hydroxide (BDH)	2.8 g dissolved in 480 ml water
Activated charcoal (Sigma)	2.0 g
Agar No. 3 (Oxoid)	12.0 g
Cysteine-HCl (BDH)	0.4 g
α -ketoglutarate (mono potassium salt, Sigma)	1.0 g
Yeast extract (Oxoid)	10.0 g
Heat sterilized at 121°C for 15 mins and cooled to 50°C before adding sterile:-	
Ferric pyrophosphate (Sigma)	0.25 g in 10 ml water
L-cysteine	0.4 g in 10 ml water

Table II. Stock solution formulations for ACES-Buffered Chemically Defined (ABCD) medium (Pine *et al.*, 1986a).

Stock solutions.	g l ⁻¹	mg l ⁻¹	Stock Solutions	g l ⁻¹	mg l ⁻¹
<u>Solution 2.</u>			<u>Solution 6.</u>		
CaCl ₂ · 2H ₂ O		55.5	sodium pyruvate	100	
MgSO ₄ · 7H ₂ O	21.4				
NH ₄ VO ₃		117	<u>Solution 7.</u>		
ZnSO ₄ · 7 H ₂ O	2.875		α-ketoglutarate	100	
<u>Solution 3.</u>			<u>Solution 8.</u>		
CoCl ₂ · 6H ₂ O		47.6	inositol		200
CuSO ₄ · 5H ₂ O		2.5	thiamine HCl		200
MnCl ₂ · 4H ₂ O		2.0	calcium -		
NaMO ₄ · 2H ₂ O		121	pantothenate		200
NiSO ₄ · 6H ₂ O		52.6	nicotinamide		100
conc. HCl		0.5 ml	biotin		10
<u>Solution 4.</u>			<u>Solution 9.</u>		
FeSO ₄ · 7H ₂ O	4.0		DL-thiocitic acid	1.0	
Conc. HCl		0.5 ml	ethanol		950 ml
<u>Solution 5.</u>			<u>Solution 10.</u>		
L- alanine	1.0		coenzyme A	1.0	
L-arginine	1.0				
L-asparagine	1.0		<u>Solution 11.</u>		
L-aspartic acid	1.0		haemin	2.0	
L-glutamine	1.0		KOH	56	
L-glutamic acid	1.0				
L-glycine	1.0				
L-histidine HCl	1.0				
L-isoleucine	1.0				
L-leucine	1.0				
L-lysine	1.0				
L-methionine	1.0				
L-phenylalanine	1.0				
L-proline	1.0				
L-serine	20.0				
L-threonine	1.0				
L-tryptophan	1.0				
L-valine	1.0				

All solutions were prepared with high quality Millipore water.

Table III. Preparation of ABCD medium (Pine *et al.*, 1986a).

Solution	Quantity
ACES buffer	10.0 g
KH ₂ PO ₄	0.22 g
Na ₂ SO ₄	0.15 g
Millipore water	500 ml
Solution 2	10 ml
Solution 3	10 ml
Solution 5	100 ml
Solution 6	10 ml
Solution 7	10 ml
Solution 8	10 ml
Solution 9	0.1 ml
Solution 10	0.1 ml
L-cysteine HCl	0.5 g
Glutathione (reduced)	0.5 g
L-tyrosine	0.05 g
Solution 4	10 ml

Adjust pH to 6.75 with 20% KOH	

Solution 11	1 ml
Millipore water up to 1 litre	

Filter sterilise by passage through 0.2 µm filter (Sartorius Ltd.)	

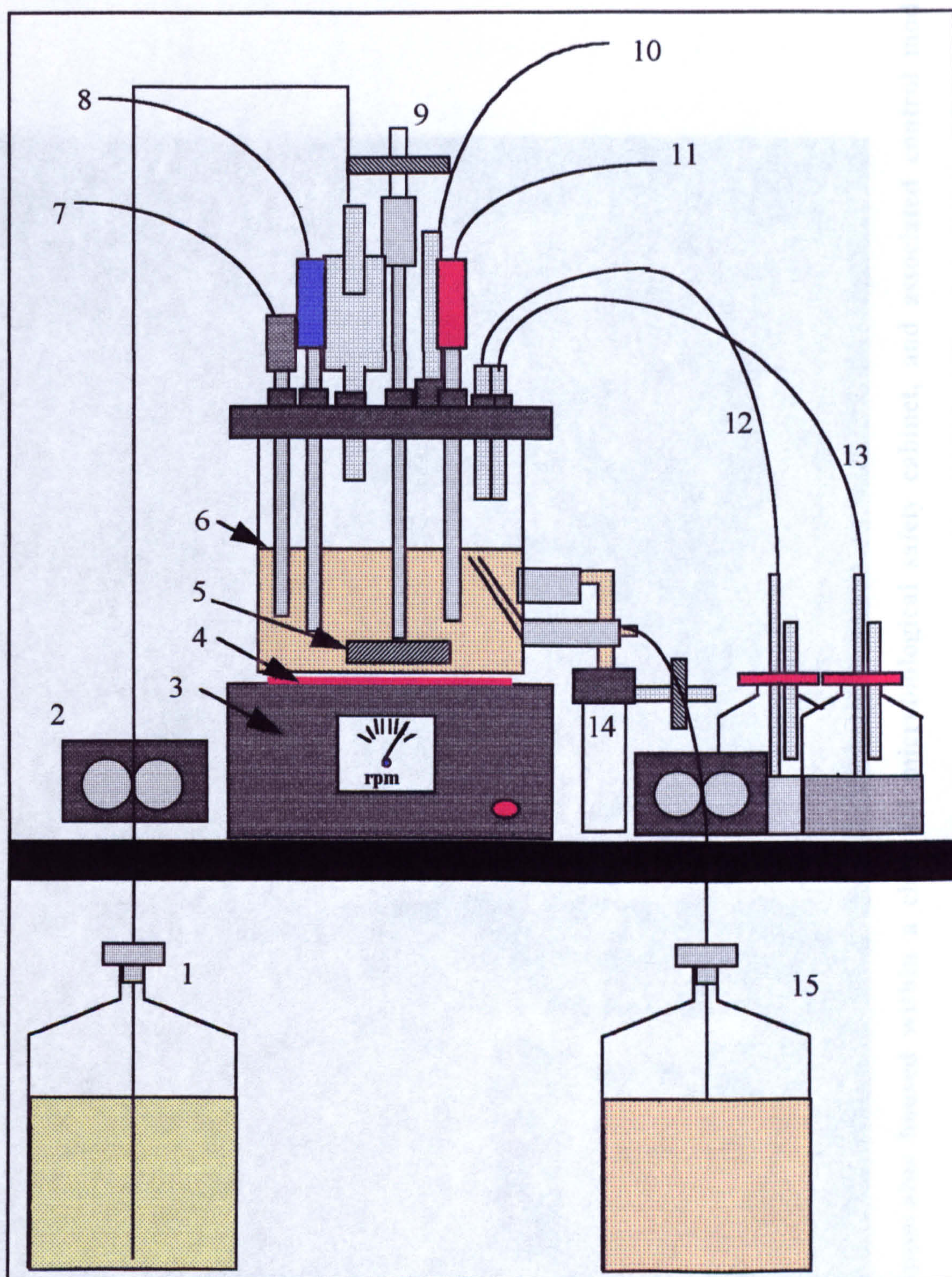
2.3 Continuous Culture.

2.3.1 Culture apparatus.

Continuous culture was performed in a one litre glass vessel fitted with a titanium top plate (Figures 1 & 2). This non-ferrous design avoided problems of iron leaching from stainless steel components of conventional fermentation systems. The culture system was operated as a chemostat by controlling nutrient addition from the medium reservoir, with the aid of a peristaltic pump (Watson Marlow). The culture volume was maintained constant at 500 ml, by an overflow tube fitted through a side arm on the culture vessel, which directed culture to the waste reservoir. Agitation was achieved by means of a magnetic bar placed in the culture vessel, which was controlled by a magnetic stirrer positioned beneath the vessel.

Culture conditions were continuously monitored and controlled by an Anglicon Microlab Fermentation System (Brighton Systems, Newhaven, UK), linked to sensor probes inserted into the culture, through sealed ports in the top plate. The oxygen concentration was monitored with the aid of a galvanic oxygen electrode (Uniprobe, Cardiff), and maintained at 4.5% (v/v) of air saturation at 37°C (equivalent to 0.31 mg l⁻¹), through feedback control of the agitation rate. Culture temperature was monitored by an Anglicon temperature probe, and maintained by an Anglicon heating pad, positioned beneath the culture vessel. An Ingold pH electrode (Mettler-Toledo, Leicester, UK) was used to monitor culture pH. The culture pH was controlled by the addition of either potassium hydroxide (1 M) or sulphuric acid (0.5 M) to the culture on demand.

The culture vessel was housed within a Class III microbiological safety cabinet. This provided protection against possible accidental liberation of aerosols from the system.



(1) medium reservoir; (2) medium addition pump and feed line; (3) magnetic stirrer unit; (4) heating pad; (5) magnetic bar; (6) culture vessel with titanium top plate; (7) temperature probe; (8) oxygen electrode; (9) air inlet and sparger; (10) vent; (11) pH electrode; (12) alkali addition; (13) acid addition; (14) sample port; (15) effluent reservoir.

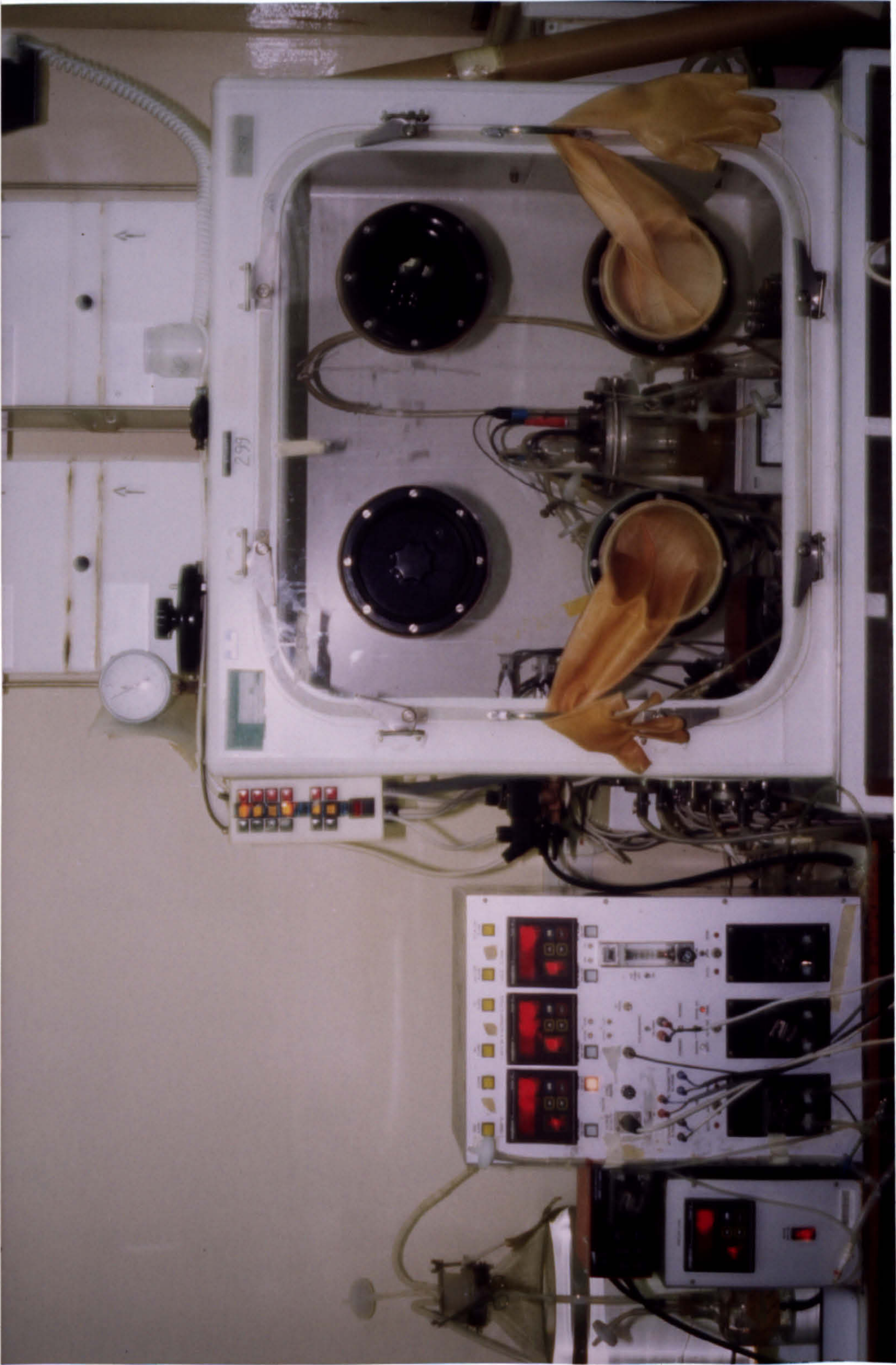


Figure 2. Continuous culture apparatus housed within a class III microbiological safety cabinet, and associated control modules.

2.3.2 Chemostat inoculation and culture.

Stock cultures stored at -70°C were plated onto BCYE agar, and incubated at 37°C . After three days growth, cultures were aseptically harvested from the agar and resuspended in sterile deionised water, to provide a dense inoculum suspension. The bacterial suspension was aseptically transferred to the culture vessel, to provide an initial culture turbidity of approximately 0.1 at 540 nm. The culture medium was purged with oxygen free nitrogen (BOC) prior to inoculation, to reduce the oxygen tension to 4.5% (v/v) of air saturation at 37°C .

After inoculation the culture was grown in batch mode until the optical density at 540 nm (OD_{540}) reached approximately 0.5 absorbance units. Continuous culture was initiated at a dilution rate of 0.025 h^{-1} , and was finally increased to 0.08 h^{-1} [equivalent to a mean generation time (MGT) of 8.7 h] once the OD_{540} reached 1.0. All cultures were established to steady state under iron-replete culture conditions at 37°C , pH 6.9, and a dissolved oxygen tension of 4.5% (v/v) air saturation at 37°C , before altering the growth environment. Steady state growth was determined by monitoring culture turbidity and biomass yield (Section 2.4).

2.4 Culture Analyses.

2.4.1 Culture purity.

Culture purity was routinely assessed by plating chemostat samples onto BCYE and NCM agar, and monitoring after 4 days incubation at 37°C , for the presence and absence of growth, respectively.

2.4.2 Optical density determination.

The optical density of culture samples, was recorded at 540 nm (OD_{540}) in a UV-260 spectrophotometer (Shimadzu Co., Japan) against a water reference. When

OD₅₄₀ measurements exceeded 1.2 absorbance units, samples were diluted 10-fold in sterile deionised water, before reading.

2.4.3 Dry weight determination.

For biomass determination, 10 ml aliquots of culture were formalized with 1% formaldehyde (v/v), for 30 minutes. The sample was then filtered through a pre-dried, pre-weighed, 0.45 µm pore sized, nylon membrane filter (Gelman Sciences), under vacuum. The membrane was rinsed with 10 ml deionised water, before re-drying in a microwave oven to a constant weight, and re-weighing.

2.4.4 Enumeration of colony forming units.

Culturability, i.e. the ability to form single colonies on BCYE agar, was determined by preparing a 10-fold dilution series of the sample in sterile deionised water, and spreading 100µl aliquots of 10⁻⁴ to 10⁻⁶ dilutions onto BCYE agar, in triplicate. The plates were incubated at 37°C for up to 5 days before counting the number of colonies formed.

2.4.5 Total Cell Count.

Total cell counts were determined by phase contrast microscopic examination of diluted samples applied to a Thoma counting chamber, using a Leitz Dialux 20 microscope (Ernst Leitz, Wetzlar, Germany). Culture samples were diluted 100-fold in deionised water before enumeration.

2.4.6 Sample collection and storage.

Cultures were grown for 10 generations after reaching steady optical density and biomass yield (cell dry wt.), before commencing sample collection. Culture samples were collected on ice and separated by centrifugation at 10,000 g for 15 min.

Supernatant samples were clarified further by passage through 0.2 µm pore size, cellulose acetate membrane filters (Sartorius Ltd.). Samples of cell paste and clarified supernatant were stored at -40 °C until analysed. For iron-limited cultures, all vessels used for collection, centrifugation and storage of samples were acid washed prior to use, by soaking in 6M hydrochloric acid and rinsing with distilled deionised water.

2.5 Chemical Analysis of Culture Supernatant and Medium Samples.

2.5.1 Amino acid analysis.

Two separate procedures were used for amino acid determination. During iron-limited studies, amino acids analysis was performed using a 4400 dedicated amino acid analyser (LKB, Cambridge). Separation was achieved by Lithium cation-exchange chromatography, with post column ninhydrin reaction and detection at 440 nm and 570 nm, on a recorder and spectra physics integrator (Phillips, Cambridge). Calibration was performed before each run, using mixed physiological fluids standards (Sigma Chem. Co.).

Separation and detection of tryptophan was achieved by reverse-phase HPLC, using a phosphate/citrate mobile phase (0.2 M Na₂HPO₄ : 0.1 M citrate : ethanol, at 3:5:2, pH 4.0), on a hypersil octadecylsilane reverse-phase column. Detection was performed at 280 nm, using a variable wavelength detector and recorder (Phillips, Cambridge). Quantitation was achieved by reference to a freshly prepared tryptophan standard solution. Cysteine concentration was determined colorimetrically using the method of Gaitonde (1967).

During studies on the influence of culture pH on the physiology of iron-limited and -replete cultures, the amino acid composition of supernatant samples was determined by HPLC separation of phenyl isothiocyanate (PITC) derivatised samples, following the procedure of Aitken *et al.* (1989). Samples were prepared for derivatisation by filtration through a 10 kDa molecular weight cut-off membrane filter (Sartorius Ltd.). Filtrate (10 µl) was mixed with 100 µl of coupling buffer (0.7

ml acetonitrile + 0.2 ml trimethylamine + 0.1 ml deionised water), vortexed and dried by vacuum centrifugation. An additional 100 μ l aliquot of coupling buffer was added to the sample along with 5 μ l of neat PITC (Sigma Chem. Co.). The reactions were vortexed and incubated at room temperature for 20 min, before drying by vacuum centrifugation and storage at -20°C under argon. Before analysis, the derivatised sample was reconstituted with 500 μ l of sodium acetate buffer (150 mM, pH 5.4), and a 20 μ l aliquot was loaded onto the column.

Separation of derivatised samples was performed on a Brownlee octadecylsilane PTC 25 column using a Beckman Gold HPLC system, operated at 40°C, and a flow rate of 1 ml min⁻¹, with detection at 254 nm. Solvent A was 50 mM sodium acetate, pH 5.4, and solvent B was 70% acetonitrile : water (v/v). The solvent gradient system was as detailed by Aitken *et al.* (1989). System calibration was performed with PITC derivatised standards (Pierce mixture H: 2.5 μ mol ml⁻¹ in 0.1 M HCl) with a column loading of 1 nmole.

2.5.2 Ammonium and phosphate determination.

Ammonium was assayed colorimetrically by the Berthelot reaction (Gordon *et al.*, 1978). Phosphate was determined by the molybdenum blue method (Basset *et al.*, 1983).

2.5.3 Iron and zinc determination.

Millimolar concentrations of iron and zinc in culture supernatants were determined by flame atomic absorption spectroscopy on a PU-9100 spectrophotometer (Philips, Cambridge). Electrothermal atomic absorption spectroscopy, was used for more sensitive determination of micromolar concentrations of iron.

The iron content of culture biomass was determined using cell paste washed twice with ultra high quality (UHQ) water (Elgastat Ltd. High Wycomb), was dried at

120°C to a constant weight. The dried material was resuspended in deionised water and analysed by electrothermal atomic absorption spectroscopy.

2.5.4 Organic carbon analysis.

The total organic carbon content (TOC) of clarified culture supernatants, was determined by infra-red detection of carbon dioxide, generated by ultra-violet promoted persulphate oxidation (Clesceri *et al.*, 1989), using a Protoc analyser (Pollution Process Monitoring, Kent). Samples of culture supernatant and uninoculated culture medium were diluted 200-fold in UHQ water before analysis. Instrument calibration was performed with a 50 mg l⁻¹ carbon stock solution, prepared with potassium hydrogen phthalate in UHQ water.

2.6 Monitoring Cellular and Colony Morphology.

2.6.1 Light microscopy.

Cell morphology was monitored by differential interference contrast (DIC) microscopy (Rogers & Keevil, 1992) using a Nikon Labophot microscope (Nikon, Telford, UK), equipped with episcopic UV illumination and a DIC analyzer. Culture samples were fixed in 1% (v/v) formaldehyde for 30 min, before preparing a dry smear on a glass slide, and viewing by episcopic DIC. Colony morphology on BCYE agar was examined using a Wild M8 stereomicroscope.

2.6.2 Electron microscopy.

Culture samples were fixed in 0.2% (v/v) formaldehyde for 2 h, before being applied to formvar/carbon filmed, 400 mesh copper EM specimen grids. These preparations were negatively stained with 1% (w/v) sodium silicotungstate before examination in a Philips EM 400T transmission electron microscope operated at 80 kV.

2.6.3 Indirect fluorescent antibody staining.

Cell paste was resuspended in sterile deionised water to an OD₅₄₀ of approximately 0.5, and applied in 5 µl aliquots to a multiwell microscope slide. The preparations were heat fixed, and coated with *L. pneumophila* serogroup 1 specific polyclonal antiserum (Dennis, 1986) for 1 h at 37 °C, in a moist atmosphere. The preparations were washed for 15 minutes with two changes of phosphate buffered saline, and a final rinse with deionised water. The antibody labelled preparations were then counter labelled with anti-rabbit IgG FITC conjugate, for 30 minutes at 37 °C, in a humid environment. The stained cells were thoroughly washed with PBS followed by distilled water before drying, and viewing with an immunofluorescent microscope, using a ×100 oil immersion objective.

2.6.4 Nile red staining.

Intracellular granules were visualized by fluorescence microscopic examination of cells stained with the fluorescent lipophilic dye, Nile red (9-diethylamino-5H-benzo[α]phenoxazine-5-one). Samples of cell paste were treated with 1% (v/v) formaldehyde for 30 minutes, pelleted by centrifugation and resuspended in sterile deionised water. Dry smears prepared on microscope slides, were stained with Nile red (25 mM Nile red in DMSO), diluted 1/500 in sterile deionised water, for 30 minutes at 25°C. The stained preparation was rinsed with sterile water and dried before fluorescence microscopic examination with a ×100 oil immersion objective.

2.7 Protein Determination.

The protein content of culture supernatants was determined by the Bio-Rad protein assay kit, using the micro assay procedure (1 to 25 $\mu\text{g ml}^{-1}$ protein). This assay is based on the principle that the absorbance maximum for an acidic solution of Coomassie Brilliant Blue G-250, shifts from 465 nm to 595 nm, when bound to protein. The most important advantage of the Bio-Rad assay is the absence of interference from many of the medium components, including amino acids, which limit the use of the other protein assays.

Samples of filter sterilized culture supernatant (0.8 ml) were reacted with 0.2 ml of undiluted dye reagent. The reactions were vortexed and the resultant absorbance was recorded at 595 nm in a UV-260 spectrophotometer, after 5 min. A standard calibration curve was prepared with bovine serum albumin (BSA, Bio-Rad). A BSA stock solution containing 1.4 mg ml^{-1} protein, was diluted in deionised water to provide a series of standards containing 25 to 1 $\mu\text{g ml}^{-1}$ protein. These standards were assayed as detailed for the sample. All absorbance readings were recorded against a blank reaction, containing 0.8 ml deionised water and 0.2 ml reagent. For each sample, control reactions were prepared with samples of the corresponding uninoculated culture medium. The absorbance readings for control reactions were normally <10% of the test reaction absorbance.

For samples such as cell extracts which contained a higher protein content (200 to 1400 $\mu\text{g ml}^{-1}$), the standard Bio-Rad protein assay procedure was used. In brief, 5 ml of dye reagent diluted 1:4 with UHQ water was reacted with 0.1 ml of sample, and mixed. After 5 min, the absorbance was recorded at 595 nm, versus a control prepared with diluent and reagent. A standard calibration curve was prepared with 0.1 ml aliquots of BSA standards, diluted in UHQ water to the range 0.2 to 1.4 mg ml^{-1} .

2.8 Preparation of Concentrated Culture Supernatants.

Samples of filter sterilized culture supernatant were concentrated 40- to 80-fold by pressure dialysis through an Amicon pressure dialysis cell, fitted with a 10 kDa molecular weight cut-off, membrane filter (Amicon Ltd.). Dialysis was performed at 4°C, with continuous agitation at 100 rpm, and under a pressure of 40 psi supplied by nitrogen gas. After dialysis, the concentrated sample was re-sterilized (0.2 µm cellulose acetate membrane filter, Sartorius), and stored in 1 ml aliquots at -40°C.

2.9 Fast Pressure Liquid Chromatography (FPLC) of Extracellular Proteins.

Samples of concentrated culture supernatant were dialysed for 20 h against two changes of 25 mM Tris-HCl buffer (pH 7.0). Aliquots of the dialysed supernatant (1.0 ml) were injected onto a HR 5/5 Mono Q anion exchange column (Pharmacia). The column was eluted with 4 column volumes of 25 mM Tris-HCl buffer (pH 7.0), before commencing a linear (0.1-0.5 M) NaCl gradient, generated over 50 ml, at a flow rate of 2.0 ml min⁻¹. The eluate was collected in 1.0 ml fractions for analysis.

2.10 Azocasein Hydrolytic Activity of Culture Supernatants.

2.10.1 Determination of azocasein hydrolytic activity.

The azocasein hydrolytic activity of culture supernatants was determined by the procedure of Gibson and Macfarlane (1988), with minor modifications. Using 1.5 ml eppendorf tubes, 0.5 ml of sample and 0.1 ml phosphate buffer (0.1 M, pH 7.0), were mixed. Azocasein (150 µl of a 50 mg ml⁻¹ solution prepared in 0.1 M phosphate buffer, pH 7.0) was added to provide an initial substrate concentration of 10 mg ml⁻¹. All reactions, prepared in triplicate, were mixed and incubated at 37°C for 2 h, before

being stopped by the addition of 0.25 ml TCA (10% w/v), with thorough mixing. For each sample, control tubes were prepared with culture supernatant as above, except azocasein was not added until after the reaction was termination with TCA. Additional control reactions were also prepared with samples of uninoculated culture medium.

After stopping the reaction, samples were allowed to stand for 30 minutes, before being microcentrifuged to sediment the precipitate. Samples of the reaction supernatant (0.5 ml) were mixed with an equal volume of 1.0 M NaOH, and the absorbance was measured at 450 nm in a UV-260 spectrophotometer. All absorbance measurements were recorded against deionised water. The net change in absorbance for each sample was calculated as the difference between the absorbance readings of the sample, and the corresponding control reaction, to which azocasein was added after reaction termination. Enzyme activity was expressed as μg substrate hydrolysed in one hour, per mg cell dry weight, to allow for differences in culture density. The extinction coefficient value of 3.4 for a 1% (w/v) azodye solution, was used to calculate activity.

2.10.2 Inhibition of azocasein hydrolysis with ethylenediaminetetraacetic acid (EDTA).

The effect of EDTA (1 and 10 mM) on enzyme activity was investigated with 6 representative iron-limited and -replete samples. For each sample, test and control reactions were prepared as outlined in Section 2.10.1. A parallel set of reactions was prepared using phosphate buffer containing either 7.5 or 75 mM EDTA (pH 7.0), instead of normal phosphate buffer. Samples were incubated with EDTA for 30 min before the addition of substrate, and the assay was completed as detailed in Section 2.10.1.

2.10.3 Recovery of hydrolytic activity.

The ability of zinc (1 mM) to relieve the inhibition of hydrolytic activity caused by 1 mM EDTA, was investigated. For each sample, 4 reactions containing 0.5 ml sample and 0.1 ml phosphate-EDTA buffer (8.5 mM EDTA in 0.1 M Phosphate buffer, pH 7.0) were prepared and incubated for 30 min. To duplicate reactions for each sample, 0.1 ml zinc (8.5 mM ZnCl₂ in deionised water) was added along with substrate (0.15 ml). Substrate plus 0.1 ml deionised water was added to the remaining two reactions. All reactions were allowed to proceed as outlined in Section 2.10.2. Test reactions prepared as outlined in Section 2.10.1, were run in parallel.

The influence of 1 mM zinc on enzyme activity in the absence of EDTA was also investigated, by preparing reactions with sample and normal buffer. After 30 min incubation reactions were commenced by the addition of 0.1 ml zinc along with substrate.

2.10.4 Inhibition of azocasein hydrolysis by anti-zinc-metalloprotease IgG.

To determine the effect of anti-zinc metalloprotease IgG [courtesy of A. Williams, (Williams *et al.*, 1987)] on the hydrolytic activity of culture supernatants, 0.1 ml of antibody prepared in phosphate buffer (0.1 M pH 7.0) was added to 0.5 ml of sample, and incubated at 37°C. The reaction was commenced after 30 min by the addition of substrate, and completed as detailed in Section 2.10.1. The titre of antibody used was sufficient to inhibit the casein precipitating activity of the sample, as determined by the caseinase assay of Conlan *et al.* (1986), and detailed in Section 2.10.5. A parallel set of control reactions were prepared with anti-serogroup antigen IgG [(courtesy of A. Williams, (Conlan & Ashworth, 1986))] substituted for the anti-zinc metalloprotease antibody, at a comparable protein concentration. This was facilitated by determining the protein concentration of both antibody preparations using the standard Bio Rad assay (Section 2.7). Normal test reactions without antibody were run in parallel.

2.10.5 Caseinase assay.

The caseinase assay was used to determine the titre of anti-zinc metalloprotease IgG, and rabbit anti-zinc metalloprotease antiserum, required to inhibit the casein precipitating activity of culture supernatant samples. The procedure followed was that of Conlan *et al.* (1986). A two-fold dilution series of the antibody was prepared in 25 mM Tris-HCl buffer (pH 7.0), and 25 μ l aliquots of each dilution were mixed with an equal volume of sample. These reactions were then transferred to a series of wells prepared in a caseinate agarose plate [1% agarose (w/v) + 1% sodium caseinate (w/v) prepared in 25 mM Tris-HCl, pH 7.0]. The agarose plate was incubated at 37°C for 24 h, and examined to identify the titre of antibody able to inhibit casein hydrolysis. Casein hydrolysis was manifested as a white ring of precipitate around the well. Figure 3 displays an example of a typical inhibition profile for two samples of culture supernatant assayed in duplicate.

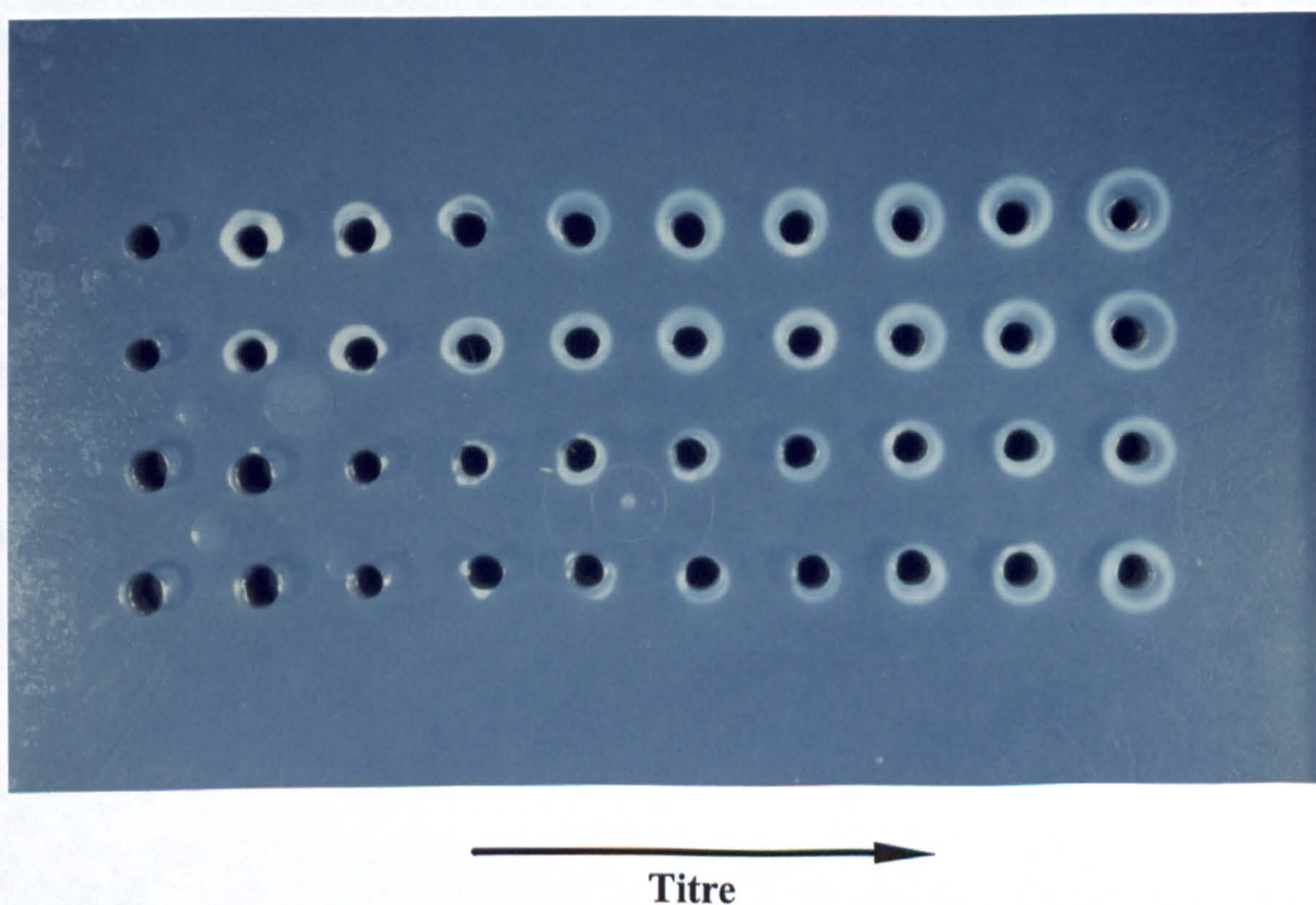


Figure 3. Caseinase assay for determination of the antibody titre capable of inhibiting the casein precipitating activity of culture supernatant samples.

2.11 Phospholipase C Activity.

The phospholipase C activity of clarified culture supernatants and cell suspensions was determined by measuring the release of *p*-nitrophenol from *p*-nitrophenylphosphorylcholine, as described by Baine (1985), with minor modifications. Filter sterilised supernatant samples (1.5 ml), were reacted with an equal volume of 10 mM *p*-nitrophenylphosphorylcholine prepared in 5 mM Tris-HCl, 2.0 mM CaCl₂ buffer (pH 7.2). Control reactions containing uninoculated culture medium and substrate were also prepared. All tubes were incubated at 37°C with gentle agitation for up to 75 h. Samples of concentrated supernatant (0.75 ml), prepared as detailed in Section 2.8, were also reacted with an equal volume of substrate-buffer reagent, and incubated at 37°C for 25 h.

To analyse cell suspensions, frozen cell paste was resuspended in 5 mM Tris-HCl, 2 mM CaCl₂ buffer (pH 7.2), and washed twice in buffer by repeated centrifugation and resuspension. The samples were finally resuspended to an optical density of 1.0 at 590 nm. Aliquots (0.5 ml) of each suspension were reacted with an equal volume of 10 mM substrate, and incubated at 37°C and 200 rpm. After 40 h incubation, the cells were sedimented by centrifugation, and the supernatant phase was removed for analysis. The hydrolysis of *p*-nitrophenylphosphorylcholine was measured by recording the reaction absorbance at 410 nm, in a UV-260 spectrophotometer. A standard calibration curve for 0-0.5 mM *p*-nitrophenol (Sigma Chem. Co.), prepared in 5 mM Tris-HCl, 2mM CaCl₂ buffer (pH 7.2), was used to quantitate *p*-nitrophenol release in the test reactions.

2.12 Human Transferrin Utilisation as a Source of Iron.

2.12.1 Preparation of diferric human transferrin.

Human apo-transferrin (Sigma Chem. Co.) was loaded with iron following the protocol of Karin & Mintz (1981) with modifications. Apo-transferrin dissolved in 0.1M Tris-HCl (pH 7.4) was dialysed for 24h against 40 mM Tris-HCl, 20 mM NaHCO₃ buffer (pH 7.4), to restore the bicarbonate content of the transferrin. The glycoprotein was then iron-loaded by the addition of ferric ammonium citrate at the rate of 1.48 µg Fe⁺⁺ per mg transferrin. The suspension was incubated at 24°C for 3 h, before redialysis against 40 mM Tris-HCl, 20 mM NaHCO₃ buffer (pH 7.4) for 24 hours at 4°C. The transferrin was redialysed for a total of 36 h against two changes of buffer and finally against UHQ water, before being freeze-dried and stored at 4°C. The saturated transferrin content was assayed spectrophotometrically at 465 nm, using the extinction coefficient value of 0.57 for a 1 % (w/v) solution of saturated transferrin

2.12.2 Growth response of iron-limited cultures to diferric transferrin.

Freeze-dried iron-loaded transferrin (Section 2.12.1) was dissolved in 10 ml Tris-HCl buffer (pH 7.4), prepared with UHQ water. After filter sterilization by passage through a 0.2 µm pore size cellulose acetate membrane filter (Sartorius Ltd.), the transferrin was added directly to the iron-limited chemostat culture, to provide an immediate increase of 2.5 µM iron. The growth response was monitored by collecting culture samples at time intervals and measuring the optical density at 540 nm (Section 2.4.2). Biomass concentration was determined at approximately 8h intervals by performing dry weight determinations (Section 2.4.3).

2.12.3 Transferrin receptor assay.

Cells from chemostat cultures were assayed for the presence of surface located transferrin receptors, following the protocol of Schryvers and Morris (1988). In brief, washed cell suspensions prepared in phosphate buffered saline (PBS), were diluted by a 2-fold series with PBS. An aliquot of each cell dilution (4 μ l) was applied directly onto nitrocellulose paper and allowed to dry. The paper was treated with blocking agent (0.05% (w/v) Tween 20 and 1% (w/v) skimmed milk powder in PBS) for 1 h, and then washed with 0.05% (w/v) Tween 20 in PBS for 15 min, with two changes of solution. The cells were reacted with human transferrin conjugated with horse radish peroxidase, 1 μ g ml⁻¹ in 0.05% (w/v) Tween 20 in PBS (Jackson Immunoresearch Labs), for 1h. After washing with three changes of PBS, the nitrocellulose sheet was reacted with 4-chloro-1-naphthol (4CN).

The 4CN reagent was prepared by dissolving 20 mg 4CN in methanol, and transferring 200 μ l to 20 ml PBS, along with 10 μ l hydrogen peroxide. Positive reactions were visible as dark purple dots, where the cells had been applied. Positive and negative control reactions were prepared with *Neisseria meningitidis* cultured in the presence of either EDDA or iron, respectively (courtesy of A. Gorringer).

2.12.4 Digestion of human transferrin by *L. pneumophila* culture supernatants.

Iron-saturated human transferrin (Sigma Chem. Co.) dissolved in 0.1M Tris-HCl, 25 mM NaHCO₃ buffer (pH 7.4), was added to filter sterilized iron-replete culture supernatant, at a final concentration of 1 mg ml⁻¹. Control reactions were prepared containing transferrin in buffer, and transferrin in supernatant containing either 10 mM EDTA or rabbit antiserum raised to purified *L. pneumophila* zinc metalloprotease (courtesy of A. Williams). The concentration of antiserum was sufficient to completely inhibit the casein precipitating activity of the supernatant, as determined by the caseinase assay (Section 2.10.5). All reactions were incubated at 37°C and sampled over a 24h period. Samples were diluted with sample buffer [2% SDS (w/v), 10% glycerol (v/v), 5% mercaptoethanol (v/v) and 0.05% bromophenol

blue (w/v), in 0.05 M Tris-HCl, pH 6.8], and boiled for 5 min before electrophoresis on precast ExcelGel SDS gradient gels (Pharmacia) at 45 mA. Protein bands were visualised by Coomassie blue staining. Similar experiments were performed with apo-transferrin and lactoferrin. The interaction of iron-limited supernatants with transferrin was also investigated.

To confirm that the zinc metalloprotease was responsible for transferrin digestion, an additional set of experiments was performed, with control reaction containing anti-zinc metalloprotease IgG [courtesy of A. Williams, (Williams *et al.*, 1987)]. The titre of antibody used was sufficient to completely inhibit the casein precipitating activity of the culture supernatant (Section 2.10.5). A corresponding control reaction was prepared with anti-*L. pneumophila* serogroup antigen IgG [courtesy of A. Williams, (Conlan & Ashworth, 1986)], added to the reaction at a comparable protein concentration. To facilitate this, the protein content of both antibody preparations was determined by the BioRad standard protein assay (Section 2.7).

2.13 Siderophore Assays.

2.13.1 Universal siderophore assay.

The universal chrome azurol S (CAS) assay was performed on iron-limited supernatants as outlined by Schwyn and Neilands, (1987). In brief, 0.5 ml of filter sterilised supernatant was reacted with an equal volume of CAS solution. Control reactions were prepared with samples of uninoculated culture medium. Absorbance was monitored at 630 nm in a UV-260 spectrophotometer, until a stable end point was reached. The iron chelating activity of samples was related to that of the commercially available siderophore, desferroxamine (Ciba-Ceigy). A standard curve was prepared with 0.5 ml aliquots of desferroxamine standards (0-20 μ M) prepared in UHQ water. A similar curve was also prepared in uninoculated iron-limited culture medium.

2.13.2 Ferric chloride binding assay.

The iron-binding activity of iron-limited and -replete culture supernatants was also analysed spectrophotometrically, by reacting 0.1 ml of sample with 0.9 ml FeCl_3 (0.12 M FeCl_3 in 0.005 N HCl) as detailed by Holzberg & Artis (1983). A differential absorption scan was performed against control reactions containing uninoculated culture media and FeCl_3 . Positive control reactions were prepared with a solution of 2.5 mM desferroxamine in UHQ water. The relationship between sample volume and absorbance was also investigated. For this assay, 0.1 to 0.5 ml aliquots of sample were reacted with 0.5 ml FeCl_3 solution, and the reaction was made up to 1.0 ml with UHQ water. Corresponding control reactions were prepared with samples of uninoculated culture medium.

2.13.3 Emery and Neilands assay.

Iron-limited and -replete supernatants were assayed for the presence of hydroxamic acids by the periodate oxidation assay of Emery and Neilands (1960), following the procedure of Holzberg and Artis (1983). Samples of culture supernatant (0.4 ml), were reacted with 1.0 ml periodic acid (2.20 mM periodic acid prepared in UHQ water). Control reactions were prepared with samples of uninoculated culture medium. Reactions were made up to 4.0 ml with UHQ water along with two drops of glycerol, before spectrophotometric analysis in quartz cuvettes, for the presence of nitroso dimers at 264 nm. Solutions of desferroxamine and catechol prepared in UHQ water (1.25 mM) were used as positive and negative controls, respectively.

2.13.4 Csaky assay.

Culture samples were assayed for the presence of hydroxamic acids by the procedure of Csaky (1948), with hydroxylamine used for standard curve preparation. The assay was performed with 30 min and 4 h hydrolysis steps.

2.13.5 Arnow assay.

The procedure of Arnow (1937) was used to assay supernatants for the presence of phenolate type siderophores. Catechol was used as a positive control, while desferroxamine served as a negative reference.

2.14 Determination of Ferric Citrate Reductase Activity.

The periplasmic, cytoplasmic and membrane fractions of iron-limited and -replete cell samples were purified following the procedure of Johnson *et al.* (1991). For iron reductase determination, 1 mg samples of freeze-dried cell fractions were reacted with 40 µg ferric citrate, 2.5 µM ferrozine and 0.01M Tris-HCl buffer (pH 7.6), in a final reaction volume of 1 ml. The reactions were allowed to stabilize for 10 min before the addition of 1µM NADH or NADPH (Sigma Chemical Co.), in 0.01M Tris-HCl buffer (pH 7.6). Activity was determined at 24°C by recording the change in absorbance over time, at 562 nm in a UV-260 spectrophotometer (Shimadzu Co. Japan). All absorbance measurements were recorded against control reactions containing all components except reductant.

The protein content of samples was determined by the Bio-Rad standard protein assay procedure, as detailed in Section 2.7. Specific iron reductase activity was calculated as the nmoles Fe^{++} formed, per mg protein in 30 minute, at 24°C.

2.15 Analysis of Serogroup Antigen.

2.15.1 Extraction of serogroup antigen.

Serogroup antigen was prepared by following the hot saline extraction procedure of Conlan and Ashworth (1986), with minor modifications. Frozen cell paste, washed twice in deionised water, was resuspended in 0.9% (w/v) saline and boiled for 1 h with regular mixing. The suspension was cooled and centrifuged for 30

min at 10,000 g. The liquid phase was removed and dialysed overnight against phosphate buffered saline. The dialysed extract was sequentially treated for 2 h at 37 °C with ribonuclease 1, deoxyribonuclease 1 (in the presence of 0.1 M MgCl_2), and proteinase K (Sigma Chem. Co.), each at a final concentration of 0.01 mg ml^{-1} . Residual enzyme activity was destroyed by boiling the extract for 5 min. The preparation was then dialysed overnight against 0.1 M Tris-HCl buffer (pH 8.2), and freeze dried.

2.15.2 Keto-2-3-deoxyoctonate determination.

Saline extracts were assayed for keto-2-3-deoxyoctonate (KDO) by a procedure adapted from Karkhanis *et al.* (1978). Extract, dissolved in UHQ water (10 mg ml^{-1}), was dispensed in 0.15 ml aliquots, along with 0.125 ml of 0.2M HCl, and heated at 100°C for 10 minutes. After cooling, 0.4 ml of periodic acid solution (25 mM periodic acid in 62.5 mM sulphuric acid), was added to each tube. After being allowed to oxidize at room temperature for 20 min, 0.6 ml of sodium arsenite [2% sodium arsenite (w/v), in 0.5 M sulphuric acid] was added with rapid mixing. The reaction was completed by adding 2.5 ml of thiobarbituric acid [0.3% (w/v) thiobarbituric acid in 10 mM HCl] and heating the tubes at 100°C for 20 min. The absorbance of the reaction mixtures were recorded at 548 nm against a control reaction prepared with UHQ water, while the reactions were still warm. The KDO concentration was determined with reference to a standard curve prepared with purified KDO (Sigma Chem. Co.). For standard curve preparation, a KDO solution (75 $\mu\text{g ml}^{-1}$) prepared with UHQ water, was diluted by a 2-fold series. Each dilution was then assayed as detailed for the sample.

2.15.3 Carbohydrate determination.

Total carbohydrate was assayed by the phenol sulphuric acid method of Dubois *et al.* (1956). Extract (1 mg in 2 ml UHQ water) was mixed with 50 μ l phenol solution [80% (w/v) in UHQ water] and 5 ml concentrated sulphuric acid. The tubes were allowed to cool for 10 min, mixed thoroughly and incubated at 30°C for 20 min, before recording absorbance at 490 nm against a control reaction prepared with UHQ water. A standard calibration curve was prepared with glucose standards (10 to 50 μ g ml^{-1}) prepared in UHQ water.

2.15.4 Protein determination.

The protein content of saline extracts (0.1 mg ml^{-1} in UHQ water) was determined by the Bio-Rad micro assay as detailed in Section 2.7.

2.15.5 SDS-PAGE of serogroup antigen.

Saline extracts were separated by SDS-PAGE using slab gels as outlined by Conlan and Ashworth (1986). The separating gel was 15% (w/v) acrylamide and 0.5% (w/v) bisacrylamide containing 4 M urea and 0.2% (w/v) SDS in 0.375 M Tris-HCl buffer (pH 8.8). Samples (5 mg ml^{-1}) in sample buffer [2% (w/v) SDS, 10% (v/v) glycerol, 5% (v/v) mercaptoethanol and 0.05% (w/v) bromophenol blue, in 0.05 M Tris-HCl, pH 6.8] were boiled for 5 min and applied to the gel at a standard loading of 60 μ g per lane. Gels were run at 45 mA and 4°C until the tracking dye reached the bottom of the gel. The gel was fixed overnight in a solution of 40% (v/v) ethanol, 5% (v/v) acetic acid in water. The lipopolysaccharide (LPS) banding profile was silver stained following the procedure of Tsai & Frasch (1981).

2.16 Analysis of Cellular Protein Expression.

2.16.1 Preparation of cell proteins.

Cell paste (approx. 1g wet wt.) was washed twice in UHQ water and finally resuspended in 20 ml of HEPES buffer (10 mM, pH 7.2). The cells were ruptured by three consecutive passages through a French pressure cell, with a pressure of 20,000 lbs per sq inch. Cell debris was removed from the bacterial suspension by centrifugation at 10,000 g and 4 °C for 30 min. Samples of the resultant cell free suspension were retained as representative of whole cell proteins.

Cell wall material was pelleted by ultracentrifugation at 100,000g and 4°C for 1 h, and washed in HEPES-EDTA buffer (10 mM HEPES, 7 mM EDTA, pH 7.2). The washed cell membrane pellets were resuspended in HEPES-EDTA buffer containing 2% (w/v) sarkosyl, and incubated at 37°C for 1 h with vigorous mixing every 15 min. The insoluble outer membrane material was pelleted at 100,000 g and 4°C for 1 h, and washed with HEPES-EDTA buffer before final resuspension in HEPES buffer and storage at -40°C. The sarkosyl soluble inner membrane material was dialysed overnight against HEPES-EDTA buffer at 4°C, before storage at -40°C.

The outer membrane preparations purified from French press extracts yielded very poor banding profiles. Although the sarkosyl extraction step was repeated on these extracts, banding resolution did not improve. Therefore, an alternative method employing a combination of lysozyme digestion and freeze-thaw was also used for the preparation of cell membranes. In brief, washed cell material (approx. 1g wet wt.) was incubated for 30 min in 10 ml Tris-EDTA buffer (10 mM Tris-HCl, 10 mM EDTA, pH 7.6) containing 0.1 mg/ml lysozyme. The suspension was then treated with three consecutive cycles of freezing and thawing. $\text{MgCl}_2 \cdot 7\text{H}_2\text{O}$ (0.1 g) and DNAase (1 µg) was added to the suspension before incubation for a further 30 min. The cell debris was removed and the outer membrane material purified as detailed above.

The protein concentration of all protein fractions was determined by the standard Bio-Rad assay as detailed in Section 2.7.

2.16.2 SDS-PAGE of protein preparations.

SDS-PAGE was performed using precast Excel gradient 8-18, SDS polyacrylamide gels (Pharmacia) with an LKB Multiphor electrophoresis system. Protein samples were diluted in sample buffer [2% (w/v) SDS, 10% (v/v) glycerol, 5% (v/v) mercaptoethanol and 0.05% (w/v) bromophenol blue, in 0.05 M Tris-HCl, pH 6.8] to a protein concentration of 1.0 mg ml⁻¹, boiled for 5 min and loaded in 8 µl aliquots. Gels were electrophoresed at 200V and 4°C, for approximately 2 h. Protein profiles were fixed and stained by the Bio-Rad silver stain plus method. Samples of molecular weight markers ranging from 14.4 to 212 kDa (Pharmacia) were run to facilitate molecular weight determination of sample proteins.

2.17 Analysis of Membrane Lipid Composition.

2.17.1 Extraction of fatty acids.

Cellular fatty acids were prepared by acid methanolysis followed by hexane:chloroform extraction as detailed by Wait (1988). In brief, freeze-dried cell material was incubated at 60°C over-night with 2 ml methanol-toluene [1:1, (v/v)] containing 50 µl concentrated sulphuric acid, in a 5 ml screw-capped tube. When cool, 1 ml saturated NaCl was added to the mixture along with 2 ml hexane-chloroform [4:1, (v/v)]. The reactions were mixed vigorously to extract the fatty acid methyl esters into the hexane phase. After separation, the organic phase was carefully removed with a Pasteur pipette to a fresh vial and rotary evaporated to dryness. The dried extracts were redissolved in trimethylpentane for gas chromatography.

2.17.2 Polar lipid extraction.

Polar lipids were extracted by a modification of the procedure of Bligh and Dyer (1959). Frozen cell paste was resuspended in deionised water, pelleted by centrifugation and freeze dried. Approximately 5 mg of lyophilized biomass was suspended in 2 ml of chloroform:methanol:distilled water [1:2:0.8 (v/v)] and vortex mixed for 2 minutes. A further 0.6 ml of chloroform was added and the mixture was vortexed for 0.5 min. Separation of the phases was encouraged by low speed centrifugation, after which the lower, mainly chloroform, layer was removed with a Pasteur pipette to a clean tube, and washed with UHQ water. The water washes were discarded, and the residual organic layer was evaporated in a vacuum centrifuge and redissolved in 30 μ l chloroform, prior to analysis by fast atom bombardment mass spectrometry.

2.17.3 Gas chromatography and mass spectrometry of fatty acid methyl esters.

Gas chromatography was performed with a Carlo-Erba 4130 chromatograph fitted with a 25 m \times 0.2 mm fused silica column, coated with a 25 μ m chemically bonded BP5 (5% phenyl polysiloxane) stationary phase (SGE Ltd. Milton Keynes, UK.). Helium was used as the carrier gas at a linear velocity of 30 cm sec⁻¹. The injector was maintained at 250°C, and samples were introduced by splitless injection (splitless time 30 seconds) at an initial oven temperature of 80 °C. After a one minute delay, the oven temperature was increased at 10°C min⁻¹ to 235°C, and this temperature was held for 15 min. The detector was maintained at 250°C.

Individual peaks were identified by gas-chromatography / mass spectrometry using a Kratos MS80 mass-spectrometer which was directly coupled to a Carlo-Erba 5160 high resolution gas chromatograph. A 25 m BPX5 (5% phenyl polysilphenylene-siloxane) column was used as detailed above. The sample was introduced by splitless injection at an initial oven temperature of 80°C. After a one minute delay, the oven temperature was programmed at 40°C min⁻¹ to 200°C, followed by 3°C min⁻¹ to 230°C and finally to 265°C at 8 °C min⁻¹ and this

temperature was held for 10 min. The injector and source temperatures were 250 and 230°C respectively. The instrument was operated at 1000 resolution and scanned at 0.6 s per decade of mass over the range 550 to 40. Electron ionization spectra were recorded at 70 eV ionization energy and 100 μ A trap current at a source temperature of 250°C.

2.17.4 Fast atom bombardment (FAB) mass spectrometry of polar lipids.

FAB mass spectra of polar lipid extracts were recorded in both positive and negative ion modes with a Kratos MS80RFA (Manchester UK) spectrometer equipped with an Ion Tech FAB gun, using xenon atoms as the bombarding particles. The liquid matrix was 3-nitrobenzyl alcohol, 1 μ l being mixed with an equal volume of sample solution on the stainless steel target. The instrument was operated at 4kV accelerating voltage and scanned at 10 seconds per decade over the range 1800-100 under the control of Mach-3 software running on a Sun Microsystems Sparcstation IPX. The instrument resolution was 1000 in all cases.

The individual phospholipid species were identified by means of collisional induced dissociation (CID) and linked scanning experiments (in the positive ion mode only). Collision induced dissociation was performed using helium as the collision gas, at a pressure sufficient to attenuate the precursor ion beam to 30% of its initial intensity. The products of collision in the field free region between the source and the electrostatic analyzer were recorded by means of computer controlled linked scans under the control of the Mach 3 software. Profiles of the individual types of phospholipids in complex mixtures were obtained by means of constant neutral loss experiments in which the mass of the neutral fragments was characteristic of a given polar head group. Thus scans for the loss of the neutral species of mass 141, 155, 169 and 172 were used to selectively record phosphatidylethanolamines, *N*-methyl phosphatidylethanolamines, di-*N*-methyl phosphatidylethanolamines and phosphatidylglycerols respectively. Phospholipids (such as phosphatidylcholine) in

which charge is retained on the polar head-group fragment were identified by B/E linked scans, using the protonated molecule as the precursor ion.

2.18 Virulence and Intracellular Growth.

2.18.1 Virulence testing.

Culture virulence was assessed using the guinea pig aerosol model as described by Baskerville *et al.* (1981), and Fitzgeorge *et al.* (1983). A Henderson apparatus was used to generate fine a particle aerosol challenge of 5 μm or less by Collison spray at 65% relative humidity, from steady state culture samples. Groups of animals were challenged with serial dilutions of the culture sample, to facilitate subsequent determination of the median lethal dose (LD_{50}). The retained dose was quantitated by plating lung macerate from guinea pigs receiving the maximum dose and sacrificed immediately after challenge, onto BCYE agar, and incubating at 37°C, as detailed by Fitzgeorge *et al.* (1983). For iron-replete samples, neat chemostat culture sample was administered as the top standard, while iron-limited cultures were concentrated 10-fold to provide the maximum challenge dose.

During preliminary experiments, 3 groups of 4 animals were challenged with the top standard and two 10-fold serial dilutions respectively. The method of Reed and Muench (1938) was used to estimate the LD_{50} value.

To facilitate a more accurate determination of the LD_{50} , and to enable the calculation of confidence intervals, the experimental design was altered, by reducing the range of dilutions used and increasing the number of animals challenged at each dose. Groups of 8 animals were challenged with neat and 2.5-fold ($0.4 \log_{10}$) serial dilutions of the sample. Six doses of iron-replete cultures were administered, while only 3 doses of iron-limited samples were used. Probit analysis was used to calculate LD_{50} values, and the exact 95% confidence interval limits were determined by the

method of Finney (1964). Potential variation between groups of animals was allowed for by incorporating a heterogeneity factor as outlined by Finney (1947).

The LD₅₀ of chemostat cultures grown at low pH was determined by administering 4 doses of the neat and 0.5 log₁₀ serial dilutions of the sample, to groups of 6 animals. The number of animals challenged in these experiments was reduced mainly for ethical reasons. For these studies estimation of the LD₅₀ and 95% confidence intervals was performed by the moving average method of Thompson (Meynell & Meynell, 1970). The probit method of Finney (1964) was not used to estimate the LD₅₀ as it requires that a minimum of six dosage levels are administered, with at least three partial responses.

2.18.2 *In vitro* macrophage assay.

Guinea-pig alveolar macrophages, obtained by lung lavage, were used to form monolayer cultures with 5×10^5 macrophages per well in a microtitre plate, as detailed by Fitzgeorge (1985). MEM Eagles medium (Imperial labs. UK) supplemented with sodium bicarbonate (10 mM), HEPES buffer (20 mM), L-glutamine (2 mM) and 5% (v/v) normal autologous guinea pig serum was used as culture medium. The monolayers were inoculated with an aliquot of bacterial suspension containing 5×10^7 colony forming units in culture medium, and incubated at 37°C for 2 hours. All non-phagocytosed bacteria were killed by treating the wells with gentamicin at 50 mg l⁻¹ for 2 hours, and removed by washing the monolayers 3 times with culture medium.

Bacterial uptake was assessed by immediately lysing the macrophages in duplicate wells with 0.8 % (w/v) digitonin for 15 min at 37°C, and enumerating the released culturable bacteria by growth on BCYE agar (Section 2.4.4). The remaining cultures were incubated in culture medium at 37°C, and duplicate wells were harvested at 24 and 48 hours. Intracellular growth was assessed by determining the total number of culturable legionellae present in both the culture medium as a result of host cell rupture, and in the remaining intact macrophages following digitonin lysis. Control reactions were included for the Corby virulent (CV) stock strain and an

avirulent variant, "CAC", obtained by repeated subculture on BCYE- α agar (Jepras & Fitzgeorge, 1986). Stock suspensions of these control cultures were harvested from BCYE agar and stored at 4°C.

2.18.3 *In vivo* infection and multiplication assay.

The infection and multiplication of iron-limited and -replete cultures in guinea pig alveolar phagocytes, was also compared by an *in vivo* assay. Suspensions of iron-limited and -replete culture (10^9 c.f.u. ml⁻¹) in sterile deionised water, were used to provide a fine particle aerosol challenge to guinea pigs. Groups of 14 animals were challenged with a single dose of each culture. The retained dose was determined by sacrificing two animals from each group immediately after challenge, and plating lung macerate onto BCYE agar (Fitzgeorge *et al.*, 1983).

A further two animals from each group were sacrificed at four hours post challenge. Alveolar macrophages collected from these animals by the pulmonary lavage procedure of Fitzgeorge (1985), were used to determine the number of legionellae associated with the host phagocytic cells *in vivo*. Phagocytic cells separated from the lavage fluid by gentle centrifugation at 200 g for 10 min, were washed with PBS and repelleted. The washed phagocytes were lysed by treatment with digitonin (0.8 % w/v) for 30 minutes, and the number of associated legionellae were enumerated by plating samples on to BCYE agar (Section 2.4.4). Samples of the lavage fluid separated from the phagocytic cells and the wash fluid were also plated on to BCYE agar to enumerate the number of extracellular legionellae. A further two animals from each group were sacrificed on each of the following 5 days, and *Legionella* growth in the guinea pig lung was determined by culturing samples of lung macerate on BCYE agar.

2.19 Poly- β -hydroxybutyrate Formation.

2.19.1 Poly- β -hydroxybutyrate extraction.

Poly- β -hydroxybutyrate (PHB) was extracted from cell paste using a modification of the method of Findlay & White (1983). Cell paste was washed twice in UHQ water and the final pellet was freeze-dried. Lyophilised cell material (0.5 g) was placed in a cellulose thimble (Whatman) and extracted in boiling chloroform (60 ml) in a Soxtec apparatus (Tekator Ltd.) for eight hours. After cooling, the chloroform was transferred to a 100 ml flask, and rotary evaporated until the crude PHB formed a film on the flask wall. The PHB was then purified by sequential washing with 3×4 ml volumes of ice cold ethanol, followed by 3×4 ml aliquots of cold diethyl ether. The residue was dried to a white solid by rotary evaporation.

2.19.2 PHB determination.

Purified extracts were dissolved in chloroform (10 - 20 ml) and assayed for PHB by the method of Slepecky & Law (1960). In summary, 20 μ l aliquots of the purified material were dispensed into screw capped glass tubes, dried, and mixed with 5 ml of concentrated sulphuric acid. The reactions were heated to 100°C for 30 minutes. Crotonic acid produced by PHB dehydration was measured at 235 nm, in a UV-260 spectrophotometer using quartz cuvettes. The PHB content of samples was determined by reference to a standard curve prepared with purified PHB from *Alcaligenes* sp. (Sigma Chem. Co.). A stock solution of PHB in chloroform was serially diluted with chloroform, to provide a range of standards between 2.0 and 0.125 mg ml⁻¹ PHB. Duplicate reactions were prepared with 20 μ l aliquots of each standard and assayed as detailed for the sample.

2.19.3 NMR spectroscopy.

^1H NMR spectra were recorded at 30°C, using a Varian Unity 500 MHz spectrometer. Approximately 3 mg of sample was suspended in 0.8 ml chloroform, residual solids were removed by centrifugation and the supernatant was transferred to 5 mm NMR tube. The spectra were referenced to residual chloroform at 7.25 ppm.

2.20 PHB Determination by Nile Red Spectrofluorimetry.

A spectrofluorometric assay employing the fluorescent lipophilic probe, Nile red (NR, Sigma Chem. Co.), was assessed for quantitative determination of the PHB content of intact cells. All cell samples were formalized with 1% (v/v) formalin for 30 min, pelleted by centrifugation, and resuspended in deionised water prior to analysis. A 25 mM NR stock solution prepared in DMSO was used to stain cell suspensions.

NR fluorescence was measured in a Perkin Elmer model LS-5B luminescence spectrometer, equipped with a xenon discharge lamp (8.3 W), separate excitation and emission reflection grating monochromators, and sample and reference photomultiplier tubes. Fluorescence was measured at fixed excitation and emission wavelengths of 545 nm and 600 nm, respectively, with both slit widths set at 2.5 nm. Readings were recorded with a fixed scale expansion factor of 2.0, and were integrated over a response time of 4 seconds. Temperature was maintained at 25°C by a thermostatically controllable cuvette holder. The instrument was auto-zeroed against a sample of unstained bacterial suspension, prior to recording fluorescence. Before quantitatively analysing cell suspensions a number of validation experiments were performed to optimize the assay.

2.20.1 Determination of excitation and emission maxima.

A washed cell suspension was prepared in deionised water to a standard optical density of 0.5 units at 540 nm, and stained with NR solution ($1 \mu\text{l ml}^{-1}$ of cells). The suspension was incubated at 25°C in the dark. The excitation/emission maxima were determined after 60 minutes using the instrument PreScan mode. Excitation and emission maxima were detected at 545 nm and 600 nm, respectively.

Excitation and emission fluorescence spectra were recorded at their corresponding emission and excitation maxima, respectively. This was achieved, by setting the emission wavelength at 600 nm, and recording the fluorescence as the excitation wavelength was increased in increments from 480 nm to 570 nm. This procedure was repeated at a fixed excitation wavelength of 545 nm, while the emission wavelength was increased in increments from 570 to 640 nm. Figure 4 shows the excitation and emission spectra for emission and excitation wavelengths of 600 and 545 nm, respectively.

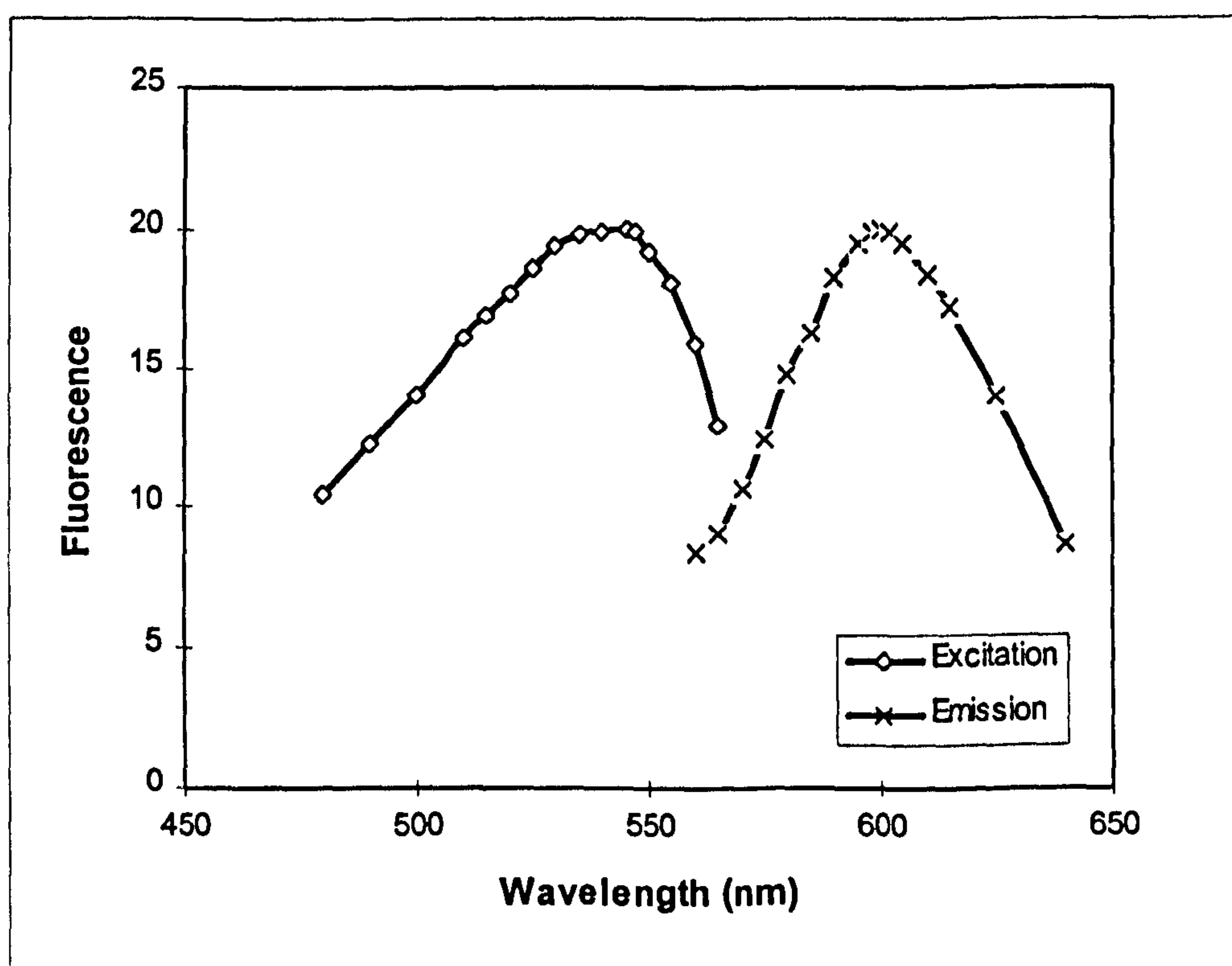


Figure 4. Excitation and emission fluorescence spectra of *L. pneumophila* stained with Nile red

2.20.2 Optimum incubation time.

To confirm the optimum incubation time required to achieve maximum fluorescence, a cell suspension (100 ml) was prepared and stained as outlined in Section 2.20.1. Samples of the stained suspension were removed at intervals over a 2.5 h incubation period, and the NR fluorescence was recorded at fixed excitation/emission wavelengths of 545 and 600 nm, respectively. Maximum fluorescence was obtained between 60 and 70 minute after adding NR to the cell suspension (Figure 5).

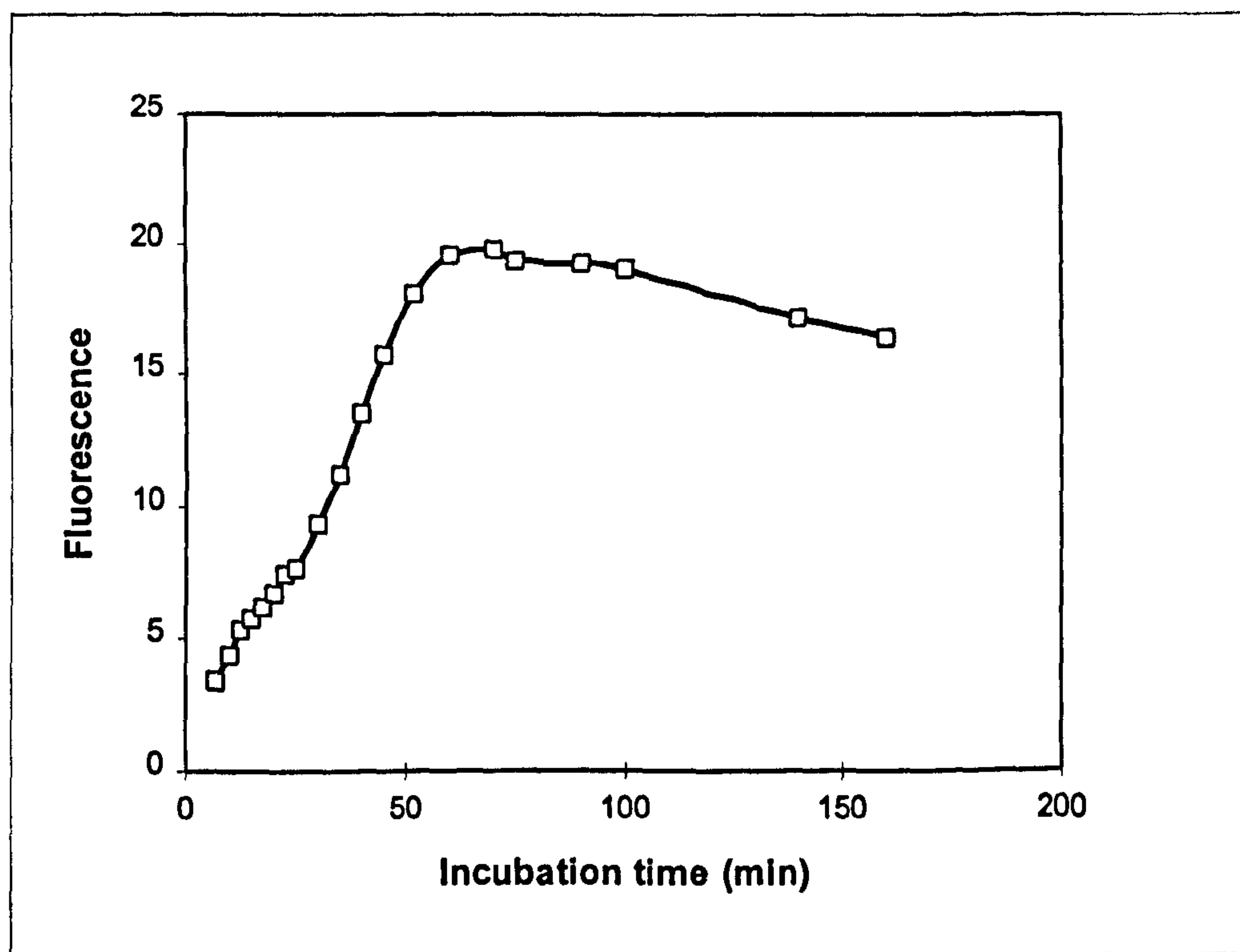


Figure 5. Relationship between Nile red fluorescence and incubation time.

2.20.3 Relationship between cell density and fluorescence.

Washed cell paste was resuspended in saline to provide bacterial suspensions ranging in optical density from 0.04 - 4.1, at 540 nm. Samples were stained with NR ($1 \mu\text{l ml}^{-1}$) for 1 h at 25°C , and the fluorescence was measured. A linear relationship was obtained between sample optical density and fluorescence, over the range tested (Figure 6).

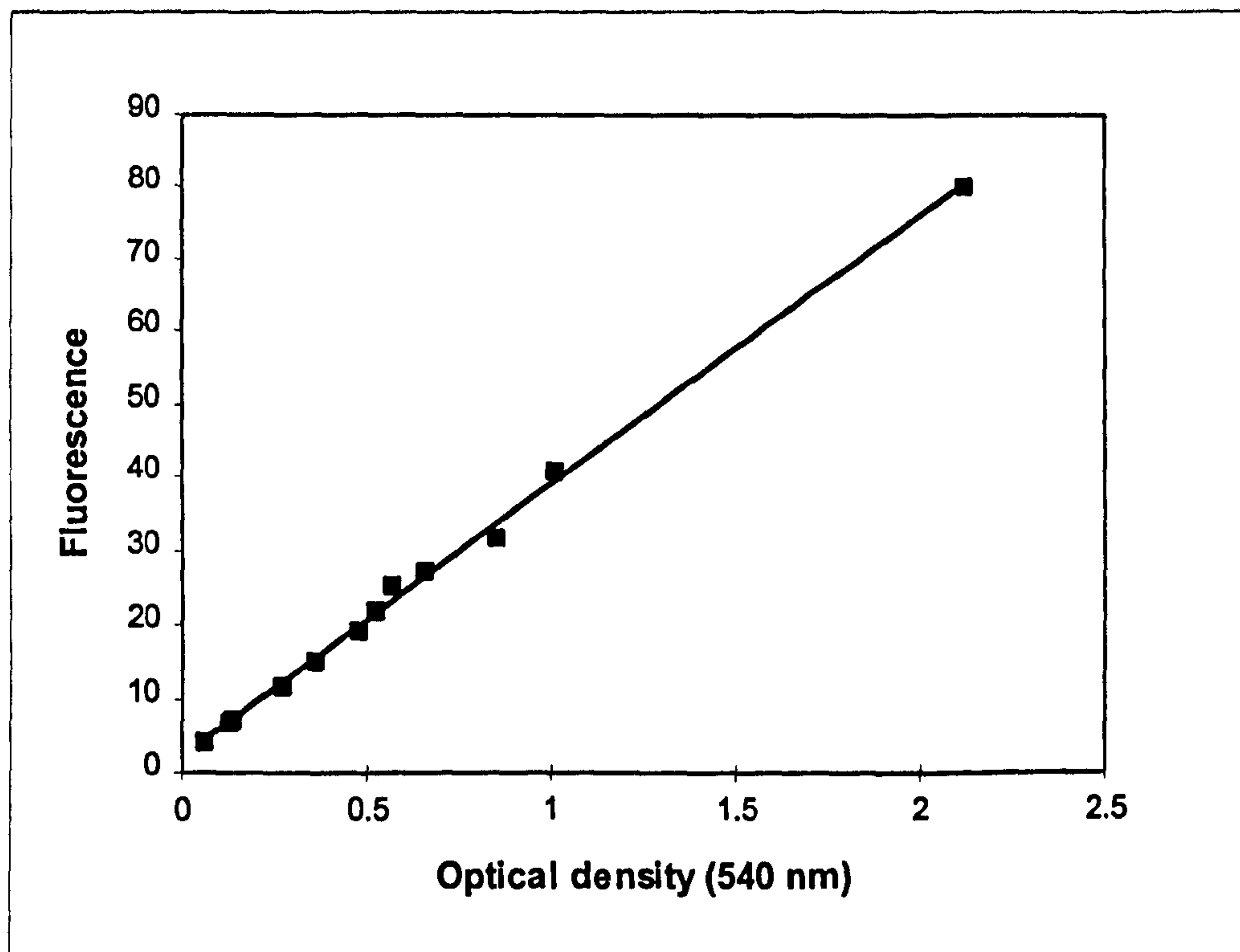


Figure 6. Relationship between sample optical density and Nile red fluorescence.

2.20.4 Influence of Nile red concentration on fluorescence.

The optimum NR concentration required to yield maximum fluorescence was investigated by varying the volume of stock NR solution added to aliquots of bacterial suspension. Fluorescence was recorded after 60 min incubation at 25°C . Optimum fluorescence was observed with $0.5 - 1.0 \mu\text{l NR ml}^{-1}$ of sample (Figure 7).

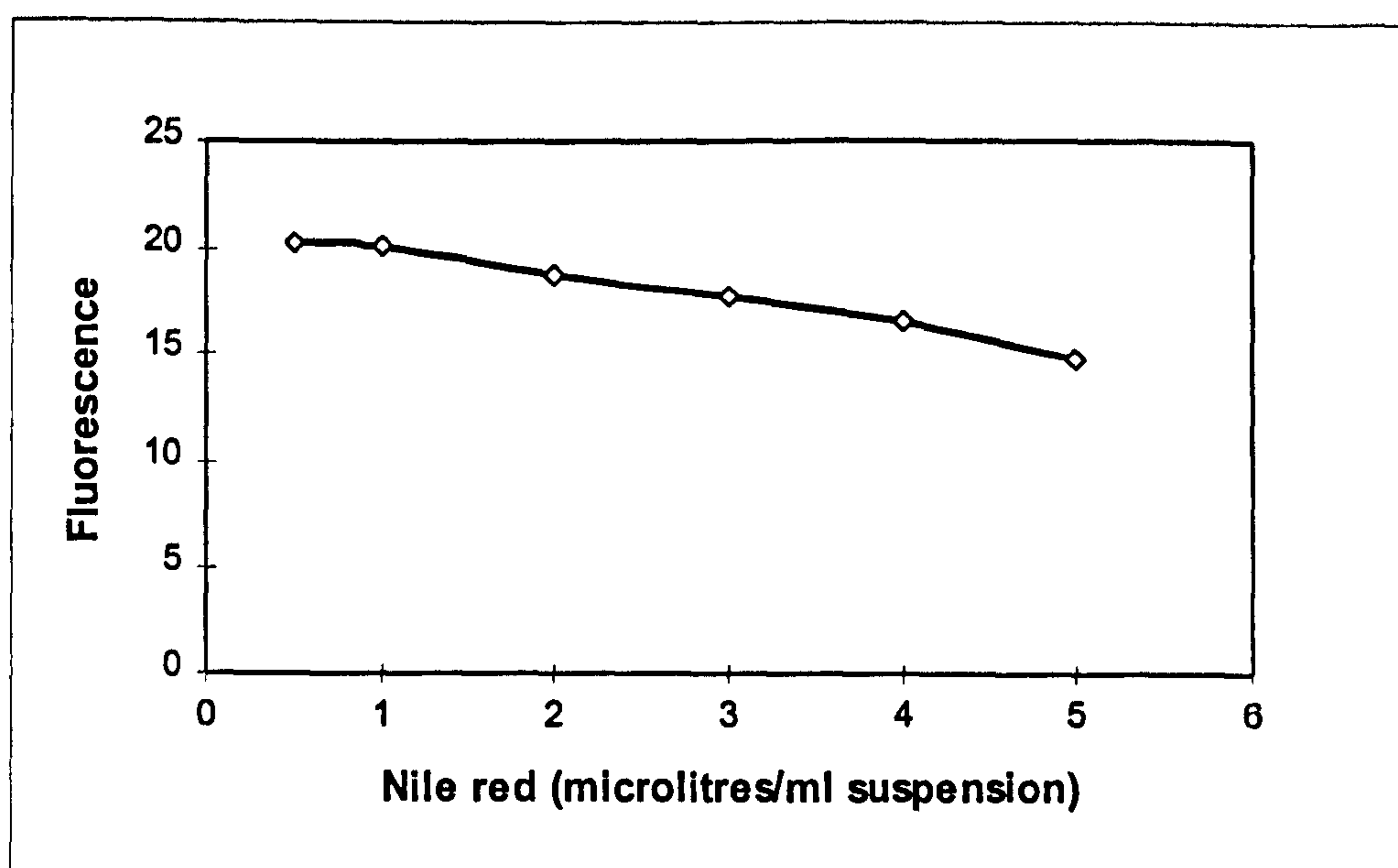


Figure 7. Influence of Nile red concentration on fluorescence.

2.20.5 Spectrofluorometric determination of the PHB content of culture samples.

Culture samples stored at -40°C were suspended in deionised water and formolized [1% (v/v) formaldehyde], for 30 min. The cells were pelleted by centrifugation, re-washed with deionised water, and finally resuspended in deionised water to a standard optical density of 0.5 at 540 nm. Aliquots were stained with $1\mu\text{l ml}^{-1}$ NR (25 mM in DMSO) for 60 min at 25°C . Fluorescence was measured at excitation/emission wavelengths of 545 nm and 600 nm, respectively, with both slit widths set at 2.5 nm. The instrument was auto-zeroed against a sample of unstained bacterial suspension, prior to recording fluorescence. Readings were recorded with a fixed scale expansion factor of 2.0, and were integrated over a response time of 4 seconds.

2.20.6 Relationship between PHB yield and Nile red fluorescence.

To investigate the relationship between the PHB content and NR fluorescence of *L. pneumophila*, samples of lyophilised cell paste were extracted for three

successive 8h periods in boiling chloroform, following the general procedure as outlined in Section 2.19.1. At the end of each 8 h extraction cycle, the extracted material was purified and quantitated as detailed in Sections 2.19.1 and 2.19.2. Samples of the cell material were also collected after each cycle.

Samples of cell paste collected before, and between, each extraction cycle were resuspended in deionised water to a standard optical density of 0.5 at 540 nm and stained with NR, as detailed in Section 2.20.5. The decrease in NR fluorescence caused by chloroform extraction was correlated with the cumulative PHB yield.

2.21 Survival of *L. pneumophila* in a Low-Nutrient Aquatic Environment.

Fresh iron-replete chemostat culture was harvested, washed three times in deionised water and resuspended in filter sterilized (0.2 μm pore size cellulose acetate filters, Sartorius) tap water, at a cell density of approximately 10^9 cells ml^{-1} . The bacterial suspension, prepared in duplicate, was incubated in the dark at room temperature (24°C), with gentle agitation (150 rpm).

2.21.1 Analysis of starved cells.

Samples of the starved suspension were removed periodically, and plated on BCYE agar to monitor culturability (Section 2.4.4). Total cell counts and optical density determinations were also performed as detailed in Section 2.4. Indirect fluorescent antibody labelling of samples was performed as detailed in Section 2.6.3. Cellular morphology was monitored by DIC microscopy (Section 2.6.1).

2.21.2 Nile red spectrofluorometric analysis of starved cells.

The PHB content of the starved culture was monitored by the Nile red spectrofluorometric assay. Samples of culture were formalized with 1% (v/v) formaldehyde and stored at -40°C, until analysis. Frozen samples of starved culture

were thawed slowly and allowed to equilibrate to room temperature. The neat cells samples were then stained by adding 1 µl NR solution per ml of cell suspension, at 25°C for 1h. Fluorescence was measured as detailed in Section 2.20.5.

2.21.3 Flow cytometry analysis of starved cells stained with Nile red.

Frozen samples of starved culture, stained with NR as outlined in Section 2.21.2, were also analysed by flow cytometry. Flow cytometry was performed using a Beckton Dickinson Immunocytometry Systems bench top flow cytometer (FACScan), operated via a Mackintosh computer system. This system analyses up to 5 parameters, [forward light scatter (FSC), side light scatter (SSC) and three fluorescence parameters at different wavelength settings (FL1, 530/30; FL2, 585/42; FL3 >650)] of individual cells, as they travel in a liquid stream past a fixed laser beam. These measurements provide information regarding cell size, internal complexity and relative fluorescence intensity. Real-time data acquisition and analysis is controlled by CellQuest software, while FACSCComp software is responsible for daily set-up and quality control. Calibration was routinely performed with CaliBRITE beads (Beckton Dickinson Immunocytometry Systems).

Samples are introduced through a stainless steel inlet tube and injected into a moving stream of sheath fluid (buffered saline) within a quartz flow cell, where they are intercepted by a 488 nm, 15 mW, air-cooled elliptical argon-ion laser beam. The resultant scattered light and fluorescence signals are detected by separate photonmultiplier tubes for SSC, FL1, FL2 and FL3, while a photodiode acts as the FSC detector.

2.21.4 Heat shock treatment of starved cells.

Samples of starved cells from the cultures prepared in Section 2.21 were incubated at 45°C for 60 min. At intervals during heat treatment, 1 ml aliquots of the suspension were removed and plated onto BCYE agar to enumerate the number of

culturable bacteria, as detailed in Section 2.4.4. After 60 min heat treatment, the suspension was cooled to 24°C and incubated at this temperature for 24 h before being re-sampled and plated onto BCYE agar.

RESULTS

3.1 Influence of Iron Limitation on the Physiology of *L. pneumophila*.

3.1.1 Growth of *L. pneumophila* in iron-replete continuous culture.

L. pneumophila strain Corby was successfully grown in chemostat culture using the ABCD medium. Following inoculation, the culture system was operated in batch mode to allow the culture to become established. Cultures displayed typical batch growth kinetics, with a lag phase of 6-8 h, before entering exponential growth with a minimum doubling time of 3.1 h (Figure 8). Continuous culture was normally initiated at a dilution rate of 0.03 h^{-1} once the culture turbidity (OD_{540}) reached 0.4, and was finally increased to 0.08 h^{-1} (equivalent to a mean generation time of 8.7 h), when the turbidity reached 1.0. Steady state iron-replete growth was achieved within 10 culture generations. Iron-replete cultures were typically dense golden-brown suspensions, containing approximately 1.3 g l^{-1} biomass (dry weight).

3.1.2 Influence of iron limitation on the growth of *L. pneumophila*.

Conversion of steady state iron-replete cultures to iron-limited conditions, resulted in a loss of culture pigmentation within 24 hours, with the culture becoming creamy-white. The culture density remained constant for 8-10 generations before decreasing by at least 50%, to a new steady state level. Steady state iron-limited growth was achieved within 10 generations from the onset of iron limitation (Figure 9). The modified iron-limited ABCD medium contained trace amounts of contaminating iron, normally $\leq 0.75 \text{ } \mu\text{M}$, which was sufficient to support steady state growth at this reduced culture density. The addition of ferrous sulphate ($2.5 \text{ } \mu\text{M}$) directly into the chemostat culture, stimulated a 2-fold increase in culture turbidity, confirming iron as the growth-limiting nutrient (Figure 10).

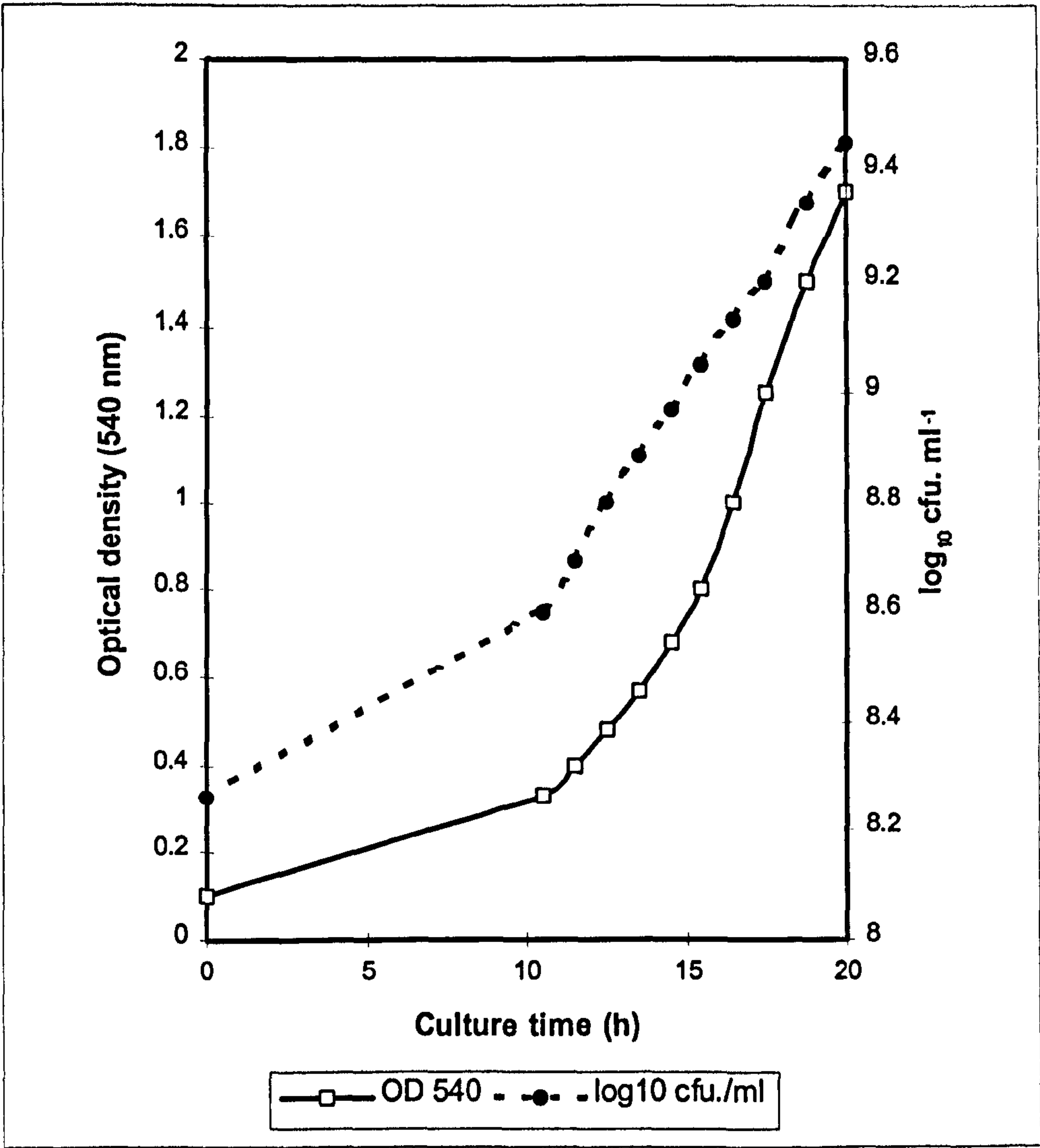


Figure 8. Batch growth of *L. pneumophila*, strain Corby, in ABCD medium.

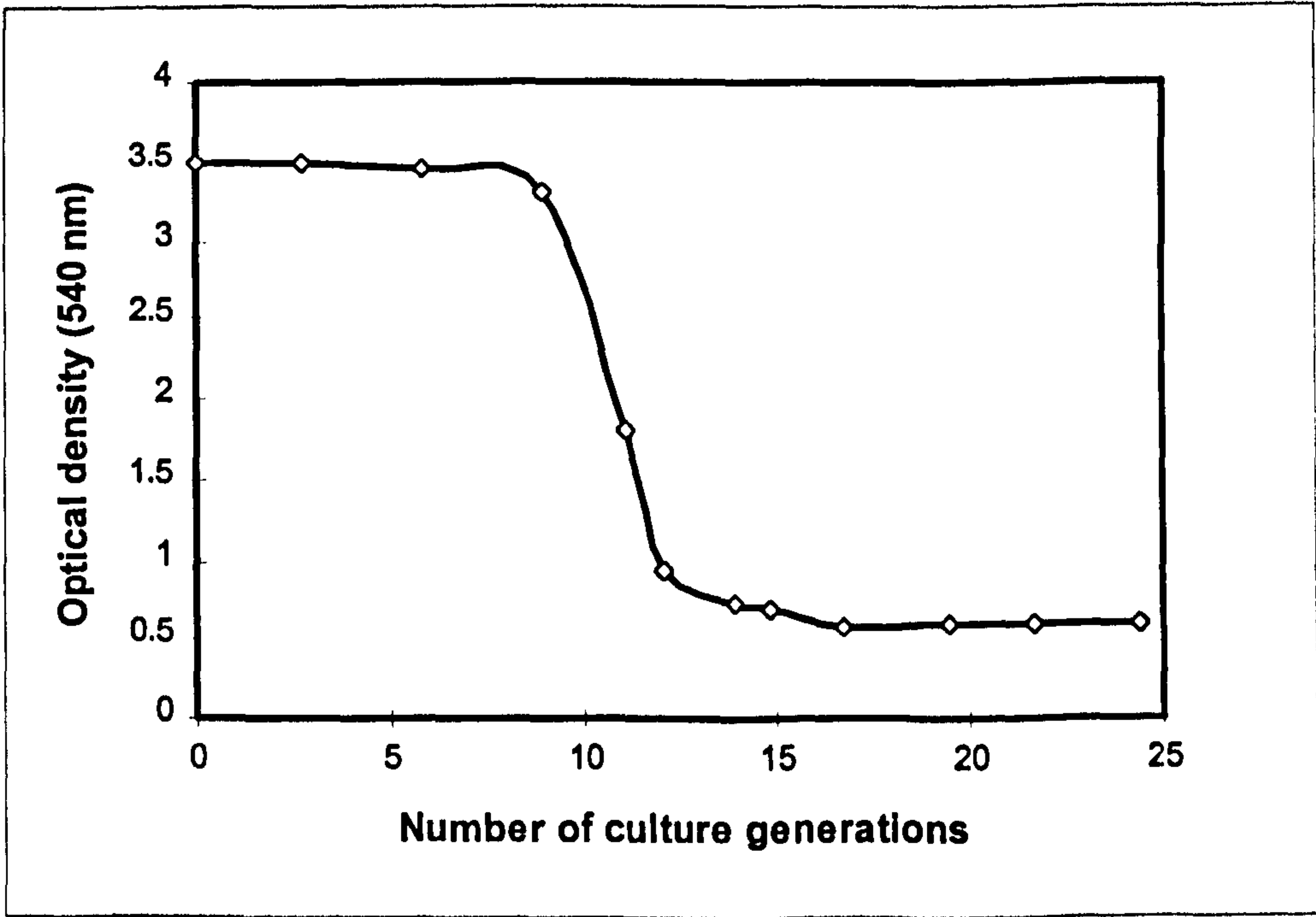


Figure 9. Growth response of a steady state iron-replete culture of *L. pneumophila* to iron limitation.

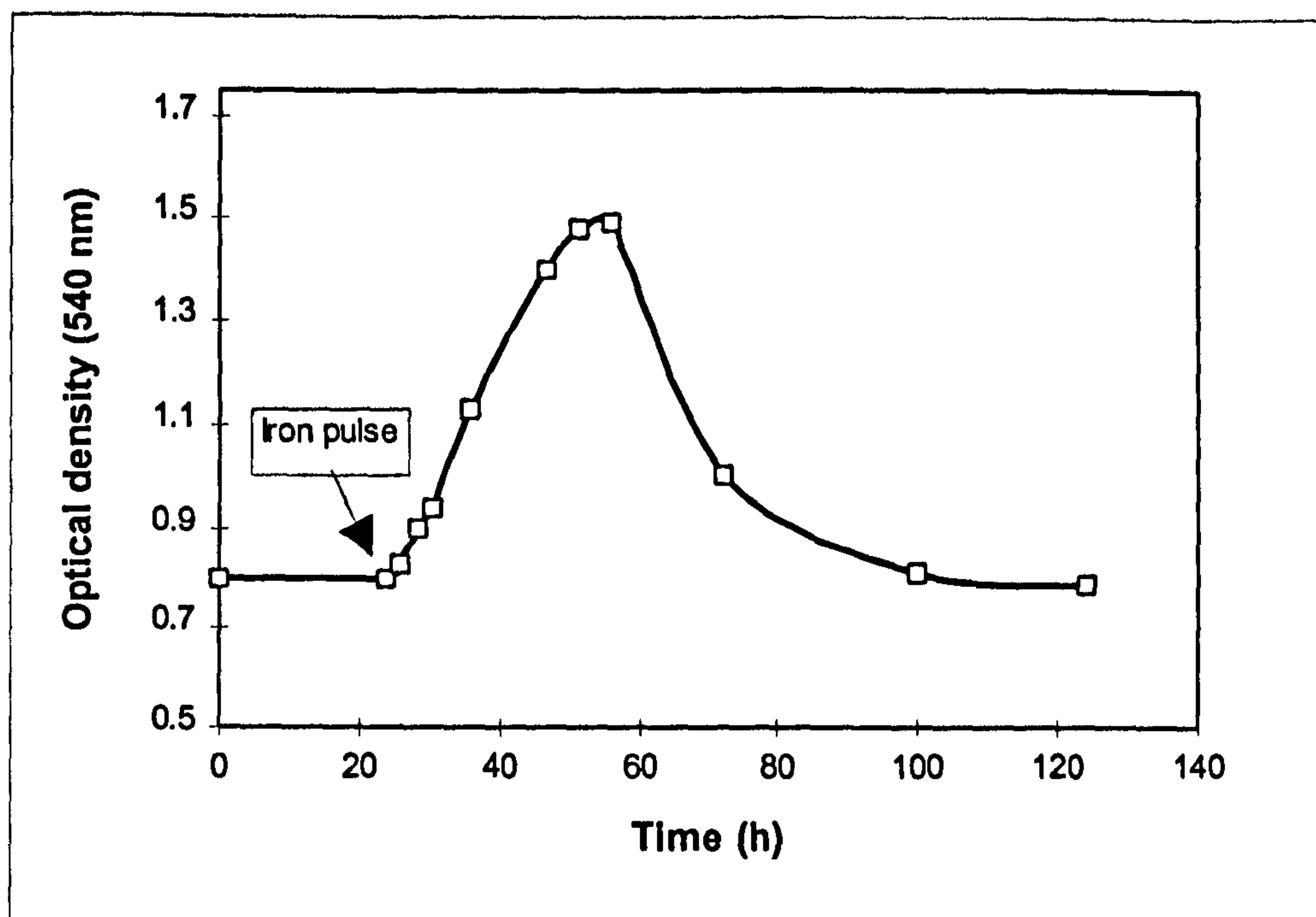


Figure 10. Growth response of an iron-limited chemostat culture of *L. pneumophila* to the addition of 2.5 μ M ferrous sulphate.

3.1.3 Nutrient utilisation by iron-limited and -replete cultures.

Table IV compares the results of biochemical analyses for iron-replete and -limited culture supernatants, and control samples of uninoculated culture medium. In iron-replete cultures, 10 amino acids were depleted below the limit of detection ($< 0.025 \mu\text{M}$). Serine, which is present in ABCD medium at a concentration at least 15-fold higher than any of the other amino acids, was also close to depletion. The metabolism of 17.2 mM serine was accompanied by the production of 16.2 mM ammonium, with a stoichiometric ratio of 1:0.95. The presence of cystine in iron-replete media and culture supernatant samples, demonstrated that oxidation of cysteine catalyzed by iron had occurred. Essential trace elements, including iron, remained in excess. Results of iron analyses indicated that approximately $3.3 \mu\text{M}$ iron was utilized during the growth of iron-replete cultures (Table IV).

In iron-limited cultures, the majority of amino acids including tyrosine and serine remained in excess, with only proline being depleted below detection (Table IV). A decrease in ammonium production in relation to serine metabolism was detected, with a stoichiometric relationship of 1:0.7 for serine metabolised and ammonium released. Iron-limited culture supernatants still contained a low concentration of iron, approximately 0.1 - 0.2 μM . Other important trace elements, namely zinc and phosphate, remained in excess (Table IV).

3.1.4 Growth characteristics of iron-limited and -replete cultures.

The growth characteristics of iron-limited and -replete cultures were calculated from analyses of representative steady state culture samples (Table V). *L. pneumophila* grew well in ABCD medium with values for culture turbidity (OD_{540}), biomass yield and culturability, comparable to those reported previously (Mauchline *et al.*, 1992). Decreasing the iron concentration caused a marked decline in these culture parameters, with 40% and 70% decreases recorded for cell dry weight and the number of colony forming units, respectively. The molar growth yield for serine (Y_{serine}), was also reduced by 25%. However, it is more appropriate to account for the metabolism of other amino acids, particularly in iron-replete culture, by calculating the molar growth yield for carbon metabolised, Y_{carbon} . A 20% decrease in the yield coefficient for carbon was demonstrated under iron-limited conditions (Table V).

The molar growth yield for iron (Y_{iron}), was increased 6-fold in response to iron limitation, indicating increased efficiency of iron metabolism. This correlated with a reduced metabolic rate (q_{iron}). Determination of the iron content of iron-limited and -replete biomass, confirmed a 54% decrease in the iron content of iron-limited cells (Table V).

Table IV. Concentration of nutrients (mM) in unused ABCD medium and in iron-limited and -replete culture supernatants.

Nutrient	Unused medium^a	Iron-replete^a	Iron-limited^a
Alanine	1.14	0.68	1.6
Arginine	0.54	ND	0.19
Aspartate	0.52	0.36	0.35
Cysteine	0.34, (0.6)	0.30	0.69
Cystine	0.22, (ND)	0.13	ND
Glutamate	1.17	0.28	0.76
Glycine	0.94	0.65	0.96
Histidine	0.32	ND	0.21
Isoleucine	0.62	ND	0.26
Leucine	0.63	ND	0.15
Lysine	0.41	ND	0.2
Methionine	0.62	0.04	0.52
Phenylalanine	0.54	ND	0.36
Proline	0.9	ND	ND
Serine	17.45	0.28	3.6
Threonine	0.53	ND	0.50
Tryptophan	0.35	0.26	0.39
Tyrosine	0.23	ND	0.17
Valine	0.83	ND	0.5
Iron^b	150.6, (0.45)	147.3	0.13
Zinc	0.07	0.07	0.07
Phosphate	1.59, (2.68)	1.04	2.27
Ammonium	6.3	22.5	15.67

^a Values for unused medium represent the means for seven samples, and values for supernatants are the means for four samples. All standard deviations were less than 18% of the mean.

^b Iron concentrations expressed as μM units.

(), Parenthesis denotes values for iron-limited medium, where they differ from those of the iron-replete culture medium.

ND, Not detected.

Table V. Comparison of the growth characteristics of iron-replete and -limited chemostat cultures of *L. pneumophila*.

Growth Characteristic	Iron-replete	Iron-limited
OD ₅₄₀	3.49	1.62
Biomass yield (g dry wt. l ⁻¹)	1.38	0.82
c.f.u ml ⁻¹ (×10 ⁹) ^a	5.4 ± 0.56	1.7 ± 0.26
<i>Y</i> _{serine} (g mol ⁻¹) ^b	80.2	59.5
<i>Y</i> _{carbon} (g mol ⁻¹) ^{bc}	5.8	4.8
<i>q</i> _{carbon} (mmol g ⁻¹ h ⁻¹) ^d	14.2	16.6
Iron metabolised (μmol l ⁻¹)	3.3	0.32
<i>Y</i> _{iron} (×10 ⁵ g mol ⁻¹) ^b	4.2	25.6
<i>q</i> _{iron} (×10 ⁻⁵ mmol g ⁻¹ h ⁻¹) ^d	19.1	3.1
Iron content (μg g ⁻¹ dry wt.)	94	44

^a ± Standard error of the mean.

^b *Y*_x, the molar growth yield, represents the biomass yield in grams dry weight per mole of substrate metabolised.

^c Calculated from total carbon analysis of culture supernatants and control culture medium, as detailed in Section 2.5.4.

^d *q*_x, the specific metabolic rate, represents the amount of substrate in mmoles metabolised per gram of biomass, in 1 hour.

3.1.5 Influence of iron concentration on the growth of iron-limited cultures.

The growth characteristics of four different iron-limited cultures are compared in Table VI. Increased concentrations of iron promoted a corresponding increase in culture turbidity and biomass yield. While the Y_{carbon} values for the different cultures varied slightly, the concentration of iron metabolised did not appear to have a direct effect on metabolic efficiency, with respect to carbon. However, some variation was observed between the Y_{iron} and q_{iron} values for the different cultures. Closer examination revealed an inverse linear relationship between Y_{iron} and the concentration of iron metabolised (Figure 11).

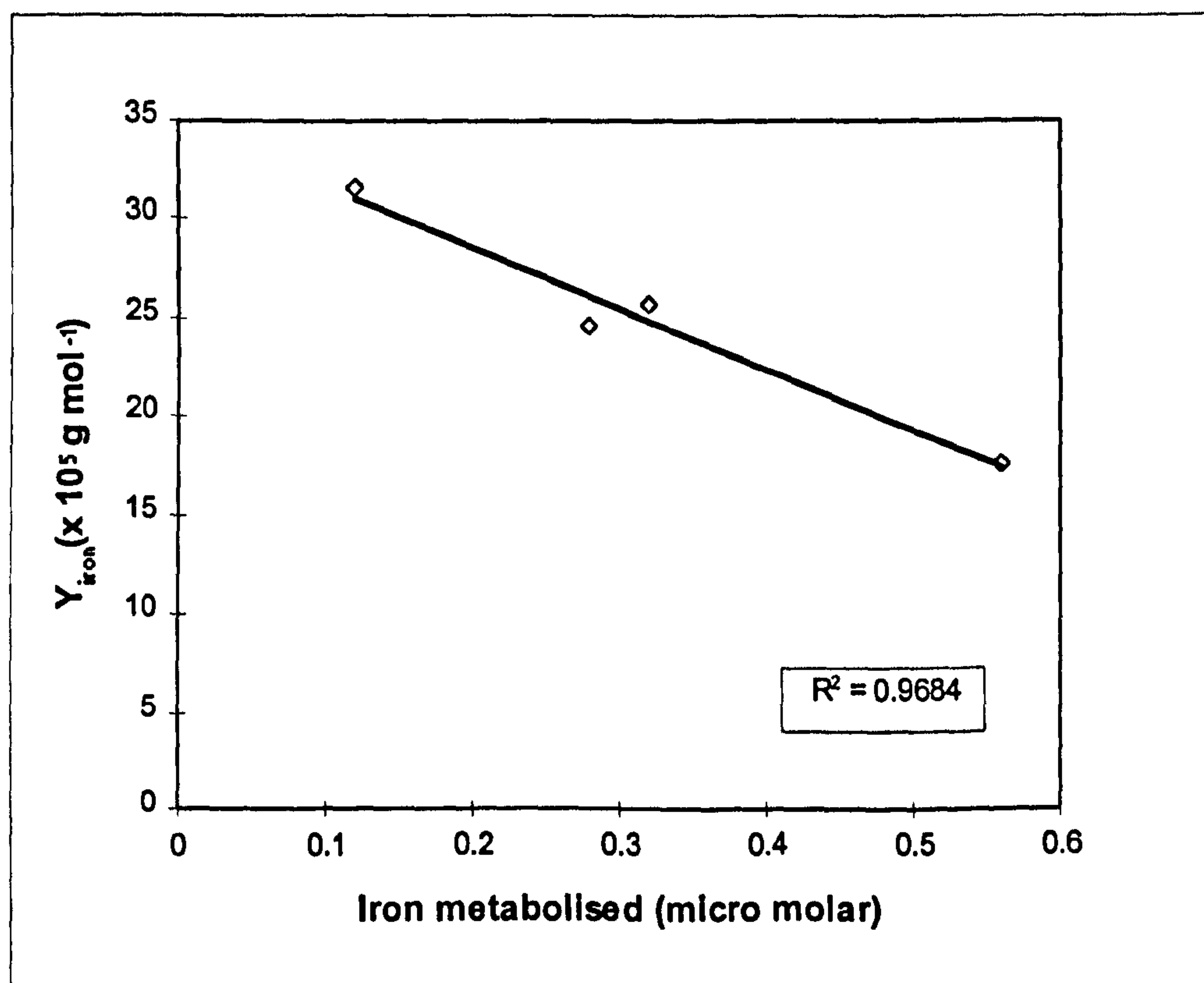


Figure 11. Relationship between the molar growth yield for iron (Y_{iron}) and the concentration of iron metabolised by iron-limited cultures of *L. pneumophila*.

Table VI. Influence of iron concentration on the growth characteristics of iron-limited cultures.

Growth Characteristic	Culture 1	Culture 2	Culture 3	Culture 4
Iron content of medium ($\mu\text{mol l}^{-1}$) ^a	0.29	0.42	0.45	0.83
Iron metabolised ($\mu\text{mol l}^{-1}$) ^a	0.12	0.28	0.32	0.56
OD ₅₄₀	0.59	1.35	1.62	2.34
Biomass (g dry wt. l ⁻¹)	0.38	0.69	0.82	0.99
c.f.u ml ⁻¹ ($\times 10^8$) ^b	5.4 \pm 0.2	18.5 \pm 0.6	17.1 \pm 0.3	20.4 \pm 0.04
Y_{carbon} (g mol ⁻¹) ^{cd}	4.5	4.0	4.8	4.0
q_{carbon} (mmol g ⁻¹ h ⁻¹) ^{ce}	17.7	20.0	16.6	20
Y_{iron} ($\times 10^5$ g mol ⁻¹) ^d	31.6	24.6	25.6	17.6
q_{iron} ($\times 10^{-5}$ mmol g ⁻¹ h ⁻¹) ^e	2.5	3.24	3.1	4.5

^a Mean values calculated from triplicate determinations for culture 1, 3 and 4, and 10 determinations for culture 2. Standard deviation was less than 10% of the mean.

^b Values represent the mean of triplicate determinations \pm s.e.m.

^c Carbon quotients were calculated from total carbon analysis of culture supernatants and uninoculated culture medium, as detailed in Section 2.5.4.

^d Y_x , the molar growth yield, represents the biomass yield in grams dry weight per mole of substrate metabolised.

^e q_x , the specific metabolic rate, represents the amount of substrate in mmoles metabolised per gram of biomass in 1 hour.

3.2 Influence of Iron Limitation on the Morphology of *L. pneumophila*.

Iron limitation produced changes in the cellular morphology of *L. pneumophila*. Iron-replete cultures were pleomorphic with cells ranging from 2 to 40 μm in length, when viewed by differential interference contrast (DIC) microscopy (Figure 12). Conversion to iron limitation, resulted in a loss of culture pleomorphism, producing uniform cultures of short rods 1-3 μm in length (Figure 12). Examination of electron micrographs did not confirm such a dramatic change in cell length, with iron-replete and -limited cells 1.5 to 3.5 and 1.5 to 2.0 μm long, respectively (Figure 13). However, iron-limited cells were approximately 20% narrower and appeared to taper towards each end (Figure 13). Both iron-limited and -replete cultures appeared to be non-flagellated when viewed by both DIC and electron microscopy.

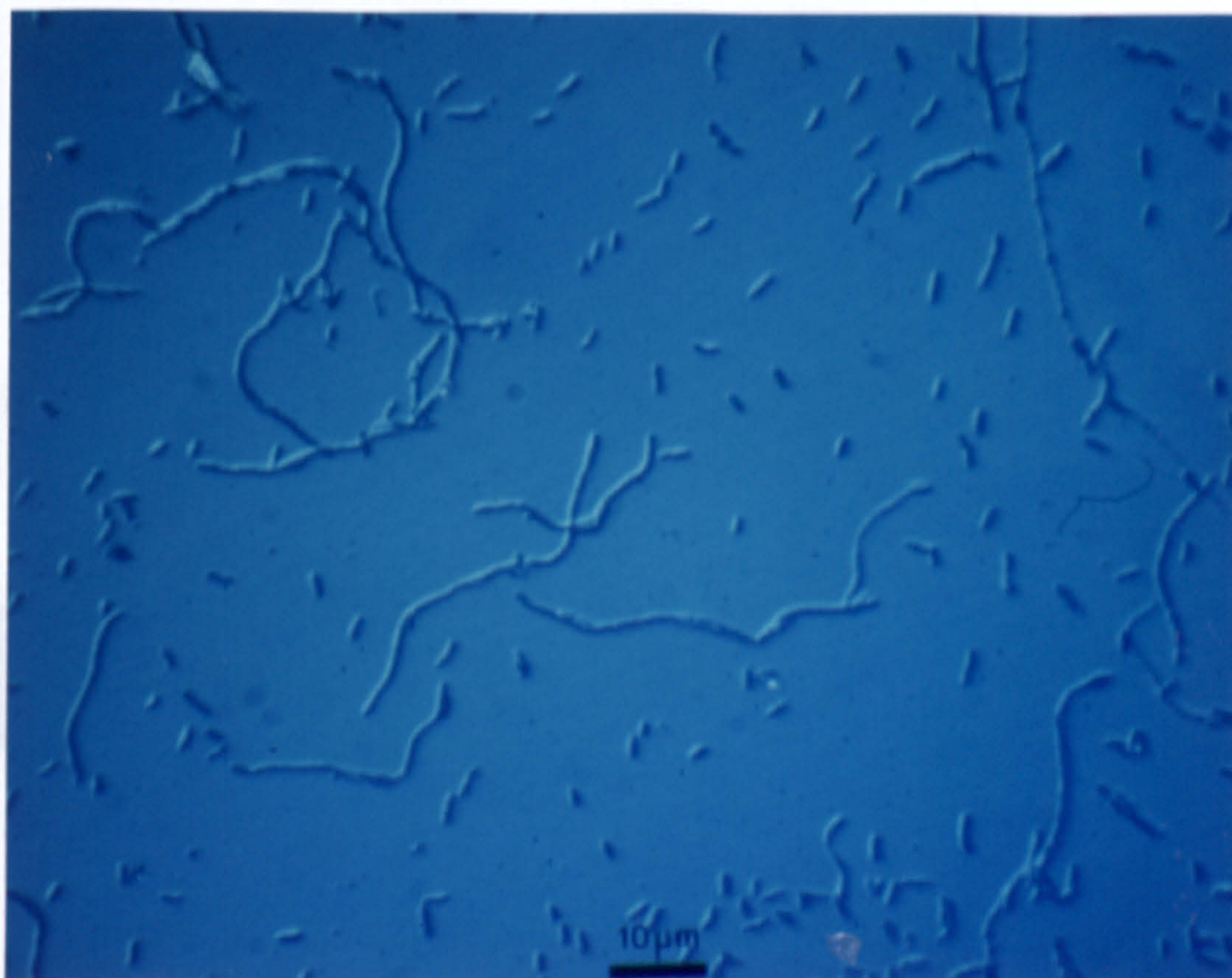
Indirect fluorescent antibody staining of iron-limited and -replete cells detected no alteration in the reaction with serogroup 1 specific polyclonal antiserum (Figure 14). Furthermore, examination of single colonies formed by plating culture samples onto BCYE agar, revealed no alteration in colony morphology, as a result of iron-limited continuous culture. Both cultures produced colonies with the characteristic ground-glass texture, within 3 days of growth at 37°C (Figure 15).

3.3 Extracellular Protein Production.

3.3.1 Influence of iron limitation on extracellular protein production.

Extracellular protein produced by iron-limited and -replete cultures was measured by the BioRad protein assay (Section 2.7). The mean protein content of iron-replete culture supernatants was almost 2-fold greater than that of iron-limited samples (Table VII). However, expression of the data as a function of biomass yield, to allow for differences in culture density, demonstrated comparable protein yields in both cultures (Table VII).

(a)



(b)



Figure 12. Cultures of *L. pneumophila* as viewed by DIC microscopy, (a) iron-replete culture exhibiting pleomorphism; (b) iron-limited culture of short rods.

(a)



(b)

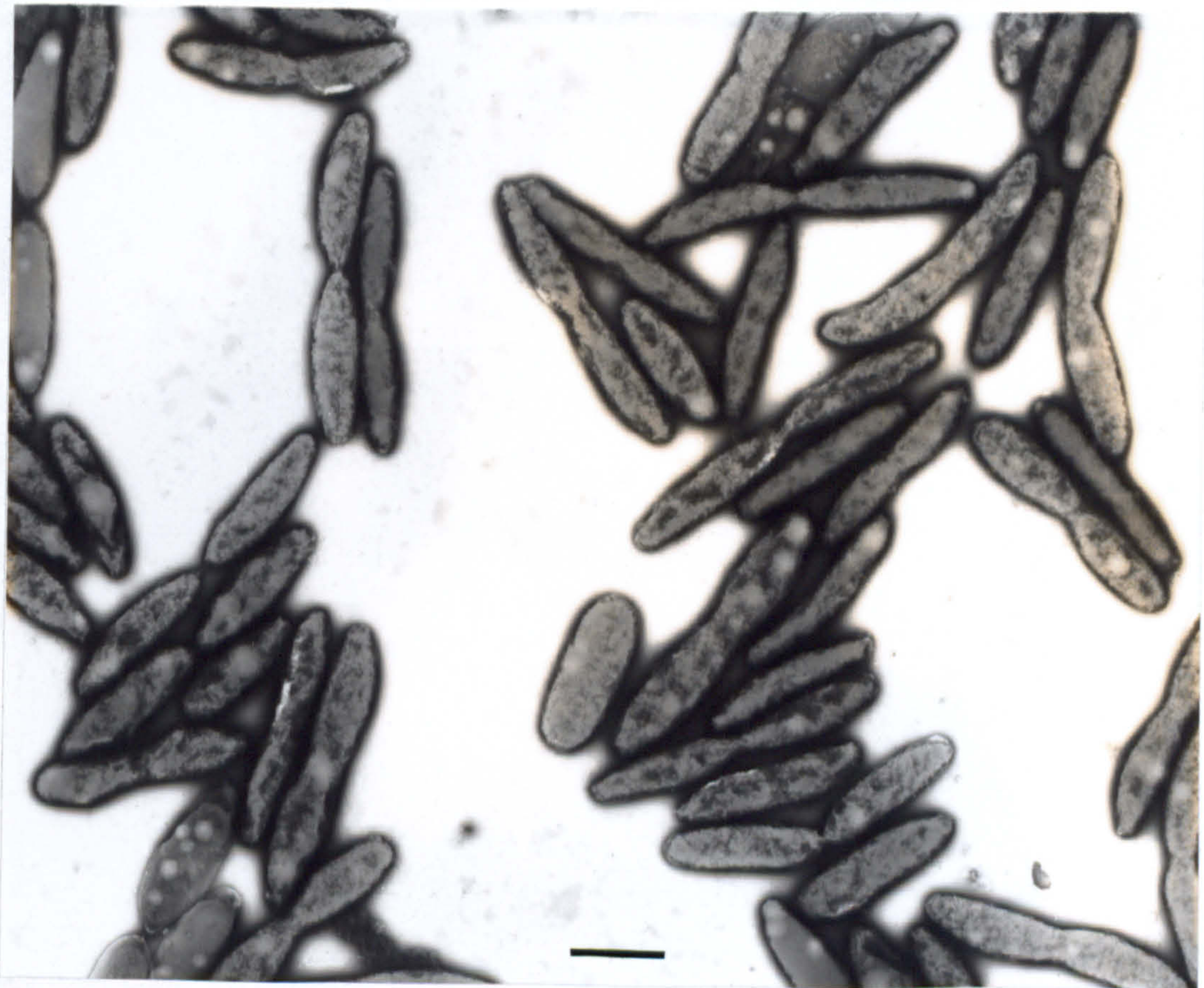
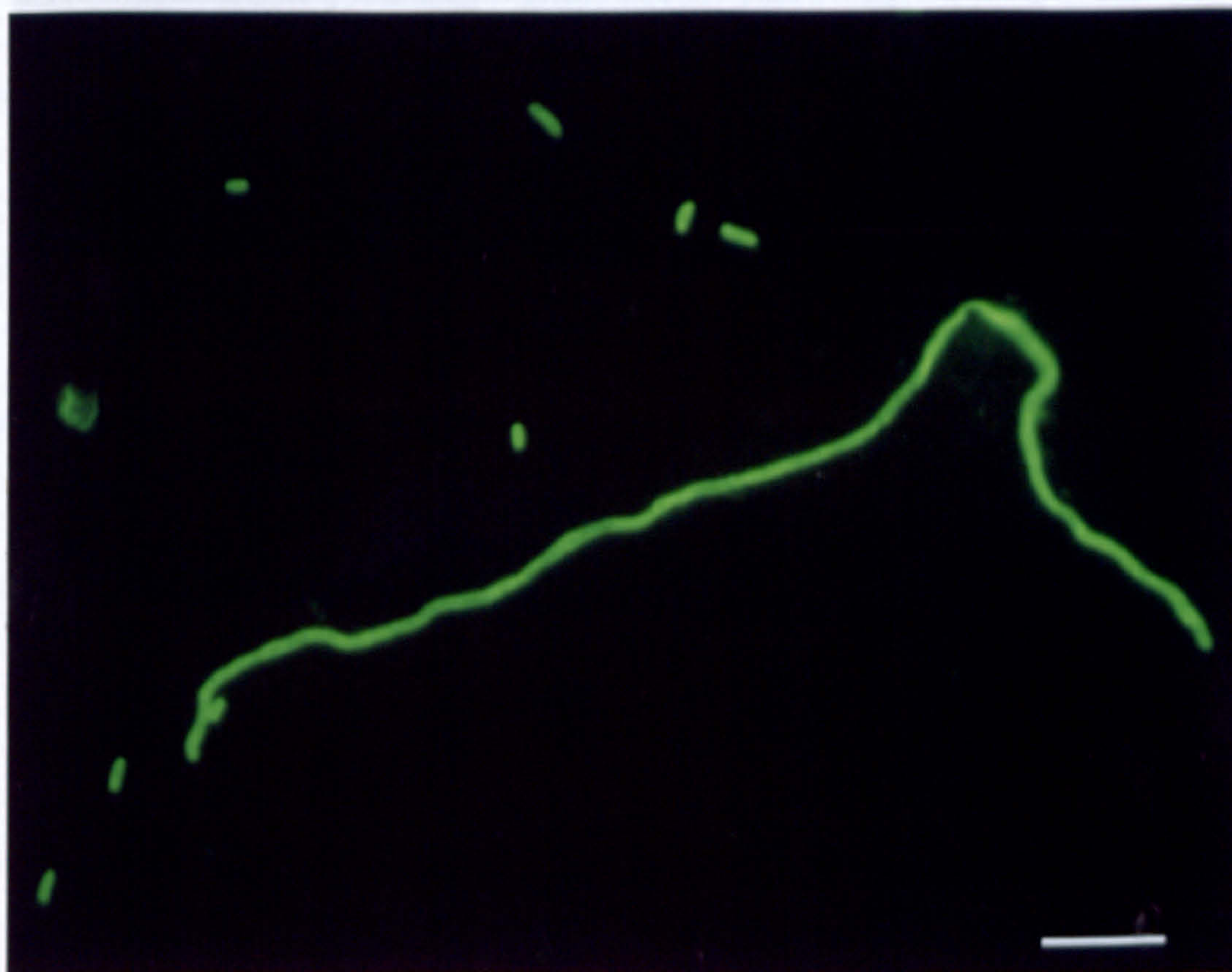


Figure 13. Transmission electron micrographs of chemostat cultures of *L. pneumophila*, (a) iron-replete cells; (b) iron-limited cells. Bar, 1 μm .

(a)



(b)

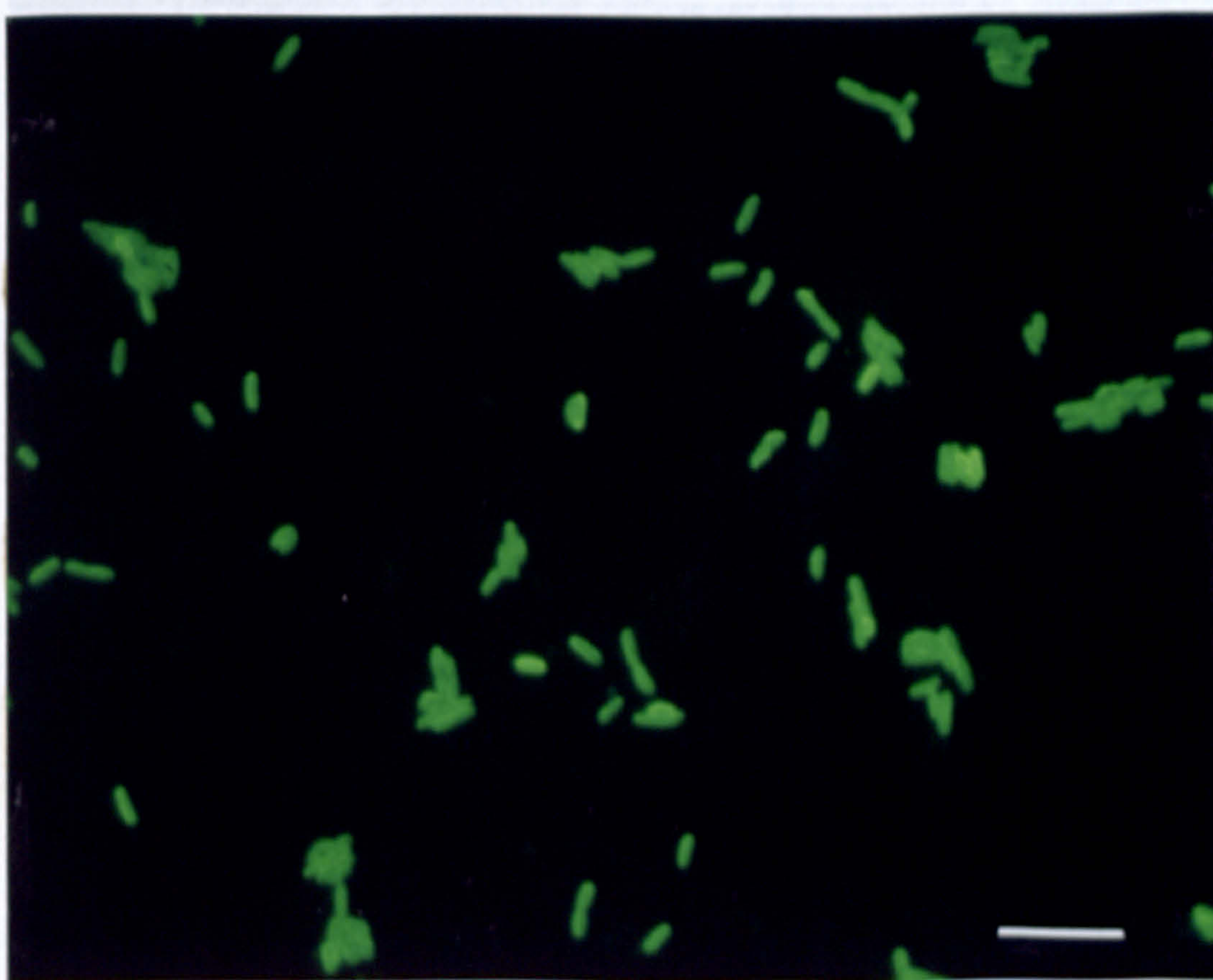
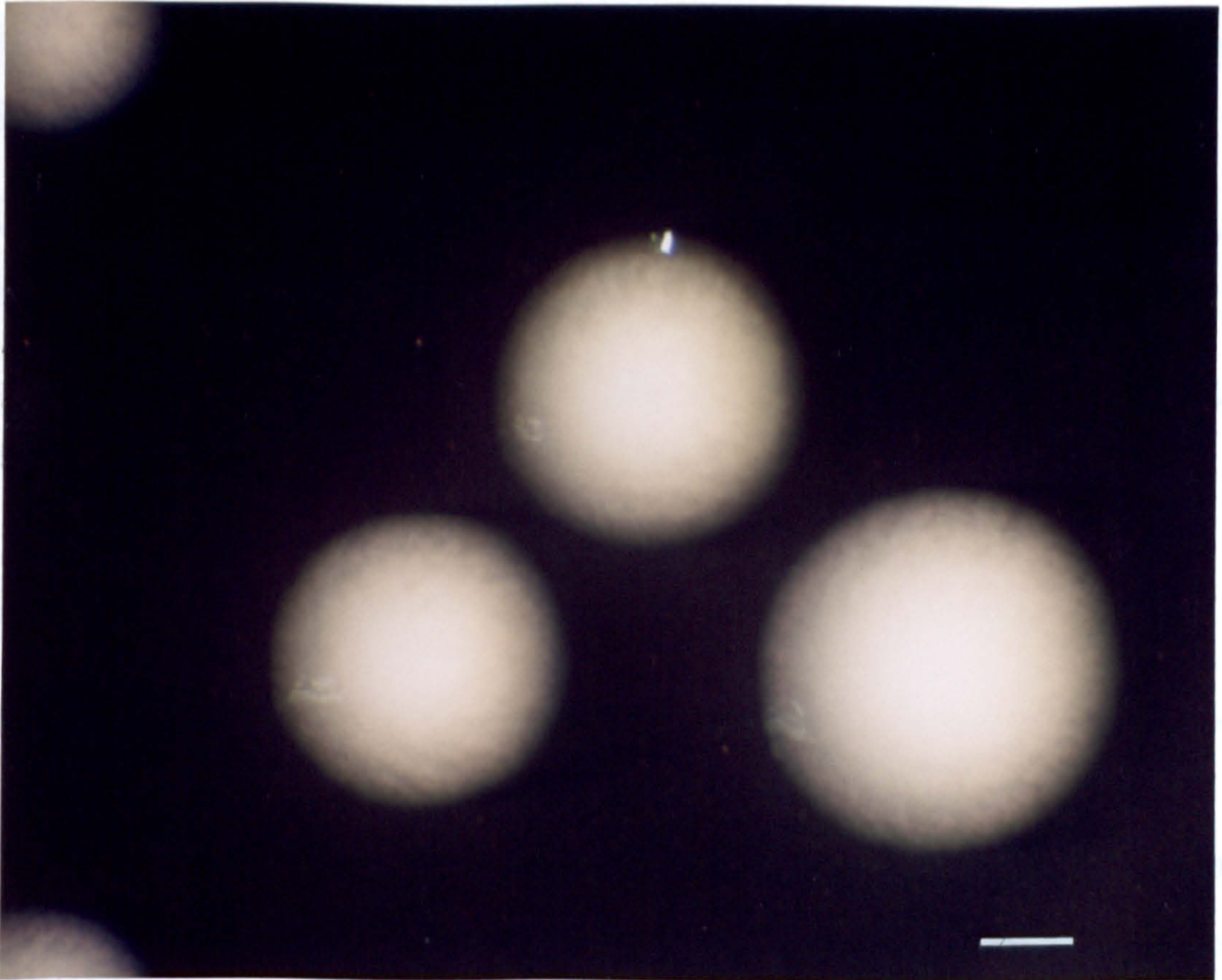


Figure 14. Indirect fluorescent antibody staining of *L. pneumophila* cultures with serogroup 1 specific polyclonal antiserum, (a) iron-replete cells; (b) iron-limited cells. Bar, 10 μm .

(a)



(b)

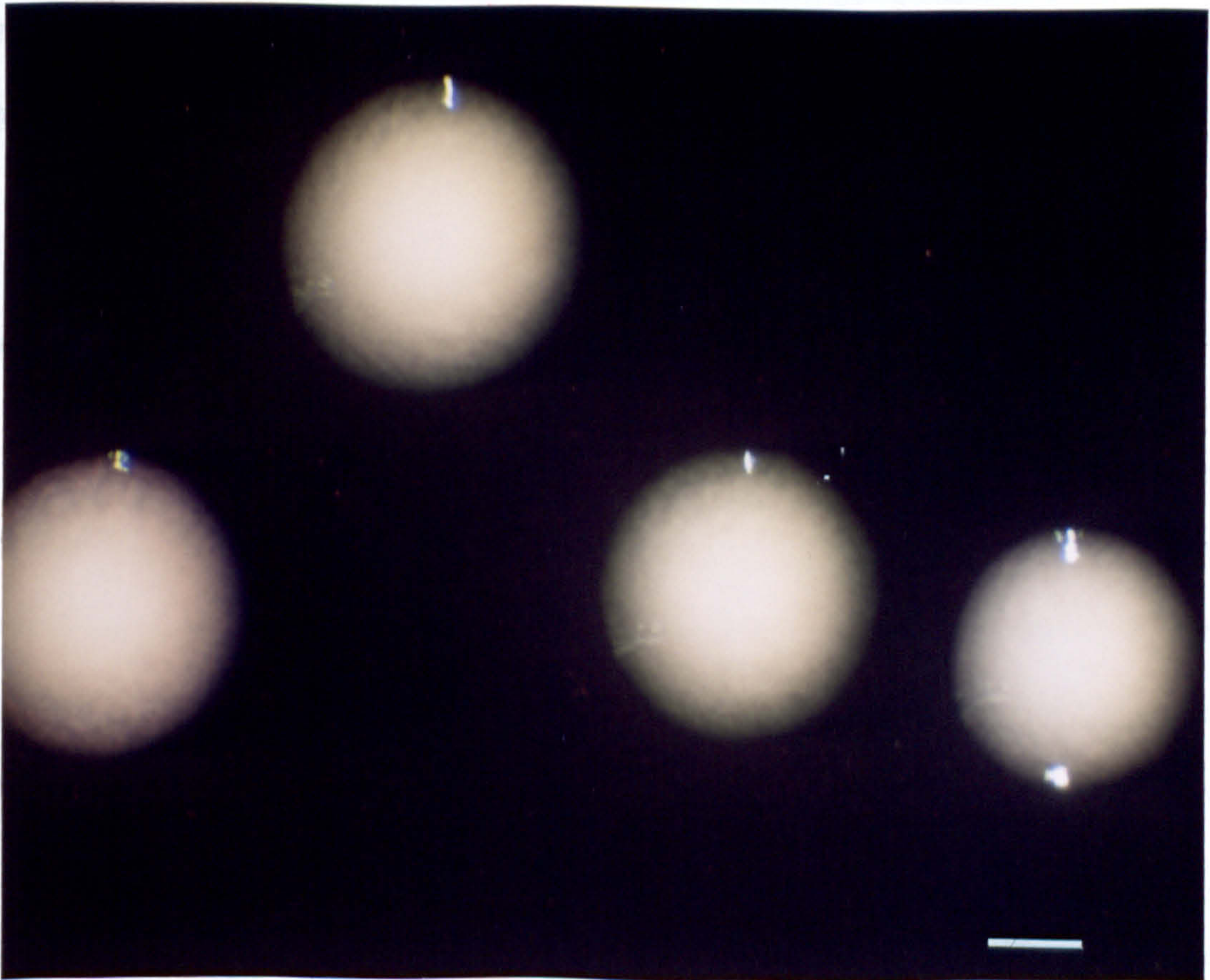


Figure 15. Colony morphology of *L. pneumophila* chemostat cultures, when grown on BCYE agar at 37°C for 3 days, (a) iron-replete; (b) iron-limited. Bar, 1 mm)

Table VII. Comparison of the extracellular protein content of iron-limited and -replete cultures^a.

Culture sample	Iron-replete ^b	Iron-limited ^c
Protein (μg ml ⁻¹ supernatant)	34.8 ± 2.6	17.6 ±2.4
Protein (μg mg ⁻¹ cell dry wt.)	24.0 ± 2.3	26.3 ± 3.2

^a For each sample, control reactions were prepared with samples of the corresponding uninoculated culture medium (Section 2.7). The absorbance of the control reaction was < 10% of the test reaction absorbance.

^b Values represent the mean of duplicate determinations on 7 samples ± s.e.m.

^c Values represent the mean of duplicate determinations on 14 samples ± s.e.m.

3.3.2 Separation of extracellular proteins by anion-exchange FPLC.

The protein content of iron-limited and -replete supernatants was separated and compared by FPLC (Section 2.9). The elution profiles for 3 different iron-replete and -limited samples were compared. Typical A₂₈₀ profiles are illustrated in Figure 16. Variation in the intensity of individual peaks was observed, both within as well as between the two sample groups. With iron-limited samples, four intense absorption peaks were consistently detected, which eluted at salt concentrations of approximately 0.12, 0.18, 0.2 and 0.25 M. Among iron-replete culture supernatants, the two most intense peaks, eluted at 0.2 and 0.25 M NaCl. Peaks eluting at 0.12 and 0.18 M NaCl appeared to be the most significantly enhanced by iron limitation (Figure 16).

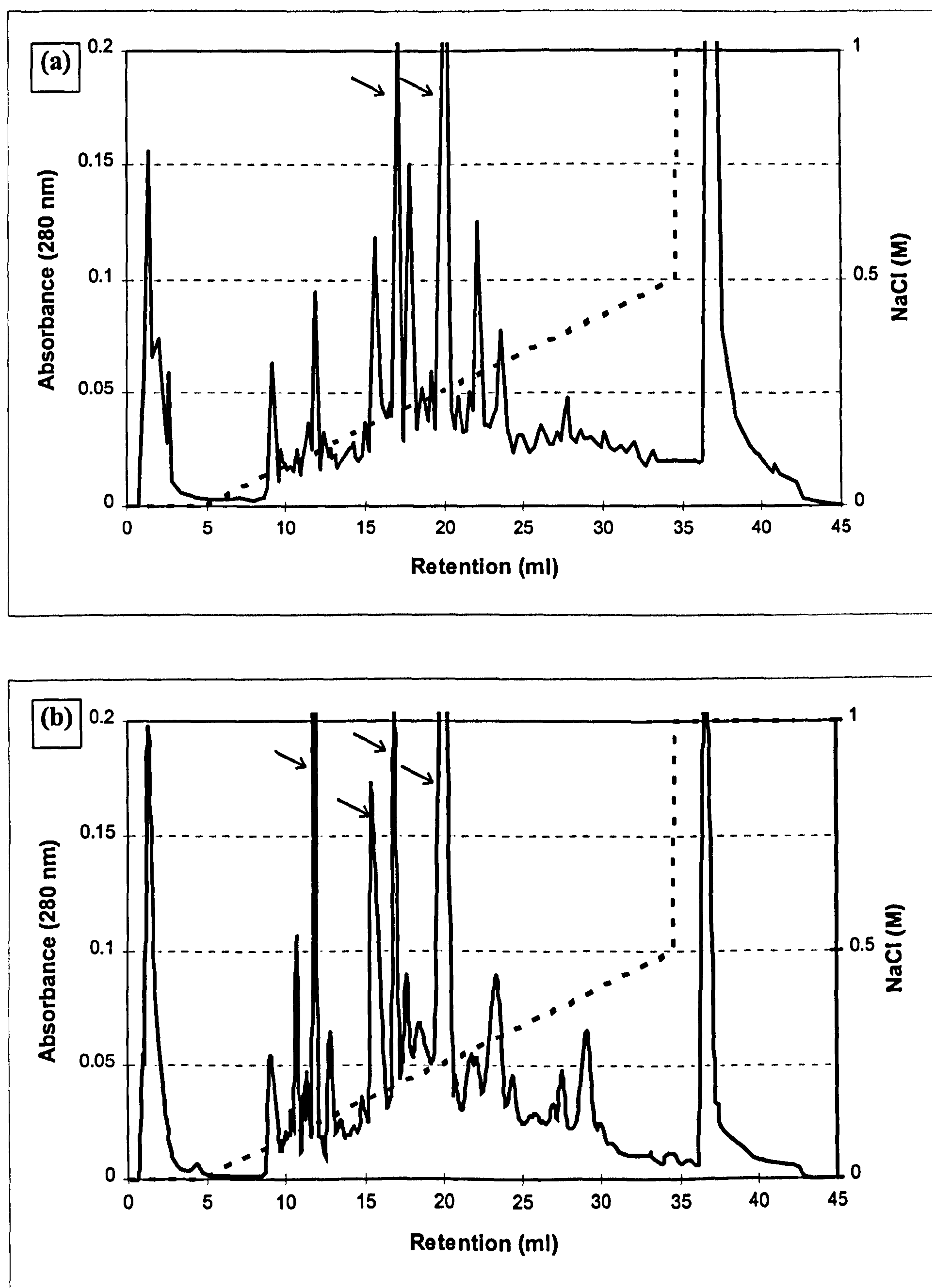


Figure 16. FPLC anion exchange elution profiles of *L. pneumophila* culture supernatants, (a) iron-replete; (b) iron-limited. Dotted line indicates NaCl gradient.

3.3.3 SDS-PAGE of FPLC fractions.

A number of fractions from both iron-limited and -replete samples were compared by SDS-PAGE with silver staining. There was insufficient protein in many of the fractions to allow band detection. However, the iron-limited fractions corresponding to 0.12 and 0.18 M NaCl were found to possess 17 and 52 kDa protein bands, respectively (Figure 17). A minor protein band migrating at 36 kDa were also detected in the iron-limited fraction eluting at 0.2 M NaCl. The corresponding iron-replete fractions did not yield detectable protein bands.

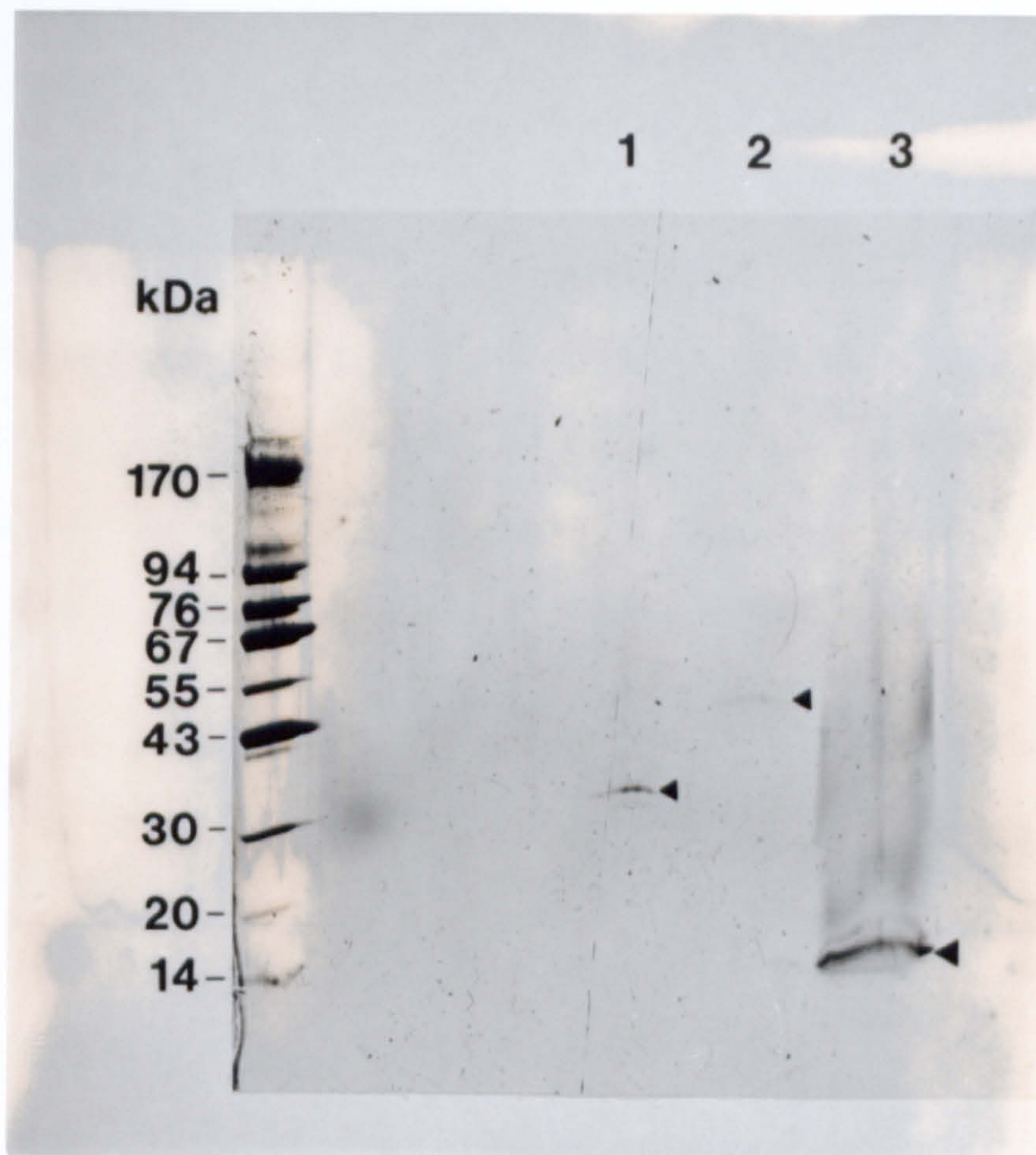


Figure 17. Silver stained SDS-PAGE of FPLC fractions. Lane 1, 2 & 3, represent 0.2, 0.18 and 0.12 M NaCl fractions from iron-limited supernatant, respectively.

3.3.4 Zinc metalloprotease activity of iron-limited and -replete supernatants.

Expression of the extracellular zinc metalloprotease was investigated by measuring the azocasein hydrolytic activity of culture supernatants (Section 2.10.1). Azocasein hydrolysis which could be inhibited by EDTA, was detected in both iron-limited and -replete supernatants. Activity was related to culture biomass to allow for differences in culture density. Calculating the mean activity for 12 representative iron-limited and -replete samples, revealed a 5-fold reduction in hydrolytic activity in response to iron limitation (Table VIII).

Pre-incubation of iron-replete samples with either 1.0 or 10 mM EDTA for 30 min before analysis (Section 2.10.2), caused 95 % inhibition of azocasein hydrolysis. A similar treatment of iron-limited samples, only inhibited activity by approximately 70% (Table VIII). The addition of 1 mM zinc to the sample after pre-incubation with 1.0 mM EDTA (Section 2.10.3), stimulated a 60% recovery in the activity of iron-replete samples, and complete recovery of iron-limited sample activity. Additional control reactions prepared with 1.0 mM zinc in the absence of chelator, demonstrated that the presence of 1.0 mM zinc caused 40% inhibition of the hydrolytic activity of iron-replete samples. No inhibition was observed with iron-limited samples (Table VIII).

For three representative iron-limited and -replete samples, control reactions were also prepared containing anti zinc-metalloprotease IgG, at a titre sufficient to inhibit the casein precipitating activity of the samples (Section 2.10.4). The hydrolytic activity of iron-limited and -replete samples was inhibited by 83 and 90% respectively, in the presence of specific antibody (Table VIII). Additional control reactions containing anti-*L. pneumophila* serogroup antigen IgG, added instead of anti-zinc metalloprotease IgG at a comparable protein concentration, demonstrated no competitive inhibition of proteolytic activity by the presence of immunoglobulin protein (Table VIII).

Analysis of the data for 4 different iron-limited cultures, revealed a linear relationship between hydrolytic activity, and the concentration of growth-limiting nutrient metabolised (Figure 18). Furthermore, the addition of iron to a steady state iron-limited culture, stimulated an increase in hydrolytic activity (Figure 19).

Table VIII. Comparison of the azocasein hydrolytic activity of iron-limited and -replete *L. pneumophila* culture supernatants.

	Iron-replete	Iron-limited
Hydrolytic activity ^a	407 ± 28.4	78 ± 9.8
10 mM EDTA (% inhibition) ^b	95	65
1.0 mM EDTA (% inhibition) ^b	95	72
1.0 mM EDTA + 1.0 mM Zinc ^c (% inhibition)	38	0
1.0 mM Zinc (% inhibition) ^d	38	0
IgG anti-zinc metalloprotease ^b (% inhibition)	90	83
IgG anti- <i>L. pneumophila</i> LPS ^b (% inhibition)	0	0

^a Activity units are µg substrate hydrolysed h⁻¹ mg⁻¹ cell dry weight ± standard error of the mean. Activity was calculated using the extinction coefficient value of 3.4 for a 1% w/v solution of azodye, at 450 nm (Section 2.10). Each value represents the mean for twelve samples.

^b Samples were incubated with either EDTA or antibody for 30 min before adding substrate (Section 2.10.2).

^c Samples were incubated in the presence of EDTA for 30 min before the addition of 1 mM zinc and substrate (Section 2.10.3).

^d Samples were incubated with 1 mM zinc for 30 min before adding substrate.

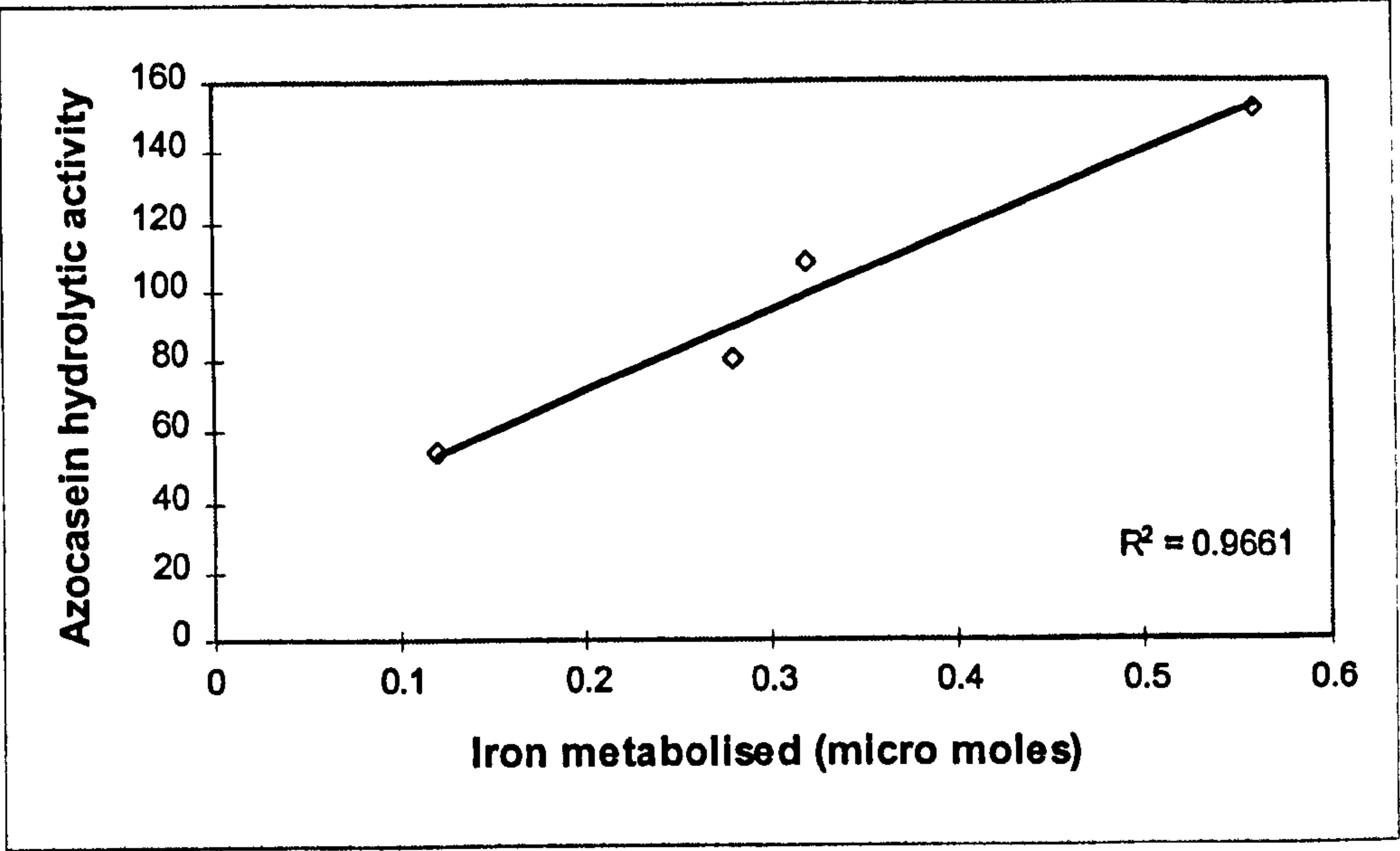


Figure 18. Relationship between the azocasein hydrolytic activity ($\mu\text{g h}^{-1} \text{mg}^{-1}$ dry wt.) of iron-limited cultures, and the concentration of iron metabolised.

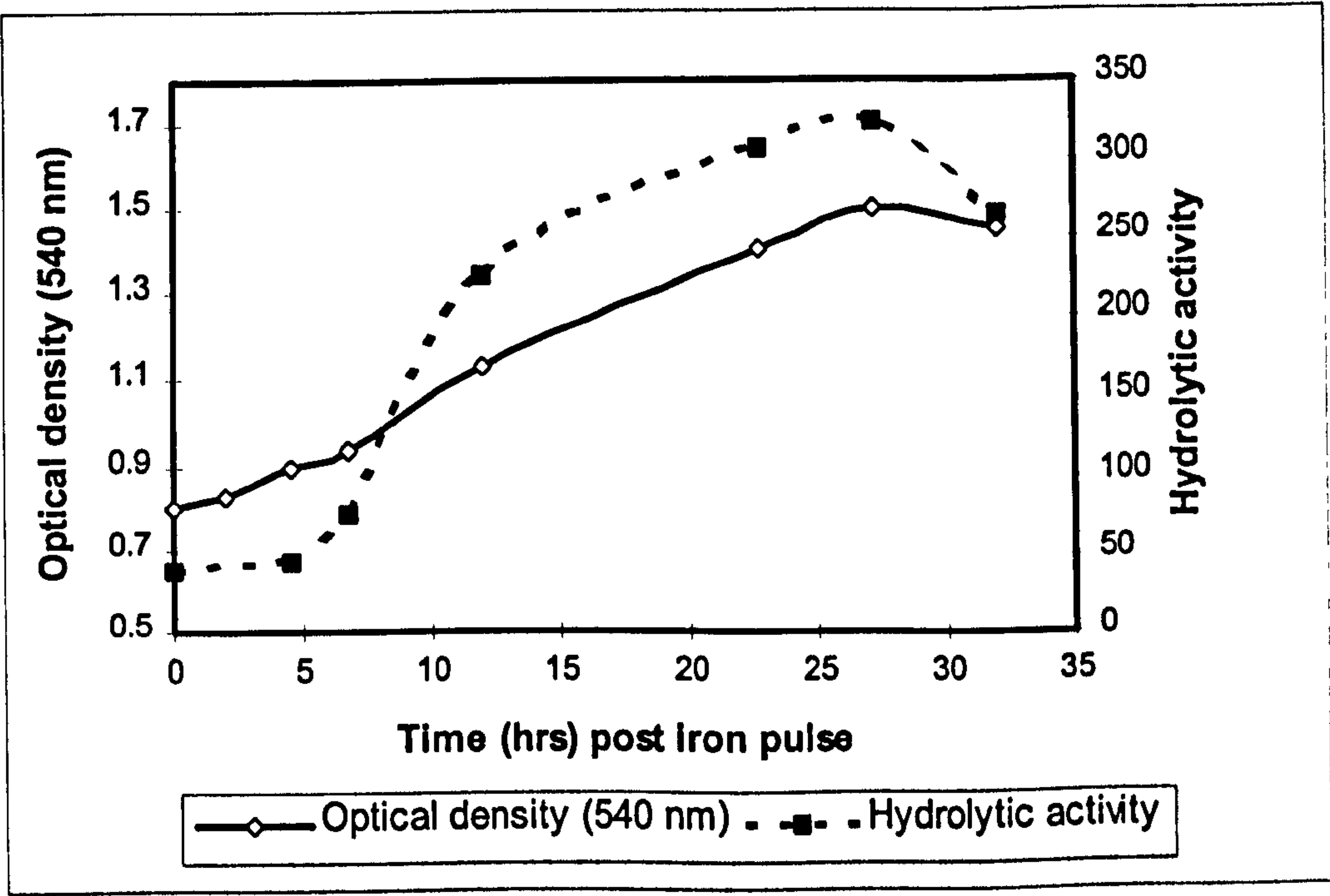


Figure 19. Increase in the azocasein hydrolytic activity ($\mu\text{g h}^{-1} \text{mg}^{-1}$ dry wt.) and the optical density of an iron-limited chemostat culture, in response to iron addition.

3.3.5 Phospholipase C activity of iron-limited and -replete cultures.

Iron-limited and -replete culture supernatant samples hydrolysed *p*-nitrophenylphosphorylcholine (Section 2.11). Results are expressed as nmoles *p*-nitrophenol released per mg cell dry weight, in 24h at 37°C. Initial assays with samples of culture supernatant indicated a 25% decrease in the extracellular activity of this enzyme under iron limitation (Table IX). However, analysis of supernatant samples concentrated 10-fold by pressure dialysis (Section 2.8), revealed no significant difference in the extracellular activity of iron-limited and -replete cultures, when corrected for differences in culture biomass yield and the concentration factor (Table IX). The enzyme activity determined from analysis of concentrated samples, was 2.5 to 4-fold higher than the activity recorded by analysis of unconcentrated samples. Analysis of washed cell suspensions also demonstrated the presence of cell associated phospholipase C activity (Section 2.11). Again, comparable activity was detected with both iron-limited and -replete cells (Table IX).

3.4 Iron Acquisition by *L. pneumophila*.

3.4.1 Ferric citrate reductase activity of iron-replete and -limited cultures.

Iron reductase activity was detected in the membrane, periplasmic and cytoplasmic fractions of both iron-limited and -replete cells (Section 2.14; Table X). With NADH as reductant, greatest activity was observed in the cytoplasmic and periplasmic fractions. The activity of the cytoplasmic fractions was comparable for both cultures. However, the activity of the periplasmic fraction was enhanced 1.7-fold, and the membrane activity was decreased by 50 %, in response to iron limitation (Table X). The activity of the different fractions was comparable to that reported by Johnson *et al.* (1991) with NADH as reductant.

Table IX. Hydrolysis of *p*-nitrophenylphosphorylcholine by iron-limited and -replete culture supernatant and cell samples.

Sample	Iron-replete (nmoles <i>p</i> -Nitrophenol)	Iron-limited (nmoles <i>p</i> -Nitrophenol)
Supernatant (neat) ^a	16.1 ± 1.1	12.1 ± 1.65
Supernatant (conc) ^b	42.1 ± 4.2	45.6 ± 3.4
Cell suspension ^c	75.5 ± 10.6	76.5 ± 9.5

^a nmoles *p*-nitrophenol liberated mg⁻¹ cell dry weight in 24 h at 37°C. Each value represents the mean of duplicate determinations for 5 different samples ± s.e.m.

^b nmoles *p*-nitrophenol liberated mg⁻¹ cell dry weight in 24 h at 37°C, based on the analysis of concentrated supernatants. Each value represents the mean of duplicate determinations for 3 different samples ± s.e.m.

^c nmoles *p*-nitrophenol liberated per unit^d of cells in 24 h at 37°C. Values represent the mean of duplicate determinations for 4 different samples ± s.e.m.

^d One unit of cells equals 1 ml of washed cells with an absorbance value of 1.0 at 590 nm.

With NADPH as reductant, the membrane activity was not significantly altered, and was comparable for both cultures (Table X). However, the periplasmic and cytoplasmic activity of both cultures was elevated 10 to 30-fold over the activity observed with NADH, and the results reported by Johnson and co-workers (1991). For both cultures, maximum activity was located in the cytoplasmic fraction and, indeed the cytoplasmic activity of both cultures was comparable. However, the activity of the iron-limited periplasmic fraction was decreased by 35% in comparison to the corresponding iron-replete fraction (Table X).

Table X. Comparison of the specific ferric citrate reductase activity^a of cell fractions from iron-limited and -replete *L. pneumophila*, with NADH or NADPH as reductant.

	NADH		NADPH	
Cell fraction	Iron-replete	Iron-limited	Iron-replete	Iron-limited
Membrane	12.6 ± 3.5	6.1 ± 1.1	10.7 ± 1.9	11.5 ± 1.8
Periplasm	17.1 ± 3.4	28.8 ± 3.5	460 ± 35.0	300 ± 38.2
Cytoplasm	19.0 ± 0.9	22.5 ± 2.9	532 ± 42.4	494 ± 18.9

^a specific activity equals nmoles Fe²⁺ formed per mg protein in 30 minutes at 24°C.

Each value represents the mean of duplicate analysis on three separate samples ± s.e.m.

3.4.2 Growth response of iron-limited cultures to human transferrin.

Iron-saturated human transferrin (Hu-Tf) was added directly to a steady state iron-limited chemostat culture, to provide an increased iron concentration of $2.5 \mu\text{M}$ (Section 2.12.2). After 5 to 6 hours a slow exponential increase in culture turbidity was detected, which resulted in a 2-fold increase in culture turbidity after 30 hours (Figure 20). Pulsing the steady state iron-limited culture with a comparable concentration of iron in the form of ferrous sulphate, produced a detectable growth response within 2 h. However, the duration of the growth response and maximum culture turbidity achieved was comparable for both iron sources (Figure 20).

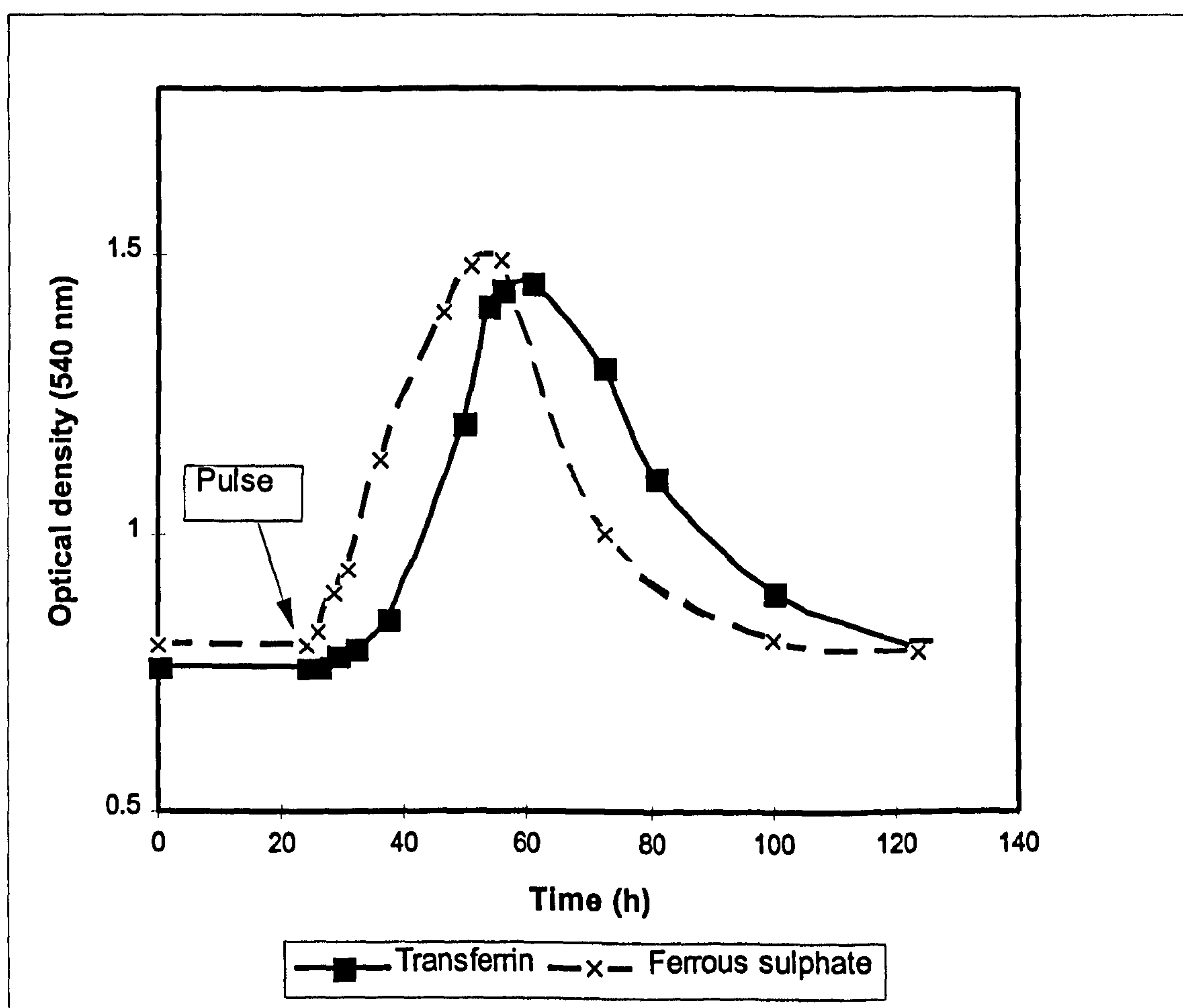


Figure 20. Growth response of a steady state iron-limited chemostat culture to $2.5 \mu\text{M}$ iron, supplied as human diferric-transferrin or ferrous sulphate.

3.4.3 Surface associated transferrin receptors.

Iron-limited and -replete cells were assayed for the presence of surface associated Hu-Tf receptors, by their ability to bind Hu-Tf conjugated with horse radish peroxidase (Section 2.12.3). This assay failed to detect the expression of surface receptors by either iron-limited or -replete cells, or by iron-limited cells pulsed with Hu-Tf during growth (Figure 21). Positive controls prepared with *N. meningitidis* cultured in the presence of EDDA confirmed the ability of the assay to detect transferrin receptors. Negative controls were prepared with *N. meningitidis* cultured in the presence of iron.

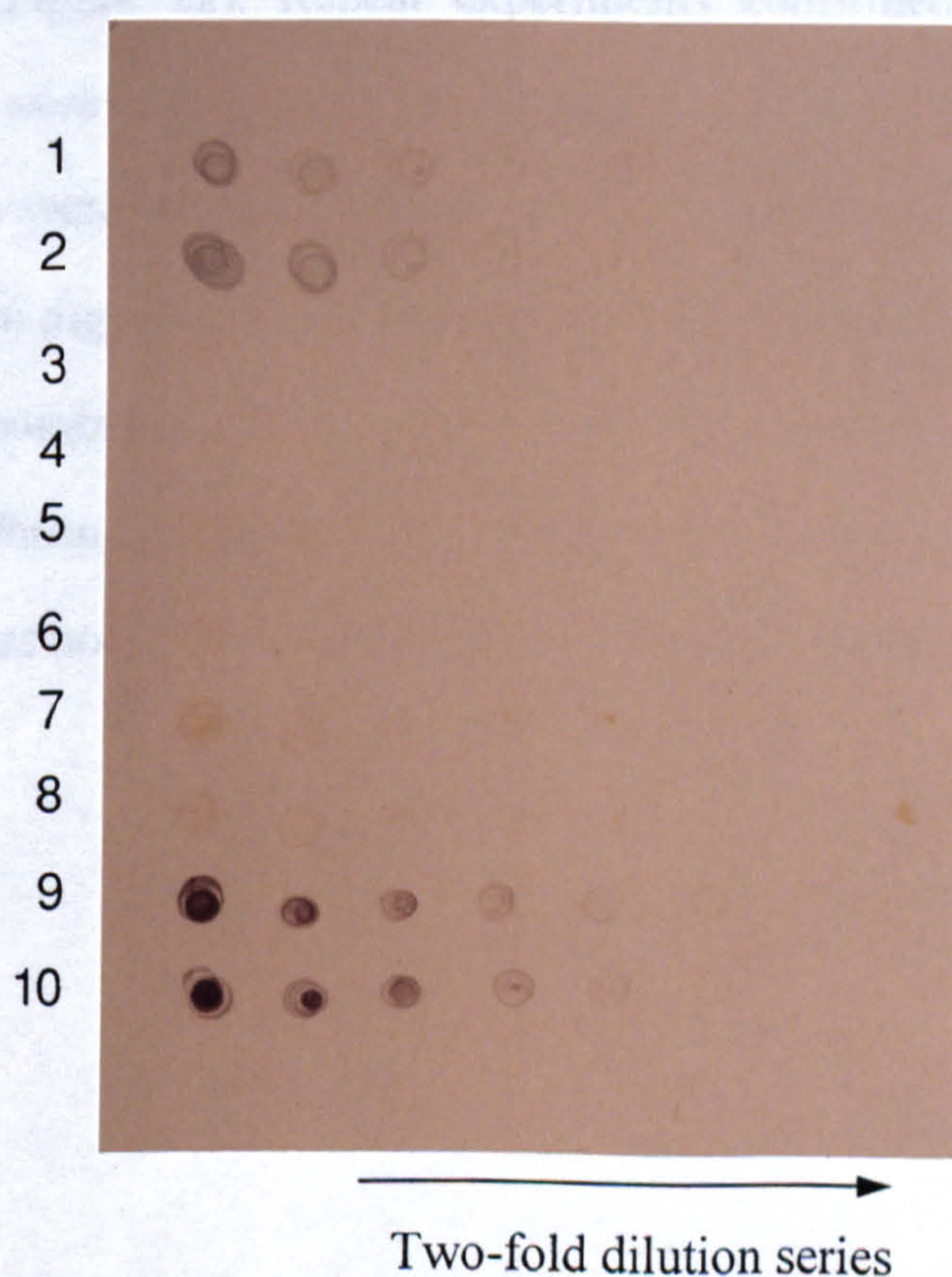


Figure 21. Analysis of *L. pneumophila* for the expression of human transferrin receptors. Rows 1 & 2, negative control, *N. meningitidis* with iron; rows 3 & 4, iron-replete *L. pneumophila*; rows 5 & 6, iron-limited *L. pneumophila*; rows 7 & 8, iron-limited *L. pneumophila* pulsed with Hu-Tf during growth; rows 9 & 10, positive control, *N. meningitidis* with EDDA.

3.4.4 Transferrin digestion by *L. pneumophila* culture supernatants.

The interaction between *L. pneumophila* culture supernatants and Hu-Tf was investigated by incubating diferric Hu-Tf in filter sterilized culture supernatant (Section 2.12.4). SDS-PAGE analysis of samples removed at time intervals, revealed digestion of Hu-Tf (Figure 22). Digestion was visible after 4 hours, with the appearance of a small 8-10 kDa band, and a corresponding decrease in the size and intensity of the original transferrin band. By 8 h and more clearly after 24 h incubation, three low molecular weight fragments of approximately 8-10, 26 and 37 kDa, with a larger band at approximately 70 kDa, were detected (Figure 22).

Control reactions demonstrated that the ion chelator EDTA could inhibit digestion, suggesting that a metalloenzyme present in the culture supernatant was responsible (Figure 22). Repeat experiments confirmed that iron-limited culture supernatants were also capable of transferrin digestion, although the low molecular weight bands were not observed (Figure 23). Additional experiments demonstrated that transferrin digestion was independent of the transferrin being saturated with iron, with a comparable cleavage profile produced with apo-transferrin (Figure 24). Human-lactoferrin, an iron-binding glycoprotein sharing considerable homology with transferrin, was not cleaved under these conditions (Figure 25).

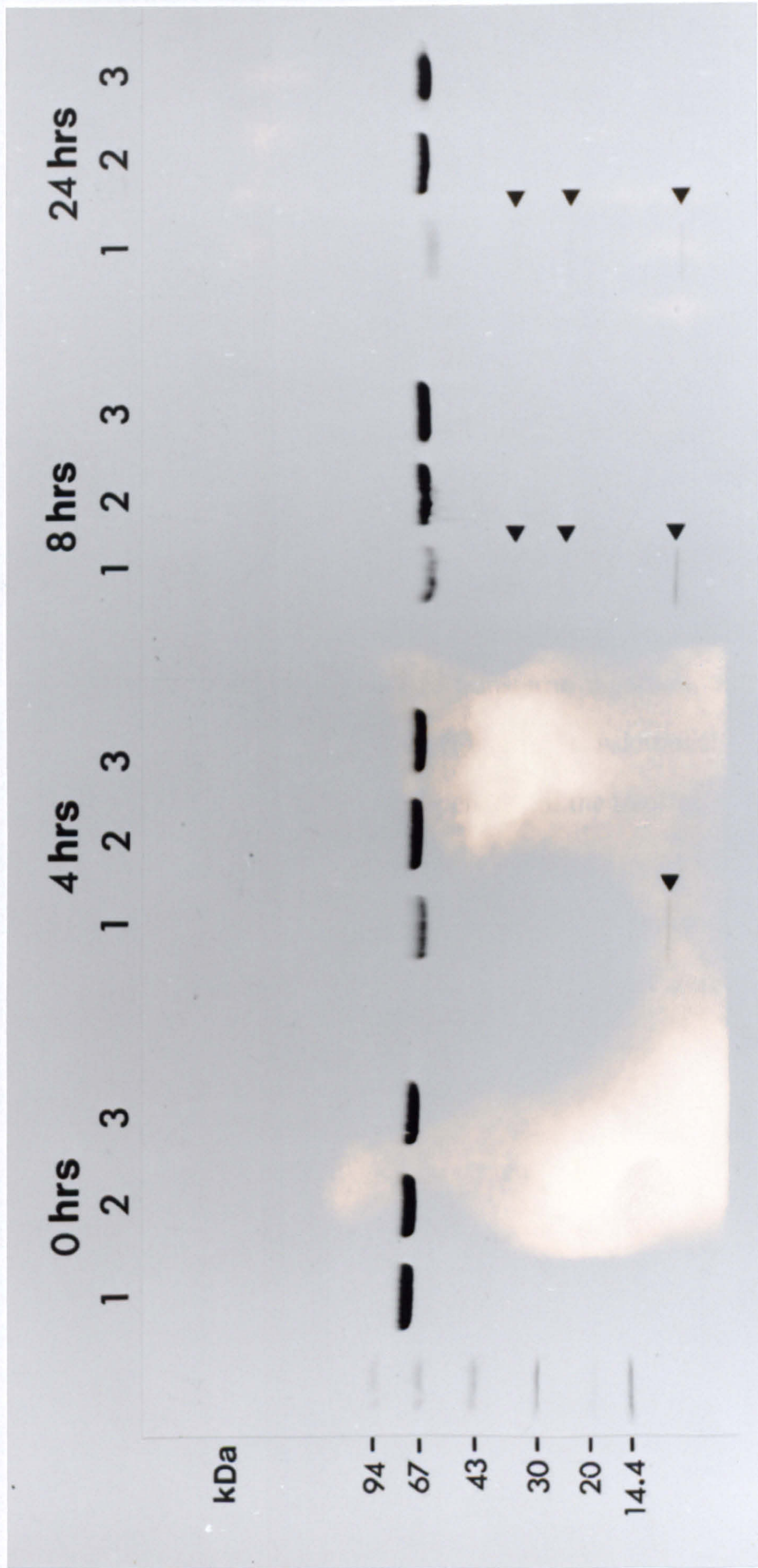


Figure 22. SDS-PAGE of iron-saturated human transferrin incubated in iron-replete culture supernatant and sampled at 0, 4, 8 and 24 hours. Lane 1, Hu-Tf incubated in culture supernatant (test reaction); lane 2, Hu-Tf incubated in supernatant containing 10 mM EDTA to inhibit metalloprotease activity; lane 3, Hu-Tf incubated in Tris buffer.

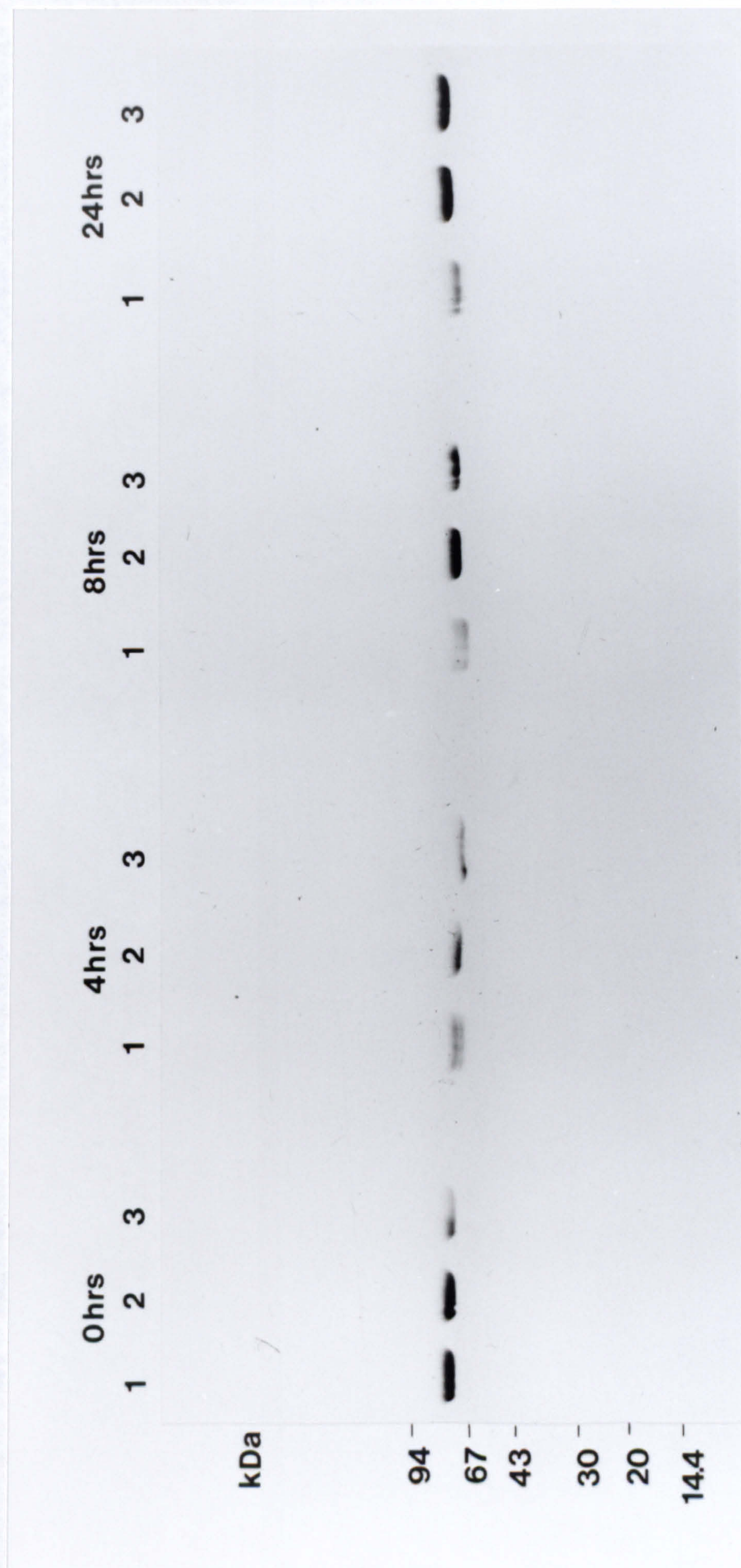


Figure 23. SDS-PAGE of iron-saturated human transferrin incubated in iron-limited culture supernatant and sampled at 0, 4, 8 and 24 hours. Lane 1, Hu-Tf incubated in culture supernatant (test reaction); lane 2, Hu-Tf incubated in supernatant containing 10 mM EDTA to inhibit metalloprotease activity; lane 3, Hu-Tf incubated in Tris buffer.

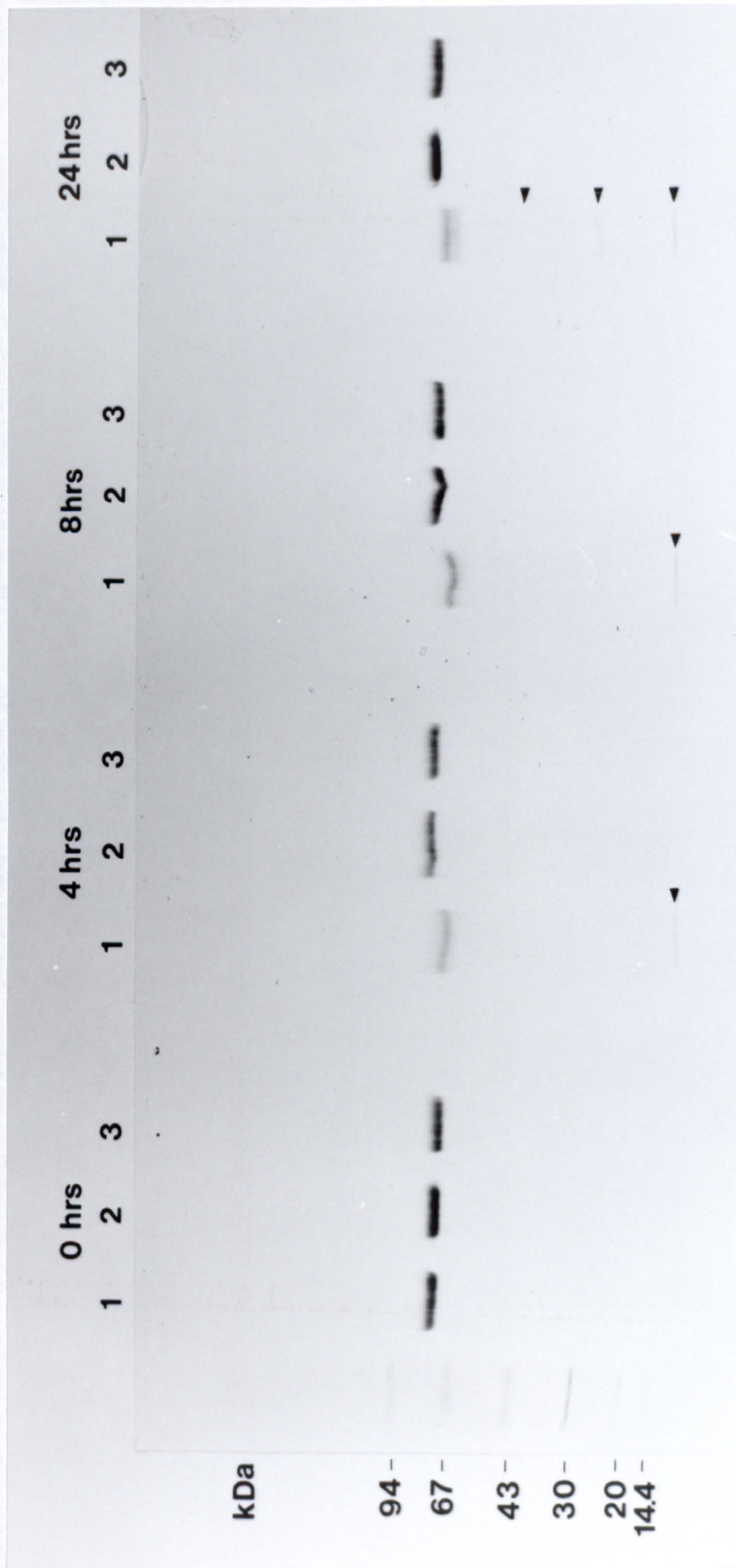


Figure 24. SDS-PAGE of iron-free human transferrin incubated in iron-replete culture supernatant and sampled at 0, 4, 8 and 24 hours. Lane 1, Hu-Tf incubated in culture supernatant (test reaction); lane 2, Hu-Tf incubated in supernatant containing 10 mM EDTA to inhibit metalloprotease activity; lane 3, Hu-Tf incubated in Tris buffer.

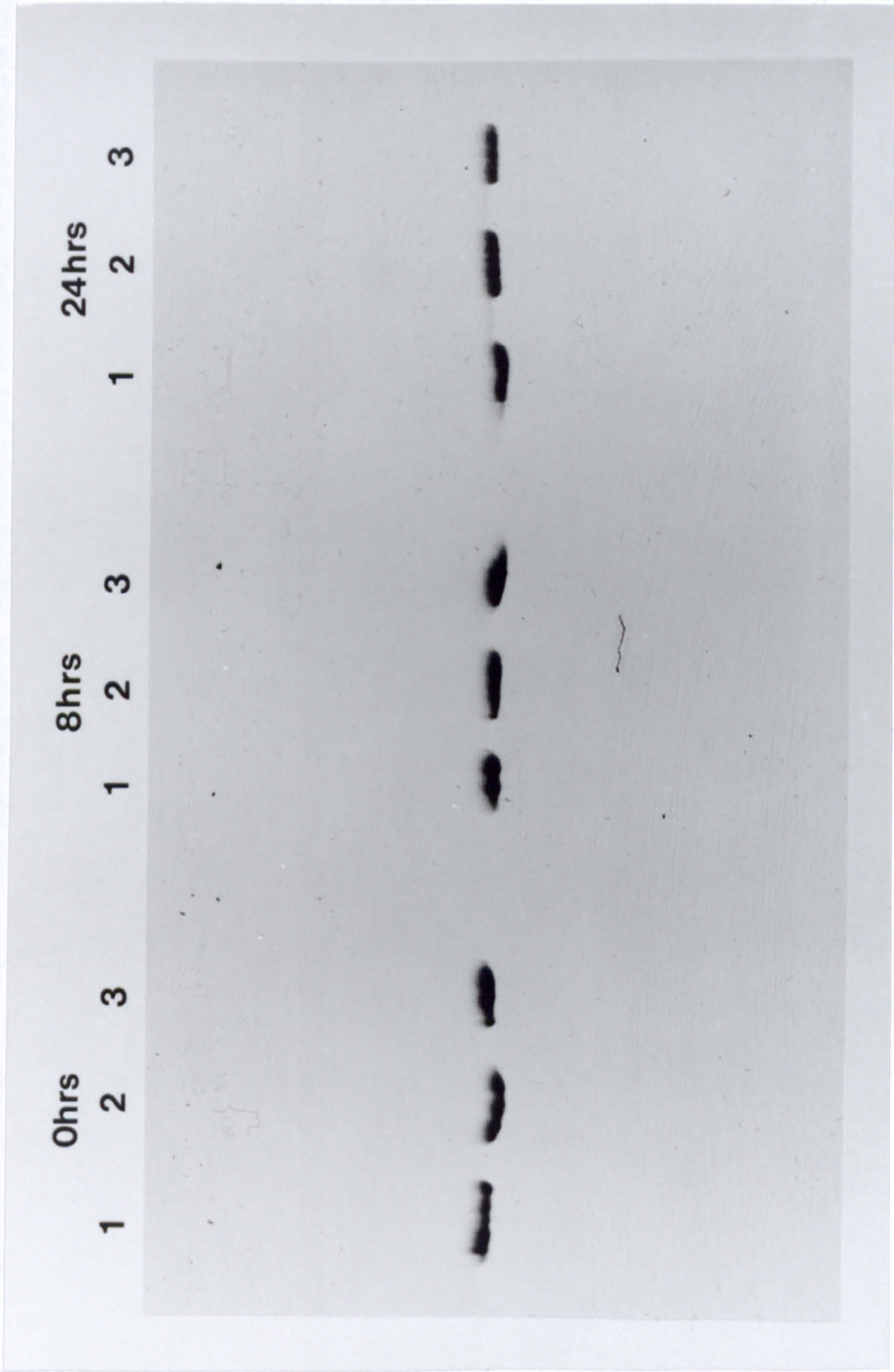


Figure 25. SDS-PAGE of human lactoferrin incubated in iron-replete culture supernatant and sampled at 4, 8 and 24 hours. Lane 1, lactoferrin incubated in culture supernatant (test reaction); lane 2, lactoferrin incubated in supernatant containing 10 mM EDTA to inhibit metalloprotease activity; lane 3, lactoferrin incubated in Tris buffer.

3.4.5 Zinc metalloprotease and transferrin digestion.

Additional experiments were conducted to investigate if the tissue destructive zinc metalloprotease was responsible for transferrin digestion. Polyclonal antiserum raised to purified *L. pneumophila* zinc metalloprotease was included in a control reaction (2.12.4). The concentration of polyclonal antiserum used was sufficient to inhibit the caseinase precipitating activity of the culture supernatant, as determined by the caseinase assay of Conlan *et al.* (1986), and described in Section (2.10.5). SDS-PAGE analysis of samples taken during the assay revealed a normal digestion profile in the test reaction (Figure 26). However, there was no evidence of transferrin digestion in the control reaction containing anti-metalloprotease serum, even after 24 h incubation (Figure 26). These observations provided additional evidence that the zinc metalloprotease is able to digest transferrin.

To confirm that serum proteins were not causing competitive inhibition of transferrin digestion, this control experiment was repeated with purified anti-zinc metalloprotease IgG (section 2.12.4). An additional control reaction was prepared containing anti-*L. pneumophila* serogroup antigen IgG, instead of anti-zinc metalloprotease IgG. Both antibodies were added at a comparable protein concentration. A normal digestion profile was observed in the test reaction, but digestion was completely inhibited in the control reaction prepared with IgG anti-zinc metalloprotease (Figure 27). Digestion was not inhibited by the presence of anti-*L. pneumophila* serogroup antigen IgG.

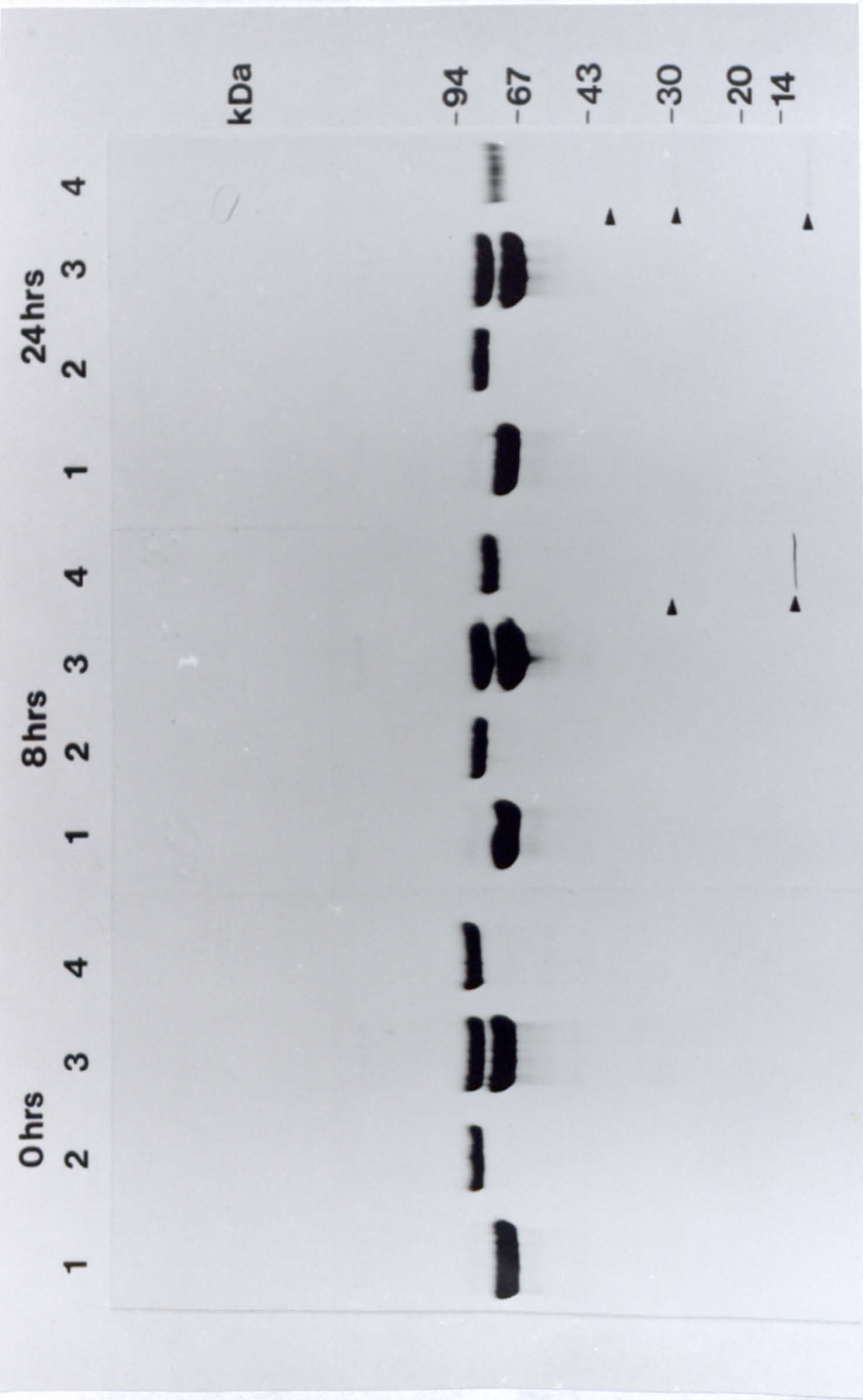


Figure 26. SDS-PAGE of human transferrin incubated in iron-replete supernatant, demonstrating inhibition of Hu-Tf digestion by anti-zinc metalloprotease antiserum. Lane 1, supernatant plus polyclonal antiserum control; lane 2, Hu-Tf incubated in culture supernatant with 10 mM EDTA; lane 3, Hu-Tf incubated in supernatant in the presence of anti-zinc metalloprotease antiserum; lane 4, Hu-Tf incubated in supernatant (test reaction). Samples were taken at 0, 8 and 24 hours.

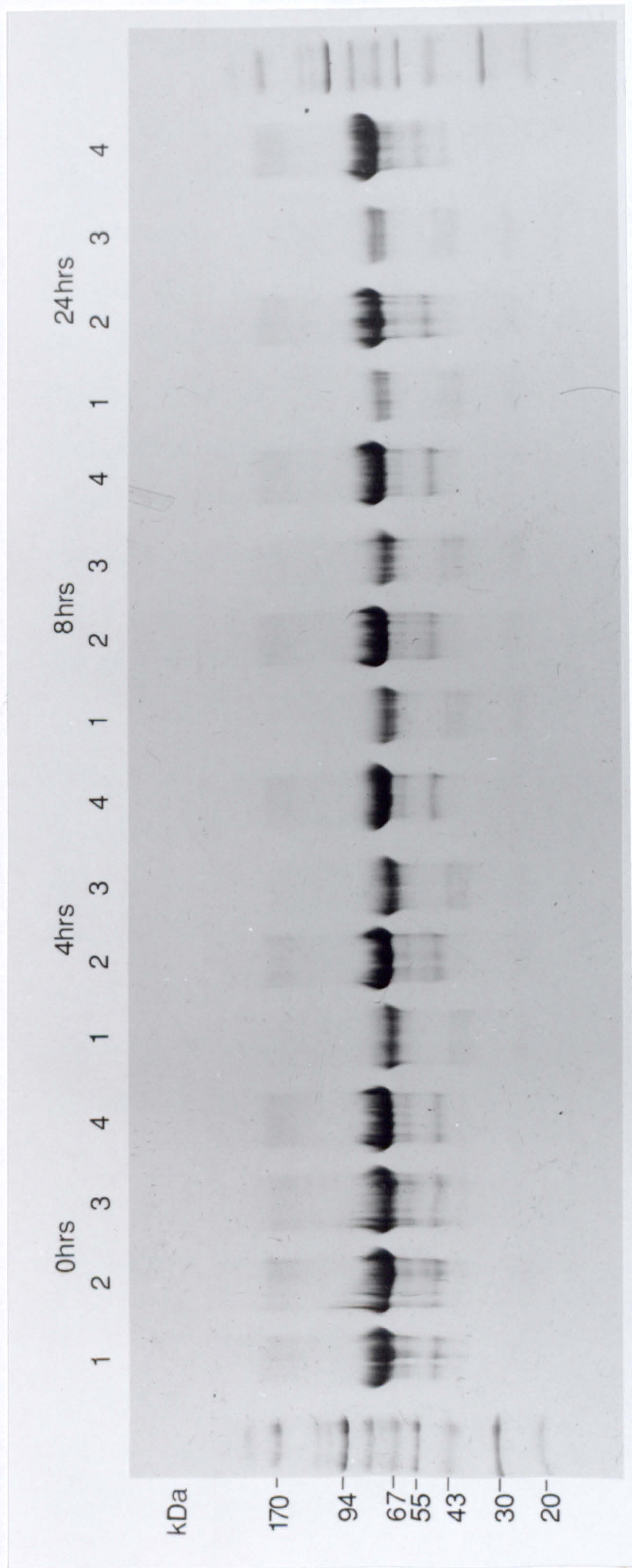


Figure 27. SDS-PAGE of human transferrin incubated in iron-replete supernatant, demonstrating inhibition of Hu-Tf digestion by anti-zinc metalloprotease IgG. Lane 1, Hu-Tf incubated in supernatant (test reaction), lane 2, Hu-Tf in supernatant in the presence of anti-zinc metalloprotease IgG; lane 3, Hu-Tf in supernatant in the presence of anti-serogroup antigen IgG; lane 4, Hu-Tf incubated in supernatant containing 10 mM EDTA. Samples were collected at 0, 4, 8 and 24 hours.

3.4.6 Universal siderophore assay.

The universal siderophore assay (Section 2.13.1) detected iron-sequestering activity in samples of iron-limited culture supernatant, by the colour transition from blue to orange, and a decrease in absorbance at 630 nm. However, control reactions prepared with samples of uninoculated culture medium, also produced a positive reaction. The final absorbance readings of the test reactions, were routinely ≤ 0.05 absorbance units less than that of the corresponding control. Absorbance readings were used to calculate absorbance/reference absorbance (A/A_{ref}) values for each sample. Using a calibration curve, prepared with desferroxamine standards (Section 2.13.1), it was estimated that the siderophore concentration of supernatants ranged from 5-10 μM desferroxamine equivalent. However, these results are based on minor differences in absorbance readings.

Desferroxamine standards (0.5 to 20 μM), prepared in uninoculated culture medium, were also assayed by this method. Figure 28 illustrates the resultant calibration curve for desferroxamine standards prepared in culture medium, along with a similar curve prepared in deionised water. A linear relationship was detected between siderophore concentration in deionised water, and absorbance. However, desferroxamine standards $\leq 7.5 \mu\text{M}$ were not detected when added to uninoculated culture medium. Desferroxamine concentrations between 10 to 20 μM produced a slight decrease in absorbance, which was ≤ 0.005 absorbance units.

3.4.7 Csaky assay for hydroxymates.

The Csaky (1948) assay failed to detect the presence of specific hydroxymate groups in culture supernatants, even after 4 h hydrolysis (Section 2.13.4). Supernatant samples concentrated 10-fold were also negative for the presence of hydroxymates. Positive reactions were obtained with desferroxamine controls.

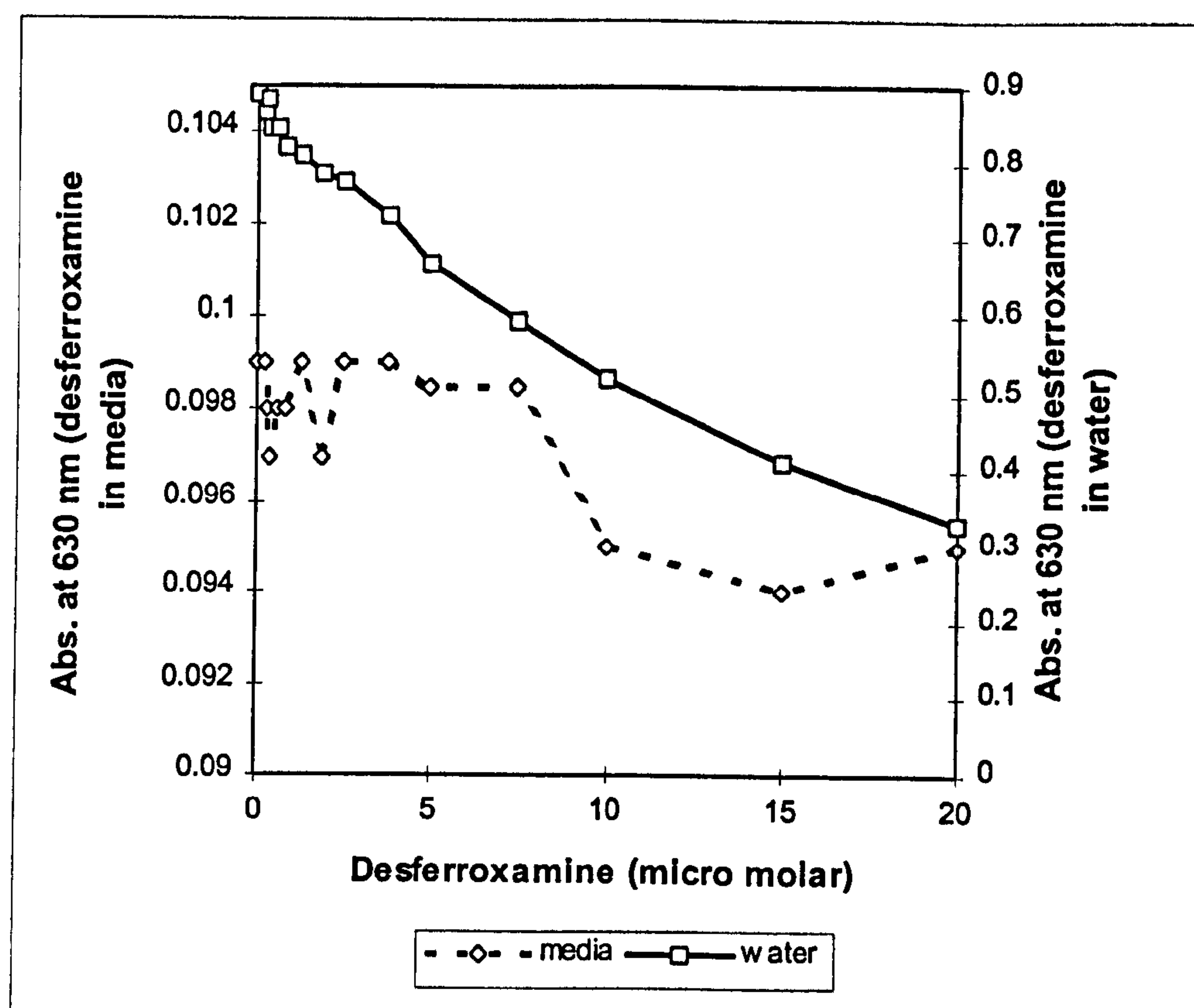


Figure 28. Comparison of desferroxamine standard calibration curves for the Universal siderophore assay, prepared in deionised water and uninoculated iron-limited ABCD culture medium.

3.4.8 Emery and Neilands assay for hydroxymates.

Culture supernatants were also assayed for hydroxymate type siderophores by the specific assay of Emery and Neilands (1960) (Section 2.13.3). Nitroso dimers formed by periodate oxidation, absorb strongly at 270 nm. Positive control reactions prepared with desferroxamine, produced a sharp absorption peak at 268 nm, with a smaller secondary peak at 210 nm (Figure 29a). Differential spectrophotometric analysis of reactions prepared with iron-limited supernatant, against control reactions prepared with uninoculated iron-limited culture medium, revealed the presence of two peaks at 235 and 284 nm (Figure 29b). Iron-replete supernatants failed to react with the assay. Furthermore, differential absorption spectra of iron-limited reactions recorded against reactions prepared with iron-replete supernatant, were comparable to those recorded against uninoculated iron-limited culture medium (Figure 29c).

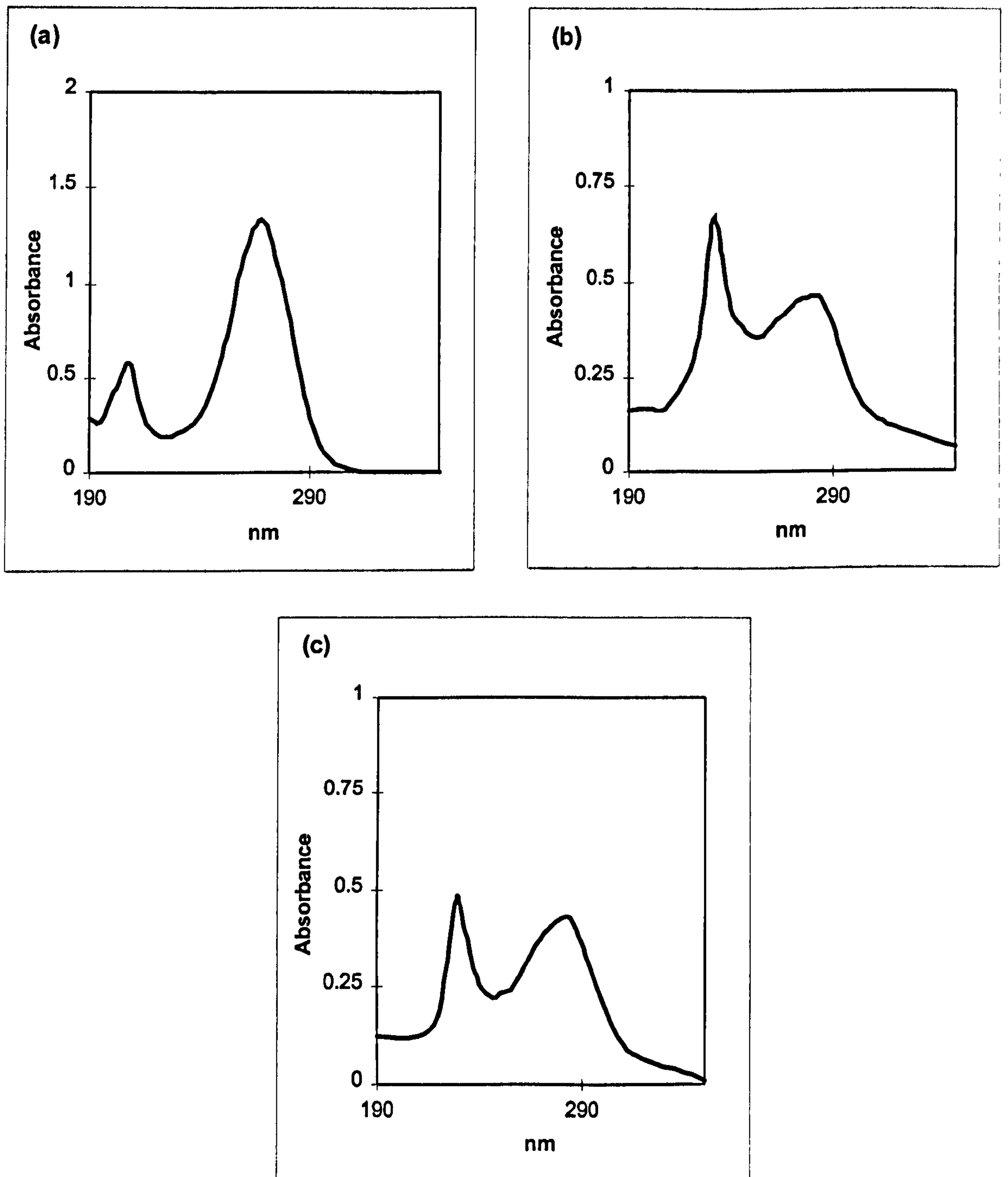


Figure 29. Differential absorption spectra of culture supernatant and standard samples following periodate oxidation, by the procedure of Emery & Neilands, (1960). (a) Desferroxamine (1.25 mM); (b) iron-limited supernatant recorded versus a control reaction prepared with iron-limited culture medium; (c) iron-limited supernatant scanned against a control reaction prepared with iron-replete supernatant.

3.4.9 Arnow assay for phenolate type siderophores.

Analyses of culture supernatants for the presence of phenolates by the assay of Arnow (1937) were also negative. Positive control reactions were prepared with a commercial preparation of catechol (Section 2.13.5).

3.4.10 Ferric chloride assay for iron-binding activity.

Iron-limited culture supernatants were also assayed for the presence of iron-chelating activity, by reaction with acidified ferric chloride (Section 2.13.2). The addition of acidified FeCl_3 to iron-limited supernatants produced a stable orange colour, indicative of a reaction with an iron chelator. However, uninoculated culture medium also produced a similar reaction, of lower intensity. Differential spectrophotometric analysis of the test reactions against the corresponding culture medium control reaction, revealed a broad asymmetric charge transfer band with λ_{max} at 470 nm (Figure 30a). Varying the proportion of supernatant in the final reaction (Section 2.13.2), revealed a linear relationship between sample volume and absorbance (Figure 31). However, iron-replete supernatant and control medium samples also yielded positive reactions, with a differential absorption peak detected at 490 to 495 nm (Figure 30b). Differential scanning of the iron-limited test reaction against the iron-replete test reaction, revealed a small asymmetric absorption band, λ_{max} at 465 nm in the iron-limited supernatant (Figure 30c). Control reactions prepared with desferroxamine produced an absorption band with λ_{max} at 521 nm (Figure 30d).

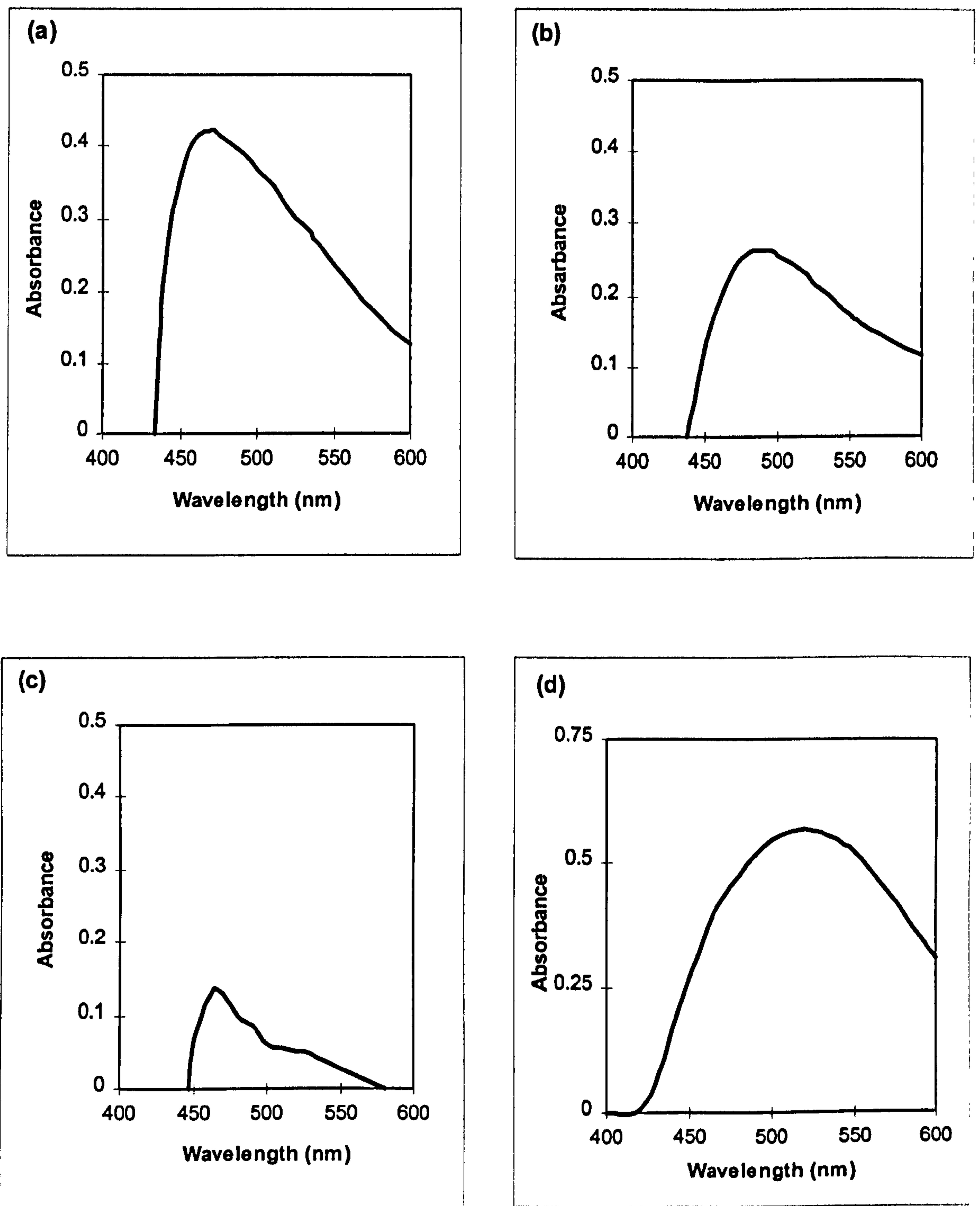


Figure 30. Differential absorption spectra of culture supernatant and standard samples reacted with acidified ferric chloride. (a) Iron-limited supernatant versus iron-limited control medium; (b) Iron-replete supernatant versus iron-replete control medium; (c) iron-limited culture supernatant versus iron-replete supernatant and (d) 2.5 mM desferrioxamine versus water control.

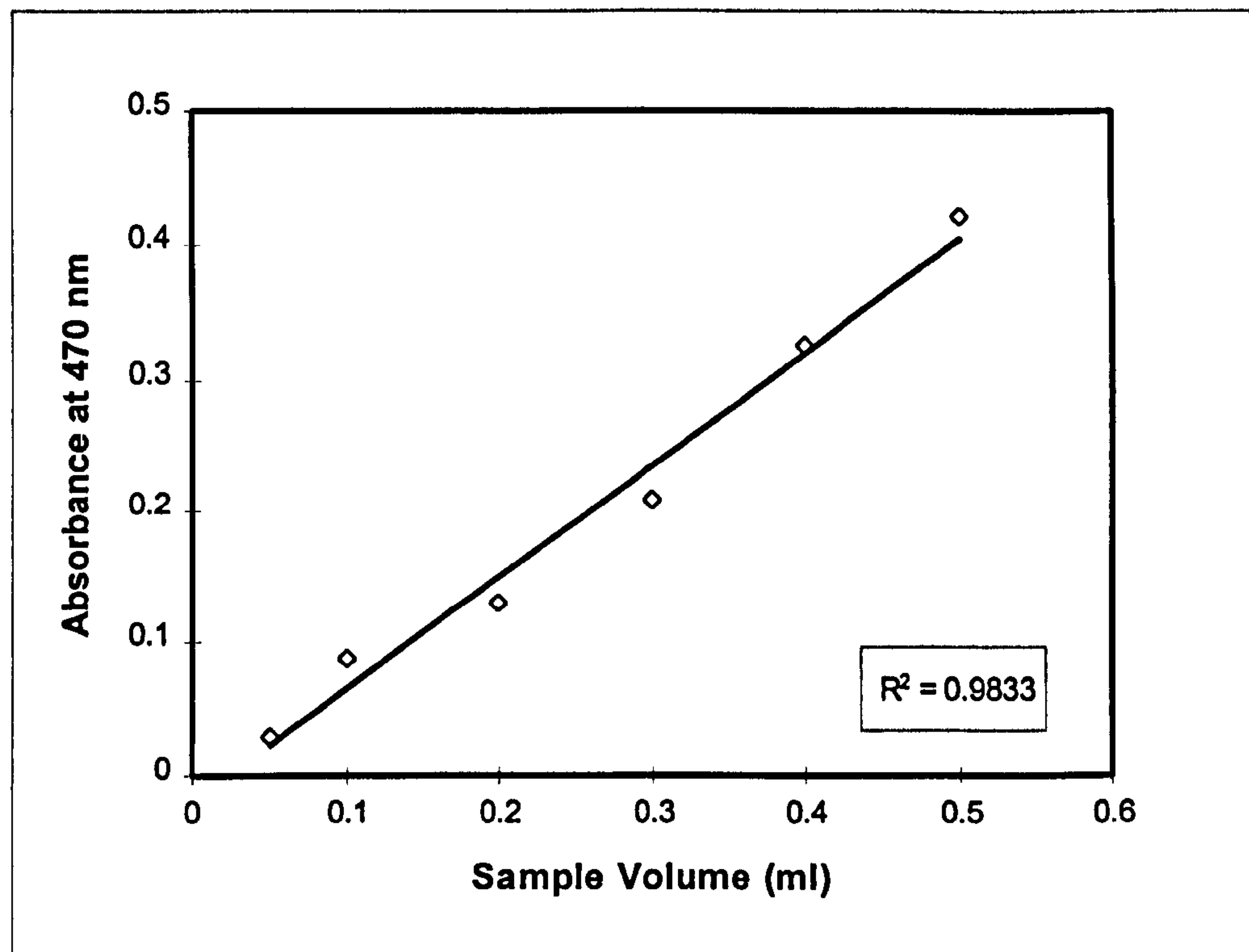


Figure 31. Relationship between sample volume and absorbance at 470 nm, following reaction with acidified ferric chloride.

Samples of iron-limited culture supernatant (0.05 to 0.5 ml) were reacted with 0.5 ml ferric chloride reagent in a final reaction volume of 1.0 ml, and the absorption profile recorded between 600 and 300 nm. Each reaction was recorded against a control reaction prepared with a comparable volume of un-inoculated culture medium and reagent (Section 2.13.2).

3.5 Influence of Iron Limitation on Membrane Lipid Composition.

3.5.1 Membrane fatty acid composition of iron-limited and -replete cells.

The fatty acid profile (Section 2.17) of iron-replete cells was comparable to those reported previously for *L. pneumophila* grown on BCYE agar and in continuous culture at 37°C (Moss *et al.*, 1977; Mauchline *et al.*, 1992). The profile was dominated by a high proportion of iso-branched fatty acids, principally 14-methyl pentadecanoic acid (i16:0). Unsaturated 9-hexadecenoic acid (16:1) was the second most abundant fatty acid (Table XI). Unbranched saturated fatty acids, hexadecanoic and dodecanoic (16:0 and 20:0), together with the anteiso-branched pentadecanoic and heptadecanoic (a15:0 and a17:0) acids, were also detected in significant proportions (Table XI).

Iron limitation promoted changes in the fatty acid profile. The proportions of the saturated iso-branched acids, i16:0 and i14:0, were significantly reduced. These changes were accompanied by an increase of the unbranched saturated 16:0, and the saturated ante-iso acids, a15:0 and a17:0. No change in the proportion of the principal unsaturated fatty acid, 16:1, occurred (Table XI).

Table XI. Influence of iron limitation on the membrane fatty acid composition (%) of *L. pneumophila* grown in chemostat culture.

Sample	i14:0	14:0	a15:0	15:0	i16:0	16:1	16:0	a17:0	17:0	18:0	20:0
Iron-replete ^a	6	1	10	1	29	22	11	4	1	3	6
Iron-limited ^a	2	2	13	1	14	22	23	9	1	5	4

^a Values for iron-limited and -replete samples, represent the mean determinations for 10 individual samples. Standard deviations are less than 15% of the means.

3.5.2 Membrane phospholipid composition of iron-limited and -replete cells.

The phospholipid profile of culture samples was recorded by positive ion fast atom bombardment mass-spectrometry (FAB-MS), (Sections 2.17.2 & 2.17.4). Representative spectra for iron-limited and -replete samples are shown in Figure 32. The mass of the protonated molecules $[M + H]^+$ produced, is diagnostic of the total number of carbon atoms, and the degree of unsaturation of the two fatty acyl groups esterified to the glycerol backbone. Signals in the region m/z 664 to 720 represent the protonated molecules of phosphatidylethanolamines, differing with respect to their fatty acyl substitution pattern, and the degree of methylation. Signals in the region m/z 746 to 788 represent the $[M + H]^+$ molecules of phosphatidylcholines. Figure 33 outlines the molecular structure of the principal phospholipid species present in *legionellae*.

Under iron-limited conditions, phospholipid signals in the region m/z 732 to m/z 762 were enhanced (Figure 34). These signals probably represent the principal phosphatidylethanolamine species, as well as some phosphatidylcholines. A number of other signals, particularly m/z 678 to 704 were also marginally increased (Figure 34). No significant decrease in the intensity of individual signals was observed.

Complementary information was provided by negative ion FAB-MS. This technique detects the deprotonated molecules $[M-H]^-$ of phosphatidylglycerols, which do not produce protonated molecules in the positive mode. Phosphatidylethanolamines will also be recorded. Representative spectra are illustrated in Figure 35. Iron limitation decreased the signals at m/z 705 and 707, which represent phosphatidylglycerols esterified with fatty acyl groups containing 31:1 and 31:0 carbon atoms, respectively. The annotation 31:1 and 31:0 indicates the combined total number of carbon atoms (31), and double bonds (1 or 0), for both fatty acyl groups. This change was compensated by a slight increase of signals m/z 719 to 735, representing phosphatidylglycerols esterified with 32 to 33 carbon atoms, respectively, between both fatty acyl groups (Figure 36).

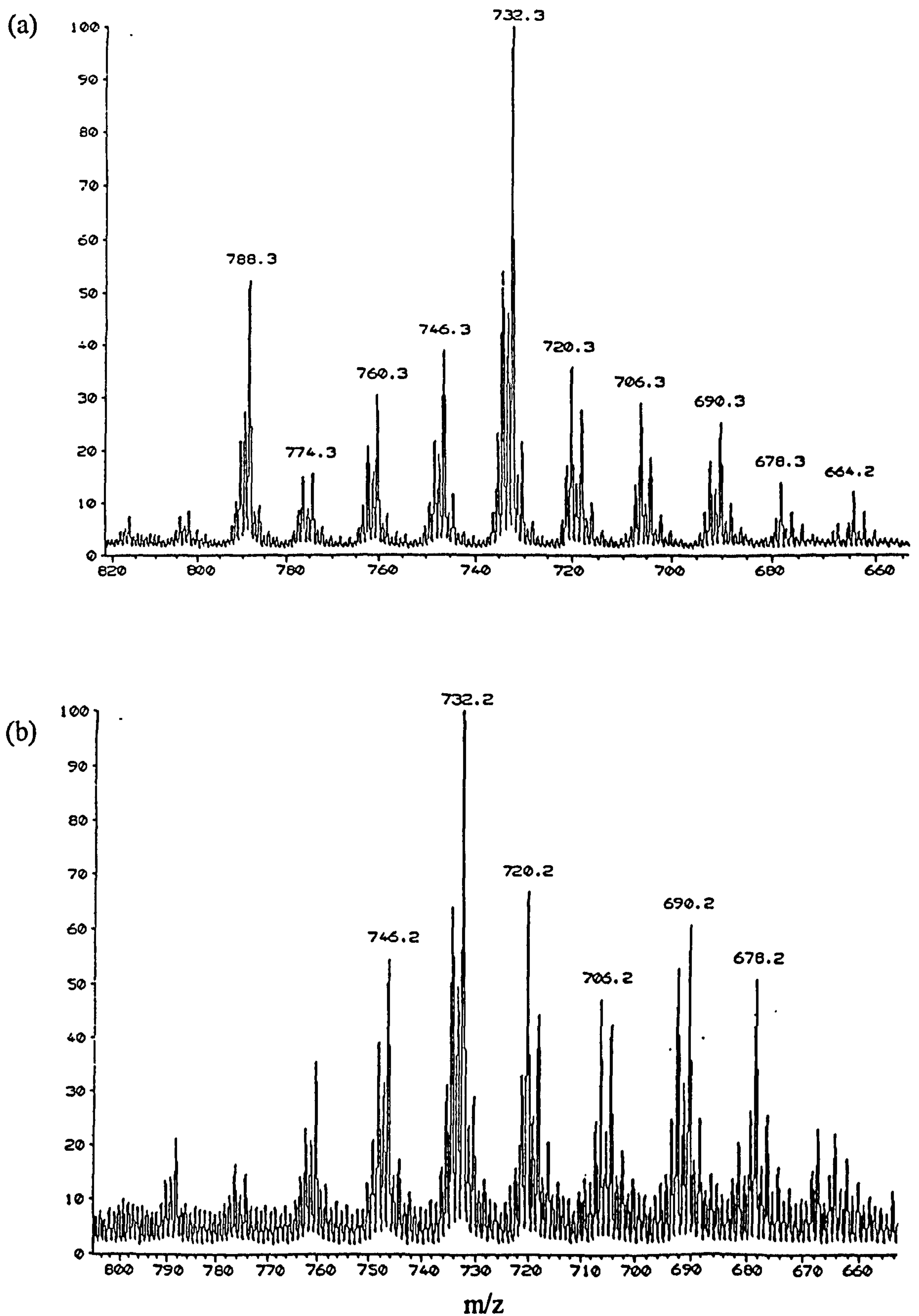
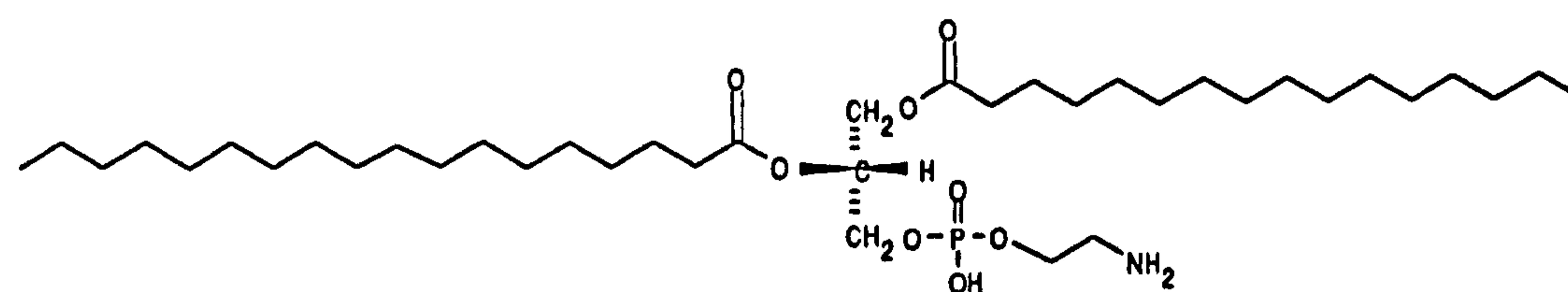
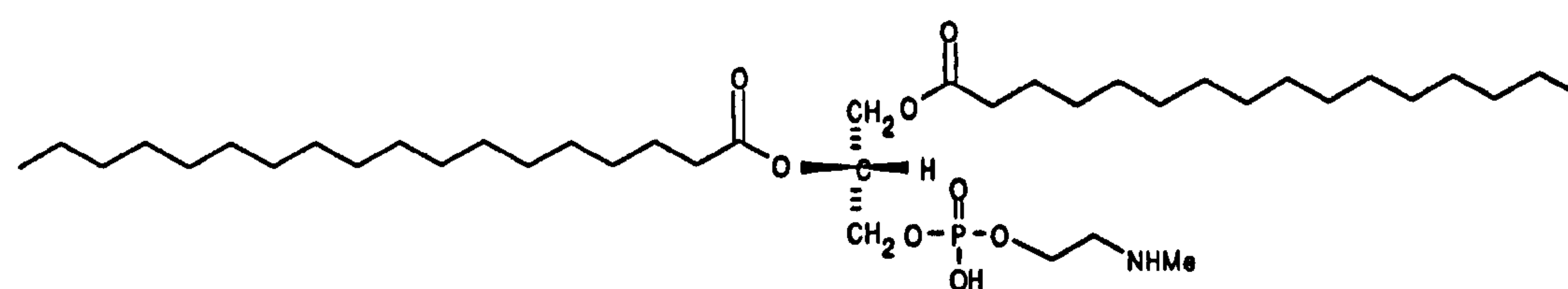


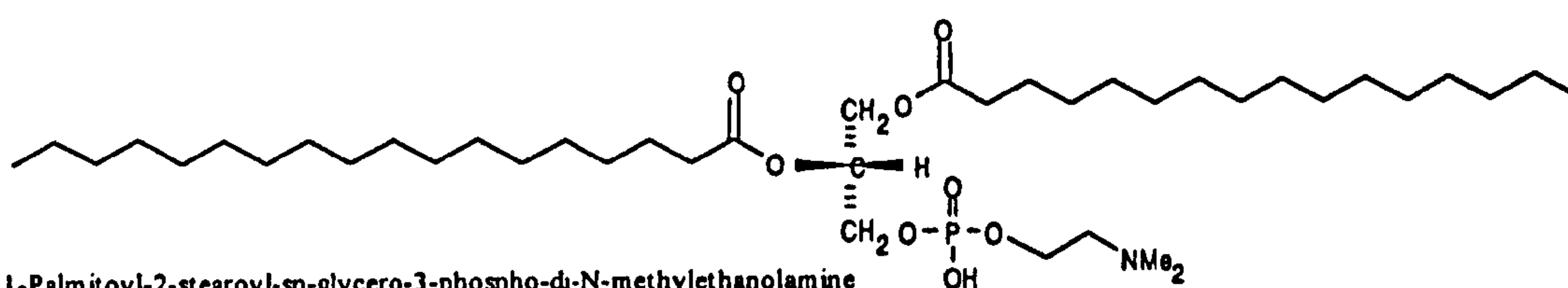
Figure 32. Positive ion FAB mass spectra of *L. pneumophila* grown in (a) iron-replete, and (b) iron-limited continuous culture.



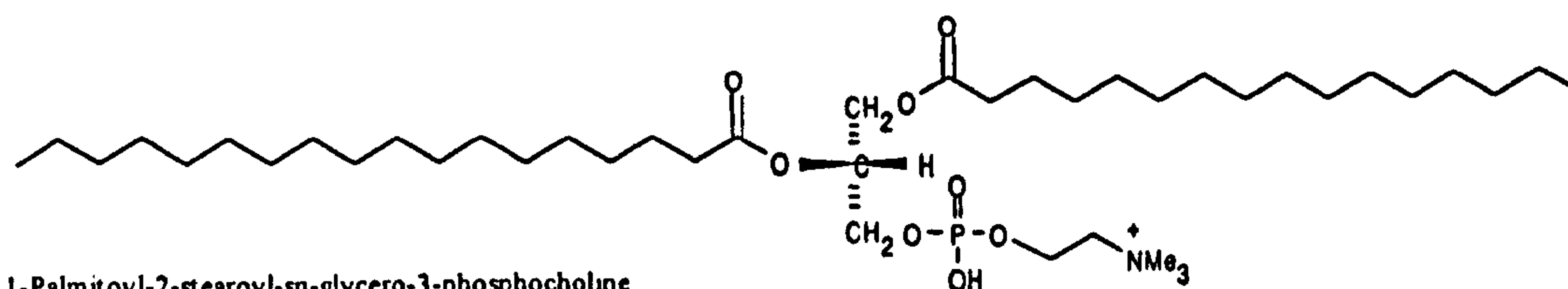
1-Palmitoyl-2-stearoyl-sn-glycero-3-phosphoethanolamine



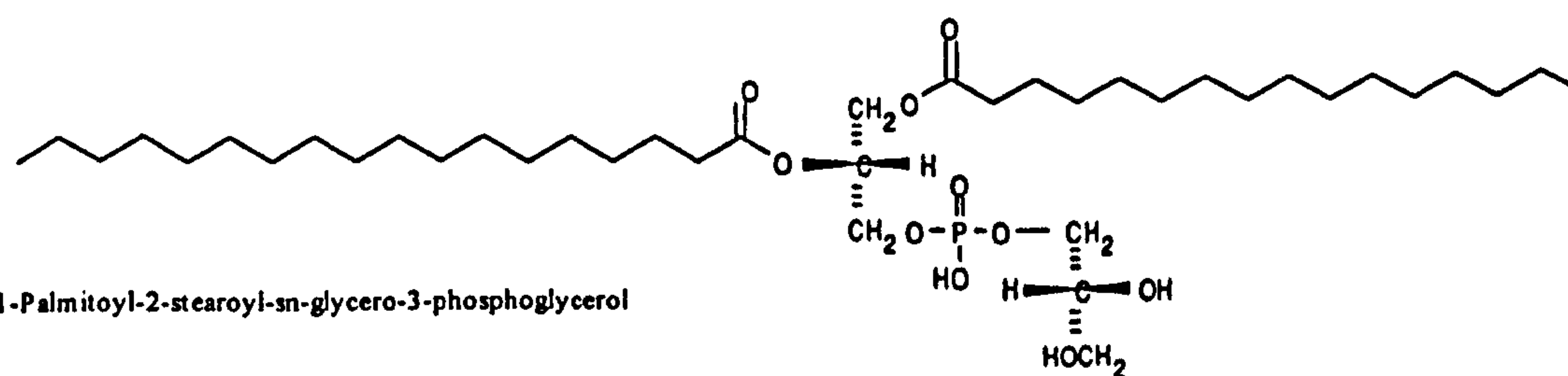
1-Palmitoyl-2-stearoyl-sn-3-phospho-N-methylethanolamine



1-Palmitoyl-2-stearoyl-sn-glycero-3-phospho-di-N-methylethanolamine



1-Palmitoyl-2-stearoyl-sn-glycero-3-phosphocholine



1-Palmitoyl-2-stearoyl-sn-glycero-3-phosphoglycerol

Figure 33. The structure of phospholipids most commonly found in legionellae.

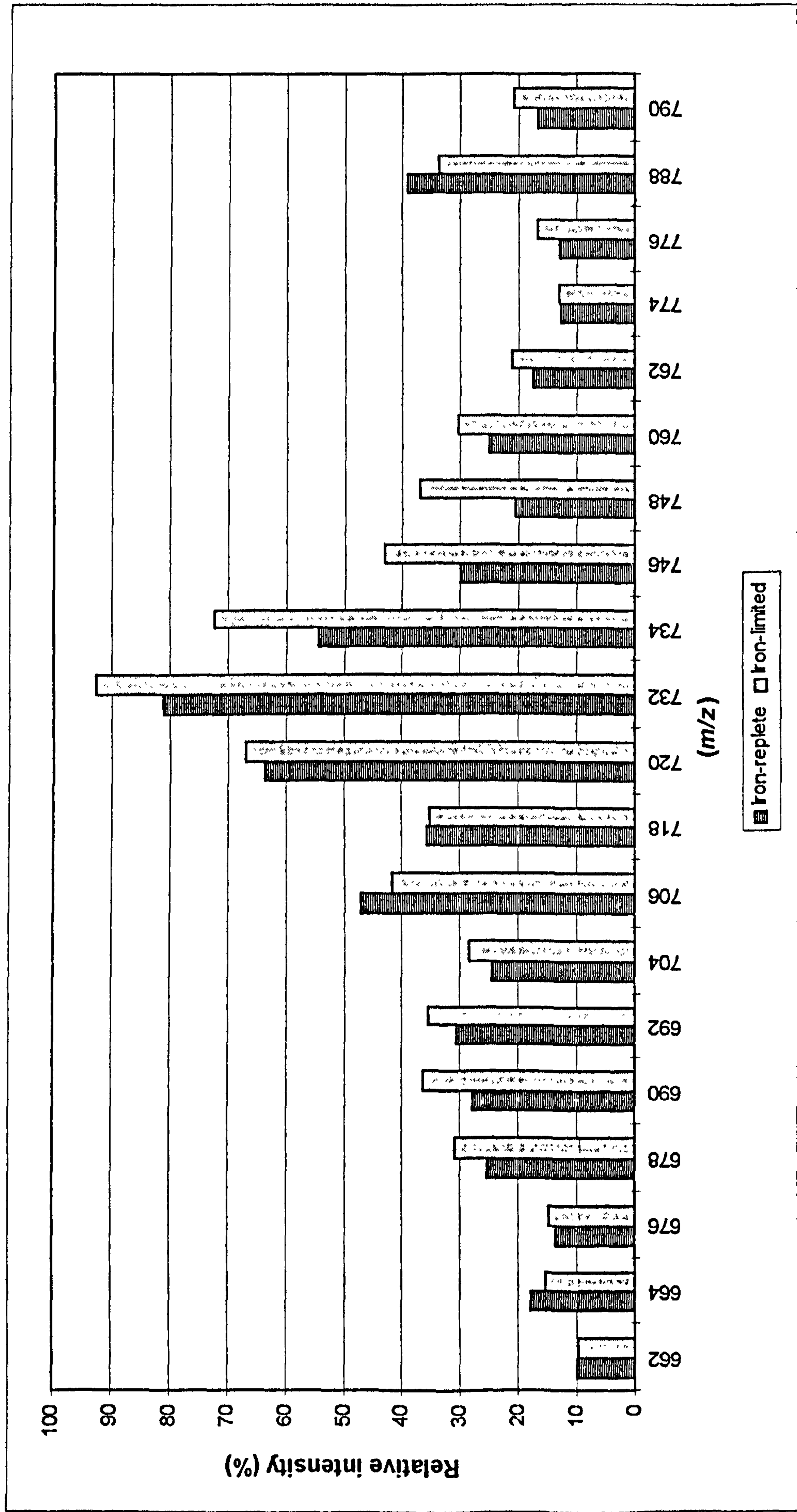
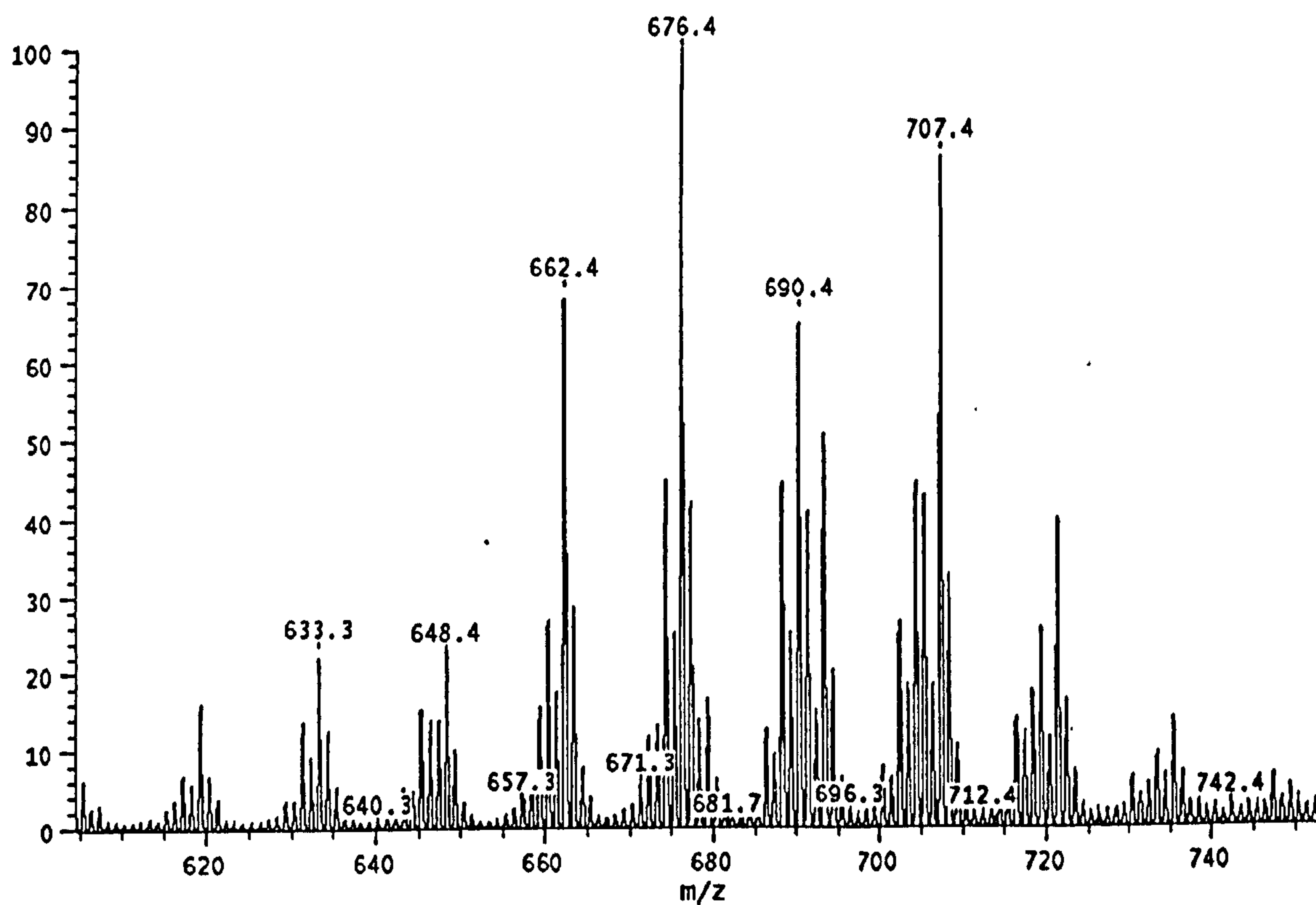


Figure 34. Comparison of the relative intensities of the protonated molecules of phosphatidylethanolamines and phosphatidylcholines from iron-limited and -replete samples of *L. pneumophila*. Each value represents the mean of 5 determinations.

(a)



(b)

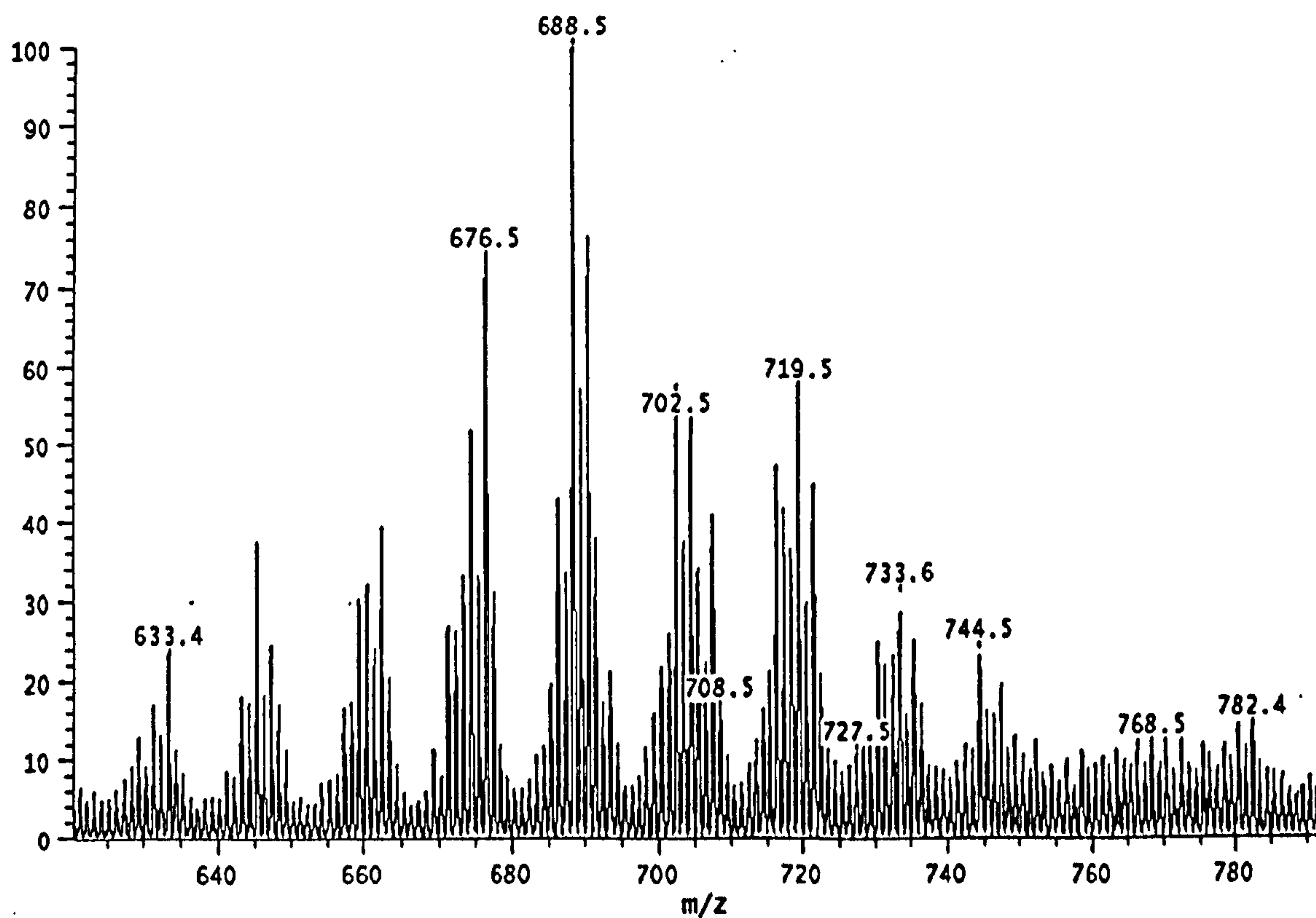


Figure 35. Negative ion FAB mass spectra of *L. pneumophila* grown in (a) iron-replete, and (b) iron-limited continuous culture.

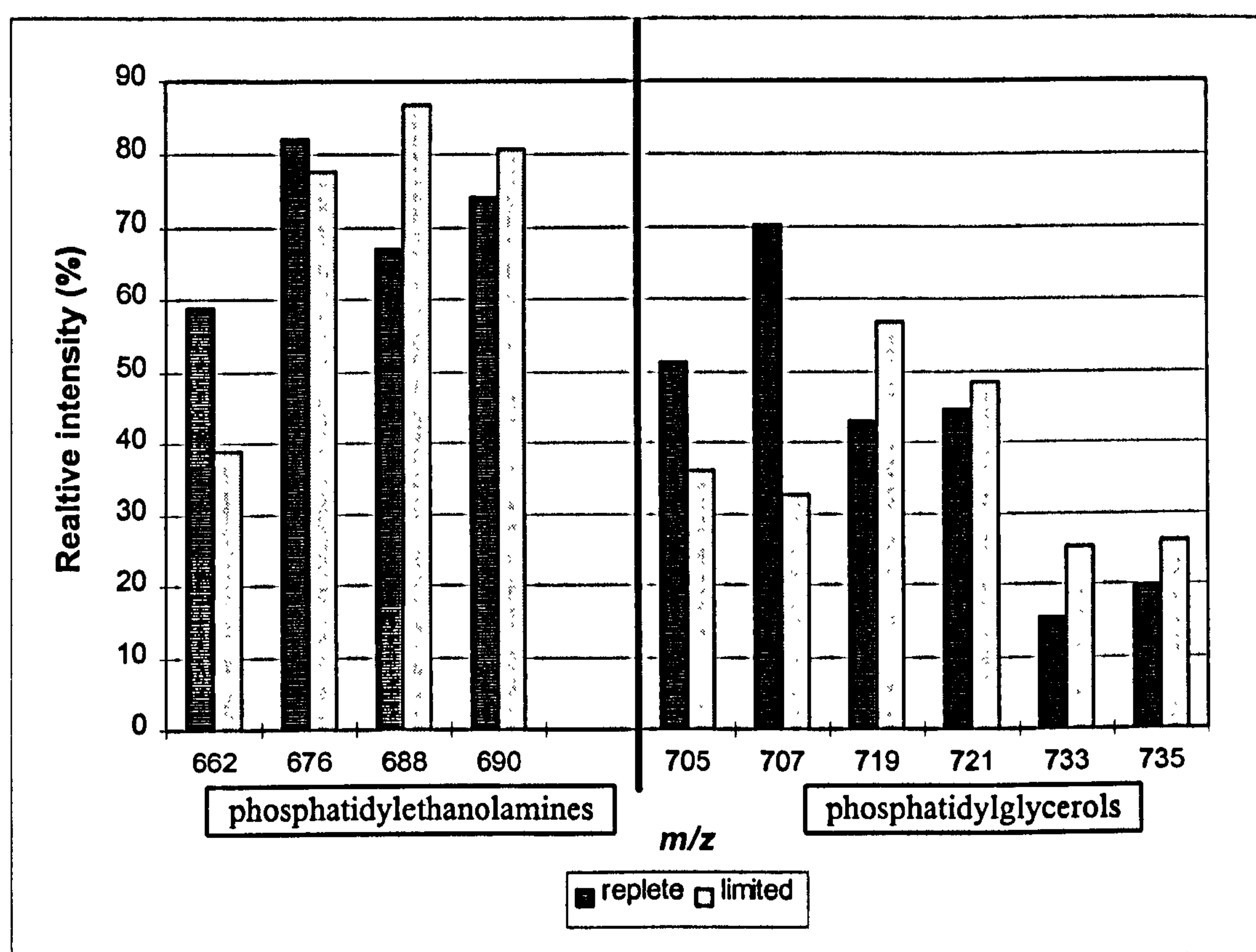


Figure 36. Comparison of the relative intensities of the deprotonated molecules of phosphatidylethanolamines and phosphatidylglycerols, from the negative ion spectra of iron-replete and -limited cultures of *L. pneumophila*. Each value represents the mean for 4 separate samples.

3.5.3 Analysis of individual phospholipid species.

Both positive and negative ion FAB-MS revealed changes in the phospholipid composition of *L. pneumophila* in response to iron limitation. However, this data provides comparatively little insight into alterations within the different phospholipid species. Different molecular species may possess the same molecular mass; for example, a phosphatidylethanolamine possessing a total of 32 carbon atoms, has the same mass (m/z 692) as an *N*-methylphosphatidylethanolamine or a di-*N*-methylphosphatidylethanolamine esterified with a combined total of 31 or 30

carbon atoms, respectively. Therefore, these three species will be represented by one signal at m/z 692.

Individual phospholipid species may be selectively analysed by performing constant neutral loss (CNL) scans, which records only species that decompose by the elimination of a selected fragment (Section 2.17.4). CNL scans were recorded for the elimination of fragments of mass 141, 155, 169 and 172, corresponding to the polar head group for phosphatidylethanolamines, *N*-methylphosphatidylethanolamines, di-*N*-methylphosphatidylethanolamines and phosphatidylglycerols, respectively. Figure 37 illustrates representative CNL scans for each molecular species.

Figures 38 and 39 compare the resultant profiles for iron-limited and -replete samples. The profiles for individual phospholipid species from iron-replete cultures were dominated by phospholipids possessing 30 to 32 fatty acyl carbon atoms. Under iron limitation the expression of phospholipids esterified with 30 and 31 saturated carbon atoms (30:0 & 31:0), were most significantly reduced. A corresponding increase of species possessing between 32 to 34 fatty acyl carbon atoms was observed, indicating an alteration in the fatty acyl substitution pattern. Phospholipids substituted with 32 carbon atoms (32:1 and 32:0) were most significantly enhanced (Figures 38 and 39). Comparable changes were observed in the profile of each of the four phospholipid species.

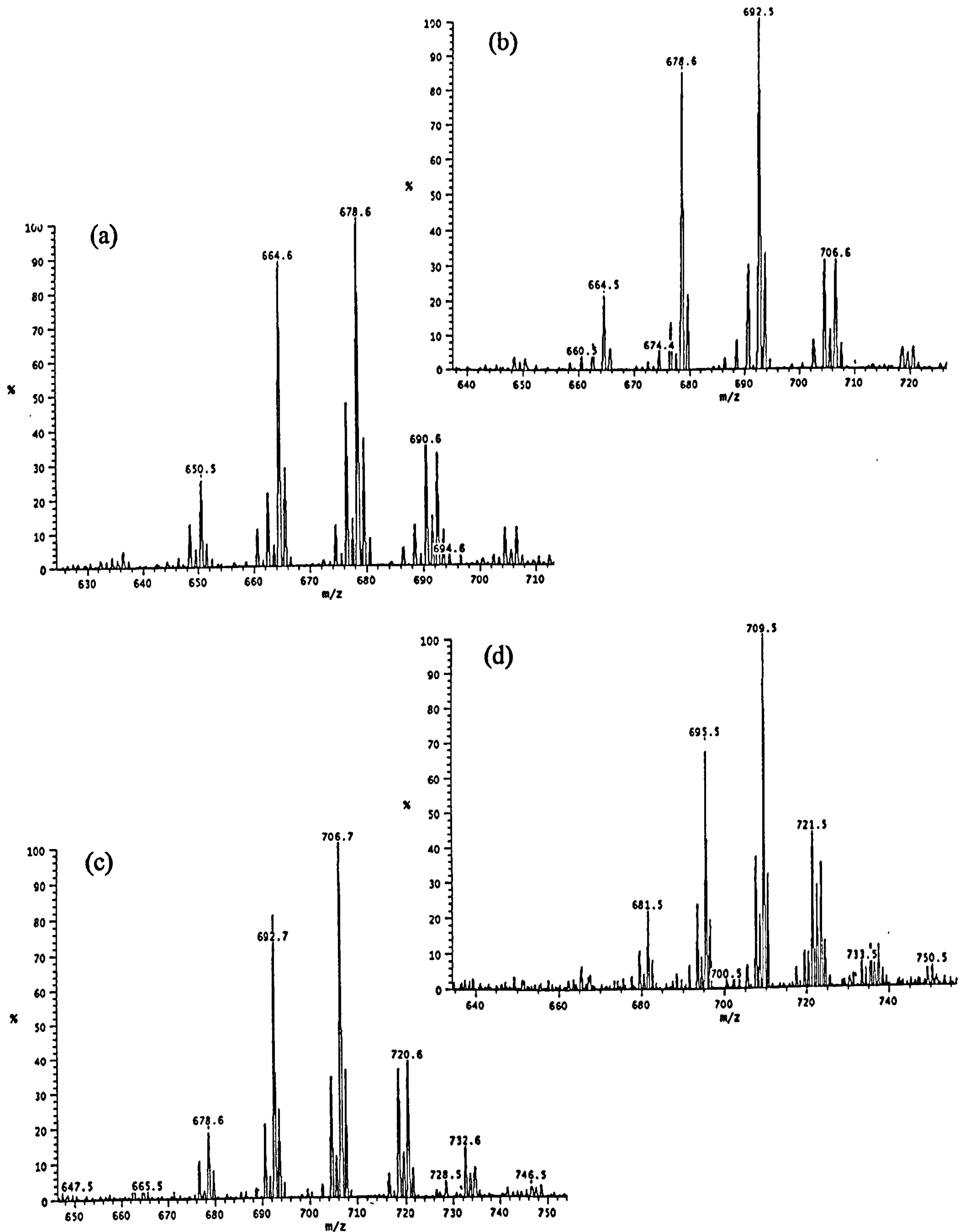


Figure 37. Constant neutral loss spectra recorded for individual phospholipid species extracted from iron-replete samples of *L. pneumophila*. (a) phosphatidylethanolamines; (b) *N*-methylphosphatidylethanolamines; (c) di-*N*-methylphosphatidylethanolamines and (d) phosphatidylglycerols.

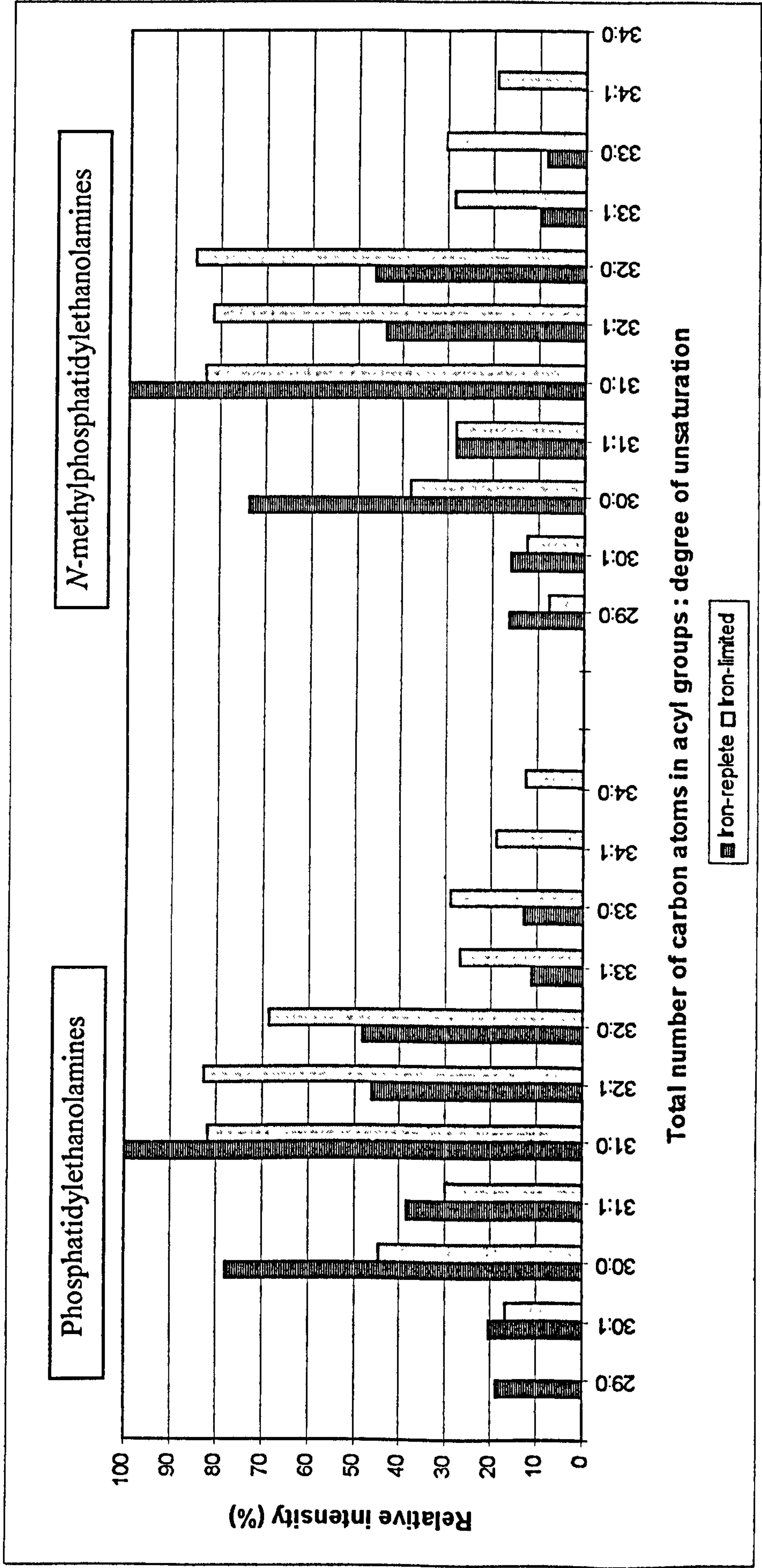


Figure 38. Comparison of the phosphatidylethanolamine and N-methylphosphatidylethanolamine profiles of iron-replete and -limited *L. pneumophila*, recorded by constant neutral loss scans for the loss of 141 and 155 mass units respectively, (i.e. loss of the polar head group). Values are the mean for 3 separate samples.

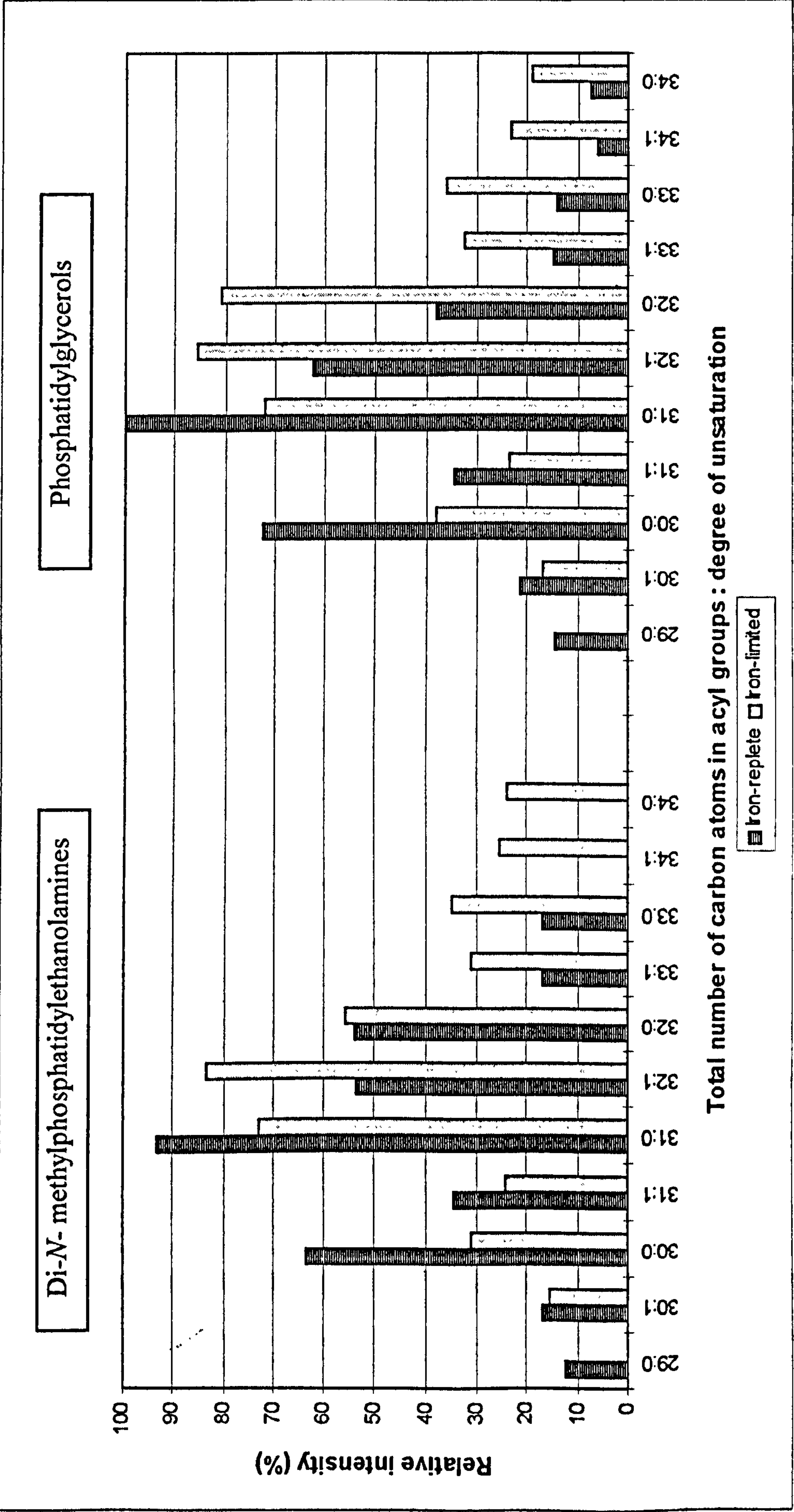


Figure 39. Comparison of the Di-N-methylphosphatidylethanolamine and phosphatidylglycerol profiles of iron-replete and -limited *L. pneumophila*, recorded by constant neutral loss scans for the loss of 169 and 172 mass units respectively, (i.e. loss of the polar head group). Values are the mean for 3 separate samples.

3.6 Analysis of Cellular Protein Expression.

3.6.1 Whole cell protein profiles of iron-limited and -replete cells.

Whole cell protein preparations from iron-limited and -replete cells were analysed by one-dimensional SDS-PAGE (Section 2.16). Figure 40 compares the SDS-PAGE profiles of two separate iron-limited and -replete culture samples. The expression of approximately 11 protein bands was influenced by iron availability. Protein bands migrating with apparent molecular weights of 18, 20, 21, 52 and 145 kDa were enhanced in response to iron limitation. Three proteins with apparent molecular weights of 23, 26 and 98 kDa appeared to be novel proteins. In addition to the induction of proteins, the expression of 3 proteins migrating at 40, 46 and 48 kDa was repressed under iron limitation (Figure 40). Table XII summarizes these changes in protein expression. No alteration in the expression of the 28 kDa major outer membrane protein was observed.

3.6.2 Cytoplasmic membrane proteins.

Following extraction of the cell membrane pellets, the sarkosyl soluble cytoplasmic membrane was also analysed by SDS-PAGE (Section 2.16). Comparison of iron-limited and -replete protein profiles, revealed the presence of approximately 7 iron-repressible cytoplasmic membrane proteins (Figure 41 and Table XII). The apparent masses of 5 of these proteins correlated with iron-repressible proteins observed in the total protein profiles (Table XII). Two additional iron-repressible protein bands migrating at 47 and 115 kDa were observed, but were not detected in the whole cell profile (Figure 41 & Table XII). Of these iron-repressible proteins, bands migrating at 47, 52, 97 and 145 kDa were the most significantly enhanced. Furthermore, one protein band at 29 kDa appeared to be down-regulated under iron-limited conditions. In both iron-replete and -limited

cultures, the principal protein bands migrated with an apparent molecular mass of 29 and 58 kDa (Figure 41).

3.6.3 Outer membrane proteins.

Analysis of sarkosyl insoluble outer membrane material purified from French press extracts, yielded very poor protein profiles, with the peptidoglycan associated outer membrane material causing bad smearing. An alternative procedure employing lysozyme in combination with freeze-thaw was used to purify cell membranes (Section 2.16.1). Improved outer membrane protein profiles were obtained with sarkosyl extracts of this material. Comparison of outer membrane protein SDS-PAGE profiles revealed the induction of two low molecular mass proteins under iron-limited conditions (Figure 42, Table XII). The most abundant of these iron-repressible proteins migrated with a molecular mass of approximately 20 kDa. Only a 15 kDa protein appeared to be novel, and was not detected in the total protein profile. In addition, two protein bands migrating at 25 and 40 kDa appeared to be repressed under iron-limited conditions (Figure 42).

The 46 and 48 kDa protein bands down-regulated, and the 23 and 26 kDa proteins induced in iron-limited whole cell protein profiles, were not observed in either membrane fraction (Table XII). This suggests that they may be cytoplasmic proteins.

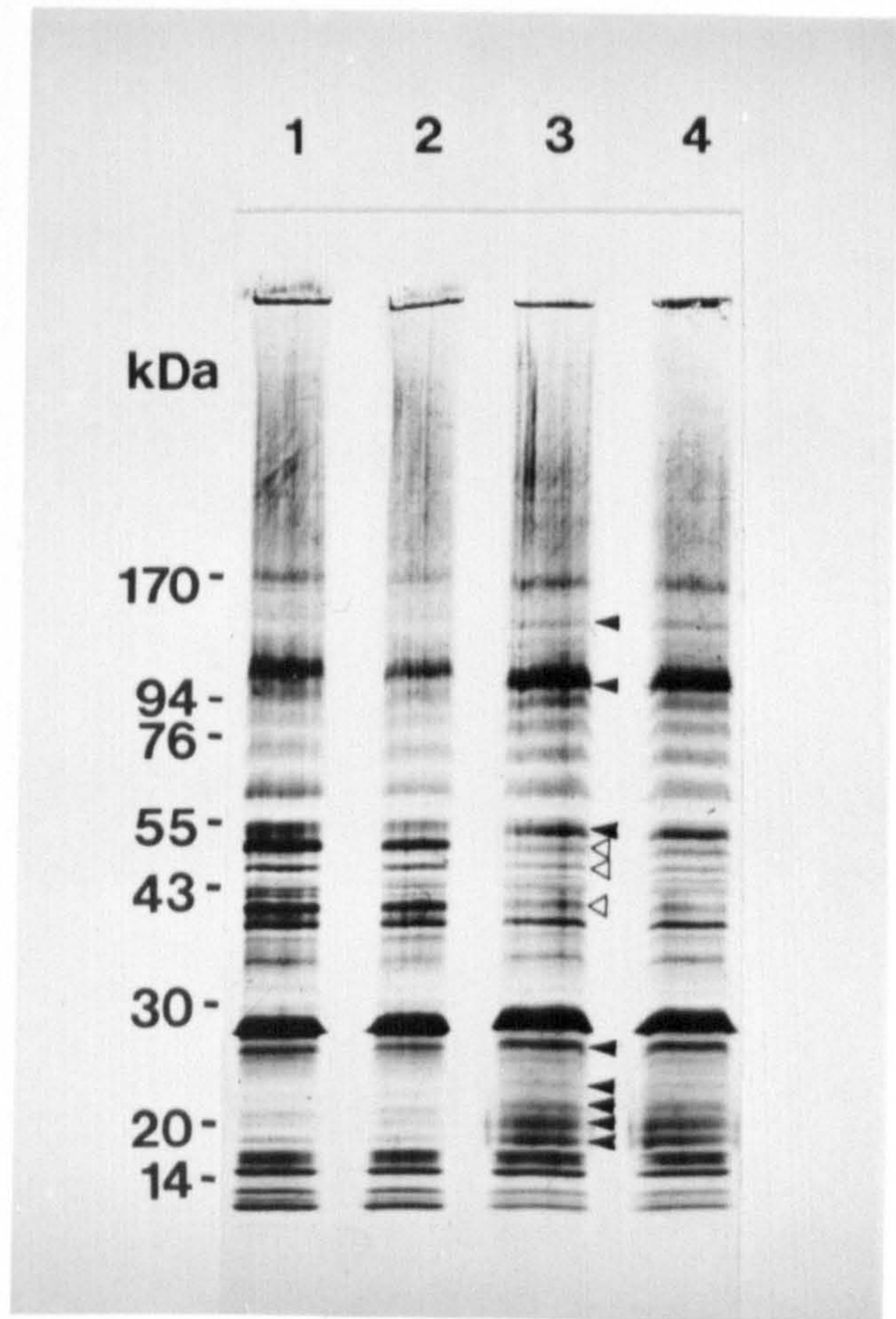


Figure 40. Silver stained SDS-PAGE total cell protein profiles of *L. pneumophila*. Lanes 1 and 2, iron-replete culture; lanes 3 and 4, iron-limited culture.

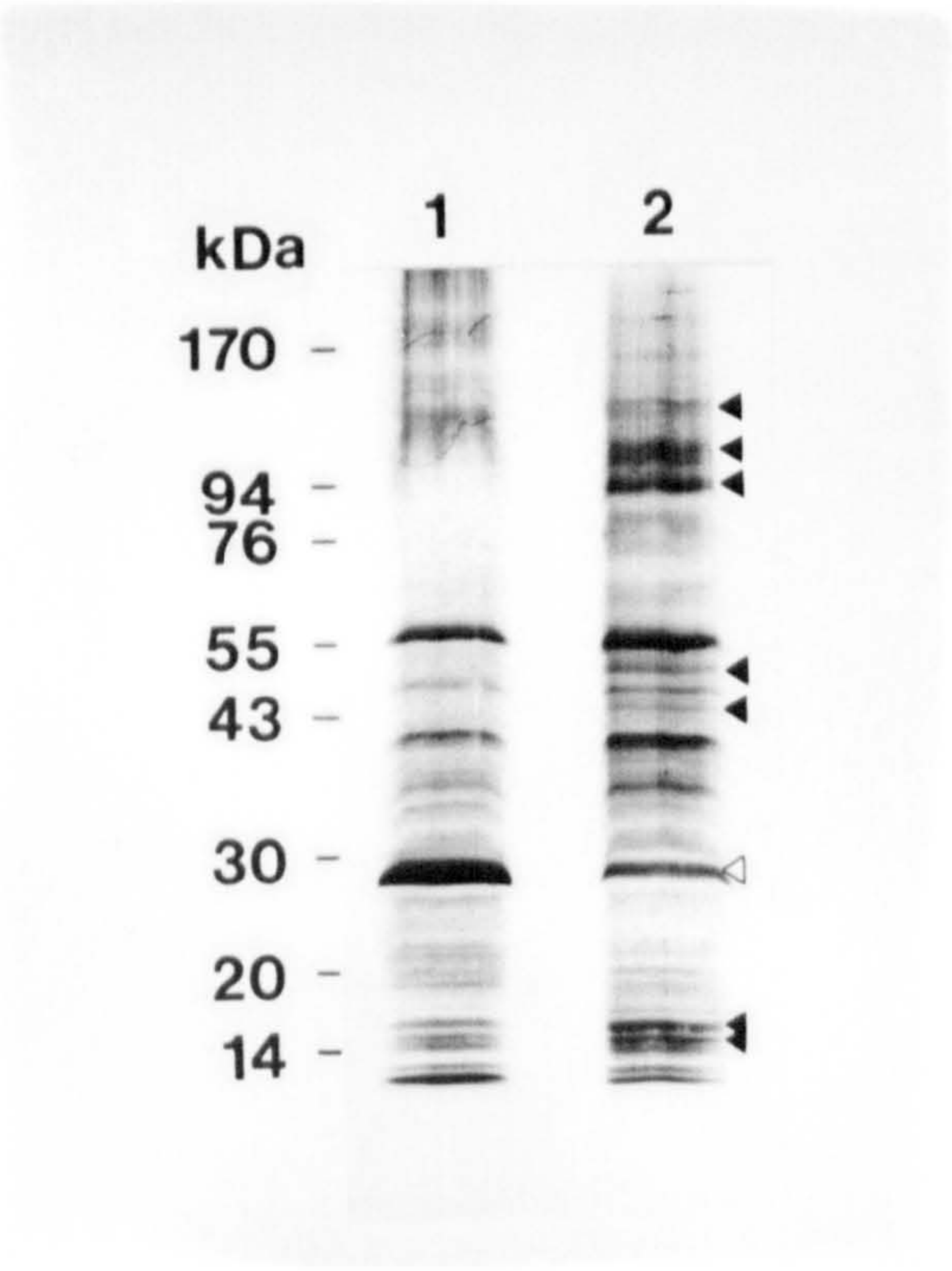


Figure 41. Silver stained SDS-PAGE cytoplasmic membrane protein profiles of *L. pneumophila*. Lane 1, iron-replete culture; lanes 2, iron-limited culture.

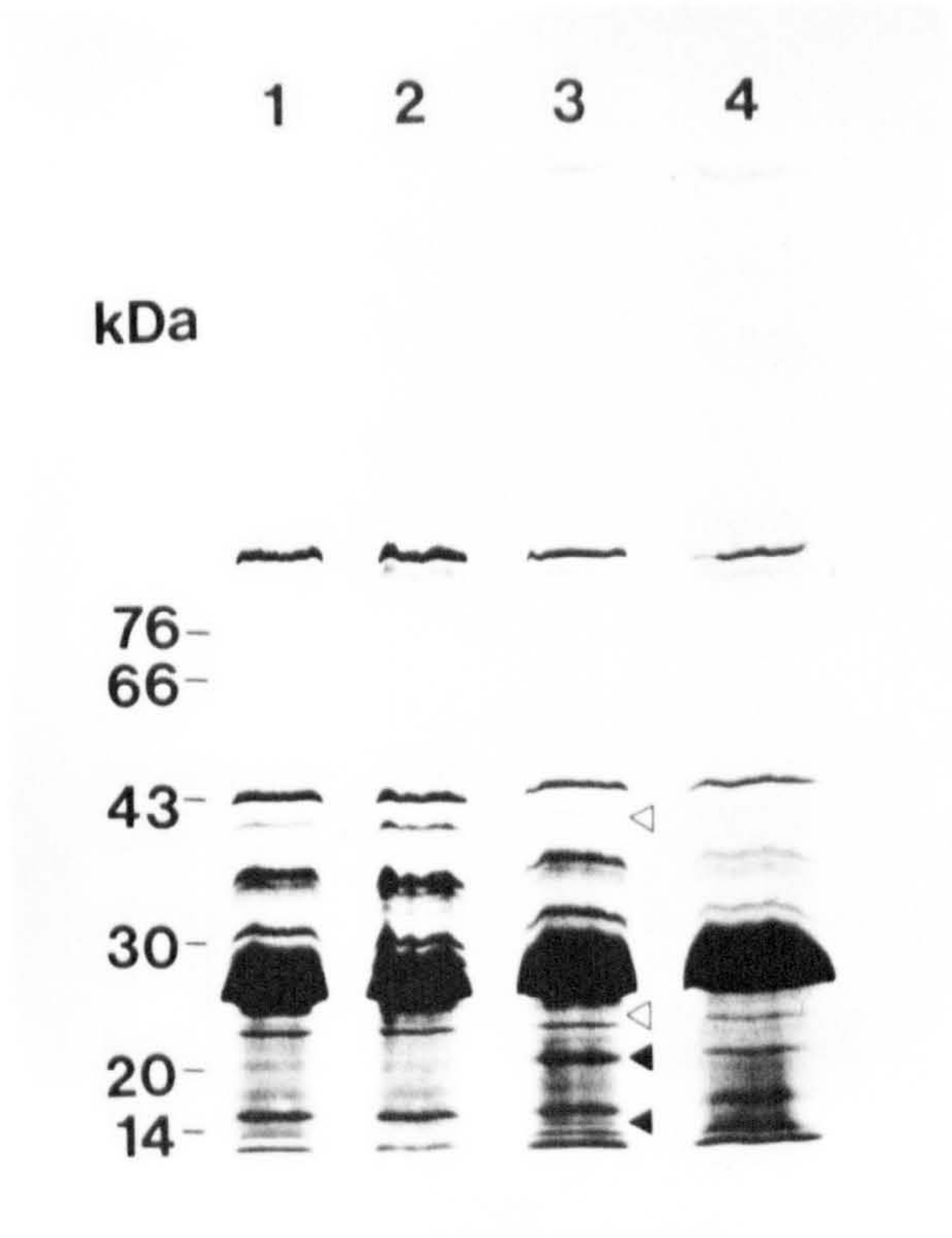


Figure 42. Silver stained SDS-PAGE outer membrane protein profiles of *L. pneumophila*. Lanes 1 and 2, iron-replete culture; lanes 3 and 4, iron-limited culture.

Table XII. Comparison of iron-regulated proteins in the whole cell, inner membrane and outer membrane fractions of iron-replete and -limited cultures of *L. pneumophila*. Values represent the apparent molecular mass (kDa) of individual proteins.

Total proteins	Inner membrane	Outer membrane
<u>up-regulated in response to iron limitation</u>		
		15
18	18	
20		20
21	21	
23		
26		
	47	
52	52	
98	97	
	115	
145	145	
<u>down-regulated in response to iron limitation</u>		
		25
	29	
40		40
46		
48		

3.7 Influence of Iron Limitation on Serogroup Antigen Expression.

3.7.1 Analysis of serogroup antigen by SDS-PAGE.

Hot saline extracts of serogroup antigen isolated from iron-replete and limited culture samples, were compared by SDS-PAGE (Sections 2.15.1 and 2.15.5). Ladder-like patterns typical of smooth-type LPS were observed for both cultures upon silver staining (Figure 43). The banding profile of both cultures appeared to be identical, with approximately 40 discrete bands visible.

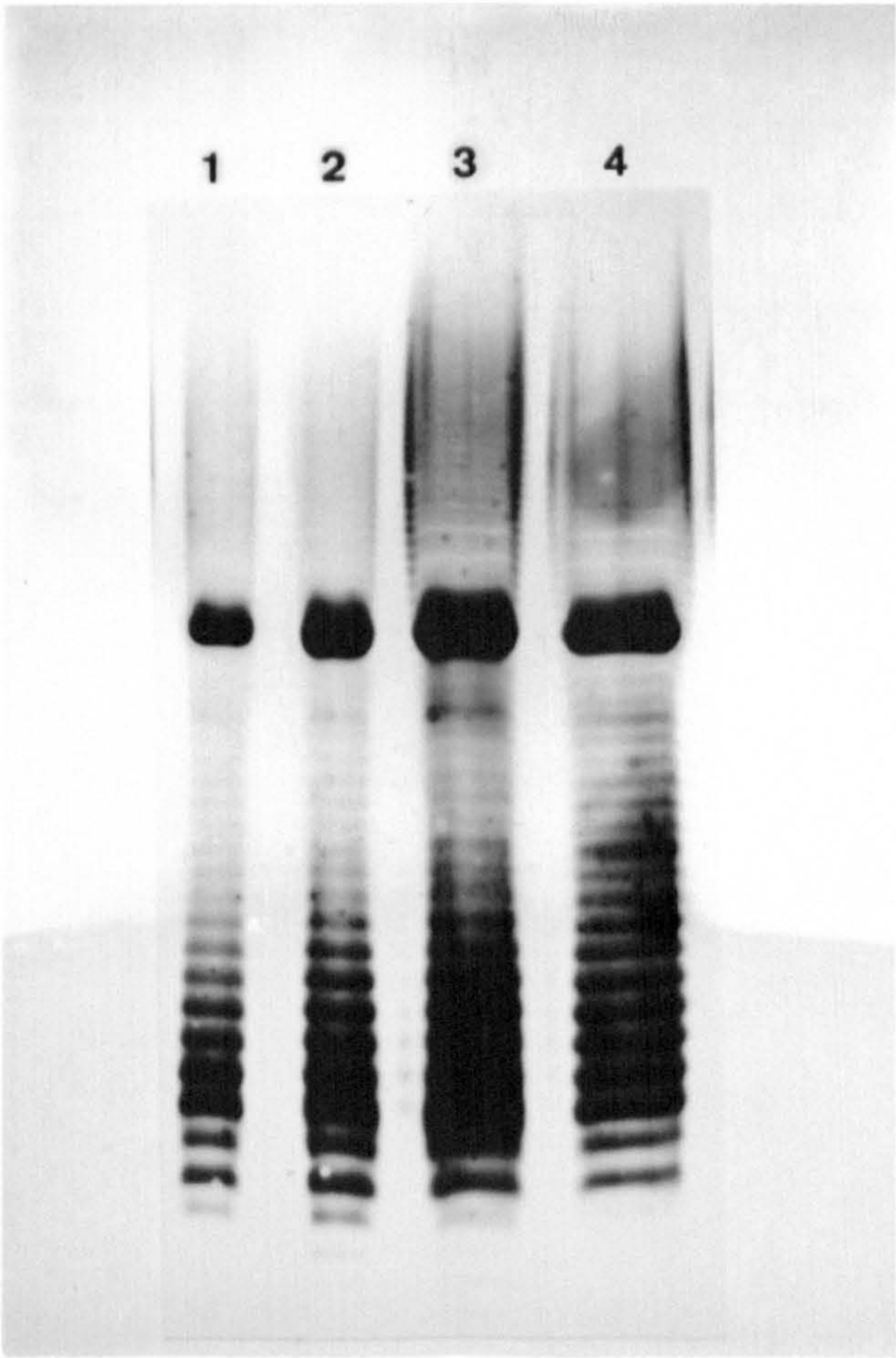


Figure 43. SDS-PAGE separation of *L. pneumophila* serogroup antigen. Lanes 1 and 2, iron-limited; lanes 3 and 4, iron-replete.

3.7.2 Chemical analyses of serogroup antigen.

The chemical composition of the saline extracts was compared by determining the carbohydrate, protein and 2-keto-3-deoxyoctonate (KDO) content (Section 2.15). The data presented in Table XIII compares the mean results for iron-limited and -replete samples, along with a control sample extracted from cells grown on BCYE agar. The chemical compositions of the iron-limited and -replete culture extracts were comparable to each other, and to the agar grown cells.

Table XIII. Chemical composition of saline extracts of serogroup antigen from iron-limited and -replete culture samples, and BCYE agar grown cells.

Sample	Carbohydrate (% dry wt.)	Protein (% dry wt.)	KDO (% dry wt.)
Iron-replete ^a	3.8	16.2	0.44
Iron-limited ^a	4.0	16.4	0.44
BCYE culture ^b	3.2	20	0.46

^a Values represent the mean results for two separate extracts

^b Values represent the mean of duplicate analysis for a single extract.

3.8 Virulence and Intracellular Growth of *L. pneumophila*.

3.8.1 Influence of iron limitation on the virulence of *L. pneumophila*.

Preliminary aerosol challenge experiments (Section 2.18.1) demonstrated that the virulence of *L. pneumophila* was attenuated during growth under iron-limited conditions. Aerosol challenge of guinea pigs with iron-replete culture produced deaths with an estimated LD₅₀ of 3.5 log₁₀ colony forming units (CFU) (Table XIV). However, when guinea pigs were challenged with steady state iron-limited cells, no deaths occurred with a maximum retained dose of 5.4 log₁₀ CFU. These initial experiments were based on challenging groups of 4 animals, with only 3 doses. This experimental design prevented the calculation of confidence intervals for the estimated LD₅₀.

Table XIV. Comparison of the LD₅₀ values for *L. pneumophila* grown in iron-limited and -replete continuous culture.

Sample	log ₁₀ LD ₅₀
Iron-replete	3.5
Iron-limited	>5.4 ^a

^a No deaths occurred at the maximum challenge.

LD₅₀ value was estimated by the method of Reed and Muench (1938).

The experimental design was modified by increasing the number of animals and the number of datum points close to the approximate LD₅₀ (Section 2.18.1). This facilitated a more accurate determination of the median lethal dose, and enabled calculation of 95% confidence intervals. Aerosol challenge of groups of 8 animals with iron-limited and -replete cultures of *L. pneumophila* confirmed that iron-replete cultures were significantly ($P < 0.05$) more virulent than the same culture grown under iron-limited conditions (Table XV). Iron-replete cells produced death with LD₅₀ of 3.79 log₁₀ CFU (Table XV). When converted to iron limitation, no deaths were observed at the maximum challenge of 5.8 log₁₀ CFU.

The culture was reverted back to iron-replete conditions, and steady state culture virulence was assessed. This demonstrated a statistically significant ($P < 0.05$) increase in virulence, with an LD₅₀ value comparable to that recorded prior to iron limitation (Table XV). This LD₅₀ value was slightly higher than that reported for the iron-replete culture prior to iron limitation, however, the 95 % confidence intervals for both iron-replete cultures overlapped. A repeat experiment confirmed that virulence modulation in response to iron limitation is a reproducible phenomenon (Table XV).

3.8.2 Intracellular growth of iron-limited and -replete cells.

An *in vitro* macrophage assay was used to compare the uptake of iron-limited and -replete cells by cultured guinea pig alveolar macrophages, and monitor subsequent intracellular multiplication (Section 2.18.2). These results were compared with those obtained with standard virulent and avirulent control cultures. In this model system there was good uptake of the virulent iron-replete cells, although the uptake frequency was lower than that of either control cultures (Figure 44). By contrast, the number of culturable iron-limited cells located intracellularly after phagocytosis, was significantly lower.

Table XV. Comparison of the LD₅₀ values and their 95% confidence intervals for *L. pneumophila* grown in chemostat culture, under iron-limited and -replete conditions.

Culture conditions	log ₁₀ LD ₅₀	95% confidence interval of LD ₅₀ ^a
Iron-replete	3.79	3.45 - 4.13
Iron-limited	>5.80 ^b	NA ^c
Iron-replete ^d	4.18	3.96 - 4.39
Repeat experiment		
Iron-replete	4.27	4.1 - 4.45
Iron-limited	>5.65 ^b	NA ^c
Iron-replete ^d	4.9	4.4 - 5.4

^a 95% fiducial limits for the median lethal dose (LD₅₀) were calculated by the method of Finney (1964).

^b No deaths occurred at the maximum challenge.

^c NA, not appropriate.

^d The culture was returned to steady state iron-replete conditions after growth under iron-limited conditions.

The difference between the number of culturable iron-limited and -replete cells located intracellularly after phagocytosis, was statistically significantly ($P < 0.01$) when tested by the un-paired t-test. However, both iron-limited and -replete cells proceeded to multiply rapidly intracellularly, with a slightly greater initial growth rate observed with the iron-limited culture. The Corby virulent control culture demonstrated good infection frequency and intracellular multiplication. The “CAC” avirulent variant also demonstrated good uptake frequency, although it was unable to multiply intracellularly (Figure 44).

3.8.3 Growth of iron-limited and -replete cultures *in vivo*.

The uptake and multiplication of iron-limited and -replete cells within guinea-pig lungs was monitored following aerosol challenge (Section 2.18.3). Figure 45 compares the uptake and growth of both cultures *in vivo*, over a 4 day period following aerosolization. Values at zero hours represent the retained dose. While there was a $0.8 \log_{10}$ difference in the retained dose for the two cultures, both cultures proceeded to multiply *in vivo*. A slightly higher growth rate was detected for the iron-replete culture, particularly during the first 24 h and after 72 h.

To investigate if there was any difference in the rate of host cell infection *in vivo*, two animals from each group were sacrificed 4 h after challenge. The alveolar phagocytic cells were recovered from each animal by performing lung lavages (Section 2.18.3). The total number of colony forming legionellae in each lavage was determined on BCYE agar. The phagocytic cells were then washed, and the number of legionellae associated with the host cells was enumerated. This assay demonstrated that the number of iron-limited cells recovered in lung lavages was 5-fold lower than that of iron-replete cells. The percentage of the total legionellae in each lavage which were associated with host cells was markedly lower (13-fold) for the iron-limited culture, in comparison to the iron-replete culture (Table XVI).

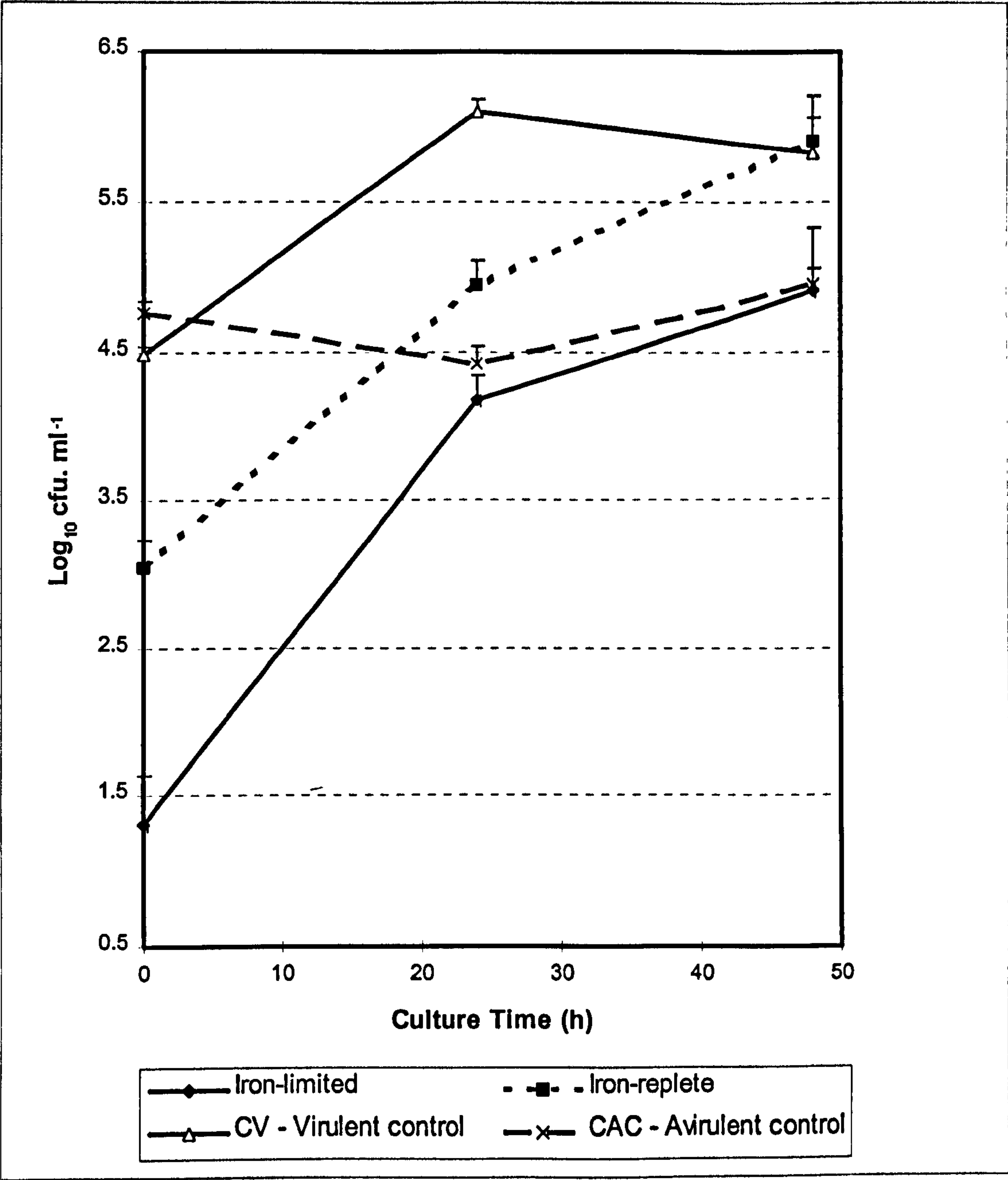


Figure 44. Comparison of the uptake and intracellular growth of iron-limited and -replete cultures of *L. pneumophila* in guinea pig alveolar macrophages cultured *in vitro*.

Each datum point for iron-limited and -replete cultures represents the mean value for 2 different culture samples, each assayed in quadruplicate. Results for control cultures represent the mean of 8 determinations. Error bars are + s.e.m.

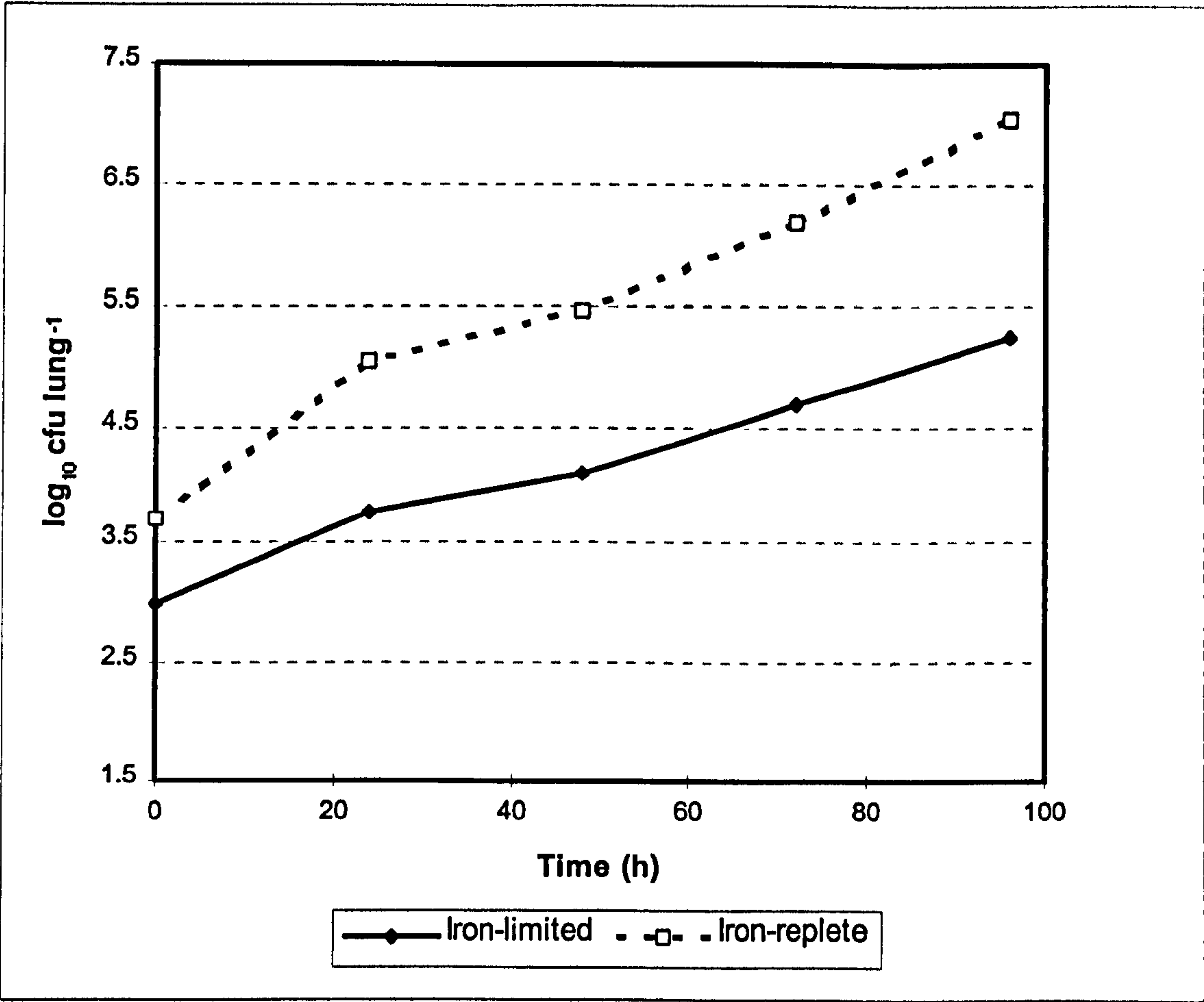


Figure 45. Comparison of the growth of iron-limited and -replete *L. pneumophila* in guinea-pig lungs.

Table XVI. Association of iron-limited and -replete cells with host phagocytic cells *in vivo* (Section 2.18.3).

	Iron-replete	Iron-limited
Total number of legionellae in lavage (log ₁₀ CFU)	3.5	2.9
Number of legionellae associated with host phagocytic cells (log ₁₀ CFU)	3.0	1.15
% legionellae association with phagocytic cells	30	2.2

3.9 Influence of Culture pH on Physiology of Iron-Replete Cultures of *L. pneumophila*.

3.9.1 Influence of pH on the growth of iron-replete cultures.

The physiological effect of altering the pH of steady state iron-replete cultures was investigated. Figure 46 illustrates a typical growth response to an incremental decrease in pH, from 6.9 to 6.0. As the pH was lowered, an increase in culture turbidity was observed at pH values from 6.7 to 6.4. Reducing the pH further to 6.0, caused a rapid transient decline in culture turbidity. The culture recovered to a final steady state turbidity which was comparable to that observed at pH 6.9. Pulsing the steady state pH 6.0 culture with 10 mM serine, stimulated a 10% increase in culture turbidity, confirming serine as the growth-limiting nutrient (Figure 47).

Increasing the culture pH from 6.9 to 7.2, caused a decline in culture turbidity, which was further augmented at pH 7.4. The turbidity declined by approximately 80%, before recovering to a new steady state level, approximately 30% lower than the original value. Raising the culture pH to 7.8 caused a further transient decline in culture turbidity, before the culture stabilized at an optical density comparable to that observed at pH 7.4 (Figure 48). As the culture pH was elevated, the culture became dark brown in colour. This colour development was observed at pH 7.4 and intensified at pH 7.8. Pulsing the steady state culture with 10 mM serine stimulated a slight increase in turbidity of 6 % (Figure 49). Pulsing the culture with 0.5 mM tyrosine in the presence of 10 mM serine, did not enhance the growth response.

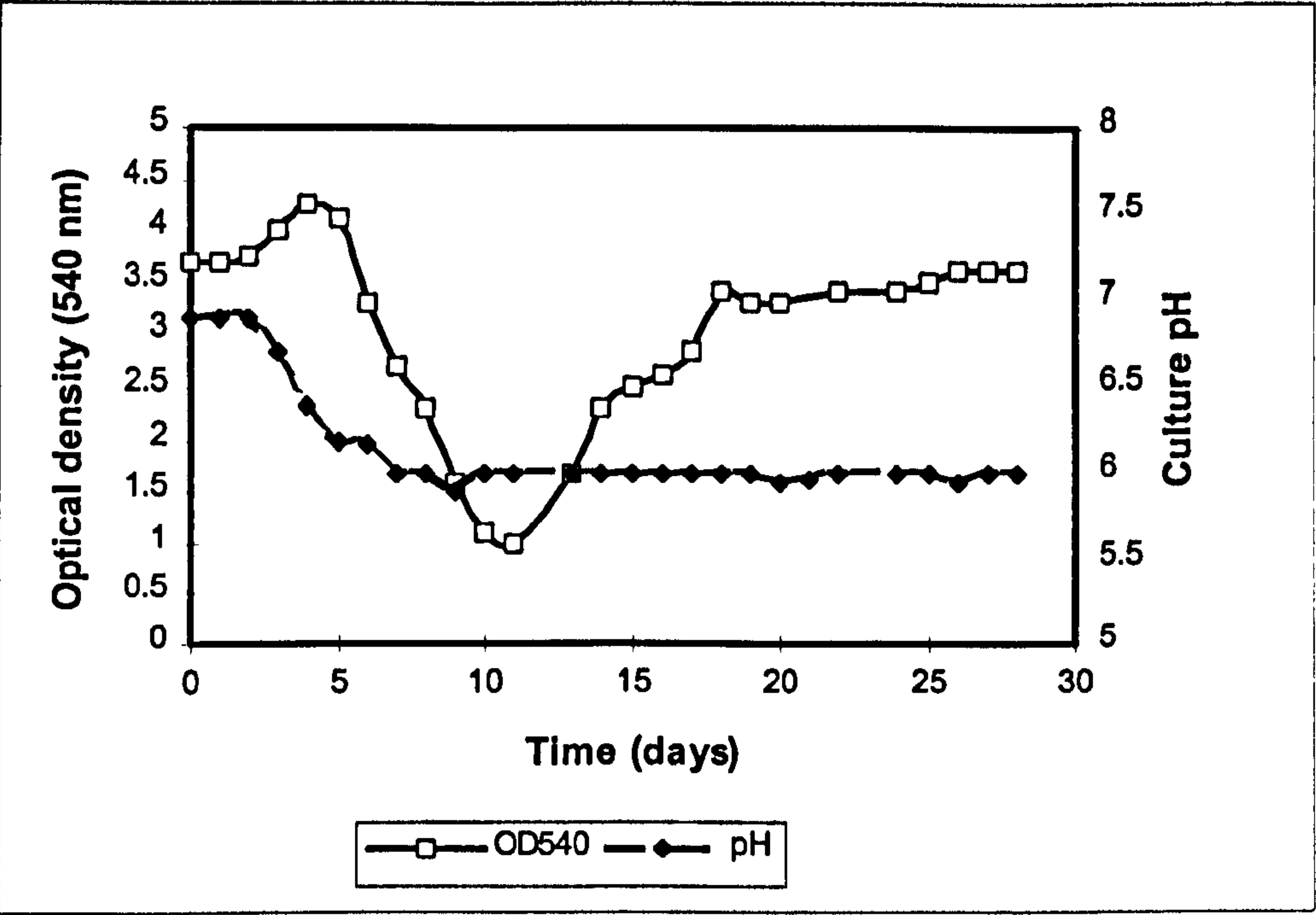


Figure 46. Growth response of a steady state iron-replete culture of *L. pneumophila* to an incremental decrease in culture pH from 6.9 to 6.0.

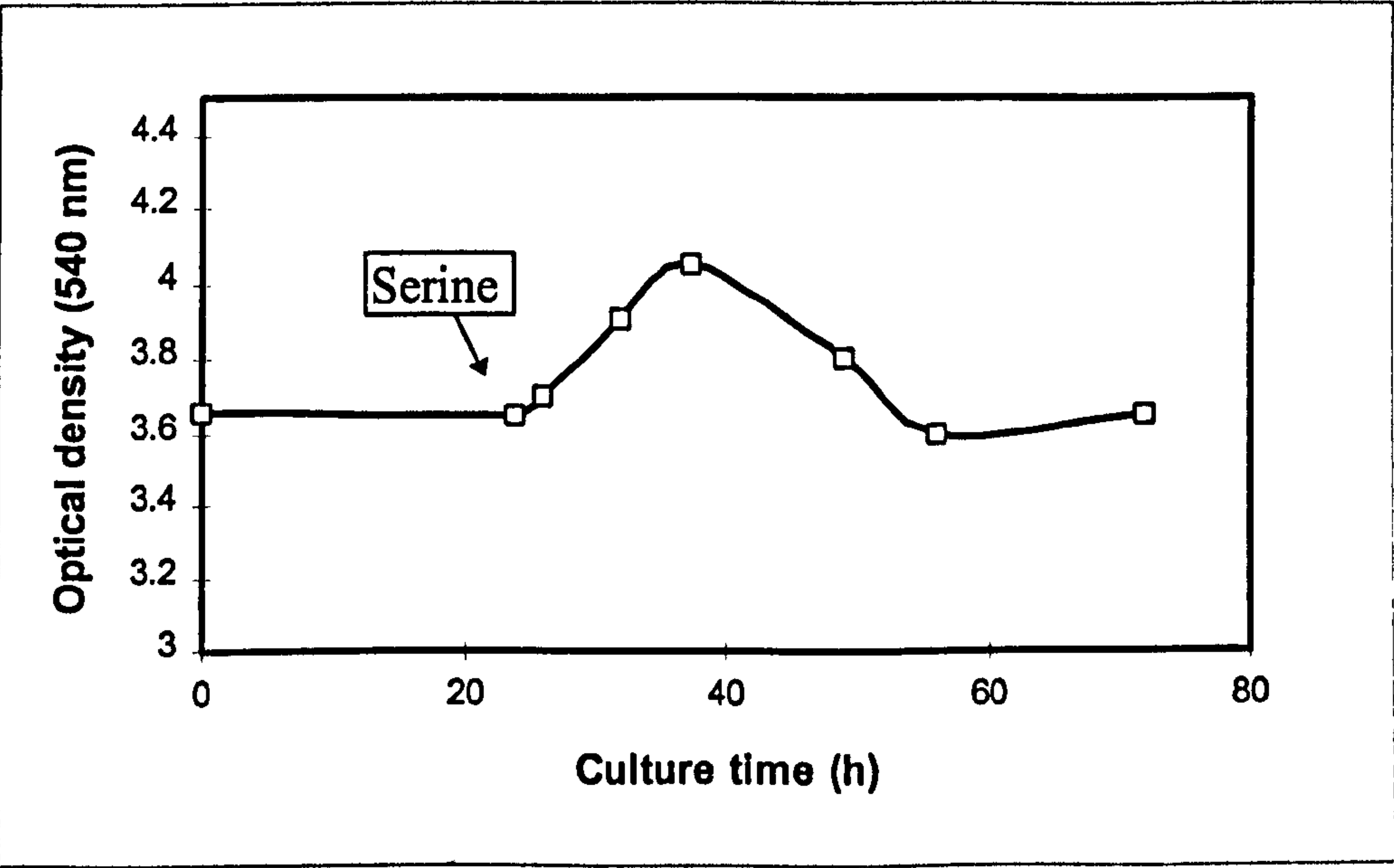


Figure 47. Growth response of a steady state pH 6.0 iron-replete culture of *L. pneumophila*, to the addition of 10 mM serine directly into the culture.

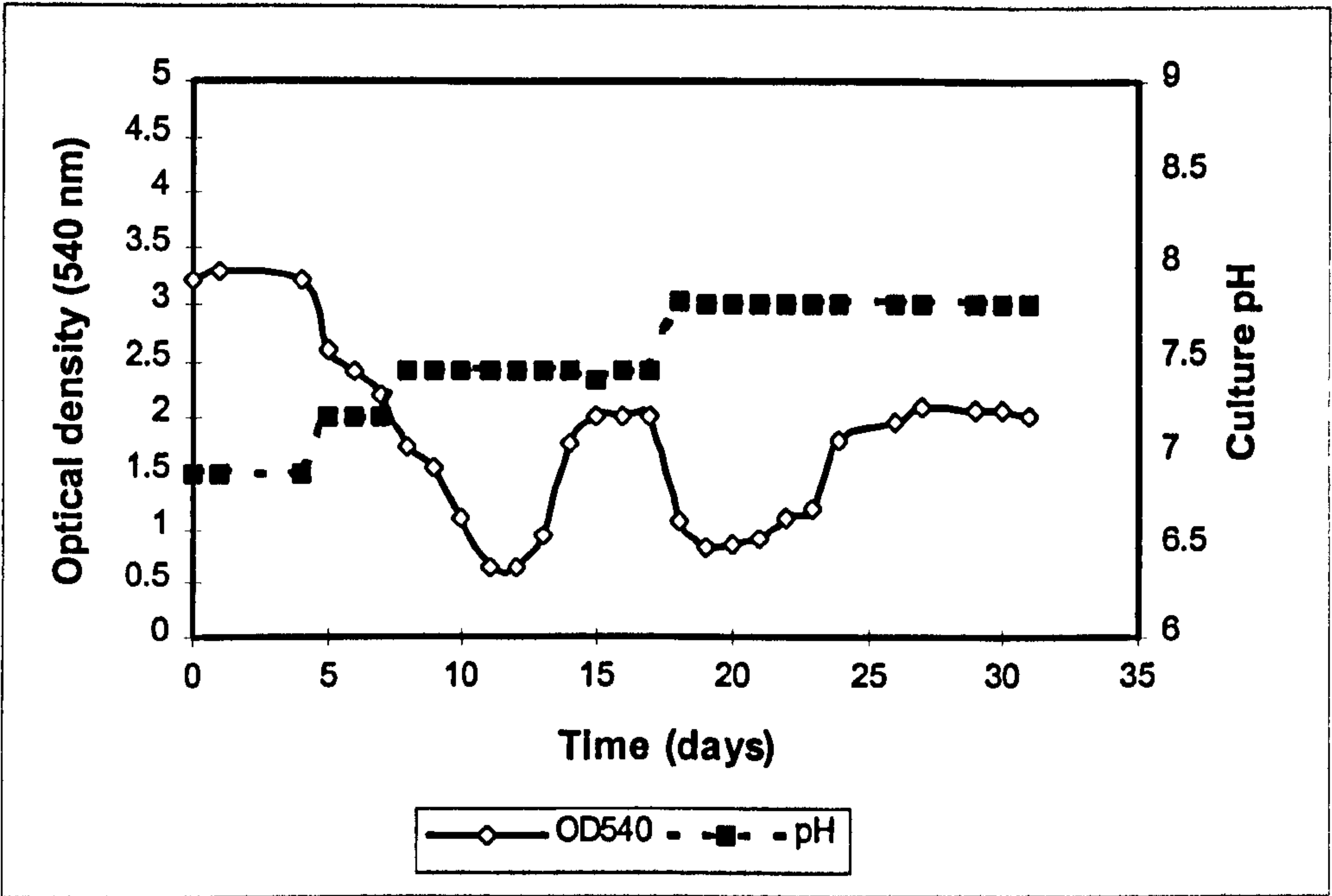


Figure 48. Growth response of a steady state iron-replete culture of *L. pneumophila* to an incremental increase in culture pH from 6.9 to 7.8.

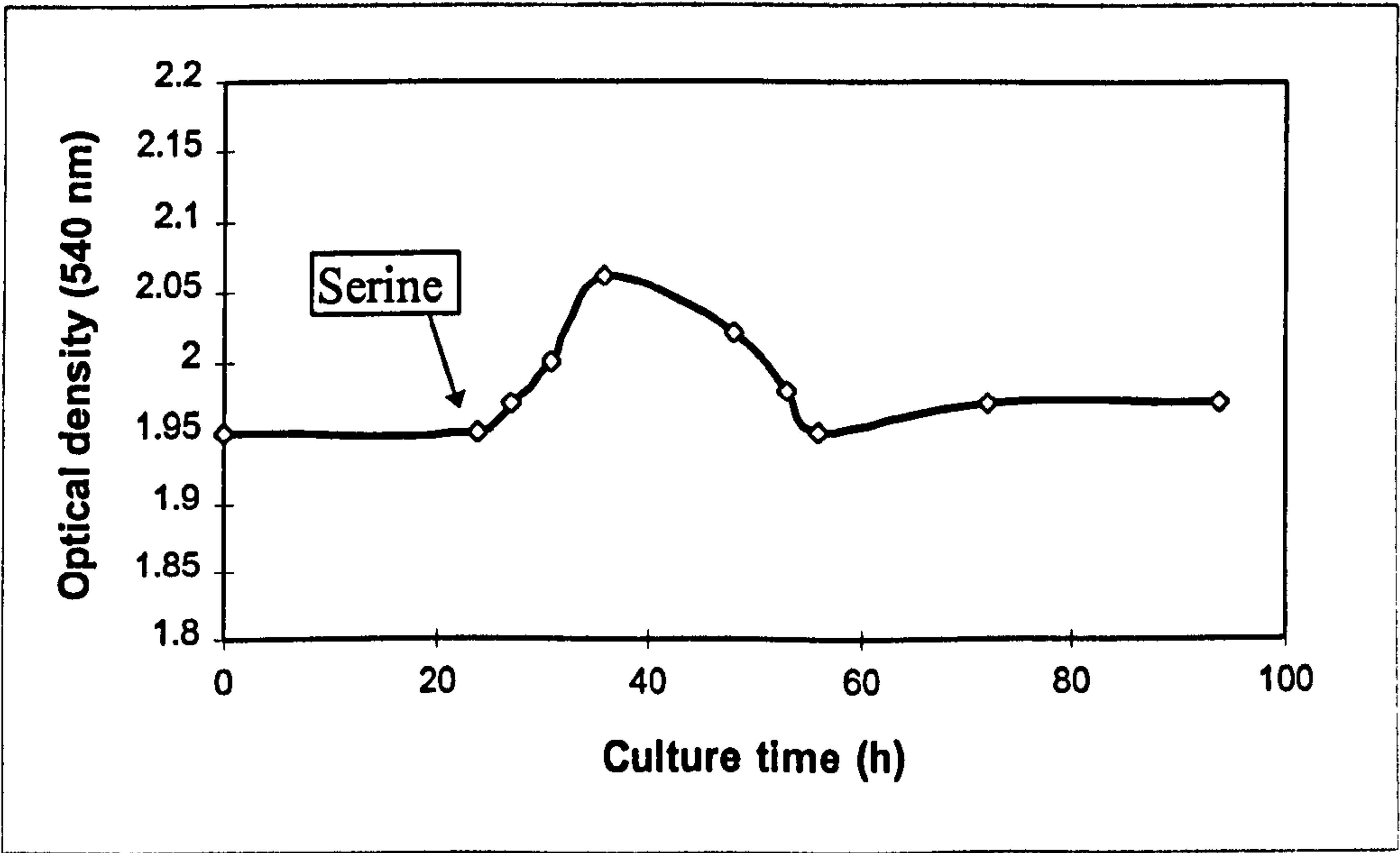


Figure 49. Growth response of a steady state pH 7.8 iron-replete culture of *L. pneumophila*, to the addition of 10 mM serine directly into the culture.

3.9.2 Nutrient utilization by iron-replete cultures grown at extremes of pH.

As previously demonstrated, growth at pH 6.9 depleted 10 amino acids, close to the limit of detection (Tables IV and XVII). When cultured at pH 6.0, 8 amino acids including serine, were depleted to ≤ 0.06 mM. A ratio of 1 : 0.9 was detected between serine metabolism and ammonium production. Growth at pH 7.8 depleted 9 amino acids to ≤ 0.06 mM (Table XVII). Serine utilization was comparable to the other cultures, with a stoichiometric ratio of 1 : 0.95 for ammonium production (Table XVII).

Figure 50 illustrates some of the key differences in amino acid metabolism between the different cultures. The metabolism of alanine and glutamate was enhanced at pH 6.0, while aspartate metabolism was increased at pH 7.8. The concentration of two amino acids, alanine and glycine, was elevated at pH 7.8, in comparison to the control uninoculated culture medium. Utilization of a number of amino acids, principally isoleucine, leucine, lysine, methionine, phenylalanine and threonine was reduced at the extremes of pH, in comparison to the pH 6.9 culture. However, of these amino acids, greater utilization was detected at pH 7.8 than at pH 6.0 (Figure 50). Trace elements remained in excess in all three cultures, with 3 to 5 μ M iron metabolised during growth (Table XVII).

3.9.3 Growth characteristics of iron-replete cultures at extremes of pH.

Table XVIII summarizes the effect of culture pH on the growth characteristics of iron-replete cultures. Quotients for the control pH 6.9 culture are comparable to those presented previously (Tables V and XVIII). Steady state growth properties were not significantly influenced by lowering the culture pH to 6.0, with culturability, optical density and biomass yield decreased by 10% (Table XVIII). Similarly, the molar growth yield for serine (Y_{serine}), was not significantly altered. A marginally greater decrease in Y_{carbon} (16%) was detected, possibly reflecting the increased

Table XVII. Comparison of the concentration of nutrients (mM)^a in unused ABCD medium and supernatant samples from and iron-replete culture grown at different pH values.

Nutrient	Unused medium	pH 6.0	pH 6.9	pH 7.8
Alanine	0.77	0.18	0.25	1.78
Arginine	0.29	ND ^b	ND	ND
Asparagine	0.48	ND	ND	0.01
Aspartate	0.39	0.38	0.18	0.09
Glutamate	0.5	ND	0.2	0.41
Glycine	0.83	0.64	0.42	1.03
Histidine	0.18	ND	ND	0.04
Isoleucine	0.58	0.16	ND	0.03
Leucine	0.77	0.36	0.04	0.06
Lysine	0.28	0.05	ND	0.01
Methionine	0.48	0.3	0.05	0.15
Phenylalanine	0.38	0.38	0.24	0.32
Proline	0.58	0.04	ND	ND
Serine	15.27	0.27	0.15	0.2
Threonine	0.62	0.19	0.1	0.14
Tyrosine	0.18	ND	ND	0.02
Valine	0.59	0.06	0.04	0.04
Iron	0.172	0.167	0.169	0.169
Phosphate	1.58	0.93	0.96	1.12
Zinc	0.1	0.09	0.09	0.09
Ammonium	4.8	18.0	19.7	19.2

^a Amino acid values are the mean concentrations calculated from analysis of 4 samples of unused medium, and three samples of culture supernatant for each growth condition. Results for trace elements represent the mean determination for 5 samples each. All standard deviations were less than 15% of the mean.

^b ND, Below the limit of detection.

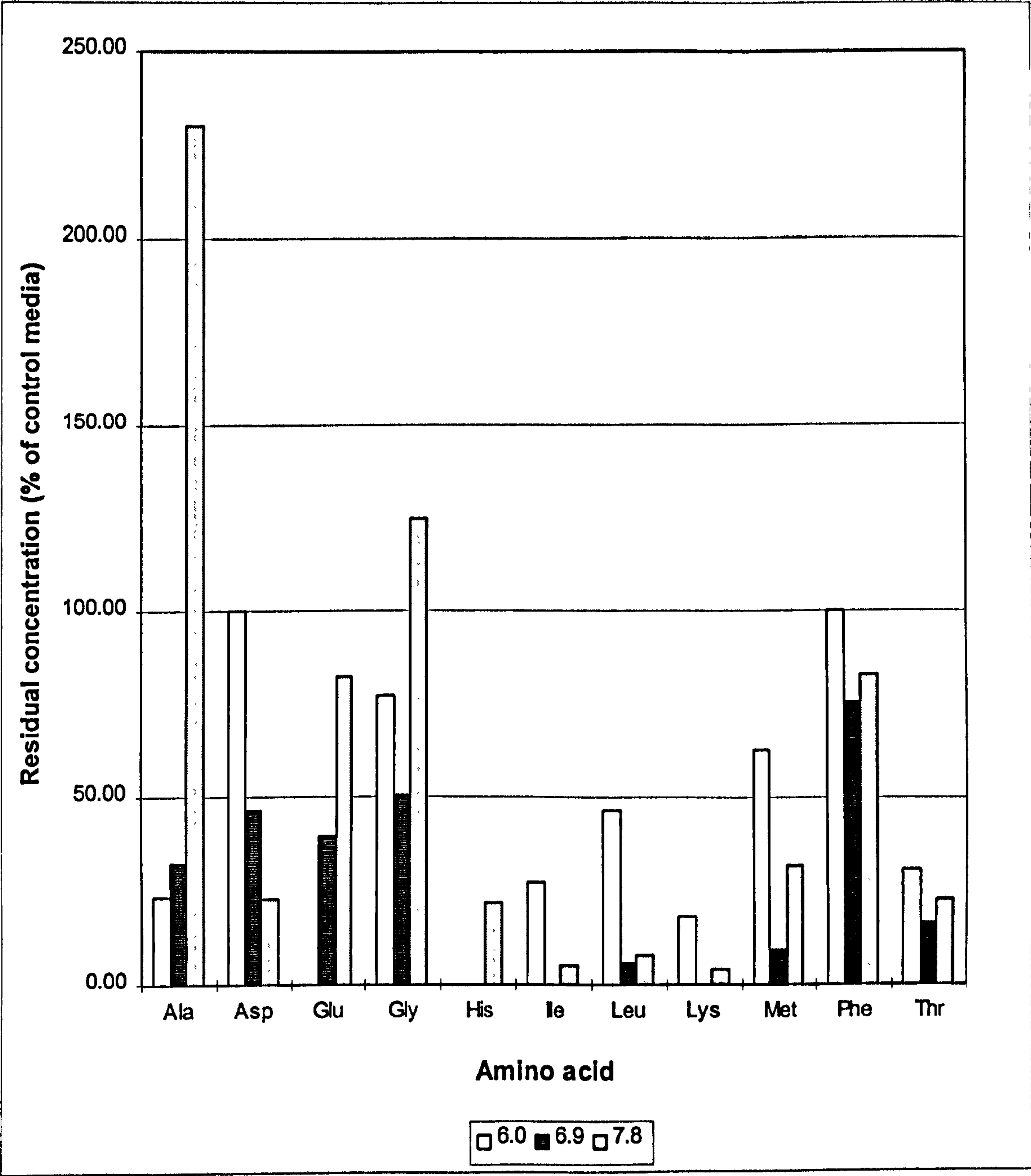


Figure 50. Comparison of residual amino acid concentrations in samples of clarified supernatant, collected from iron-replete cultures of *L. pneumophila* grown at different pH values.

Values represent the mean residual concentration present in the culture supernatants, expressed as a percentage of the concentration present in uninoculated culture medium.

utilisation of glutamate and alanine, as discussed in Section 3.9.2. A more pronounced 55% decrease in the molar growth yield for iron (Y_{iron}), was calculated.

Increasing the culture pH to 7.8 had a more dramatic physiological impact, with steady state biomass yield and turbidity reduced by 30 and 40 %, respectively. More significantly, an 80% decrease in culturability was detected (Table XVIII). The molar growth yield for serine, (Y_{serine}), was reduced by 30% in comparison to the pH 6.9 culture. However, only a 7% decrease in the molar growth yield for carbon metabolised (Y_{carbon}), was demonstrated. Iron analyses also indicated reduced metabolic efficiency at pH 7.8, with Y_{iron} diminished by 30% (Table XVIII). Phosphate utilisation was not significantly influenced by culture pH.

3.10 Influence of pH on the Morphology of Iron-Replete cultures.

3.10.1 Cellular morphology.

The influence of culture pH on the cellular morphology of *L. pneumophila* was monitored by DIC microscopy (Section 2.6.1). Iron-replete cells grown at pH 6.9 were previously demonstrated to be pleomorphic (Figure 12). Decreasing the culture pH to 6.0 resulted in a loss of pleomorphism, producing suspensions of short rods between 2 to 4 μm in length (Figure 51a). Cultures grown at pH 7.8 retained their pleomorphic features, however the majority of the cells were approximately 4 to 5 μm long, with the occasional cell extending to 20 μm . The long filamentous forms observed at pH 6.9, were not detected at pH 7.8. Many of the cells appeared slightly curved (Figure 51b).

Table XVIII. Comparison of the growth properties of iron-replete chemostat cultures grown at pH 6.9, 6.0 and 7.8.

Growth characteristic	pH 6.9 ^a	pH 6.0 ^b	pH 7.8 ^b
OD ₅₄₀	3.5	3.3	2.1
Biomass (g dry wt. l ⁻¹)	1.3	1.2	0.9
c.f.u ml ⁻¹ (× 10 ⁹) ^c	5.8 ± 0.5	5.3 ± 0.4	1.3 ± 0.6
<i>Y</i> _{serine} (g mol ⁻¹)	86	80	61
<i>Y</i> _{carbon} (g mol ⁻¹) ^d	4.4	3.7	4.1
<i>q</i> _{carbon} (mmol g ⁻¹ h ⁻¹) ^d	18.0	21.0	19.5
Iron metabolised (μmol l ⁻¹)	3	5	3
<i>Y</i> _{iron} (× 10 ⁵ g mol ⁻¹)	4.3	2.4	3.1
<i>q</i> _{iron} (× 10 ⁻⁵ mmol g ⁻¹ h ⁻¹)	18.0	33.3	26.1
<i>Y</i> _{Phosphate} (× 10 ³ g mol ⁻¹)	2.09	1.85	2.04

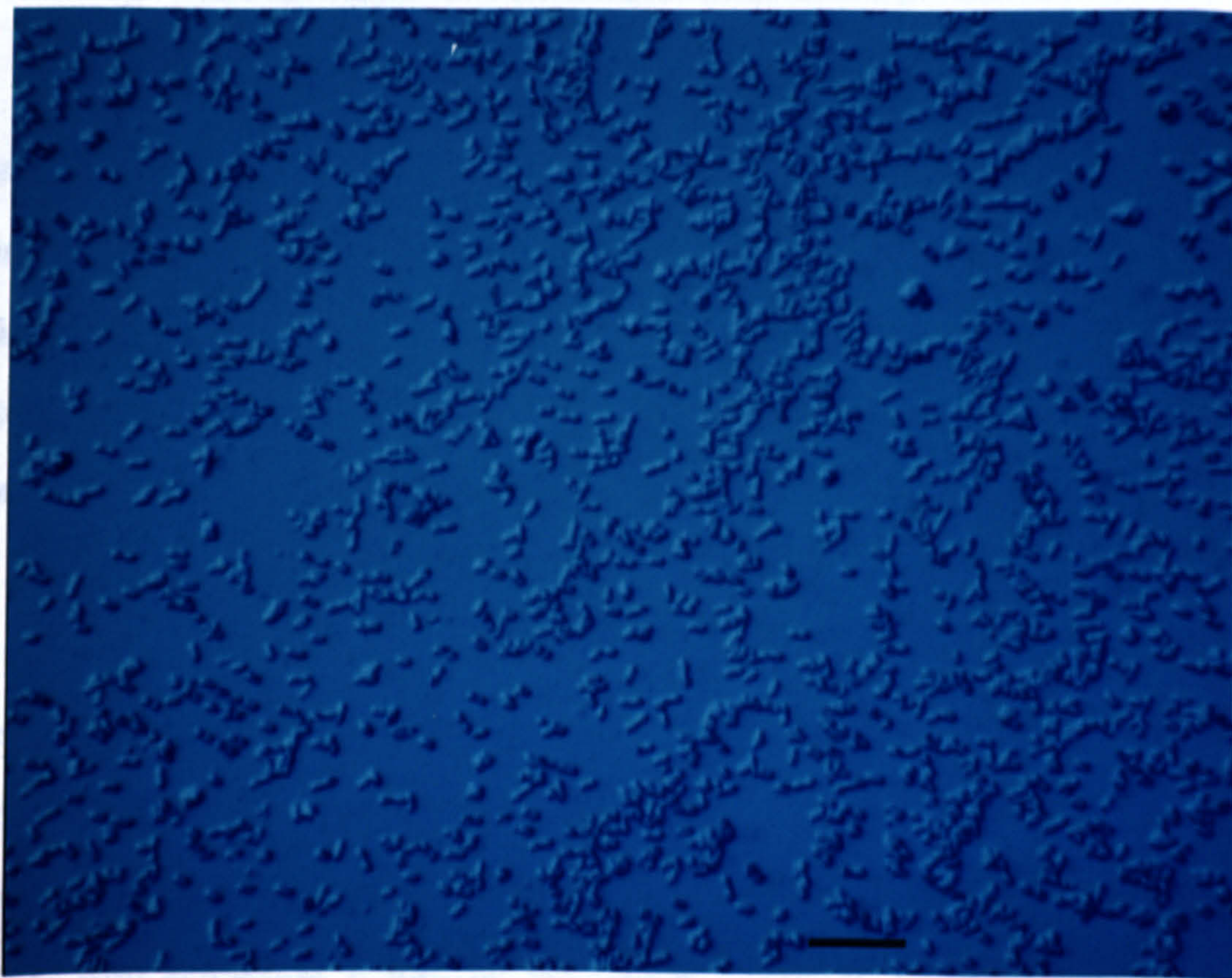
^a Values for pH 6.9 cultures represent the mean values calculated from 4 separate steady state cultures.

^b Values for pH 6.0 and 7.8 cultures are based on analysis of two steady state cultures.

^c ± Standard error of the mean.

^d Calculated from total organic carbon analysis performed on samples of clarified culture supernatant and uninoculated medium (see Section 2.5.4). Values are the mean of at least 4 separate determinations.

(a)



(b)

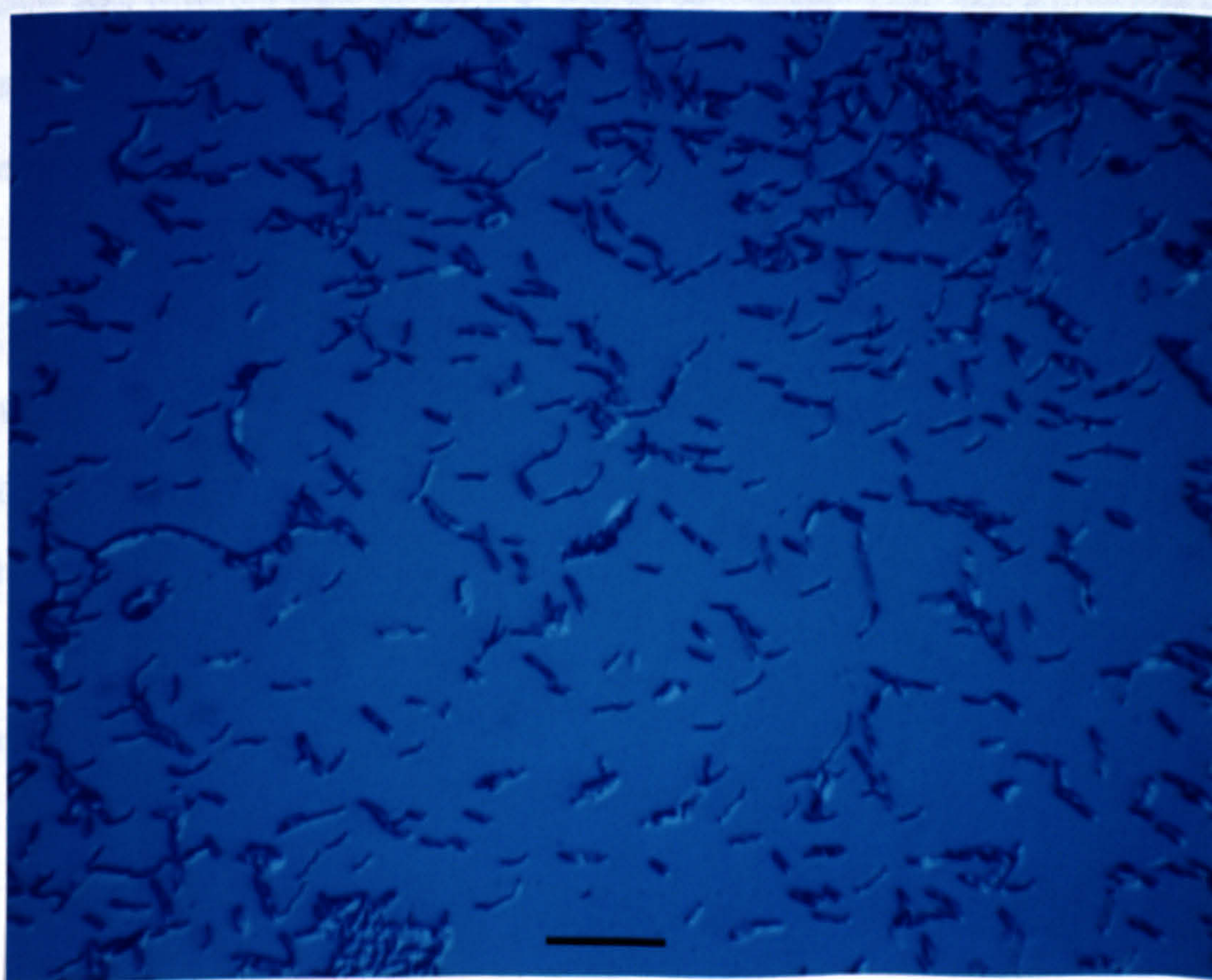


Figure 51. Cellular morphology of iron-replete cultures of *L. pneumophila* grown at (a) pH 6.0, and (b) pH 7.8, as viewed by DIC microscopy. Bar, 10 μm .

3.10.2 Colony morphology.

The colony morphology of culture samples grown on BCYE agar was monitored. No morphological changes were detected during the first pH 6.0 chemostat run. However, during the second pH 6.0 experiment, a small colony variant (SCV) was selected. On 4-day old BCYE agar cultures, normal colonies were 3 to 4 mm in diameter, however, the variant colonies were considerably smaller, at approximately 1.5 to 2.0 mm in diameter (Figure 52a).

Appearance of the SCV, coincided with the recovery in culture turbidity after the pH had been decreased to pH 6.0, as illustrated in Figure 46. Over a period of 7 days, the number of variant colonies increased steadily, until they reached 95% of the population. The culture composition of 95% SCV and 5% normal colony type, remained stable during subsequent steady state growth, for 14 days. The culture still reacted with serogroup 1 specific polyclonal antiserum (Figure 52b). When the culture was reverted back to pH 6.9, the normal colony type became re-established over a period of approximately 7 days, and the SCV decreased below the limit of detection.

Changes in colony morphology were also observed at elevated pH. During the first experiment, a small colony variant became apparent as the culture adapted to growth at pH 7.4 (Figures 53). This variant population increased to represent approximately 40% of the culture, but declined below the limit of detection as the culture entered a steady state at pH 7.8. The colony morphology remained normal for the rest of the experiment. During a repeat experiment, no alteration in colony morphology was observed.

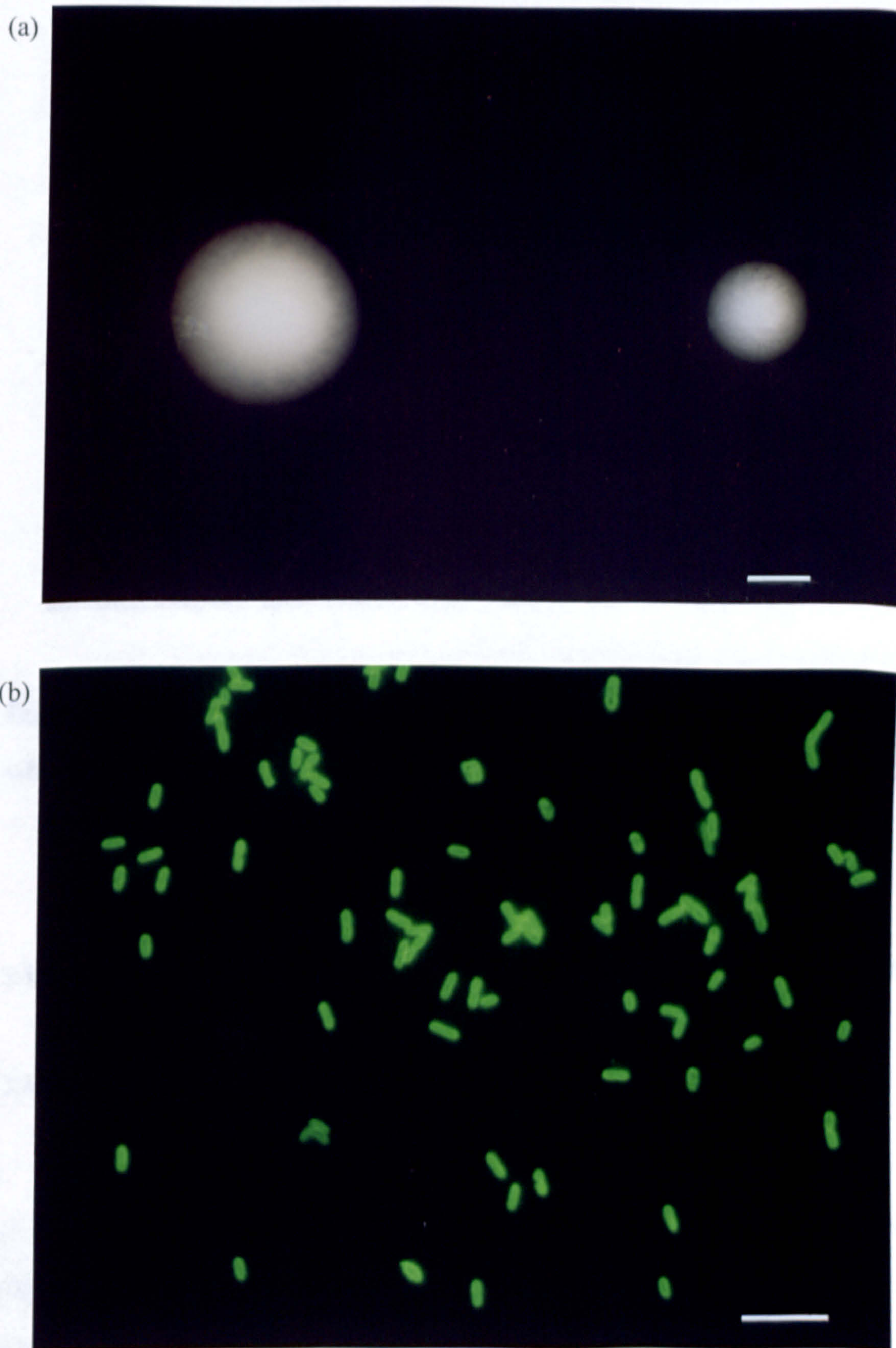


Figure 52. (a) Normal and variant colony morphologies of iron-replete pH 6.0 cells, when grown on BCYE agar for 4 days at 37°C (Bar, 1 mm); (b) indirect fluorescent antibody staining of the pH 6.0 chemostat culture with serogroup 1 specific polyclonal antiserum (Bar, 10 μ m).

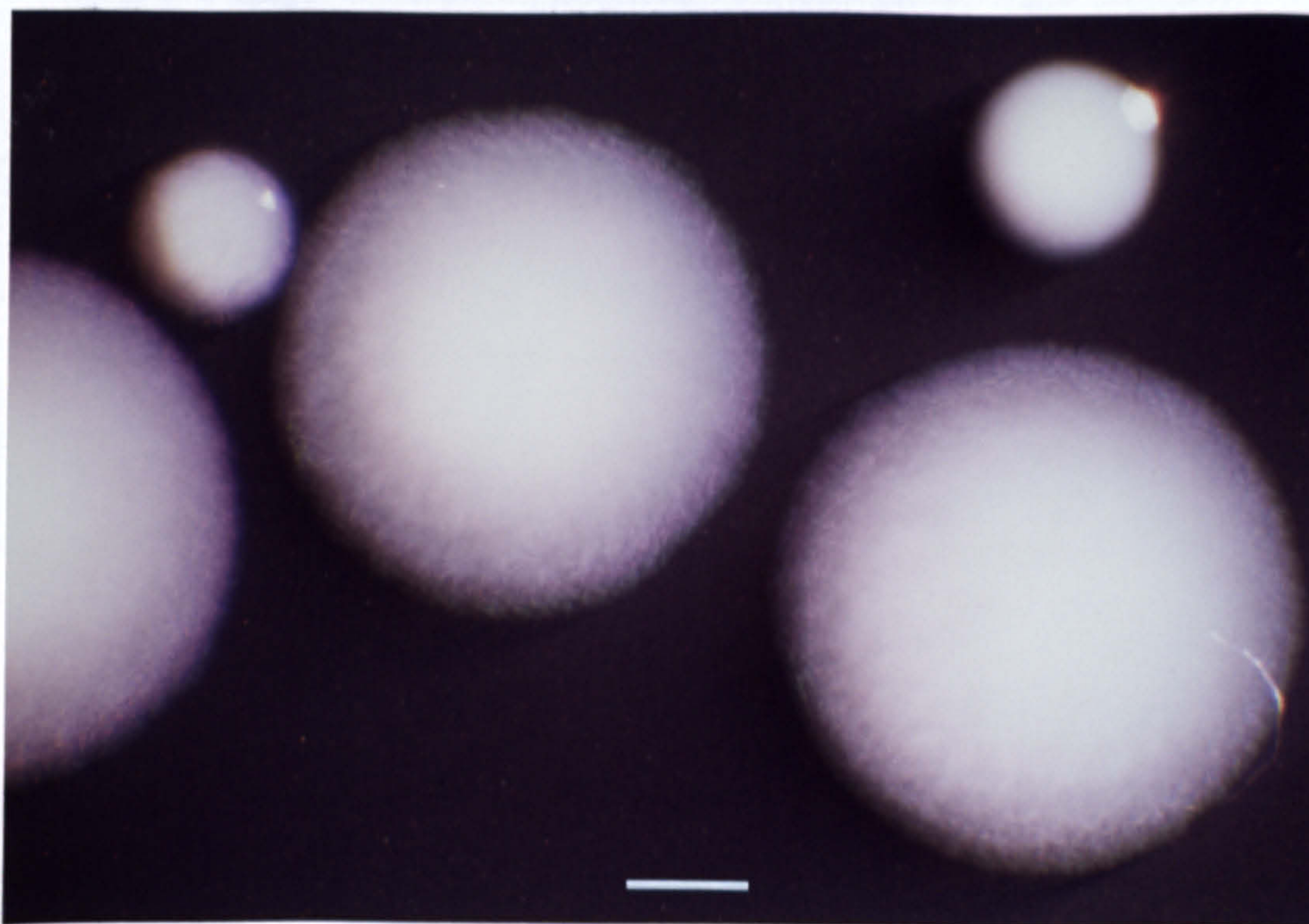


Figure 53. Normal and variant colony morphologies of iron-replete pH 7.4 cells, when grown on BCYE agar for 4 days at 37°C. Bar, 1 mm.

3.11 Influence of Culture pH on the Physiology of Iron-limited *L. pneumophila*.

3.11.1 Growth response of iron-limited cultures to low and high pH.

Decreasing the pH from 6.9 to 6.0 also had a major impact on the steady state growth of iron-limited cultures. As the pH was lowered, a slight increase in culture turbidity was observed at pH 6.4 (Figure 54). Reducing the pH further to 6.0 caused a transient decline in turbidity, before the culture recovered to a steady state turbidity 35% lower than that observed at pH 6.9 (Figure 54). Pulsing the steady state pH 6.0 culture with 2.5µM ferrous sulphate, stimulated an increase in culture turbidity, confirming iron as the growth-limiting nutrient (Figure 55).

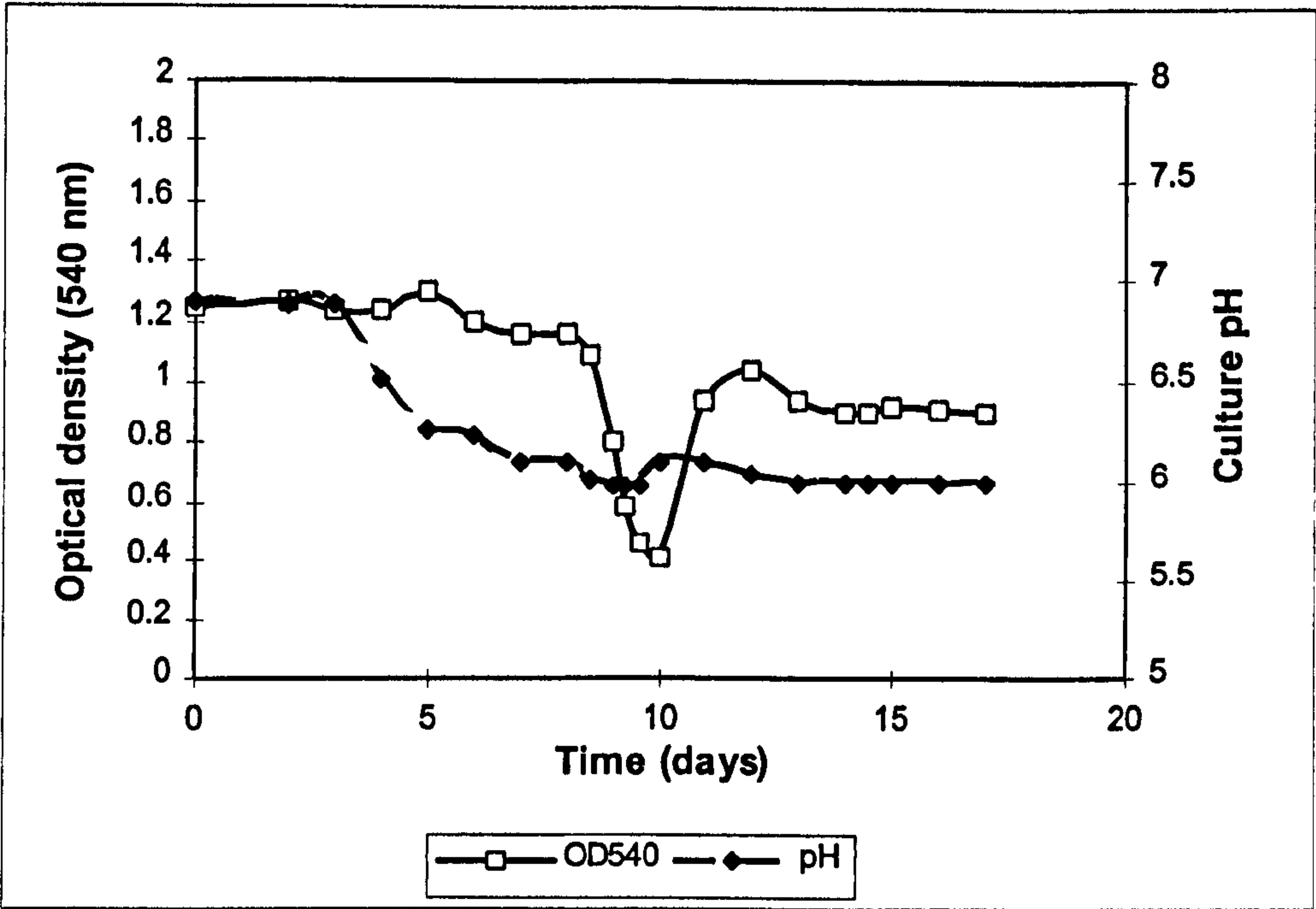


Figure 54. Growth response of a steady state iron-limited chemostat culture of *L. pneumophila* to an incremental decrease in culture pH from 6.9 to 6.0.

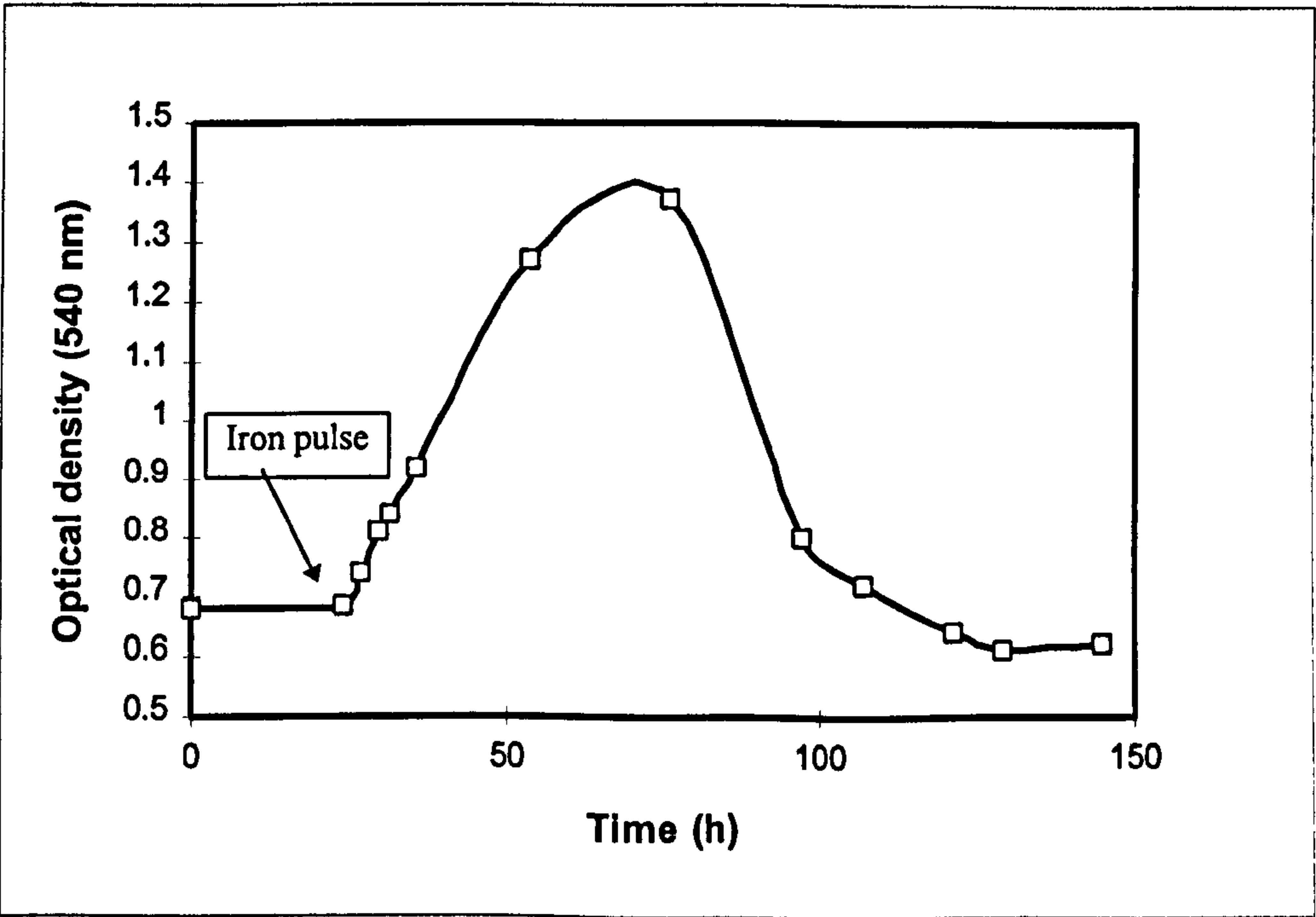


Figure 55. Growth response of a steady state iron-limited (pH 6.0) chemostat culture to the addition of 2.5 μ M ferrous sulphate directly into the culture.

The growth response of steady state iron-limited cultures to an increase in culture pH, was similar to that observed with the replete culture (Figures 48 and 56). A modest pH increase of 0.4 pH units, stimulated a transient decline in culture turbidity, followed by recovery to 50% of the original value. Increasing the culture pH further to 7.8 stimulated a further decline, to produce a final steady state density 60% lower than observed at pH 6.9. Pulsing the steady state pH 7.8 culture with ferrous sulphate (2.5 μ M) produced an increase in culture turbidity, confirming iron as the growth-limiting nutrient (Figure 57).

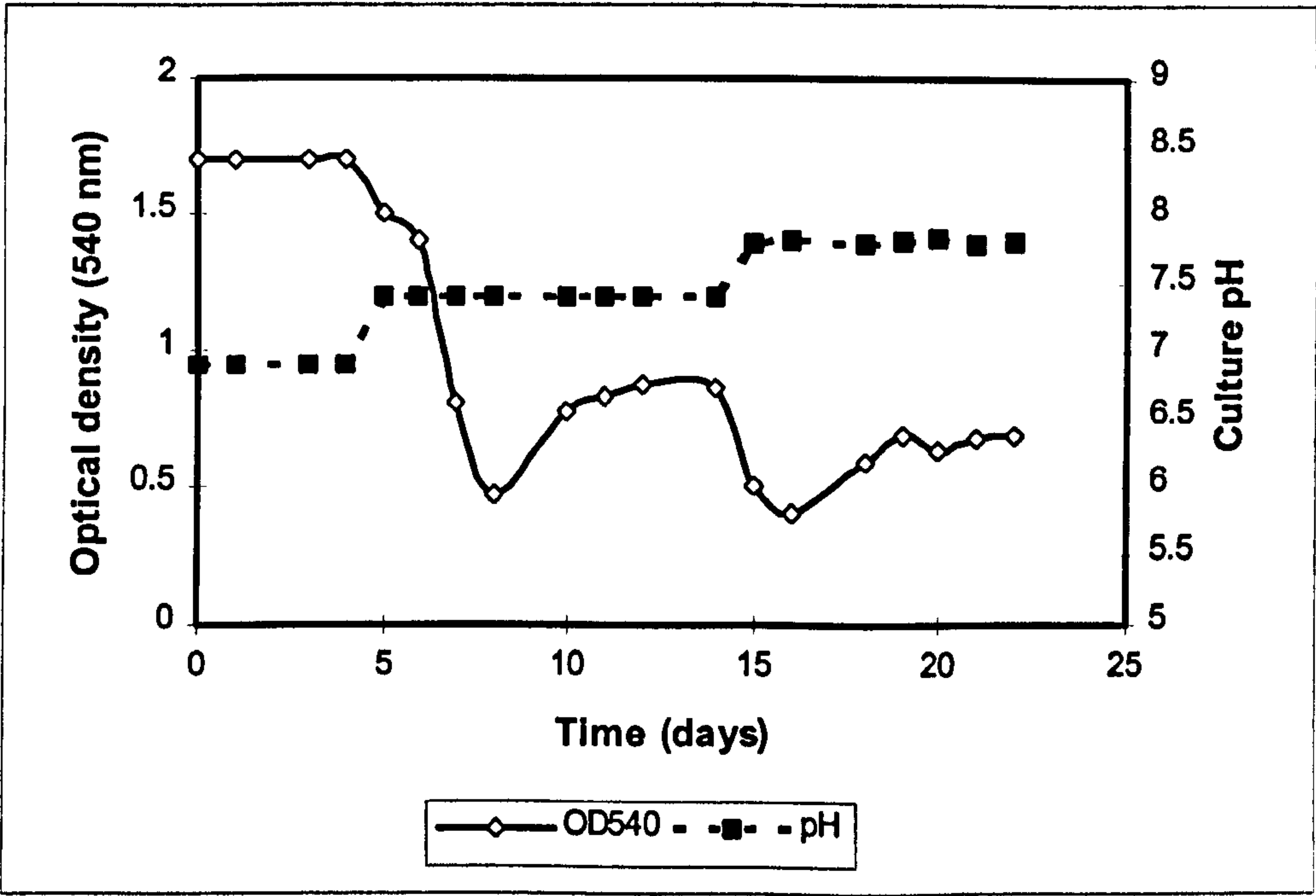


Figure 56. Growth response of a steady state iron-limited chemostat culture of *L. pneumophila* to an incremental increase in culture pH from 6.9 to 7.8.

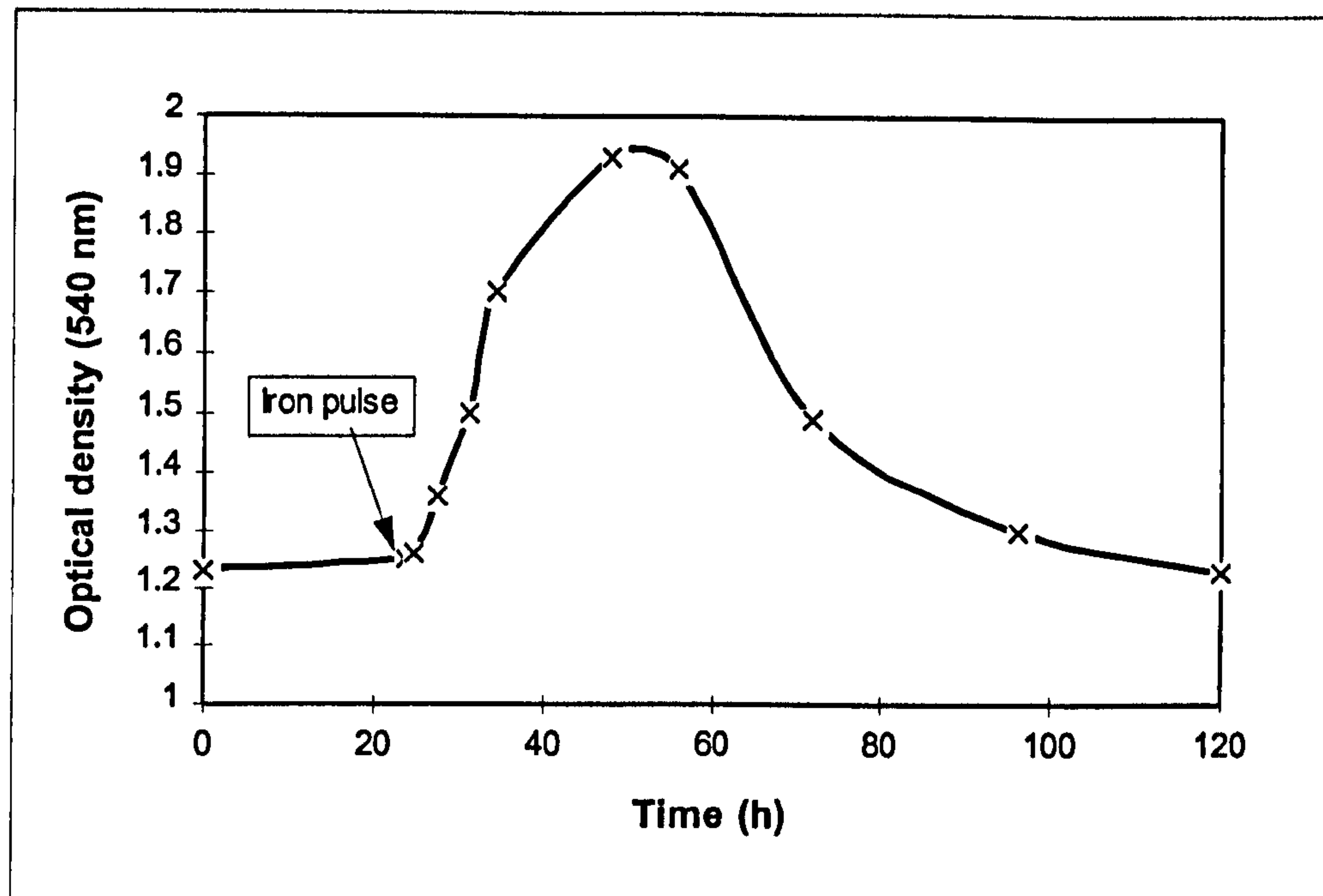


Figure 57. Growth response of a steady state iron-limited (pH 7.8) chemostat culture of *L. pneumophila* to the addition of 2.5 μ M ferrous sulphate.

3.11.2 Nutrient utilization by iron-limited cultures at different pH values.

As previously demonstrated (Section 3.1.3), under iron-limited conditions at pH 6.9, the majority of amino acids including serine remained in excess (Table XIX). At pH 6.0, all amino acids remained in excess, with only arginine, asparagine and glutamine depleted to less than 50% of their original concentration (Table XIX and Figure 58). With the exception of glutamate and glycine, utilization of all amino acids was significantly reduced in comparison to the pH 6.9 culture. Metabolism of serine was reduced by 50 %, however, a molar ratio of 1:1.1 was calculated for serine utilization and ammonium production (Table XIX and Figure 58).

By contrast, at pH 7.8 many amino acids were utilized to a comparable or greater extent than in the control pH 6.9 culture. In particular, serine, arginine, asparagine and aspartate utilization was enhanced. A ratio of 1 : 0.86 was determined for serine metabolism and ammonium release. As observed with iron-replete cultures (Section 3.9.2), the concentration of both alanine and glycine was elevated in response to increased culture pH (Table XIX and Figure 58).

Table XIX. Comparison of the concentration of nutrients (mM)^a in unused culture medium and iron-limited cultures grown at different pH values

Nutrient	Unused Medium	pH 6.0	pH 6.9	pH 7.8
Alanine	0.9	1.11	1.34	1.84
Arginine	0.37	0.18	0.1	0.07
Asparagine	0.57	0.19	0.07	0.01
Aspartate	0.41	0.33	0.18	0.13
Glutamate	0.64	0.11	0.26	0.71
Glycine	1.02	0.89	0.95	1.25
Histidine	0.29	0.25	0.1	0.1
Isoleucine	0.72	0.61	0.23	0.26
Leucine	0.89	0.83	0.35	0.38
Lysine	0.22	0.22	0.11	0.16
Methionine	0.65	0.73	0.35	0.41
Phenylalanine	0.36	0.36	0.24	0.25
Proline	0.7	0.49	ND ^b	0.02
Serine	15.58	10.12	5.17	3.18
Threonine	0.73	0.6	0.36	0.34
Tyrosine	0.22	0.2	0.1	0.1
Valine	0.67	0.57	0.37	0.47
Phosphate	2.55	2.41	2.3	2.0
Zinc	0.10	0.1	0.1	0.09
Ammonium	4.5	10.4	12.3	15.2

^a Results represent the mean values calculated from analysis of 4 samples of unused medium and three samples of culture supernatant under each condition. All standard deviations were less than 15% of the mean.

^b ND, below the limit of detection.

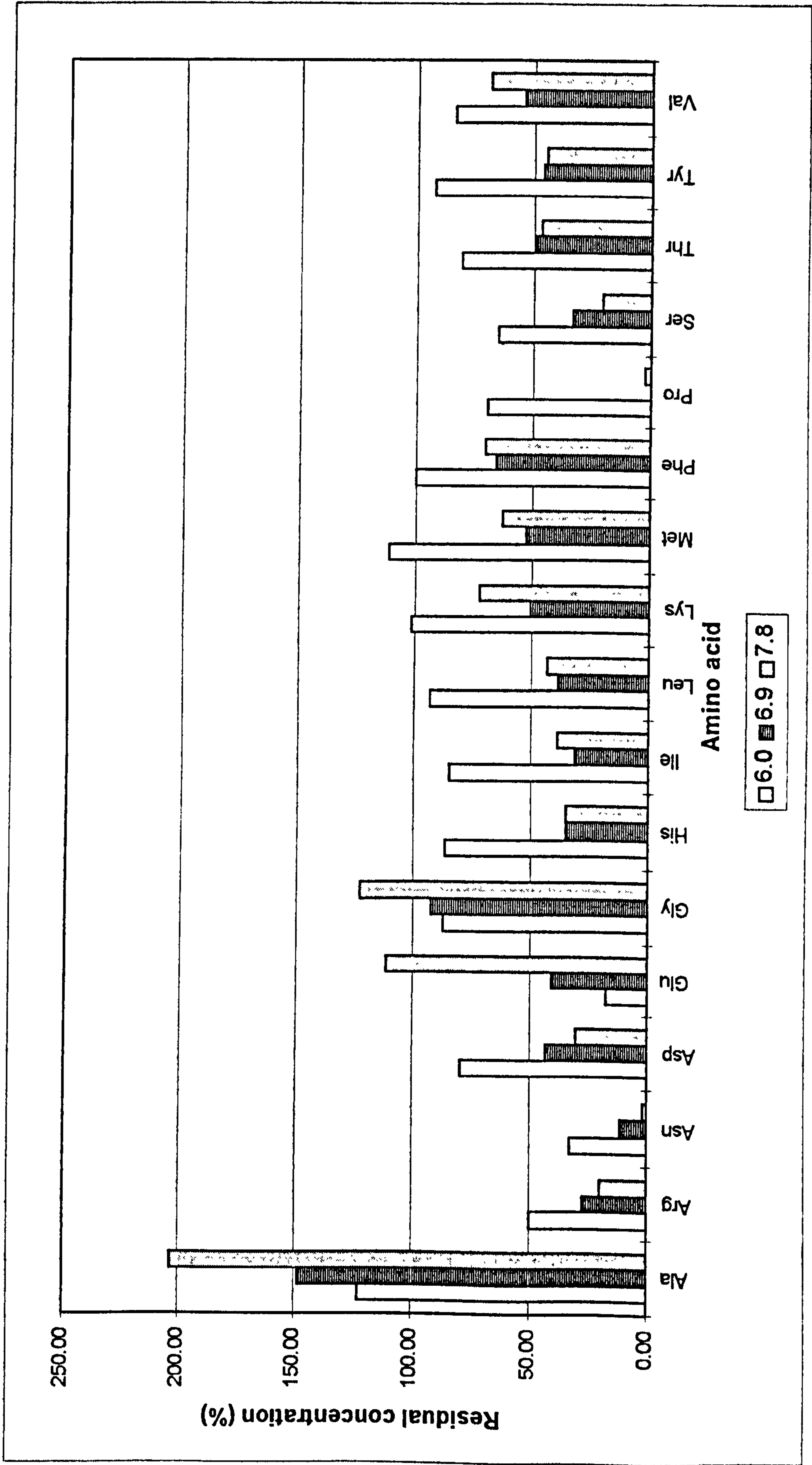


Figure 58. Comparison of residual amino acid concentrations in samples of clarified supernatant collected from iron-limited cultures of *L. pneumophila* grown at different pH values. Values represent the mean residual concentration present in the culture supernatants expressed as a percentage of the concentration present in uninoculated culture medium.

3.11.3 Growth characteristics of iron-limited cultures at extremes of pH.

Decreasing the pH of iron-limited cultures to 6.0 had a more dramatic physiological impact than observed with replete cultures (Section 3.9.3). Culture viability and biomass yield were reduced by 65 and 40%, respectively, in comparison to the control pH 6.9 culture (Table XX). Serine metabolism was also reduced, resulting in a 15% increase in the molar growth yield for serine (Y_{serine}). Carbon analysis revealed a more significant 30% decrease in the yield coefficient for carbon metabolised, and a corresponding increase in the specific metabolic rate (q_{carbon}). The metabolic quotients for iron (Y_{iron} and q_{iron}) also indicated reduced metabolic efficiency, with a 15% decrease in the molar growth yield for iron (Table XX).

Biomass yield and culture turbidity also declined dramatically in response to elevated pH. As observed under iron-replete conditions (Section 3.9.3), the most dramatic change was in culturability, with a 90% decrease observed (Table XX). The metabolic efficiency of the culture was also diminished, with 55 and 35% decreases recorded for Y_{serine} and Y_{carbon} , respectively, correlating with increased metabolic activity (q_{carbon}). Iron analysis revealed a 6-fold decrease in the yield coefficient for iron metabolised (Y_{iron}). Furthermore, the molar growth yield for phosphate was reduced 4-fold in response to elevated pH (Table XX).

Table XX. Comparison of the growth properties of iron-limited cultures of *L. pneumophila* grown at pH 6.9, 6.0, and 7.8.

Growth characteristic	pH 6.9 ^{ab}	pH 6.0 ^a	pH 6.9 ^{ab}	pH 7.8 ^a
OD ₅₄₀	1.3	0.9	1.63	0.67
Biomass (g dry wt. l ⁻¹)	0.7	0.42	0.75	0.4
c.f.u ml ⁻¹ (× 10 ⁸) ^c	17.8 ± 0.3	6.4 ± 0.6	13.5 ± 0.3	1.6 ± 0.4
<i>Y</i> _{serine} (g mol ⁻¹)	67	77	71	32
<i>Y</i> _{carbon} (g mol ⁻¹) ^d	4.0	2.9	4.4	2.8
<i>q</i> _{carbon} (mmol g ⁻¹ h ⁻¹) ^d	20	27.6	18	28.5
Iron metabolised (μmol l ⁻¹)	0.28	0.2	0.22	0.72
<i>Y</i> _{iron} (× 10 ⁵ g mol ⁻¹)	25	21	34	5.55
<i>q</i> _{iron} (× 10 ⁻⁵ mmol g ⁻¹ h ⁻¹)	3.2	3.8	2.3	14.4
<i>Y</i> _{Phosphate} (× 10 ³ g mol ⁻¹)	2.8	3.0	3.0	0.72

^a Each set of data represents steady state values for a single culture.

^b Properties of steady state culture, prior to altering the culture pH.

^c ± Standard error of the mean.

^d Calculated from total carbon analysis of samples of clarified culture supernatant and uninoculated culture medium (Section 2.5.4). Values represent the mean of at least 3 determinations.

3.12 Influence of pH on the Morphology of Iron-Limited *L. pneumophila*.

3.12.1 Cellular morphology.

Iron-limited cultures of short rods, 3 to 5 μm long, became more pleomorphic at pH 6.0, with cells ranging from 1.5 to 5 μm in length. A high proportion of cells appeared as coccobacilli, approximately 2 μm in length (Figure 59). Indirect fluorescent antibody staining with serogroup 1 specific polyclonal antiserum (Section 2.6.3), revealed no alteration in serogroup reactivity (Figure 60). Iron-limited cells grown at pH 7.8 were more uniform in size, approximately 3 to 5 μm in length, and comparable to the control pH 6.9 culture. The curved appearance observed in iron-replete pH 7.8 cultures (Section 3.10.1), was more pronounced under iron-limited conditions, with many cells appearing sickle-shaped (Figure 61).

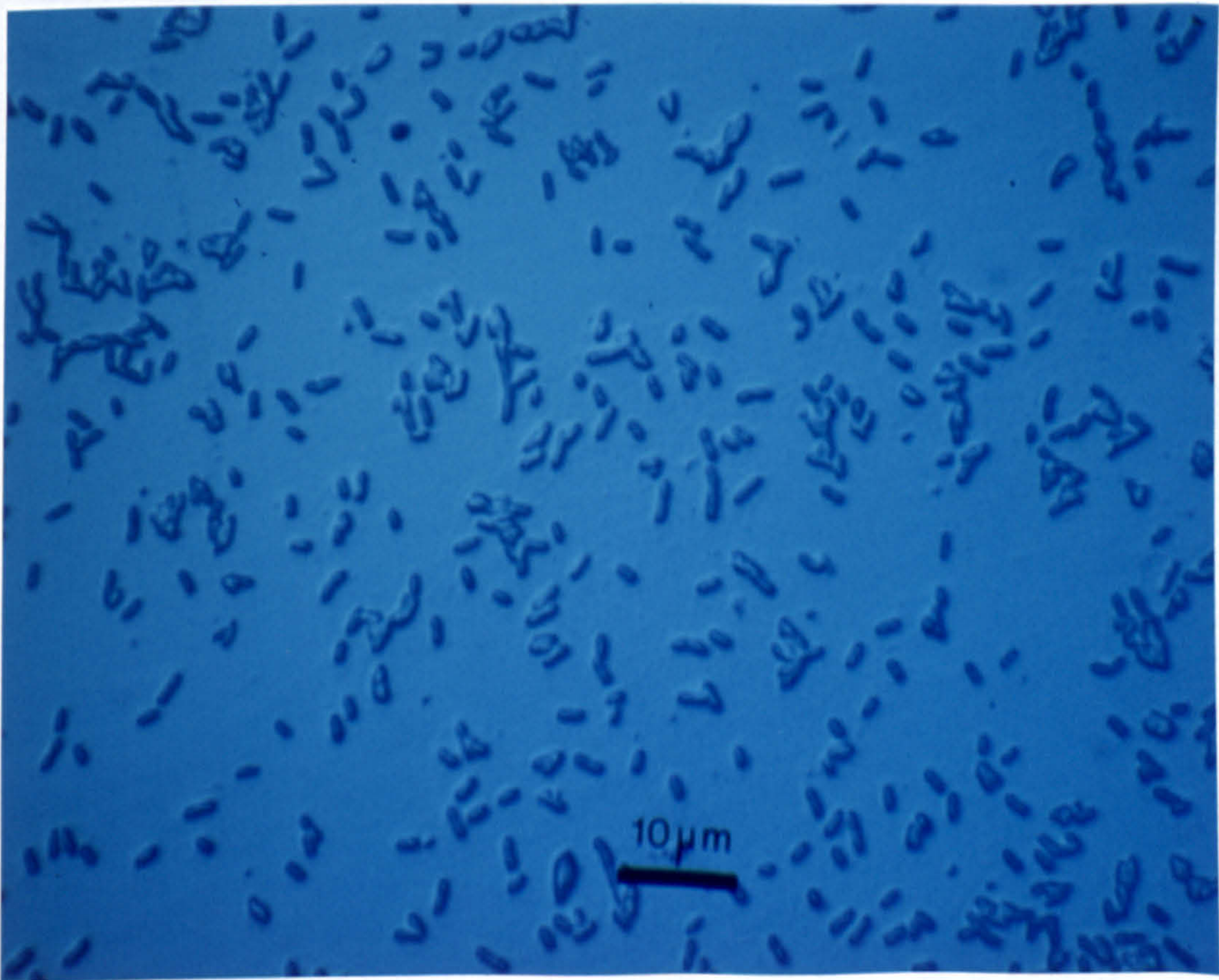


Figure 59. Cellular morphology of *L. pneumophila* cultured under iron-limited conditions at pH 6.0, as viewed by DIC microscopy.

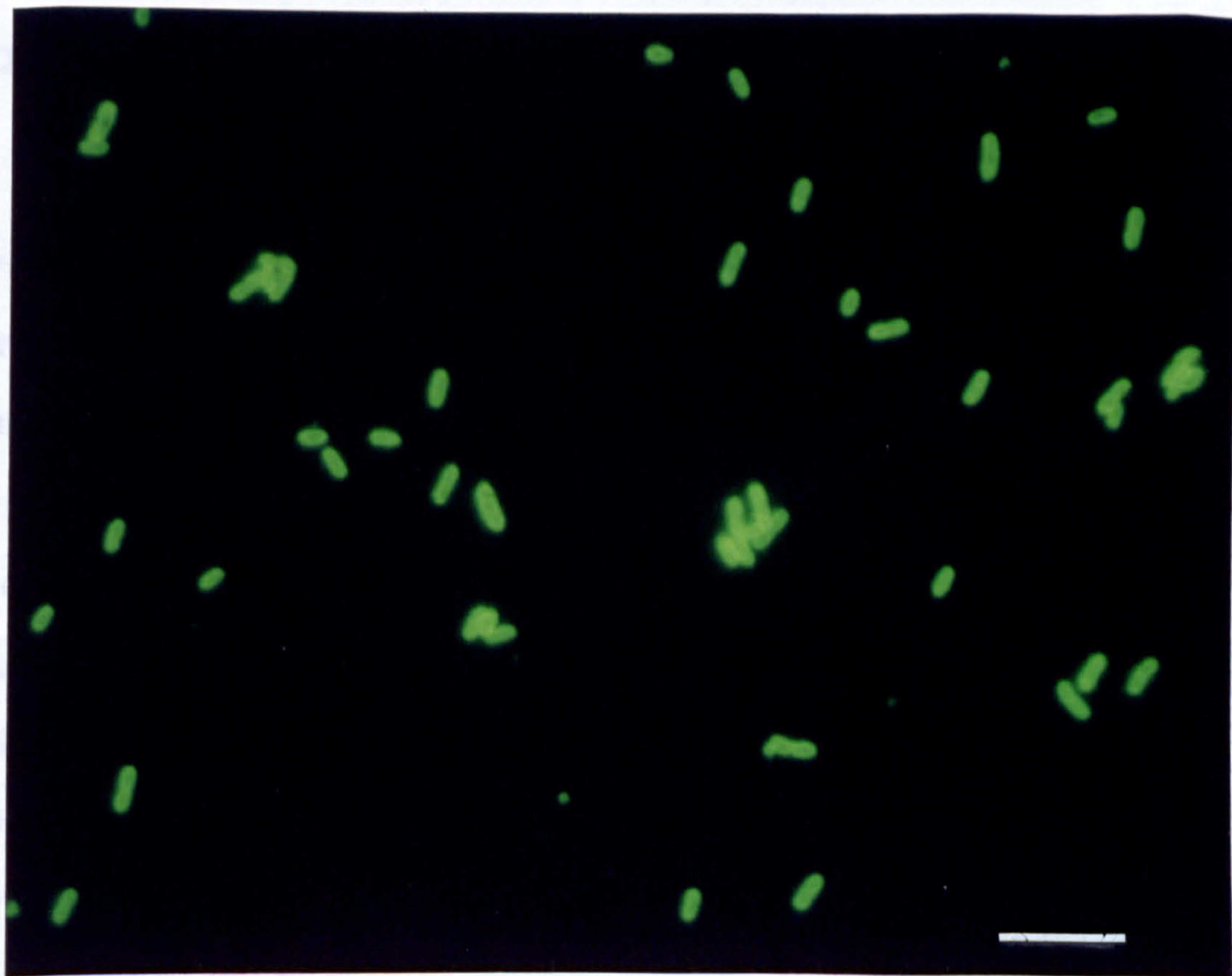


Figure 60. Indirect fluorescent antibody labelling of iron-limited pH 6.0 cultures of *L. pneumophila* with serogroup 1 specific polyclonal antiserum. Bar, 10 μm .

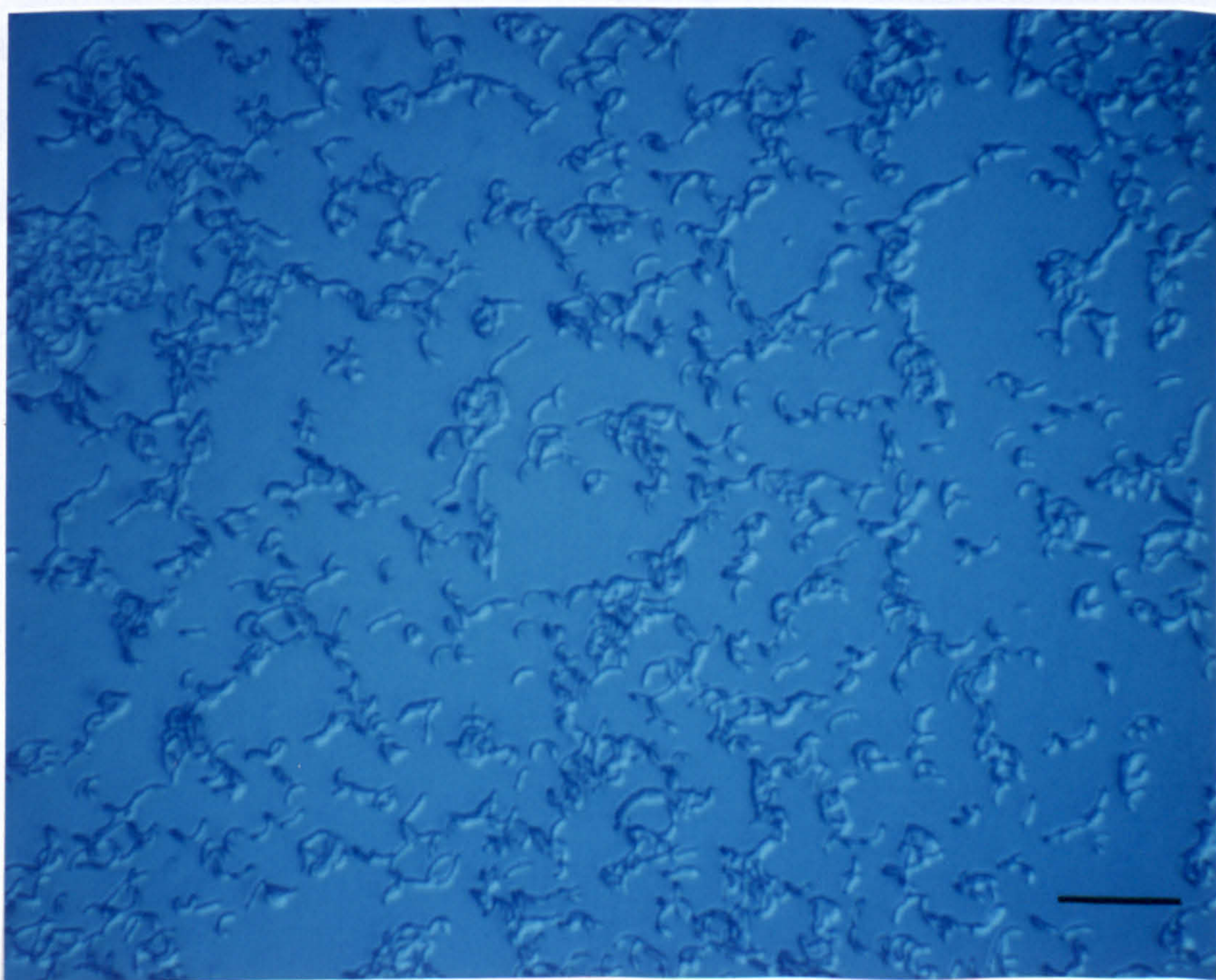


Figure 61. Cellular morphology of *L. pneumophila* cultured under iron-limited conditions at pH 7.8, as viewed by DIC microscopy. Bar, 10 μm .

3.12.2 Colony morphology.

During iron-limited growth at pH 6.0, a small colony variant (SCV) was observed on BCYE agar cultures of chemostat samples, collected 7 days after the culture entered steady state. As with iron-replete pH 6.0 cultures (Section 3.10.2), the variant colony was approximately 50% smaller in diameter than the normal colony type, and steadily increased in numbers over a two week period to finally represent 98% of the culture (Figure 62a). Cells representing both normal and variant colony types, from 4-day old BCYE agar cultures, reacted with serogroup 1 specific polyclonal antiserum. Cells from the normal colony type were pleomorphic, ranging between 5 to 10 μm in length (Figure 63a). Cells from the SCV were more variable in length, ranging from 2 to approximately 100 μm long (Figure 63b). The small colony phenotype remained stable for three successive passages on BCYE agar.

During a repeat experiment another variant, similar in size to the normal colony type, was observed. Colony colour was the most distinguishing feature, with the variant possessing a light centre and a darker outer rim (Figure 62b). The variant population did not increase above 35% of the total population. Changes in colony morphology were not observed during iron-limited growth at pH 7.8.

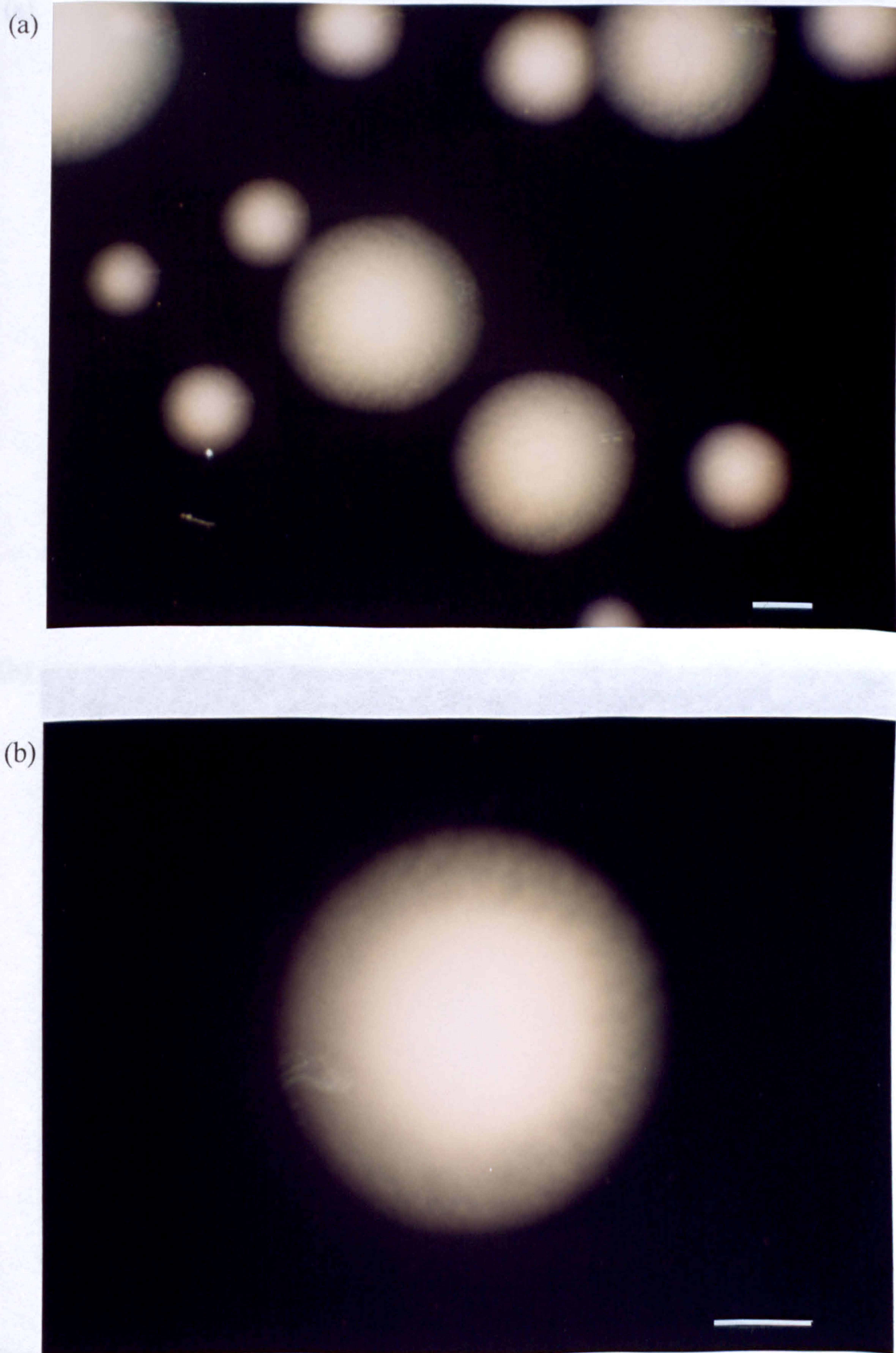


Figure 62. Normal and variant colony morphologies observed in iron-limited pH 6.0 cultures, when grown on BCYE agar for 4 days at 37°C, (a) small colony variant; (b) normal sized variant with a light coloured centre. Bar, 1 mm.

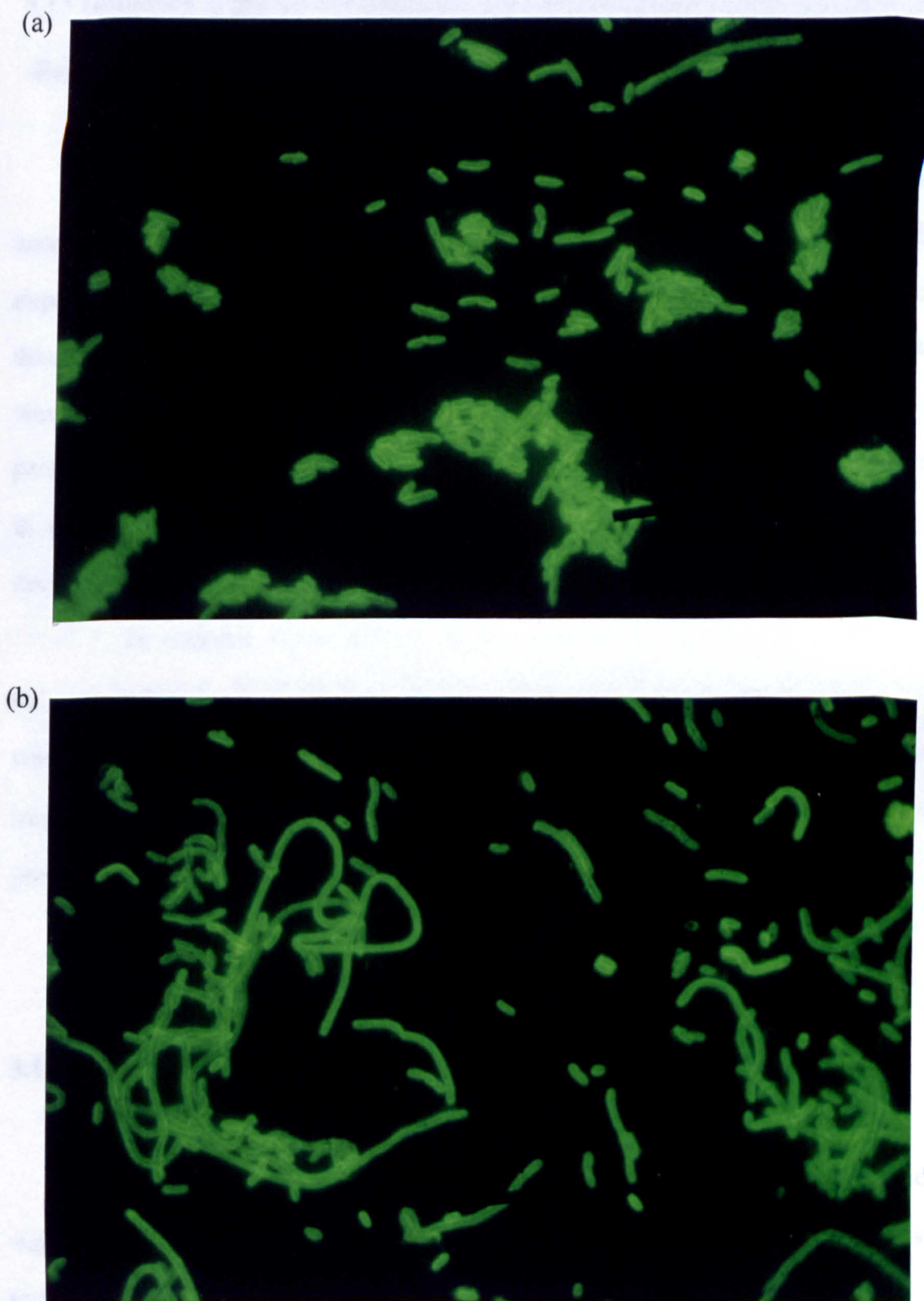


Figure 63. Indirect fluorescent antibody staining of cells from normal and variant colonies observed during growth of iron-limited pH 6.0 culture samples on BCYE agar, (a) normal; (b) small variant colony type.

3.13 Influence of pH on Extracellular Protein Production by Iron-Limited and -Replete Cultures.

The BioRad protein assay was used to determine the extracellular protein content of samples of clarified culture supernatant (Section 2.7). Protein yields are expressed as μg protein per mg cell dry weight, to allow for differences in culture density. Extracellular protein production by both iron-limited and -replete cultures, was reduced markedly by decreasing the culture pH to 6.0 (Table XXI). The most pronounced decrease was detected with iron-replete cultures, with a 10-fold decrease in extracellular protein yield. Under iron-limited conditions, the protein yield was decreased 3-fold (Table XXI).

In contrast to the effects of low pH, increasing the pH of iron-replete cultures, induced a 2-fold increase in extracellular protein yield, while a 40% increase was detected in iron-limited cultures (Table XXI). The protein content of control iron-limited and -replete cultures grown at pH 6.9, was comparable to values reported previously (Tables VII and XXI).

3.14 Influence of pH on Expression of Azocasein Hydrolytic Activity.

The azocasein hydrolytic activity (Section 2.10.1) of control iron-limited and -replete cultures (pH 6.9) was comparable to values presented previously (Tables VIII and XXII), with iron limitation reducing activity markedly. Culture pH also influenced enzyme activity (Table XXII). The hydrolytic activity of iron-replete cultures was diminished by 50% and 30%, when cultured at pH 6.0 and 7.8, respectively. Under iron-limited conditions, a slight increase in hydrolytic activity was detected at pH 6.0, while increasing the pH to 7.8 caused a 30% reduction in activity (Table XXII).

Table XXI. Influence of culture pH on extracellular protein production by iron-limited and -replete cultures of *L. pneumophila*.

Culture pH	Protein concentration ($\mu\text{g mg}^{-1}$ cell dry weight)	
	Iron-replete	Iron-limited
6.0	1.8 ± 0.6	6.4 ± 0.6
6.9	18.0 ± 1.5	21.0 ± 2.8
7.8	41.1 ± 3.2	29.4 ± 6.6

Values represent the mean \pm s.e.m. for 4 separate samples assayed in duplicate.

Table XXII. Influence of culture pH on the azocasein hydrolytic activity^a of iron-limited and -replete cultures.

Culture pH	Hydrolytic Activity ^a	
	Iron-replete	Iron-limited
6.0	199 ± 15	105 ± 9.2
6.9	420 ± 18	90 ± 14.5
7.8	298 ± 46	65 ± 5.5

^a Units of hydrolytic activity are mg substrate hydrolysed $\text{h}^{-1} \text{mg}^{-1}$ cell dry weight \pm s.e.m. Each mean value was calculated from duplicate analysis of at least three different samples.

3.15 Influence of Growth at pH 6.0 on the Virulence of *L. pneumophila*.

The virulence of iron-replete and -limited cultures grown at pH 6.0 was investigated using the guinea-pig aerosol model (Section 2.18.1). Previous experiments demonstrated that iron-replete cells grown at pH 6.9 are significantly more virulent than iron-limited cultures (Section 3.8.1). Aerosol challenge of guinea-pigs with the first iron-replete pH 6.0 culture which appeared morphologically normal on BCYE agar (Section 3.10.2), failed to cause death, although animals did have an elevated temperature 3 days post challenge, suggesting infection. Unfortunately, these animals received a very low dose, with a retained lung count of $3.0 \log_{10}$ c.f.u. per lung. This retained lung count, was almost 10-fold lower than previous LD_{50} values for normal replete cultures.

During the second chemostat experiment, the normal iron-replete culture (pH 6.9) established before altering the pH, was confirmed to be virulent (Table XXIII). However, due to a high retained dose, all the animals died, even at the lowest dose of $4.28 \log_{10}$ c.f.u. per lung. For two previous challenge experiments with this strain grown under similar culture conditions, a mean LD_{50} value of $4.0 \log_{10}$ was obtained (Section 3.8.1). When converted to pH 6.0, aerosol challenge with a steady state iron-replete sample produced death with a 50% lethal dose (LD_{50}) of $3.5 \log_{10}$ (Table XXIII). Therefore, this pH 6.0 culture, which produced a small colony variant morphology on BCYE agar (Section 3.10.2), was found to be highly virulent.

Under iron-limited conditions, no deaths were observed with the control pH 6.9 culture, in agreement with previous results (Tables XV and XXIV). When the pH of the culture was reduced to 6.0, aerosol challenge with steady state iron-limited culture, which produced a small colony morphology on BCYE agar (as described in Section 3.12.2), produced deaths with an LD_{50} value of 5.4 (Table XXIV). During a repeat experiment, aerosol challenge with a steady state pH 6.0 sample (which possessed a normal sized variant population of 35%; Section 3.12.2), produced no deaths at a retained dose of $5.1 \log_{10}$ (Table XXIV).

Table XXIII. Comparison of LD₅₀ values for *L. pneumophila* cultured under iron-replete conditions at pH 6.9 and 6.0.

Culture conditions	log ₁₀ LD ₅₀	95% confidence interval of LD ₅₀
Iron-replete pH 6.9 ^a	4.0	3.4 - 4.4
Iron-replete pH 6.0 ^b	3.5	3.2 - 3.8

^a Mean LD₅₀ value and combined 95% confidence interval for two previous challenge experiments presented in Section 3.8.1.

^b LD₅₀ and 95 % confidence intervals were calculated by the method of moving averages (Meynell & Meynell, 1970).

Table XXIV. Comparison of LD₅₀ values for *L. pneumophila* cultured under iron-limited conditions at pH 6.9 and 6.0.

Culture conditions	log ₁₀ LD ₅₀
Iron-limited pH 6.9 ^a	> 5.6
Iron-limited pH 6.0 ^b	5.4
Iron-limited pH 6.0 ^{a,c}	> 5.1

^a No deaths occurred at the maximum challenge.

^b Small colony variant population (Section 3.12.2), LD₅₀ calculated by the method of Reed & Muench (1937).

^c Culture contained a normal colony size variant population of 35% (Section 3.12.2).

3.16 Influence of pH on Membrane Lipid Composition of Iron-Replete Cells.

3.16.1 Lipid composition of replete pH 6.0 cultures with different colony phenotypes.

Sections 3.9 and 3.10 described the continuous growth of *L. pneumophila* under iron-replete conditions at pH 6.0, and revealed morphological differences between two separate cultures, when subsequently grown on BCYE agar. One experiment maintained the normal colony phenotype, while during the second experiment a stable small colony variant was selected. The membrane lipid composition of these two cultures was compared (Section 2.17). For ease, the two cultures will be referred to as normal and variant.

Comparison of the membrane fatty acid composition of these two cultures did not reveal significant differences (Figure 64). Both profiles were dominated by a high proportion of iso-branched 14-methylpentadecanoic acid (i16:0), and unsaturated hexadecanoic acid (16:1). The variant strain possessed a slightly elevated proportion of i16:0, mainly at the expense of hexadecanoic (16:0) and dodecanoic acid (20:0).

Analysis of intact membrane phospholipids by positive ion FAB-MS, also revealed little difference in the membrane lipid composition of these two cultures (Figure 65). Both profiles were dominated by phosphatidylethanolamine signals m/z 732 and m/z 734, and phosphatidylcholine signals m/z 788 and 790. In view of the close similarity between the fatty acid and phospholipid profiles of these two cultures, data for both cultures was combined in the following section to assess the influence of culture pH on the lipid composition of *L. pneumophila*.

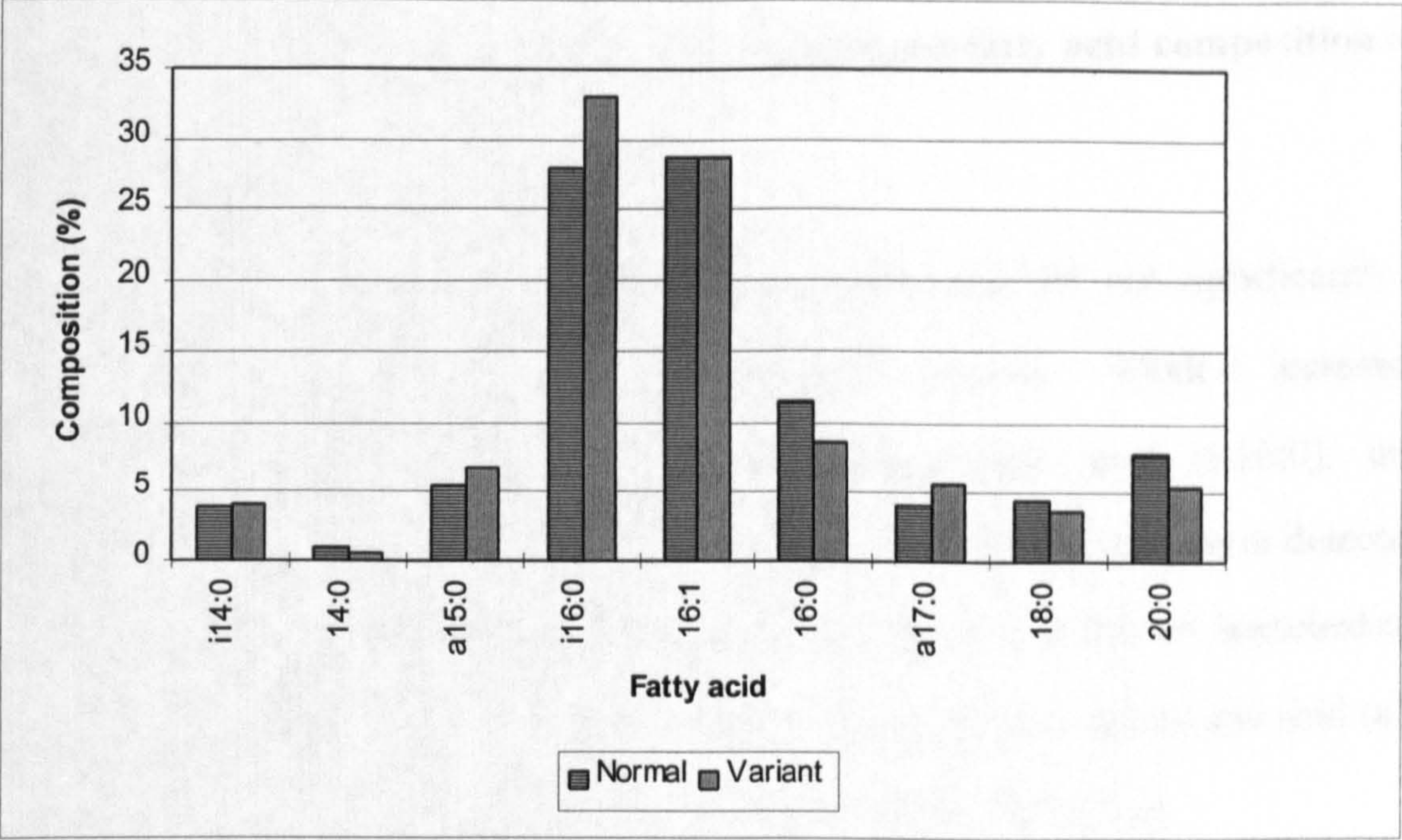


Figure 64. Comparison of the fatty acid profiles of iron-replete (pH 6.0) cultures which exhibited different colony morphologies on BCYE agar.

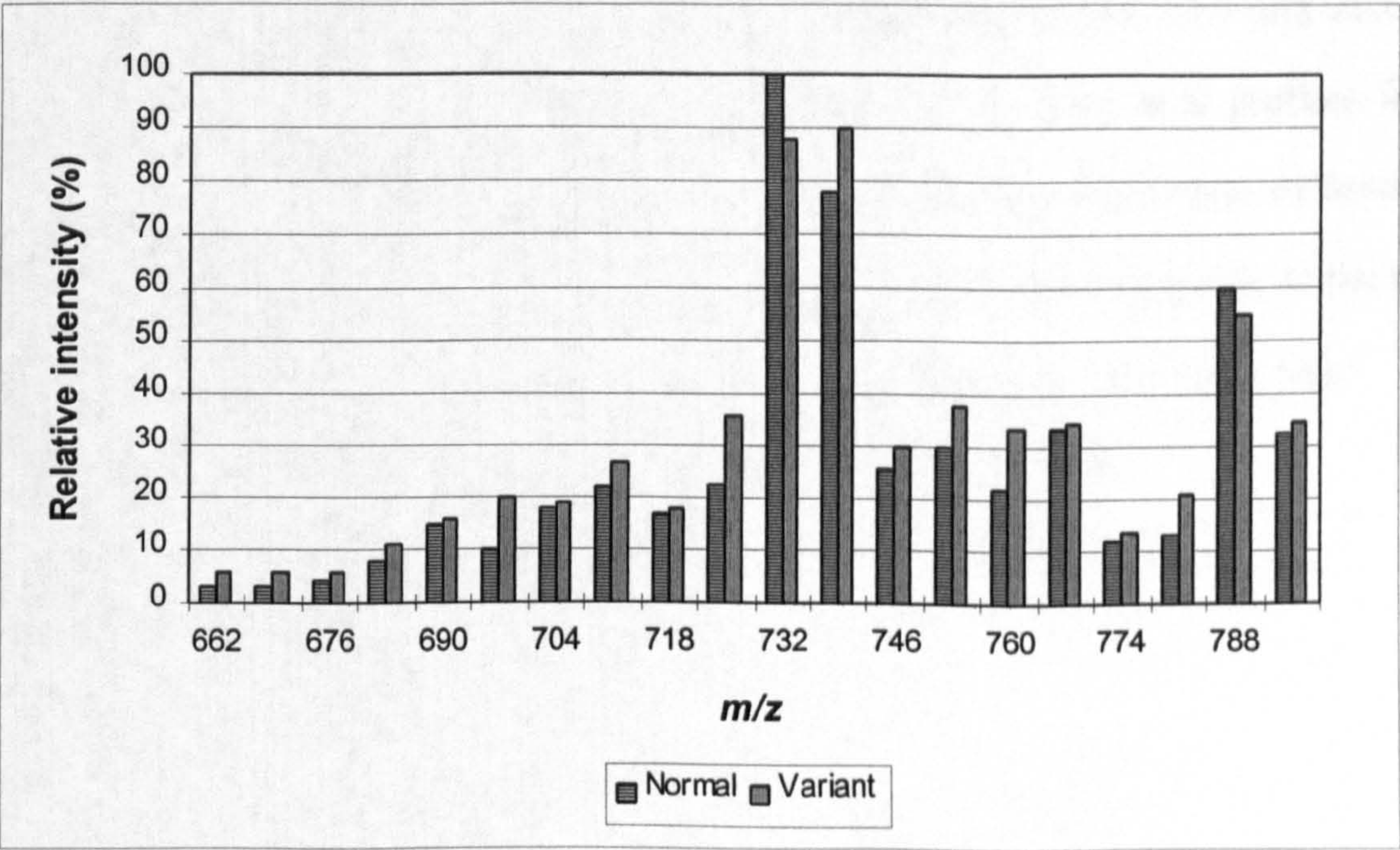


Figure 65. Comparison of the relative intensities of the protonated molecules of phosphatidylethanolamines and phosphatidylcholines, for two iron-replete pH 6.0 cultures of *L. pneumophila*, which displayed different colony morphologies when cultured on BCYE agar.

3.16.2 Influence of culture pH on the membrane fatty acid composition of iron-replete cells.

Decreasing the culture pH from 6.9 to 6.0 did not significantly alter the membrane fatty acid profile of iron-replete cultures. Modest increases in the proportions of iso-branched 14-methylpentadecanoic acid (i-16:0), unsaturated hexadecenoic acid (16:1) and saturated dodecanoic acid (20:0), were detected (Figure 66). These increases occurred mainly at the expense of shorter branched-chain fatty acids, 12-methyltridecanoic acid (i14:0) and 12-methyltetradecanoic acid (a15:0), and the unbranched saturated hexadecanoic acid (16:0) (Figure 66).

Increasing the culture pH to 7.8 had a more pronounced effect on the fatty acid profile. The proportions of iso-branched i14:0 and i16:0, and the anteiso-branched a15:0 fatty acids, were elevated in response to growth at pH 7.8. A corresponding decrease in the proportion of unbranched fatty acids, principally 16:1, and 16:0 was observed. Longer chain saturated fatty acids, 18:0 and 20:0 were also slightly diminished (Figure 66). Comparison of the fatty acid profiles for all three replete cultures revealed a progressive increase in the proportion of branched chain fatty acids, i14:0, a15:0 and i16:0, occurring mainly at the expense of the unbranched 16:1, 16:0 and 20:0, as the pH was elevated from 6.0 to 7.8 (Figure 66).

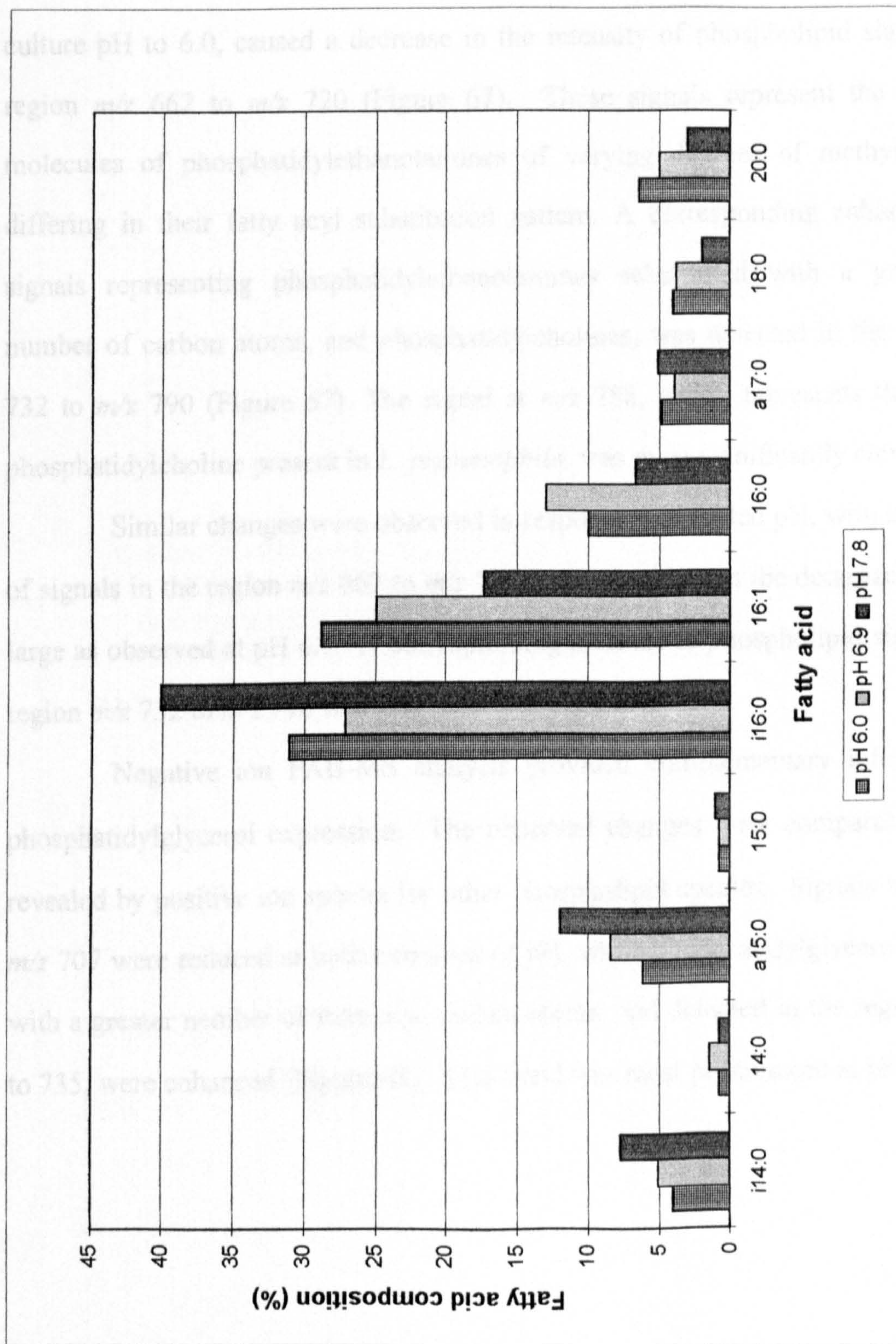


Figure 66. Influence of culture pH on the membrane fatty acid composition (%) of iron-replete cultures of *L. pneumophila*. Each values represent the mean of 4 separate determinations.

3.16.3 Effect of culture pH on the phospholipid composition of iron-replete cells.

Alterations in the membrane phospholipid composition in response to pH, were demonstrated by positive ion FAB-MS analysis (Section 2.17.4). Lowering the culture pH to 6.0, caused a decrease in the intensity of phospholipid signals in the region m/z 662 to m/z 720 (Figure 67). These signals represent the protonated molecules of phosphatidylethanolamines of varying degrees of methylation, and differing in their fatty acyl substitution pattern. A corresponding enhancement of signals representing phosphatidylethanolamines substituted with a greater total number of carbon atoms, and phosphatidylcholines, was detected in the region m/z 732 to m/z 790 (Figure 67). The signal at m/z 788, which represents the principal phosphatidylcholine present in *L. pneumophila*, was most significantly elevated.

Similar changes were observed in response to elevated pH, with the majority of signals in the region m/z 662 to m/z 720 reduced, although the decrease was not as large as observed at pH 6.0. A corresponding increase in phospholipid signals in the region m/z 732 to m/z 790 was also detected (Figure 67).

Negative ion FAB-MS analysis provided complementary information on phosphatidylglycerol expression. The observed changes were comparable to those revealed by positive ion spectra for other phospholipid species. Signals m/z 705 and m/z 707 were reduced at both extremes of pH, while phosphatidylglycerols esterified with a greater number of fatty acyl carbon atoms, and detected in the region m/z 719 to 735, were enhanced (Figure 68). This trend was most pronounced at pH 6.0.

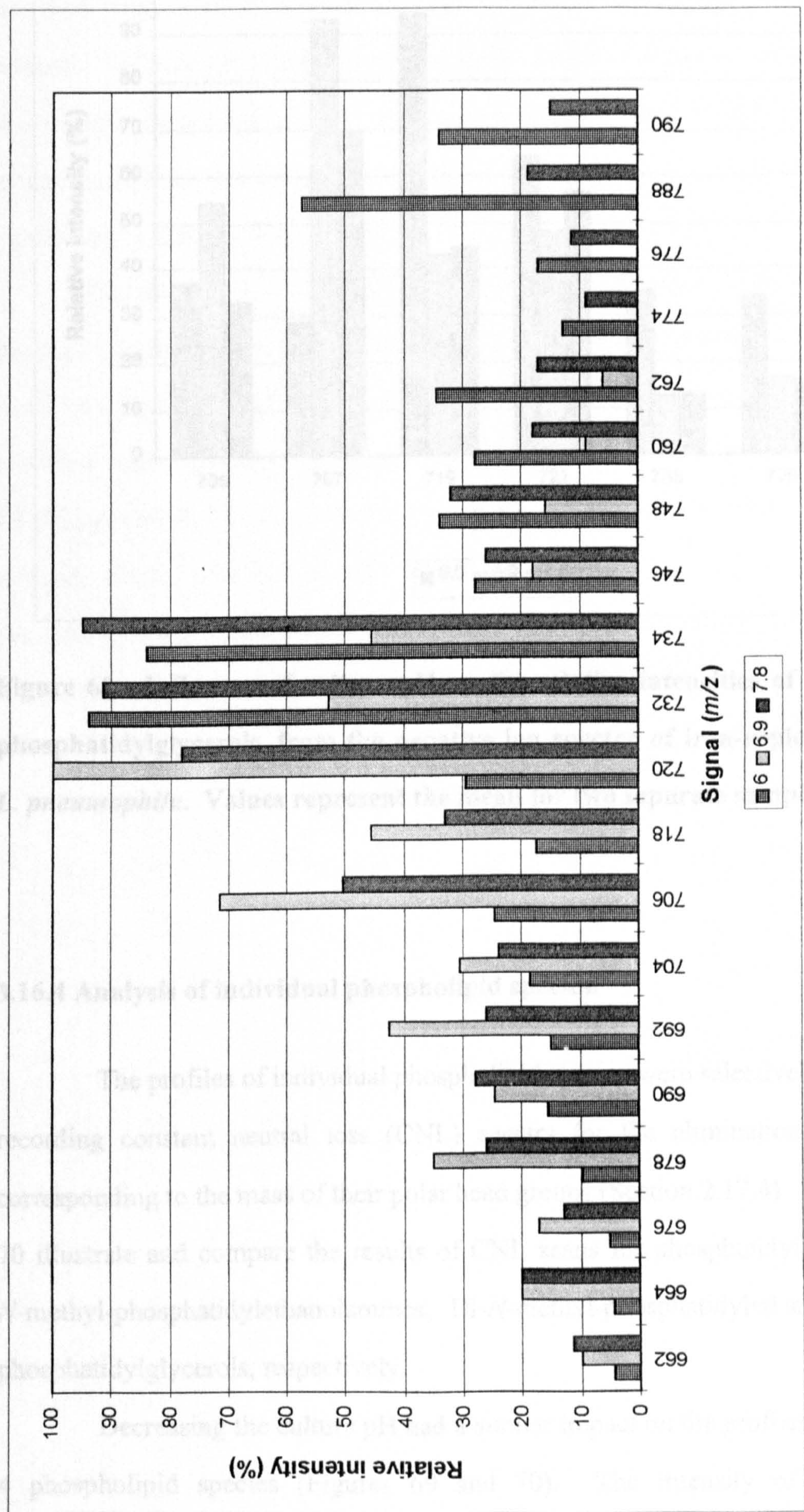


Figure 67. Influence of culture pH on the relative intensities of the protonated molecules of phosphatidylethanolamines and phosphatidylcholines of iron-replete cultures of *L. pneumophila*. Each value represents the mean of two separate samples.

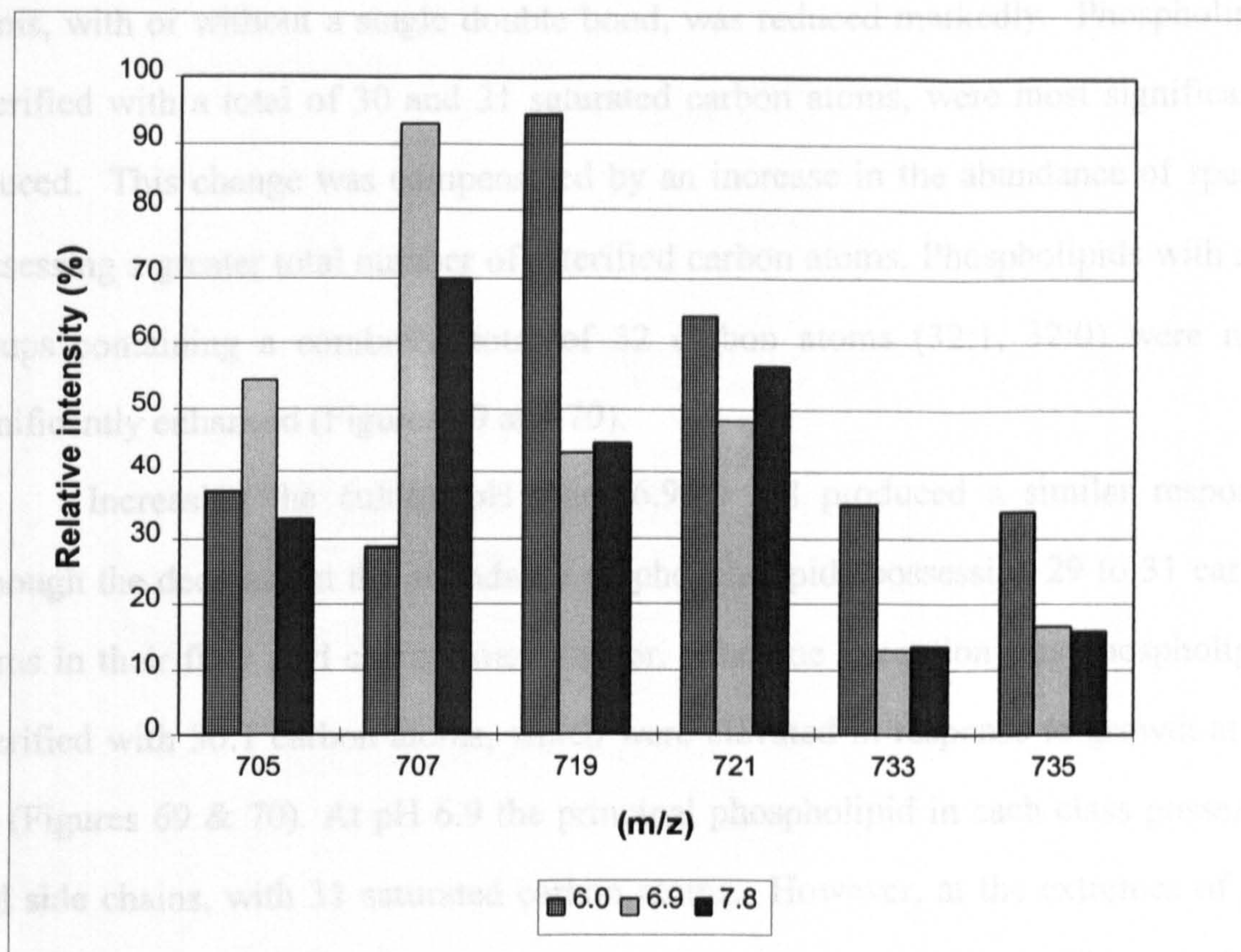


Figure 68. Influence of culture pH on the relative intensities of deprotonated phosphatidylglycerols, from the negative ion spectra of iron-replete cultures of *L. pneumophila*. Values represent the mean for two separate samples.

3.16.4 Analysis of individual phospholipid species.

The profiles of individual phospholipid species were selectively analysed, by recording constant neutral loss (CNL) spectra for the elimination of fragments corresponding to the mass of their polar head groups (Section 2.17.4). Figures 69 and 70 illustrate and compare the results of CNL scans for phosphatidylethanolamines, *N*-methyl-phosphatidylethanolamines, Di-*N*-methyl-phosphatidylethanolamines and phosphatidylglycerols, respectively.

Decreasing the culture pH had a similar impact on the profiles of each of the 4 phospholipid species (Figures 69 and 70). The intensity of phospholipids substituted with fatty acyl groups containing a combined total of 29 to 31 carbon

atoms, with or without a single double bond, was reduced markedly. Phospholipids esterified with a total of 30 and 31 saturated carbon atoms, were most significantly reduced. This change was compensated by an increase in the abundance of species possessing a greater total number of esterified carbon atoms. Phospholipids with acyl groups containing a combined total of 32 carbon atoms (32:1, 32:0) were most significantly enhanced (Figures 69 and 70).

Increasing the culture pH from 6.9 to 7.8 produced a similar response, although the decrease in the abundance of phospholipids possessing 29 to 31 carbon atoms in their fatty acyl chains, was smaller. The one exception was phospholipids esterified with 30:1 carbon atoms, which were elevated in response to growth at pH 7.8 (Figures 69 & 70). At pH 6.9 the principal phospholipid in each class possessed acyl side chains, with 31 saturated carbon atoms. However, at the extremes of pH, phospholipids esterified with a total of 32 carbon atoms, with or without a single double bond, became the major phospholipid in each group.

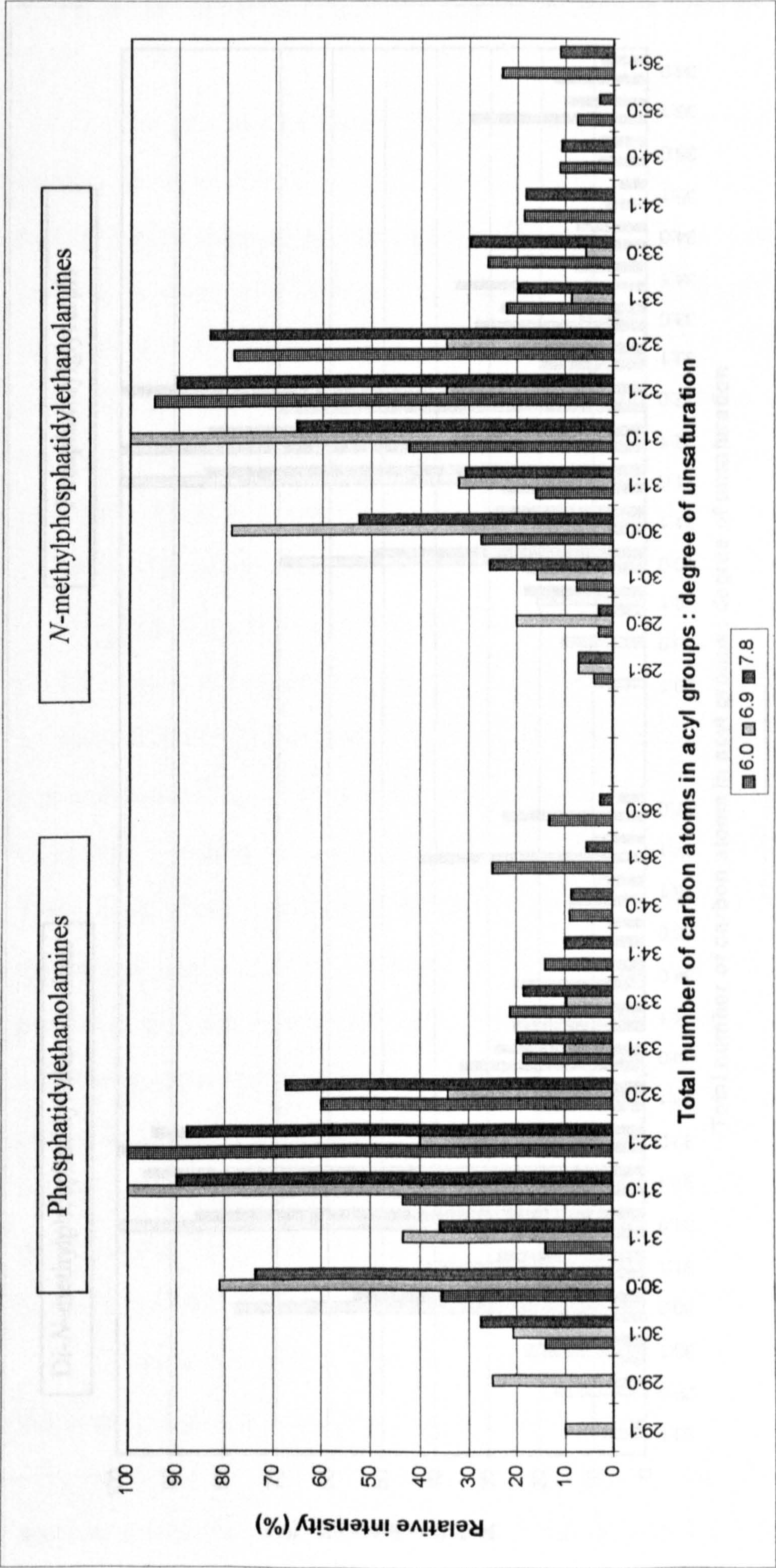


Figure 69. Influence of culture pH on the phosphatidylethanolamine and N-methylphosphatidylethanolamine profiles of iron-replete cultures of *L. pneumophila*, recorded by constant neutral loss scans for the loss of 141 and 155 mass units respectively. Values are the means for two samples.

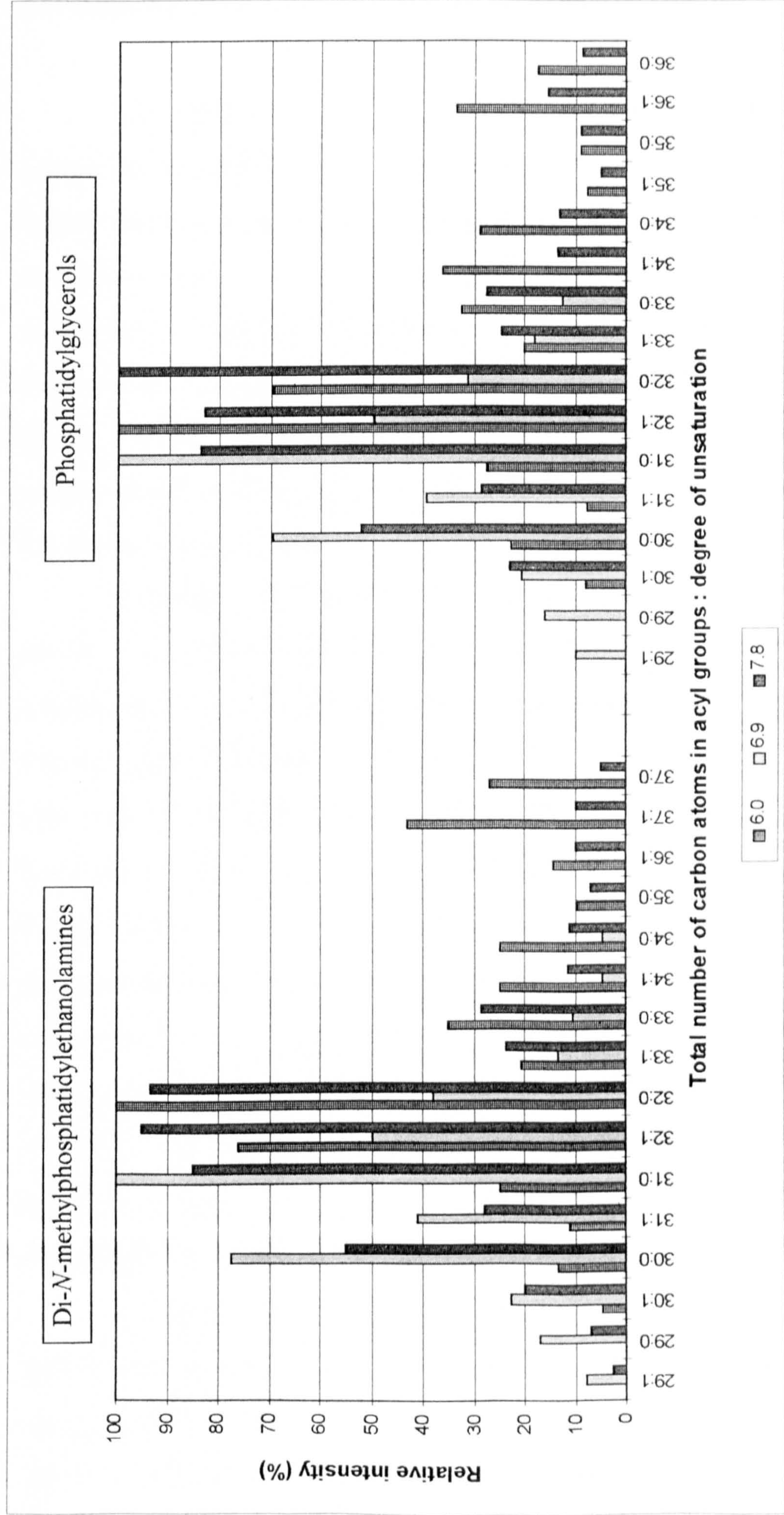


Figure 70. Influence of culture pH on the di-*N*-methylphosphatidylethanolamine and phosphatidylglycerol profiles of iron-replete cultures of *L. pneumophila*, recorded by constant neutral loss scans for the loss of 169 and 172 mass units respectively. Values are the means for two samples.

3.17 Influence of pH on Cellular Protein Expression by Iron-Replete Cells.

The influence of culture pH on cellular protein expression by iron-replete cultures was investigated (Section 2.16). Whole cell protein extracts were compared by SDS-PAGE followed by silver staining (Figure 71). Comparison of the profiles revealed a number of changes in response to environmental pH which are summarised in Table XXV. Increasing the culture pH to 7.8 resulted in the reduced expression of 4 protein bands, migrating with apparent molecular masses of 24, 40, 65, and 114 kDa (lanes 5 and 6 Figure 71; Table XXV). The expression of 3 other proteins migrating with molecular masses of 21, 31, and 35 kDa was enhanced at pH 7.8. None of these proteins appeared to be novel (Figure 71 and Table XXV).

Alterations in protein expression were also detected in response to growth at pH 6.0. Lane 2 illustrates the profile for the virulent pH 6.0 culture, which produced a variant small colony morphology on BCYE agar (Section 3.10.2). The expression of 5 protein bands of apparent molecular weight 24, 31, 35, 40 and 50 kDa was reduced, while only 1 protein band, migrating at 54 kDa, was enhanced (lane 2 Figure 71; Table XXV). Lane 1 illustrates the protein profile for the pH 6.0 culture which displayed a normal colony morphology on BCYE agar. Comparison with the pH 6.9 profile revealed that the expression of 6 proteins was clearly induced. These proteins migrated at 23, 31, 47, 54, 64, and 70 kDa (lane 1 Figure 71, and Table XXV). One protein band (42 kDa) appeared to be repressed in this culture. Only one of the induced proteins (54 kDa) was enhanced in the previous pH 6.0 culture. Therefore, the protein profiles of the two pH 6.0 cultures which produced different colony morphologies on BCYE agar, differed markedly.

Comparison of the profiles at both extremes of pH, revealed very few similarities in protein modulation. Two proteins migrating at 24 and 42 kDa were repressed at pH 7.8 and in the variant pH 6.0 culture. Only one protein with an apparent molecular mass of 31 kDa, was enhanced at pH 7.8 and in the normal phenotype pH 6.0 culture (Table XXV).

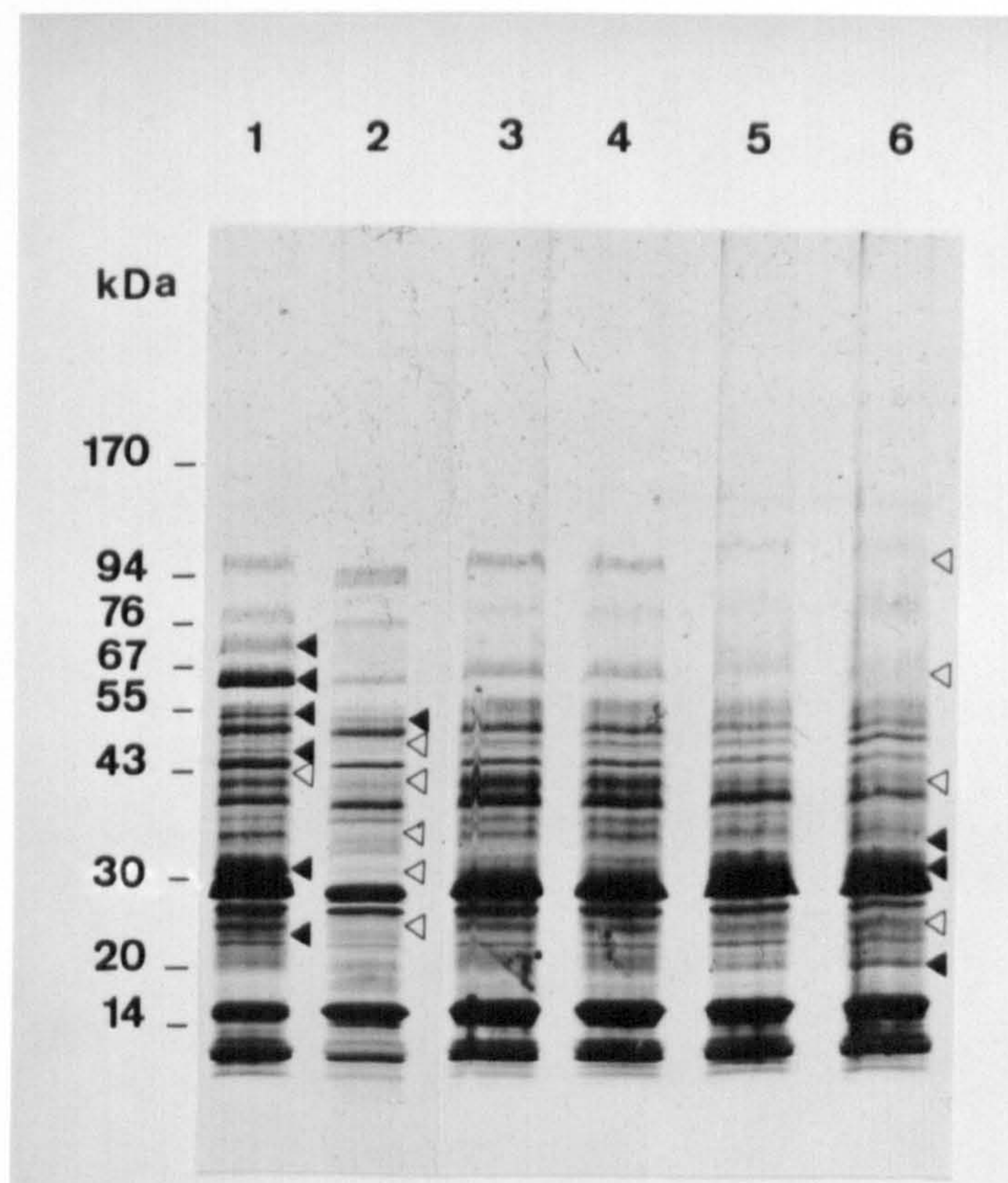


Figure 71. Comparison of silver stained SDS-PAGE whole cell protein profiles of *L. pneumophila*, grown in iron-replete culture at different pH values. Lanes 1 and 2, pH 6.0; lanes 3 and 4, pH 6.9; lanes 5 and 6, pH 7.8.

Table XXV. Summary of alterations in whole cell protein expression by iron-replete cultures of *L. pneumophila* in response to pH. Quoted values correspond to their apparent molecular mass (kDa) on SDS-PAGE.

pH 7.8 lanes 5 & 6	pH 6.0 (variant) lane 2	pH 6.0 (normal) lane 1
<u>up-regulated</u>		
21		
		23
31		31
35		
		47
	54	55
		64
		70
<u>down-regulated</u>		
24	24	
	31	
	35	
40	40	
		42
	50	
65		
114		

3.18 Serogroup Antigen Expression by Iron-Replete Cultures at Extremes of pH.

SDS-PAGE of hot saline extracts (Section 2.15) produced profiles with poor banding resolution, however, ladder-like patterns typical of smooth-type LPS were discernible in all extracts (Figure 72). The banding profile of cultures grown at pH 6.9 and 7.8 (lanes 1 & 2, and lanes 5 & 6, respectively) was similar. The banding profile of cultures grown at pH 6.0 (lanes 3, 4, 7 and 8) demonstrated a slight increase in the intensity of lower molecular weight bands. This increase was most prominent with extracts from the virulent pH 6.0 culture which displayed a small colony variant morphology (lanes 7 & 8). Lanes 3 and 4 represent the pH 6.0 culture which displayed a normal colony morphology, as discussed in Section 3.10.2.

The protein, carbohydrate and KDO composition of these extracts was compared (Section 2.15; Table XXVI). The chemical composition of the control iron-replete culture samples was comparable to results reported previously (Table XIII). Furthermore, the composition of the control pH 6.9 extracts pH 7.8 extracts was comparable. This is in agreement with the observations of the banding profile. Minor differences in the chemical composition of the pH 6.0 extracts were detected, with a slightly elevated carbohydrate and a diminished protein content (Table XXVI). These differences were most pronounced in the culture displaying the variant colony phenotype.

Table XXV. Antigenic properties of *L. pneumophila* serogroup 9A-10A antigens extracted at various pH values.

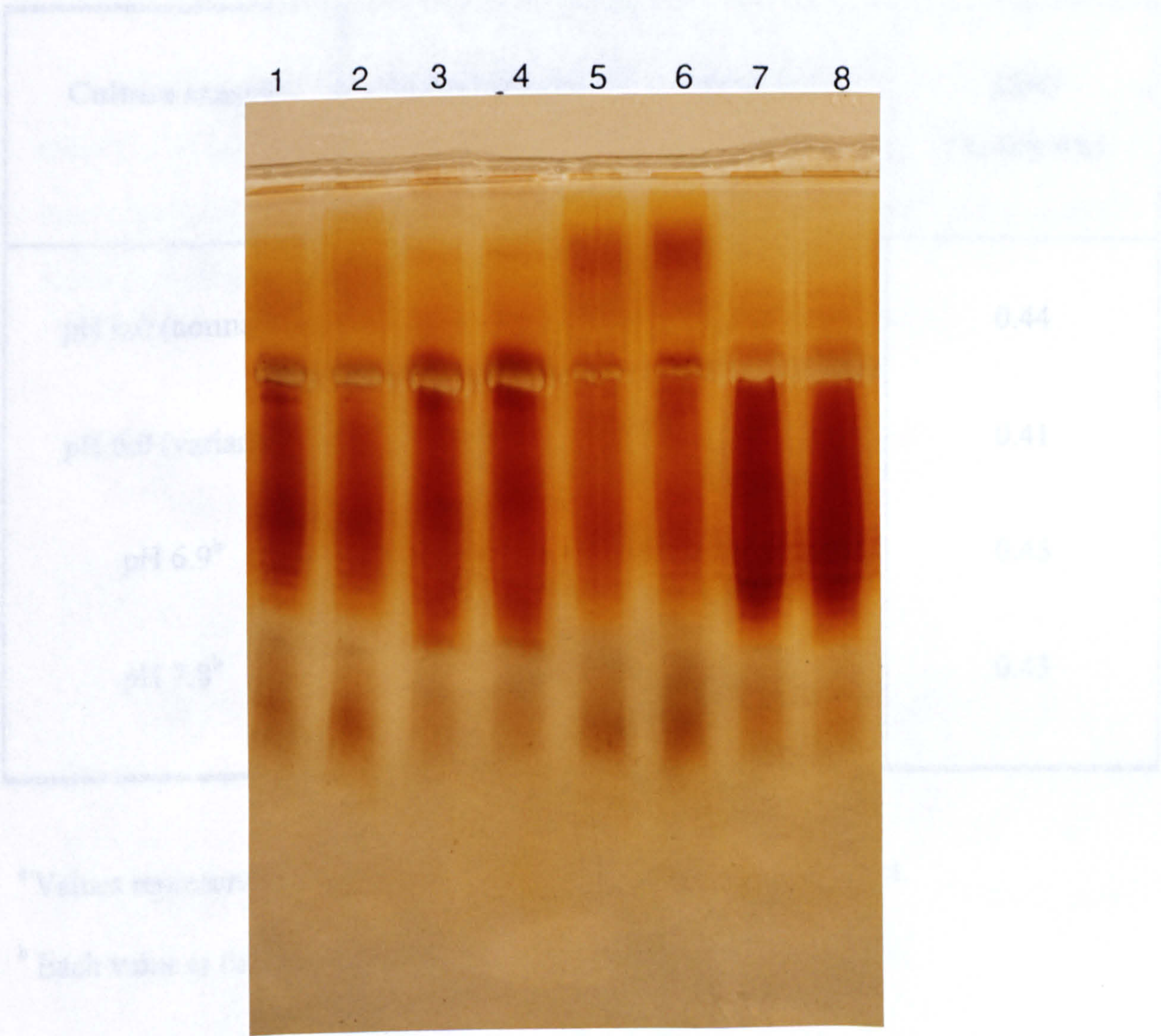


Figure 72. SDS-PAGE profiles of *L. pneumophila* serogroup antigen, extracted in hot saline. Lanes 1 and 2, pH 6.9; lanes 3 and 4, pH 6.0, normal phenotype; lanes 5 and 6, pH 7.8; lanes 7 and 8, pH 6.0, virulent small colony variant (Section 3.10.2).

Table XXVI. Influence of culture pH on the chemical composition of saline extracts of serogroup antigen from iron-replete cultures of *L. pneumophila*.

Culture sample	Carbohydrate (% dry wt.)	Protein (% dry wt.)	KDO (% dry wt.)
pH 6.0 (normal) ^a	4.4	8.3	0.44
pH 6.0 (variant) ^a	4.9	9.3	0.41
pH 6.9 ^b	4.0	14.5	0.45
pH 7.8 ^b	3.9	15.3	0.43

^a Values represent the mean for duplicate analysis of a single extract.

^b Each value is the mean result for two samples assayed in duplicate.

3. 19 Physiology of Poly- β -hydroxybutyrate Formation by *L. pneumophila*.

3. 19.1 Intracellular granule formation by iron-limited and -replete cells.

During morphological examination of chemostat cultures by electron microscopy, inclusion bodies resembling intracellular granules were observed in both iron-limited and -replete cells grown at pH 6.9. Figure 73 illustrates the characteristic appearance of these intracellular inclusions.

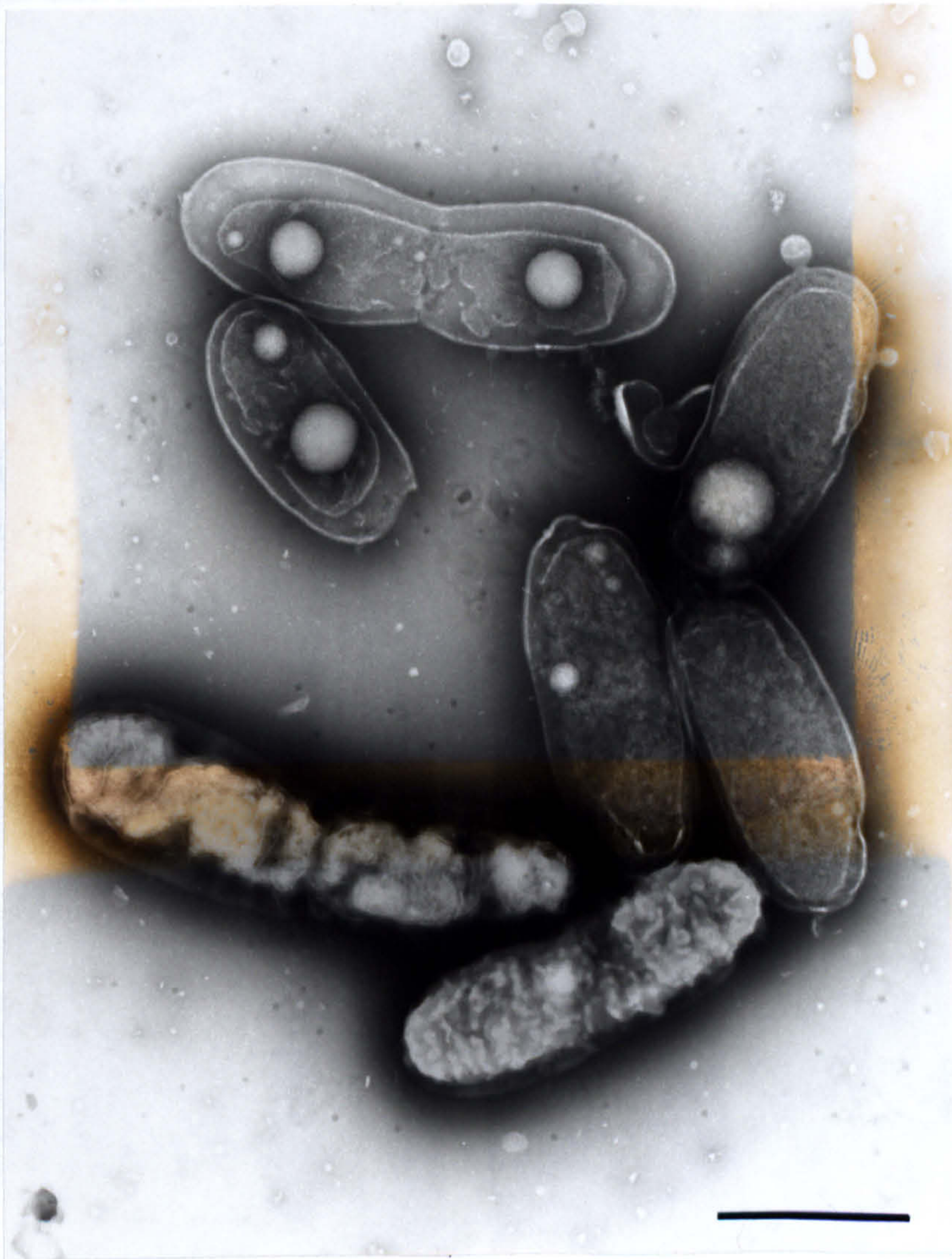


Figure 73. Electron micrograph of chemostat grown cells revealing the presence of intracellular granule-like inclusions. Bar, 1 μ m.

3.19.2 Nile red staining of intracellular inclusions.

Laser confocal microscopic examination of culture samples following staining with Nile red (Section 2.6.4), revealed bright orange fluorescing granules, located intracellularly in both iron-limited and -replete cells, demonstrating the hydrophobic nature of these inclusions (Figures 74 & 75). The granule content of the pleomorphic iron-replete cells normally varied between 1-4 granules depending on the cell length. Occasionally long cells containing up to 15 granules were observed (Figures 74). Iron-limited cells typically contained 1-3 granules per cell (Figure 75).

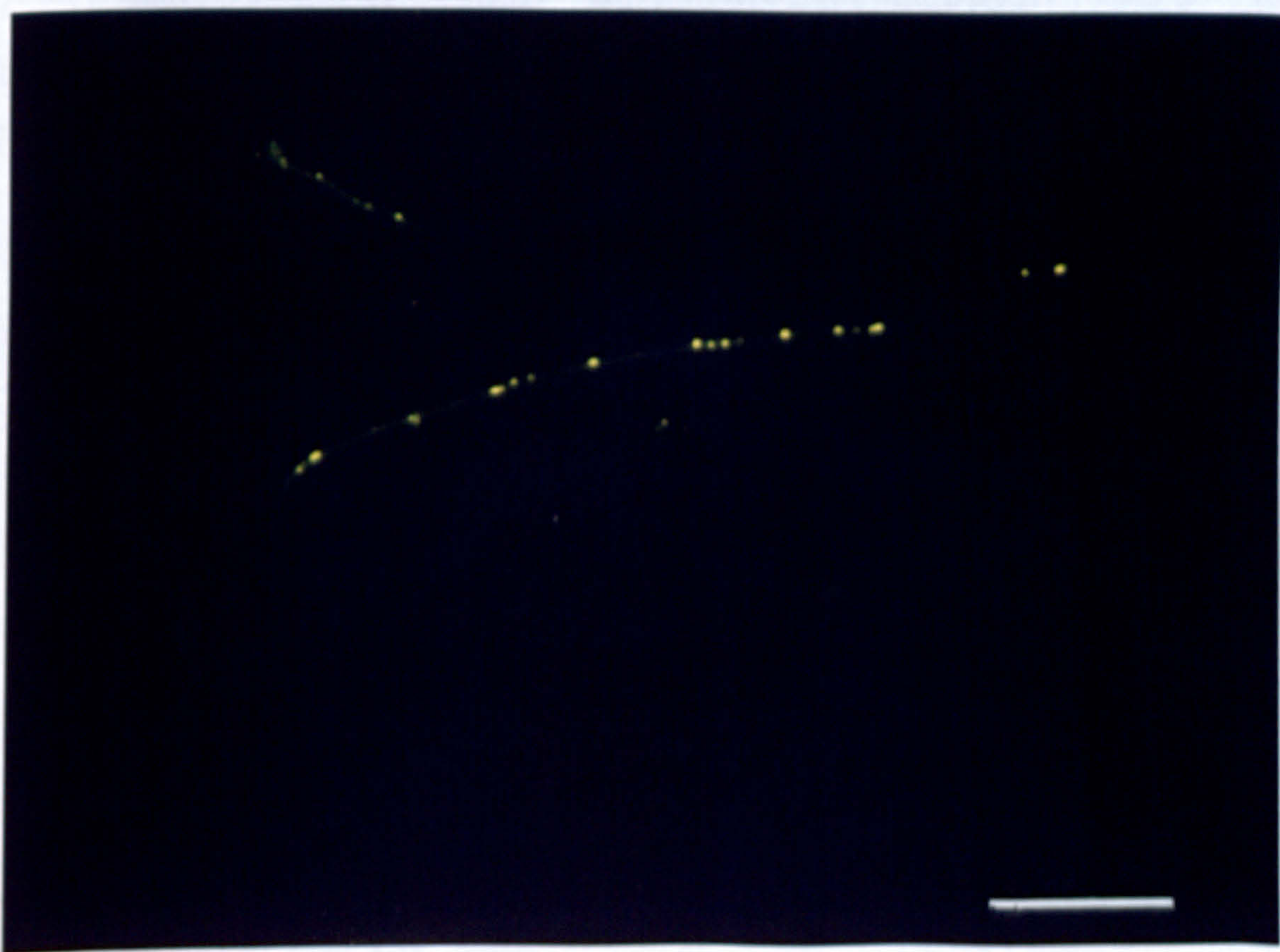


Figure 74. Laser confocal microscopic examination of *L. pneumophila* stained with the fluorescent lipophilic dye, Nile red, and counter stained with FITC. The figure shows a long iron-replete cell containing multiple intracellular granules of varying fluorescence intensity. Bar, 10 μm .

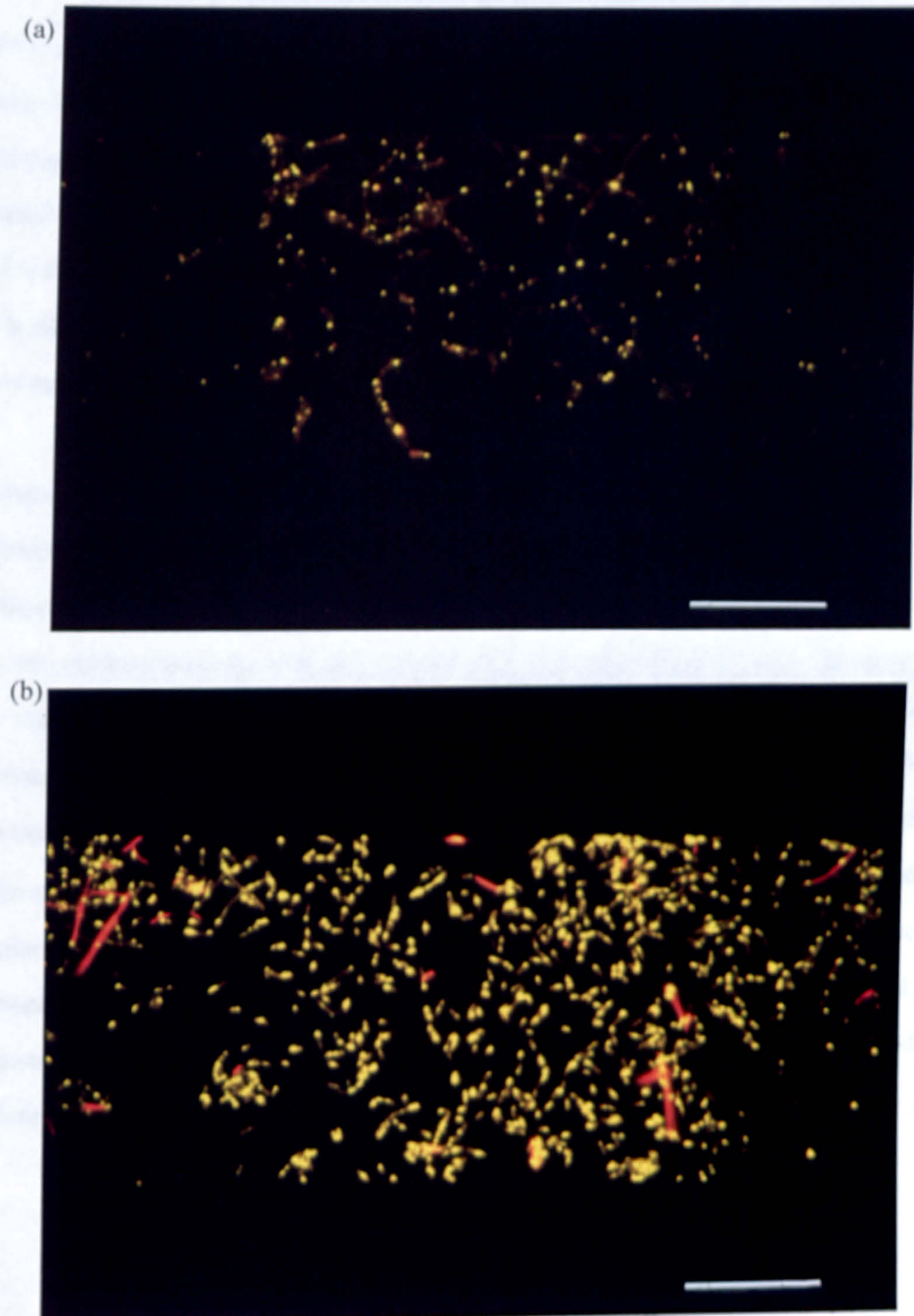


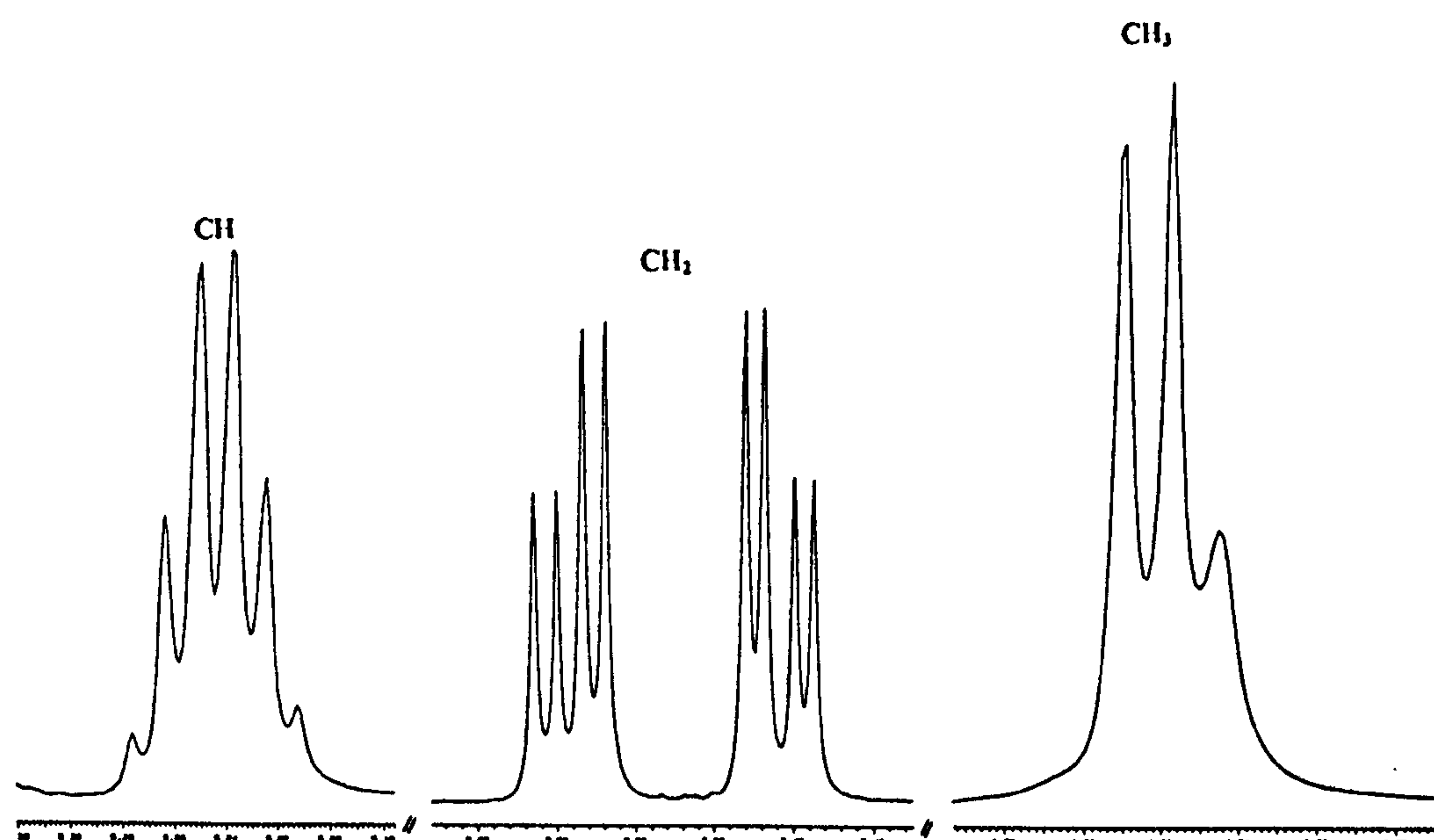
Figure 75. Laser confocal microscopic examination of *L. pneumophila* stained with the fluorescent lipophilic dye, Nile red, (a) iron-replete; (b) iron-limited. Bar, 10 μm .

3.19.3 Analysis of PHB by ^1H NMR spectroscopy.

Purification of hot chloroform extracts from iron-limited and -replete cell pastes, yielded a white membrane-like material which was characterized by ^1H NMR spectroscopy (Section 2.19). Figure 76 compares the expanded ^1H NMR spectra for both samples. The ^1H NMR spectra of the purified material contained 3 clusters of signals which were characteristic of a polymer of hydroxybutyric acid. The chemical shifts, multiplicities and coupling constants ($^3J_{\text{H,H}}$), of these signals corresponded to the methyl, methylene and methine protons (Figure 76 & Table XXVII), and were in close agreement with published spectra of authentic PHB (Doi *et al.*, 1986).

The chemical shift of the doublet at 1.25-1.28 ppm is consistent with methyl protons, which being highly shielded are observed at high field (low ppm). Furthermore, the multiplicity of this peak indicated coupling to the spin of the adjacent methine proton. Methylene proton resonance was detected at 2.4-2.65 ppm. The two clusters indicated vincinal coupling of the two methylene protons, producing two resonance peaks for each proton, which are further split through coupling to the methine proton. The multiplet resonance at 5.22-5.27 was assigned to methine protons, with the chemical shift indicating reduced shielding, and a lower density of electrons in the local environment. The four peaks of the methine signal indicated coupling to the magnetic fields associated with each of the methylene protons. The chemical shifts and coupling constants for both samples were effectively identical, indicating no structural difference in the purified polymer from iron-limited and -replete cells (Tables XXVII).

(a)



(b)

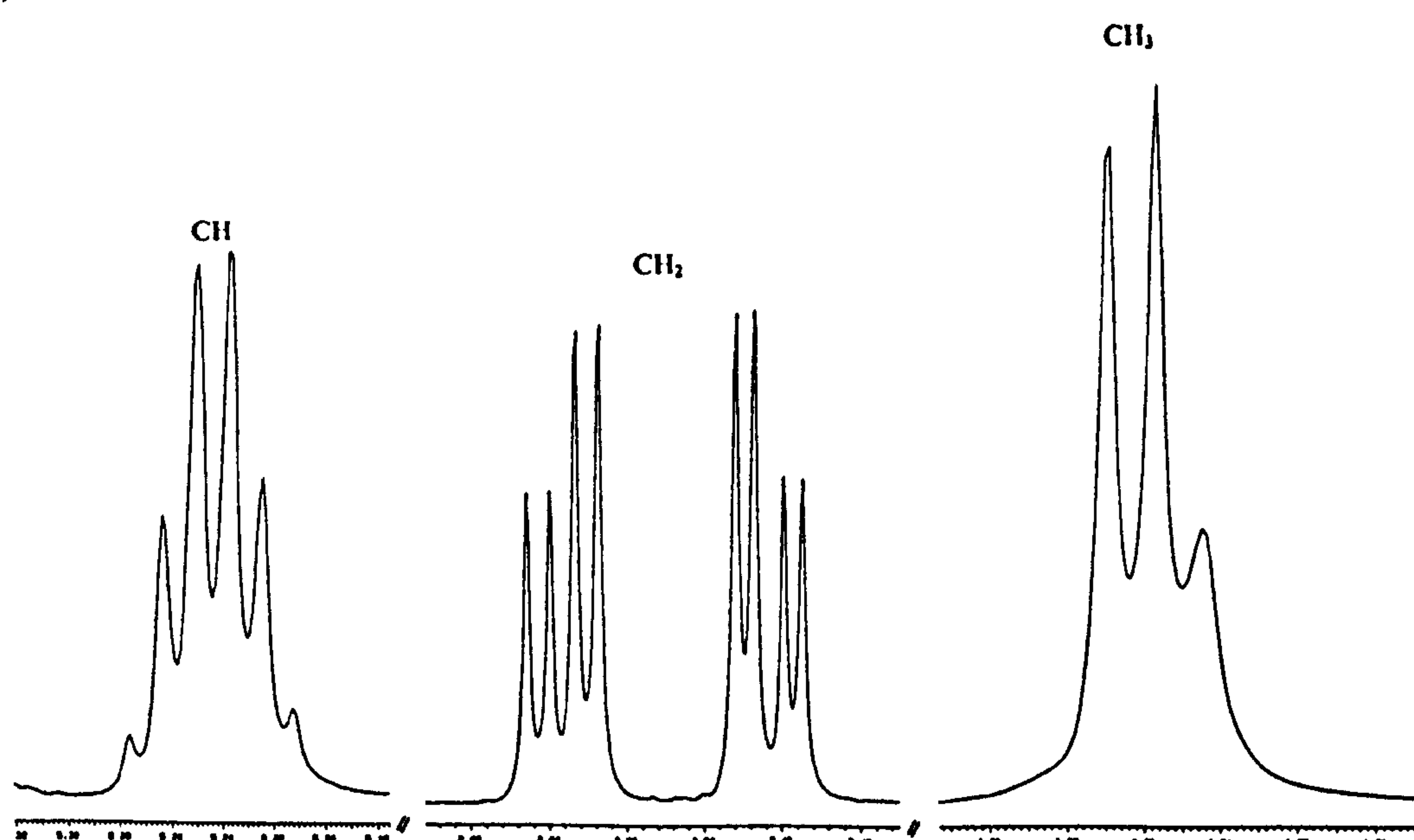


Figure 76. ^1H NMR spectrum at 500 MHz of PHB purified from (a) iron-replete and (b) iron-limited cultures of *L. pneumophila*. Chemical shifts are in ppm downfield from trimethylsilane.

Two important parameters are the resonance frequency or chemical shift (measured in ppm), which is an indication of the degree of electron shielding in the vicinity of the nucleus, and coupling to other nuclei (spin-spin-coupling) which is revealed by the multiplicity of the peak, and is commonly measured as the coupling constant between ^1H nuclei, ($^3J_{\text{H,H}}$).

Table XXVII. Comparison of the chemical shifts and coupling constants from ¹H NMR spectra of purified hot chloroform extracts from iron-limited and -replete cultures of *L. pneumophila*.

Proton	Chemical shift (ppm, relative to trimethylsilane)	
	Iron-replete	Iron-limited
CH	5.243	5.244
CH ₂ a	2.593	2.593
CH ₂ b	2.459	2.459
CH ₃	1.264	1.265
Coupled protons	Proton coupling constants ³ J _{H,H} (Hz) ± 0.3 Hz	
CH-CH ₂ a	7.3	7.3
CH-CH ₂ b	5.5	5.8
CH-CH ₃	6	6.5

3.19.4 Comparison of the PHB content of iron-limited and -replete cells.

The PHB content of the purified material from chloroform extracts was chemically quantitated by dehydration to crotonic acid (2.19.2). This assay detected low yields of PHB for both iron-limited and -replete cultures. The PHB yield from iron-limited cells represented 4.7 % cell dry weight, while the polymer content of iron-replete samples was approximately 60% lower (Table XXVIII). The PHB yield from both cultures was low, considering the microscopic observation of multiple granules in many cells.

Table XXVIII. Comparison of the PHB content of iron-replete and -limited samples of *L. pneumophila*.

PHB Content (% cell dry weight)	
Iron -replete ^a	Iron-limited ^b
1.9 ± 0.8	4.7 ± 1.0

^a Value represents the mean ± s.e.m. for four samples.

^b Value represents the mean ± s.e.m. for three samples.

3.19.5 Relationship between Nile red fluorescence and PHB content.

Samples of cell paste were extracted for three successive 8h periods in boiling chloroform. The PHB extracted during each 8h cycle was quantitated by dehydration to crotonic acid (Section 2.19.2). The cumulative PHB yield was correlated with the NR spectrofluorescence of the cell paste, which was also determined after each extraction cycle (as detailed in Section 2.20.6). Figures 77 and 78 illustrates that there is an inverse linear relationship between the decrease in NR spectrofluorescence and the PHB yield, for two representative samples, labelled A and B.

This study also shows that one 8 h extraction cycle, produced poor recovery of PHB. Less than 50% of the total PHB yield was extracted from sample A, during the first 8h (Figure 77). Furthermore, repeated extraction of sample A produced a cumulative PHB yield equivalent to 16 % cell dry weight. Sample B which possessed a low initial NR spectrofluorescence, yielded less than 1% PHB, confirming the relationship between NR spectrofluorescence and PHB content (Figure 78). Both

samples possessed a high background fluorescence of comparable intensity, even after 24 h chloroform extraction (Figures 77 and 78).

Comparison of the PHB yield and NR spectrofluorescence for a number of different samples (Sections 2.19 and 2.20.5), also demonstrated a linear relationship between spectrofluorescence and PHB content (Figure 79). From this relationship it can be extrapolated that a fluorescence reading of approximately 9.0 represents the cell associated background fluorescence in the absence of PHB, under these assay conditions.

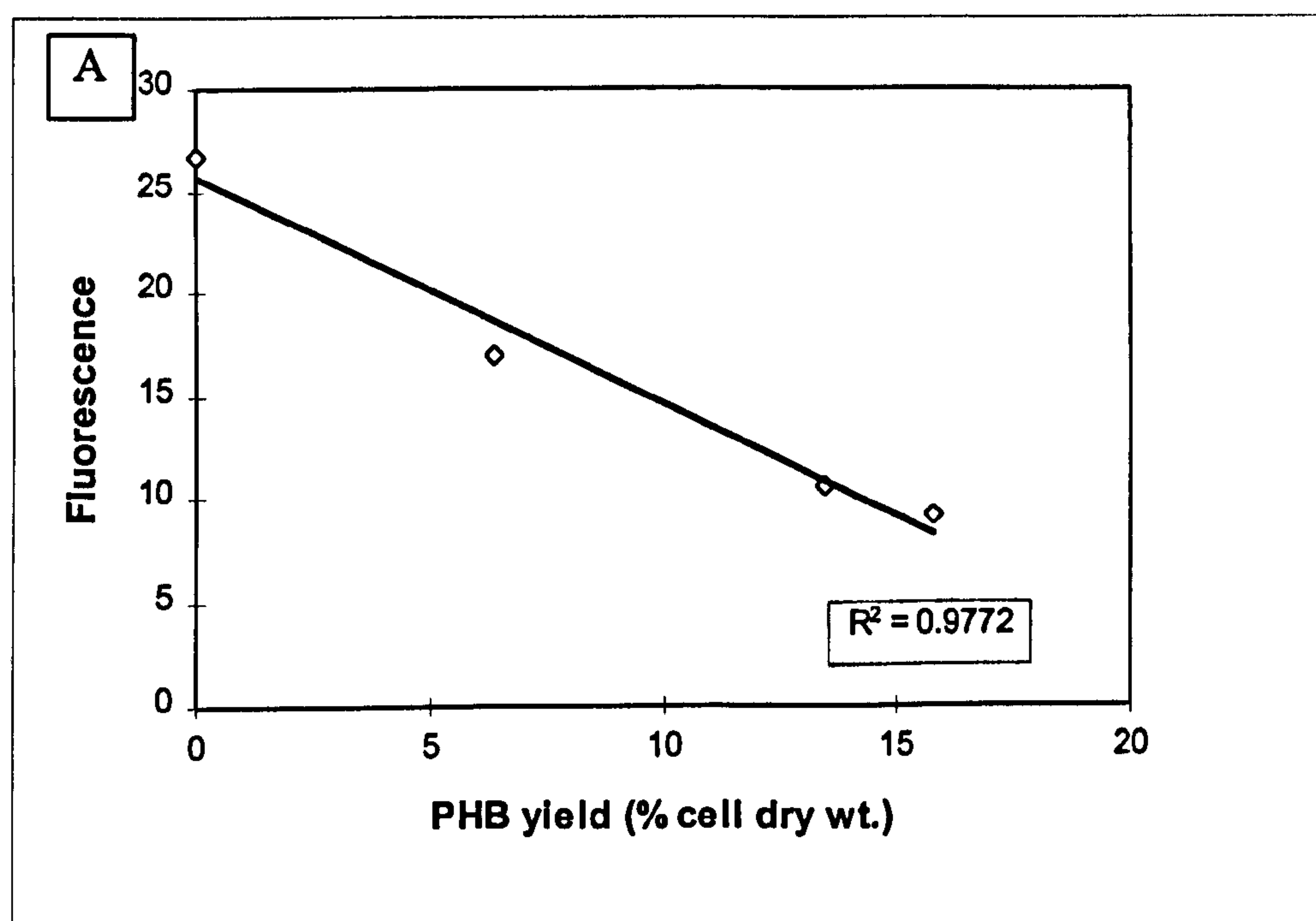


Figure 77. Relationship between Nile red spectrofluorescence and PHB yield, for a *L. pneumophila* sample possessing high initial spectrofluorescence, after extraction for three successive 8 h cycles in boiling chloroform (Section 2.20.6).

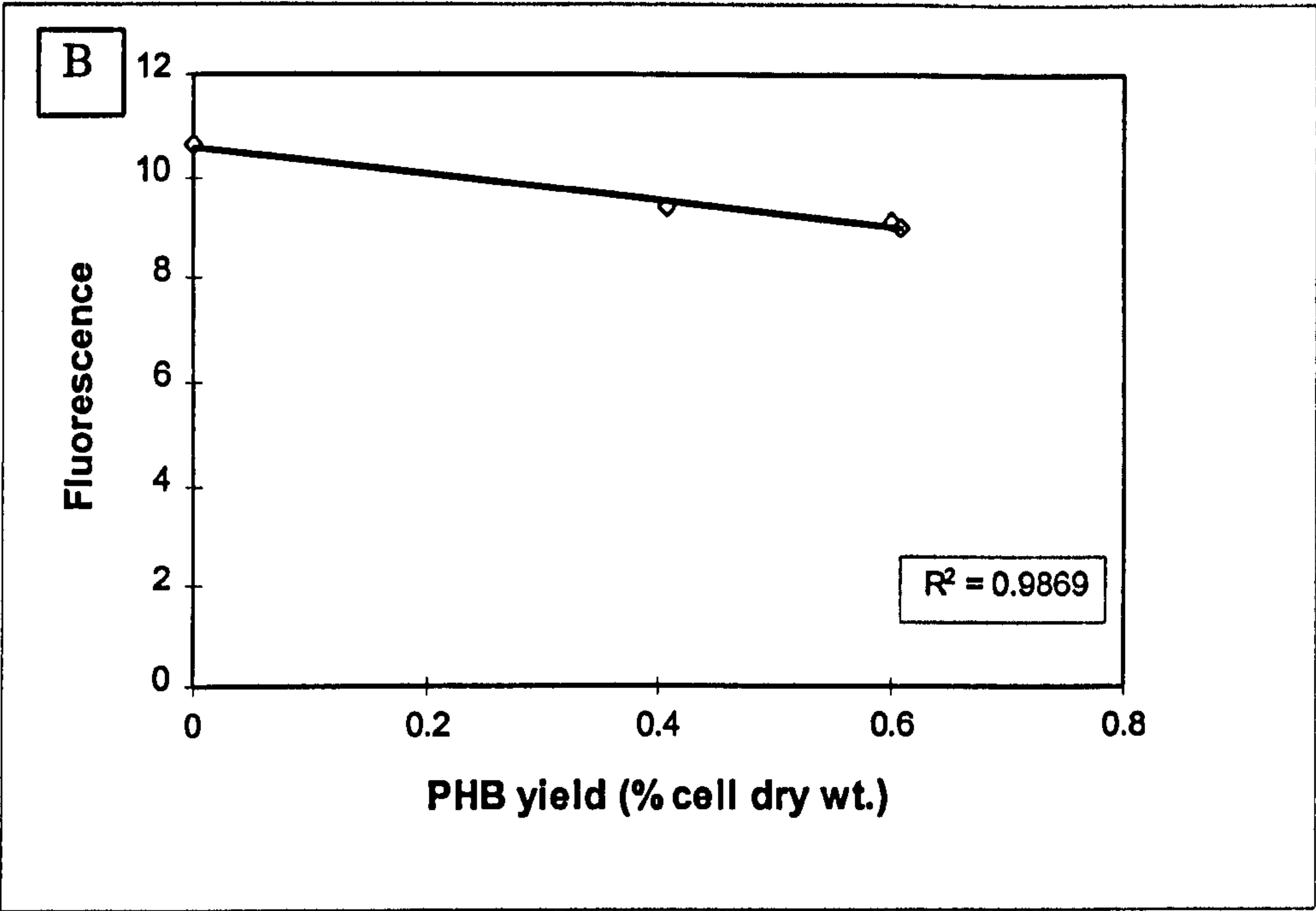


Figure 78. Relationship between Nile red spectrofluorescence and PHB yield, for a *L. pneumophila* sample possessing low initial spectrofluorescence, after extraction for three successive 8 h cycles in boiling chloroform (Section 2.20.6).

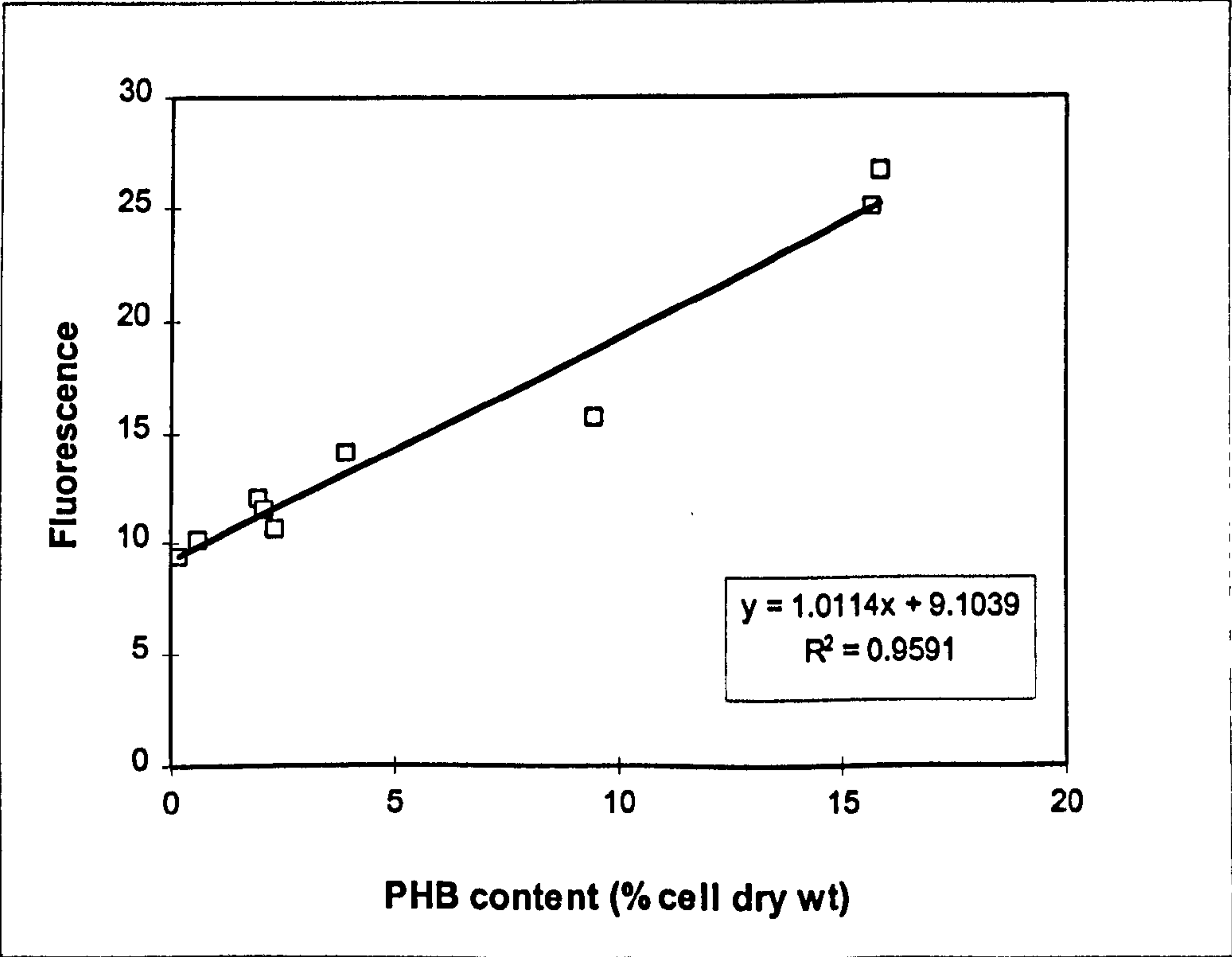


Figure 79. Relationship between PHB content of *L. pneumophila* samples and Nile red fluorescence.

3.19.6 Spectrofluorometric analysis of iron-limited and -replete samples.

A number of different iron-limited and -replete samples grown at pH 6.9 were assayed spectrofluorometrically (Section 2.20.5). Figure 80 illustrates the fluorescence readings for nine separate iron-limited and -replete samples, prepared to a standard optical density. This data demonstrates that the NR spectrofluorescence of iron-limited samples normally exceeds that of iron-replete samples, with mean fluorescence values of 21 and 13, respectively (Table XXIX). Using the equation from figure 79, these values correspond to a mean PHB content for iron-limited and -replete cells of 11.7 and 4.2 % cell dry weight, respectively (Table XXIX). This data agrees with the previous observation made in Section 3.19.4, that PHB accumulation is elevated during iron-limited growth.

Table XXIX. Comparison of the mean NR spectrofluorescence and calculated PHB content for iron-replete and -limited samples of *L. pneumophila*.

Culture sample	Mean fluorescence (\pm sd.)	Mean PHB content (% cell dry wt.) ^a
Iron-replete	13.3 \pm 3.9	4.2
Iron-limited	21.1 \pm 4.1	11.7

^a Calculated using the equation of the line from Figure 79 ($y = 1.0114x + 9.1039$), which defines the relationship between the NR fluorescence and PHB content of samples of *L. pneumophila*.

3.19.7 Relationship between PHB content and culture biomass yield.

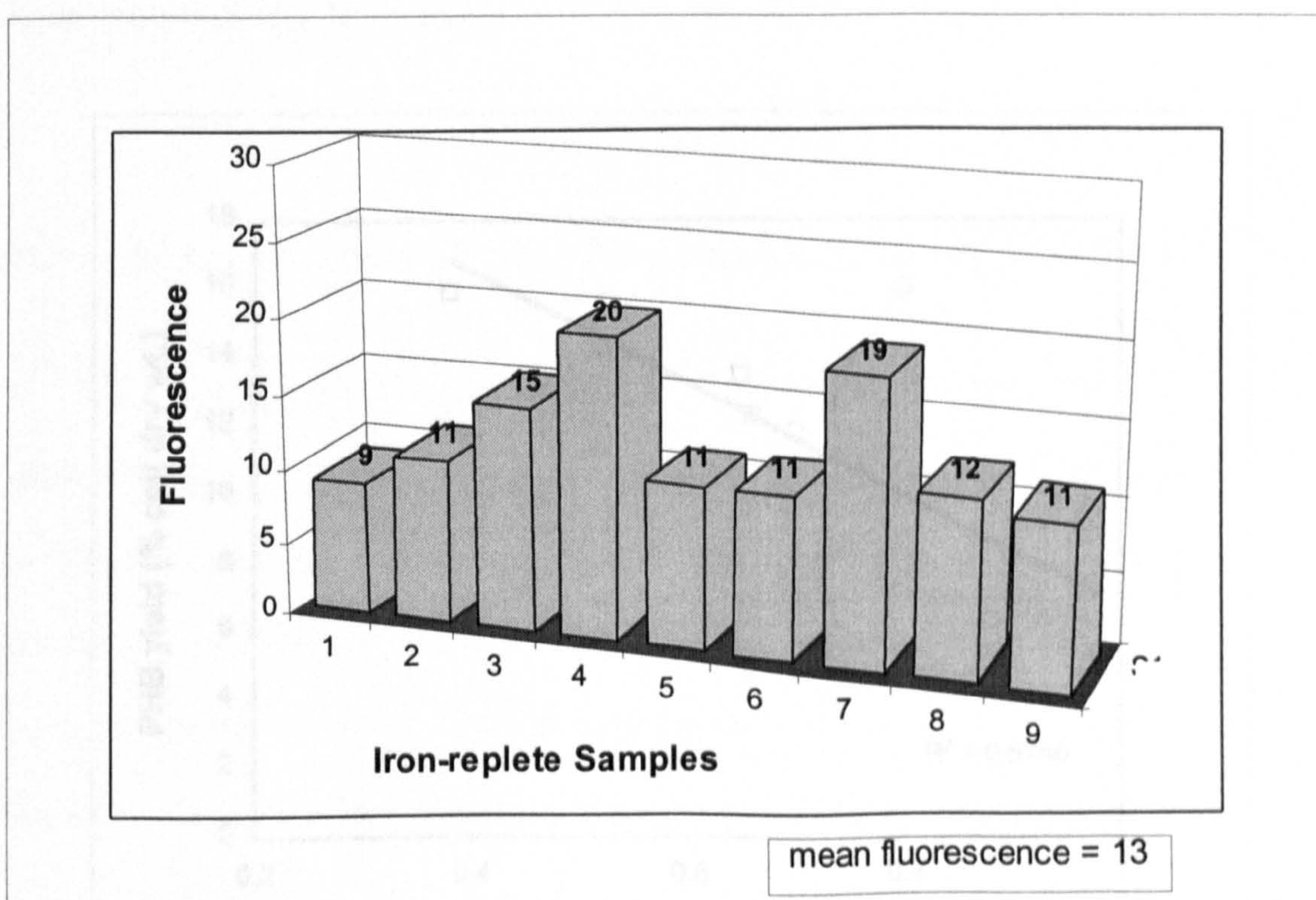
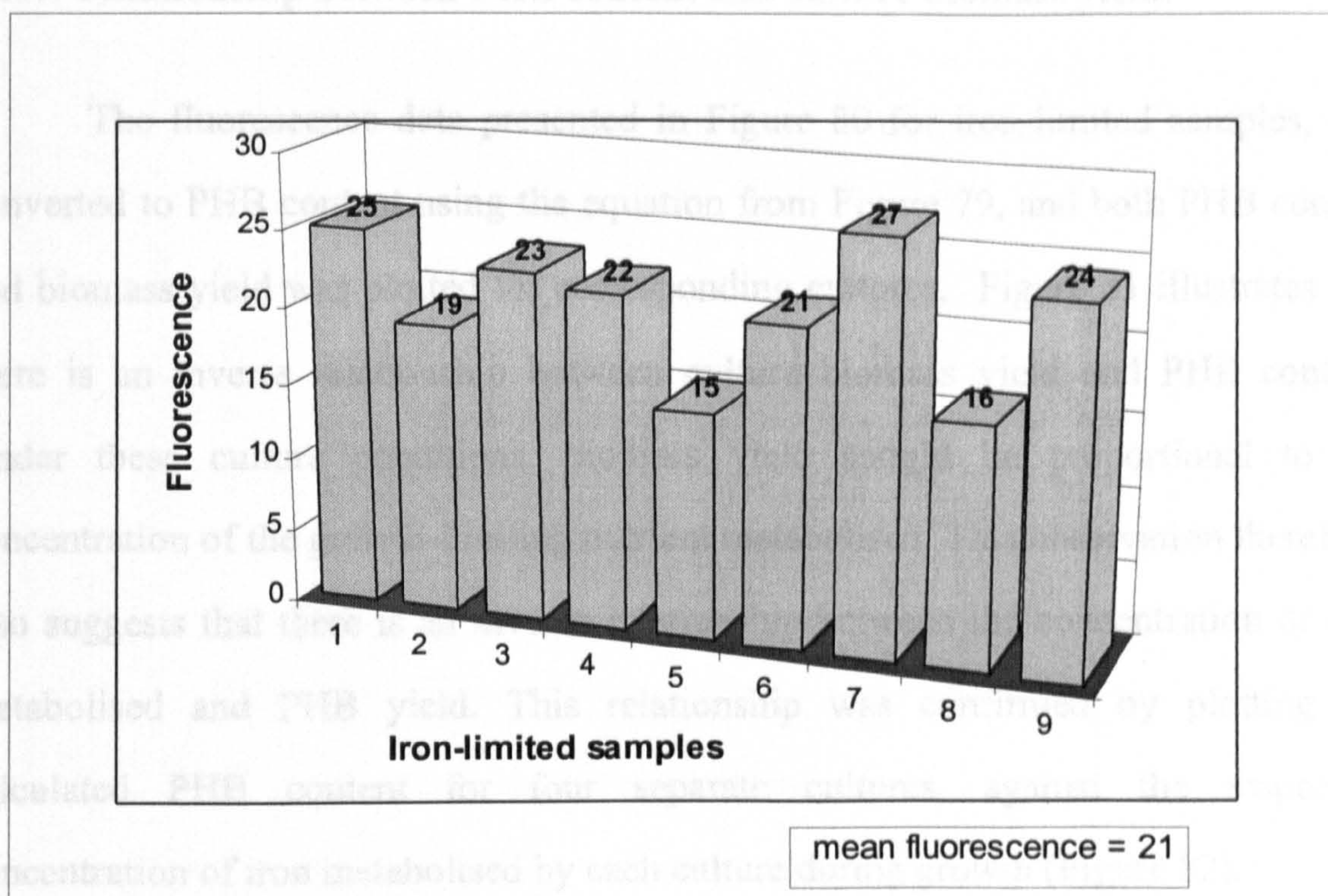


Figure 80. Comparison of NR spectrofluorescence values for iron-limited and -replete samples of *L. pneumophila*. All samples were prepared to a standard optical density at 540 nm (Section 2.20.5).

3.19.7 Relationship between PHB content and culture biomass yield.

The fluorescence data presented in Figure 80 for iron-limited samples, was converted to PHB content using the equation from Figure 79, and both PHB content and biomass yield was plotted for corresponding cultures. Figure 81 illustrates that there is an inverse relationship between culture biomass yield and PHB content. Under these culture conditions, biomass yield should be proportional to the concentration of the growth-limiting nutrient metabolised. This observation therefore, also suggests that there is an inverse relationship between the concentration of iron metabolised and PHB yield. This relationship was confirmed by plotting the calculated PHB content for four separate cultures, against the respective concentration of iron metabolised by each culture during growth (Figure 82).

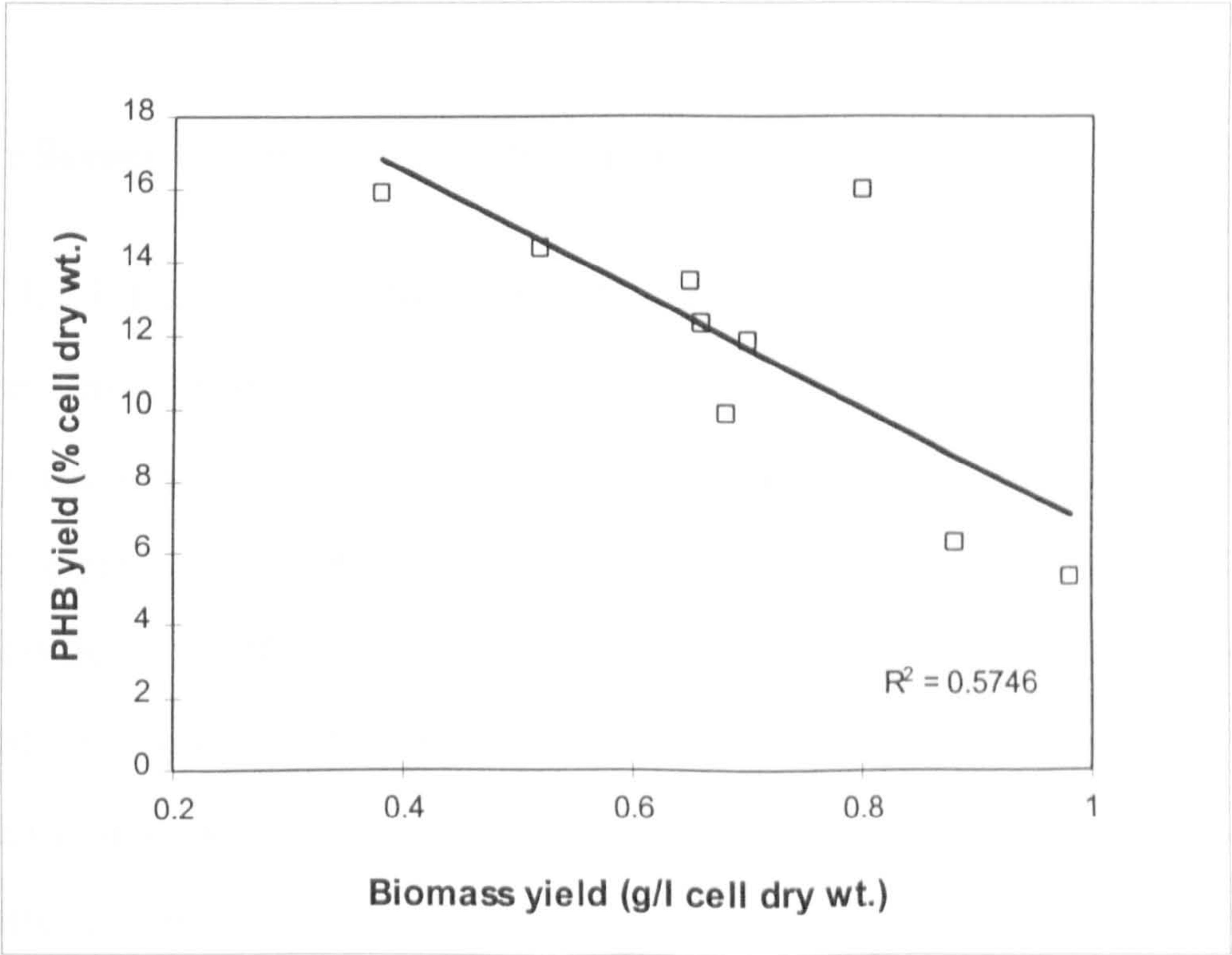


Figure 81. Relationship between PHB content and the biomass yield of iron-limited cultures of *L. pneumophila*.

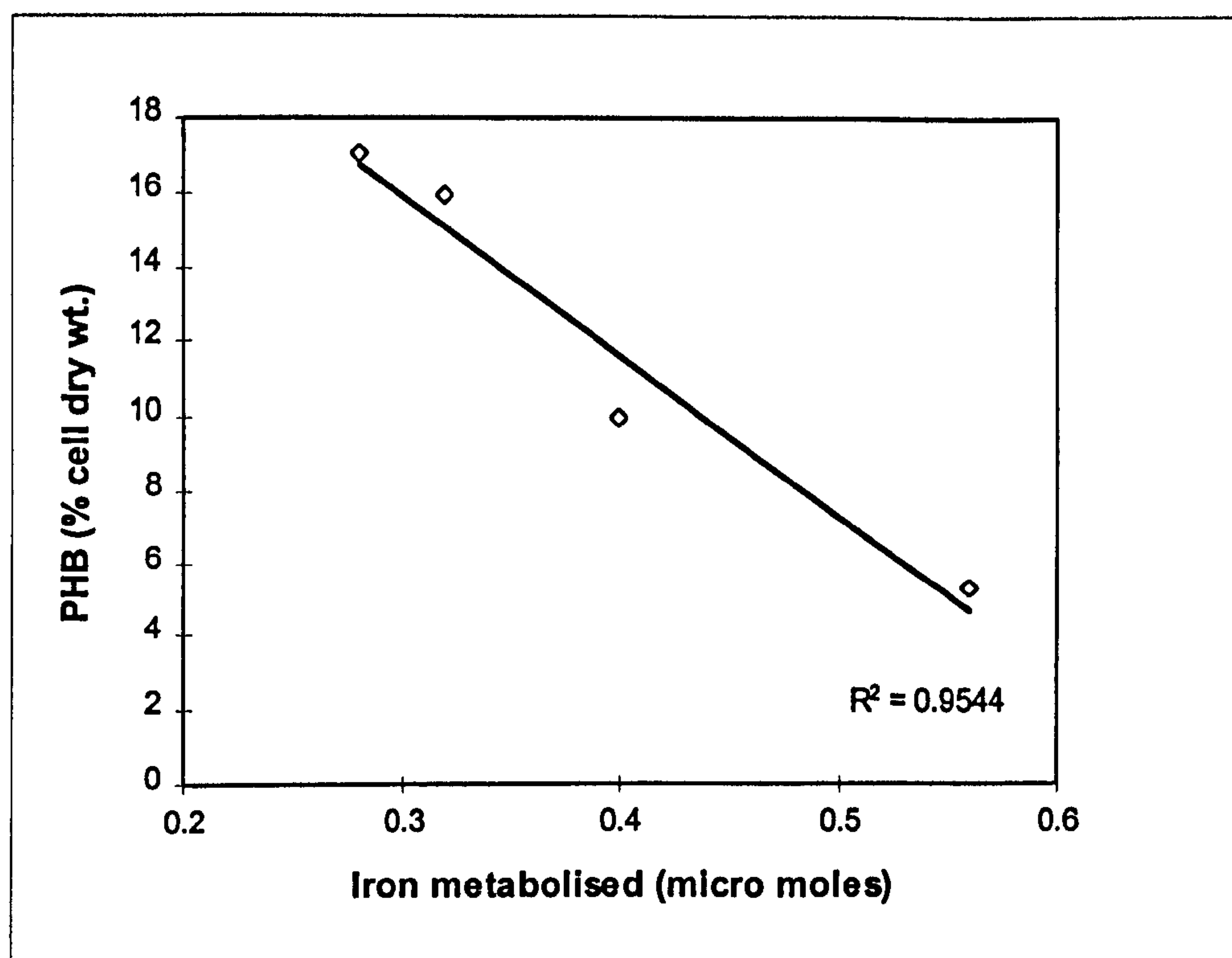


Figure 82. Relationship between calculated PHB content and the concentration of iron metabolised, by iron-limited cultures of *L. pneumophila*.

3.19.8 Influence of culture pH on PHB accumulation by *L. pneumophila*.

The influence of culture pH on PHB accumulation, was monitored by fluorescent microscopic examination of iron-limited and -replete samples stained with NR (Section 2.6.4). Iron-replete cultures grown at pH 6.0 contained 1 to 2 fluorescing granules per cell, confirming PHB formation (Figure 83a). Intracellular granules were also visible in iron-limited cultures grown at pH 6.0. While some cells contained 2 to 3 granules, the majority contained a single polar granule (Figure 83b).

Examination of cultures grown at pH 7.8 revealed changes in granule content. Approximately 50% of iron-replete cells appeared devoid of granules, with the remaining cells containing 1 to 2 brightly fluorescing granules (84a). The decrease in granule content was more striking in iron-limited cultures at pH 7.8. Virtually no intracellular fluorescing granules were visible (Figure 84b).

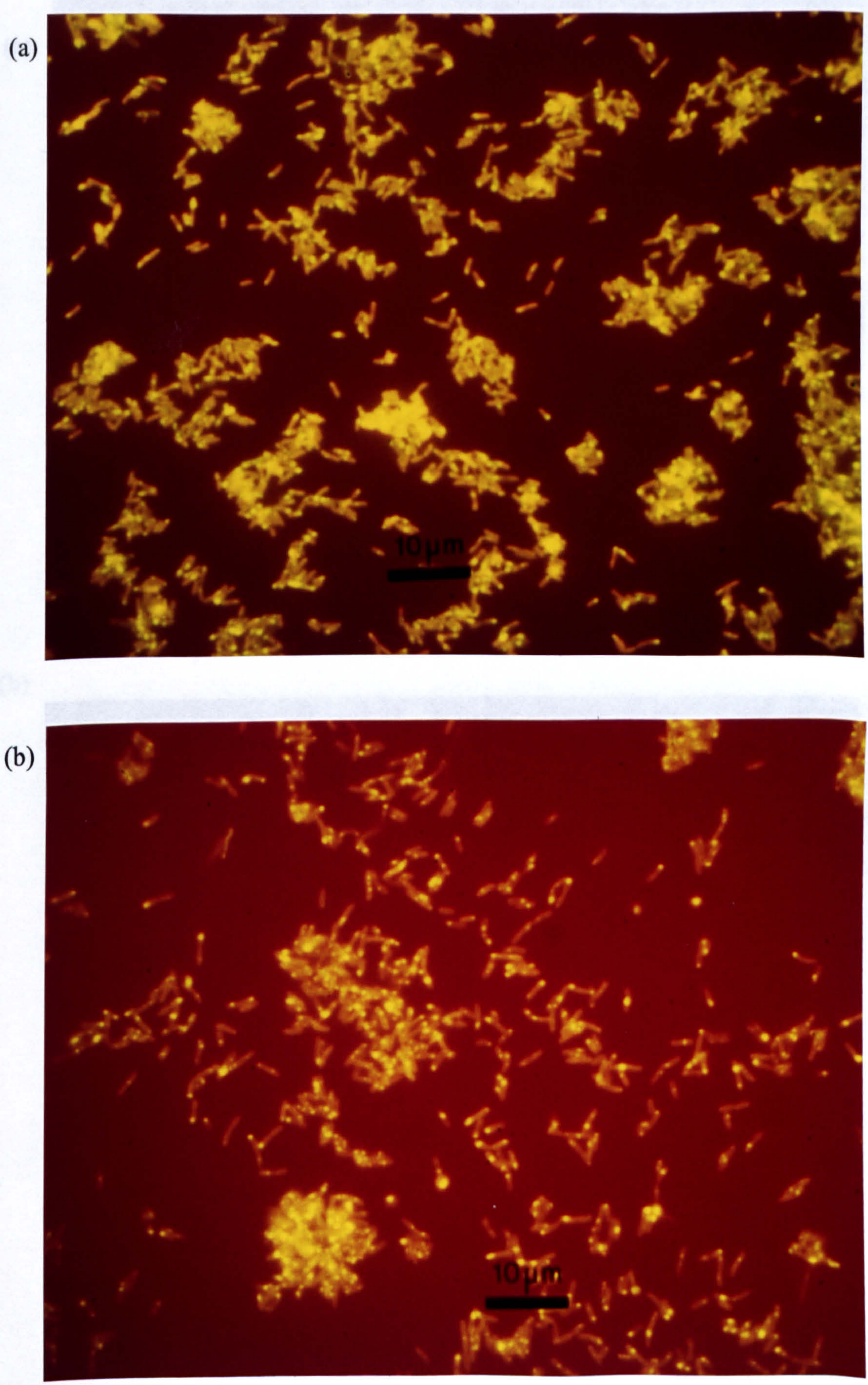


Figure 83. Fluorescent microscopic examination of culture samples grown at pH 6.0 and stained with NR, (a) iron-replete; (b) iron-limited.

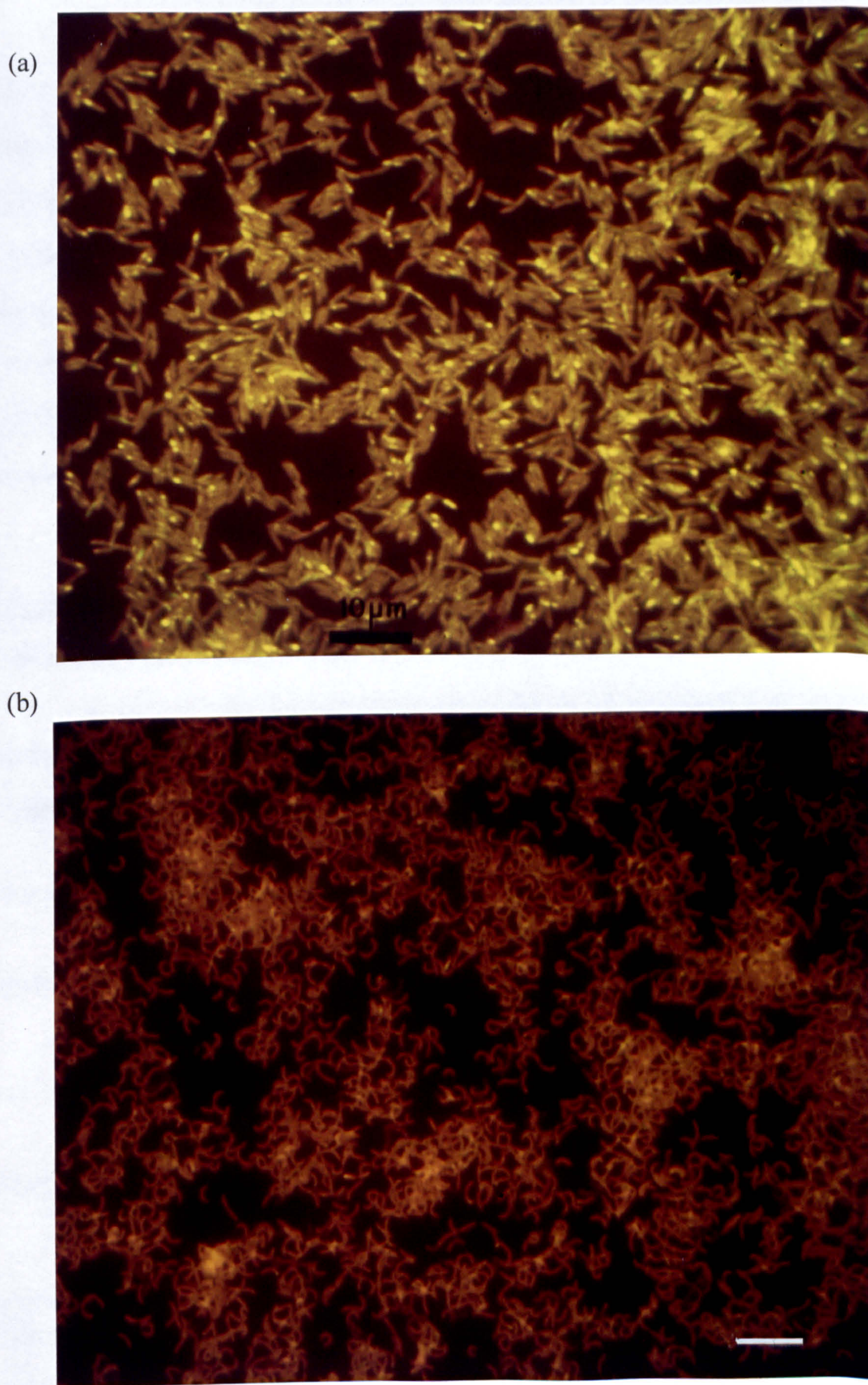


Figure 84. Fluorescent microscopic examination of culture samples grown at pH 7.8 and stained with NR, (a) iron-replete; (b) iron-limited. Bar, 10 μm .

Representative samples were also assayed spectrofluorometrically (Section 2.20.5). Decreasing the pH of iron-replete cultures from 6.9 to 6.0, induced a 40% increase in PHB content (Table XXX). By contrast, increasing the pH to 7.8 caused a comparable decrease in PHB content, in agreement with microscopic observations. Analysis of iron-limited cultures detected a 20% decrease in PHB content, in response to lowering the pH from 6.9 to 6.0. However, increasing the pH to 7.8 had a more dramatic effect on iron-limited samples, with virtually no PHB detected (Table XXX). Results for control iron-replete and limited cultures grown at pH 6.9 were in close agreement to previous determinations (Table XXIX).

Table XXX. Influence of culture pH on the mean NR spectrofluorescence and calculated PHB content of iron-replete and -limited cultures.

Culture	pH	Mean fluorescence \pm sd.	Mean PHB content (% cell dry wt.) ^a
Iron-replete ^b	6.0	15.6 \pm 1.7	6.4
	6.9	13.7 \pm 1.5	4.5
	7.8	12.1 \pm 1.7	2.9
Iron-limited ^c	6.0	20.6 \pm 1.9	10.5
	6.9	24.1 \pm 2.0	13.6
	7.8	9.4 \pm 0.2	0.3

^a PHB content was calculated from the spectrofluorescence data using the equation of the line from Figure 79.

^b Values represent the mean determination for 5 separate samples.

^c Values represent the mean determination for 4 separate samples.

3.20 Survival of *L. pneumophila* in a Low Nutrient Environment.

3.20.1 PHB content and the survival of *L. pneumophila* in a low nutrient environment.

The survival of *L. pneumophila* in filter sterilized tap water was investigated (Section 2.21). *L. pneumophila* grown in iron-replete culture, survived in a culturable state for a period in excess of 600 days, when incubated in this low nutrient environment (Figure 85). Initially, culturability declined rapidly, with the number of colony forming units decreasing by 60 % within the first 7 days. After this initial phase, the rate of loss of culturability decreased, with 25% of the population still culturable after 75 days, and 10% culture positive after 130 days (Figure 85). Spectrofluorometric analysis of samples stained with NR (Section 2.21.2), demonstrated a decrease in the fluorescence of the suspension during this period, indicating PHB utilization (Figure 85).

Figure 86 illustrates the relationship between the decline in culturability, and spectrofluorescence, both expressed as a percentage of their respective values at day zero. The relationship between the loss of culturability, and the decrease in spectrofluorescence changed with time, and can be divided into at least three different phases. The first phase which occurred during the first 7 days of starvation, is characterized by a rapid decline in both culturability and fluorescence. Although there is a linear relationship between both parameters, a greater decline in percentage culturability occurred. During the second stage (days 8 and 75), both rates of decline were reduced markedly. However, fluorescence decreased by 40% without a proportional loss of culturability, indicating PHB utilisation to support survival. The last phase which occurred over a period of 530 days, displayed significantly reduced rates of PHB utilization and loss of culturability. The decline in culturability during this final stage was more directly coupled to PHB utilization (Figure 86).

The total cell count of the starved suspension was monitored using phase contrast microscopy (Section 2.21.1). This revealed that after an initial decline of 25

% during the first week, the total number of intact cells remained relatively constant during the experiment, despite the decline in culturability (Figure 85). However, turbidity (OD_{540}) measurements, revealed a progressive decline in the optical density of the suspension, which appeared to follow a similar trend to the decrease in fluorescence (Figure 87). Figure 88 illustrates that the relationship between the percentage decrease in optical density and fluorescence is non-linear. With prolonged starvation, the decrease in optical density appears to become independent of the decrease in fluorescence.

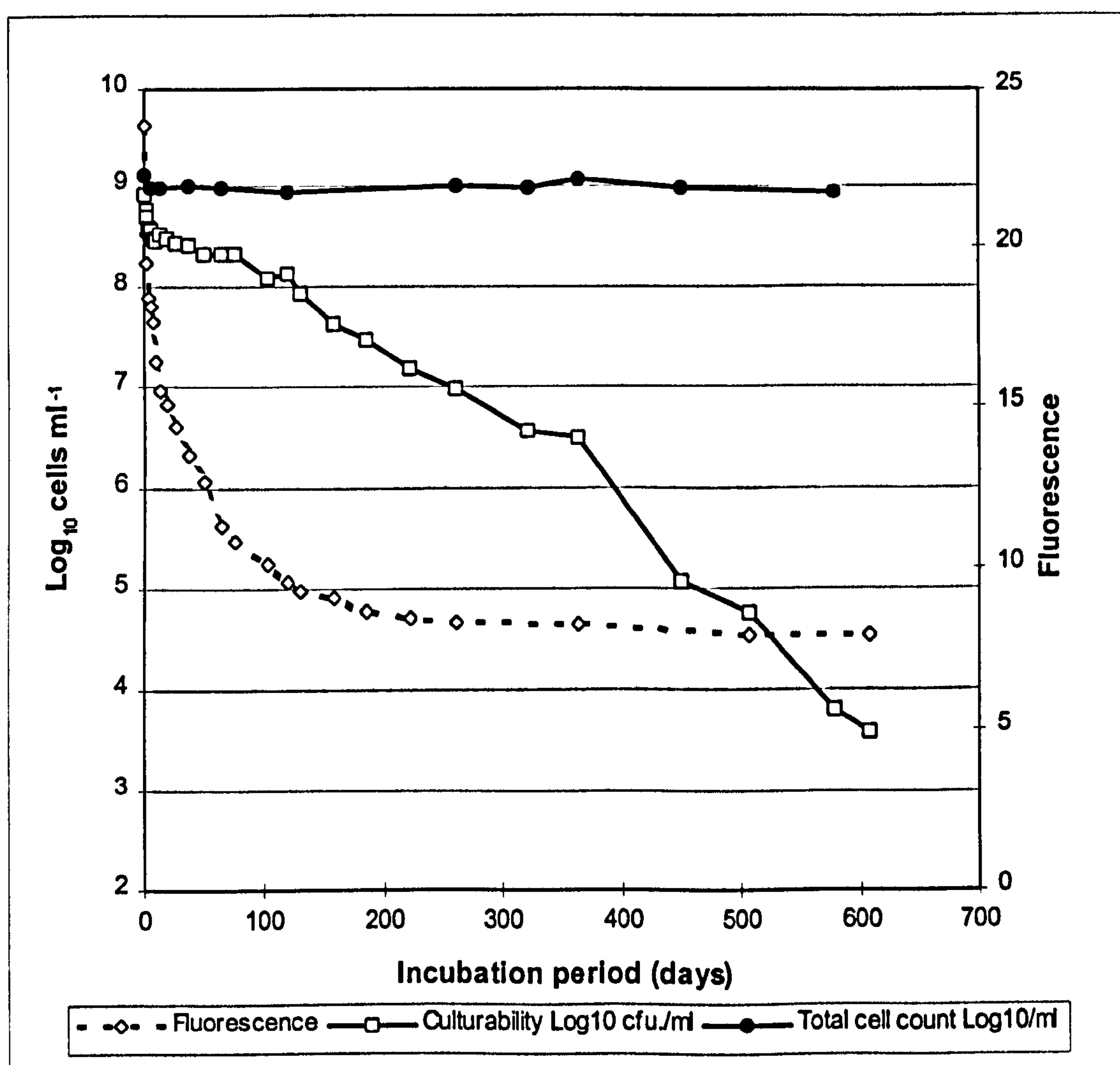


Figure 85. Influence of starvation on the culturability (formation of colonies on BCYE agar), total cell count (enumerated by phase contrast microscopy), and NR spectrofluorescence, of a suspension of *L. pneumophila* incubated in filter sterilized tap water at 24°C.

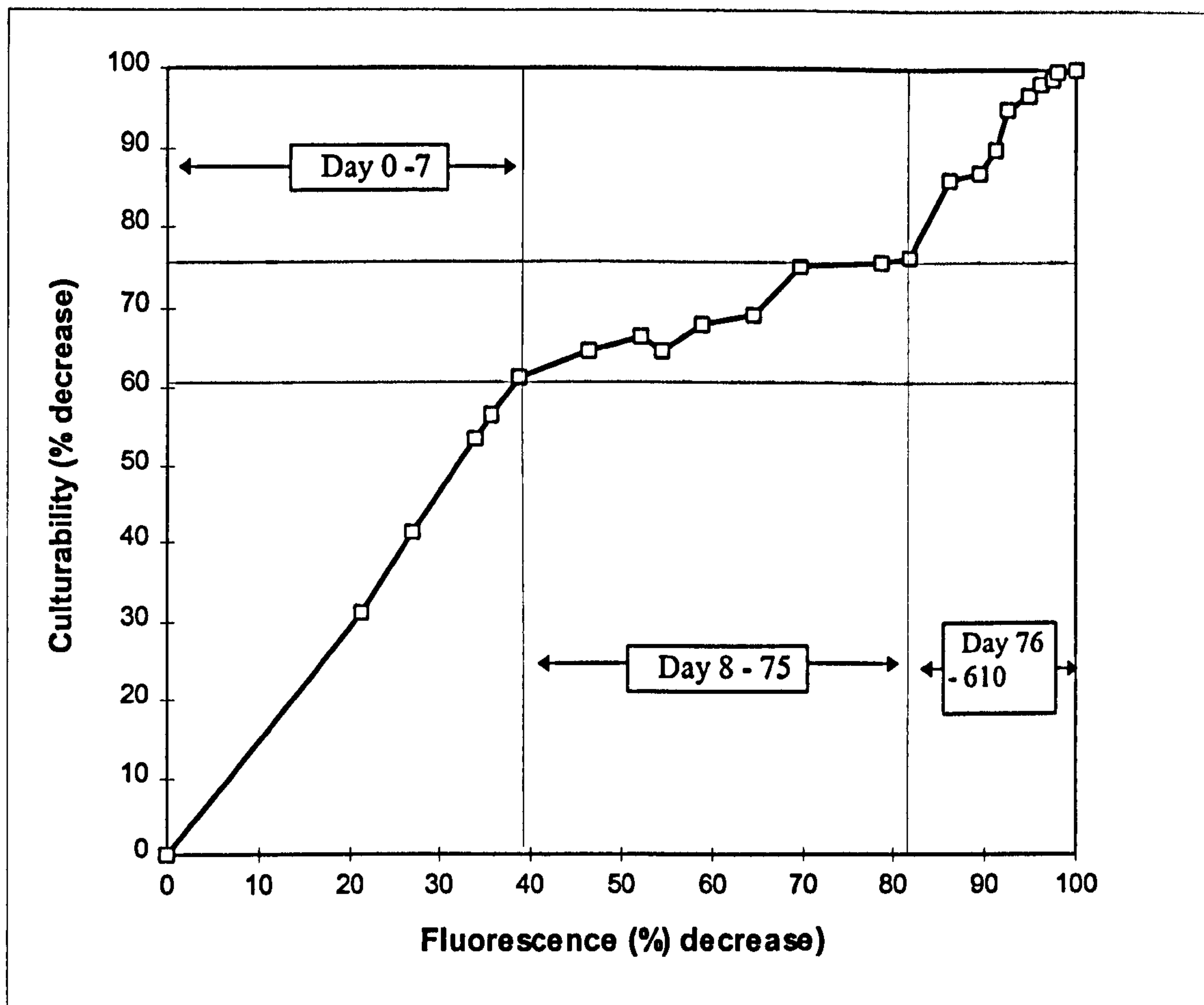


Figure 86. The relationship between the decline in culturability and NR spectrofluorescence, both expressed as a percentage of their respective values at day zero.

For this illustration, the assumption is made that the stable fluorescence reading at the end of the experiments represents the background cellular fluorescence, and 100% PHB utilization has occurred. This background fluorescence reading was subtracted from the fluorescence readings for each sample to provide a net fluorescence reading associated with the PHB.

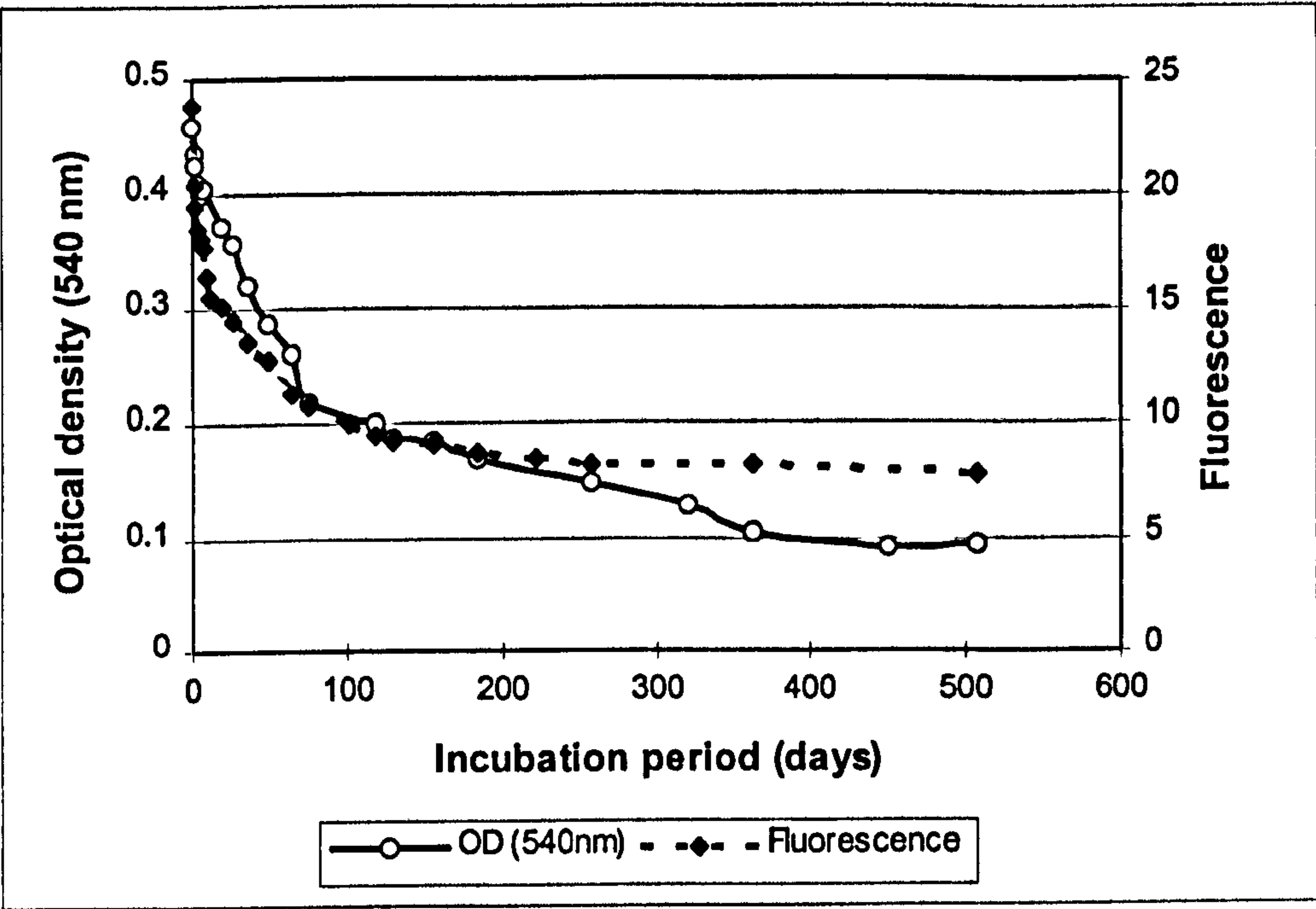


Figure 87. Influence of starvation on the optical density (540 nm), and NR spectrofluorescence of a suspension of *L. pneumophila*.

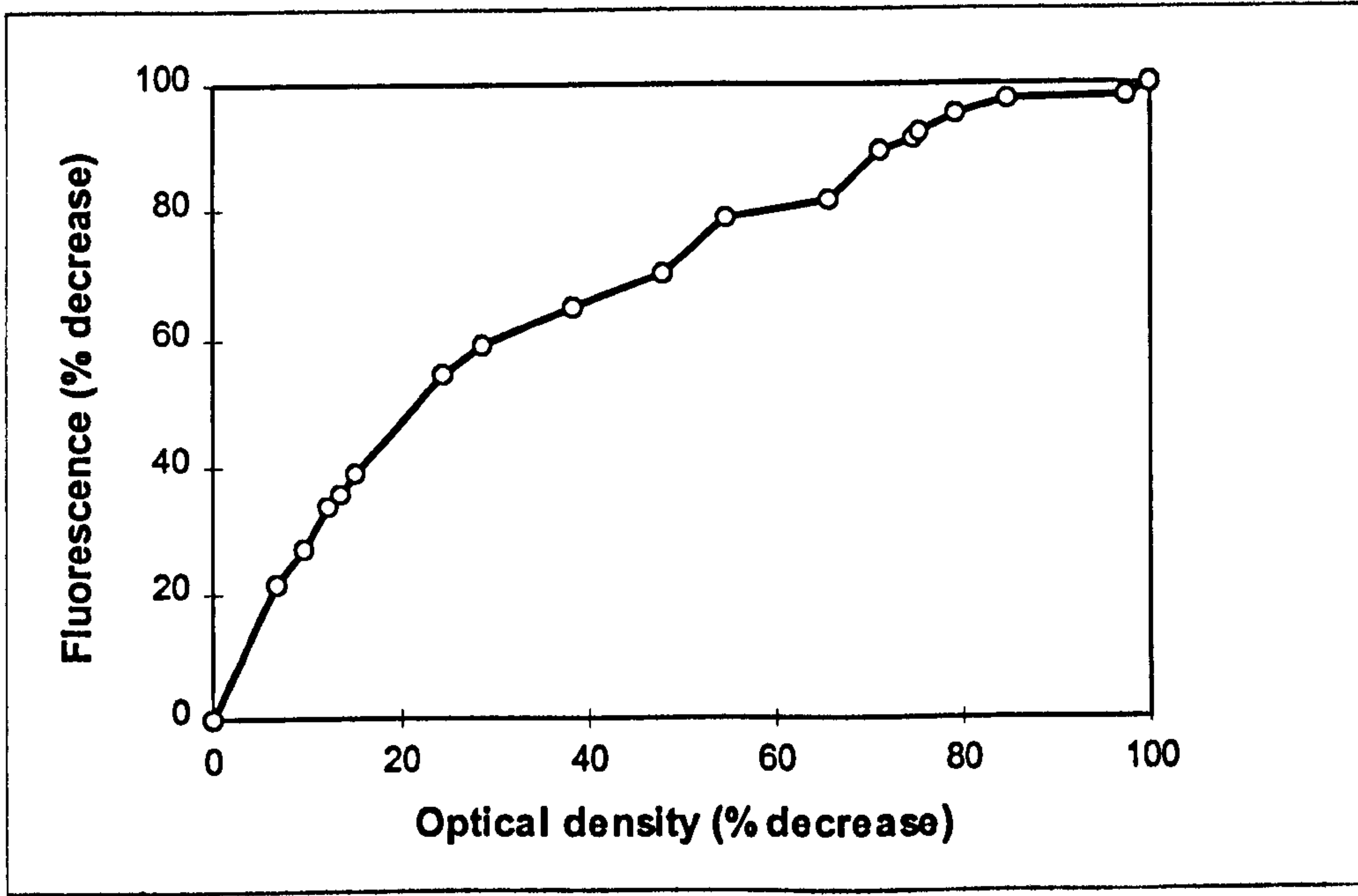


Figure 88. Relationship between the decrease in NR spectrofluorescence and optical density, both expressed as a percentage of their respective values at day zero.

A repeat study was performed with a different culture sample, possessing a calculated PHB content 35% greater than that of the previous culture, based on NR spectrofluorescence. This study confirmed the relationship between PHB content and survival in a low nutrient environment (Figure 89). However, this second culture demonstrated enhanced survival, in comparison to the previous study. The culturability of the suspension decreased to 10% after approximately 380 days, as opposed to 130 days in the first experiment.

Figure 90 illustrates the relationship between the decline in culturability and fluorescence, both expressed as a percentage of values at day zero. As observed with the previous culture (Figure 86), the relationship between loss of culturability and PHB utilization changes with time, with at least three different phases recognised (Figure 90). During the first week of starvation, the most rapid decline in culturability and fluorescence occurred, and both parameters appeared to be directly coupled. This phase was followed by a survival stage where a significant decrease in fluorescence, i.e. PHB utilization, occurred without a proportionate decrease in culturability. However, once the fluorescence was decreased by approximately 80%, the rate of culturability loss increased in relation to PHB utilization (Figure 90).

The enhanced survival of this second culture is likely to reflect the higher PHB content of this culture. Figure 91 compares the relationship between NR fluorescence and the survival (expressed as % culturability) for both cultures. Culture 1, which possessed a lower initial fluorescence demonstrated a more rapid loss of culturability. With culture 2, increased PHB utilization is associated with a more gradual decline in culturability, indicating enhanced survival. However, as the fluorescence of both cultures approaches depletion, the loss of culturability accelerates.

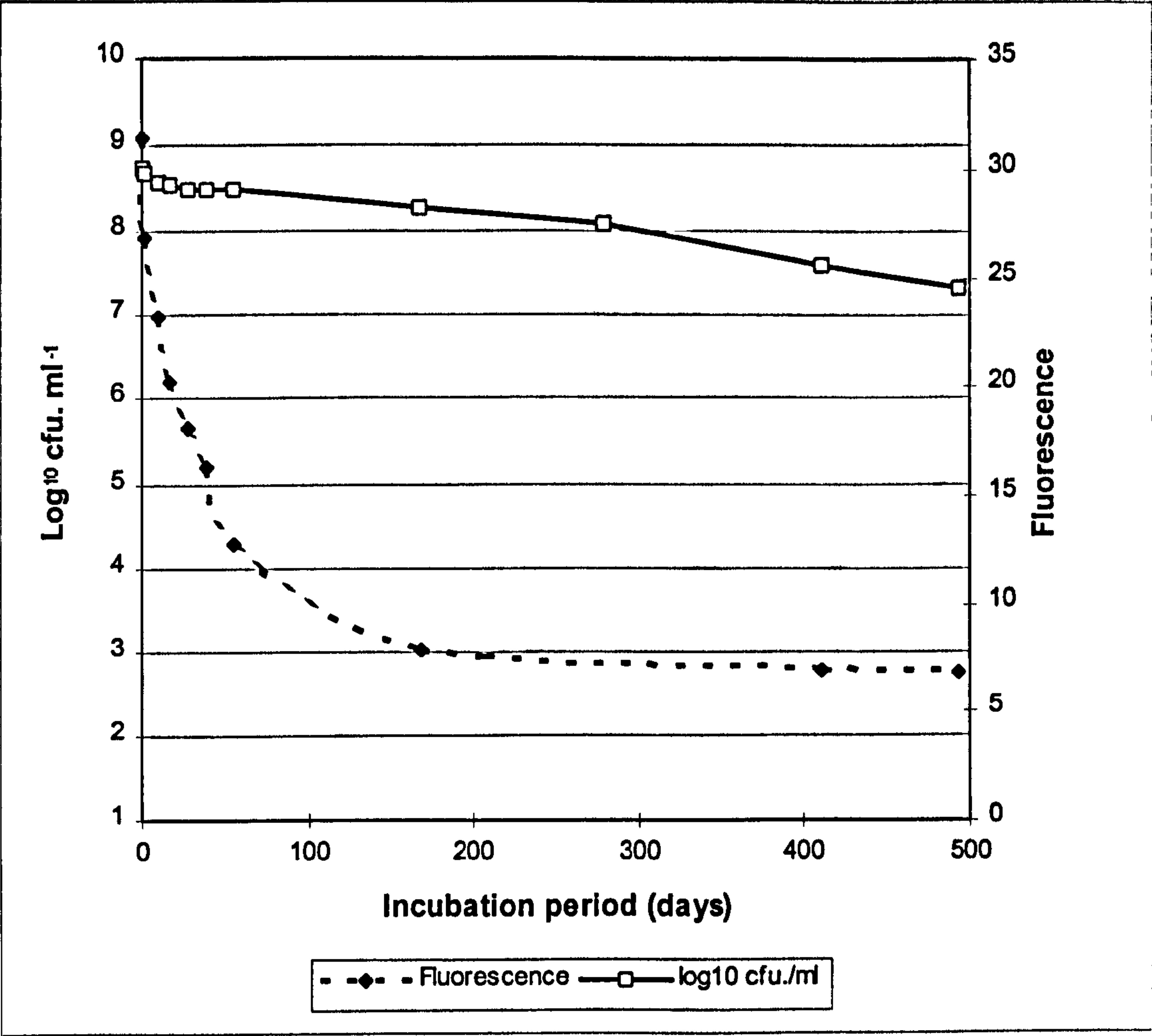


Figure 89. Influence of nutrient starvation on the culturability and NR spectrofluorescence of a suspension of *L. pneumophila*.

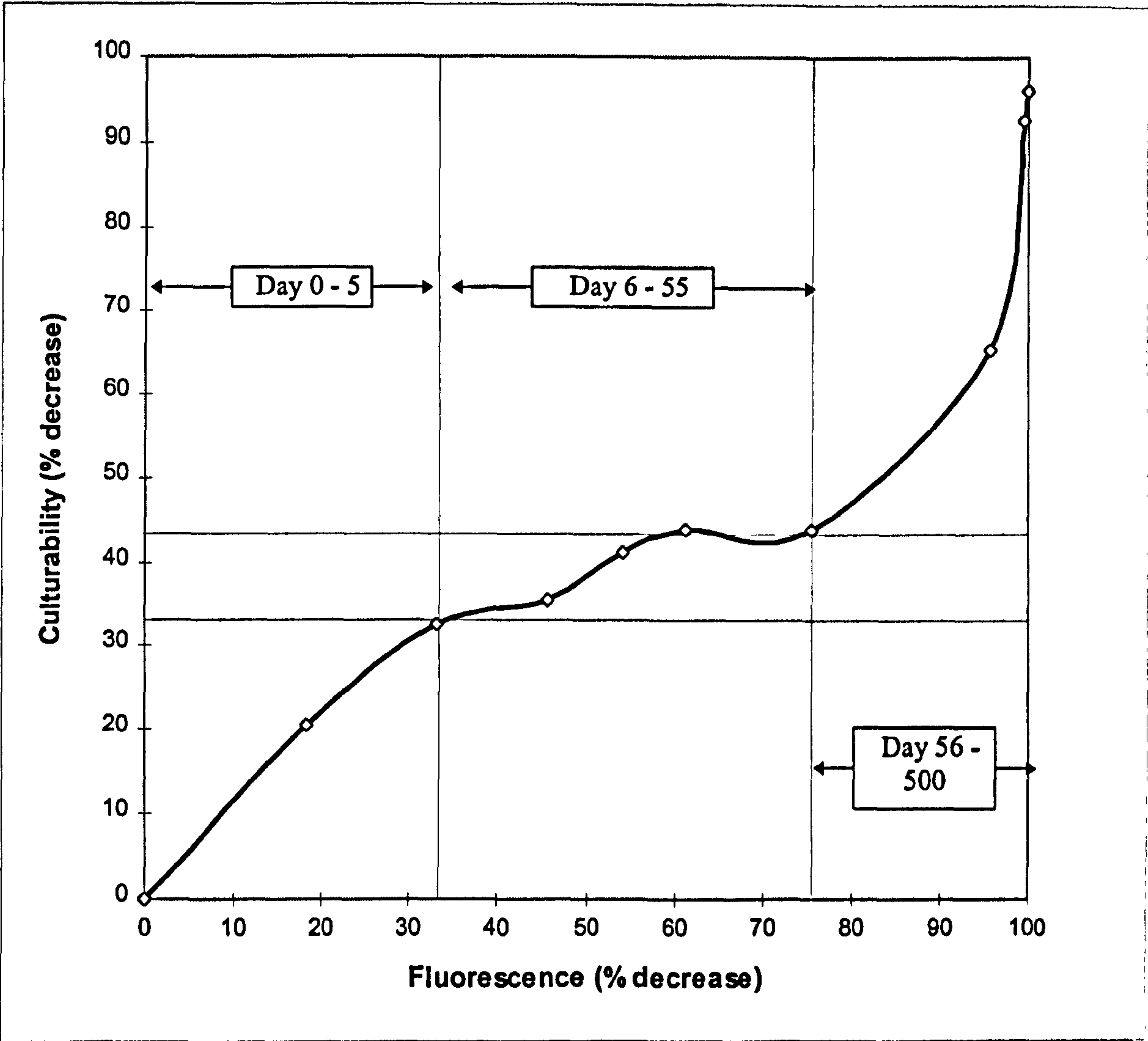


Figure 90. The relationship between the decline in culturability and NR spectrofluorescence, both expressed as a percentage of their respective values at day zero.

The stable background fluorescence reading recorded at the end of the experiment was subtracted from the fluorescence readings for each sample, to provide a net fluorescence value associated with the PHB.

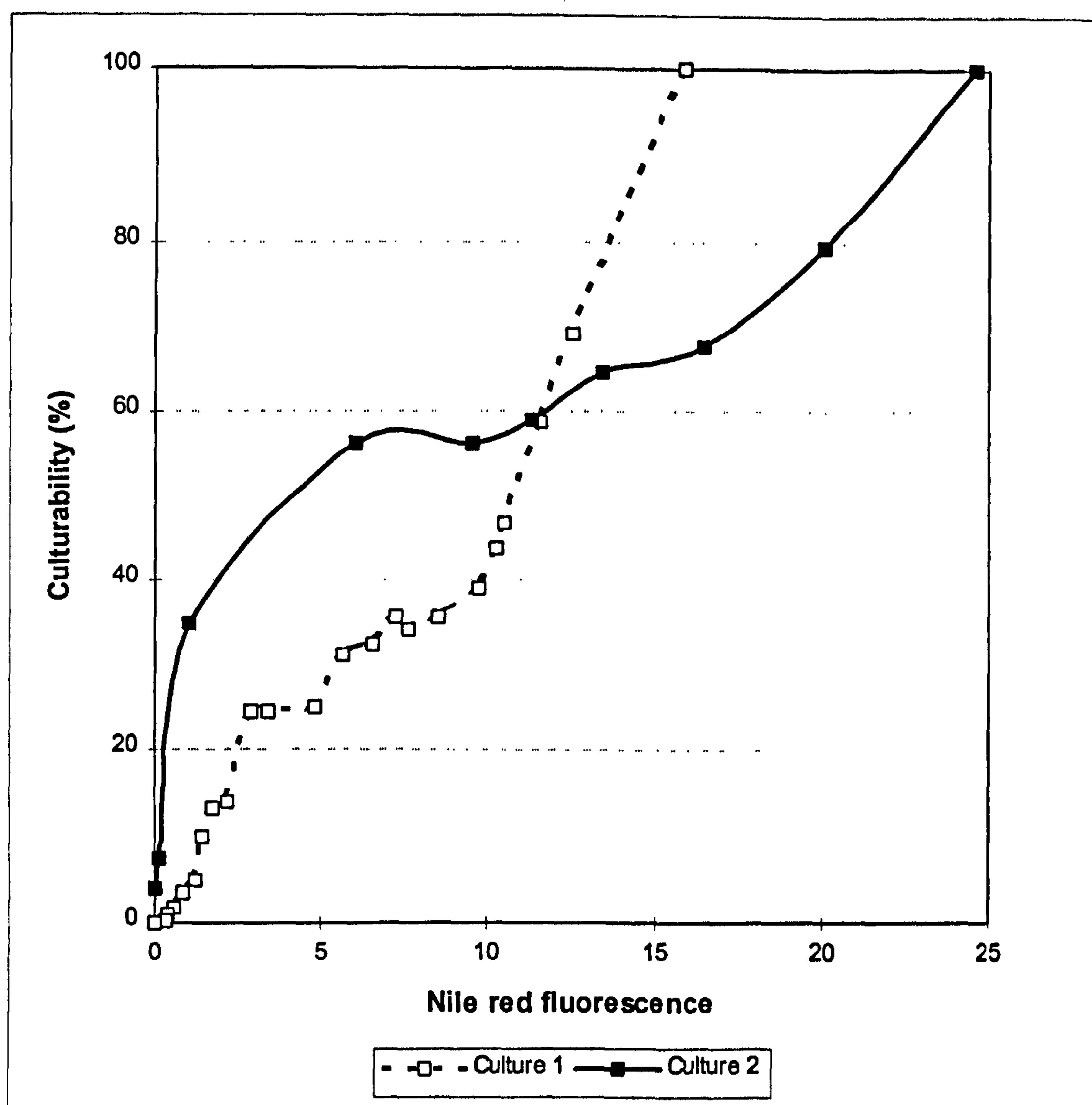


Figure 91. Comparison of the relationship between culturability (expressed as a percentage of original values at day 0) and NR spectrofluorescence, for two cultures of *L. pneumophila* incubated under starvation conditions. The initial calculated PHB content of cultures 1 and 2 was 14 and 21 % cell dry weight, respectively.

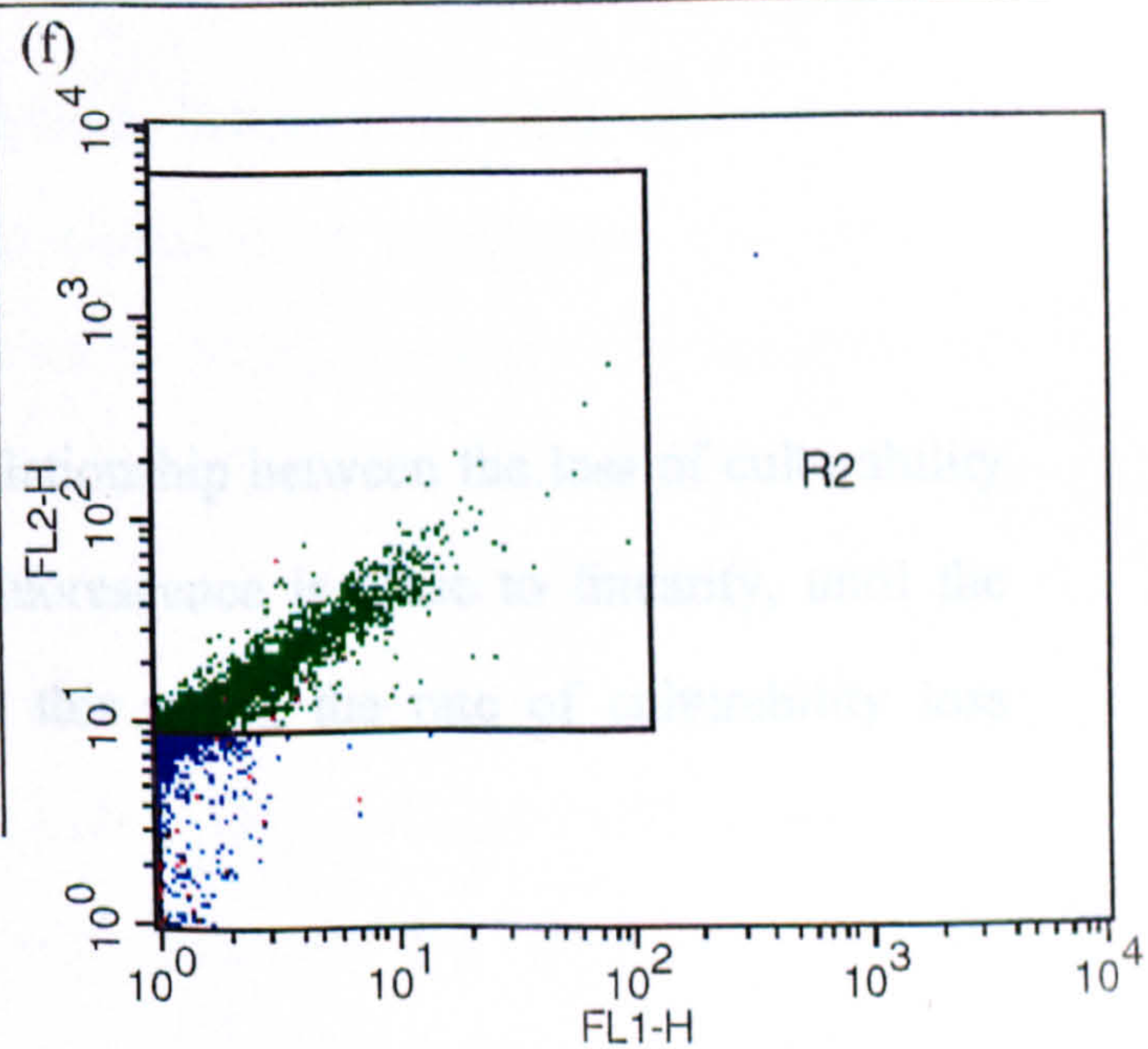
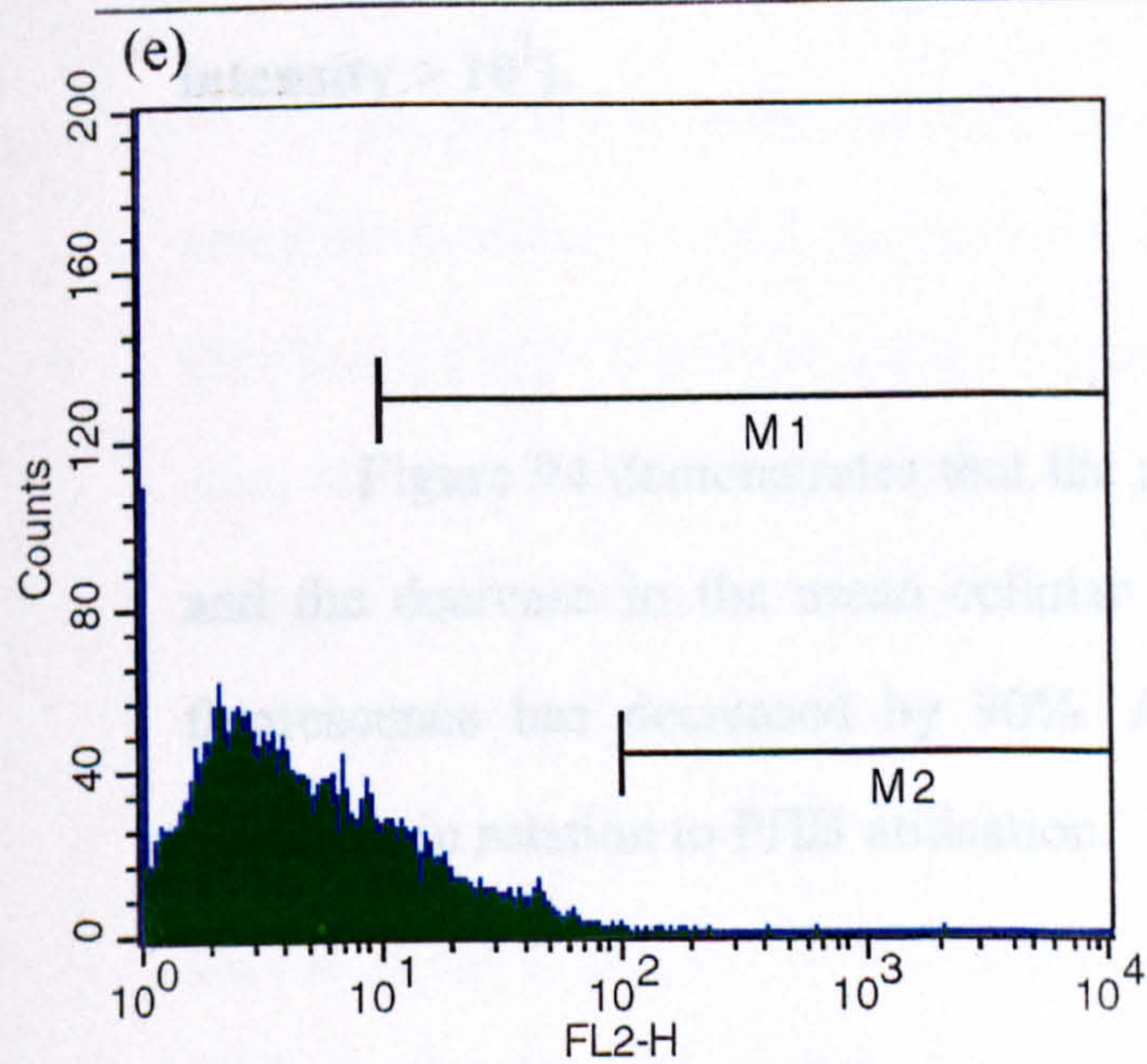
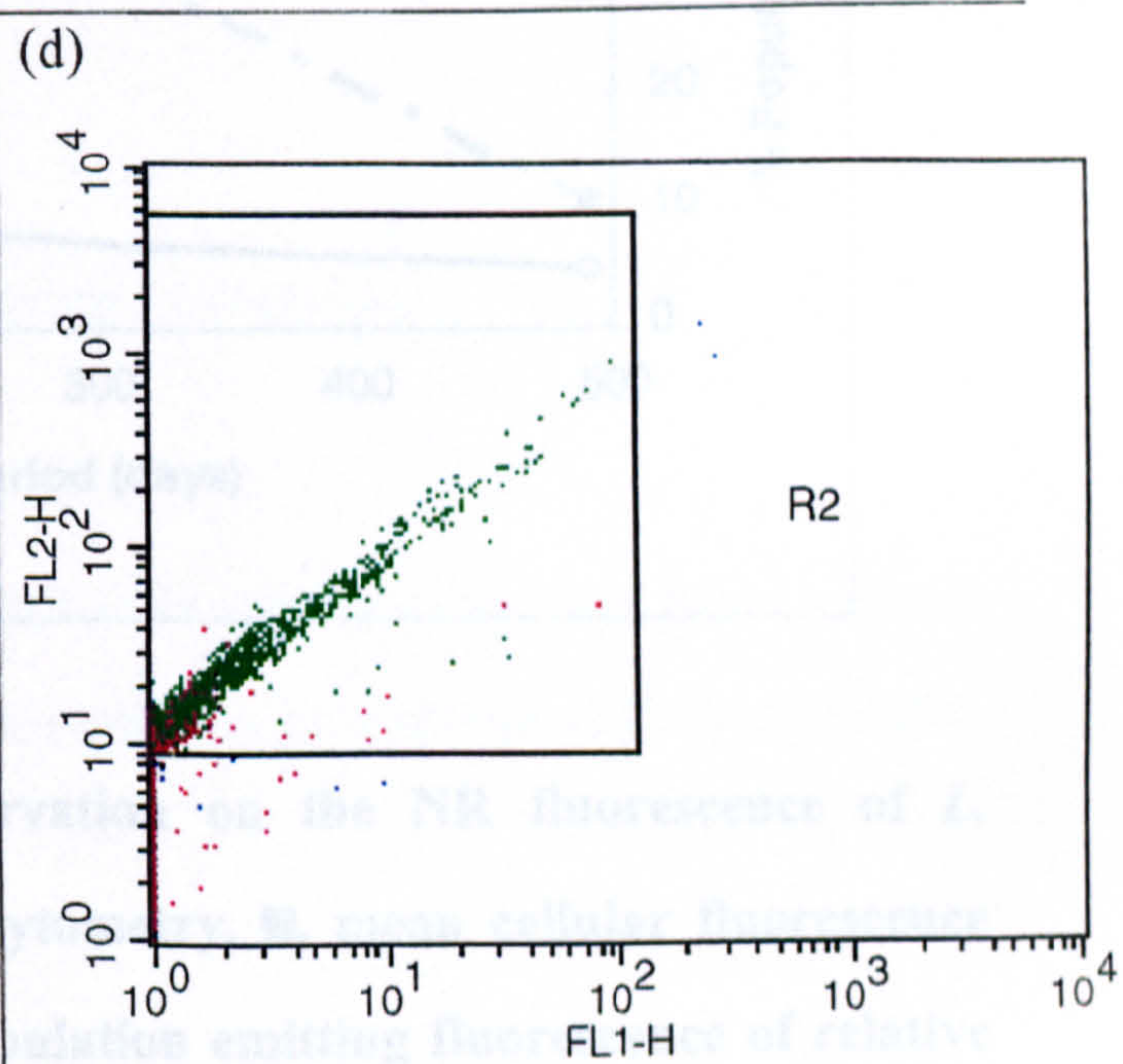
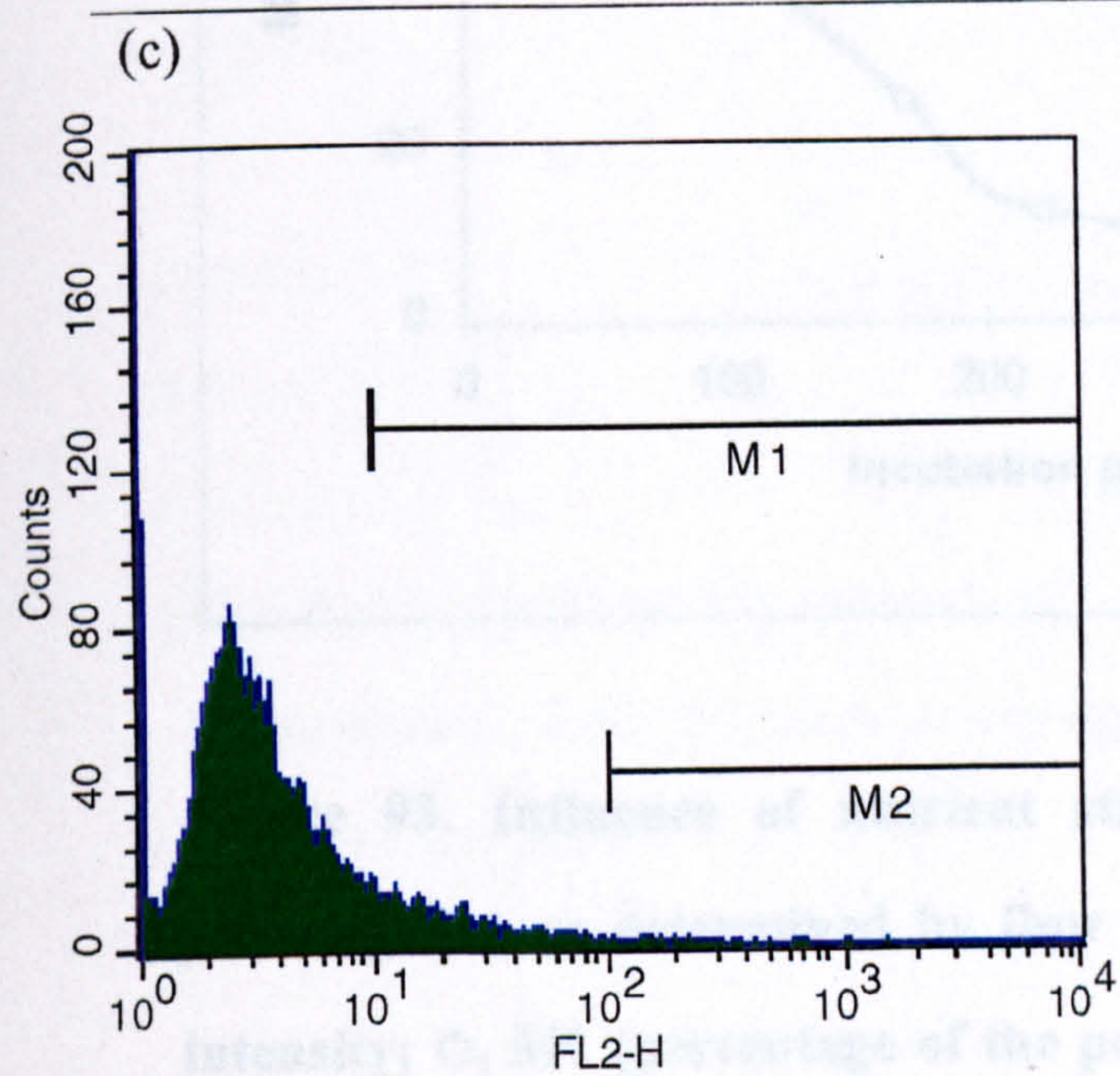
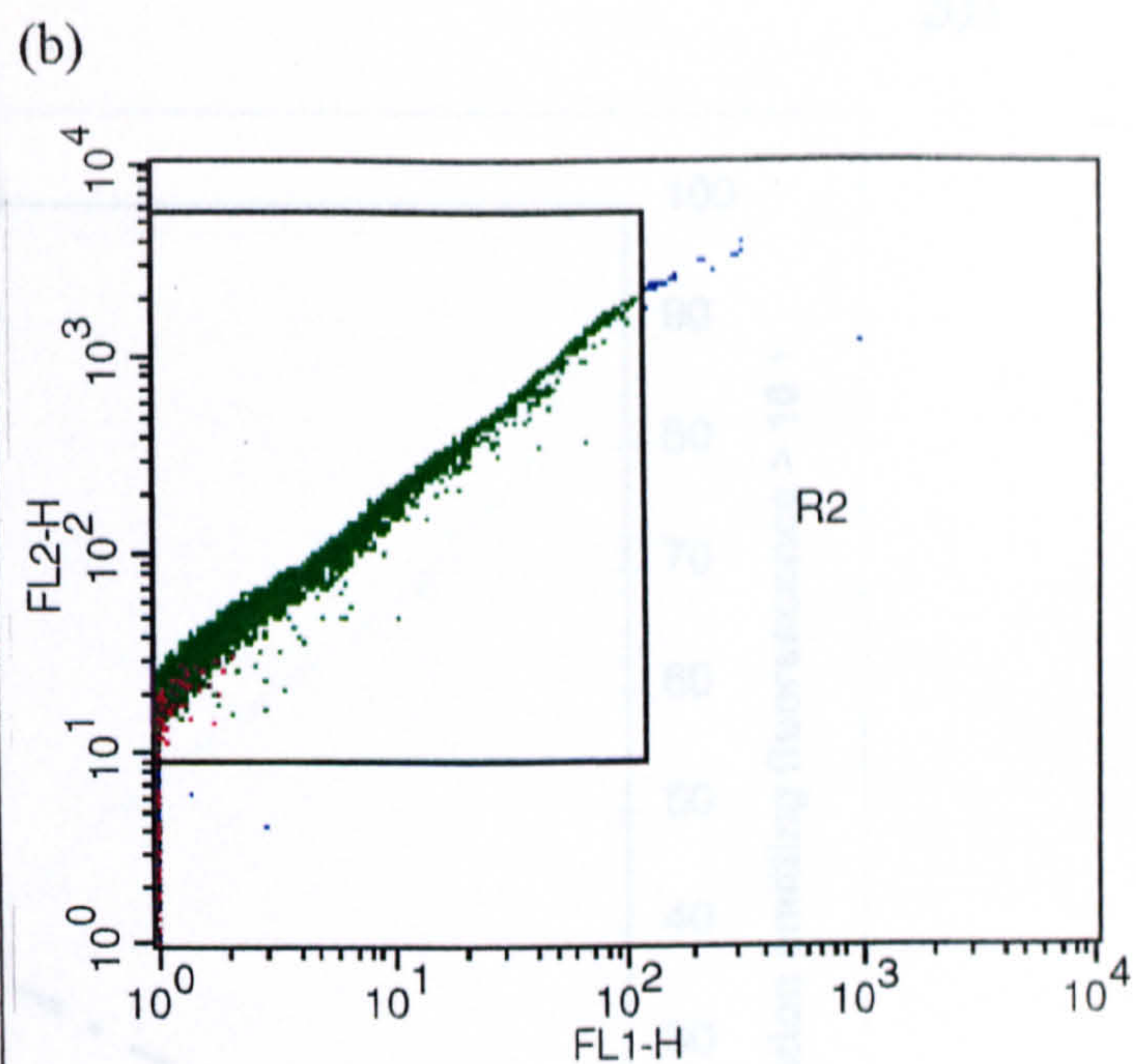
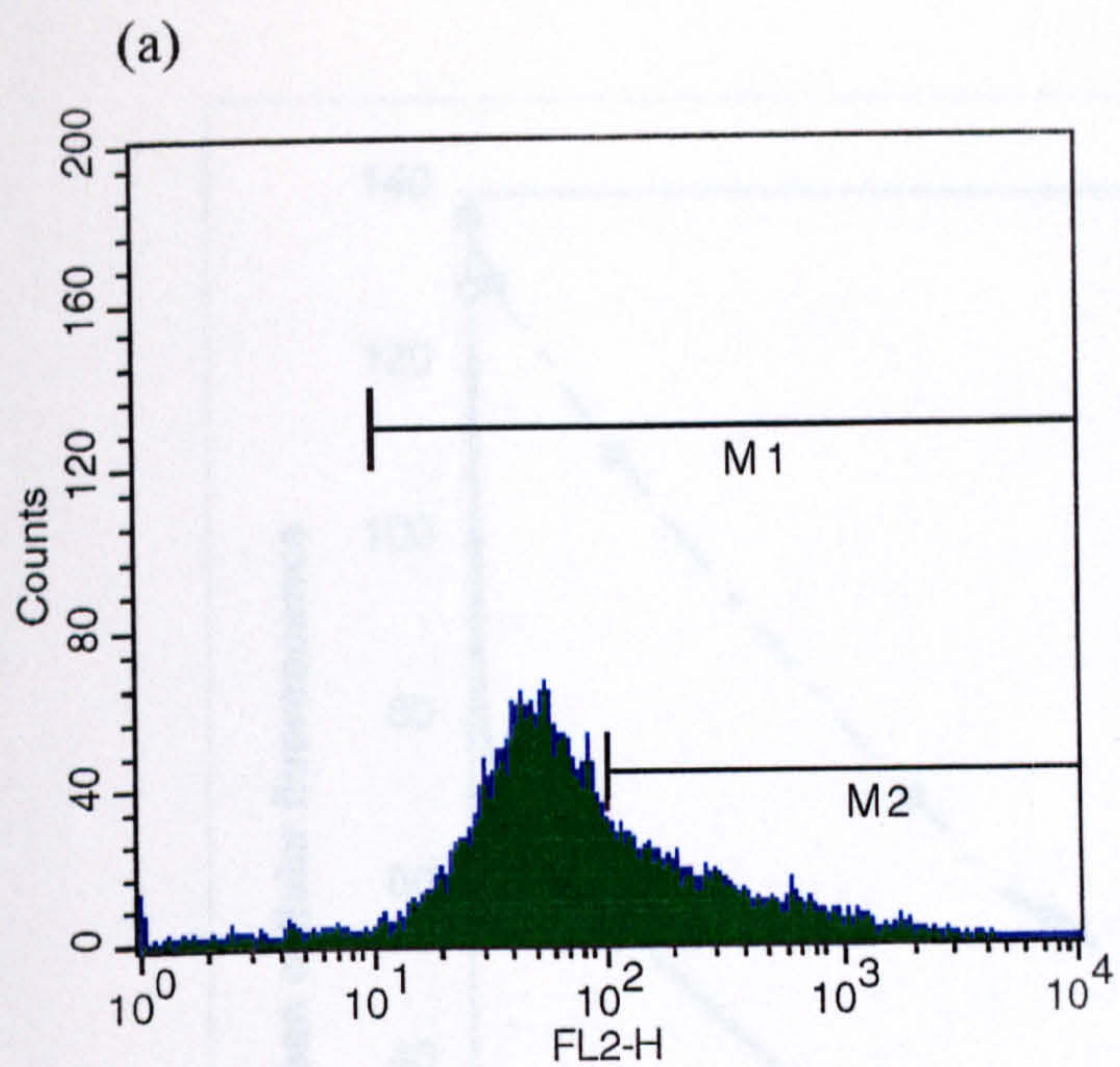
3.20.2 Flow Cytometry analysis of starved cells.

Samples collected from the second survival culture and stored at -40°C , were subsequently analysed by flow cytometry following staining with NR (Section 2.21.3). Figure 92 compares the cellular fluorescence of the suspension at day 0 (a & b) and after 490 days (c & d) starvation. At day 0, the majority of cells emitted a fluorescence intensity between 10^1 to 10^3 (relative to the background fluorescence of the unstained sample), with 98% of cells occurring within the gated regions M1 and R2 (fluorescence intensity $> 10^1$). However, after 490 days incubation under starvation conditions, a dramatic decrease in the relative fluorescence intensity of the cells was demonstrated. Approximately 90% of the starved population produced a fluorescence intensity $< 10^1$ (Figure 92 c & d). This low intensity fluorescence of the culture at day 490, was comparable to the background fluorescence of the unstained culture at day 0, (Figure 92 e & f).

The changes in cellular fluorescence with time are illustrated further in Figure 93. Six representative samples collected and stored during the course of the study, were stained with NR and analysed. The percentage of the population emitting a fluorescence of intensity greater than 10^1 (M1) declined by 50 % during the first 10 days of starvation. This rate of decline then slowed, and remained constant for approximately 200 days, until 95% of the population emitted a fluorescence of intensity $< 10^1$ (Figure 93). Values for the mean cellular fluorescence intensity, revealed a more gradual decline in cellular fluorescence during starvation (Figure 93). These observations are in close agreement with the spectrofluorometric data presented in Figure 89.

Figure 92. Flow cytometry analysis of the changes in cellular NR fluorescence in response to nutrient starvation, (a & b) day 0, pre-starvation; (c & d) after 490 days incubation in a low nutrient environment; (e & f) negative control, unstained cells at day 0. All plots represent the results from analysis of 10,000 events.

For histogram plots, the x-axis represents fluorescence intensity recorded by detector FL2 (580 ± 25 nm). The y-axis represents the number of cells counted at a particular intensity. Dot plots display the distribution of each event based on the intensity of cellular fluorescence recorded by detectors FL1 (500 ± 25 nm) and FL2 (580 ± 25 nm).



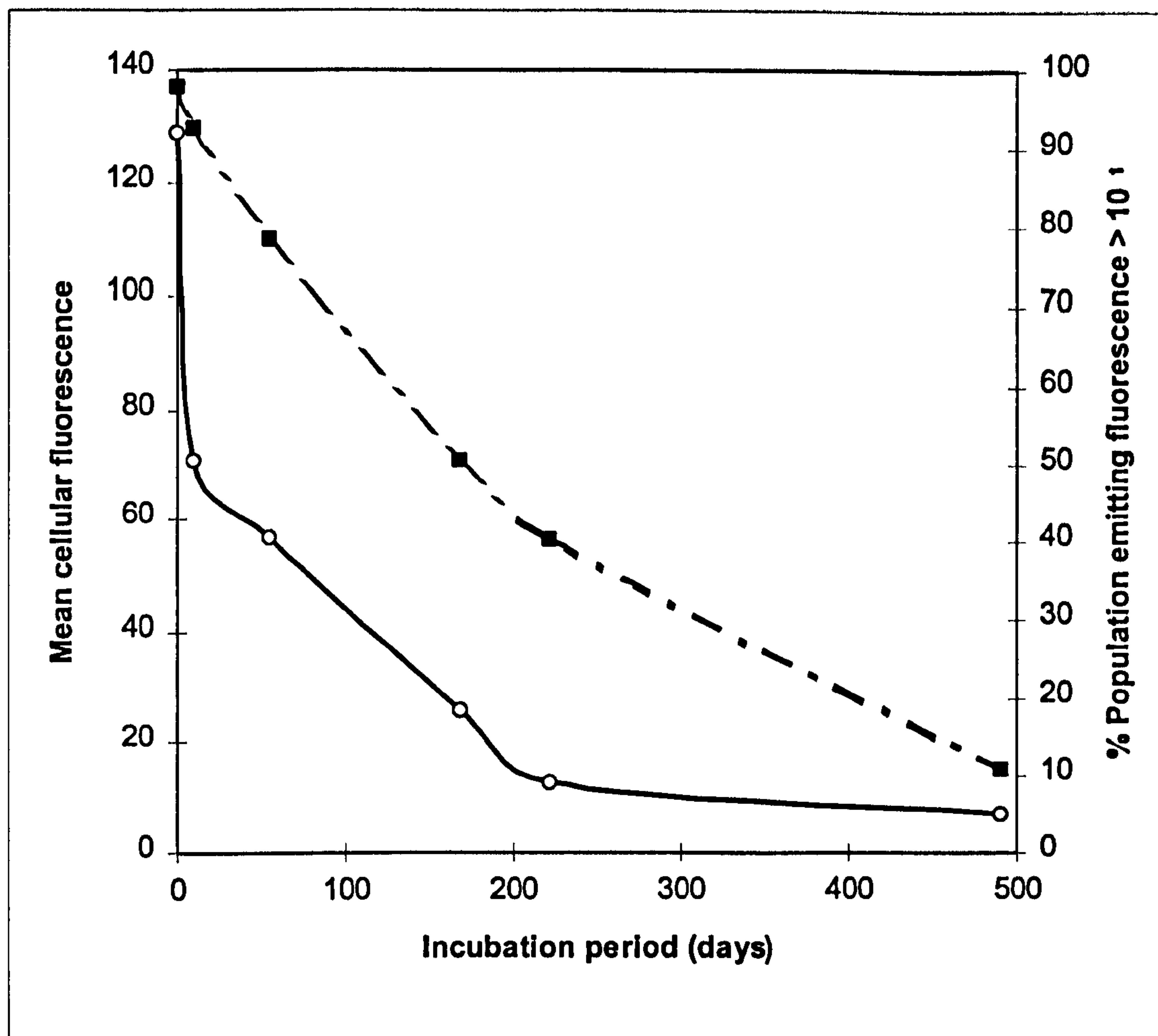


Figure 93. Influence of nutrient starvation on the NR fluorescence of *L. pneumophila*, as determined by flow cytometry. ■, mean cellular fluorescence intensity; ○, M1 (percentage of the population emitting fluorescence of relative intensity > 10¹).

Figure 94 demonstrates that the relationship between the loss of culturability and the decrease in the mean cellular fluorescence is close to linearity, until the fluorescence has decreased by 90%. At this point, the rate of culturability loss increases in relation to PHB utilisation.

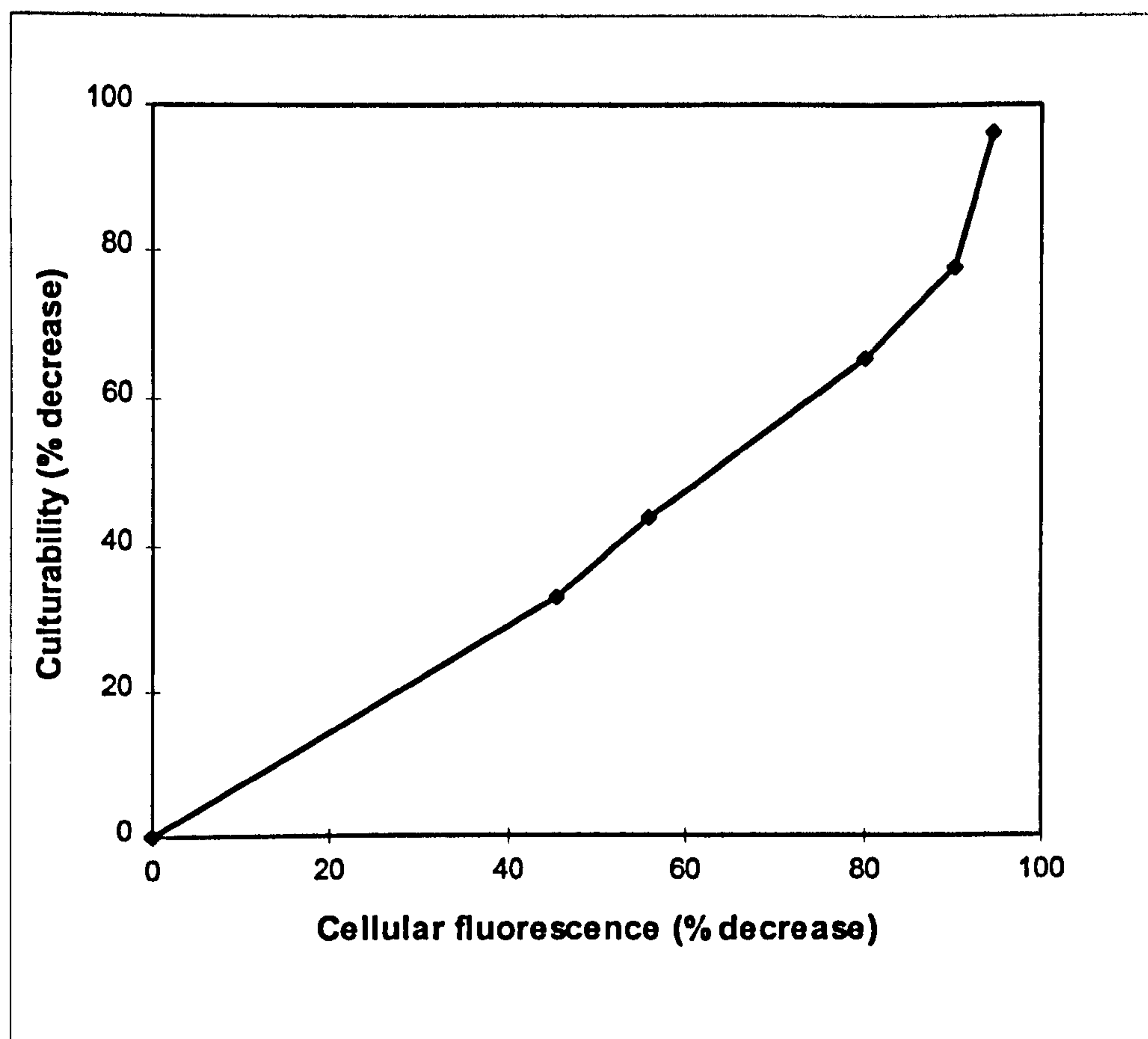


Figure 94. Relationship between the decline in culturability, and mean cellular fluorescence. Both parameters are expressed as a percentage of their respective values at day zero.

In addition to the changes in cellular fluorescence, flow cytometry also revealed changes in cell complexity (an indicator of granularity) and cell size (Section 2.21.3). Figure 95 shows acquisition dot plots, depicting cell granularity and size, for samples collected at day 0 (a), and after 490 days incubation (b). The y-axis represents the side-scatter (SSC) of the cells, and provides an indication of the relative granularity or internal complexity of the cells. Cell length is indicated along the x-axis by the forward scatter (FSC). The plots were divided into the gated regions shown in figure 95, to allow changes in cell complexity and length to be analysed further. Comparison of the plots revealed a dramatic change in the population distribution as a result of starvation.

At day 0, the cells are widely distributed, indicating a wide range of cell complexity and size. A low percentage of the cells (7 %) are positioned in the region R1, which represents small cells of low internal complexity, and debris. After 490 days starvation, the percentage of the population located in R1 increased to 86%, indicating a significant decrease in cell size and complexity (Figure 95 and Table XXXI). Analysis of the whole plot, also confirmed changes in both cell complexity and size. During starvation, the mean cell complexity (y-mean) decreased by 80%, from 382 to 86 (Figure 95 and Table XXXI). Examination of the x-axis data also revealed a 30% decrease in the mean cell length (Table XXXI).

Graphical analysis of data for the 6 representative samples confirmed a steady decrease in both cell complexity and length over time, indicated by a decrease in the y-mean and x-mean values for the whole plot (Figure 96). As observed with the spectrofluorometric and culturability data for the culture, the most rapid decline in cell complexity occurred during the early stages of starvation (Figure 96).

The relationship between the decline in mean cellular fluorescence and complexity was close to linearity, until the cellular fluorescence was decreased by approximately 90%; at this point the cell complexity continued to decrease, without a proportional decrease in fluorescence (Figure 97). A linear relationship was observed between the decline in percentage culturability and mean cell complexity (Figure 98).

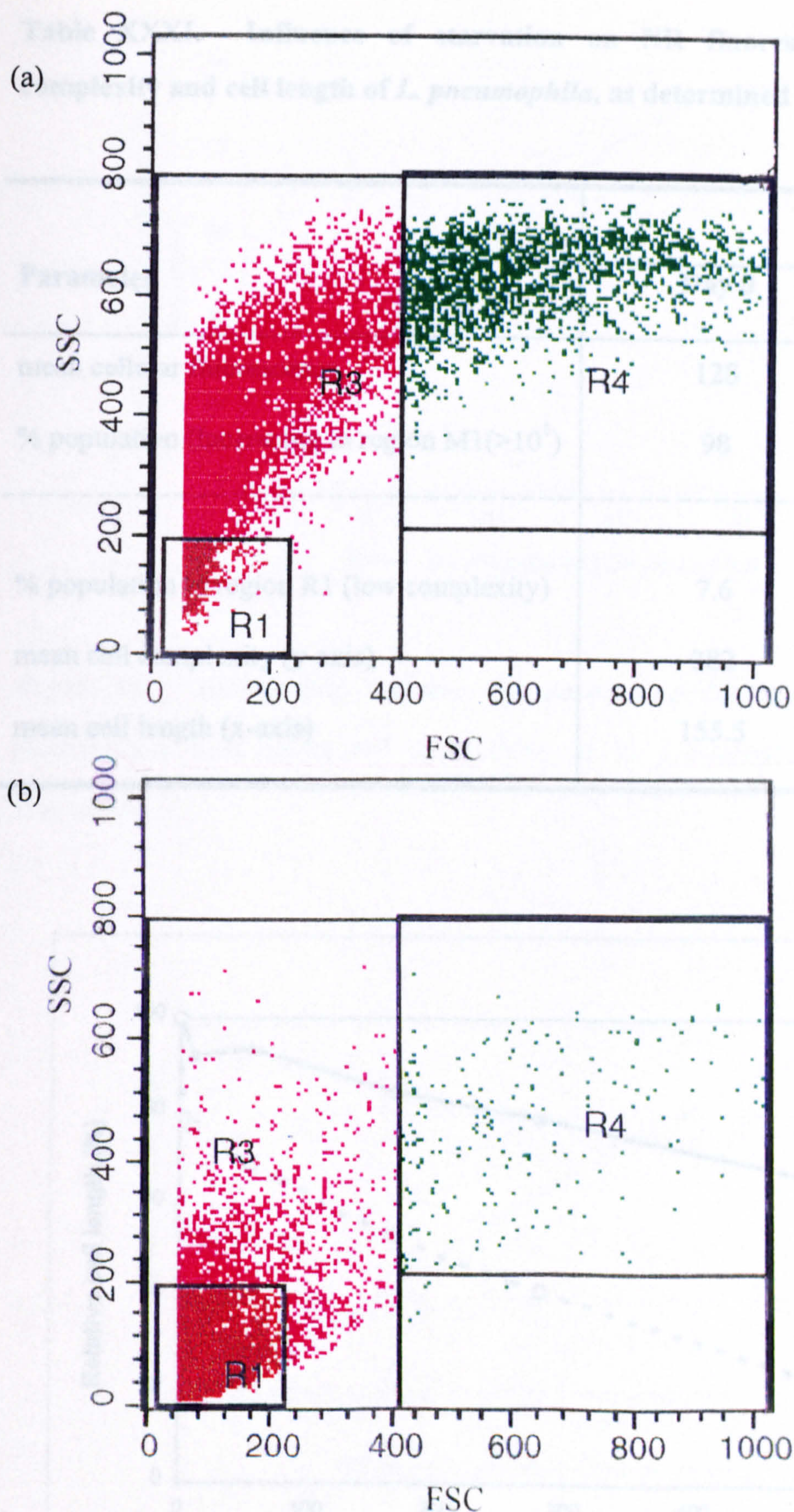


Figure 95. Comparison of dot plots representing the relative cell complexity and size distribution for *L. pneumophila* at (a) day 0, and (b) 490 days post incubation in filter sterilized tap water. SSC - side scatter representative of relative complexity/granularity; FSC - forward scatter representative of relative cell length.

Table XXXI. Influence of starvation on NR fluorescence, intracellular complexity and cell length of *L. pneumophila*, as determined by flow cytometry.

Parameter	Sample	
	Day 0	Day 490
mean cellular fluorescence	128	7
% population fluorescing in region M1(>10 ¹)	98	11
<hr/>		
% population in region R1 (low complexity)	7.6	86
mean cell complexity (y-axis)	382	86
mean cell length (x-axis)	155.5	103

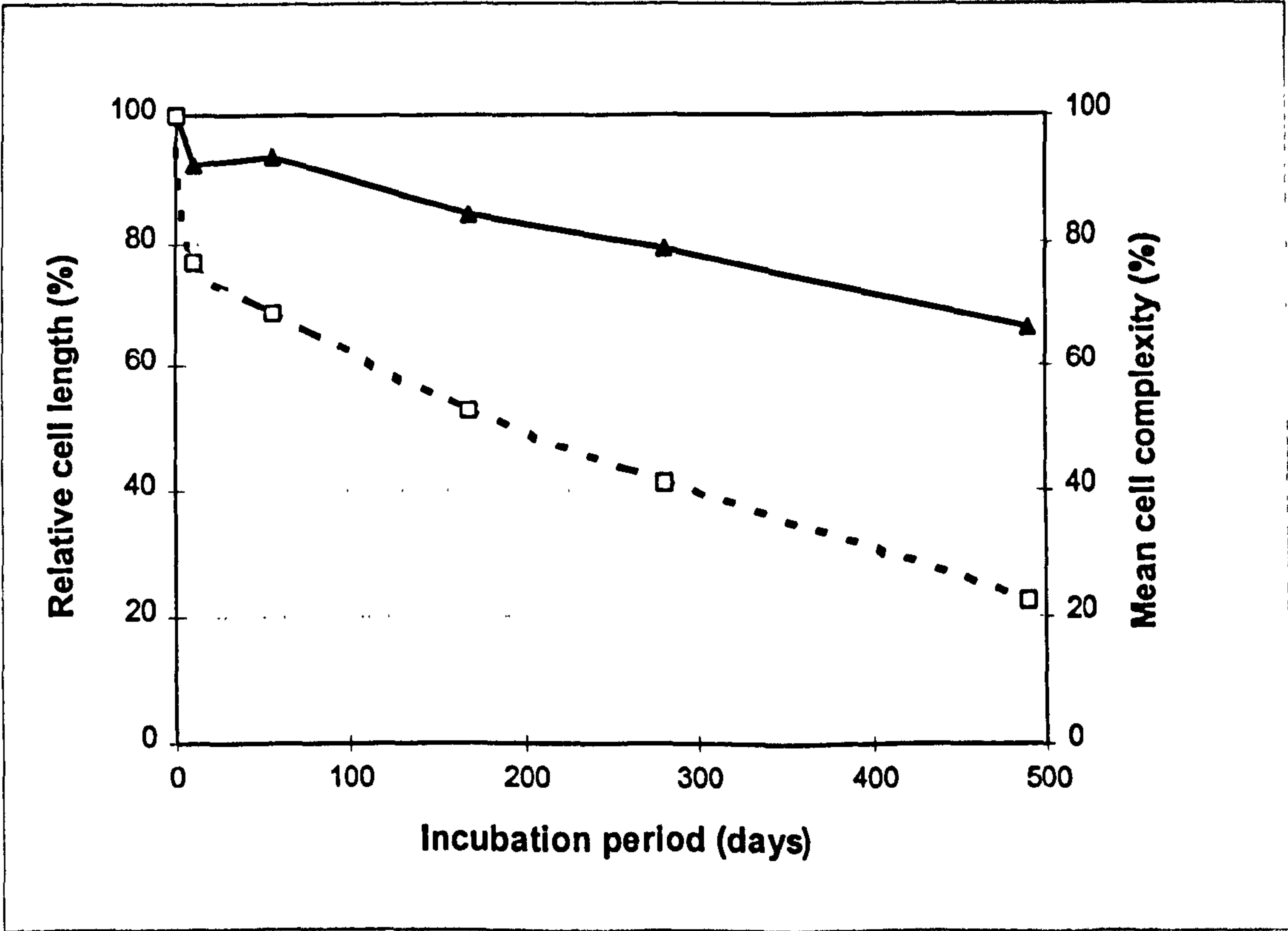


Figure 96. Influence of starvation on mean cell length (Δ) and mean cell complexity (□), expressed as a percentage of their respective values at day 0. Results are based on the analysis of 10,000 events for each sample.

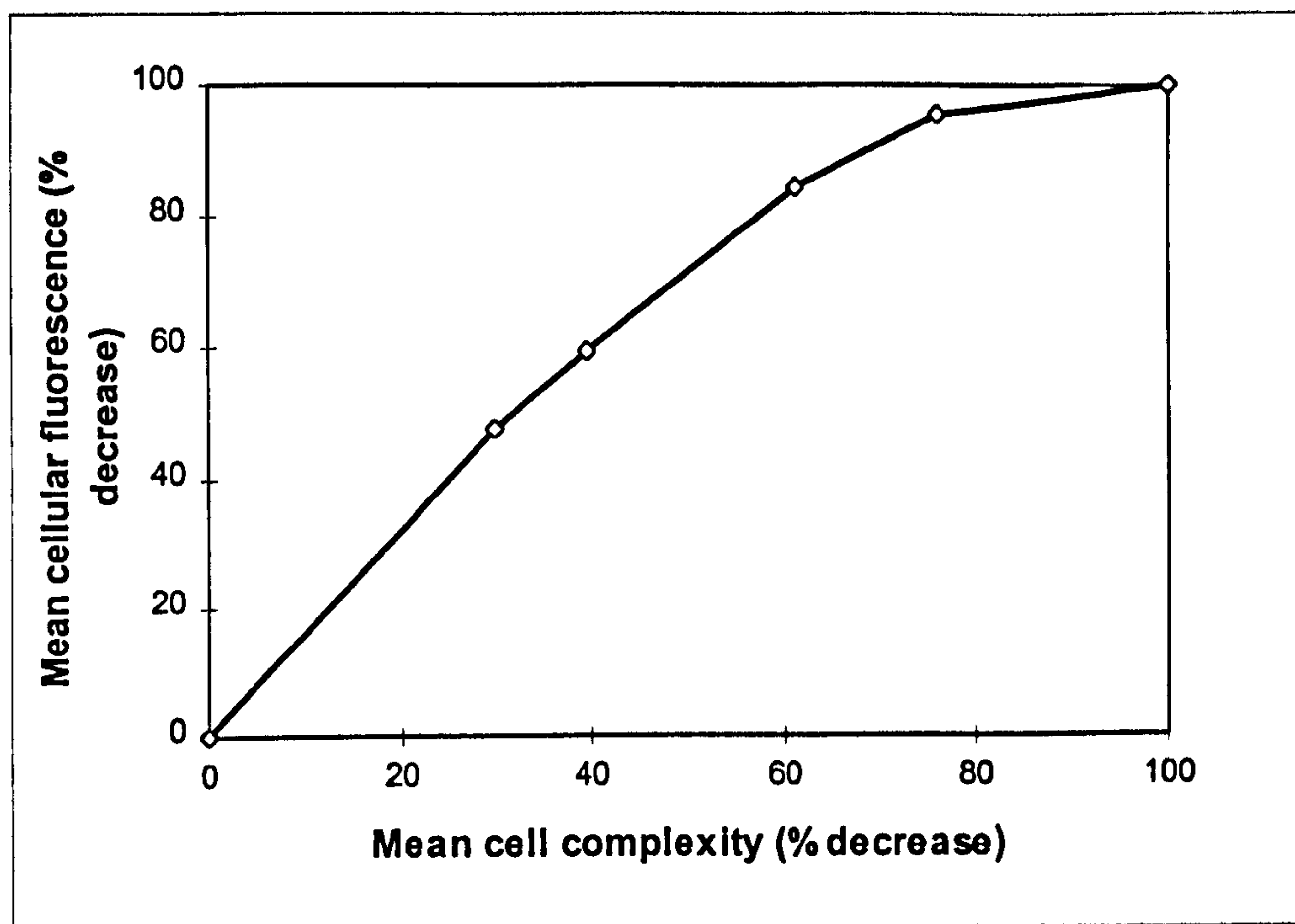


Figure 97. Relationship between the percentage decrease in mean cellular fluorescence and mean cell complexity of *L. pneumophila*, in response to starvation.

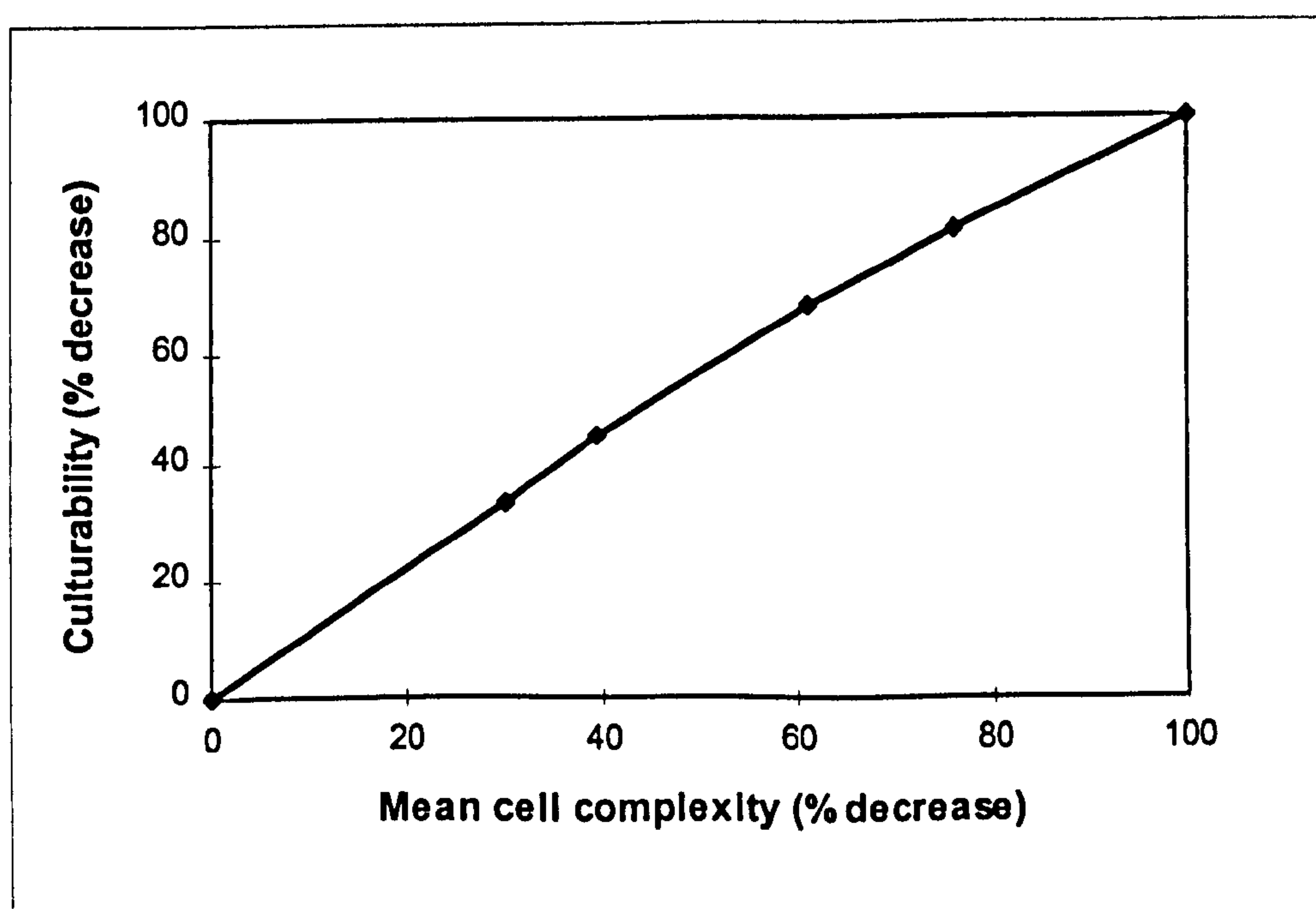


Figure 98. Relationship between the decrease in culturability and mean cell complexity, both expressed as a percentage of their respective values at day 0.

3.20.3 Morphological examination of starved cells.

Samples collected from the first study were also examined by fluorescence microscopy following NR staining (Section 2.6.4). At day 0, the majority of the cells contained brightly fluorescing lipophilic granules, with multiple granules visible in longer cells (Figure 99a). After 260 days incubation, a marked decrease in the granule content of the culture was clearly visible. Indeed, many cells appeared to contain no granules (Figure 99b). Examination of NR stained samples collected after 500 days starvation revealed virtually no intracellular granules (Figure 99c). Microscopic examination of cells stained with serogroup specific polyclonal antiserum, after 260 days starvation, revealed no alteration in serogroup reactivity, or in cellular morphology (Figure 100).

DIC microscopy of cells revealed some alterations in cell morphology in response to starvation. At day 0, all cells appeared to be intact with no evidence of cell debris (Figure 101a). However, after 600 days starvation, a high proportion of the cells appeared ghost-like, giving the appearance of cell debris (Figure 101b).

Alterations in colony size on BCYE agar also became apparent after prolonged starvation. Samples plated onto BCYE agar at day 0, produced colonies approximately 4 to 5 mm in diameter after 4 days growth. However, after 600 days starvation, colonies were found to range from 1 to 5 mm in diameter after 4 days growth. Despite differences in colony size, other colony features including colour and 'ground-glass' texture, appeared normal (Figure 102).

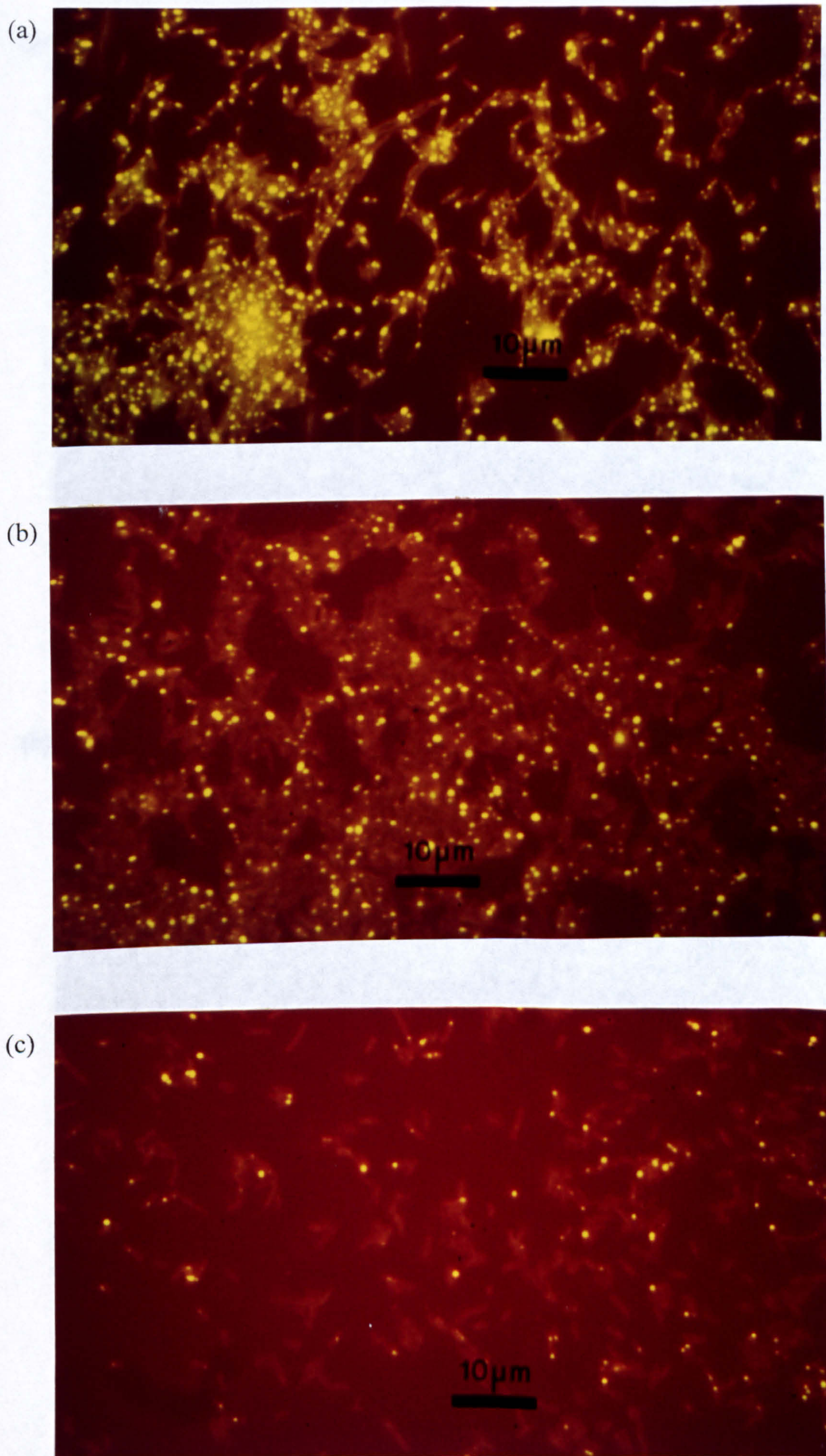


Figure 99. Fluorescent microscopic examination of NR stained samples of starved culture collected at (a) day 0, (b) day 260 and (c) day 500.

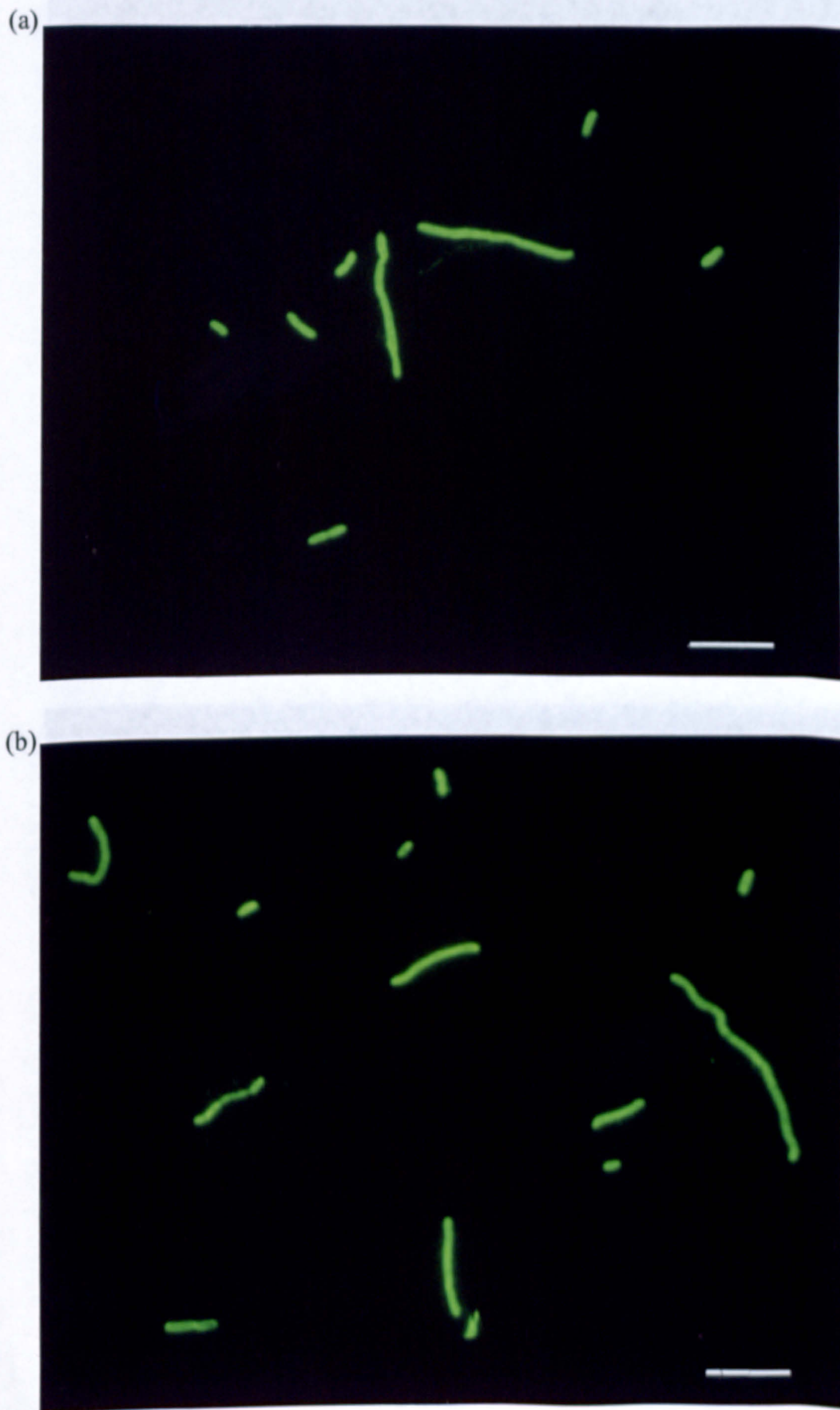
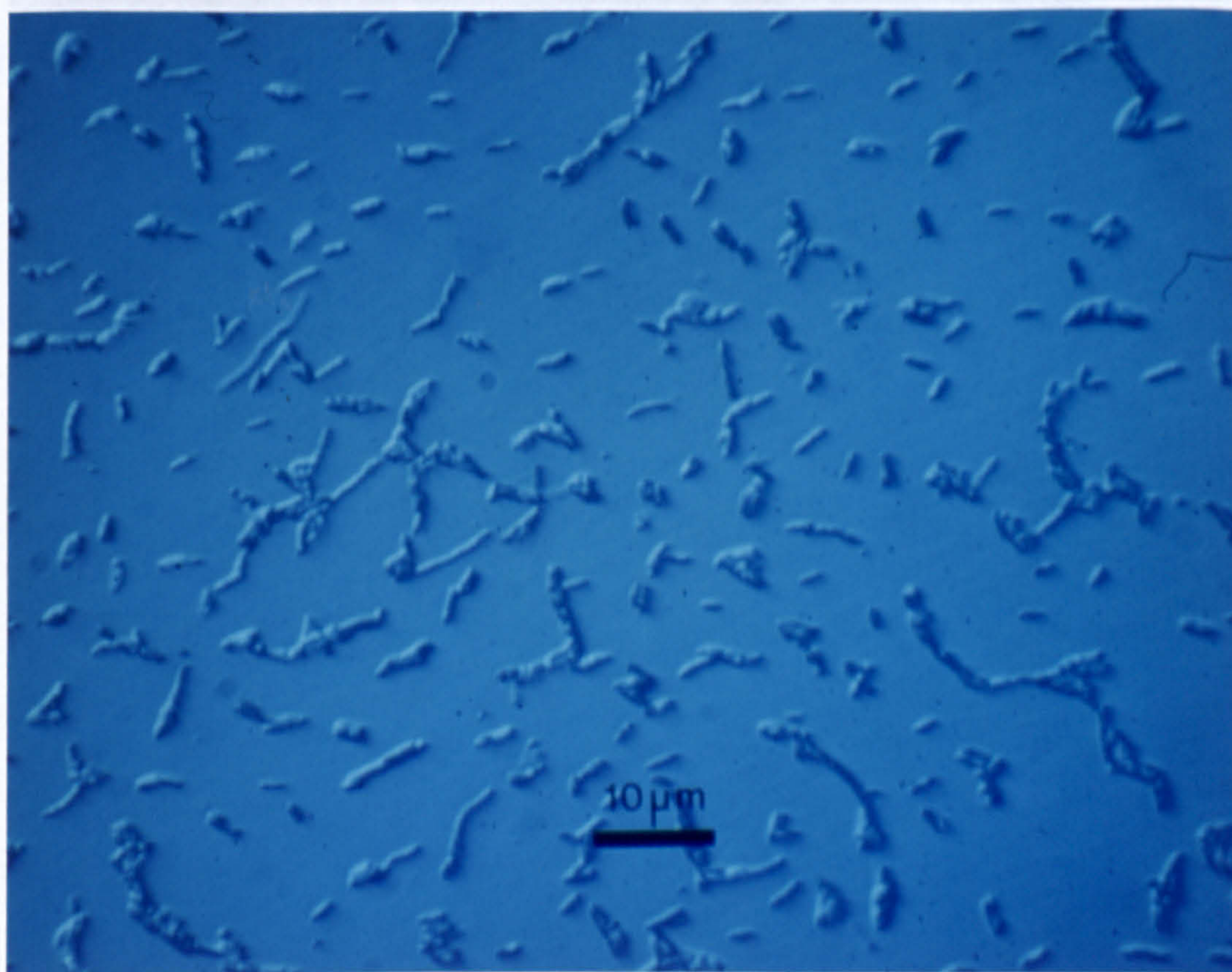


Figure 100. Fluorescent microscopic examination of starved cells stained with serogroup 1 specific polyclonal antiserum, (a) day 0; (b) day 260. Bar, 10 μm .

(a)



(b)

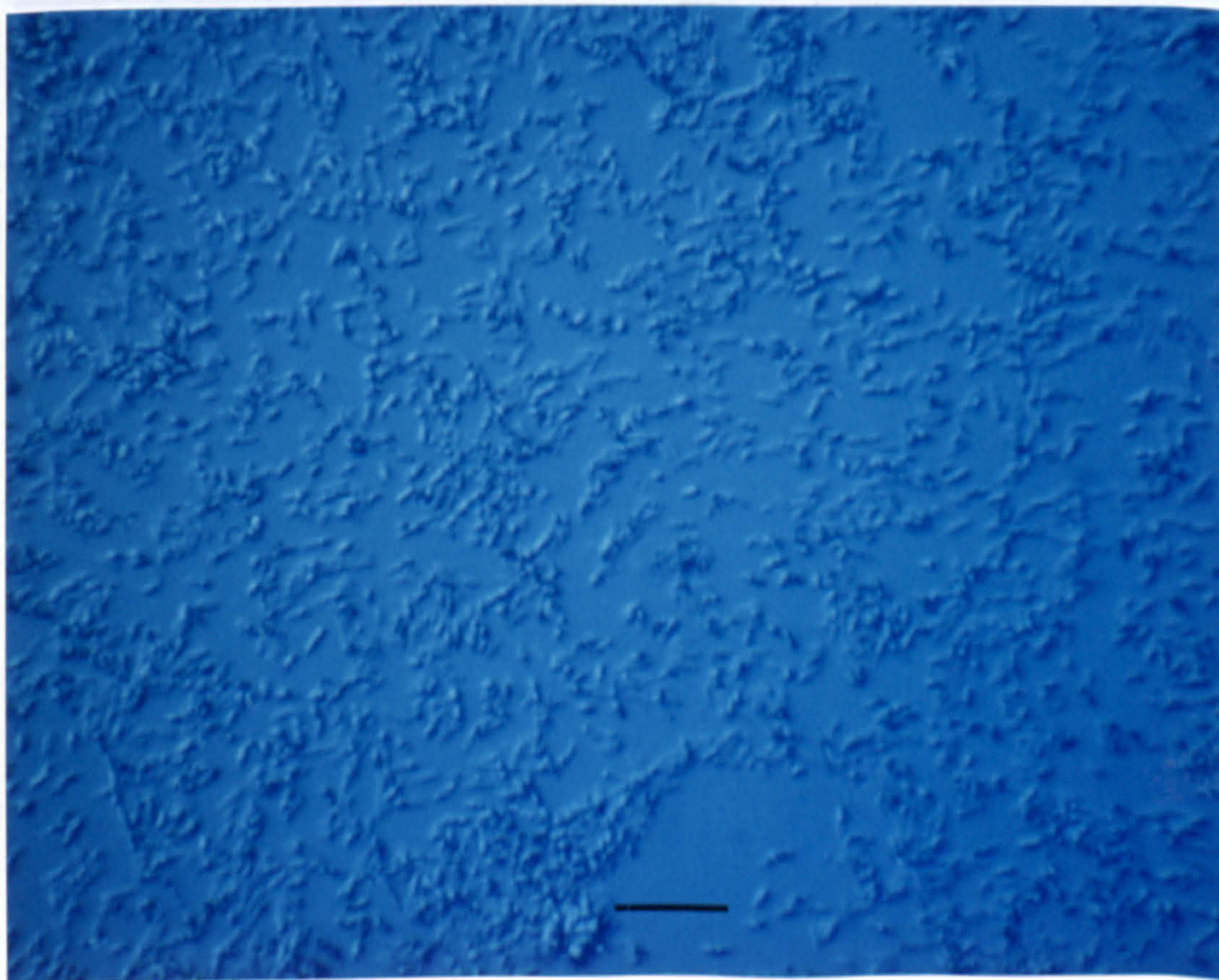


Figure 101. Influence of starvation on the cellular morphology of *L. pneumophila*, as viewed by DIC microscopy, (a) day 0; (b) after 500 days starvation, (Bar, 10 μm).

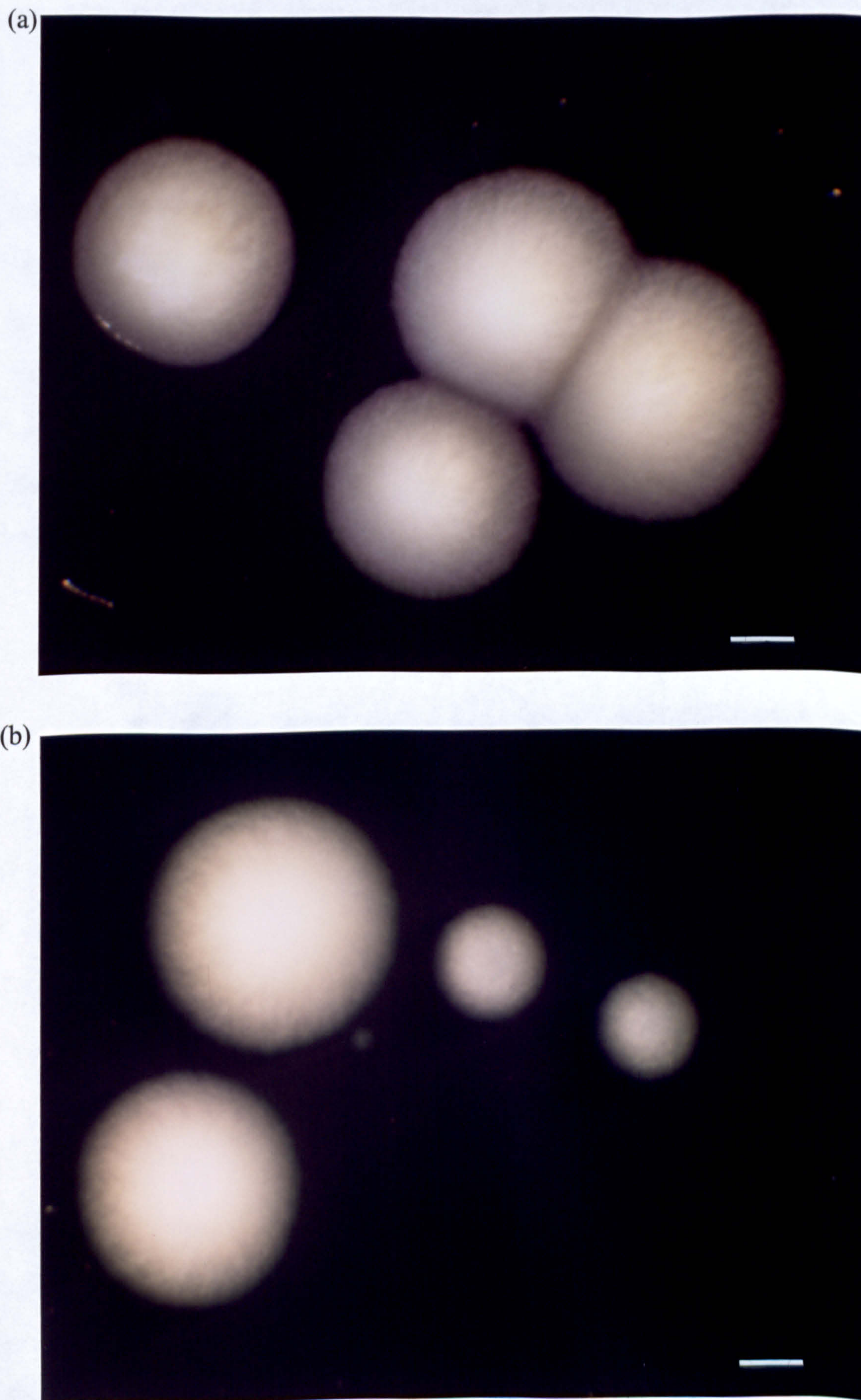


Figure 102. Colony morphology of starved cells after growth on BCYE agar, (a) day 0; (b) day 600. Bar, 1 mm.

3.20.4 Heat shock treatment of nutrient stressed *L. pneumophila*.

The non-culturable cells observed in these survival studies may be in a viable, but dormant state. A heat shock experiment was performed on samples from the first culture after 600 days starvation, to investigate if non-culturable cells could be rendered culture positive (Section 2.21.4). Incubating the starved cell suspension at 45°C for up to 60 min, and then plating them directly onto BCYE agar, failed to increase culturability. Indeed, a 30% decline in recovery was observed after 30 minutes heat shock (Figure 103). The suspension was also incubated at 24°C after heat shock, and culturability was monitored after 24 h. Again no increase in culturability was detected.

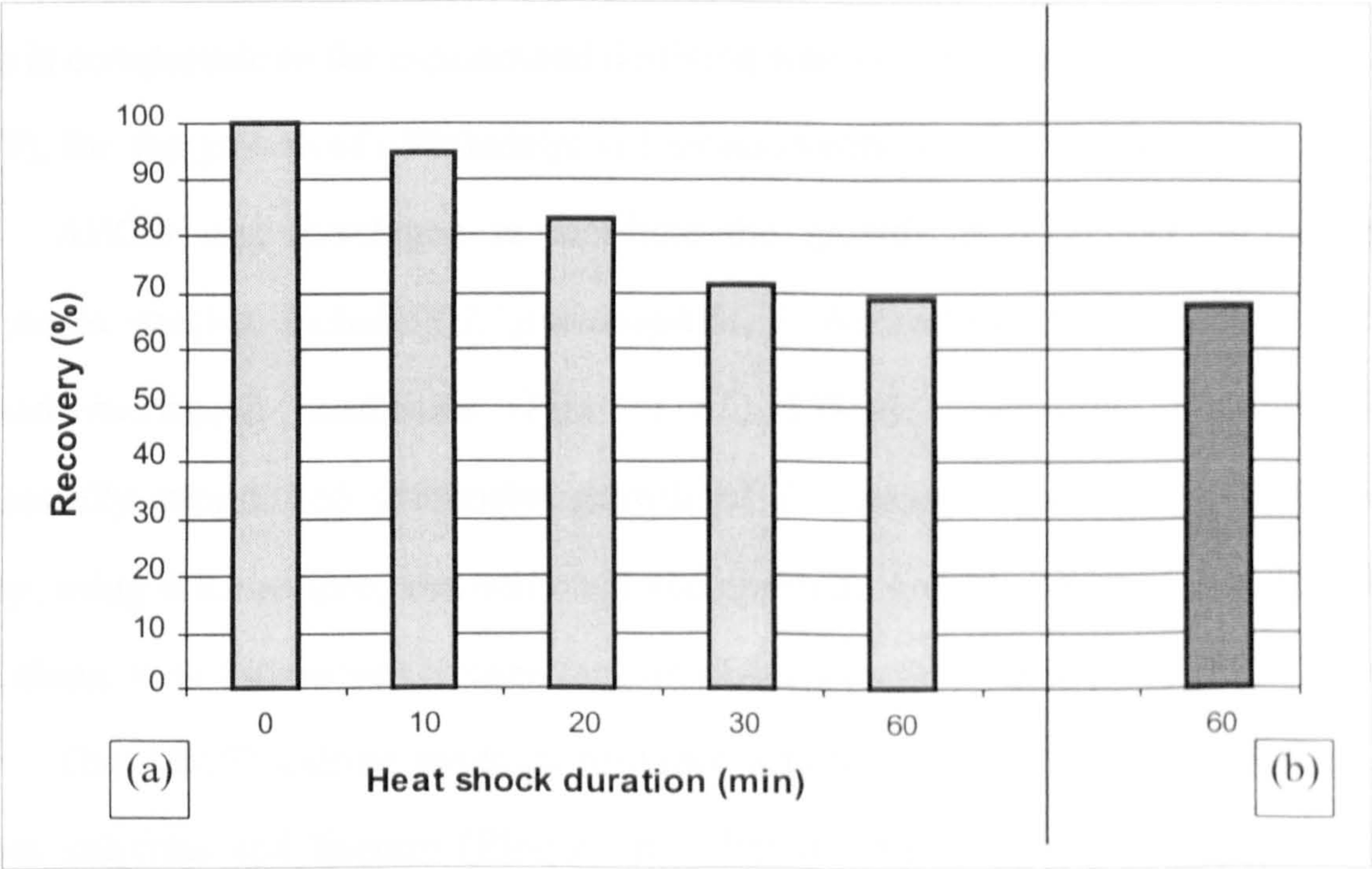


Figure 103. Recovery of *L. pneumophila* on BCYE agar after heat shock treatment at 45°C for up to 60 minutes. (a) Plated directly onto BCYE agar after heat treatment; (b) incubated at 24°C for 24 h after 60 min heat shock, and then plated onto BCYE agar.

DISCUSSION

4.1 Physiology of *L. pneumophila* Grown in Chemostat Culture.

4.1.1 Influence of iron limitation on growth and metabolism of *L. pneumophila*.

The ABCD culture medium provided a suitable nutritional environment for the growth of the *L. pneumophila* in continuous culture under iron-replete conditions, with a mean generation time of 8.7 h (Section 3.1.1). A minimum doubling time of 3.1 h was calculated during the initial batch phase of culture establishment. This value is comparable to the exponential doubling time of 3.8 h reported by Wang *et al.* (1979), for the growth of a Philadelphia 1 strain in complex Feeley-Gorman broth.

ABCD was developed to facilitate the growth of a number of different *Legionella* species, including *L. pneumophila*, *L. bozemanii* and *L. dumoffii* under defined nutritional conditions (Pine *et al.*, 1986a). Mauchline *et al.* (1992) successfully established chemostat growth of *L. pneumophila*, strains 74/81 and Corby, using this medium, and demonstrated optimum growth under microaerophilic conditions, with a dissolved oxygen tension of 4.5% (v/v) air saturation, at 37°C.

The ABCD culture medium provides a rich supply of iron, in the form of ferrous sulphate and haemin (Pine *et al.*, 1986a). The omission of iron from the medium produced a marked decline in steady state growth, confirming previous observations that iron is essential for the growth of *L. pneumophila* (Feeley *et al.*, 1978; Reeves *et al.*, 1981). These cultures achieved steady state growth with a reduced culture density, indicating that a limited concentration of iron was still present (Section 3.1.2). Indeed, iron is a ubiquitous contaminant of chemical reagents, water and laboratory glassware. Pulsing these steady state cultures with ferrous sulphate, stimulated an increase in culture turbidity, confirming iron as the growth-limiting nutrient. Therefore, the omission of iron from the culture medium,

together with the non-ferrous design of the culture system, provided a suitable environment for the continuous growth of *L. pneumophila* under iron-limited conditions.

Amino acid analysis demonstrated that serine was close to depletion in iron-replete cultures (Section 3.1.3). A stoichiometric relationship close to 1:1 for serine metabolism and ammonium production, confirmed that serine provided the principal source of carbon and energy for the growth of *L. pneumophila*. This is in agreement with the observations of Mauchline *et al.* (1992). Tyrosine, which was previously demonstrated to be the growth limiting-nutrient under these culture conditions, was depleted below the limit of detection (Mauchline *et al.*, 1992). A number of other amino acids were also depleted during iron-replete growth, either for incorporation directly into biomass, or for energy generation. It is generally agreed that arginine, cysteine, isoleucine, leucine, methionine, serine, threonine and valine are essential for the growth of *L. pneumophila*, while proline, glutamate, phenylalanine and tyrosine also help promote growth. Of these, serine, glutamate, threonine and glutamine are the principal carbon and energy sources for the growth of *L. pneumophila* (Pine *et al.*, 1979; George *et al.*, 1980; Ristroph *et al.*, 1980; Tesh & Miller, 1981). All of these essential and growth promoting amino acids, with the exception of cysteine and glutamate, were reduced close to or below the limit of detection in iron-replete cultures.

Under iron-limited conditions, the majority of amino acids including serine remained in excess, with only proline completely depleted (Section 3.1.3). A decrease in ammonium production for serine metabolised was demonstrated in comparison to the iron-replete culture, suggesting increased incorporation into biomass formation, as deamination of serine should produce a stoichiometric release of ammonia. Iron concentrations $\leq 0.7 \mu\text{M}$ supported sub-optimal growth. Furthermore, $3 \mu\text{M}$ iron was utilized during iron-replete growth. Previous reports on the iron requirements of *L. pneumophila* vary considerably. Reeves *et al.* (1981) observed that metal requirements were strain dependent, with a Philadelphia 1 strain requiring $20 \mu\text{M}$

iron for optimum batch growth. Ristroph *et al.* (1980) reported that approximately 4.5 μM iron was needed for optimum growth. The observation of this study is in closer agreement with Johnson *et al.* (1991), who found that 3 μM iron supported the growth of a virulent strain of *L. pneumophila*. Residual iron $\leq 0.15 \mu\text{M}$, was routinely detected in iron-limited culture supernatants. This low concentration of iron is likely to reflect a combination of experimental error and assay sensitivity, as well as the affinity of *L. pneumophila*'s iron transport system, expressed as the substrate utilization constant K_s .

Iron limitation caused a decrease in several steady state culture properties, with biomass yield and culturability reduced by 40 and 70%, respectively (Section 3.1.4). This suggests that the mean weight of individual cells increased in response to iron limitation. The yield coefficients for both serine and carbon (Y_{serine} , Y_{carbon}) were reduced by approximately 20%, indicating reduced efficiency of biomass formation and increased metabolic activity (q_{serine} , q_{carbon}). A similar increase in metabolic activity was reported for iron-limited cultures of *N. gonorrhoea* (Keevil *et al.*, 1989). By contrast, the molar growth yield for iron, Y_{iron} , increased 6-fold in response to iron limitation. Increased efficiency of iron utilization was also supported by the observation that the iron content of iron-limited biomass was reduced by approximately fifty percent.

Micro-organisms respond to nutrient limitation by modulating their metabolism in a number of different ways. This may include, (1) increased transport of the growth-limiting nutrient; (2) controlled fluxes of the limiting-nutrient to ensure fulfilment of essential cellular functions; (3) modulated metabolism of non-limiting nutrients to avoid the accumulation of metabolic intermediates at inhibitory concentrations; this may involve energy spillage reactions such as, metabolite excretion and futile cycles, and (4) controlled biosynthesis of other cellular components (Tempest & Neijssel, 1976; Harder & Dijkhuizen, 1983; Russell & Cook, 1995).

The increase in Y_{iron} and the decrease in the iron content of iron-limited cells demonstrates that *L. pneumophila* optimizes utilization of the growth-limiting nutrient for the maintenance of essential cellular functions. Iron is an integral component of respiratory iron-sulphur proteins and cytochromes, the synthesis of which may be modified in response to iron-deficiency. For example, the non-haem iron content of *E. coli* was reduced 1.8-fold in response to iron-limited growth (Hubbard *et al.*, 1986). Iron-deficient growth of *Azobacterium vinelandii* resulted in the formation of NADH dehydrogenase containing only 2 moles Fe/S per mole FMN, compared to 4 moles in the iron-sufficient enzyme. In iron-deficient *Clostridium pasteurianum*, ferredoxin was replaced by a novel metal-free flavoprotein, flavodoxin (Light & Clegg, 1974).

However, such changes in the biochemical composition of iron-limited cells may compromise their metabolic efficiency with respect to carbon and energy substrate utilisation. Impaired energy coupling, and reduced respiratory chain activity has been demonstrated for iron-limited *E. coli* and *Micrococcus denitrificans*, and the yeasts *Torulopsis utilis*, *Candida utilis* and *Candida guilliermondii* (Light & Garland, 1971; Rainnie & Bragg, 1973; Light & Clegg, 1974; Hubbard *et al.*, 1986). Furthermore, iron limitation may lead to impairment of key metabolic enzymes, such as aconitase. Indeed, the major iron containing protein of *L. pneumophila* is an aconitase with 4 Fe atoms per molecule, when fully saturated (Mengaud & Horwitz, 1993). Therefore, the reduced yield coefficients for carbon and serine, which were demonstrated during iron-limited growth (Section 3.1.4), may reflect reduced energy conversion through impaired metabolic pathway and respiratory chain function.

This reduced conversion efficiency may also point to the channelling of excess metabolic intermediates into energy spilling reactions. During carbon-limited growth, carbon conversion into biomass is high, and diversion into extracellular products is minimised. However, when metabolism becomes uncoupled through limitation of an essential nutrient other than the carbon and energy source, bacteria may adopt energy spilling reactions, to avoid the accumulation of metabolic

intermediates at inhibitory concentrations, and to regenerate reduced co-factors. Such reactions include, increased respiration which may be uncoupled from ATP synthesis, futile cycles and metabolite excretion (Tempest & Neijssel, 1984 & 1992; Dawes, 1986a; Russell & Cook, 1995).

Alternatively, some bacteria respond to unbalanced growth by accumulating storage polymers such as poly- β -hydroxybutyrate (PHB) (Dawes, 1986a & b). PHB synthesis is a reductive process which serves as an electron sink for excess reducing power. Acetyl-CoA acyl transferase, CoA-SH and NADH are key regulatory elements in PHB metabolism. During balanced growth, CoA-SH levels are high and polymer synthesis is inhibited. However, when growth is limited by an essential nutrient other than the carbon source, NADH concentrations increase and inhibit the early events of the TCA cycle, namely citrate synthetase and isocitrate dehydrogenase. This results in an accumulation of acetyl CoA, which relieves the inhibition exerted by CoA-SH, leading to 3-hydroxybutyric acid formation (Dawes 1986b; Steinbüchel & Schlegel, 1991).

Indeed, these studies did demonstrated an increase in polymer synthesis during iron-limited growth (Sections 3.19.4 & 3.19.6). Formation of storage polymer normally produces an increase in the molar growth yield (Srienc *et al.*, 1984; Dawes, 1986a). However, despite demonstrating PHB yields of up to 16% cell dry wt. among iron-limited cells, the yield coefficients for both carbon and serine metabolised were still diminished in comparison to the iron-replete control culture (Section 3.1.4). This suggests that in addition to channelling excess carbon into polymer formation, other aspects of the metabolic behaviour of *L. pneumophila* were modulated in response to iron limitation. As discussed, these may include impaired respiratory chain function as well as additional energy spillage reactions, such as metabolite excretion and futile cycles.

The molar growth yield for iron was inversely related to the concentration of iron metabolised by *L. pneumophila* (Section 3.1.5). Monod (1942) demonstrated that there was a linear relationship between biomass formation and the quantity of carbon

and energy source metabolised, producing a constant yield coefficient. However, the advent of continuous culture studies demonstrated that yield coefficients (Y_{glc} , Y_{phos} , Y_{ATP}) are dependent on the specific growth rate, partly due to changes in endogenous metabolism, and the structural composition of cells (Herbert, 1956; Button, 1985 & 1993; Russell & Cook, 1995).

However, in this study, changes in the yield coefficient for iron (Y_{iron}) occurred even though the growth rate remained constant. Therefore, the relationship between biomass concentration and the influent concentration of limiting-nutrient should be governed by the equation:

$$X = Y_{X/A} (A_o - A_{\text{out}})$$

where X is biomass, $Y_{X/A}$ is the yield of cells per substrate consumed, A_o is the concentration of substrate in fresh medium, and A_{out} is the concentration of substrate outside the cells (Button, 1985). However, as with other micro-organisms, where nutrient limitation and growth rate can influence growth yields by promoting the formation of storage compounds, and conservation of cellular components; the increase in Y_{iron} at lower concentrations of limiting-nutrient probably reflects increased PHB formation (Robertson & Button, 1979; Button, 1985; Dawes, 1988). At lower concentrations of iron, the amount of excess carbon source is increased, and may be channelled into increased PHB formation. Indeed, an inverse relationship was also demonstrated between PHB yield and the concentration of iron metabolised by these cultures (Section 3.19.7).

4.1.2 Influence of pH on growth and metabolism of iron-replete *L. pneumophila*.

The steady state growth of iron-replete cultures of *L. pneumophila* was also modulated by changes in environmental pH. Culture density increased within the pH range of 6.7 to 6.4, suggesting enhanced growth efficiency under these conditions (Section 3.9.1). This is in agreement with reports that optimum growth of *L. pneumophila* in batch culture occurs between pH 6.5 and 6.9 (Feeley *et al.*, 1978;

Warren & Miller, 1979; Pine *et al.*, 1979). Decreasing the culture pH further to 6.0, promoted a rapid decline in culture density. Cultures were less tolerant to elevated culture pH, with an increase from pH 6.9 to 7.2 also promoting a decline in culture turbidity (Section 3.9.1). The decreases in culture turbidity observed with the transitions to pH 6.0 and 7.2 were transient, indicating either phenotypic adjustment of the culture, or selection of genotypic variants more functionally suited to the imposed conditions. Cultures which became adapted to growth at pH 7.2 were still sensitive to a further increase in pH to 7.8. Both steady state iron-replete cultures established at pH 6.0 and 7.8, were growth-limited by the principal carbon and energy source, serine.

Steady state iron-replete cultures established at extremes of pH depleted a number of amino acids during growth, indicating no significant decrease in metabolic activity in comparison to the control pH 6.9 culture (Section 3.9.2). However, the metabolism of alanine, aspartate, glutamate and glycine appeared to be influenced by culture pH. Glutamate metabolism was enhanced at pH 6.0, and reduced at pH 7.8, relative to the control pH 6.9 culture. This is in accordance with the metabolic studies of Weiss *et al.* (1980), who observed that optimum incorporation and CO₂ release from glutamate occurred at pH 5.5 and 6.1, respectively. Keen and Hoffman (1984) proposed a model for the interaction between serine and glutamate metabolism, via the Krebs cycle. Glutamate-aspartate transaminase catalyses the transfer of the amino group from glutamate to oxaloacetate, yielding α -ketoglutarate and aspartate. Regeneration of the oxaloacetate pool may be achieved by the sequential action of serine dehydratase and pyruvate carboxylase.

In contrast to glutamate metabolism, aspartate utilization was enhanced at pH 7.8, possibly as a consequence of reduced glutamate metabolism. According to Keen and Hoffman (1984), aspartate is formed during glutamate metabolism, by transfer of the amino group to oxaloacetate. However, in the absence of these events at alkaline pH, the cells are possibly more dependent on exogenous aspartate, resulting in its utilization.

The concentration of both alanine and glycine was increased in pH 7.8 culture supernatant, in comparison to the uninoculated culture medium (Section 3.9.2). Microbial biosynthesis of alanine may proceed by a number of different routes, for example, transamination or direct reductive amination of pyruvate. Serine is readily converted to glycine by serine transhydroxymethylase. The physiological significance of alanine and glycine release is unclear, although it is possible that they represent a form of energy spillage reaction which was induced under these culture conditions. The high metabolic activity observed at pH 7.8 will ensure a rapid turn-over of Krebs cycle intermediates and reduced co-factors, thereby inhibiting the PHB biosynthetic pathway. In this case, excess pyruvate and serine are possibly channelled into alanine and glycine formation. Indeed, the PHB content of these iron-replete cultures grown at pH 7.8 was reduced. Alternatively, alanine and glycine formation may represent a mechanism for reducing the ammonium content of the cytoplasm, helping to maintain a constant intracellular pH.

The growth efficiency of steady state iron-replete cultures was only slightly reduced at pH 6.0. However, elevated pH exerted a greater impact, with biomass yield reduced by 30%. Culturability on BCYE agar was most significantly reduced (80%) (Section 3.9.3). The transfer of these cells from medium at pH 7.8 into deionised water, and plating onto BCYE agar, may have caused pH shock. Such changes in the growth environment, combined with possible alterations in membrane composition and stability during growth at pH 7.8, may have compromised their ability to respond to the new growth environment used in determining culturability. The yield coefficient for serine metabolised, was also diminished by 30% at elevated pH, suggesting reduced efficiency of biomass formation. However, a corresponding decrease in Y_{carbon} was not detected. The discrepancy between these two quotients may reflect altered fluxes in amino acid metabolism, possibly the release of glycine and alanine at the expense of serine.

The molar growth yield for iron was reduced at both extremes of pH under iron-replete conditions (Section 3.9.3). This may partly be due to experimental error

involved in iron determination. It may also reflect increased energy expenditure for the maintenance of cellular functions such as intracellular pH and solute transport, which may promote an increase in the respiratory chain content of these cells, to meet the increased energy demand.

These studies demonstrate that altering the external pH above 7.2 and below 6.3 influenced the growth and metabolism of *L. pneumophila*. Numerous investigations have demonstrated that the maintenance of a constant internal pH (pH_i), between 7.6 and 7.8, is essential for the growth of bacterial neutrophiles. This is achieved mainly through the action of the primary proton pumps along with Na^+/H^+ and K^+/H^+ antiporters (Plack & Rosen, 1980; Kroll & Booth, 1983; Nakamura *et al.*, 1984; Booth, 1985). Studies with *S. faecalis* and *E. coli* have revealed that rapid fluctuations in the external pH (pH_o), cause a collapse in pH homeostasis and temporary cessation of growth, until the pH homeostatic mechanism begins to function and the pH gradient (ΔpH_i) is restored and maintained (Zilberstein *et al.*, 1984).

It is likely that potassium transport plays a prominent role in maintaining the intracellular pH and transmembrane pH gradient of *L. pneumophila*, as sodium is growth inhibitory to legionellae (Barbaree *et al.*, 1983). The transmembrane pH gradient (ΔpH) generated by the homeostatic mechanism, combines with the membrane electrochemical potential ($\Delta\psi$), to form the proton motive force, which drives various transmembrane energy requiring processes, such as ATP synthesis and metabolite accumulation. Therefore, the transient decline in culture density in response to acidification or alkalinization of the culture medium, was probably due to a collapse of pH homeostasis, before the cells began to raise or lower their cytoplasmic pH, respectively (Section 3.9.1). Furthermore, the decrease in steady state culture properties, particularly at high pH, is probably due to increased dissipation of the proton motive force for the maintenance of intracellular pH and solute transport, leading to an uncoupling of ATP formation.

4.1.3 Growth response of iron-limited cultures to changes in culture pH.

Micro-organisms may encounter combinations of environmental stresses such as nutrient-limitation and extremes of pH, both in their natural habitat as well as during infection. The growth response of iron-limited cultures to high and low pH was reminiscent of the behaviour of iron-replete cultures, although the physiological impact was more severe (Section 3.11.1). Pulse experiments with ferrous sulphate confirmed that these steady state cultures established at pH 6.0 and 7.8 were indeed iron-limited. The metabolic activity of iron-limited cultures was severely diminished at low pH, with only three amino acids depleted to less than 50% of their original concentration. By contrast, growth at pH 7.8 did not reduce metabolism, with many amino acids utilized to a comparable or greater extent than by the control pH 6.9 culture (Section 3.11.2). However, all amino acids remained in excess in steady state pH 6.0 and 7.8 iron-limited cultures. As with iron-replete cultures, the metabolism of alanine, glycine, glutamate and aspartate was influenced by culture pH.

The influence of low pH on the physiology of *L. pneumophila* was more severe under iron-limited conditions than observed with iron-replete cultures. Culturability, biomass yield and serine metabolism were all reduced markedly (Section 3.11.3). The molar growth yield for carbon metabolised (Y_{carbon}) indicated a 30% decrease in the efficiency of biomass formation. However, the metabolic quotients for iron (Y_{iron} and q_{iron}) were not significantly affected by low pH.

The effect of high pH on steady state iron-limited culture properties was more comparable to events under replete conditions, with biomass yield and culturability on BCYE agar most significantly reduced (Section 3.11.3). Both Y_{serine} and Y_{carbon} were reduced markedly by 55 and 35%, respectively, indicating reduced growth efficiency. The yield coefficient for iron was also reduced, possibly reflecting an increase in cellular iron requirements, in accordance with the increased metabolic activity and energy dissipation, associated with growth at pH 7.8. The molar growth yield for phosphate was reduced 4-fold in response to elevated pH, a phenomenon which was not observed at pH 6.0 or under iron-replete conditions. Increased

phosphate utilization may signify alterations in the composition of membrane components, particularly phospholipids.

Therefore, the combined effects of iron limitation in conjunction with perturbations in extracellular pH, had a more significant effect on the growth and metabolic efficiency of *L. pneumophila*. As discussed previously, iron limitation may impair energy conversion efficiency, by causing changes in the structure and function of the respiratory chain. Coupled with this, disruption of the proton motive force, and increased energy expenditure for the maintenance of cellular functions, such as solute transport and homeostasis, may have reduced growth efficiency further.

4.2 Influence of Growth Environment on Cellular and Colony Morphology.

The cellular morphology of *L. pneumophila* was influenced by both iron availability and culture pH. Iron-replete cultures were pleomorphic, however, conversion to iron limitation or decreasing the pH of iron-replete cultures resulted in a loss of pleomorphism, encouraging the formation of uniform suspensions of short rods (Sections 3.2 & 3.10.1). The combined effects of iron limitation and low pH, also produced cultures of short coccobacilli (Section 3.12.1). Despite these changes in cellular morphology, no change in reactivity with serogroup specific polyclonal anti-serum was detected. At pH 7.8, iron-replete cultures retained their pleomorphic characteristics, although long filamentous forms were absent, while iron-limited cultures became uniform suspensions of short rods (Sections 3.10.1 and 3.12.1). A unique feature of these pH 7.8 cells was their curved appearance. This curved feature was more prominent with iron-limited cells.

Flagella expression was not observed in any of these cultures. Previous studies have also noted the absence of flagella expression during *in vitro* growth at 37°C, while growth at low temperature was reported to induce expression (Barker *et al.*, 1986; Dennis, 1986; Ott *et al.*, 1991; Mauchline *et al.*, 1992). Motility appears to be an important feature of the intracellular growth of legionellae in amoebae, with

cells becoming highly motile during the later stages of infection and lysis of the host cell (Rowbotham, 1986; Barker *et al.*, 1992; Cirillo *et al.*, 1994). However, flagella expression is not essential for virulence in the guinea pig model (Pruckler *et al.*, 1995).

Alterations in the cellular morphology of *L. pneumophila* in response to the growth environment have been reported previously. Batch growth in defined media was reported to encourage the formation of filamentous cells, while cells cultured in complex media retained their single cell morphologies (Pine *et al.*, 1979; Warren & Miller, 1979). Mauchline *et al.* (1992) also demonstrated the pleomorphic nature of chemostat cultures grown in ABCD medium, and reported a loss of pleomorphism at reduced growth temperatures. Therefore, the physico-chemical properties of the growth environment, including temperature, pH and iron availability all have a pronounced effect on the cellular morphology of *L. pneumophila*.

The mechanism by which iron and pH influence cellular morphology is unclear. For some bacteria such as *Campylobacter jejuni*, growth in iron-limited medium promotes cell elongation, suggesting that iron-deficiency may affect DNA synthesis and cell division (Light & Clegg, 1974; Field *et al.*, 1986). This phenomenon was not observed during this study. It is possible that the formation of short bacilli represents part of a controlled physiological response to environmental stresses, producing a more resistant phenotype. Indeed intracellular growth in amoebae has been associated with the formation of short flagellated cells, which are more resistant to antimicrobial agents (Barker *et al.*, 1992 & 1995; Cirillo *et al.*, 1994). The observation that cells became sickle-shaped when cultured at high pH may also be an indicator of cellular stress, particularly as this phenomenon was augmented in iron-limited cultures.

The distinctive colony morphology of *L. pneumophila* on BCYE agar was not altered as a result of iron-limited growth at pH 6.9. However, during iron-replete growth at pH 6.0, a small colony variant was selected over a period of 7 days (Section 3.10.2). The slow transition kinetics associated with the change in culture

composition suggested selection of a genotypic variant in response to environmental pressure, as opposed to induction of a novel phenotype (Lancaster *et al.*, 1988; Keevil *et al.*, 1989). This variant population was not observed during a repeat experiment, confirming that the small colony morphology was not a phenotypic response to growth at pH 6.0. This observation also suggests that the variant population was the result of a mutational event, which was selected under these growth conditions.

A small colony variant also emerged with slow transition kinetics during iron-limited growth at pH 6.0 (Section 3.12.2). In support of a genotypically altered variant, the small colony phenotype was stable for three subcultures on normal BCYE agar. In this case, cells from both the variant and normal colonies reacted with serogroup specific antiserum, indicating no major alteration in epitope expression. The only striking difference was the enhanced pleomorphism of cells from the variant colony, with many cells extending to 100µm long, possibly indicating a defect in cell division when cultured on BCYE agar. However, these long filamentous forms were not detected in the chemostat culture sample. During a repeat experiment a large colonial variant was selected but in this instance it did not become established as the dominant cell type in the chemostat (Section 3.12.2).

These observations demonstrate that growth of *L. pneumophila* at low pH in particular, provides a potent stimulus for the selection of genotypic variants. Small colony variants were selected in three separate experiments, suggesting that possibly a common mutational event was involved. Other genotypic alterations in culture composition may have occurred without being detected. Chemostat growth provides a strong selective pressure, encouraging the selection of natural spontaneous mutants or existing variants, which are physiologically more suited to the prevailing growth conditions. This normally results in replacement of the parent population (Powell, 1958; Pechurkin, 1980). In the case of the experiments reported here, the parental population was not completely displaced, and the normal colony phenotype became re-established once the original pH was restored. This indicates that the parent population was still capable of growth at pH 6.0, although less efficiently than the

variant population. Wash-out of the variant population occurred when the pH was restored to 6.9, indicating that the variant was functionally more suited to growth at low pH, possibly due to altered transport and homeostatic capabilities.

Both iron levels and the pH of the growth environment have been reported to influence the colony morphology of other bacteria, such as, *N. gonorrhoeae* and *N. meningitidis* (Magnusson *et al.*, 1979; Brener *et al.*, 1981). These alterations were attributed to changes in surface charge associated with altered membrane components, such as lipopolysaccharide and cell surface proteins (Brener *et al.*, 1981).

4.3 Influence of Iron Limitation and pH on the Virulence of *L. pneumophila*.

In addition to the morphological and physiological effects, this study clearly demonstrates that iron availability has a dramatic effect on the virulence of *L. pneumophila* in the guinea pig aerosol model (Section 3.8.1). The virulence of chemostat cultures was significantly attenuated in response to growth under iron-limited conditions. Furthermore, the virulent phenotype was restored when the iron-limited avirulent culture was reverted back to iron-replete conditions. No signs of genotypic selection were observed, suggesting that virulence modulation was the result of phenotypic down-regulation of virulence determinants. Virulence attenuation in response to iron limitation was confirmed by three separate experiments.

These results were complemented by those from *in vitro* macrophage assays, which demonstrated a significantly lower number of culturable iron-limited cells located within alveolar macrophages after infection, in comparison to the virulent replete and control cultures (Section 3.8.2). However, intracellular iron-limited cells proceeded to multiply rapidly after phagocytosis, demonstrating that they were not defective in the subsequent stages of the infection cycle. Therefore, a number of subtle differences comprising a combination of reduced phagocytosis and/or reduced survival after uptake, appear to coincide with a significant decrease in the virulence

of *L. pneumophila* in response to iron limitation. Reduced association between iron-limited cells and host phagocytic cells, in comparison to iron-replete cells, was also demonstrated *in vivo* following infection (Section 3.8.3).

This avirulent iron-limited phenotype differed considerably from the avirulent “CAC” control culture, which although able to enter and survive within mononuclear phagocytes, was unable to multiply intracellularly (Jepras *et al.*, 1985). Horwitz (1987) also characterized an avirulent mutant of *L. pneumophila* which was unable to multiply within human monocytes, due to an inability to inhibit phagosome-lysosome fusion. These observations led to the assumption that avirulence was due to an inability to multiply within host phagocytic cells, as opposed to reduced phagocytosis (Jepras *et al.*, 1985; Horwitz, 1987). However, these studies employed naturally-occurring less virulent or genotypically altered strains, as opposed to the phenotypically modulated cultures used in this study. Interestingly, *mip* mutants defective for macrophage and protozoa infection, were still capable of intracellular multiplication and causing death at a reduced rate (Engleberg *et al.*, 1989; Cianciotto *et al.*, 1990; Cianciotto & Fields, 1992; Wintermeyer *et al.*, 1995).

The results of this study are in contrast to the role of iron in regulating the virulence of many pathogens, such as *E. coli*, *V. cholerae*, *N. gonorrhoeae*, *N. meningitidis*, and *P. aeruginosa*. With these pathogens, the transcription of virulence determinants including iron acquisition mechanisms and toxin expression, is normally induced in response to iron limitation through the action of the iron-responsive regulatory locus, *fur* (Keevil *et al.*, 1989; Goldberg *et al.*, 1990; Prince *et al.*, 1991; Gross, 1993; Thomas & Sparling, 1994 & 1996). However, it is possible that other environmental stimuli are required in addition to iron limitation, for induction of a virulent *L. pneumophila* phenotype; with virulence representing the cumulative action of numerous response regulons governing the products of many genes (Gross, 1993). A classic example of this was provided by Brener *et al.* (1981), who demonstrated that the virulence of *N. meningitidis* was enhanced by iron-limited growth at low pH.

However, this study demonstrates that growth of iron-limited cultures of *L. pneumophila* at a low pH, comparable to that encountered intracellularly during infection, does not lead to a significant enhancement of culture virulence (Section 3.15). While deaths were observed with one iron-limited pH 6.0 culture, the LD₅₀ was significantly higher (1.5 log₁₀ units) than that recorded for iron-replete cultures grown at either pH 6.9 or 6.0 (Sections 3.8.1 and 3.15).

Iron-replete cells grown at pH 6.0 were highly virulent for the guinea pig aerosol model, with an LD₅₀ marginally lower than that of the iron-replete pH 6.9 culture (Section 3.15). While this culture produced a variant morphology on BCYE agar probably reflecting a genotypic modification, the virulent phenotype was retained, and iron-replete growth at pH 6.0 was conducive to the expression of a highly virulent phenotype. Therefore, iron availability appears to exert greater regulatory control over *L. pneumophila* virulence than the pH of the growth environment. Mauchline and co-workers (1994), demonstrated that growth temperature participates in the reversible induction of *L. pneumophila* virulence, with the culture significantly more virulent when cultured at 37°C. Therefore, these observations support the theory that numerous environmental stimuli may participate in regulating the virulence of *L. pneumophila*.

The important finding of this study that iron is essential to induce expression of a virulent *L. pneumophila* phenotype, is supported by previous observation. Numerous studies have demonstrated that intracellular growth is iron-dependant, and mutants which are defective for iron-acquisition and assimilation are also defective for intracellular infection (Byrd & Horwitz, 1989 & 1991; Gebran *et al.*, 1994a; Pope *et al.*, 1996). *L. pneumophila* may encounter a range of stressful physicochemical conditions in aquatic habitats, including iron-restriction (Fliermans *et al.*, 1981; Wadowsky *et al.*, 1988; Rogers & Keevil, 1992; Fields, 1993; States *et al.*, 1994). Under these conditions, down-regulation of virulence determinants and other non-essential cellular components may represent part of the survival strategy of this environmental micro-organism, helping to conserve vital carbon and energy reserves.

Therefore, based on the observations of this study, it would appear essential for *L. pneumophila* to encounter an iron rich environment prior to aerosolization, to induce expression of a virulent phenotype. Once infection is established, the legionellae may then be able to acquire iron from the host cells' iron binding and storage proteins. One of the few niches in aquatic habitats that may fulfil this requirement is the intra-protozoal environment. Although little is known about the nature of this environment, the ability of *L. pneumophila* to multiply to high cell densities suggests that it provides a relatively rich source of nutrients, in comparison to the extracellular medium (Barker *et al.*, 1993; Fields, 1993). Indeed it has been proposed that adaptation to intracellular growth within protozoa may pre-condition legionellae for infection and survival within human phagocytic cells (Barker & Brown, 1995; Fields, 1996). It is also possible that the increased concentration of nutrients encountered in the sediment of water systems and cooling tower ponds, together with leached metal ions from water pipes, could participate in inducing the virulence of *L. pneumophila*.

The virulence determinants elaborated by *L. pneumophila* to mediate infection and growth in human macrophages are still poorly characterized. Recent transcomplementation studies have identified a number of loci, such as *dot*, for defect in organelle trafficking, *icm*, for intracellular multiplication, and the early stage macrophage-induced locus (*eml*), which are essential for intracellular survival and multiplication (Marra *et al.*, 1992; Berger & Isberg, 1993; Berger *et al.*, 1994; Brand *et al.*, 1994; Abu Kwaik & Pederson, 1996). However, the precise function of these determinants, and the means by which their expression is regulated intracellularly, awaits further characterization.

4.4 Extracellular Protein Production and Iron Acquisition Mechanisms.

4.4.1 Pigment formation.

In this study, iron-replete cultures developed a dark brown colour during growth at elevated pH (Section 3.9.1). Production of a melanin-like pigment by *L. pneumophila* has been associated with the late exponential phase of batch cultivation, and slow growth in continuous culture (Warren & Miller, 1979; Berg *et al.*, 1985). Baine *et al.* (1978) proposed that pigment formation was mediated by either a tyrosinase or a *o*-monooxygenase. However, recently a gene encoding a 39 kDa protein termed legiolysin (Lly), which confers the phenotypic characteristic of culture medium browning in late stationary phase, has been cloned and characterized (Wintermeyer *et al.*, 1991 & 1994; Steinert *et al.*, 1995). The *lly* sequence is proposed to catalyses the formation of homogentisate from 4-hydroxyphenylpyruvate, a product formed following transamination of L-tyrosine. Spontaneous aggregation of homogentisate may lead to the formation of a melanin-like pigment (Wintermeyer *et al.*, 1991 & 1994; Steinert *et al.*, 1995). Although, pigment formation is not essential for intracellular survival, it does appear to enhance the survival of *L. pneumophila* in response to light stress (Wintermeyer *et al.*, 1994; Steinert *et al.*, 1995).

Interestingly, tyrosine utilisation was comparable in all three iron-replete cultures grown at different pH values, even though intense pigment formation was only observed at high pH. Therefore, elevated culture pH appears to stimulate pigment production. This observation may explain why pigment formation occurs during the late exponential phase of batch growth, at which point the culture pH will have increased due to microbial activity. Pigment formation as revealed by culture browning, was not observed under iron-limited conditions. Therefore, both iron and environmental pH appear to participate either directly or indirectly in regulating pigment production. It is possible that iron may function as a cofactor for legiolysin

activity, which would account for the lack of pigment formation in iron-limited cultures at elevated pH.

4.4.2 Extracellular protein production.

Iron-limited and -replete cultures grown at pH 6.9 produced comparable extracellular protein yields (Section 3.3.1). However, anion exchange chromatography of culture supernatants resolved two individual protein peaks which were enhanced in response to iron limitation (Section 3.3.2). SDS-PAGE analysis identified two low molecular mass proteins in these iron-repressed fractions. As the virulence of *L. pneumophila* was attenuated in response to iron limitation, these proteins are unlikely to represent important virulence determinants. More extensive chromatographic studies are required in conjunction with biochemical assays, to purify and characterize both proteins. Iron inducible extracellular proteins correlating with culture virulence were not detected by this investigation.

Culture pH had a more pronounced effect on extracellular protein production, particularly during carbon-limited, iron-replete growth at pH 6.0 (Section 3.13). This suggests that in response to pH stress, these carbon-limited cells reduced synthesis of non-essential extracellular products, thereby optimising energy generation for other cellular functions. Similarly, extracellular protein production by iron-limited cultures was reduced by lowering the pH to 6.0 (Section 3.13). By contrast, growth at pH 7.8 stimulated an increase in extracellular protein production. This increase was most pronounced under iron-replete conditions, and correlates with the increase in pigment production which may have interfered with the assay (Sections 3.9.1 and 3.13).

4.4.3 Zinc metalloprotease.

The mean azocasein hydrolytic activity of pH 6.9 cultures was reduced 5-fold in response to iron limitation (Section 3.3.4). Conlan (1987) demonstrated that azocasein hydrolysis was specific to the zinc metalloprotease, although the possible

existence of additional azocasein hydrolytic enzymes was not ruled out. In this study the relatively non-specific ion chelator, EDTA, inhibited the hydrolytic activity of culture supernatants, confirming the activity of a metalloenzyme. EDTA was more effective at inhibiting the activity of iron-replete samples. However, this difference may be due to an artefact generated by calculating the residual activity after EDTA treatment, as a percentage of the initial activity, which was considerably lower for iron-limited samples. This seems likely, considering both iron-limited and -replete reactions containing EDTA, produced a comparable change in absorbance (Δ absorbance $\cong 0.05$) in relation to their respective controls. Zinc was found to relieve the inhibition imposed by EDTA, indicating that zinc was able to act as a cofactor for the enzyme.

The presence of anti-zinc metalloprotease IgG also caused 80 to 90 % inhibition of the hydrolytic activity present in iron-replete and -limited samples (Section 3.3.4). The activity of control reactions containing IgG anti-serogroup antigen was not inhibited, confirming that the added immunoglobulin was not causing unspecific competitive inhibition of proteolytic activity. Taken together, these experiments demonstrate that extracellular activity of the zinc metalloprotease is reduced in response to iron limitation. Zinc remained in excess in both iron-limited and -replete cultures (Section 3.1.3).

This phenomenon was reversible, with protease activity increasing in response to iron-addition to steady state iron-limited cultures. Surprisingly, the hydrolytic activity of iron-limited cultures was not constant, but was directly related to the concentration of iron-metabolised (Section 3.3.4). It is possible that this relationship is also an artefact created by expressing enzyme activity as a function of biomass yield. As discussed in Section 4.1, the yield coefficient for iron increased with decreasing iron concentrations, probably as a result of increased PHB formation.

The metalloprotease activity of iron-replete cultures was also influenced by extremes of pH, however, the decrease was less significant than that observed in

response to iron limitation (Section 3.14). Altering the pH of iron-limited cultures did not influence protease expression.

Although some reports suggest that the metalloprotease is not essential for virulence, many believe that it aids pathogenesis by degrading important human immunoregulatory proteins, eliciting pulmonary damage, and interfering with the response of host inflammatory cells (Baskerville *et al.*, 1986; Conlan *et al.*, 1986; Blander *et al.*, 1990; Rechnitzer & Kharazmi, 1992; Hell *et al.*, 1993; Mintz *et al.*, 1993). *In vivo* production in the lungs of experimentally infected guinea pigs has also been demonstrated (Conlan *et al.*, 1988). This study indicates that environmental parameters, in particular iron availability, influences metalloprotease expression. However, the precise regulatory mechanism is unclear. The iron-responsive regulatory protein Fur, normally acts as a repressor of gene expression, although there is increasing evidence that Fur also acts as a positive regulatory element, and that iron may participate in regulating gene expression independently of Fur (Neiderhoffer *et al.*, 1990; Thomas & Sparling, 1996). The inverse relationship between metalloprotease activity and the concentration of iron metabolised, could also indicate low level constitutive expression of this enzyme, with increased iron acting as an inducer of expression, resulting in a cascading effect. Such a phenomenon may be of significance *in vivo*, leading to high level expression during the later destructive stages of infection. The modest reduction in proteolytic activity in response to pH perturbation, points to a physiological adjustment of cellular metabolism, rather than a direct regulatory role of environmental pH in protease expression.

4.4.4 Phospholipase C activity.

Iron-limited and -replete culture samples possessed comparable extracellular and cell associated *p*-nitrophenylphosphorylcholine hydrolytic activity (Section 3.3.5), indicating that phospholipase C expression is independent of iron, and that there is no correlation between enzyme expression and virulence. Phospholipase C activity constitutes an important virulence determinant for many human pathogens,

for example, *Listeria monocytogenes* and *P. aeruginosa* (Berka & Vasil, 1982; Geoffroy *et al.*, 1991). This enzyme possesses the potential to aid pathogenesis through the disruption of pulmonary surfactant, inflammatory cell membranes and the phagocytic cell respiratory burst. However, a precise function in *Legionella* pathogenesis has not been demonstrated, and these studies suggest that it is not of major importance (Baine, 1988; Dowling *et al.*, 1992).

4.4.5 Ferric citrate reductase.

Ferric reductase activity was demonstrated in the cell fractions isolated from both iron-limited and -replete cells grown at pH 6.9 (Section 3.4.1). Optimum activity was detected with NADPH as reductant, and was located mainly in the periplasmic and cytoplasmic cell compartments. Comparable reductase activity was demonstrated in both iron-limited and -replete cell fractions, indicating that expression is independent of iron availability, and may be constitutive. The presence of ferric citrate reductase activity in *L. pneumophila* cell fractions was originally demonstrated by Johnson *et al.* (1991). They subsequently identified two distinct enzymes, one periplasmic and the other cytoplasmic, the expression of which appeared to be independent of iron, in agreement with the observations of this study (Poch & Johnson, 1993).

There are a number of differences between the results of this study and those reported by Johnson and co-workers (1991), particularly regarding the cellular location of the activity, the amount of activity, and its requirement for reductant. Firstly, Johnson and co-workers reported that ferric reductase activity was located primarily in the periplasmic fraction. This is in contrast to observations with other bacteria, where the enzyme is generally cytoplasmic (Cox, 1980; Moody & Dailey, 1985). However, this study demonstrates high NADPH-dependent activity located in both the periplasm and cytoplasm. Secondly, the specific activity of the periplasmic and cytoplasmic fractions with NADPH was 10 to 30-fold greater than the activity detected by Johnson and co-workers (1991). Thirdly, in this study NADPH yielded

optimum activity for both iron-limited and -replete cultures, with the periplasmic and cytoplasmic activity elevated 10 to 30-fold over activity in the presence of NADH. While Johnson and colleagues (1991) observed no difference in the activity of virulent cell fractions with either reductant, he did record a 2-fold increase in the activity of avirulent cell fractions with NADPH. This led Johnson and co-workers to speculate that the intracellular growth of avirulent cells may be limited during infection, due to their requirement of NADPH for optimum reductase activity. However, the observations of this study, where the virulent iron-replete and avirulent iron-limited cultures both required NADPH for optimum activity, do not support this hypothesis.

Many of the inconsistencies highlighted between these two studies may reflect differences in the physiological status of the cultures used, as well as strain variations. Johnson and co-workers (1991) employed batch culture methods, which expose bacteria to environmental extremes as well as changing growth rates. In this study the cells were physiologically adapted to growth in a controlled environment at a constant growth rate. Furthermore, the avirulent strain used by Johnson and colleagues was selected by repeated subculture on charcoal yeast extract medium and Muller-Hinton agar, in contrast to the phenotypically less virulent iron-limited culture used in this study.

Iron reductases are an important component of the iron-acquisition apparatus of a number of bacteria including *P. aeruginosa* and *L. monocytogenes* (Cox, 1980; Cowart & Foster, 1985). The present study confirms the presence of *L. pneumophila* ferric-citrate reductase activity which preferentially uses NADPH as reductant, and is located in both the cytoplasmic and periplasmic cell compartments. These observations support the view that ferric reductase activity forms an integral part of the *L. pneumophila*'s iron-transport machinery, and suggest that expression of this activity may be constitutive. As proposed by Poch and Johnson (1993), it is possible that this enzyme may have even greater activity for other biologically important iron-sources.

4.4.6 Human transferrin as a potential iron-source.

Iron-loaded human transferrin stimulated the growth of iron-limited chemostat cultures, indicating that it provided a source of iron (Section 3.4.2). A number of bacterial pathogens, for example *Neisseria spp.* and *Haemophilus influenza*, express specific iron-repressible membrane receptors which mediate iron acquisition from transferrin (Schryvers & Morris, 1988; Morton & Williams, 1990). However, analysis of iron-limited culture samples failed to detect the presence of membrane associated transferrin receptors on iron-limited cells (Section 3.4.3). This is in agreement with previous observations (Reeves *et al.*, 1983).

In vitro experiments demonstrated digestion of human transferrin by *L. pneumophila* zinc metalloprotease (Section 3.4.5), providing further evidence of the broad spectrum proteolytic activity of this enzyme. It is possible that amino peptidases may also participate in transferrin degradation, once the zinc metalloprotease has performed the initial cleavage. Lactoferrin, an iron-binding glycoprotein sharing considerable homology with transferrin, was not cleaved. These observations provide evidence that human transferrin may represent a potentially important iron-source for *L. pneumophila in vivo*, with the degradative action of the zinc metalloprotease possibly mediating iron release. In agreement with this observation, Müller (1981) reported a slight anodic shift and decrease in the intensity of a transferrin band, when studying the interaction between *L. pneumophila* and transferrin by an agar immunodiffusion assay.

These findings contradict a number of previous reports which have demonstrated the bacteriostatic activity of apo-transferrin for *L. pneumophila*, associated with its iron chelating activity (Quinn & Weinberg, 1988, Goldoni *et al.*, 1991). Quinn and Weinberg (1988) observed that the antagonistic effect of transferrin on the growth of legionellae in serum could be reversed by the addition of iron. This led them to conclude that the inability of legionellae to obtain iron from transferrin, contributed to the pathogen's inability to cause disseminated infection. Furthermore, Johnson *et al.* (1991) demonstrated that *L. pneumophila* cell suspensions failed to

capture iron, when incubated with labelled human transferrin. These studies, however, were performed over short time courses using either washed or very dilute suspensions of iron-depleted cells, incubated under low nutrient conditions. Hence, it is likely that the amount of protease present was minimal, and expression was probably not induced to levels sufficient to produce a detectable response. This seems likely considering the previous observation that iron may act as an inducer of protease expression (Section 4.4.3).

The homologous *P. aeruginosa* metalloenzyme, elastase, cleaves transferrin, releasing iron, which is then transported to the cell by the siderophore pyoverdine (Doring *et al.*, 1988). However, the possibility of the zinc metalloprotease fulfilling a similar role during *Legionella* infections, is difficult to contemplate for a number of reasons. Firstly, *L. pneumophila* is believed to obtain iron directly from the intracellular labile pool during infection, and the addition of apo-transferrin to monocyte cultures inhibits intracellular multiplication of *L. pneumophila* (Byrd & Horwitz, 1989; Gebran *et al.*, 1994a). Secondly, although monocytes obtain iron by interacting with transferrin, the transferrin-receptor complex is recycled within a vacuole. Furthermore, monocytes respond to infection by down-regulating the expression of transferrin receptors (Byrd & Horwitz, 1989). Thirdly, the present study demonstrated that metalloprotease expression is down-regulated under iron-limited growth conditions. If transferrin digestion represented a critical iron acquisition mechanism, then metalloprotease expression would normally be derepressed under such conditions. Furthermore, protease deficient mutants were competent for *in vivo* growth in guinea pigs (Szeto & Shuman, 1990; Blander, *et al.*, 1990).

The significance of transferrin in *Legionella* iron acquisition during infection remains to be elucidated. It is possible, that transferrin may become a more accessible iron source during the later destructive stages of infection, coinciding with increased levels of metalloprotease (Conlan *et al.*, 1988). Under these circumstances the metalloprotease could possibly perform dual roles, mediating both iron acquisition and tissue destruction. Transferrin digestion may also be of significance to

L. pneumophila by aiding resistance to the bactericidal effects of serum proteins (Horwitz & Silverstein, 1981a).

4.4.6 Siderophore activity.

The universal siderophore assay of Schwyn and Neilands (1987) detected the presence of iron-sequestering activity in iron-limited culture supernatants (Section 3.4.6). However, components of the uninoculated culture medium also reacted with the assay, rendering it unsuitable for detecting iron-chelators elaborated during microbial growth. This was confirmed by the inability to quantitate authentic exogenous siderophore added to the culture medium. A recent study identified cysteine as a medium component responsible for false-positive results with this assay (Liles & Cianciotto, 1996). Other medium components, such as phosphate, will also cause interference (Schwyn and Neilands, 1987). The specific hydroxamate and phenolate assays of Csáky (1948) and Arnow (1937) also failed to detect siderophore production by iron-limited cultures, confirming previous observations with batch grown cultures of *L. pneumophila* (Reeves *et al.*, 1983).

The absence of hydroxamate type siderophores was confirmed by the specific assay of Emery and Neilands (1960) which failed to detect the presence of nitrosodimers, formed by oxidation of hydroxylamine groups which absorb maximally between 265 to 270 nm (Section 3.4.8). Oxidation products were detected in iron-limited culture supernatants, however, their λ_{\max} was not characteristic of nitrosodimers. The identity and physiological significance of these oxidation products was not investigated further.

Iron-limited samples reacted with ferric chloride, to produce a charge transfer band with λ_{\max} at 470 nm (3.4.10). Iron-binding compounds, such as aerobactin, typically have an absorption maxima in the range of 400 to 500 nm, when reacted with Fe^{3+} (Neilands, 1981; Agiato & Dyer, 1992; Okujo & Yamamoto, 1994). A positive reaction was also observed with iron-replete samples, although the λ_{\max} was shifted to a longer wavelength. Whether the difference in λ_{\max} between iron-limited

and -replete reactions represents two distinct chemical entities, is unclear. Different chelate complexes do produce different characteristic values of λ_{\max} (Atkin *et al.*, 1970).

Considerable uncertainty surrounds the issue of siderophore production by *L. pneumophila*, with most laboratories supporting the view that *L. pneumophila* does not elaborate siderophores (Reeves *et al.*, 1983; Liles & Cianciotto, 1996). Much of the data from this study agrees with these observations. However, the ferric chloride assay indicates that a component of culture supernatants elaborated during growth, is capable of binding iron. Whether it serves a role in iron transport or requires iron as a functional cofactor, is unclear. Cysteine does not appear to be responsible for this reaction, as amino acid analysis demonstrated that the cysteine content of supernatant and control media samples, was comparable (Section 3.1.3). The identity and functional role of this iron-binding agent warrants further investigation. Interestingly, a *L. pneumophila* Fur-regulated gene encoding a protein which has homology with aerobactin synthetase has recently been identified, supporting the theory that *L. pneumophila* may elaborate siderophore activity (Hickey & Cianciotto, 1997).

In recent years, a number of structurally novel chelators have been identified, for example, Rhizobactin and Yersinophore (Smith *et al.*, 1985; Chambers & Sokol, 1994). Furthermore, certain α -keto acids possessing aromatic or hetero-aromatic side chains generated by L-amino acid deaminases, have been demonstrated to possess siderophore activity (Drechsel *et al.*, 1993). These compounds produced ligand to metal charge transfer bands in the region 400 to 500. Characterization of mutants which are defective for iron acquisition, will provide valuable information on the iron acquisition mechanisms employed by *L. pneumophila* (Pope *et al.*, 1996).

4.5 Influence of Growth Environment on Membrane Composition.

4.5.1 Membrane lipid composition.

The bacterial cell envelope is a structurally and functionally flexible organelle, mediating interactions between bacteria and the environment. To function, cell membranes must remain fluid, and not undergo transition to form a rigid crystalline phase, particularly as environmental temperature decreases (Rose, 1989). Fluidity can be maintained in response to decreasing temperature, by increasing the proportion of membrane fatty acids and phospholipids of lower melting point. This may be achieved by increasing the proportion of unsaturated fatty acids, reducing fatty acyl chain length, switching from branched to unbranched fatty acids, increasing the ratio of anteiso to iso fatty acids, as well as by altering the phospholipid type (Rogers *et al.*, 1980; Melchoir, 1982; Rose, 1989). Indeed, Mauchline *et al.* (1992) demonstrated an increase in the proportion of unsaturated fatty acids and phospholipids containing unsaturated fatty acid substituents, when the growth temperature of *L. pneumophila* was lowered from 37 to 24°C.

The fatty acid composition of iron-replete cells was dominated by i16:0, and was similar to that reported previously for *L. pneumophila* grown on BCYE agar at 37°C, and in chemostat culture with ABCD medium (Moss *et al.*, 1977; Mauchline *et al.*, 1992). Iron limitation induced changes in the fatty acid profile (Section 3.5.1), the most significant of which was an increase in the proportion of unbranched and anteiso branched fatty acids, at the expense of iso-branched acids, in particular i16:0. These changes are consistent with a slight decrease in membrane melting temperature for the maintenance of fluidity. However, no significant change in fatty acyl chain length, or the degree of unsaturation was detected.

Positive and negative ion FAB-MS (Section 3.5.2) confirmed previous observations that phosphatidylethanolamines, phosphatidylcholines and phosphatidylglycerols are the principal polar lipids species of *L. pneumophila* (Finnerty *et al.*, 1979; Hindahl & Ingleski, 1984; Mauchline *et al.*, 1992). Spectra

revealed a modest enhancement of signals representing the principal phosphatidylethanolamine species, and some phosphatidylcholines, in response to iron-limited growth at pH 6.9. Phosphatidylglycerol species esterified with a greater number of fatty acyl carbon atoms were also slightly enhanced. Of particular significance for membrane fluidity was the increase of phosphatidylcholines which have a lower melting temperature than phosphatidylethanolamines with similar fatty acyl substituents (Wilkinson & Nagle, 1981).

Selective constant neutral loss (CNL) analysis of individual phospholipid species, demonstrated a universal increase of phospholipid species esterified with a greater total number of carbon atoms. Phospholipids substituted with 32 carbon atoms were most significantly enhanced, at the expense of species esterified with 30 to 31 carbon atoms (Section 3.5.3). Furthermore, a slight increase in the degree of unsaturation was suggested by a decrease in phospholipids possessing saturated acyl groups, and an increase of phospholipids with a mono-unsaturated fatty acyl substituent. These changes indicate a change in the fatty acyl substitution pattern on the glycerol back-bone, and may reflect the significant changes which were observed among the whole cell fatty acids, in particular the increase of unbranched 16:0 at the expense of 16:0.

Therefore, iron limitation altered the membrane fatty acid and phospholipid composition of *L. pneumophila*. However, the combined changes, in particular the increase of unbranched and anteiso branched fatty acids, and the alteration in fatty acyl substitution pattern, do not indicate a significant change in melting temperature. These alterations may represent a balanced set of alterations designed to maintain optimum fluidity and membrane function, in response to the stressful iron-limited environment. The phospholipid data presented in this study are qualitative results; as the signal intensity reflects the relative ease of desorption rather than the concentration of each phospholipid species in the extracts. Perhaps more significant alterations in the absolute amounts of the different phospholipid species may have occurred. With *P. cepacia*, an increase in the phosphatidylethanolamine :

phosphatidylglycerol ratio was demonstrated when cells were cultured under iron-depleted conditions (Anwar *et al.*, 1983).

Barker *et al.* (1993) also noted alterations in the fatty acid content of *L. pneumophila* in response to different *in vitro* growth conditions. However, the fatty acid profile reported by Barker *et al.* (1993) for iron-depleted cells, differs considerably from the iron-limited profile presented in this study. In particular, i16:0 which was reduced markedly in response to iron limitation, was the dominant acid of iron-depleted cells, while 16:0 was present at a 3-fold lower concentration among iron-depleted cells. Furthermore, the proportion of anteiso fatty acids was considerably higher among iron-depleted cells, than observed with the iron-limited cells of this study. Barker and colleagues (1993) also demonstrated that cyclopropane-17 was present in cells cultured under nutrient sufficient conditions but was absent in iron-depleted cultures. This fatty acid was not detected in this study, in agreement with the observation of Mauchline *et al.* (1992), who noted that cyclopropane acids are associated with slower growing mature cells. It is possible that the marked differences between these studies reflect the different culture methods employed, influencing the physiological state of the cells.

Decreasing the culture pH from 6.9 to 6.0 did not significantly alter the membrane fatty acid composition of *L. pneumophila* (Section 3.16.2). A slight increase in fatty acyl chain length, in particular among the branched acids, and a modest increase in the degree of unsaturation was detected. However, there was no significant changes in the proportion or type of fatty acid branching. When cultured at pH 7.8, the proportion of branched chain fatty acids, in particular iso-branched acids increased more significantly, mainly at the expense of straight chain saturated and unsaturated species. These changes are indicative of an increase in melting temperature and membrane rigidity.

Changes in the membrane phospholipid composition as revealed by FAB-MS, followed a similar trend at both extremes of pH (Section 3.16.3). Of particular importance for membrane fluidity, was the increase of phosphatidylcholine signals

which have a lower melting temperature (Wilkinson & Nagle, 1981). The principal phosphatidylcholine signals present in *L. pneumophila* (m/z 788 and 790), were most significantly elevated at pH 6.0. Signals representing phosphatidylethanolamines substituted with a greater number of carbon atoms, were also enhanced, with a corresponding decrease of phosphatidylethanolamines esterified with fewer total carbon atoms. Comparable changes were revealed among the phosphatidylglycerols by negative ion FAB/MS. CNL analysis confirmed the observations of positive and negative ion FAB mass spectra, with a general enhancement of phospholipid species possessing a greater number of total carbon atoms, in particular 32:1 and 32:0, at both extremes of pH (Section 3.16.4). There was no evidence of a change in the proportion of unsaturated substituents. Comparable changes were detected in each of the 4 phospholipid species examined, at both extremes of pH. As discussed previously, this increase of phospholipid species esterified with a greater number of carbon atoms, probably reflects an alteration in fatty acyl substitution patterns, as no significant increase in fatty acyl length was revealed by whole cell fatty acid analysis. More extensive analysis of the fatty acyl groups esterified to the glycerol backbone are required to investigate this further. This could be achieved by using phospholipase A₂ to remove the acyl group from position 2 of the phospholipid, followed by analysis of the hydrolysis product by FAB-MS (Embley & Wait, 1994).

Overall, growth at extremes of pH induced changes in the fatty acid and phospholipid composition of the cell envelope, however, once again a universal shift in lipid composition which would be indicative of a change in melting temperature was not observed. At pH 7.8, the increase of branched chain fatty acids was possibly counter balanced by the increase of phosphatidylcholine species.

4.5.2 Membrane protein expression.

Comparison of whole cell protein profiles of iron-limited and -replete cultures grown at pH 6.9 demonstrated that the expression of 8 protein bands was induced in response to iron limitation (Section 3.6.1). Five of these protein bands were low

molecular mass proteins, migrating between 18 and 26 kDa. Only two high molecular weight proteins migrating at 98 and 145 kDa, were induced. Two up-regulated low molecular mass proteins of 15 and 20 kDa, were also identified in the outer membrane protein fraction of iron-limited cells (Section 3.6.3). Expression of the 29 kDa major outer membrane protein and the 24 kDa Mip protein, did not appear to be influenced by iron availability. This is in agreement with the report that Mip expression is not regulated by *in vitro* stresses (Abu Kwaik & Engleberg, 1994). The induction of high molecular weight outer membrane proteins between 60 to 85 kDa, which are typically associated with iron-repressible iron-transport systems in other organisms, was not observed with iron-limited cells (Neilands, 1982; Brown & Williams, 1985; Williams *et al.*, 1990). Similarly, Barker *et al.* (1993) reported the induction of only two iron-repressible outer membrane proteins in iron-depleted *L. pneumophila*, and noted the absence of high molecular weight iron-repressible outer membrane proteins.

Analysis of the sarkosyl soluble fraction of the cell envelope (Section 3.6.2), located 7 iron-repressible proteins to the cytoplasmic membrane, 5 of which corresponded to bands detected in the whole cell protein profiles. Two of these were high molecular weight proteins migrating at 97 and 145 kDa. The major cytoplasmic membrane protein, has been characterized as a 60 kDa member of the Hsp60 family of heat shock proteins, and exhibits homology with the *E. coli* GroEL protein (Hoffman *et al.*, 1989 & 1990). In this study a major band migrating at approximately 58 kDa, was detected in both iron-limited and -replete cells. The expression of this protein, which may correspond to the major cytoplasmic membrane protein, was not influenced by iron limitation.

The physiological role and significance of these iron-repressible cytoplasmic and outer membrane proteins is unclear. As we have demonstrated that the virulence of iron-limited *L. pneumophila* is attenuated, these proteins are unlikely to play a significant role in pathogenesis. It is possible that some of these proteins may represent components of an iron transport system. Recently a *L. pneumophila* gene,

hbp, encoding a haemin binding protein with a predicted mass of 15.5 kDa, has been identified. Although, expression appeared to be iron-repressible, this protein was not essential for intracellular growth (O'Connell *et al.*, 1996). Whether, the 15 kDa iron-repressible OMP detected in this study was this haemin binding protein, was not investigated.

In addition to iron-repressible proteins, two iron-inducible proteins migrating at 25 and 40 kDa were observed in the outer membrane fractions, and one 29 kDa protein was detected in the cytoplasmic membrane. Two additional iron-induced proteins with molecular masses of 46 and 48 kDa were detected in the whole cell protein fraction, but were not observed in either membrane, suggesting that they may be cytoplasmic proteins (Section 3.6). The potential correlation between their down regulation and virulence attenuation under iron limitation requires further investigation. It is possible that some of these proteins may also represent non-essential iron-containing proteins, which are down regulated to optimize growth efficiency. Seven iron containing proteins have been identified in the cytoplasmic and periplasmic fractions of *L. pneumophila* (Mengaud & Horwitz, 1993). The major iron-containing protein (MICP) is a 98 kDa cytoplasmic aconitase, which contains 4 iron atoms per molecule. Preliminary studies indicated that iron does not participate in regulating aconitase expression (Mengaud & Horwitz, 1993). Among the remaining iron containing proteins, an iron superoxide dismutase (FeSOD) which is essential for viability, and is expressed independently of iron, has been identified (Sadosky *et al.*, 1994). The remaining iron containing proteins which migrated between 85 and 500 kDa on non-denaturing PAGE, have not been characterized (Mengaud & Horwitz, 1993).

Iron is an important environmental signal regulating protein expression in a wide range of bacteria, including human pathogens such as *P. aeruginosa*, *Neisseria* sp., *E. coli* and *S. typhimurium* (Neilands, 1982; Anwar *et al.*, 1983; West & Sparling, 1985; Schryvers & Morris, 1988; Williams, 1988; Foster & Hall, 1992). The regulatory action of iron is normally mediated by Fur (ferric uptake regulator),

which functions primarily to repress gene expression in the presence of Fe^{++} (Bagg & Neilands, 1987; Gross, 1993; Prince *et al.*, 1993). In addition, Fur may also act as a positive regulator of many iron-induced genes (Foster & Hall, 1992; Thomas & Sparling, 1996). A Fur homologue has been identified in *L. pneumophila* although its regulatory role has not been fully elucidated (Hickey & Cianciotto, 1994).

Apart from a potential role in iron transport, it is possible that some of these iron-induced proteins may represent stress proteins. A number of studies have confirmed the induction of *L. pneumophila* stress proteins, both in response to the intracellular environment of macrophages and to *in vitro* stress stimuli (Abu Kwaik *et al.*, 1993; Abu Kwaik & Engleberg, 1994; Susa *et al.*, 1996). Abu Kwaik & Pederson (1996) proposed that stress induced proteins may participate in the formation of the replicative phagosome and adaptation to the intracellular environment. Indeed, a number of loci which are essential for intracellular survival and multiplication, such as *eml*, *dotA* and *icm* have been identified (Marra *et al.*, 1992; Berger & Isberg, 1993; Berger *et al.*, 1994; Abu Kwaik & Pederson, 1996). Furthermore, a 19 kDa global stress protein, GspA, is induced intracellularly and upon exposure to several stress stimuli *in vitro* (Abu Kwaik & Engleberg, 1994).

Fluctuations in environmental pH may also modulate microbial gene expression. With *S. typhimurium* significant overlap was identified between iron-Fur and pH regulated protein synthesis. A subset of genes which were members of the acid tolerance response module, were influenced by both iron and acid, and were controlled by Fur (Foster & Hall, 1992).

In this study analysis of the virulent pH 6.0 culture which displayed a small colony phenotype on BCYE agar (Section 3.10.2), identified only one pH induced protein band (Section 3.17). In addition 5 minor proteins were repressed in comparison to the virulent cultures grown at pH 6.9. One of these protein bands migrated with an apparent molecular mass of 24 kDa. Whether this 24 kDa protein corresponds to Mip, was not investigated. A second 24 kDa protein distinct from Mip has been observed in *L. pneumophila* cultured in macrophages (Miyamoto *et al.*,

1993). Therefore, while this culture was genotypically more suited to growth at low pH, a significant change in protein composition was not observed. Furthermore, these alterations in protein expression did not have a significant impact on culture virulence. Whether the regulation of these protein bands is the result of phenotypic modulation or mutational disruption of gene expression was not determined.

The whole cell protein profile of the second replete pH 6.0 culture which displayed a wild-type colony phenotype, demonstrated a marked change in protein expression in comparison to both the variant pH 6.0 culture, and the control pH 6.9 culture (Section 3.17). In contrast to observations with the variant culture, only one minor protein was down-regulated, and 6 proteins were induced. While the physiological significance or the cellular location of these proteins has not been determined, the induction of a large number of proteins is indicative of a stress response. One of these proteins, which appeared as a major protein band of apparent molecular mass 64 kDa, may be the Hsp60 major cytoplasmic membrane protein, which is induced in response to intracellular growth and *in vitro* stress stimuli (Hoffman *et al.*, 1990). The marked difference in the protein profile of the two pH 6.0 cultures suggest that possibly the variant population was more suited to growth at pH 6.0, and as a result a stress response may not have been induced.

Growth of *L. pneumophila* at pH 7.8 also induced changes in cellular protein expression, with three minor proteins bands induced and 4 proteins down-regulated. Two of these repressed proteins migrated at 24 and 65 kDa, possibly corresponding to Mip and the major cytoplasmic membrane Hsp60 protein. Only one protein migrating at 31 kDa appeared to be induced at both extremes of pH. There was no evidence of the more dramatic changes normally associated with stress response.

Very few similarities were detected between the protein responses to iron limitation and extremes of pH, indicating that these stimuli induce different sets of genes, probably mediated through different regulatory networks. Changes in iron-availability and pH may have had a more significant impact on protein expression, and further studies would require the application of two-dimensional SDS-PAGE.

4.5.3 Serogroup antigen expression.

SDS-PAGE analysis of hot saline serogroup antigen extracts from iron-limited and -replete cultures revealed a ladder-like banding pattern, typically associated with smooth type LPS (Section 3.7.1). The profile for iron-limited and -replete cultures grown at pH 6.9 was comparable, as was the chemical composition of both extracts. Similar banding profiles have been reported by a number of researchers (Conlan & Ashworth, 1986; Hindahl & Iglewski, 1986; Nolte *et al.*, 1986). This distinct banding profile is generated by differences in the number of repeating units in the O-side chain, which is a highly hydrophobic homopolymer of nonulosonic acid lacking free hydroxyl groups. The narrow distance between bands, reflects a difference of only 356 Da, equivalent to one nonulosonic acid residue (Knirel *et al.*, 1994). Barker *et al.* (1993) also reported that the LPS profile of nutrient-sufficient and iron-depleted cells was comparable. Therefore, there was no alteration in the LPS structure or chemical composition correlating with reduced virulence under iron limitation. Conlan & Ashworth (1986) also reported that the LPS profiles of virulent and avirulent strains of *L. pneumophila* were similar.

The influence of growth at extremes of pH on serogroup antigen expression by iron-replete cultures was also investigated (Section 3.18). An increase in the staining intensity of low molecular mass LPS bands was observed with iron-replete pH 6.0 cultures, suggesting a decrease in the number of repeating units in the O-specific side chain. This effect was most prominent in the pH 6.0 culture which displayed a small colony variant morphology on BCYE agar. A modest increase in the carbohydrate content of these pH 6.0 extracts, was also demonstrated. Despite these changes in LPS structure, these cultures remained highly virulent in the guinea pig model, with an LD₅₀ marginally lower than that of the control pH 6.9 culture (Section 3.15). This alteration may have increased the hydrophobicity of the cell surface, resulting in the formation of a more discrete colony morphology. Increased surface hydrophobicity would also enhance survival in aerosols by reducing water

loss through desiccation (Dennis & Lee, 1988). No change in the banding profile or chemical composition of extracts from cultures grown at elevated pH was detected.

Thus of the various environmental shifts investigated in this study, only low pH appeared to influence the gross LPS structure. LPS, in particular its O-specific side chain, contributes to the pathogenicity of a number of bacteria including *Salmonellae* and *E. coli*. As with other bacterial species, *L. pneumophila* LPS is highly antigenic and represents the principal serogroup antigen (Gabay & Horwitz, 1985; Ciesielski *et al.*, 1986; Nolte *et al.*, 1986). However, *L. pneumophila* LPS possesses low endotoxic activity, induces a weak pyrogenic response in rabbits and is not considered to be an important virulence determinant (Wong *et al.*, 1979; Conlan & Ashworth, 1986; Otten *et al.*, 1986).

4.6 The Physiology of Poly- β -hydroxybutyrate Accumulation.

PHB is a linear head to tail polymer of β -hydroxybutyrate, which is normally accumulated by bacteria in the form of discrete cytoplasmic granules. Depending on the organism and on the physiological conditions applied to the cell, PHB may function as a carbon and / or energy storage compound, or as an electron sink for reducing power, which may accumulate during unbalanced growth, as well as under oxygen-limited growth conditions (Steinbüchel & Schlegel, 1991).

Intracellular inclusions resembling PHB granules, were observed within the cytoplasm of iron-replete and -limited cells (Section 3.19.1). This observation is in agreement with a number of ultrastructural studies (Chandler *et al.*, 1979; Rodgers & Davey, 1982). PHB formation by *L. pneumophila*, has been confirmed by chemical analysis. However, very low yields of polymer (< 4.3%), were detected in chemostat cultures, and poor correlation was observed between the number of intracellular granules and PHB yield (Mauchline *et al.*, 1992).

Laser confocal fluorescent microscopic examination of Nile red stained cells, revealed bright yellow-orange fluorescing inclusions, in both iron-replete and -limited

cells cultured at pH 6.9, confirming that these granules were lipophilic in nature (Section 3.19.2). Nile red has been used extensively for the detection and visualisation of neutral and polar lipid inclusions, in a variety of eukaryotic cell types (Fowler & Greenspan, 1985; Greenspan *et al.*, 1985; Brown *et al.*, 1992). The colour of the observed fluorescence is directly proportional to the hydrophobicity of the surrounding environment. Therefore, in highly hydrophobic environments, a spectral blue shift produces yellow-gold fluorescence (515 - 560 nm). Interaction with other cellular components such as membrane phospholipids produces orange-red fluorescence (>610 nm) (Fowler & Greenspan, 1985; Greenspan & Fowler, 1985; Greenspan *et al.*, 1985; Brown *et al.*, 1992).

This differential staining property has been exploited in the development of quantitative flow cytometry assays (Greenspan *et al.*, 1985; Dive *et al.*, 1992; Hassall, 1992; Smyth & Wharton, 1992). Nile blue A, a basic oxazine dye containing traces of the oxidized product, Nile red, has been used for the visualization of intracellular PHB granules in *Bacillus megaterium* and *Azobacter chroococcum* (Ostle & Holt, 1982).

Hot chloroform extraction of chemostat cell paste produced a white solid membrane like material. This material yielded ^1H NMR carbon spectra with coupling constants and chemical shifts consistent with that for authentic PHB (Doi *et al.*, 1986; Reusch, 1992). Furthermore, purified material from both iron-limited and -replete cells yielded comparable ^1H spectra, indicating no alteration in the molecular structure of the polymer (Section 3.19.3). Quantitative measurement of the purified material by dehydration to crotonic acid, confirmed low yields of PHB (2% cell dry wt.) under iron-replete conditions (Section 3.19.4). These results are in close agreement with the observations of Mauchline *et al.* (1992). Iron-limited growth induced a 2.5 fold increase in polymer accumulation. However, as noted by Mauchline *et al.* (1992), these PHB yields did not appear to correlate well with the number of intracellular granules observed during microscopic studies.

By performing 3 sequential chloroform extractions on representative samples, it was demonstrated that a single extraction cycle in chloroform provided poor PHB recovery (approximately 50 % of final yield; Section 3.19.5). Similar observations have been reported by Ramsay (1994), who demonstrated that recovery of PHB from *A. eutrophus*, even after 10 successive chloroform extractions, was still only 70 to 80 %. Repeated extraction of cell paste demonstrated that *L. pneumophila* has the potential to accumulate more significant concentrations of PHB, than was previously thought. A maximum yield of 16 % cell dry weight was detected. Poor recovery is likely to have been responsible for the poor yields observed during initial experiments and in previous studies (Mauchline *et al.*, 1992). This improved recovery correlated better with the granule content of *L. pneumophila*.

Solvent extraction and colorimetric determination of PHB is time consuming, hazardous, and requires large amounts of cell material, particularly when PHB concentrations are low. A spectrophotometric assay based on the lipophilic probe, NR, was evaluated as a fast quantitative measure of PHB accumulation (Sections 2.20 & 3.19). A linear relationship was demonstrated between the PHB content of culture samples and NR spectrofluorescence. Samples of *L. pneumophila* cell paste possessed a high background fluorescence reading, even after repeated chloroform extraction (Section 3.19.5). This fluorescence is likely to represent the background fluorescence associated with other cellular components, as well as residual PHB. While the excitation/emission wavelengths used provided maximum fluorescence, more selectivity for granule associated fluorescence may have been achieved at shorter wavelengths, excitation 450-500 nm and emission 528-578 nm (Greenspan *et al.*, 1985). Nevertheless, these results demonstrated that the contribution of background fluorescence was independent of initial PHB content, and the correlation between fluorescence and PHB content was retained even at very low PHB concentrations (Section 3.19.5). These initial experiments confirmed that the NR spectrofluorometric assay is a sensitive quantitative method, for the determination of PHB.

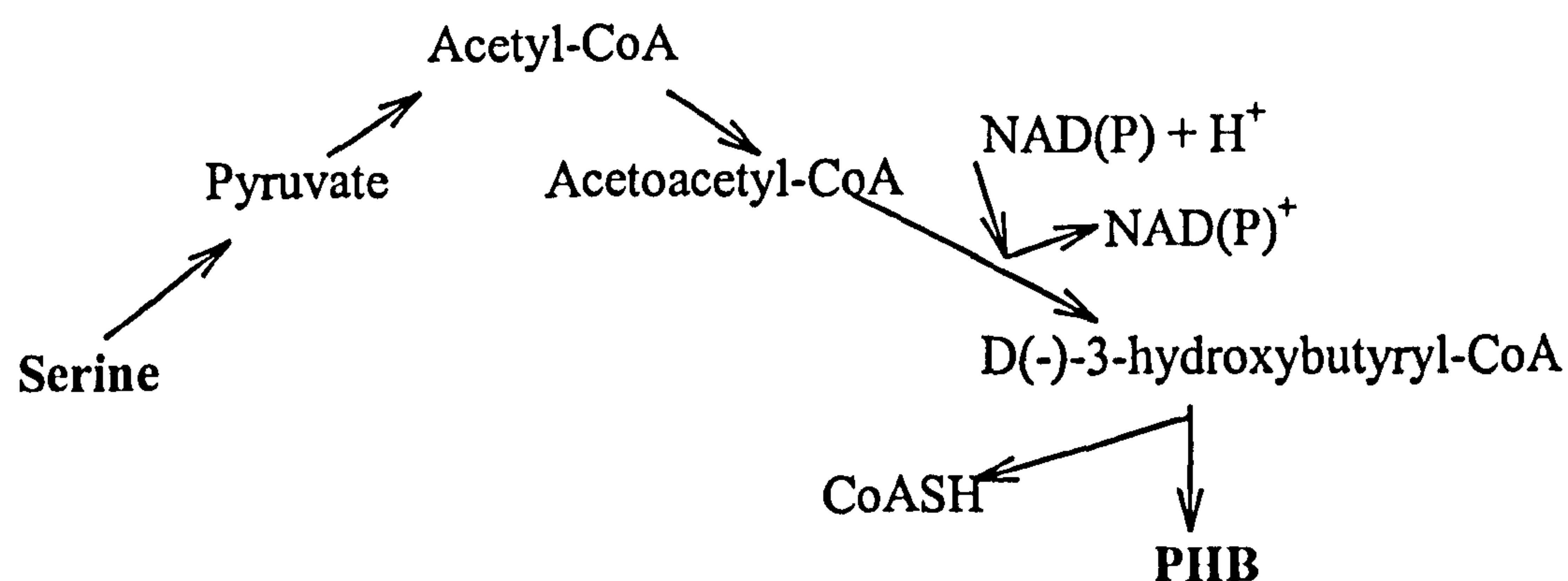
Spectrofluorometric analysis of pH 6.9 culture samples, demonstrated a 3-fold increase in PHB accumulation under iron-limited conditions (Section 3.19.6). In addition, the PHB content of iron-limited cultures was found to be inversely related to the concentration of iron metabolised (Section 3.19.7). These observations are in agreement with the physiology of PHB formation, when growth is limited by an essential nutrient other than the carbon and energy source (Steinbüchel & Schlegel, 1991). Furthermore, as the concentration of available iron is decreased, the concentrations of excess carbon and energy source will increase, which may be channelled into increased PHB accumulation. The majority of iron-replete samples emitted a low fluorescence intensity, indicating a low PHB content. However, two exceptions were observed and indeed one sample yielded 15% PHB, when extracted. It is possible that these differences may have been caused by oxygen-limitation during growth, caused by decreased electrode performance.

Iron-limited and -replete cultures grown at pH 6.0 also possessed brightly fluorescing intracellular granules (Section 3.19.8). However, at pH 7.8 a dramatic decrease in the number of intracellular granules was observed. This decrease was most prominent in iron-limited cultures. Spectrofluorometric data supported these microscopic observations. Decreasing the pH did not significantly reduce the calculated PHB content of either iron-limited or -replete cultures. However, at pH 7.8 the PHB content of iron-replete and -limited cultures was reduced 2- and 45-fold, respectively (Section 3.19.8). This decrease in PHB accumulation at elevated pH may reflect reduced grow efficiency associated with increased energy expenditure for the maintenance of essential cellular functions. Furthermore, as discussed in Section 4.1, excess serine may have been channelled into glycine release.

Therefore, this study demonstrates that *L. pneumophila* has the potential to accumulate significant concentrations of storage polymer. PHB formation is promoted during unbalanced growth, when growth is impaired due to limited availability of an essential nutrient other than carbon and energy source (Dawes & Senior, 1973; Dawes, 1986b; Steinbüchel & Schlegel, 1991). Regulation of PHB

metabolism is achieved at the enzyme level, with acetyl-CoA acyl transferase, CoA-SH and NADH as key regulatory elements. During balanced growth CoA-SH levels are high and polymer synthesis is inhibited. However, under conditions where growth is limited by an essential nutrient other than the carbon and energy source, NADH concentrations increase resulting in inhibition of early events of the TCA cycle, namely citrate synthetase and isocitrate dehydrogenase. This leads to an accumulation of acetyl CoA, which relieves the inhibition exerted by CoA-SH, leading to 3-hydroxybutyric acid formation.

Degradation of the polymer by 3-hydroxybutyrate dehydrogenase is also under the control of NADH and acetoacetate. Therefore, synthesis and breakdown of PHB is linked to the metabolic state of the cell, and to the carbon flux through intermediary metabolism. Based on the established pathways of PHB formation in other bacteria, it is likely the PHB formation in *L. pneumophila* proceeds via acetyl-CoA as follows:



Biochemical pathway of PHB formation from serine (Dawes, 1986b).

4.7 Relationship between PHB Reserves and Survival of *L. pneumophila* in a Low-Nutrient Environment.

PHB is recognized as an important endogenous carbon and energy reserve which enhances microbial survival under starvation conditions, and is therefore likely to make an important contribution to the persistence of *L. pneumophila* in low

nutrient aquatic environments, outside the protozoan host. This hypothesis is supported by the observation that legionellae are able to metabolise 3-hydroxybutyric acid, the monomeric unit released by hydrolysis of PHB (Mauchline & Keevil, 1991). Indeed, previous investigations have demonstrated that legionellae can survive in a culturable state for many months when incubated as a pure culture in either sterile stream or tap water (Skaliy & McEachern, 1979; Wang *et al.*, 1979; Hussong *et al.*, 1987; West *et al.*, 1993)

The current study demonstrates that *L. pneumophila* can maintain a vegetative state for prolonged periods (at least 600 days), when incubated in a low nutrient tap water environment, without the addition of exogenous nutrients (Section 3.20.1). Nile red spectrofluorometric analysis confirmed PHB utilisation during starvation. The relationship between the percentage decrease in culturability and NR spectrofluorescence, revealed at least three distinct physiological stages in the survival response of the suspension. A rapid decline in both culturability and spectrofluorescence was recorded during the first week of starvation. This initial phase is likely to represent the adaptive phase to starvation, with the expenditure of carbon and energy reserves for the induction of stress proteins and nutrient scavenging mechanisms. A proportion of the population possessing limited PHB reserves, may be unable to become physiologically adapted to the encountered stresses, resulting in a loss of culturability. This initial phase was followed by a survival stage, where the rates of culturability loss and PHB utilization decreased considerably (Section 3.20.1). However, spectrofluorescence decreased at a much faster rate than culturability. Therefore, PHB utilization appeared to be supporting the survival of *L. pneumophila*, and at the end of this survival stage, the PHB content was depleted by at least 80%. During the final stage, the residual PHB content approached depletion, promoting an increase in the rate at which culturability declined. This relationship between PHB content and survival of *L. pneumophila* was demonstrated with two separate cultures possessing different initial PHB

contents. A repeat experiment performed with cells possessing a higher PHB content, demonstrated enhanced survival.

Culture turbidity also declined in response to starvation, indicating a decrease in cell refractivity due to a loss of electron dense intracellular granules (Srienc *et al.*, 1984). The rate of decline in optical density increased in relation to the rate of PHB utilisation, with time. This suggests that in addition to PHB utilization contributing to the decrease in optical density, the incidence of cell disruption may also have increased with prolonged starvation. Monitoring the total cell count by phase contrast microscopy did not confirm this observation. However, it is difficult to discriminate between normal intact cells and partially disrupted cells by phase contrast microscopy.

Analysis of the light scattering and NR fluorescence properties of individual cells by flow cytometry, confirmed spectrofluorometric observations (Section 3.20.2). After 490 days starvation, the fluorescence of 90% of the population had declined to background levels. A linear relationship existed between the percentage decrease in culturability and mean cellular fluorescence, until the cellular fluorescence was depleted by 90 %, at which point there was an increase in the rate of culturability loss in relation to PHB utilization. The light scattering properties of the starved cells also revealed a significant decrease in the mean cell complexity, supporting a decrease in cell granularity and PHB content, in agreement with optical density measurements. The relationship between the decrease in mean cellular fluorescence and cell complexity was non-linear, and indicated a progressive increase in cell disruption with time, in agreement with the observations from optical density measurements. However, a linear relationship was observed between the decline in cell complexity and loss of culturability (Section 3.20.2).

Fluorescent microscopic examination of starved cells following staining with NR also provided visual evidence of PHB utilization (Section 3.20.3). After prolonged starvation a marked decrease in the number of intracellular granules was observed. Furthermore, after 500 days starvation, many cells were morphologically

ghost-like, when viewed by DIC microscopy. This morphological appearance suggested that many of the cells were in a disrupted state.

In addition, starvation appeared to influence the ability of culturable cells to form colonies on BCYE agar. Samples cultured after prolonged starvation produced colonies ranging considerably in diameter, as well as taking longer to appear on culture plates (Section 3.20.3). This variation in colony size may reflect the different physiological states of the starved population, and their potential for growth on nutrient rich media. It is possible that the smaller cells possess lower residual carbon and energy reserves, resulting in a reduced ability to initiate nutrient acquisition from their new environment.

During this study a significant decrease in the culturability of the suspension was demonstrated (Section 3.20.1). It is possible that many of these non-culturable cells were still in a viable state. *L. pneumophila* has been reported to enter a dormant state when exposed to low nutrient environments (Hussong *et al.*, 1987). Colbourne and Dennis (1989) demonstrated that heat shock treatment rendered *L. pneumophila* culture positive. However, West *et al.* (1993) failed to confirm dormancy among a non-culturable population of *L. pneumophila*, using comparable heat shock methods. Attempts to revive potentially non-culturable cells in this study by heat shock were also unsuccessful (Section 3.20.4).

Taken together, these observations provide strong evidence that PHB provides a critical energy reserve, aiding the survival and persistence of *L. pneumophila* in low nutrient environments. A number of studies have noted the formation of inclusions resembling PHB granules during intracellular growth in aquatic amoebae (Anand *et al.*, 1983; Fields *et al.*, 1986; Rowbotham, 1986; Vandenesch *et al.*, 1990). Therefore, as well as supporting the proliferation of legionellae and providing protection in hostile environments, amoebae may also make a significant contribution to the persistence of legionellae by inducing a PHB-rich phenotype which is physiologically more prepared for extracellular survival. Furthermore, these observations on the survival of *L. pneumophila* support the hypothesis that in their natural habitat,

legionellae may manifest a range of different phenotypes differing in their ability to survive in a culturable state, as well as possibly differing in their ability to resist chemical inactivation, survive aerosolization and cause human infection.

4.8 Conclusion.

This study illustrates that *L. pneumophila* is a physiologically versatile micro-organism, capable of adapting to environmental stresses commonly encountered in its natural habitat as well as during infection. Continuous culture in a controlled iron-limited environment and at extremes of pH under iron-limited and -replete conditions, induced significant changes in cellular morphology, metabolic activity and membrane composition. Although common microbial iron acquisition and transport mechanisms were not detected, diferric human transferrin was identified as a potentially important iron source for the growth of *L. pneumophila in vivo*, with the zinc metalloprotease possibly mediating iron-release. An important feature of the physiological response of *L. pneumophila* to iron-limited, carbon-excess growth, was the accumulation of significant intracellular reserves of poly- β -hydroxybutyrate. PHB supported long-term survival of *L. pneumophila* in a culturable state under starvation conditions, demonstrating the critical role of PHB in aiding the persistence of *L. pneumophila* in low-nutrient aquatic environments following release from the amoebal host.

In addition to physiological adaptation, the virulence of *L. pneumophila* was modulated in response to these changes in environmental conditions. Growth of iron-replete cells at pH 6.9 and 6.0 induced the expression of a highly virulent phenotype. However, in contrast to the role of iron in up-regulating the virulence of many human pathogens, the virulence of iron-limited cultures was significantly attenuated in guinea pigs, demonstrating that iron is essential for expression of a virulent phenotype. Virulence attenuation correlated with reduced phagocytosis and / or

reduced intracellular survival following uptake by alveolar macrophages. Decreasing the pH of iron-limited cultures to 6.0 did not induce expression of a virulent phenotype. Therefore, common environmental stresses have a significant impact on the physiology and virulence of *L. pneumophila*, leading to the expression of several distinct phenotypes which differ in their ability to persist in nature and cause human disease.

4.9 Future work.

A number of areas have been highlighted during this study which warrant further attention, in particular the issue of iron acquisition. Although previous reports and much of the data from this study suggests that *L. pneumophila* does not elaborate siderophore activity, the ferric chloride binding assay provided a clear indication of iron chelating activity in culture supernatants, and is worthy of further investigation. Traditionally, chemical extraction in conjunction with chemical and biological assays and mass spectrometry have been used to isolate and identify iron chelators. However, such techniques have proved unsuccessful with studies of *L. pneumophila*. A more promising approach is the characterization of mutants defective for iron acquisition. Interestingly, this method has recently identified a *L. pneumophila* iron and Fur-regulated (*frgA*) gene which encodes a protein which shares homology with aerobactin synthetase (Hickey & Cianciotto, 1997). Characterization of this protein, and additional mutants defective in iron acquisition, will advance our understanding of *L. pneumophila* iron acquisition, and the mechanism by which iron modulates pathogenicity.

Human transferrin was identified as a potential iron source for the growth of *L. pneumophila*, and may be of significance *in vivo*. Additional experiments employing human transferrin loaded with radiolabelled iron (^{55}Fe -transferrin) would help elucidate the importance of this interaction. These experiments could be

performed with actively growing iron-limited cultures, as well as washed iron-limited cells in the presence and absence of metalloprotease.

Spectrofluorometric and flow cytometric analysis of Nile red stained cells provided an important insight into the relationship between PHB and the survival of *L. pneumophila* under starvation conditions. A worthy extension of this study would be the use of vital fluorescent stains such as 5-cyano-2,3-ditolyl tetrazolium chloride (CTC), in conjunction with flow cytometry to investigate the relationship between culturability, metabolic activity and PHB utilization in response to starvation. This approach would also help address the issue of dormancy in relation to legionellae survival. It would also be interesting to determine the effect of long-term starvation on virulence, and resistance to antimicrobial agents and aerosolisation.

In addition to iron-limitation and extremes of pH, other environmental stresses, such as phosphate limitation, are likely to have a significant effect on the physiology and virulence of *L. pneumophila*, leading to an even greater diversity of environmental phenotypes. Phosphate is an essential nutrient for microbial growth, required for nucleotide and membrane phospholipid biosynthesis. Indeed, Barker *et al.* (1993) demonstrated alterations in the envelope composition of *L. pneumophila* during phosphate-depleted growth. Studies of *L. pneumophila* grown in phosphate-limited continuous culture would help elucidate other aspects of the organisms physiological response to phosphate limitation, including metabolic activity and efficiency, polymer formation and virulence modulation.

REFERENCES

- Abshire, K. Z., and F. C. Neidhardt. 1993. Analysis of proteins synthesized by *Salmonella typhimurium* during growth within a host macrophage. *J. Bacteriol.* 175:3734-3743.
- Abu Kwaik, Y. 1996. The phagosome containing *Legionella pneumophila* within the protozoan *Hartmannella vermiformis* is surrounded by rough endoplasmic reticulum. *Appl. Environ. Microbiol.* 62:2022-2028.
- Abu Kwaik, Y., B. I. Eisenstein, and N. C. Engleberg. 1993. Phenotypic modulation by *Legionella pneumophila* upon infection of macrophages. *Infect. Immun.* 61:1320-1329.
- Abu Kwaik, Y., and N. C. Engleberg. 1994. Cloning and molecular characterization of a *Legionella pneumophila* gene induced by intracellular infection and by various *in vitro* stress conditions. *Mol. Microbiol.* 13:243-251.
- Abu Kwaik, Y., B. S. Fields, and N. C. Engleberg. 1994. Protein expression by the protozoan *Hartmannella vermiformis* upon contact with its bacterial parasite *Legionella pneumophila*. *Infect. Immun.* 62:1860-1866.
- Abu Kwaik, Y., and L. L. Pederson. 1996. The use of differential display-PCR to isolate and characterize a *Legionella pneumophila* locus induced during the intracellular infection of macrophages. *Mol. Microbiol.* 21:543-556.
- Agiato, L., and D. W. Dyer. 1992. Siderophore production and membrane alterations by *Bordetella pertussis* in response to iron starvation. *Infect. Immun.* 60:117-123.
- Aitken, A., M. J. Geisow, J. B. C. Findlay, C. Holmes, and A. Yarwood. 1989. Peptide preparation and characterization, p. 43-68. *In* J. B. C. Findlay and M. J. Geisow (eds.), *Protein sequencing: a practical approach*. IRL Press, Oxford.
- Amano, K., and J. C. Williams. 1983. Partial characterization of peptidoglycan-associated proteins of *Legionella pneumophila*. *J. Biochem.* 94:601-606.

- Anand, C. M., A. R. Skinner, A. Malic, and J. B. Kurtz. 1983. Interaction of *Legionella pneumophila* and a free living amoeba (*Acanthamoeba palestinensis*). J. Hyg. (Camb.) 91:167-178.
- Anwar, H., M. R. W. Brown, R. M. Cozens, and P. A. Lambert. 1983. Isolation and characterization of the outer and cytoplasmic membranes of *Pseudomonas cepacia*. J. Gen. Microbiol. 129:499-507.
- Arnow, L. E. 1937. Colorimetric determination of the components of 3,4-dihydroxyphenylalanine-tyrosine mixtures. J. Biol. Chem. 118:531-537.
- Arnow, P. M., T. Chou, D. Weil, E. N. Shapiro, and C. Kretzschmar. 1982. Nosocomial Legionnaires' disease caused by aerosolized tap water from respiratory devices. J. Infect. Dis. 146:460-467.
- Atkin, C. L., J. B. Neilands, and H. J. Phaff. 1970. Rhodotorulic acid from species of *Leucosporidium*, *Rhodospiridium*, *Rhodotorula*, *Sporidiobolus*, and *Sporobolomyces*, and a new alanine-containing ferrichrome from *Cryptococcus melibiosum*. J. Bacteriol. 103:722-733.
- Bagg, A., and J. B. Neilands. 1987. Ferric uptake regulation protein acts as a repressor, employing iron(II) as a cofactor to bind the operator of an iron transport operon in *Escherichia coli*. Biochem. 26:5471-5477.
- Baine, W. B. 1985. Cytolytic and phospholipase C activity in *Legionella* species. J. Gen. Microbiol. 131:1383-1391.
- Baine, W. B. 1988. A phospholipase C from the Dallas 1E strain of *Legionella pneumophila* serogroup 5: purification and characterization of conditions for optimal activity with an artificial substrate. J. Gen. Microbiol. 134:489-498.
- Baine, W. B., J. K. Rasheed, J. C. Feeley, G. W. Gorman, and L. E. Casida, Jr. 1978. Effect of supplemental L-tyrosine on pigment production in cultures of the Legionnaires' disease bacterium. Curr. Microbiol. 1:93-94.
- Barbaree, J. M., B. S. Fields, J. C. Feeley, G. W. Gorman, and W. T. Martin. 1986. Isolation of protozoa from water associated with a legionellosis outbreak and

demonstration of intracellular multiplication of *Legionella pneumophila*. Appl. Environ. Microbiol. 51:422-424.

Barbaree, J. M., A. Sanchez, and G. N. Sanden. 1983. Tolerance of *Legionella* species to sodium chloride. Curr. Microbiol. 9:1-5.

Barker, J., and M. R. W. Brown. 1994. Trojan horses of the microbial world: protozoa and the survival of bacterial pathogens in the environment. Microbiol. 140:1253-1259.

Barker, J., and M. R. W. Brown. 1995. Speculations on the influence of infecting phenotype on virulence and antibiotic susceptibility of *Legionella pneumophila*. J. Antimicrob. Chemother. 36:7-21.

Barker, J., M. R. W. Brown, P. J. Collier, I. Farrell, and P. Gilbert. 1992. Relationship between *Legionella pneumophila* and *Acanthamoeba polyphaga*: physiological status and susceptibility to chemical inactivation. Appl. Environ. Microbiol. 58:2420-2425.

Barker, J., I. D. Farrell, and J. G. P. Hutchinson. 1986. Factors affecting growth of *Legionella pneumophila* in liquid medium. J. Med. Microbiol. 22:97-100.

Barker, J., P. A. Lambert, and M. R. W. Brown. 1993. Influence of inter-amoebic and other growth conditions on the surface properties of *Legionella pneumophila*. Infect. Immun. 61:3503-3510.

Barker, J., H. Scaife, and M. R. W. Brown. 1995. Intraphagocytic growth induces an antibiotic-resistant phenotype of *Legionella pneumophila*. Antimicrob. Agents Chemother. 39:2684-2688.

Bartlett, C. L. R., J. B. Kurtz, J. G. Hutchinson, G. C. Turner, and A. E. Wright. 1983. *Legionella* in hospital and hotel water supplies. Lancet ii:1315.

Bartlett, C. L. R., A. D. Macrae, and J. T. Macfarlane. 1986. Clinical aspects and diagnosis of *Legionella* infections, p. 37-55. In C. L. R. Bartlett, A. D. Macrae, and J. T. Macfarlane (eds.), *Legionella* infections. Edward Arnold, London.

- Baskerville, A., J. W. Conlan, L. A. E. Ashworth, and A. B. Dowsett. 1986. Pulmonary damage caused by a protease from *Legionella pneumophila*. Br. J. Exp. Path. 67:527-536.
- Baskerville, A., R. B. Fitzgeorge, M. Broster, P. Hambleton, and P. J. Dennis. 1981. Experimental transmission of Legionnaires' disease by exposure to aerosols of *Legionella pneumophila*. Lancet ii:1389-1390.
- Basset, J., R. C. Denney, G. Jeffery, and T. Mendham. 1983. Vogles text book of quantitative inorganic analysis, 4th edition.
- Bellinger-Kawahara, C., and M. A. Horwitz. 1990. Complement component C3 fixes selectively to the major outer membrane protein (MOMP) of *Legionella pneumophila* and mediates phagocytosis of liposome-MOMP complexes by human monocytes. J. Exp. Med. 172:1201-1210.
- Berg, J. D., J. C. Hoff, P. V. Roberts, and A. Martin. 1985. Growth of *Legionella pneumophila* in continuous culture. Appl. Environ. Microbiol. 49:1534-1537.
- Berger, K. H., and R. R. Isberg. 1993. Two distinct defects in intracellular growth complemented by a single genetic locus in *Legionella pneumophila*. Mol. Microbiol. 7:7-19.
- Berger, K. H., J. J. Merriam, and R. R. Isberg. 1994. Altered intracellular targeting properties associated with mutations in the *Legionella pneumophila* *dotA* gene. Mol. Microbiol. 14:809-822.
- Berka, R. M., and M. L. Vasil. 1982. Phospholipase C (heat-labile hemolysin) of *Pseudomonas aeruginosa*: purification and preliminary characterization. J. Bacteriol. 152:239-245.
- Black, W. J., F. D. Quinn, and L. S. Tompkins. 1990. *Legionella pneumophila* zinc metalloprotease is structurally and functionally homologous to *Pseudomonas aeruginosa* elastase. J. Bacteriol. 17:2608-2613.
- Blackmon, J. A., R. A. Harley, M. D. Hicklin, and F. W. Chandler. 1979. Pulmonary sequelae of acute Legionnaires' disease pneumonia. Ann. Intern. Med. 90:552-554.

- Blanchard, D. K., H. Friedman, W. E. Stewart II, T. W. Klein, and J. Y. Djeu. 1988. Role of gamma interferon in induction of natural killer activity by *Legionella pneumophila* in vitro and in an experimental murine infection model. *Infect. Immun.* 56:1187-1193.
- Blander, S. J., and M. A. Horwitz. 1989a. Vaccination with the major secretory protein of *Legionella pneumophila* induces cell-mediated and protective immunity in a guinea pig model of Legionnaires' disease. *J. Exp. Med.* 169:691-705.
- Blander, S. J., and M. A. Horwitz. 1989b. Vaccination with the major secretory protein of *Legionella* induces humoral and cell-mediated immune responses and protective immunity across different serogroups of *Legionella pneumophila* and different species of *Legionella*. *J. Immunol.* 147:285-291.
- Blander, S. J., L. Szeto, H. A. Shuman, and M. A. Horwitz. 1990. An immunoprotective model, the major secretory protein of *Legionella pneumophila*, is not a virulence factor in a guinea-pig model of Legionnaires' disease. *J. Clin. Invest.* 86:817-824.
- Bligh E. G. and W. J. Dyer. 1959. A rapid method of total lipid extraction and purification. *Can. J. Biochem. Physiol.* 37: 911-917.
- Bollin, G. E., J. F. Plouffe, M. F. Para, and B. Hackman. 1985a. Aerosols containing *Legionella pneumophila* generated by shower heads and hot-water faucets. *Appl. Environ. Microbiol.* 50:1128-1131.
- Bollin, G. E., J. F. Plouffe, M. F. Para, and R. B. Prior. 1985b. Difference in virulence of environmental isolates of *Legionella pneumophila*. *J. Clin. Microbiol.* 21:674-677.
- Booth, I. R. 1985. Regulation of cytoplasmic pH in bacteria. *Microbiol. Rev.* 49:359-378.
- Bortner, C. A., R. D. Miller, and R. R. Arnold. 1986. Bactericidal effect of lactoferrin on *Legionella pneumophila*. *Infect. Immun.* 51:373-377.

- Bozue, J. A., and W. Johnson. 1996. Interaction of *Legionella pneumophila* with *Acanthamoeba castellanii*: uptake by coiling phagocytosis and inhibition of phagosome-lysosome fusion. *Infect. Immun.* 64:668-673.
- Brand, B. C., A. B. Sadosky, and H. A. Shuman. 1994. The *Legionella pneumophila icm* locus: a set of genes required for intracellular multiplication in human macrophages. *Mol. Microbiol.* 14:797-808.
- Brener, D., I. W. DeVoe, and B. E. Holbein. 1981. Increased virulence of *Neisseria meningitidis* after *in vitro* iron-limited growth at low pH. *Infect. Immun.* 33:59-66.
- Brenner, D. J. 1986. Classification of *Legionellaceae*, current status and remaining questions. *Isr. J. Med. Sci.* 22:620-632.
- Brenner, D. J., A. G. Steigerwalt, and J. E. McDade. 1979. Classification of the Legionnaires' disease bacterium: *Legionella pneumophila*, genus novum, species nova, of the family *Legionellaceae*, familia nova. *Ann. Intern. Med.* 90:656-658.
- Brown, M. R. W., H. Anwar, and P. A. Lambert. 1984. Evidence that mucoid *Pseudomonas aeruginosa* in the cystic fibrosis lung grows under iron-restricted conditions. *FEMS Microbiol. Lett.* 21:113-117.
- Brown, M. R. W., P. J. Collier, and P. Gilbert. 1990. Influence of growth rate on susceptibility to antimicrobial agents: modification of the cell envelope and batch and continuous culture studies. *Antimicrob. Agents Chemother.* 34:1623-1628.
- Brown, W. J., T. R. Sullivan, and P. Greenspan. 1992. Nile red staining of lysosomal phospholipid inclusions. *Histochem.* 97:349-354.
- Brown, M. R. W., and P. Williams. 1985. The influence of environment on envelope properties affecting survival of bacteria in infections. *Ann. Rev. Microbiol.* 39:527-556.
- Buchmeier, N. A., and F. Heffron. 1990. Induction of *Salmonella* stress proteins upon infection of macrophages. *Sci.* 248:730-732.
- Butler, C. A., E. D. Street, T. P. Hatch, and P. S. Hoffman. 1985. Disulfide-bonded outer membrane proteins in the genus *Legionella*. *Infect. Immun.* 48:14-18.

- Button, D. K. 1985. Kinetics of nutrient-limited transport and microbial growth. *Microbiol. Rev.* 49:270-297.
- Button, D. K. 1993. Nutrient-limited microbial growth kinetics: overview and recent advances. *Antonie van Leeuwenhoek* 63:225-235.
- Byrd, T. F., and M. A. Horwitz. 1989. Interferon-gamma activated human monocytes downregulate transferrin receptors and inhibit the intracellular multiplication of *Legionella pneumophila* by limiting the availability of iron. *J. Clin. Invest.* 83:1457-1465.
- Byrd, T. F., and M. A. Horwitz. 1991 Lactoferrin inhibits or promotes *Legionella pneumophila* intracellular multiplication in non-activated and interferon gamma-activated human monocytes depending upon its degree of iron saturation. *J. Clin. Invest.* 88:1103-1112.
- Carrington, C. B. 1979. Pathology of Legionnaires' disease. *Ann. Intern. Med.* 90:496-498.
- Chambers, C. E., and P. A. Sokol. 1994. Comparison of siderophore production and utilization in pathogenic and environmental isolates of *Yersinia enterocolitica*. *J. Clin. Microbiol.* 32:32-39.
- Chandler, F. W., R. M. Cole, M. D. Hicklin, J. A. Blackmon, and C. S. Callaway. 1979. Ultrastructure of the Legionnaires' disease bacterium. *Ann. Intern. Med.* 90:642-647.
- Cianciotto, N. P., B. I. Eisenstein, C. H. Mody, and N. C. Engleberg. 1990. A mutation in the *mip* gene results in an attenuation of *Legionella pneumophila* virulence. *J. Infect. Dis.* 162:121-126.
- Cianciotto, N. P., B. I. Eisenstein, C. H. Mody, G. B. Toews, and N. C. Engleberg. 1989. A *Legionella pneumophila* gene encoding a species-specific surface protein potentiates initiation of intracellular infection. *Infect. Immun.* 57:1255-1262.

- Cianciotto, N. P., and B. S. Fields. 1992. *Legionella pneumophila* mip gene potentiates intracellular infection of protozoa and human macrophages. Proc. Natl. Acad. Sci. (USA) 89:5188-5191.
- Ciesielski, C. A., M. J. Blaser, and W. L. Wang. 1984. Role of stagnation and obstruction of water flow in isolation of *Legionella pneumophila* from hospital plumbing. Appl. Environ. Microbiol. 48:984-987.
- Ciesielski, C. A., M. J. Blaser, and W. L. Wang. 1986. Serogroup specificity of *Legionella pneumophila* is related to lipopolysaccharide characteristics. Infect. Immun. 51:397-404.
- Cirillo, J. D., S. Falkow, and L. S. Tompkins. 1994. Growth of *Legionella pneumophila* in *Acanthamoeba castellanii* enhances invasion. Infect. Immun. 62:3254-3261.
- Clesceri, L. S., A. E. Greenberg, and R. R. Trussell. 1989. Standard methods for the examination of water and waste water, 17th edition. American Public Health Association, Washington, DC.
- Colbourne, J. S., and P. J. Dennis. 1989. The ecology and survival of *Legionella pneumophila*. J. IWEM 3:345-350.
- Colville, A., J. Crowley, D. Dearden, R. C. B. Slack, and J. V. Lee. 1993. Outbreak of Legionnaires' disease at University Hospital Nottingham. Epidemiology, microbiology and control. Epidemiol. Infect. 110:105-116.
- Conlan, J. W. 1987. Studies of lipopolysaccharide and extracellular proteases from legionellae of differing virulence. PhD thesis, CNAA, UK.
- Conlan, J. W., and L. A. E. Ashworth. 1986. The relationship between the serogroup antigen and lipopolysaccharide of *Legionella pneumophila*. J. Hyg. (Camb.) 96:39-48.
- Conlan, J. W., A. Baskerville, and L. A. E. Ashworth. 1986. Separation of *Legionella pneumophila* proteases and purification of a protease which produces lesions like those of Legionnaires' disease in guinea-pig lung. J. Gen. Microbiol. 132:1565-1574.

- Conlan, J. W., A. Williams, and L. A. E. Ashworth. 1988. *In vivo* production of a tissue-destructive protease by *Legionella pneumophila* in the lungs of experimentally infected guinea-pigs. *J. Gen. Microbiol.* 134:143-149.
- Costerton, J. W., Z. Lewandowski, D. E. Caldwell, D. R. Korber, and H. M. Lappin-Scott. 1995. Microbial biofilms. *Ann. Rev. Microbiol.* 49:711-745.
- Cowart, R. E., and B. G. Foster. 1985. Differential effects of iron on the growth of *Listeria monocytogenes*: minimum requirements and mechanism of action. *J. Infect. Dis.* 151:721-730.
- Cox, C. D. 1980. Iron reductases from *Pseudomonas aeruginosa*. *J. Bacteriol.* 141:199-204.
- Csáky, T. Z. 1948. On the estimation of bound hydroxylamine in biological materials. *Acta Chem Scand* 2: 450-454.
- Davis, G. S., W. C. Winn, and H. N. Beaty. 1981. Legionnaires' disease. *Clin. Chest. Med.* 2:145-166.
- Dawes, E. A. 1986a. Energetics of microbial growth, p. 52-59. *In* E. A. Dawes (ed.), *Microbial energetics*. Blackie, London.
- Dawes, E. A. 1986b. Microbial energy reserve compounds, p. 145-165. *In* E. A. Dawes (ed.), *Microbial energetics*. Blackie, London.
- Dawes, E. A. 1988. Polyhydroxybutyrate: an intriguing biopolymer. *Biosci. Reports.* 8:537-547.
- Dawes, E. A., and P. J. Senior. 1973. The role and regulation of energy reserve polymers in micro-organisms. *Adv. Microb. Physiol.* 10:135-266.
- Dennis, P. J. L. 1986. Environmental factors affecting the survival and pathogenicity of *Legionella pneumophila*. Ph. D. Thesis. University of Warwick, Coventry, U. K.
- Dennis, P. J., D. J. Brenner, W. L. Thacker, R. Wait, G. Vesey, A. G. Steigerwalt, and R. F. Benson. 1993. Five new *Legionella* species isolated from water. *Int. J. Syst. Bacteriol.* 43:329-337.
- Dennis, P. J., D. Green, and B. P. C. Jones. 1984. A note on the temperature tolerance of *Legionella*. *J. Bacteriol.* 56:349-350.

- Dennis, P. J., and J. V. Lee. 1988. Differences in aerosol survival between pathogenic and non-pathogenic strains of *Legionella pneumophila* serogroup 1. J. Appl. Bacteriol. 65:135-141.
- Dive, C., T. M. Yoshida, D. J. Simpson, and B. L. Marrone. 1992. Flow cytometric analysis of steroidogenic organelles in differentiating granulosa cells. Biol. Reprod. 47:520-527.
- Doi, Y., M. Kunioka, Y. Nakamura, and K. Soga. 1986. ¹H and ¹³C NMR analysis of poly (β -hydroxybutyrate) isolated from *Bacillus megaterium*. Macromols. 19:1274-1276.
- Dondero, T. J. Jr., R. C. Rendtorff, G. F. Mallison, R. M. Weeks, J. S. Levy, E. W. Wong, and W. Schaffner. 1980. An outbreak of Legionnaires' disease associated with a contaminated air-conditioning cooling tower. New. Eng. J. Med. 302:365-370.
- Doring, G., M. Pfestorf, K. Botzenhart, M. A. Abdallah. 1988. Impact of proteases on iron uptake of *Pseudomonas aeruginosa* pyoverdin from transferrin and lactoferrin. Infect. Immun. 56:291-293
- Dorman, C. J. 1994. Genetics of Bacterial Virulence. Blackwell Scientific Publications.
- Dournon, E. 1988. Isolation of legionellae from clinical specimens, p. 13-30. In T. G. Harris and A. G. Taylor (eds.), A laboratory manual for *Legionella*. John Wiley & Son, Chichester.
- Dowling, J. N., A. K. Saha, and R. H. Glew. 1992. Virulence factors of the family *Legionellaceae*. Microbiol. Rev. 56:32-60.
- Drechsel, H., A. Thieken, R. Reissbrodt, G. Jung, and G. Winkelmann. 1993. α -Keto acids are novel siderophores in the genera *Proteus*, *Providencia*, and *Morganella* and are produced by amino acid deaminases. J. Bacteriol. 175:2727-2733.
- Dreyfus, L. A., and B. H. Iglewski. 1986. Purification and characterization of an extracellular protease of *Legionella pneumophila*. Infect. Immun. 51:736-743.

- Drlica, K. 1992. Control of bacterial DNA supercoiling. *Mol. Microbiol.* 6:425-433.
- Dubois, M., K. A. Gilles, J. K. Hamilton, P. A. Rebers, and F. Smith. 1956. Colorimetric method for determination of sugars and related substances. *Anal. Chem.* 28: 350-356.
- Edelstein, P. H. 1981. Improved semi-selective medium for isolation of *Legionella pneumophila* from contaminated clinical and environmental specimens. *J. Clin. Microbiol.* 14:298-303.
- Elliott, J. A., and W. C. Winn, Jr. 1986. Treatment of alveolar macrophages with cytochalasin D inhibits uptake and subsequent growth of *Legionella pneumophila*. *Infect. Immun.* 51:31-36.
- Embley, T. M., and R. Wait. 1994. Structural lipids of eubacteria, p.121-161. *In* M. Goodfellow and A. D. O'Donnell (eds.), *Chemical methods in prokaryotic systematics*. Wiley & Sons Ltd.
- Emery, T., and J. B. Neilands. 1960. Periodate oxidation of hydroxylamine derivatives. Products, scope, and application. *J. Am. Chem. Soc.* 82:4903-4904.
- Engleberg, N. C., C. Carter, D. R. Weber, N. P. Cianciotto, and B. I. Eisenstein. 1989. DNA sequence of *mip*, a *Legionella pneumophila* gene associated with macrophage infectivity. *Infect. Immun.* 57:1263-1270.
- Feeley, J. C., R. J. Gibson, G. W. Gorman, N. C. Langford, J. K. Rasheed, D. C. Mackel, W. B. Baine. 1979. Charcoal-yeast extract agar: primary isolation medium for *Legionella pneumophila*. *J. Clin. Microbiol.* 10:437-441.
- Feeley, J. C., and G. W. Gorman. 1980. *Legionella*, p. 318-324. *In* E. H. Lennette, A. Balows, W. J. Hausler, Jr., and J. P. Truant (eds.), *Manual of clinical microbiology*, 3rd edition. American Society for Microbiology, Washington, D.C.
- Feeley, J. C., G. W. Gorman, R. E. Weaver, D. C. Mackel, and H. W. Smith. 1978. Primary isolation media for Legionnaires' disease bacterium. *J. Clin. Microbiol.* 8:320-325.

Field, L. H., V. L. Headley, S. M. Payne, and L. J. Berry. 1986. Influence of iron on growth, morphology, outer membrane protein composition, and synthesis of siderophores in *Campylobacter jejuni*. *Infect. Immun.* 54:126-132.

Fields, B. S. 1993. *Legionella* and protozoa: interaction of a pathogen and its natural host, p. 129-136. *In* J. M. Barbaree, R. F. Breiman, and A. P. Dufour (eds.), *Legionella: current status and emerging perspectives*. American Society for Microbiology, Washington DC.

Fields, B. S. 1996. The molecular ecology of legionellae. *Trends in Microbiol.* 4:286-290.

Fields, B. S., J. M. Barbaree, E. B. Shotts, Jr., F. C. Feeley, W. A. Morrill, G. N. Sanden, and M. J. Dykstra. 1986. Comparison of guinea pig and protozoan models for determining virulence of *Legionella* species. *Infect. Immun.* 53:553-559.

Fields, B. S., G. N. Sanden, J. M. Barbaree, W. E. Morrill, R. M. Wadowsky, E. H. White, and J. C. Feeley. 1989. Intracellular multiplication of *Legionella pneumophila* in amoebae isolated from hospital hot water tanks. *Curr. Microbiol.* 18:131-137.

Findlay, R. H., and D. C. White. 1983. Polymeric beta-hydroxyalkanoates from environmental samples and *Bacillus megaterium*. *Appl. Environ. Microbiol.* 45:71-78.

Finnerty, W. R., R. A. Makula, and J. C. Feeley. 1979. Cellular lipids of the Legionnaires' disease bacterium. *Ann. Intern. Med.* 90:631-634.

Finney, D. J. 1947. Probit analysis. Cambridge University Press, Cambridge.

Finney, D. J. 1964. Probit Analysis, 2nd ed. Cambridge University Press, Cambridge.

Fitzgeorge, R. B. 1985. The effect of antibiotics on the growth of *Legionella pneumophila* in guinea-pig alveolar phagocytes infected in vivo by an aerosol. *J. Infect.* 10:189-193.

Fitzgeorge, R. B., A. Baskerville, M. Broster, P. Hambleton, and P. J. Dennis. 1983. Aerosol infection of animals with strains of *Legionella pneumophila* of

different virulence: comparison with intraperitoneal and intranasal routes of infection. *J. Hyg. (Camb.)* 90:81-89.

Fliermans, C. B., W. B. Cherry, L. H. Orrison, S. J. Smith, D. L. Tison, and D. H. Pope. 1981. Ecological distribution of *Legionella pneumophila*. *Appl. Environ. Microbiol.* 41:9-16.

Foster, J. W., and H. K. Hall. 1992. The effect of *Salmonella typhimurium* ferric uptake regulator (*fur*) mutations on iron- and pH-regulated protein synthesis. *J. Bacteriol.* 174:4317-4323.

Fowler, S. D., and P. Greenspan. 1985. Application of Nile red, a fluorescent hydrophobic probe, for the detection of neutral lipid deposits in tissue sections: comparison with oil red O. *J. Histochem. Cytochem.* 33:833-836.

Fraser, D. W., T. R. Tsai, W. Orenstein, W. E. Parkin, H. J. Beecham, R. G. Sharrar, J. Harris, G. F. Mallison, S. M. Martin, J. E. McDade, C. C. Shepard, and P. S. Brachman. 1977. Legionnaires' disease: description of an epidemic of pneumonia. *N. Eng. J. Med.* 297:1189-1197.

Friedman, R. L., B. H. Iglewski, and R. D. Miller. 1980. Identification of a cytotoxin produced by *Legionella pneumophila*. *Infect. Immun.* 29:271-274.

Friedman, R. L., J. E. Lochner, R. H. Bigley, and B. H. Iglewski. 1982. The effects of *Legionella pneumophila* toxin on oxidative processes and bacterial killing of human polymorphonuclear leukocytes. *J. Infect. Dis.* 146:328-334.

Friedman, S., K. Spitalny, J. Barbaree, Y. Faur, and R. McKinney. 1987. Pontiac fever outbreak associated with a cooling tower. *Am. J. Pub. Health.* 77:568-572.

Gabay, J. E., M. Blake, W. D. Niles, and M. A. Horwitz. 1985. Purification of *Legionella pneumophila* major outer membrane protein and demonstration that it is a porin. *J. Bacteriol.* 162:85-91.

Gabay, J. E., and M. A. Horwitz. 1985. Isolation and characterization of the cytoplasmic and outer membranes of the Legionnaires' disease bacterium (*Legionella pneumophila*). *J. Exp. Med.* 161:409-422.

- Gaitonde, M. K. 1967. A spectrofluorometric method for the direct determination of cysteine in the presence of other naturally occurring amino acids. *J. Biochem.* 104:627-633.
- Garrity, G. M., A. Brown, and R. M. Vickers. 1980. *Tatlockia* and *Fluoribacter*: two new genera of organisms resembling *Legionella pneumophila*. *Int. J. Syst. Bacteriol.* 30:609-620.
- Gebran, S. J., C. Newton, Y. Yamamoto, R. Widen, T. W. Klein, and H. Friedman. 1994a. Macrophage permissiveness for *Legionella pneumophila* growth modulated by iron. *Infect. Immun.* 62:564-568.
- Gebran, S. J., Y. Yamamoto, C. Newton, T. W. Klein, and H. Friedman. 1994b. Inhibition of *Legionella pneumophila* growth by gamma interferon in permissive A/J mouse macrophages: role of reactive oxygen species, nitric oxide, tryptophan and iron (III). *Infect. Immun.* 62:3197-3205.
- Geoffroy, C., J. Raveneau, J. Beretti, L. Lecroisey, J. Vazquez-Boland, J. E. Alouf, and P. Berche. 1991. Purification and characterization of an extracellular 29-kilodalton phospholipase C from *Listeria monocytogenes*. *Infect. Immun.* 59:2382-2388.
- George, J. R., L. Pine, M. W. Reeves, and W. K. Harrell. 1980. Amino acid requirements of *Legionella pneumophila*. *J. Clin. Microbiol.* 11:286-291.
- Gibson, S. A. W., and G. T. Macfarlane. 1988. Studies on the proteolytic activity of *Bacteroides fragilis*. *J. Gen. Microbiol.* 134:19-27.
- Gibson, F. C. III, A. O. Tzianabos, and F. G. Rodgers. 1994. Adherence of *Legionella pneumophila* to U-937 cells, guinea-pig alveolar macrophages, and MRC-5 cells by a novel, complement-independent binding mechanism. *Can. J. Microbiol.* 40:865-872.
- Glick, T. H., M. B. Gregg, B. Berman, G. Mallison, W. W. Rhodes, Jr., and I. Kassanoff. 1978. Pontiac fever: an epidemic of unknown etiology in a health department: I. clinical and epidemiologic aspects. *Am. J. Epidemiol.* 107:149-160.

- Goldberg, M. B., S. A. Boyko, and S. B. Calderwood. 1990. Transcriptional regulation by iron of a *Vibrio cholerae* virulence gene and homology of the gene to the *Escherichia coli* Fur system. *J. Bacteriol.* 172:6863-6870.
- Goldoni, P., P. Visca, M. Castellani Pastoris, P. Valenti, and N. Orsi. 1991. Growth of *Legionella* spp. under conditions of iron restriction. *J. Med. Microbiol.* 34:113-118.
- Gordon, S.A., A. Fleck, and J. Bell. 1978. Optimal conditions for the estimation of ammonium by the Berthelot reaction. *Ann. Clin. Biochem.* 15:270-275.
- Greenspan, P., and S. D. Fowler. 1985. Spectrofluorometric studies of the lipid probe, Nile red. *J. Lipid. Res.* 26:781-789.
- Greenspan, P., E. P. Mayer, and S. D. Fowler. 1985. Nile red: a selective fluorescent stain for intracellular lipid droplets. *J. Cell Biol.* 100:965-973.
- Griffiths, E. 1987a. Iron in biological systems, p. 1-25. *In* J. J. Bullen, and E. Griffiths (eds.), *Iron and infection: molecular, physiological and clinical aspects*. John Wiley & Sons Ltd., New York.
- Griffiths, E. 1987b. The iron-uptake systems of pathogenic bacteria, p. 69-137. *In* J. J. Bullen and E. Griffiths (eds), *Iron and infection: molecular, physiological and clinical aspects*. John Wiley & Sons Ltd., New York.
- Gross, R. 1993. Signal transduction and virulence regulation in human and animal pathogens. *FEMS Microbiol. Rev.* 104:301-326.
- Hantke, K. 1984. Cloning of the repressor protein gene of iron-regulated systems in *Escherichia coli* K12. *Mol. Gen. Genet.* 197:337-341.
- Harder, W., and L. Dijkhuizen. 1983. Physiological responses to nutrient limitation. *Ann. Rev. Microbiol.* 37:1-23.
- Harrison, T. G., and N. A. Saunders. 1994. Taxonomy and typing of legionellae. *Rev. Med. Microbiol.* 5:79-90.
- Hassall, D. G. 1992. Three probe flow cytometry of a human foam-cell forming macrophage. *Cytometry.* 13:381-388.
- Hedlund, K. W. 1981. *Legionella* toxin. *Pharmac. Ther.* 15:123-130.

- Hell, W., A. Essig, S. Bohnet, S. Gatermann, and R. Marre. 1993. Cleavage of tumor necrosis factor- α by *Legionella* exoprotease. *APMIS* 101:120-126
- Herbert, D., R. Elsworth, and R. C. Telling. 1956. The continuous culture of bacteria; a theoretical and experimental study. *J. Gen. Microbiol.* 14:601-622.
- Herwaldt, L. A., G. W. Gorman, T. McGrath, S. Toma, B. Brake, A. W. Hightower, J. Jones, A. L. Reingold, P. A. Boxer, P. W. Tang, C. W. Moss, II. Wilkinson, D. J. Brenner, A. G. Steigerwalt, and C. V. Broome. 1984. A new *Legionella* species, *Legionella feeleyi* species nova, causes Pontiac fever in an automobile plant. *Ann. Intern. Med.* 100:333-338.
- Hickey, E. K., and N. P. Cianciotto. 1994. Cloning and sequencing of the *Legionella pneumophila* *fur* gene. *Gene*. 143:117-121.
- Hickey, E. K., and N. P. Cianciotto. 1997. An iron- and Fur-repressed *Legionella pneumophila* gene that promotes intracellular infection and encodes a protein with similarity to the *Escherichia coli* aerobactin synthetase. *Infect. Immun.* 65:133-143.
- Hindahl, M. S., and B. H. Iglewski. 1984. Isolation and characterization of the *Legionella pneumophila* outer membrane. *J. Bacteriol.* 159:107-113.
- Hindahl, M. S., and B. H. Iglewski. 1986. Outer membrane proteins from *Legionella pneumophila* serogroups and other *Legionella* species. *Infect. Immun.* 51:94-101.
- Hoffman, P. 1984. Bacterial physiology, p. 61-67. *In* C. Thornsberry, A. Balows, J. C. Feeley, and W. Jakubowski (eds.), *Legionella*: proceedings of the second international symposium. American Society for Microbiology, Washington, D.C.
- Hoffman, P. S., C. A. Butler, and F. D. Quinn. 1989. Cloning and temperature-dependent expression in *Escherichia coli* of a *Legionella pneumophila* gene coding for a genus-common 60-kilodalton antigen. *Infect. Immun.* 57:1731-1739.
- Hoffman, P. S., L. Houston, and C. A. Butler. 1990. *Legionella pneumophila* *htpAB* heat shock operon: nucleotide sequence and expression of the 60-kilodalton antigen in *L. pneumophila*-infected HeLa cells. *Infect. Immun.* 58:3380-3387.

- Hoffman, P. S., and L. Pine. 1982. Respiratory physiology and cytochrome content of *Legionella pneumophila*. *Curr. Microbiol.* 7:351-356.
- Holzberg, M., and W. M. Artis. 1983. Hydroxymate siderophore production by opportunistic and systemic fungal pathogens. *Infect. Immun.* 40:1134-1139.
- Horwitz, M. A. 1983a. Formation of a novel phagosome by the Legionnaires' disease bacterium (*Legionella pneumophila*) in human monocytes. *J. Exp. Med.* 158:1319-1331.
- Horwitz, M. A. 1983b. The Legionnaires' disease bacterium (*Legionella pneumophila*) inhibits phagosome-lysosome fusion in human monocytes. *J. Exp. Med.* 158:2108-2126.
- Horwitz, M. A. 1984. Phagocytosis of the Legionnaires' disease bacterium (*Legionella pneumophila*) occurs by a novel mechanism: engulfment within a pseudopod coil. *Cell.* 36:27-33.
- Horwitz, M. A. 1987. Characterization of avirulent mutant *Legionella pneumophila* that survive but do not multiply within human monocytes. *J. Exp. Med.* 166:1310-1328.
- Horwitz, M. A. 1992. Interactions between macrophages and *Legionella pneumophila*. *Curr. Top. Microbiol. Immunol.* 181:265-282.
- Horwitz, M. A., and F. R. Maxfield. 1984. *Legionella pneumophila* inhibits acidification of its phagosome in human monocytes. *J. Cell. Biol.* 99:1936-1943.
- Horwitz, M. A., and S. C. Silverstein. 1980. The Legionnaires' disease bacterium (*Legionella pneumophila*) multiplies intracellularly in human monocytes. *J. Clin. Invest.* 66:441-450.
- Horwitz, M. A., and S. C. Silverstein. 1981a. Interaction of the Legionnaires disease bacterium (*Legionella pneumophila*) with human phagocytes. I. *L. pneumophila* resists killing by polymorphonuclear leukocytes, antibody, and complement. *J. Exp. Med.* 153:386-397.
- Horwitz, M. A., and S. C. Silverstein. 1981b. Interaction of the Legionnaires disease bacterium (*Legionella pneumophila*) with human phagocytes, II. Antibody

promotes binding of *L. pneumophila* to monocytes but does not inhibit intracellular multiplication. J. Exp. Med. 153:398-406.

Horwitz, M. A., and S. C. Silverstein. 1981c. Activated human monocytes inhibit the intracellular multiplication of Legionnaires' disease bacterium. J. Exp. Med. 154:1618-1635.

Hubbard, J. A. M., K. B. Lewandowska, M. N. Hughes, and R. K. Poole. 1986. Effects of iron limitation of *Escherichia coli* on growth, the respiratory chains and gallium uptake. Arch. Microbiol. 146:80-86.

Hughes, M. S., and T. W. Steele. 1994. Occurrence and distribution of *Legionella* species in compost plant materials. Appl. Environ. Micro. 60:2003-2005.

Hussong, D., R. R. Colwell, M. O'Brien, E. Weiss, A. D. Pearson, R. M. Weiner, and W. D. Burge. 1987. Viable *Legionella pneumophila* not detectable by culture on agar media. Biotechnol. 5:947-950.

Jantzen, E., A. Sonesson, T. Tangen, and J. Eng. 1993. Hydroxy-fatty acid profiles of *Legionella* species: Diagnostic usefulness assessed by principal component analysis. J. Clin. Microbiol. 31:1413-1419.

Jepras, R. I., and R. B. Fitzgeorge. 1986. The effect of oxygen-dependent antimicrobial systems on strains of *Legionella pneumophila* of different virulence. J. Hyg. (Camb.) 97:61-69.

Jepras, R. I., R. B. Fitzgeorge, and A. Baskerville. 1985. A comparison of virulence of two strains of *Legionella pneumophila* based on experimental aerosol infection of guinea-pigs. J. Hyg. (Camb.) 95:29-38.

Johnson, W., L. Varner, and M. Poch. 1991. Acquisition of iron by *Legionella pneumophila*: role of iron reductase. Infect Immun. 59:2376-2381.

Joly, J. R., R. M. McKinney, J. O. Tobin, W. F. Bibb, I. D. Watkins, and D. Ramsay. 1986. Development of a standardized subgrouping scheme for *Legionella pneumophila* serogroup 1 using monoclonal antibodies. J. Clin. Microbiol. 23:768-771.

- Karin, M., and B. Mintz. 1981. Receptor mediated endocytosis of transferrin in developmentally totipotent mouse teratocarcinoma stem cells. *J. Biol. Chem.* 256:3245-3252
- Karkhanis, Y. D., J. Y. Zeltner, J. J. Jackson, and D. J. Carlo. 1978. A new improved microassay to determine 2-keto-3-deoxyoctonate in lipopolysaccharide of gram negative bacteria. *Anal. Biochem.* 85:995-601.
- Kaufmann, A. F., J. E. McDade, C. M. Patton, J. V. Bennett, P. Skaliy, J. C. Feeley, D. C. Anderson, M. E. Potter, V. F. Newhouse, M. B. Gregg, and P. S. Brachman. 1981. Pontiac fever: isolation of the etiologic agent and demonstration of its mode of transmission. *Am. J. Epidemiol.* 114:337-347.
- Keen, M. G., and P. S. Hoffman. 1984. Metabolic pathways and nitrogen metabolism in *Legionella pneumophila*. *Curr. Microbiol.* 11:81-88.
- Keen, M. G., and P. S. Hoffman. 1989. Characterization of a *Legionella pneumophila* extracellular protease exhibiting hemolytic and cytotoxic activities. *Infect. Immun.* 57:732-738.
- Keevil, C. W., D. B. Davies, B. J. Spillane, and E. Mahenthiralingam. 1989. Influence of iron-limited and -replete continuous culture on the physiology and virulence of *Neisseria gonorrhoeae*. *J. Gen. Microbiol.* 135:851-863.
- Kilvington, S., and J. Price. 1990. Survival of *Legionella pneumophila* within cysts of *Acanthamoeba polyphaga* following chlorine exposure. *J. Appl. Bacteriol.* 68:519-525.
- Kim, M. J., J. E. Rogers, M. C. Hurley, and N. C. Engleberg. 1994. Phosphatase-negative mutants of *Legionella pneumophila* and their behavior in mammalian cell infection. *Microb. Path.* 17:51-62.
- King, C. H., B. S. Fields, E. B. Shotts, Jr., and E. H. White. 1991. Effects of cytochalasin D and methylamine on intracellular growth of *Legionella pneumophila* in amoebae and human monocyte-like cells. *Infect. Immun.* 59:758-763.

- Klein, T. W., Y. Yamamoto, H. K. Brown, and H. Friedman. 1991. Interferon-gamma induced resistance to *Legionella pneumophila* in susceptible A/J mouse macrophages. *J. Leukocyte. Biol.* 49:98-103.
- Knirel, Y. A., E. T. Rietschel, R. Marre, and U. Zähringer. 1994. The structure of the O-specific chain of *Legionella pneumophila* serogroup 1 lipopolysaccharide. *Eur. J. Biochem.* 221:239-245.
- Kroll, R. G., and I. R. Booth. 1983. The relationship between intracellular pH, the pH gradient and potassium transport in *Escherichia coli*. *Biochem. J.* 216:709-716.
- Kuchta, J. M., S. J. States, A. M. McNamara, R. M. Wadowsky, and R. B. Yee. 1983. Susceptibility of *Legionella pneumophila* to chlorine in tap water. *Appl. Environ. Microbiol.* 46:1134-1139.
- Lambert, M. A., and C. W. Moss. 1989. Cellular fatty acid compositions and isoprenoid quinone contents of 23 *Legionella* species. *J. Clin. Microbiol.* 27:465-473.
- Lancaster, M. J., C. W. Keevil, D. C. Ellwood, and R. C. W. Berkeley. 1988. Effect of environmental phosphate concentration on protein export by *Bacillus licheniformis* NCIB 6346. *Arch. Microbiol.* 150:547-551.
- Leland, D. S., and R. B. Kohler. 1991. Evaluation of the L-CLONE *Legionella pneumophila* serogroup 1 urine antigen latex test. *J. Clin. Microbiol.* 29:2220-2223.
- Light, P. A., and R. A. Clegg. 1974. Metabolism in iron-limited growth, p. 35-61. *In* Neilands, J. B. (ed.), *Microbial iron metabolism: a comprehensive treatise*. Academic Press, New York
- Light, P. A., and P. B. Garland. 1971. A comparison of mitochondria from *Torulopsis utilis* grown in continuous culture with glycerol, iron, ammonium, magnesium or phosphate as the growth-limiting nutrient. *Biochem. J.* 124:123-134.
- Liles, M. R., and N. P. Cianciotto. 1996. Absence of siderophore-like activity in *Legionella pneumophila* supernatants. *Infect. Immun.* 64:1873-1875.
- Litwin, C. M., S. A. Boyko, and S. B. Calderwood. 1992. Cloning, sequencing, and transcriptional regulation of the *Vibrio cholerae fur* gene. *J. Bacteriol.* 174:1897-1903.

- Loewen, P. C., and R. Hengge-Aronis. 1994. The role of the sigma factor σ^S (KatF) in bacterial global regulation. *Ann. Rev. Microbiol.* 48:53-80.
- Magnusson, K., E. Kihlström, L. Norlander, A. Norqvist, J. Davies, and S. Normark. 1979. Effect of colony type and pH on surface charge and hydrophobicity of *Neisseria gonorrhoeae*. *Infect. Immun.* 26:397-401.
- Marra, A., M. A. Horwitz, and H. A. Shuman. 1990. The HL-60 model for the interaction of human macrophages with the Legionnaires' disease bacterium. *J. Immunol.* 144:2738-2744.
- Marra, A., S. J. Blander, M. A. Horwitz, and H. A. Shuman. 1992. Identification of a *Legionella pneumophila* locus required for intracellular multiplication in human macrophages. *Proc. Natl. Acad. Sci. (USA)* 89:9607-9611.
- Marston, B. J., J. F. Plouffe, R. F. Breiman, T. M. File, Jr., R. F. Benson, M. Moyenudden, W. L. Thacker, K. -H. Wog, S. Skelton, B. Hackman, S. J. Salstrom, and J. M. Barbaree. 1993. Preliminary findings of a community-based pneumonia incidence study, p. 36-37. *In* J. M. Barbaree, R. F. Breiman, and A. P. Dufour (eds), *Legionella: current status and emerging perspectives*. American Society for Microbiology, Washington, DC.
- Matsiota-Bernard, P., C. Léfèbre, M. Sedqui, P. Cornillet, and M. Guenounou. 1993. Involvement of tumour necrosis factor alpha in intracellular multiplication of *Legionella pneumophila* in human monocytes. *Infect. Immun.* 61:4980-4983.
- Mauchline, W. S., R. Araujo, R. Wait, A. B. Dowsett, P. J. Dennis, and C. W. Keevil. 1992. Physiology and morphology of *Legionella pneumophila* in continuous culture at low oxygen concentration. *J. Gen. Microbiol.* 138:2371-2380.
- Mauchline, W. S., B. W. James, R. B. Fitzgeorge, P. J. Dennis, and C. W. Keevil. 1994. Growth temperature reversibly modulates the virulence of *Legionella pneumophila*. *Infect. Immun.* 62:2995-2997.
- Mauchline, W. S., and C. W. Keevil. 1991. Development of the BIOLOG substrate utilisation system for identification of *Legionella* spp. *Appl. Environ. Microbiol.* 57:3345-3349.

- Mayaud, C., and E. Dournon. 1988. Clinical features of Legionnaires' disease, p. 5-11. *In* T. G. Harris and A. G. Taylor (eds.), *A laboratory manual for Legionella*. John Wiley & Son, Chichester.
- McCusker K. T., B. A. Braaten, M. W. Cho, and D. A. Low. 1991. *Legionella pneumophila* inhibits protein synthesis in chinese hamster ovary cells. *Infect. Immun.* 59:240-246.
- McDade, J. E., D. J. Brenner, and F. M. Bozeman. 1979. Legionnaires' disease bacterium isolated in 1947. *Ann. Intern. Med.* 90:659-661.
- McDade, J. E., C. C. Shepard, D. W. Fraser, T. R. Tsai, M. A. Redus, and W. R. Dowdel. 1977. Legionnaires' disease: isolation of a bacterium and demonstration of its role in other respiratory disease. *N. Eng. J. Med.* 297:1197-1203.
- Mekalanos, J. J. 1992. Environmental signals controlling expression of virulence determinants in bacteria. *J. Bacteriol.* 174:1-7.
- Melchoir, D. L. 1982. Lipid phase transitions and regulation of membrane fluidity in prokaryotes. *Curr. Top. Memb. Transp.* 17:263-316.
- Mengaud, J. M., and M. A. Horwitz. 1993. The major iron-containing protein of *Legionella pneumophila* is an aconitase homologous with the human iron-responsive element-binding protein. *J. Bacteriol.* 175:5666-5676.
- Meyer, R. D. 1983. Legionella infections: a review of five years of research. *Rev. Infect. Dis.* 5:258-278.
- Meynell, G. G., and Meynell, E. 1970. *Theory and practice in experimental bacteriology*, 2nd ed. Cambridge University Press, Cambridge.
- Miller, R. D., and K. A. Kenep. 1993. Risk assessments for Legionnaires' disease based on routine surveillance of cooling towers for legionellae, p. 40-43. *In* J. M. Barbaree, R. F. Breiman, and A. P. Dufour (eds.), *Legionella: current status and emerging perspectives*. American Society for Microbiology, Washington, DC.
- Miller, J. F., J. J. Mekalanos, and S. Falkow. 1989. Coordinate regulation and sensory transduction in the control of bacterial virulence. *Sci.* 243:916-922.

Mintz, C. S., R. D. Miller, N. S. Gutsell, and T. Malek. 1993. *Legionella pneumophila* protease inactivates interleukin-2 and cleaves CD4 on human T cells. *Infect. Immun.* 61:3416-3421.

Mintz, C. S., D. R. Schultz, P. I. Arnold, and W. Johnson. 1992. *Legionella pneumophila* lipopolysaccharide activates the classical complement pathway. *Infect. Immun.* 60:2769-2776.

Miyamoto, H., S. Yoshida, H. Taniguchi, M. H. Qin, H. Fujio, and Y. Mizuguchi. 1993. Protein profiles of *Legionella pneumophila* Philadelphia-1 grown in macrophages and characterization of a gene encoding a novel 24 kDa *Legionella* protein. *Microb. Path.* 15:469-484.

Moffat, J. F., W. J. Black, and L. S. Tompkins. 1994. Further molecular characterization of the cloned *Legionella pneumophila* zinc metalloprotease. *Infect. Immun.* 62:751-753.

Moffat, J. F., and L. S. Tompkins. 1992. A quantitative model of intracellular growth of *Legionella pneumophila* in *Acanthamoeba castellanii*. *Infect. Immun.* 60:296-301.

Moll, H., A. Sonesson, E. Jantzen, R. Marre, and U. Zahringer. 1992. Identification of 27-oxo-octacosanoic acid and heptacosane-1,27-dioic acid in *Legionella pneumophila*. *FEMS Microbiol. Letters.* 97:1-6.

Monod, J. 1942. *Récherches sur la croissance des cultures bactériennes*, p. 210. Hermann et Cie, Paris.

Monod, J. 1950. La technique de culture continue; théorie et applications. *Ann. Inst. Pasteur.* 79:390-410.

Moody, M. D., and H. A. Dailey. 1985. Ferric iron reductase of *Rhodopseudomonas sphaeroides*. *J. Bacteriol.* 163:1120-1125.

Morton, D. J., and P. Williams. 1990. Siderophore-independent acquisition of transferrin-bound iron by *Haemophilus influenza* type b. *J. Gen. Microbiol.* 136:927-933.

- Moss, C. W., and S. B. Dees. 1979. Cellular fatty acid composition of WIGA, a rickettsia-like agent similar to the Legionnaires' disease bacterium. *J. Clin. Microbiol.* 10:390-391.
- Moss, C. W., R. E. Weaver, S. B. Dees, and W. B. Cherry. 1977. Cellular fatty acid compositions of isolates from Legionnaires' disease. *J. Clin. Microbiol.* 6:140-143.
- Muder, R. R., V. L. Yu, and A. H. Woo. 1986. Mode of transmission of *Legionella pneumophila*. *Arch. Intern. Med.* 146:1607-1612.
- Müller, H. E. 1980. Proteolytic action of *Legionella pneumophila* on human serum proteins. *Infect. Immun.* 27:51-53.
- Müller, H. E. 1981. Enzymatic profile of *Legionella pneumophila*. *J. Clin. Microbiol.* 13:423-426.
- Müller, H. E. 1983. Induction of proteinases in *Legionella* by growth on agar containing serum. *Zbl Bakt Hyg A* 256:211-221.
- Myerowitz, R. L., A. W. Pasculle, J. N. Dowling, G. J. Pazin, M. Puerzer, R. B. Yee, C. R. Rinaldo, Jr., and T. R. Hakala. 1979. Opportunistic lung infection due to "Pittsburgh pneumonia agent". *New. Eng. J. Med.* 301:953-958.
- Nakamura, T., H. Tokuda, and T. Unemoto. 1984. K^+/H^+ antiporter functions as a regulator of cytoplasmic pH in a marine bacterium, *Vibrio alginolyticus*. *Biochim. Biophys. Acta* 776:330-336.
- Nash, T. W., D. M. Libby, and M. A. Horwitz. 1984. Interaction between the Legionnaires' disease bacterium (*Legionella pneumophila*) and human alveolar macrophages. Influence of antibody, lymphokines and hydrocortisone. *J. Clin. Invest.* 74:771-782.
- Nash, T. W., D. M. Libby, and M. A. Horwitz. 1988. Gamma interferon activated human alveolar macrophages inhibit the intracellular multiplication of *Legionella pneumophila*. *J. Immunol.* 140:3978-3981.

- Neiderhoffer, E. C., C. M. Naranjo, K. L. Bradley, and J. A. Fee. 1990. Control of *Escherichia coli* superoxide dismutase (*sodA* and *sodB*) genes by the ferric uptake regulation (*fur*) locus. *J. Bacteriol.* **172**:1930-1938.
- Neilands, J. B. 1974. Iron and its role in microbial physiology, p. 4-31. *In* J. B. Neilands (ed.), *Microbial iron metabolism: a comprehensive treatise*. Academic Press, New York.
- Neilands, J. B. 1981. Microbial iron compounds. *Ann. Rev. Biochem.* **50**:715-731.
- Neilands, J. B. 1982. Microbial envelope proteins related to iron. *Ann. Rev. Microbiol.* **36**:285-309.
- Nolte, F. S., C. A. Conlin, and M. A. Motley. 1986. Electrophoretic and serological characterization of the lipopolysaccharide of *Legionella pneumophila*. *Infect. Immun.* **52**:676-681.
- Nolte, F. S., G. E. Hollick, and R. G. Robertson. 1982. Enzymatic activities of *Legionella pneumophila* and Legionella-like organisms. *J. Clin. Microbiol.* **15**:175-177.
- Novick, A., and L. Szilard. 1950. Description of the chemostat. *Sci.* **122**:715-716.
- O'Connell, W. A., E. K. Hickey, and N. P. Cianciotto. 1996. A *Legionella pneumophila* gene that promotes hemin binding. *Infect. Immun.* **64**:842-848.
- Okujo, N., and S. Yamamoto. 1994. Identification of the siderophores from *Vibrio hollisae* and *Vibrio mimicus* as aerobactin. *FEMS Microbiol. Lett.* **118**:187-192.
- Oldham, L. J., and F. G. Rodgers. 1985. Adhesion, penetration and intracellular replication of *Legionella pneumophila*: an *in vitro* model of pathogenesis. *J. Gen. Microbiol.* **131**:697-706.
- Olson, E. R., 1993. Influence of pH on bacterial gene expression. *Mol. Microbiol.* **8**:5-14.
- Ostle, A. G., and J. G. Holt. 1982. Nile blue A as a fluorescent stain for poly- β -hydroxybutyrate. *Appl. Environ. Microbiol.* **44**:238-241.
- Ott, M., P. Messner, J. Heesemann, R. Marre, and J. Hacker. 1991. Temperature-dependent expression of flagella in *Legionella*. *J. Gen. Microbiol.* **137**:1955-1961.

- Otten, S., S. Iyer, W. Johnson, and R. Montgomery. 1986. Serospecific antigens of *Legionella pneumophila*. J. Bacteriol. 167:893-904.
- Otto, B. R., A. M. J. J. Verweij-van Vught, and D. M. MacLaren. 1992. Transferrin and heme-compounds as iron sources for pathogenic bacteria. Crit. Rev. Microbiol. 18:217-233.
- Pasculle, A. W., J. C. Feeley, R. J. Gibson, L. G. Cordes, R. L. Myerowitz, C. M. Patton, G. W. Gorman, C. L. Carmack, J. W. Ezzell, and J. N. Dowling. 1980. Pittsburgh pneumonia agent: direct isolation from human lung tissue. J. Infect. Dis. 141:727-732.
- Payne, N. R., and M. A. Horwitz. 1987. Phagocytosis of *Legionella pneumophila* is mediated by human monocyte complement receptors. J. Exp. Med. 165:1377-1389.
- Pearlman, E., A. H. Jiwa, N. C. Engleberg, and B. I. Eisenstein. 1988. Growth of *Legionella pneumophila* in human macrophage-like (U937) cell line. Microb. Path. 5:87-95.
- Pechurkin, N. S. 1980 Questions of stability and microevolution of continuous microbial cultures, p. 137-150. In B. Sikyta, Z. Fencel, and V. Polacek (eds.), Continuous cultivation of microorganisms. Proceedings of the 7th International Symposium, Prague.
- Pine, L., M. J. Franzus, and G. B. Malcolm. 1986a. Guanine is a growth factor for *Legionella* species. J. Clin. Microbiol. 23:163-169.
- Pine, L., J. R. George, M. W. Reeves, and W. K. Harrell. 1979. Development of a chemically defined liquid medium for growth of *Legionella pneumophila*. J. Clin. Microbiol. 9:615-626.
- Pine, L., P. S. Hoffman, G. B. Malcolm, R. F. Benson, and M. J. Franzus. 1986b. Role of keto acids and reduced-oxygen-scavenging enzymes in the growth of *Legionella* species. J. Clin. Microbiol. 23:33-42.
- Pirt, S. J. 1972. Prospects and problems in continuous flow culture of microorganisms. J. Appl. Chem. Biotech. 22:55-64.

- Pirt, S. J. 1975. Principles of microbe and cell cultivation. Blackwell Scientific, Oxford.
- Plack, R. H. Jr., and B. P. Rosen. 1980. Cation/Proton antiporter systems in *Escherichia coli*. J. Biol. Chem. 255:3824-3825.
- Plouffe, J. F., L. R. Webster, and B. Hackman. 1983. Relationship between colonization of hospital buildings with *Legionella pneumophila* and hot water temperatures. Appl. Environ. Microbiol. 46:769-770.
- Poch, M. T., and W. Johnson. 1993. Ferric reductases of *Legionella pneumophila*. Bio Metals. 6:107-114.
- Pope, C. D., W. A. O'Connell, and N. P. Cianciotto. 1996. *Legionella pneumophila* mutants that are defective for iron acquisition and assimilation and intracellular multiplication. Infect. Immun. 64:629-636.
- Powell, E. O. 1958. Criteria for the growth of contaminants and mutants in continuous culture. J. Gen. Microbiol. 18:259-268.
- Prince, R. W., C. D. Cox, and M. L. Vasil. 1993. Coordinate regulation of siderophore and exotoxin A production: molecular cloning and sequencing of the *Pseudomonas aeruginosa fur* gene. J. Bacteriol. 175:2589-2598.
- Prince, R. W., D. G. Storey, A. I. Vasil, and M. L. Vasil. 1991. Regulation of *tox A* and *reg A* by *Escherichia coli fur* gene and identification of a Fur homologue in *Pseudomonas aeruginosa* PA103 and PA01. Mol. Microbiol. 5:2823-2831.
- Pruckler, J. M., R. F. Benson, M. Moyenuddin, W. T. Martin, and B. S. Fields. 1995. Association of flagellum expression and intracellular growth of *Legionella pneumophila*. Infect. Immun. 63:4928-4932.
- Quinn, F. D., and L. S. Tompkins. 1989. Analysis of a cloned sequence of *Legionella pneumophila* encoding a 38kD metalloprotease possessing haemolytic and cytotoxic activities. Mol. Microbiol. 3:797-805.
- Quinn, F. D., and Weinberg, E. D. 1988. Killing of *Legionella pneumophila* by human serum and iron-binding agents. Curr Microbiol. 17:111-116.

- Rainnie, D. J., and P. D. Bragg. 1973. The effect of iron deficiency on respiration and energy-coupling in *Escherichia coli*. J. Gen. Microbiol. 77:339-349.
- Ramsay, J. A. 1994. PHA: its separation from microbial biomass and its biodegradation, p. 49-58. In G. Braunegg (ed.), Physiology, kinetics, production and use of biopolymers. Proceedings of the European Federation of Biotechnology, Austria.
- Rechnitzer, C. 1994. Pathogenic aspects of Legionnaires' disease: interaction of *Legionella pneumophila* with cellular host defenses. APMIS. 102:Suppl. 43.
- Rechnitzer, C., and J. Blom. 1989. Engulfment of the Philadelphia strain of *Legionella pneumophila* within pseudopod coils in human phagocytes. APMIS. 97:105-114.
- Rechnitzer, C., and A. Kharazmi. 1992. Effect of *Legionella pneumophila* cytotoxic protease on human neutrophil and monocyte function. Microb. Path. 12:115-125.
- Reed, L. J. and H. Muench. 1938. A simple method of estimating fifty percent endpoints. Am. J. Hyg. 27:493-497.
- Reeves, M. W., L. Pine, S. H. Hunter, J. R. George, and W. K. Harrell. 1981. Metal requirements of *Legionella pneumophila*. J. Clin. Microbiol. 13:688-695.
- Reeves, M. W., L. Pine, J. B. Neilands, and A. Balows. 1983. Absence of siderophore activity in *Legionella* species grown in iron-deficient media. J. Bacteriol. 154:324-329.
- Reingold, A. L., B. M. Thomason, B. J. Brake, L. Thacker, H. W. Wilkinson, and J. N. Kuritsky. 1984. *Legionella* pneumonia in the United States: the distribution of serogroups and species causing human illness. J. Infect Dis. 149:819.
- Reusch, R. N. 1992. Biological complexes of poly- β -hydroxybutyrate. FEMS Microbiol. Rev. 103:119-130.
- Ristroph, J. D., K. W. Hedlund, and R. G. Allen. 1980. Liquid media for growth of *Legionella pneumophila*. J. Clin. Microbiol. 11:19-21.

- Robertson, B. R., and D. K. Button. 1979. Phosphate-limited continuous culture of *Rhodotorula rubra*: kinetics of transport, leakage, and growth. *J. Bacteriol.* 138:884-895.
- Rodgers, F. G., and M. R. Davey. 1982. Ultrastructure of the cell envelope layers and surface details of *Legionella pneumophila*. *J. Gen. Microbiol.* 128:1547-1557.
- Rogers, J., and C. W. Keevil. 1992. Immunogold and fluorescein immunolabelling of *Legionella pneumophila* within an aquatic biofilm visualized by using episcopic differential interference contrast microscopy. *Appl. Environ. Microbiol.* 58:2326-2330.
- Rogers, H. J., H. R. Perkins, and J. B. Ward. 1980. Microbial cell walls and membranes. Chapman & Hall, NY.
- Rose, A. H. 1989. Influence of the environment on microbial lipid composition, p. 255-277. In C. Ratledge and S. G. Wilkinson (eds.), *Microbial lipids Volume II*. Acad. Press Ltd.
- Rosenfeld, J. S., F. Kueppers, T. Newkirk, R. Tamada, J. J. Meissler Jr. and T. K. Eisenstein. 1986. A protease from *Legionella pneumophila* with cytotoxic and dermal ulcerative activity. *FEMS Microbiol. Lett.* 37:51-58.
- Rowbotham, T. J. 1980. Preliminary report on the pathogenicity of *Legionella pneumophila* for fresh-water and soil amoebae. *J. Clin. Pathol.* 33:1179-1183.
- Rowbotham, T. J. 1986. Current views on the relationship between amoebae, legionellae and man. *Isr. J. Med. Sci.* 22:678-689.
- Russell, J. B., and G. M. Cook. 1995. Energetics of bacterial growth: balance of anabolic and catabolic reactions. *Microbiol. Rev.* 59:48-62.
- Sadosky, A. B., J. W. Wilson, H. E. Steinman, and H. A. Shuman. 1994. The iron superoxide dismutase of *Legionella pneumophila* is essential for viability. *J. Bacteriol.* 176:3790-3799.
- Saha, A. K., J. N. Dowling, K. L. LaMarco, S. Das, A. T. Remaley, N. Olomu, M. T. Pope, and R. H. Glew. 1985. Properties of an acid phosphatase from *Legionella*

micdadei which blocks superoxide anion production by human neutrophils. Arch. Biochem. Biophys. 243:150-160.

Schryvers, A. B., and L. J. Morris. 1988. Identification and characterization of the transferrin receptor from *Neisseria meningitidis*. Mol. Microbiol. 2:281-288.

Schwyn, B., and J. B. Neilands. 1987 Universal chemical assay for the detection and determination of siderophores. Anal. Biochem. 160:47-56.

Simonson, C., D. Brener, and I. W. DeVoe. 1982. Expression of a high-affinity mechanism for acquisition of transferrin iron by *Neisseria meningitidis*. Infect. Immun. 36:107-113.

Skaliy, P., and H. V. McEachern. 1979. Survival of the Legionnaires' disease bacterium in water. Ann. Intern. Med. 90:662-663.

Skerrett, S. J., and T. R. Martin. 1991. Alveolar macrophage activation in experimental legionellosis. J. Immunol. 147:337-345.

Skerrett, S. J., and T. R. Martin. 1992. Recombinant murine interferon- γ reversibly activates rat alveolar macrophages to kill *Legionella pneumophila*. J. Infect. Dis. 166:1354-1361.

Slepecky, R. A., and J. H. Law. 1960. A rapid spectrophotometric assay for alpha, beta-unsaturated acids and beta-hydroxy acids. Anal. Chem. 32:1697-1699.

Smith, M. J., N. J. Shoolery, B. Schwyn, I. Holden, and J. B. Neilands. 1985. Rhizobactin, a structurally novel siderophore from *Rhizobium meliloti*. J. Am. Chem. Soc. 107:1739-1743.

Smyth, M., and W. Wharton. 1992. Differentiation of A31T6 proadipocytes to adipocytes: a flow cytometric analysis. Exp. Cell Res. 199:29-38.

Srienc, F., B. Arnold, J. E. Bailey. 1984. Characterization of intracellular accumulation of poly- β -hydroxybutyrate (PHB) in individual cells of *Alcaligenes eutrophus* H16 by flow cytometry. Biotech. Bioeng. 26:982-987.

Staggs, T. M., and R. D. Perry. 1991. Identification and cloning of a *fur* regulatory gene in *Yersinia pestis*. J. Bacteriol. 173:417-425.

States, S. J., L. F. Conley, M. Ceraso, T. E. Stephenson, R. S. Wolford, R. M. Wadowsky, A. M. McNamara, and R. B. Yee. 1985. Effects of metals on *Legionella pneumophila* growth in drinking water plumbing systems. *Appl. Environ. Microbiol.* **50**:1149-1154.

States, S. J., L. F. Conley, J. M. Kuchta, B. M. Oleck, M. J. Lipovich, R. S. Wolford, R. M. Wadowsky, A. M. McNamara, J. L. Sykora, G. Keleti, and R. B. Yee. 1987. Survival and multiplication of *Legionella pneumophila* in municipal drinking water systems. *Appl. Environ. Microbiol.* **53**:979-986.

States, S. J., R. M. Wadowsky, J. M. Kuchta, R. S. Wolford, L. F. Conley, and R. B. Yee. 1994. *Legionella* in drinking water, p. 340-367. In G. A. McFeters (ed.), *Drinking water microbiology: progress and recent developments*. Springer-Verlag, New York.

Steele, T. W. 1993. Interactions between soil amoebae and soil legionellae, p140-142. In J. M. Barbaree, R. F. Breiman, and A. P. Dufour (eds.), *Legionella: current status and emerging perspectives*. American Society for Microbiology, Washington, D.C.

Steinbüchel, A., and H. G. Schlegel. 1991. Physiology and molecular genetics of poly(β -hydroxyalkanoic acid) synthesis in *Alcaligenes eutrophus*. *Mol. Microbiol.* **5**:535-542.

Steinert, M., H. Engelhard, M. Flügel, E. Wintermeyer, and J. Hacker. 1995. The Lly protein protects *Legionella pneumophila* from light but does not directly influence its intracellular survival in *Hartmannella vermiformis*. *Appl. Environ. Microbiol.* **61**:2428-2430.

Stout, J. E., V. L. Yu, and M. G. Best. 1985. Ecology of *Legionella pneumophila* within water distribution systems. *Appl. Environ. Microbiol.* **49**:221-228.

Summersgill, J. T., M. J. Raff, and R. D. Miller. 1990. Interactions of virulent and avirulent *Legionella pneumophila* with human monocytes. *J. Leukocyte Biol.* **47**:31-38.

- Susa, M., J. Hacker, and R. Marre. 1996. De novo synthesis of *Legionella pneumophila* antigens during intracellular growth in phagocytic cells. *Infect. Immun.* 64:1679-1684.
- Swanson, M. S., and R. R. Isberg. 1995. Association of *Legionella pneumophila* with the macrophage endoplasmic reticulum. *Infect. Immun.* 63:3609-3620.
- Szeto, L., and H. A. Shuman. 1990. The *Legionella pneumophila* major secretory protein, a protease, is not required for intracellular growth or cell killing. *Infect. Immun.* 58:2585-2592.
- Tempest, D. W., and O. M. Neijssel. 1976. Microbial adaptation to low-nutrient environments, p. 283-294. *In* A. C. R. Dean, D. C. Ellwood, C. G. T. Evans and J. Melling (eds.), Continuous culture 6: applications and new fields. Ellis Horwood LTD., Chichester.
- Tempest, D. W., and O. M. Neijssel. 1982. The status of Y_{ATP} and maintenance energy as biologically interpretable phenomena. *Ann. Rev. Microbiol.* 38:459-486.
- Tempest, D. W., and O. M. Neijssel. 1992. Physiological and energetic aspects of bacterial metabolite overproduction. *FEMS. Microbiol. Lett.* 100:169-176.
- Tesh, M. J., and R. D. Miller. 1981. Amino acid requirements for *Legionella pneumophila* growth. *J. Clin. Microbiol.* 13:865-869.
- Tesh, M. J., and R. D. Miller. 1982. Growth of *Legionella pneumophila* in defined media: requirement for magnesium and potassium. *Can. J. Microbiol.* 28:1055-1058.
- Tesh, M. J., S. A. Morse, and R. D. Miller. 1983. Intermediary metabolism in *Legionella pneumophila*: utilization of amino acids and other compounds as energy sources. *J. Bacteriol.* 154:1104-1109.
- Thacker, S. B., J. V. Bennett, T. F. Tsai, D. W. Fraser, J. E. McDade, C. C. Shepard, K. H. Williams, Jr., W. H. Stuart, H. B. Dull, and T. C. Eickhoff. 1978. An outbreak in 1965 of severe respiratory illness caused by the Legionnaires' disease bacterium. *J. Infect. Dis.* 138:512-519.

- Thacker, W. L., B. B. Plikaytis, and H. W. Wilkinson. 1985. Identification of 22 *Legionella* species and 33 serogroups with the slide agglutination test. *J. Clin. Microbiol.* 21:779-782.
- Thomas, C. E., and P. F. Sparling. 1994. Identification and cloning of a *fur* homologue from *Neisseria meningitidis*. *Mol. Microbiol.* 11:725-737.
- Thomas, C. E., and P. F. Sparling. 1996. Isolation and analysis of a *fur* mutant of *Neisseria meningitidis*. *J. Bacteriol.* 178:4224-4232.
- Thorpe, T. C., and R. D. Miller. 1981. Extracellular enzymes of *Legionella pneumophila*. *Infect. Immun.* 33:632-635.
- Tison, D. L., and R. J. Seidler. 1983. *Legionella* incidence and density in potable drinking water supplies. *Appl. Environ. Microbiol.* 45:337-339.
- Tobin J. O'H., M. S. Dunnill, M. French, P. J. Morris, J. Beare, S. Fisher-Hoch, R. G. Mitchell, M. F. Muers. 1980. Legionnaires' disease in a transplant unit: isolation of the causative agent from shower baths. *Lancet* ii:118-121.
- Tsai, C. M., and C. E. Frasch. 1981. A sensitive silver stain for detecting lipopolysaccharide in polyacrylamide gels. *Anal. Biochem.* 119:115-119.
- Tyndall, R. L., and E. L. Domingue. 1982. Cocultivation of *Legionella pneumophila* and free-living amoebae. *Appl. Environ. Microbiol.* 44:954-959.
- Vandenesch, F., M. Surgot, N. Bornstein, J. C. Paucod, D. Marmet, P. Isoard, and J. Fleurette. 1990. Relationship between free amoebae and *Legionella*: studies *in vitro* and *in vivo*. *Intern. J. Med. Microbiol.* 272:265-275.
- Verbrugh, H. A., D. A. Lee, G. R. Elliott, W. F. Keane, J. R. Hoidal, and P. K. Peterson. 1985. Opsonization of *Legionella pneumophila* in human serum: key roles for specific antibodies and the classical complement pathway. *Immunol.* 54:643-653.
- Veríssimo, A., G. Marrão, F. Gomes da Silva, and M. S. da Costa. 1991. Distribution of *Legionella* spp. in hydrothermal areas in continental Portugal and the island of São Miguel, Azores. *Appl. Environ. Microbiol.* 57:2921-2927.
- Wadowsky, R. M., L. J. Butler, M. K. Cook, S. M. Verma, M. A. Paul, B. S. Fields, G. Keleti, J. L. Sykora, and R. B. Yee. 1988. Growth-supporting activity for

Legionella pneumophila in tap water cultures and implication of hartmannellid amoebae as growth factors. Appl. Environ. Microbiol. 54:2677-2682.

Wadowsky, R. M., R. Wolford, A. M. McNamara, and R. B. Yee. 1985. Effect of temperature, pH, and oxygen level on the multiplication of naturally occurring *Legionella pneumophila* in potable water. Appl. Environ. Microbiol. 49:1197-1205.

Wadowsky, R. M., and R. B. Yee. 1983. Satellite growth of *Legionella pneumophila* with an environmental isolate of *Flavobacterium breve*. Appl. Environ. Microbiol. 43:1447-1449.

Wadowsky, R. M., and R. B. Yee. 1985. Effect of non-*Legionellaceae* bacteria on the multiplication of *Legionella pneumophila* in potable water. Appl. Environ. Microbiol. 49:1206-1210.

Wadowsky, R. M., R. B. Yee, L. Mezmar, E. J. Wing, and J. N. Dowling. 1982. Hot water systems as sources of *Legionella pneumophila* in hospital and non-hospital plumbing fixtures. Appl. Environ. Microbiol. 43:1104-1110.

Wait, R. 1988. Confirmation of the identity of legionellae by whole cell fatty acid and isoprenoid quinone profiles, p. 69-101. In T. G. Harrison, and A. G. Taylor (eds.), A laboratory manual for *Legionella*. John Wiley & Son, Chichester.

Wang, W. L. L., B. J. Martin, J. Cravens, and M. A. Johnson. 1979. Growth, survival, and resistance to the Legionnaires' disease bacterium. Ann. Intern. Med. 90:614-618.

Warren, W. J., and R. D. Miller. 1979. Growth of Legionnaires' disease bacterium (*Legionella pneumophila*) in chemically defined medium. J. Clin. Microbiol. 10:50-55.

Watkins, I. D., J. O'H. Tobin, P. J. Dennis, W. Brown, R. S. Newnham, and J. B. Kurtz. 1985. *Legionella pneumophila* serogroup 1 subgrouping by monoclonal antibodies - an epidemiological tool. J. Hyg. (Camb.) 95:211-216.

Weinberg, E. D. 1974. Iron and susceptibility to infectious disease. Sci. 184:952-956.

- Weiss, E., M. G. Peacock, and J. C. Williams. 1980. Glucose and glutamate metabolism of *Legionella pneumophila*. *Curr. Microbiol.* 4:1-6.
- West, A. A., J. Rogers, J. V. Lee, and C. W. Keevil. 1993. Lack of dormancy in *Legionella pneumophila*? p. 201-203. In J. M. Barbaree, R. F. Breiman, and A. P. Dufour (eds.), *Legionella: current status and emerging perspectives*. American Society for Microbiology, Washington, D.C.
- West, S. E. H., and P. F. Sparling. 1985. Response of *Neisseria gonorrhoeae* to iron limitation: alterations in expression of membrane proteins without apparent siderophore production. *Infect. Immun.* 47:388-394.
- Wilkinson, D. A., and J. F. Nagle. 1981. Dilatometry and calorimetry of saturated phosphatidylethanolamine dispersions. *Biochem.* 20:187-192.
- Williams, P. 1988. Role of the cell envelope in bacterial adaptation to growth *in vivo* in infections. *Biochimie.* 70:987-1011.
- Williams, A., A. Baskerville, A. B. Dowsett, and J. W. Conlan. 1987. Immunocytochemical demonstration of the association between *Legionella pneumophila*, its tissue destructive protease, and pulmonary lesions in experimental Legionnaires' disease. *J. Path.* 153:257-264.
- Williams, P., D. J. Morton, K. J. Towner, P. Stevenson, and E. Griffiths. 1990. Utilization of enterobactin and other exogenous iron sources by *Haemophilus influenza*, *H. parainfluenza* and *H. paraphrophilus*. *J. Gen. Microbiol.* 136:2343-2350.
- Winn, W. C. Jr. 1988. Legionnaires' disease: historical perspective. *Clin. Microbiol. Rev.* 1:60-81.
- Winn, C. W. Jr., and R. L. Myerowitz. 1981. The pathology of the *Legionella* pneumonias. *Prog. Hu. Path.* 12:401-422.
- Wintermeyer, E., M. Flugel, M. Ott, M. Steinert, U. Rdest, K. Mann, and J. Hacker. 1994. Sequence determination and mutational analysis of the *lly* locus of *Legionella pneumophila*. *Infect. Immun.* 62:1109-1117.

- Wintermeyer, E., B. Ludwig, M. Steinert, B. Schmidt, G. Fischer, and J. Hacker. 1995. Influence of site specifically altered Mip proteins on intracellular survival of *Legionella pneumophila* in eukaryotic cells. *Infect. Immun.* 63:4576-4583.
- Wintermeyer, E., U. Rdest, B. Ludwig, A. Debes, and J. Hacker. 1991. Characterization of legiolysin (*lly*), responsible for hemolytic activity, colour production and fluorescence of *Legionella pneumophila*. *Mol. Microbiol.* 5:1135-1143.
- Wong, K. H., C. W. Moss, D. H. Hochstein, R. J. Arko, and W. O. Schalla. 1979. "Endotoxicity" of the Legionnaires' disease bacterium. *Ann. Intern. Med.* 90:624-627.
- Woo, A. H., A. Goetz, and V. L. Yu. 1992. Transmission of *Legionella* by respiratory equipment and aerosol generating devices. *Chest.* 102:1586-1590.
- Yamamoto, Y., T. W. Klein, and H. Friedman. 1994. *Legionella* and macrophages, p. 329-348. In B. S. Zwillling, and T. K. Eisenstein (eds.), *Macrophage-pathogen interactions*. Marcel Dekker, Inc.
- Yee, R. B., and R. M. Wadowsky. 1982. Multiplication of *Legionella pneumophila* in unsterilized tap water. *Appl. Environ. Microbiol.* 43:1330-1334.
- Zilberstein, D., V. Agmon, S. Schuldiner, and E. Padan. 1984. *Escherichia coli* intracellular pH, membrane potential, and cell growth. *J. Bacteriol.* 158:246-252.